

THE URBAN FORM AND SOLAR RADIATION

— IN TROPICAL ARID CLIMATES

INVESTIGATION OF THE INTERRELATIONSHIPS WITH THE
AID OF AN EVALUATIVE COMPUTER MODEL WITH
GENERATIVE POTENTIALS : WITH PARTICULAR
REFERENCE TO KHARTOUM

MOHAMED YOUSIF NUMAN
B.Sc. (ARCH.), KHARTOUM
M.BLDG.Sc., SYDNEY



PH.D.

DEPARTMENT OF ARCHITECTURE
UNIVERSITY OF EDINBURGH

1977

DECLARATION

This thesis is my own work.

ABSTRACT

The thesis is concerned with the interactions between solar irradiance and buildings in urban situations in tropical arid regions. It attempts to reveal the effects of the geometry and surface reflectance of buildings on the initial, inter-reflected and final irradiance on the external surfaces of buildings and define their interrelationships. A computerised mathematical model is developed to simulate the interactions at the external surfaces of buildings, embodies the relevant physical processes and factors involved and enables the irradiance load to be evaluated. The model is used to carry out systematic and detailed investigations for the most common forms of buildings and urban configurations for Khartoum, a location typical of the tropical arid regions. These identify the ranges, the significance and the effects of the geometrical parameters and surface reflectance of buildings on the initial, interreflected and final irradiance load and define their interrelationships. On this basis, simplified economical solution procedures for the evaluation of the initial and interreflected irradiance are developed, irradiance indices and measures of form performance are established and guidelines for the manipulation of the form parameters for the control of the irradiance load are defined. The generative potentials of the model, its capabilities, flexibility and applicability in the design process in minimising the irradiance load on buildings are illustrated.

In order to carry out the programme of work described above, a major preliminary investigation of solar and sky radiation in tropical arid conditions had to be carried out. This is also presented in the thesis.

ACKNOWLEDGEMENTS

This thesis was supervised by Professor C B Wilson, Professor of Architectural Science in the Department of Architecture. I would like to express my sincere gratitude to him for his constant guidance, enthusiastic and resourceful support.

In compiling and operating the computer, I received generous assistance from many people in the Edinburgh Regional Computing Centre for which I am grateful.

My thanks are due to Dr F Smith, Post Doctoral Research Fellow in the Department of Architecture, for his advice and useful comments on the technical specification of the computer programs package.

My thanks go to my fellow research students in the Department for their constructive discussions, comments and suggestions.

My sincere thanks are also due to Mrs Linda Halstead who undertook the difficult task of typing this thesis with great patience, efficiency and co-operation. I am also most grateful to Miss Ingrid Clouston for her generous help in typing part of the manuscript and proof-reading of the text.

Most of all, my sincere gratitude goes to my wife, Nagat, who shared my years of study in Edinburgh, supported and cared for me with patience and grace.

During my period of study in Edinburgh, I received financial support from the British Council and later from the University of Khartoum for which I am thankful.

CONTENTS

	<u>page no</u>
CHAPTER I : A GENERAL INTRODUCTION	
1. Origin of the Problem	1
2. Analysis of Previous Studies on the Control of the Irradiance Field	3
2.1 Constructional Control	4
2.2 Control Over Form, Spacing and Orientation of Buildings	5
3. The Definition of the Problem, the Approach and the Method of Investigation	8
3.1 Conception of the Problem	9
3.2 The Approach and the Method of Investigation	11
3.3 Outline of the Study	13
3.4 Layout of the Thesis	16
CHAPTER II : DEFINITION OF A MODEL EMBODYING THE INTER-ACTIONS BETWEEN THE URBAN FORM AND SOLAR RADIATION	
1. Introduction	19
2. The Physical System	23
2.1 The System	23
2.2 The Input	25
2.3 The Output	25
2.4 Definition of the System and Subsystem Boundaries	27
2.5 Previous Studies	(31)
2.6 An Outline of a Model for the System	(32)
3. Solar Radiation : The Excitation Source of the System	35
3.1 The Solar Spectrum	35
3.2 The Solar Constant	35
3.3 The Solar Energy Received on the Earth's Surface	36
4. Parameters of the Physical System, the Physical Structure	43
4.1 Geometrical Parameters	43
4.2 Physical Parameters : Reflectivity for Solar Radiation	45

The Structure of the Model, Formulation
of the Factors and the Irradiance
Transfer Function

5.	Transfer Function	52
6.	Initial Irradiance Function	53
6.1	The Direct Radiation	53
6.2	The Diffuse Sky Radiation	56
6.3	The Global Irradiance	61
6.4	Shadows and the Obstruction of the Direct Solar Rays	61
6.5	Diffusion and the Obstruction of the Diffuse Sky Radiation	65
6.6	Shadow and Diffusion Factors	70
6.7	Initial Irradiance Functions of Surfaces	73
7.	Interreflected Irradiance	74
7.1	Configuration and Form Factors	74
7.2	Long Wave Radiation Exchange Between Building Surfaces	79
8.	Final Irradiance Transfer Function	81
9.	Theoretical Analysis of Irradiance Transfer Function	85
9.1	Analysis of Initial Irradiance Function	85
9.2	Analysis of the Final Irradiance Function	88

CHAPTER III : THE MATHEMATICAL MODEL AND ITS COMPUTER
APPLICATION

1.	Introduction	93
2.	The Choice of a Mathematical Model	95
2.1	Physical Models	95
2.2	Analogue Computers	97
2.3	The Digital Computer Mathematical Model	102
3.	Sun Geometry	105
3.1	Fundamental Solar Angles	107
3.2	The Angular Parameters of the Sun	112

4.	Standardisation and Prediction of Irradiance and Illuminance of Surfaces of Different Inclinations and Orientations in Tropical Regions	115
4.1	Standard Tropical Atmosphere	117
4.2	Direct Incident Irradiance	120
4.3	Direct Solar, Diffuse Sky and Global Irradiance on a Horizontal Surface	121
4.4	Solar and Sky Illuminance	124
4.5	Diffuse Irradiance and Illuminance of Vertical and Inclined Surfaces	129
4.6	Zenith Luminance and Intensity	142
5.	The Evaluation of the Shaded Direct and the Obstructed Diffuse Sky Radiation	144
5.1	Formulation of the Shadow Geometry	144
5.2	The Obstructed Sky Component and Radiation	149
5.3	The Initial Irradiance Model	155
6.	The Building Description	157
6.1	Geometrical Description of the Built Form	157
6.2	The Physical Parameters of the Built Form	161
7.	The Evaluation of the Form Factors	163
7.1	Formulation of the Configuration and Form Factors for Finite Surfaces	163
7.2	The Form Factors of Infinitely Long Surfaces	168
8.	The Numerical Evaluation of Double Integral Functions	169

CHAPTER IV : TECHNICAL SPECIFICATION OF THE COMPUTER PROGRAMS PACKAGE

1.	Introduction	171
2.	The Operation and Organisation of the Model Program Package	172
2.1	Hardware and Software Background	172
2.2	The Programming Language	173

	<u>page no</u>
2.3 The Data Structure	173
2.4 The Layout and Organisation of the Program Package and its Output	175
3. Description of the Main Subroutines	177
3.1 The Shadow Subroutine SHGT	177
3.2 The Sky Component Subroutine SKYCOM	182
3.3 The Form Factor Subroutine FOFACT	183
3.4 The Initial Irradiance Subroutine IRRILL	189
3.5 The Sun Geometry Subroutine SUNGT	190
3.6 The Assembly and Solution of the Final Irradiance Transfer Functions, The Subroutine MATRIX	190
4. The Flow Charts	191
CHAPTER V : EXPLORATORY INVESTIGATIONS	
1. Introduction	202
2. The Computational Errors	204
2.1 Roundoff Error	204
2.2 Truncation Error	204
2.3 Inherent Error	211
3. Verification of the Approximate Techniques Used to Simplify the Evaluation of Model Output	212
3.1 The Weighted Average Reflectance of Facade	213
3.2 The Weighted Average Initial Irradiance of Facade	215
4. The Overall Performance and Accuracy of the Model	220
CHAPTER VI : INVESTIGATION WITH THE MODEL : THE EFFECTS OF ORIENTATION, PLAN PROPORTION AND CONFIGURATION OF FORM AND SURROUNDINGS ON THE INITIAL IRRADIANCE LOAD	
1. Introduction	223
2. Evaluation of the Surfaces Initial Irradiance Load	227

	<u>page no</u>
2.1 Measures of the Surface's Irradiance Input	227
2.2 The Average Daily Total as a Measure of Irradiance Input of Surfaces	228
3. Initial Irradiance and the Geometrical Parameters of Form	231
3.1 Configuration and Ranges of Form Parameters	231
3.2 The Evaluation of the Initial Irradiance of Vertical and Horizontal Surfaces	234
4. Analysis of the Variation and Distribution of the Average Daily Total Initial Irradiance with the Geometrical Parameters of Form	236
4.1 The Distribution of the Initial Irradiance of the Vertical Surface	236
4.2 The Distribution of the Initial Irradiance of the Ground Surface Separating Two Vertical Facades	249
5. Irradiance and Shadow Factor Indices	258
5.1 Initial Irradiance Index of the Vertical Surface	259
5.2 Initial Irradiance Index of the Ground	264
5.3 Development of Simplified Shadow Factor Index for Block-Spacing Criteria	268
6. The Evaluation of Form Geometry, Plan Proportion and Orientation in Terms of Total Initial Irradiance Load	272
6.1 Generation of Geometric Configuration of Block and Surroundings and the Evaluation of the Total Initial Irradiance Load	273
6.2 The Evaluation of the Total Irradiance Load of a Building Block	278
6.3 Analysis of the Results : The Relations Between Optimum Plan Proportion of Block, Orientation and Geometric Configuration of Urban Form	281

6.4	Variation of the Optimum Irradiance Load with the Parameters of Form	295
6.5	Consideration of the Optimum Plan Proportion and the Initial Irradiance Load for Maximum Shadow Factor	301
7.	Concluding Remarks	303

CHAPTER VII : INVESTIGATION WITH THE MODEL : THE EFFECTS OF THE GEOMETRICAL AND PHYSICAL PARAMETERS OF THE FORM ON THE INTERREFLECTED AND FINAL IRRADIANCE

1.	Introduction	308
2.	Evaluation of the Interreflected and Final Irradiance Load of the Facades	311
2.1	Geometrical Representation of the Block's Finite Facades by a Model of Infinitely Long Surfaces	311
2.2	Evaluation of the Daily Average Interreflected Irradiance Load	317
3.	The Effects of the Geometrical and Physical Parameters on the Interreflected Irradiance	318
3.1	Components of the Interreflected Irradiance	318
3.2	Coefficients of the Interreflected Irradiance Components and their Variations with the Parameters of the System	320
3.3	The Effects of the Geometrical and Physical Parameters of the Form on the Instantaneous Initial Irradiance and Interreflected Irradiance and its Components	332
3.4	The Effects of Form Parameters on the Hourly Distribution of the Interreflected and Final Irradiance	350
3.5	Effects of the Parameters of the Form on the Daily Average Inter-Reflected Irradiance	357

	<u>page no</u>
4. Development of Form Performance Index for the Interreflected Irradiance	367
5. The Effects of Orientation, Geometric Configuration of Surroundings and Reflectance of Surfaces on the Optimum Plan Proportion and Final Irradiance Load of the Block	373
5.1 Evaluation of Optimum Form of Block for Minimum Irradiance Load	373
5.2 Variation of the Optimum Plan Proportion with Orientation and Parameters of the Form	375
5.3 Variation of the Optimum Final Irradiance Load on Building Block with its Form Parameters and Orientation	383
6. Concluding Remarks	389
 CHAPTER VIII : GENERAL CONCLUSION	
1. Practical Interpretation of the Results	400
2. Further Development of the Evaluative Model and its Generative Potentials	404
 APPENDICES	 408
 BIBLIOGRAPHY	 466

PRINCIPAL SYMBOLS USED

S.T.S.	Standard tropical sky or atmosphere	
I_o	Solar constant	W/m^2
I_{cn}	Direct normal irradiance, standard tropical atmosphere	W/m^2
I_{ch}	Direct horizontal irradiance, standard tropical atmosphere	W/m^2
I_{DN}	Direct normal irradiance	W/m^2
I_{Dh}	Direct horizontal irradiance	W/m^2
I_{dh}	Diffuse horizontal irradiance	W/m^2
I_{Gh}	Global horizontal irradiance	W/m^2
I_{Ds}	Direct incident irradiance of an inclined surface	W/m^2
I_{ds}	Diffuse irradiance of an inclined surface	W/m^2
I_{Gs}	Global irradiance of an inclined surface	W/m^2
CN	Clearness number	dimensionless
K_s	Luminous efficacy of sun radiation	Lm/W
K_d	Luminous efficacy of sky radiation	Lm/W
K_g	Luminous efficacy of global radiation	Lm/W
E_{DN}	Direct normal illuminance	KLx
E_{Dh}	Direct horizontal illuminance	KLx
E_{dh}	Horizontal sky illuminance	KLx
E_{Gh}	Horizontal global illuminance	KLx
E_{ds}	Sky illuminance of an inclined surface	KLx
E_{GS}	Global illuminance of an inclined surface	KLx
E_{DS}	Direct illuminance of an inclined surface	KLx
L_p	Luminance of a point in the sky	cd/m^2
L_z	Zenith luminance	cd/m^2
I_p	Radiant intensity of a point in the sky	W/m^2
I_z	Zenith radiant intensity	W/m^2
T	Turbidity factor of the sky, Linke	
R	Sky component of a fully exposed surface	
R_s	Sky component of a partially exposed surface (clear sky)	dimensionless
R_{ob}	Obstructed sky component (clear sky)	dimensionless
S_F	Shadow factor of a surface	dimensionless

SF_{av}	Area weighted average shadow factor of a surface	dimensionless
SF_d	Daily average shadow factor of a surface	dimensionless
γ_0	Solar altitude	degrees
α_0	Solar azimuth	degrees
ϵ_0	Solar zenith distance	degrees
γ_s	Surface inclination, angle surface makes with the horizon	degrees
α_s	Surface orientation, angle between normal of the surface and true north measured clockwise	degrees
θ	The angle the direct solar beam makes with the normal to the surfaces	degrees
δ	Angular distance between a point in the sky and the sun	degrees
ϵ	Zenith distance of a point in the sky	degrees
δ_0	Solar declination	degrees
E	Equation of time	seconds
H	hour angle	degrees
γ_{ob}	Altitude angle of obstruction, from a reference point on the surface	degrees
γ_{om}	Altitude angle of obstruction, at ground level for a surface	degrees
α_{ob}	Azimuthal angular width of obstruction	degrees
A	Area of a surface	m^2
A_s	Shaded area of a surface	m^2
Rd	Proportion of street width to height of block	dimensionless
Rh	Proportion of height of obstruction to height of block	dimensionless
$F_{i,j}$	Form factor, the fraction of energy leaving surface 'i' that is incident on surface 'j'	dimensionless
ρ	Reflectance of a surface for solar radiation; ρ_f : facade reflectance, ρ_g : ground reflectance and ρ_s : surrounding reflectance	dimensionless
ρ_{av}	Area weighted average reflectance of a surface	dimensionless
I_I	Initial irradiance of a surface	W/m^2
I_{yt}	Yearly total initial irradiance of a vertical surface	W/m^2
I_{dt}	Daily average initial irradiance of a vertical surface	W/m^2
I_{xv}	Standard irradiance index of a vertical surface	KW/m^2

I_{dth}	Daily average initial irradiance of ground	W/m^2
I_{xg}	Standard irradiance index of ground	KW/m^2
I_F	Final irradiance of a surface	W/m^2
I_R	Total interreflected irradiance of a surface	W/m^2
I_{rd}	Daily average interreflected irradiance of a surface	W/m^2
I_{rf}	Facade component of the interreflected irradiance initiated by facade irradiance input I_{If}	W/m^2
I_{rg}	Ground component of the interreflected irradiance initiated by ground irradiance input I_{Ig}	W/m^2
I_{rs}	Surrounding component of the interreflected irradiance, initiated by surrounding irradiance input I_{Is}	W/m^2
a_{cf}	Coefficient of the facade component of the interreflected irradiance	dimensionless
a_{cg}	Coefficient of the facade component of the interreflected irradiance	dimensionless
a_{cs}	Coefficient of the ground component of the interreflected irradiance	dimensionless
I_{Px}	Form performance index for interreflected irradiance	dimensionless
P	Plan proportion of a rectangular block for minimum initial irradiance	dimensionless
P_f	Plan proportion of a rectangular block for minimum final irradiance	dimensionless
C_p	Volume correction factor	m

CHAPTER 1
INTRODUCTION

INTRODUCTION

1. ORIGIN OF THE PROBLEM

1.1.1 The development of technology, the rapid social changes and the rigorous demands of modern urban life confront urban architecture with numerous and complex environmental problems. In order to tackle such problems it has become essential for the designer to acquire detailed knowledge about the physical environment and its interactions with buildings, establish comprehensive information and data on the performance characteristics of building materials and psychophysical requirements of man and develop adequate skills, techniques and design tools to produce a balanced environmental design. Much existing knowledge refers to the problems of the temperate regions where most of the industrialised developed countries are found. It cannot be directly applied to the tropical regions which contain most of the developing countries. ✓

1.1.2 The problems of the tropical arid regions are particularly acute because of the characteristically high intensity and duration of insolation which makes solar irradiance the most important environmental physical field. It is this which is the concern of the study reported in this thesis. A primary objective of environmental design in these regions is the control of the solar irradiance field by minimising its thermal and glare effects while utilising and enhancing

its positive visual aspects. However, there is a lack of adequate knowledge, data and design tools and this limits the designer's ability to achieve natural control of the irradiance environment by manipulating the geometrical, spatial and physical characteristics of a building's elements. In addition, most designers in these regions have been influenced by western ideas and technology and have adopted building styles, materials and techniques without carefully scrutinising their suitability to the local climatic conditions. Similarly, they have relied heavily on mechanical means for cooling, ventilation and lighting which may not be justified in the context of the meagre financial and energy resources of many developing countries.

1.1.3 The information needed by the designer is the direct output of research. It is therefore justifiable that recent interests in building research should be directed towards problems arising in the tropical regions. This study considers aspects of the problems of solar irradiance and buildings in tropical regions which have not previously received full consideration. In particular, an attempt is made to investigate the interaction between solar irradiance and buildings in urban situations taking into account the relevant physical processes involved and to define the inter-relationships between the initial and final irradiance load received on the external surfaces of buildings and the geometrical and physical parameters of the form.

2. ANALYSIS OF PREVIOUS STUDIES ON THE CONTROL OF THE IRRADIANCE FIELD

2.0.1 Several aspects of the problems of solar irradiance and buildings have already been studied at length. These may be classified into two main areas :

(i) Psychophysical studies dealing with the problems of daylighting and the thermal stress. These have led to the development of theories of daylighting and thermal exchange and to recommendations for optimum levels and indices of thermal and visual comfort. The relevance of their findings to tropical conditions is evident.

Accordingly, they may be interpreted and incorporated into the process of architectural design. However, there is a need for further studies regarding the direct and reflected sunlight which constitutes the main source of interior illumination in the tropics.

(ii) Studies which dealt with the basic physics and mechanics of thermal and irradiative transfer, the physical characteristics of building materials and the performance of buildings.

2.0.2 On the basis of these studies, two possible means have emerged of enabling the designer to exercise control over the irradiance environment in the tropical arid regions without mechanical aids :

- (i) by constructional control, and
- (ii) by controlling the form, orientation and spacing of buildings.

The extent to which the designer is able to incorporate successfully either or both means in the design depends on the extent of the studies in understanding the physical phenomena and making accurate formulations of them. At present the psychophysical aspects seem to be better understood than the physical. The following discussion, therefore, considers the limitations of physical studies with regard to the two possible means of controlling the irradiance environment.

2.1 Constructional Control

2.1.1 The principles of thermal transfer and the characteristics of building materials and construction are by now well established. This is illustrated by the volume of completed research and by the numerous books, manuals, and other publications concerning this field which are currently in circulation (eg, Billington 1952, 1967, ASHRAE 1963, Van Straaten 1967, Givoni 1969, Ragsdale 1972, Koenigsberger et al 1973). Similarly, the geometry of the sun's movement and the performance of the different shading devices is well documented (eg, Olgyay 1957, 1967, Nicol 1964, Bussat et al 1972, and so on).

2.1.2 The designer is therefore able to control the thermal built environment, calculate and regulate the thermal and irradiance transfer by the following basic techniques :

- (i) the selection of the type of construction, such as the cavity or multi-layer wall,
- (ii) the selection of the type of materials and finishes, such as insulation, thermal capacity and reflective materials, and
- (iii) the use of added design features such as louvre systems and shading devices.

2.1.3 In general the use of these constructional methods adds considerably to the initial cost of a building. At the same time, the designer is required to estimate the magnitude of the irradiance load received on the external surfaces of the building. No standard practical method has yet been presented for the prediction of the direct solar and diffuse sky irradiance, for the tropical regions, and to account for the shading created by surrounding buildings.

2.2 Control Over Form, Spacing and Orientation of Buildings

2.2.1 The magnitude of the final irradiance received on the external surfaces of buildings which ^{some of it} is eventually transmitted to the internal enclosures through the openings and the materials of the external walls is composed of two main

components, initial irradiance and interreflected irradiance. The two components are determined by the following physical processes :

(i) The shading of the direct solar and the obstruction of the diffuse sky radiation by adjacent buildings determines the initial irradiance load.

(ii) The externally interreflected irradiance is determined by the multiple interreflection between the external surfaces of buildings and the ground space between them.

2.2.2 It is apparent that the manipulation of the geometrical and angular parameters of buildings provides a practical possibility for the control of the final irradiance load, the factors determining it and ultimately the thermal and visual built environment. However, previous studies considering these aspects seemed to place emphasis on only some of the factors involved. These studies may be classified as follows :

(i) Studies which are mainly concerned with the optimisation and the minimisation of the irradiance load (eg, work by Buchberg and Naruishi 1967, Olgyay 1967, 1969, Kuba 1969, Valko 1969, 1970 and 1972, Tappuni 1973). These studies mainly deal with the initial irradiance load. They treated buildings simply as free standing and isolated units and do not take into account the shading and obstruction of the direct and diffuse sky radiation caused by the surroundings.

They therefore fail to explore the potential of the shading effects for reducing the irradiance load. Similarly, they under-estimate the externally interreflected irradiance. The limitations of these studies are mainly due to the complex formulation and evaluation procedures required for the estimation of the shading and interreflection effects. ✓

(ii) Studies which recognise the importance of the externally reflected component in determining the final output of the physical system (eg, Hopkinson 1963, Plant et al 1965, 1967, 1969 and 1973, Narasimhan 1969). These studies show the dependence of interior illumination on such parameters as height, separation and reflectance of opposite facades. They consider a limited configuration of building facades and reflectances. The choices of the initial irradiances appear to have been made rather arbitrarily, although, in general, they represent the irradiances for certain typical positions of the sun. They do not consider the variation of the initial irradiance with variation of the geometrical parameters of the form. It is apparent that these studies, too, faced the difficulties of estimating the initial irradiance and accounting for the shading and obstruction effect of neighbouring buildings on the direct and diffuse solar irradiance. ✓

3. THE DEFINITION OF THE PROBLEM, THE APPROACH AND THE METHOD OF INVESTIGATION

3.0.1 The present study considers the problem of interaction between the solar irradiance and buildings in urban situations typical of tropical arid regions. The determining factors may be summarised as :

- (i) the dominance of the solar irradiance in the tropical arid regions,
- (ii) the lack of adequate information and procedures for the evaluation of the irradiance load,
- (iii) the lack of adequate understanding of the interaction between the irradiance field and buildings, the inter-relationship between the factors and the parameters involved and their significance in determining the irradiance load,
- (iv) the lack of adequate tools, data and information needed by the designer to enable him to manipulate the geometrical and physical parameters of buildings for the control of the thermal and visual effects of the solar irradiance within the desirable levels for human comfort, and
- (v) the inadequacy of existing architectural practice and its failure to exploit the natural possibilities for controlling the irradiance field.

3.1 Conception of the Problem

3.1.1 Buildings, as physical structures, interact with and modify the irradiance field. Therefore, the interaction between solar irradiance and building is conceived as a single physical system. The system is specified by the urban built form which comprises solids and voids. These represent the physical structures enclosing the internal spaces and the external spaces formed between them. They are defined by the spatial, geometrical and physical characteristics of their surfaces. The solar irradiance field acting on the system is the excitation source. It is composed of the direct solar and diffuse sky radiation with their temporal variations, spectral distribution and directional characteristics. The ultimate output of the system is the thermal and luminous built environment. /

3.1.2 External and internal subsystems, defining the spaces contained within the solids and the voids of the system, are distinguished. The distinction is made with respect to the two main levels of input and output of the system and the irradiance transfer processes determining them. The study deals mainly with the external subsystem as defined by the external surfaces of buildings and the ground between them. This choice was prompted by three main factors :

- (i) The geometry of the external subsystem governs the primary input to the system which is the initial irradiance of the external surfaces.

(ii) The output of the external subsystem, being the final irradiance of the external surfaces is the primary output of the system. It forms the input to the internal subsystem and determines the ultimate output of the system, thermal and luminous built environment.

(iii) This area has not yet been fully considered in an integrated form, particularly regarding the formulation of the interactions and the physical processes involved, and the significance of the parameters of the form in determining the primary output.

3.1.3 The study continues with the construction of a model which defines the external subsystem by the spatial, geometrical and physical characteristics of its surfaces. The model expresses the interactions between the solar irradiance field and the external surfaces of buildings. It embodies the main physical processes involved :

- (i) the partial or total shading and obstruction of the direct solar and diffuse sky radiation which determine the initial irradiance of the external surfaces, representing the primary input of the system; and
- (ii) the interreflection between the external surfaces which determines their final irradiance and represents the primary output of the system.

3.1.4 To simplify the formulation of the model certain assumptions have been made :

- (i) it is assumed that surfaces are perfect diffusers,
- (ii) the interreflection between the external surfaces and internal surfaces of the enclosures through openings is ignored as being insignificant, and
- (iii) the long-wave radiation exchange between the external surfaces is similarly considered to have no practical significance.

3.2 The Approach and the Method of Investigation

3.2.1 The physics of the problem was defined first and, on this basis, a mathematical model was formulated. This involved the derivation of mathematical expressions for the prediction of the quantities of the irradiance and illuminance on surfaces of different orientations and inclinations for standard tropical sky. The model then accounts for the relevant physical processes and factors involved. It defines the quantitative relationships between the output and the parameters of the subsystem.

3.2.2 The availability of high speed digital computers with their capacity for rapid and repetitive calculation provided a practical tool for use in conducting the investigations.

The study was, therefore, conducted with the aid of a computer orientated mathematical model. With it, it was possible to overcome the practical difficulties generally associated with experimental investigations and measurements in the field and the laboratory such as the limited ranges of parameters and geometrical configurations of forms which may be considered, the inconsistency of the natural irradiance data, the climatic conditions and so on. It also provided the means to study alternative configurations of urban forms and establish the effects of wide ranges and combinations of the parameters on the output. Computer models are being extensively used nowadays for analysing and solving various complex architectural problems and in design application. The model developed in conjunction with this study may be incorporated with related models towards a synthesis of a total architectural solution.

3.2.3 As is generally the case, the implementation of the model on a computer raised numerous difficulties. These were surmounted prior to conducting the investigation and mainly related to the following points :

- (i) the development and choice of the numerical methods for the evaluation of the various factors and the output;
- (ii) the compilation of efficient computer programmes and routines for the evaluation of the different factors and the output;

- (iii) the optimisation and the evaluation of the accuracy of the numerical methods, the individual routines and the overall accuracy of the model with respect to the computation time; and
- (iv) the derivation of simpler methods and compilations of routines, on the basis of the results obtained, with the object of finding more economical solution procedures.

3.2.4 A computer programme package was prepared which encompassed the model. The programmes were coded in FORTRAN which is a standard language for scientific problems. For efficient and direct utilisation of the package in evaluative and generative studies particular features of the programmes were emphasised, such as :

- (i) simplicity of input and output,
- (ii) flexibility of use with different routines, which evaluate the different factors, separately or jointly, and
- (iii) efficiency and accuracy of the routines.

3.3 Outline of the Study

3.3.1 The model was then used in a series of investigations.

The scope of these was limited by two main factors :

(i) The solar irradiance field is greatly influenced by the geographical location of the site. The study is therefore confined to Khartoum, a location typical of the tropical arid region.

(ii) It was found to be impractical to study all possible combinations of geometrical shapes of building and urban configurations. The study therefore, deals with the most common forms of buildings and urban configurations. These are mainly rectilinear blocks arranged in parallel rows. Wide ranges and combinations of the parameters of this sub-system are considered.

3.3.2 The output of the model was produced at different levels of detail. At the most basic level, output was obtained from the different subroutines. This produced detailed information and data needed in practical application, such as the position of the sun, form factors, sky components, direct normal solar irradiance and illuminance, and so on.

3.3.3 The higher level of output was achieved by running the model programmes package at two main stages :

(i) The first stage dealt with the initial irradiance load on both the individual surfaces and all the vertical facades of the blocks. It explored the variation of the irradiance load, the optimum irradiance and the optimum plan proportion of the block with the variation of the system's parameters and their significance, mainly orientation, facade height,

street width proportion and height of the obstruction.

The minimum irradiance and maximum shadow factor were used as the criteria for the optimum plan proportion of the block.

(ii) The second stage dealt with the externally interreflected and final irradiance load. It also showed the variation of the interreflected irradiance with the variation of the geometrical and physical parameters of the system and their significance in determining the components of the externally interreflected irradiance. The minimum final irradiance load was used as a criterion for defining the relative effectiveness of various geometrical configurations of the surroundings.

3.3.4 The investigation which was carried out illustrates the application of the model in the study of similar specific design problems and the potential of the model in the synthesis of architectural solutions. It also shows the interrelationship between the form's parameters, their initial and their final irradiance load. Further, it shows the significance of the parameters of the form and their ranges in affecting the initial and final irradiance load. General recommendations are given regarding the optimum plan proportion, orientation of the block and configuration of surroundings with respect to minimum initial and final irradiance load on the block. The data obtained forms the basis for developing simplified procedures and indices for the evaluation of irradiance load and measures of form performance.

3.4 Layout of the Thesis

3.4.1 The thesis is presented in eight chapters. The first is an introductory chapter outlining the need for such a study. The main arguments and investigations covered by the thesis are presented in six following chapters. These may be grouped into three main parts.

3.4.2 The first part, given in Chapter II, deals with the definition of the model embodying the interactions between the form and solar radiation. It discusses the definition of the system's boundary, components and parameters. It gives the formulation of the physical processes and the factors involved, and presents the assumptions made.

3.4.3 The second part deals with the development of the mathematical model and its computer implementation. This is presented in Chapters III, IV and V. In these, the numerical methods and procedures which were used are discussed and considerations which influenced the programming techniques are presented. The accuracy of the model is investigated and the error involved with the numerical methods and the simplified procedures used for calculating the factors and the final output are evaluated. The layout of the model programme package as well as the individual routines are described and illustrated with the aid of high level flow charts. The discussion is supported by six appendices.

These illustrate the output generated, at the basic level, by the different subroutines. They include tables of the sun's position for Khartoum, irradiance data for standard tropical atmosphere, tables of sky component and form factors. A list of the individual subroutines is also provided. ✓

3.4.4 A mathematical model is developed to standardise and simplify the prediction of the direct solar and diffuse sky irradiance and illuminance of surfaces of different orientations and inclinations in tropical arid regions. This furthers the concept of the standard tropical atmosphere and involves the derivation of mathematical expressions for direct evaluation of the direct solar, diffuse sky and global irradiance and illuminance of vertical and horizontal surfaces as functions of the solar altitude and atmospheric clearness. Data for the sky component is prepared and tabulated in the appendix for the evaluation of the diffuse sky irradiance and illuminance of surfaces of different orientations, inclinations and obstructions. This work was presented in a paper to COMPLES International Conference on Solar Energy which was held in Madrid in September 1974. It has also been published in : COMPLES Revue Internationale D'Helio-technique 1er Semestre 1975, under the title : Standardisation and Prediction of Irradiance and Illuminance of Surfaces of Different Inclinations and Orientation in Tropical Regions.

3.4.5 The third part, which is contained in Chapters VI and VII, describes and discusses the investigations carried out with the model. This part includes the generation of the initial, interreflected and final irradiance data with the model at higher levels of output, and analyses their variation with the system's parameters. The development of initial irradiance indices for horizontal and vertical surfaces and measures of form performance are discussed with regard to the interreflected and final irradiance. The interrelation between optimum plan proportion and orientation and configuration of form in terms of minimum initial and final irradiance load are investigated as are the variations of the externally reflected irradiance and the factors influencing it. Diagrams are presented to illustrate and explain the different interrelationships.

3.4.6 The last chapter summarises the findings of the study. It discusses further development of the model and suggests further investigations.

CHAPTER II

DEFINITION OF A MODEL EMBODYING THE INTERACTIONS BETWEEN THE URBAN FORM AND SOLAR RADIATION

DEFINITION OF A MODEL EMBODYING THE INTERACTIONS BETWEEN THE URBAN FORM AND SOLAR RADIATION

1.0 INTRODUCTION

1.0.1 The solar electromagnetic radiation is one of the major components of the environmental physical fields which exist on the Earth's surface and engulf man and his built structures. These built structures, being specially created by man to contain him^{self} and his activities, modify the irradiance field, as well as the other environmental physical fields, and provide man with thermal and luminous environment tailored to his specification. ✓

1.0.2 The interrelations between man and buildings through the irradiance field may be formulated as an interaction between a physical and a psychophysical system and illustrated by the flow diagram shown in Figure 2.1. ✓

1.0.3 The physical system is specified as buildings which are physical structures with certain geometrical and physical characteristics. The physical irradiance field composed of solar and sky radiation, with their temporal variations, spectral distributions and directional characteristics is the excitation source acting on buildings. A primary output of the system is a set of final irradiance patterns over the external surfaces of buildings. This ultimately gets transmitted to the inside and directly yield the thermal and luminous built environment which is the ultimate output of the system.

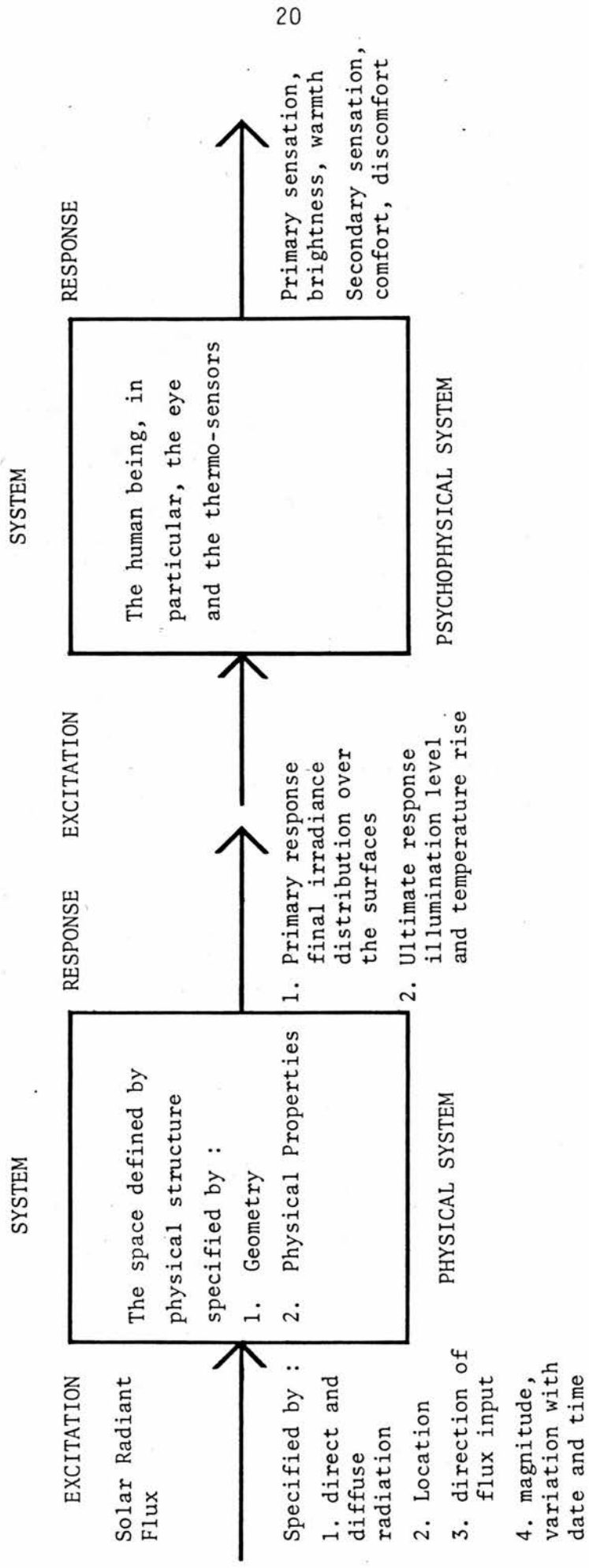


Figure 2.1 The Relations Between Physical and Psychophysical Systems for Solar Radiation (O'Brien and Howard 1959)

It is possible to define the physical processes involved in this system by considering the interaction of solar radiation and buildings in an urban situation in dry sunny climates.

These processes may be divided into four stages defining :

- (i) The initial irradiance received from the sun and sky on the external surfaces of buildings taking into account the shading of direct radiation and the obstruction of diffuse sky radiation by adjacent buildings. ✓
- (ii) The final irradiance patterns of the external surfaces due to the initial fluxes and the multiple inter-reflection between the external surfaces.
- (iii) The transmission and conduction of the final irradiance from the external surfaces to the inside cavities and the initial irradiance of the surfaces of the inside cavities.
- (iv) The final irradiance at the surfaces of the inside cavities or at any specified point after interreflection inside. This ultimately creates the luminous and thermal built environment, eg, inside temperature, illumination level, and so on. ✓

1.0.4 The psychophysical system, the human being and in particular, the eye and the thermo-sensors, is excited by the thermal and visual built environment. That is, the output of physical system would be the excitation source, the stimulus, of the psychophysical system which will respond with the human

sensations, primary and secondary.

1.0.5 It is possible to construct a model of a physical system which expresses the interactions between solar radiation and buildings in an urban situation, in tropical arid regions, and takes into consideration the most important of the physical processes involved. The discussion which follows in this chapter suggests a structure for a model, which considers the first two stages of the physical processes of the physical system, and discusses its development by :

- (i) defining the boundary of the system;
- (ii) defining the components and parameters of the system;
- (iii) formulating the factors and the physical processes involved; and
- (iv) presenting the basic assumptions made.

2. THE PHYSICAL SYSTEM

2.1 The System

2.1.1 The urban structure, in the real world, comprises human artifacts, natural surrounding of trees, vegetation and topological features, ground space and the sky above it. The built form is that part of it being regarded as a system (for the purpose of this study) acted on by solar radiation as the excitation source. The built form may be viewed as a combination of solids and voids, as illustrated by the diagram of Figure 2.2. The external shells of the structures, enclosing the internal spaces, define the solids. It is assumed here that, the various elements of the external shell, eg, windows, walls and so on, form a unit membrane composed of surface elements with different geometrical and physical characteristics. The voids represent the open spaces formed between the building blocks which are open on the sky-side. They are defined by the surfaces of the external shells and the horizontal ground.

2.1.2 It may be possible to define the boundary of the system, for which a model is to be constructed, by defining the physical processes that determine its input and output. These processes and interactions are illustrated by the diagrams shown in Figure 2.3, which represents cross-sections through an urban built-up area.

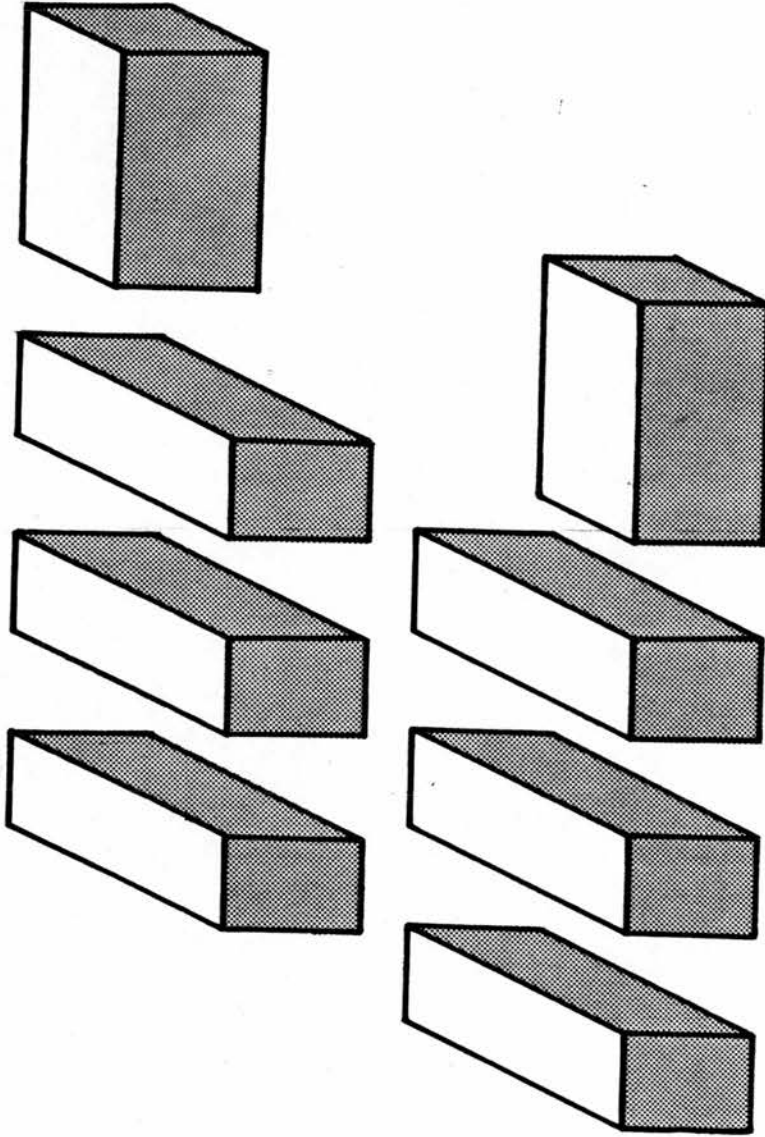


Figure 2.2 The Urban Form as a Combination of Solids and Voids

2.2 The Input

2.2.1 The direct solar and diffuse sky radiation are the two components of the irradiance source of the system. The irradiance received on ground spaces and external vertical surfaces of the urban form will be coming through the open sky-side of the form. Two factors will determine the magnitude and distribution of the initial irradiance received on these surfaces, as explained by the diagram, Figure 2.3:

- (i) the total or partial shading of direct radiation from the surfaces by adjacent buildings, and
- (ii) the obstruction of diffuse sky radiation by adjacent buildings.

The initial irradiance of a surface is due to either the diffuse or both the direct and diffuse radiation. The input to the system is then a set of initial irradiances received on the external surfaces of the urban form.

2.3 The Output

2.3.1 Primary Output

The initial radiant flux received on the external surfaces is partly transmitted or absorbed and partly reflected and rereflected in a process of multiple reflection. The final irradiance received at the external surfaces, which may be regarded as the primary output of the system, is the sum of initial and interreflected irradiance. This is illustrated

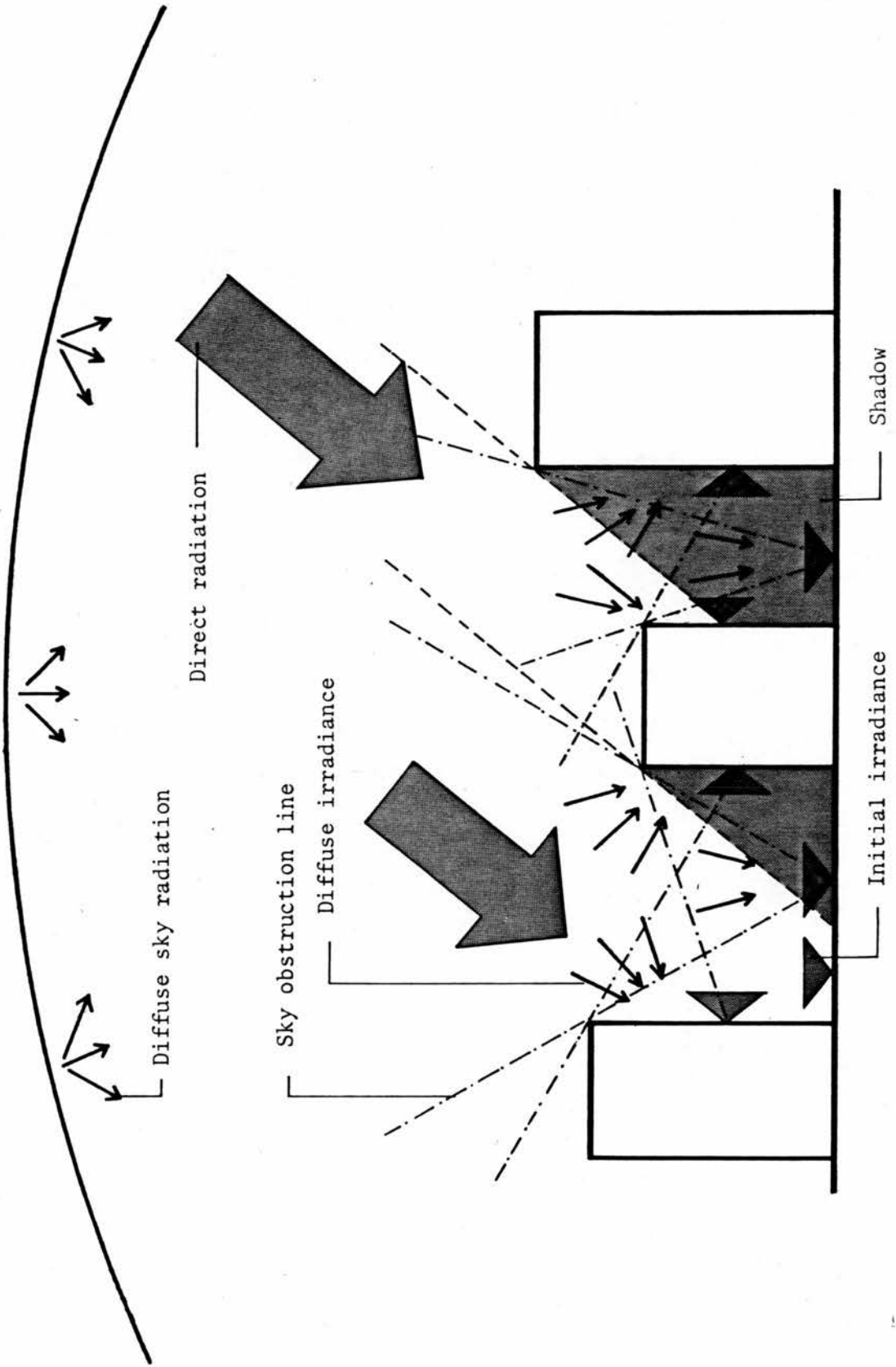


Figure 2.3 The Initial Irradiance of Vertical Surfaces and Ground as Determined by the Shading and Obstruction of Direct and Diffuse Radiation

by the diagram of Figure 2.4.

2.3.2 The Ultimate Output of the System

The final irradiance of the external surfaces is ultimately transmitted and conducted to the inside spaces through the openings and materials of the external walls. Within the inside spaces the process of multiple reflection between the inside surfaces is repeated. With the presence of openings on the shell, radiation is exchanged between internal and external surfaces. The diagram shown in Figure 2.5 illustrates these processes. Internal surfaces also exchange long wave low temperature radiation. The ultimate output of the system is the thermal and visual built environment which directly act on man.

2.4 Definition of the System and the Subsystems Boundaries

2.4.1 From the above discussion two points are evident :

- (i) Although the irradiance source is external to the system, the actual input to it, the initial irradiance of the external surfaces, is determined by the geometry of the urban form, apart from the fact that it is also dependent on the geometry of the sun.
- (ii) The output, primary or ultimate, is determined by the multiple interreflection processes which are governed

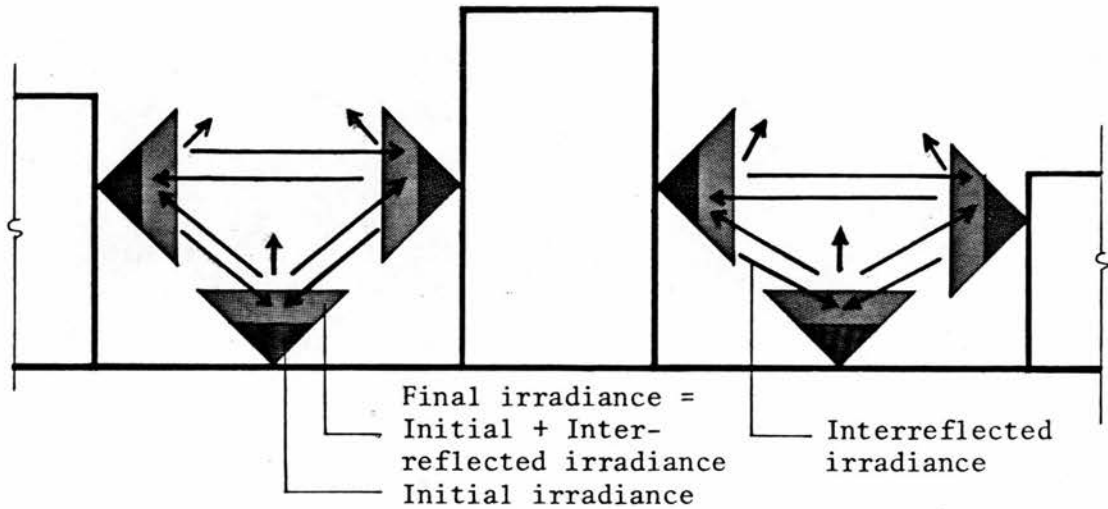


Figure 2.4 The Final Irradiance of External Surfaces is the Sum of Initial and Interreflected Components

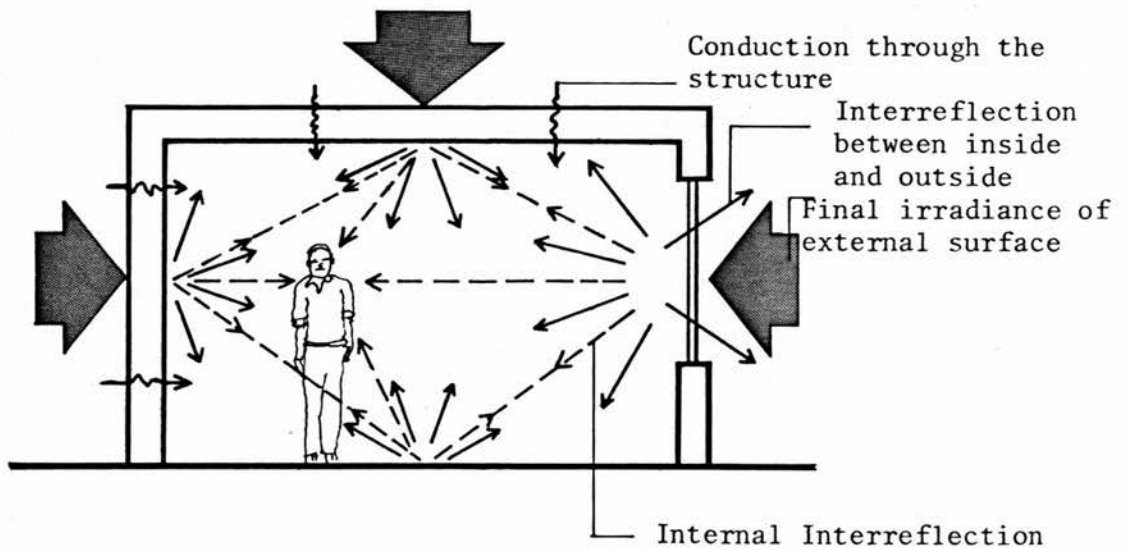


Figure 2.5 Irradiance Transfer Processes that Determine the Thermal and Luminous Built Environment

by the geometrical and physical characteristics of the form.

2.4.2 It may be simpler then to define the physical system by the geometrical and physical characteristics of the built urban form. The irradiance transfer processes in the system may be divided into two stages. The first stage takes place within the void part of the urban form and the second stage takes place within the solid part of it. Thus, we may distinguish two subsystems forming the physical system.

2.4.3 The external subsystem, which comprises the void spaces formed between the external shells of the urban built form and which are open at least on the sky-side is specified by the physical, geometrical and spatial characteristics of the various surface elements of the shells. The input of this subsystem is the initial irradiance of the surfaces which are determined by the geometry of the sun and the form, taking into account the shading of the direct radiation and the obstruction of the diffuse sky radiation by adjacent buildings. Each set of surface configurations, for a particular sun position, has a corresponding set of initial irradiance inputs to the external subsystem. Multiple interreflection between the surfaces of the external subsystem is determined by their geometrical and reflectance properties. The final irradiance of a surface is the sum of initial and reflected radiation. For each mode of irradiance input, to a form configuration, there is a corresponding set of final irradiance patterns over its

surfaces. The output of the subsystem is the set of final irradiances of the surfaces.

2.4.4 The internal subsystem, which is defined as the internal spaces, in which human activities are performed, enclosed by the external shell, is specified by the geometrical and physical properties of the bounding elements. The input to this subsystem is the output of the external subsystem, the final irradiance of the external surfaces, which is ultimately transmitted through windows and openings and conducted through the materials. With interreflection between the internal surfaces, the ultimate output of this subsystem is the thermal and luminous environment in the enclosed spaces.

2.4.5 In order to simplify the formulation of the subsystems the irradiance exchange between internal and external surfaces of the system, through opening on the shell, has been ignored. Windows are usually very small in hot arid regions and the magnitude of this irradiance exchange is not significant.

2.4.6 Long wave radiation (in the wavelength region $3.0 \mu < \lambda < \infty$) is not included in this study. The magnitude of this radiation involved is very small and most building materials are nearly black in this region. The magnitude of this radiation exchanged between the surfaces of the system is also of no practical significance.

2.5 Previous Studies

2.5.1 Analysing some of the previous studies, dealing with irradiance transfer, radiation load on buildings and daylighting for both arid regions with sunny climates and temperate regions with diffuse skies, in terms of the structure of the physical system suggested above may throw light on those areas not yet fully considered by research workers.

2.5.2 Studies dealing with the thermal irradiance load on the external shells of buildings (Buchberg and Naruishi 1967, Olgyay 1967, 1969, Givoni 1969, Kuba 1969, Valko 1969, 1970 and Tappuni 1973) were mainly concerned with the initial irradiance input to the external subsystem. They did not consider the final irradiance or take into account the external interreflection. Apparently, this is because of the complex calculations needed to estimate the reflected irradiance and the multiple reflection (Dresler 1954, O'Brien 1959). In tropical arid regions the magnitude of the externally reflected radiation is of too high an order to ignore.

2.5.3 Studies on daylighting have mostly been related to overcast skies. These studies may be viewed to relate to internal subsystem. The input to this subsystem is the sum of direct component initial irradiance, and externally reflected component. The externally reflected component is evaluated on the assumption that, the final luminance of the opposing facade is only a fraction of the luminance of that part of the sky being obstructed

by the facade, which usually is taken as 10 percent (Hopkinson and others 1966). However, in his book of 1963, Hopkinson was first to recognise that such approximate solutions which ignore the multiple reflection between the external surfaces cannot be applied successfully in dry sunny climates. He realised the need for further comprehensive studies investigating the town-planning of tropical buildings in relation to reflected sunlight, especially to size, position, reflectance of facades and street width.

2.5.4 Subsequently, exploratory studies of natural lighting design and interior illumination in sunny tropical regions have taken into consideration the external multiple reflection (Plant 1965, 1967, 1969 and 1973, Narasimhan 1969). These studies recognised the dominant role of the reflected component of the output of the external subsystem, being an input determining the final output of the internal subsystem. Hence, these studies have shown the dependency of interior illumination on such parameters as the height, separation and reflectance of facades. However, as the choice of the initial irradiance of the external surfaces, input, was arbitrary, they were not able to include the shading of direct radiation and the obstruction of diffuse radiation and indicate the effects of the geometrical parameters of the form in determining the initial irradiance of the external surfaces.

2.6 An Outline of a Model for the System

2.6.1 It may be concluded that the thermal and visual performances of buildings are determined by the final irradiance loads and

their distribution over the external surfaces of buildings, the output of the external subsystem. It seems logical then to study the external subsystem explicitly and in more detail, to take into account all the factors involved, eg, the shading and obstruction of direct and diffuse radiation and the multiple interreflection and to bring forward the interrelationships between the output and the different parameters of the system.

2.6.2 The study conducted here deals with the external subsystem.

Any reference to the physical system in what follows will be to the external subsystem. The model being used here to represent this system shows a typical section of an urban form of two street facades of buildings and the horizontal ground space separating them as illustrated by the diagram of Figure 2.6. The initial irradiance of the surfaces is the input and the final irradiance is the output.

2.6.3 The first step in this study requires that the various components and parameters of the system be defined and the factors determining the physical processes which govern its input and output be specified. The relationships between the system parameters will be formulated and quantitatively established in terms of a transfer function. This is useful in describing the physics of the problem and indicating the significant factors, the assumptions and approximations which may be required in order to obtain a practical solution. This will provide a base for the construction of a mathematical or analogue model.

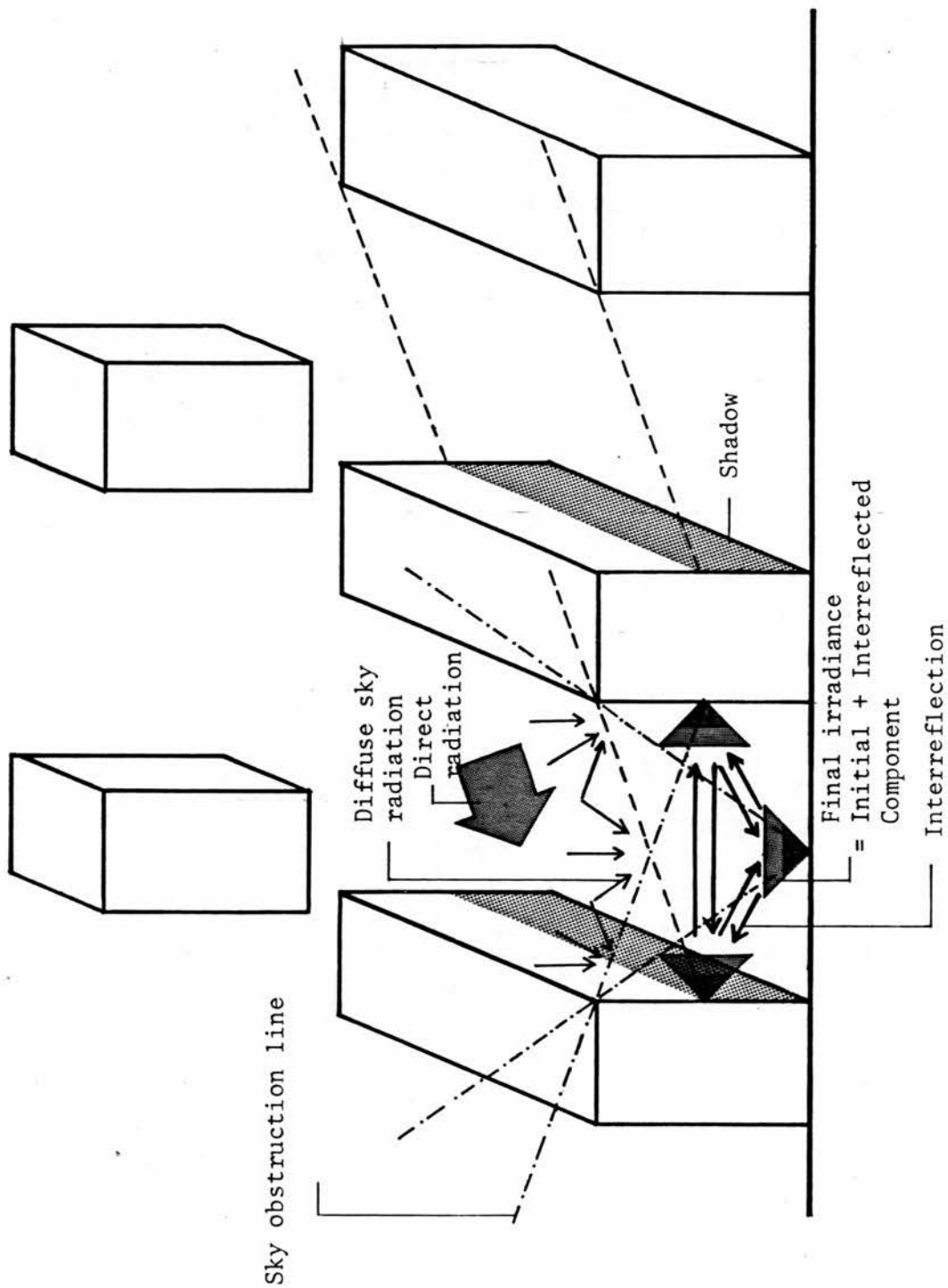


Figure 2.6 The Model of External System Showing a Section of Street Facades, Geometrical Parameters of Form and Initial and Final Irradiance

3. SOLAR RADIATION : THE EXCITATION SOURCE OF THE SYSTEM

3.1 The Solar Spectrum

3.1.1 Solar radiation is electromagnetic radiation emitted by the sun. Outside the Earth's atmosphere the solar spectrum extends from a fraction of a micron ($1 \text{ cm} = 10^4 \mu$) to hundreds of meters. The spectral radiant energy varies with the wavelength, with the maximum energy emitted at a wavelength of about 0.5μ . 98 percent of the total solar energy is emitted between 0.25μ and 3.0μ , and nearly 50 percent is radiated in the visible band which lies between 0.35μ and 0.75μ (Robinson 1966, Brinkworth 1972). The solar spectrum is usually divided into three regions :

- | | |
|-------------------------|-----------------------|
| (i) Ultra-Violet (u.v.) | $0.28 \mu - 0.35 \mu$ |
| (ii) Visible | $0.35 \mu - 0.75 \mu$ |
| (iii) Infra-red (i.r.) | $0.75 \mu - 3.0 \mu$ |

3.2 The Solar Constant

3.2.1 A minute fraction of the total energy radiated by the sun in all directions, strikes the Earth. The quantity of solar energy at normal incidence outside the Earth's atmosphere and at mean solar-distance is called the solar constant I_0 ($\text{Cal cm}^{-2} \text{ min}^{-1}$). A standard value for the solar constant (and its spectral distribution) has been prepared by NASA

(1971, Thekaekara 1973) from measurements of the solar spectral irradiance which were carried out using space-craft and satellites. This value is given as

$$I_0 = 1.94 \pm 0.03 \text{ cal cm}^{-2} \text{ min}^{-1}$$

$$= 1353 \pm 21 \text{ W m}^{-2}$$

3.3 The Solar Energy Received on the Earth's Surface

3.3.1 The fraction of the solar energy received on the Earth's surface is influenced by a number of factors (Robinson 1966). The more important of these factors are listed below.

3.3.2 Physical and Meteorological Factors

(i) Atmospheric absorption

In the upper atmosphere, virtually all the radiation of wavelengths shorter than 0.28μ is absorbed by ozone. In the lower atmosphere, wavelengths greater than 3.0μ , in the i.r. region, are strongly absorbed by atmospheric water, carbon dioxide and other atmospheric constituents.

(ii) Atmospheric scattering

This is caused by air molecules, dust particles, water droplets and clouds. Most of the scattering is within the visible and infra-red bands. Part of this scattered radiation is received on the Earth's surface as diffuse radiation.

3.3.3 Geographical Factors

The depletion of the solar energy in the atmosphere is a function of the distance travelled by the solar beam through the atmosphere (as shown by the diagram of Figure 2.7) which is dependent on the solar altitude. This is a function of :

- (i) The latitude and longitude of the place;
- (ii) The altitude of the place above sea level; and
- (iii) Time.

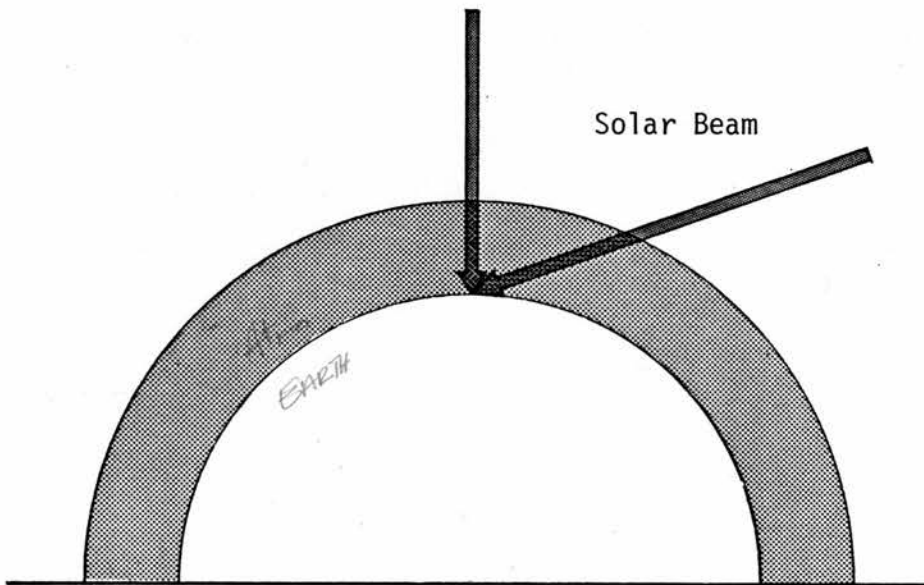


Figure 2.7 The Path of the Solar Beam Through the Atmosphere

3.3.4 The cumulative effects of these factors on the solar radiation are :

- (i) They cause the depletion of the direct solar beam and reduce its intensity to little more than half the value at the top of the atmosphere.
- (ii) They scatter the radiation resulting in the diffuse radiation coming from all parts of the sky, though not being uniformly distributed over the clear tropical sky.
- (iii) They influence the spectral energy distribution of both the direct and diffuse sky radiation where the two spectral energy distributions are different, as shown by Figures 2.8 (a), (b), (c) and (d). Hence, they influence the ratios by which the energy is shared between the visible and the invisible parts of the spectrum for both the direct and the diffuse sky radiation.

3.3.5 Solar radiation which is within the wavelength region 0.28μ to 3.0μ is usually referred to as short-wave radiation to differentiate it from radiation emitted by low temperature surfaces (for instance, those heated by the absorption of solar radiation) which is regarded as long-wave radiation with wave length greater than 5.0μ (Holden 1963, Van Straaten 1967 and Hassal 1969).

3.3.6 The statistical analysis of solar radiation data, obtained by different research workers in different parts of

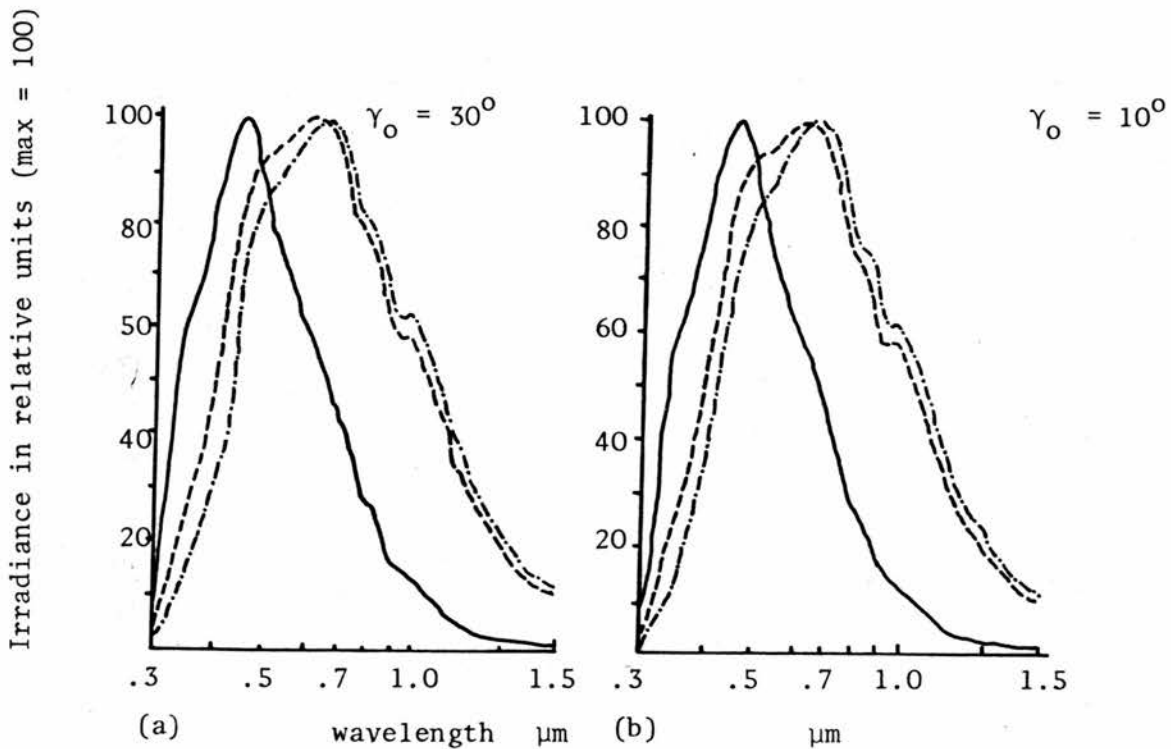
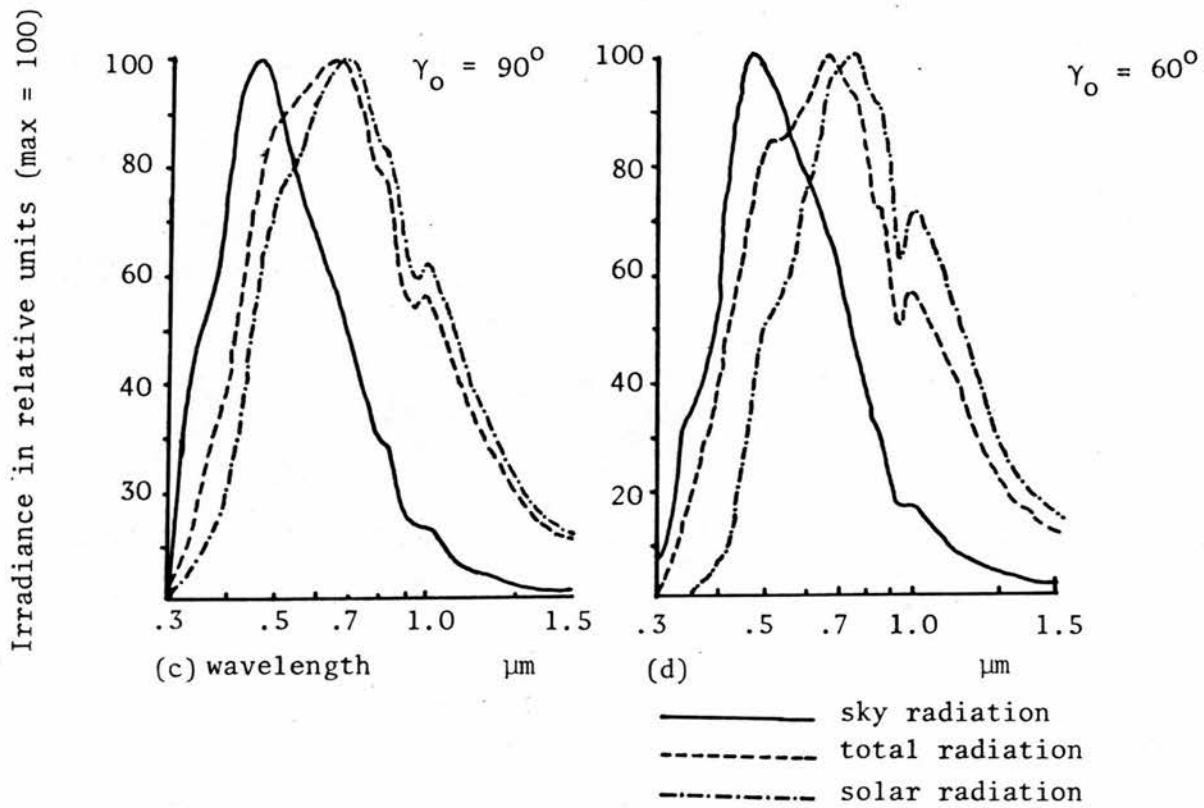


Figure 2.8 Relative Spectral Distribution of Solar, Sky and Total Radiation at Different Altitudes of the Sun (Krochmann 1969)

the world, has suggested simple functions to express the direct and diffuse radiation (Parmelee 1954, Liu and Jordan 1960, Ballantyne 1965, Loudon 1965, Sharma and Pal 1965, Kittler 1972 and Krochmann 1973). The direct normal irradiance, the radiant flux on a surface perpendicular to the solar beam, is given as a function of $\sin \gamma_0$, where γ_0 is the solar altitude. The function has the general form

$$I_{DN} = I_0 f(\sin \gamma_0) \quad \dots 2.1(a)$$

$$E_{DN} = E_0 f(\sin \gamma_0) \quad \dots 2.1(b)$$

The diffuse sky radiation on a horizontal surface is given as a linear function of the direct horizontal irradiance. Similarly it is expressed by the function

$$I_{dh} = f(I_{DN}, \sin \gamma_0) \quad \dots 2.2(a)$$

$$E_{dh} = f(E_{DN}, \sin \gamma_0) \quad \dots 2.2(b)$$

Sharma and Pal (1965) suggested that, any appropriate mathematical expression for estimating solar radiation should include the relative air mass as one of the variables. The air mass accounts for the length of the path of the solar beam through the atmosphere, which determines the absorption and scattering of the solar radiation, and is expressed by $\text{cosec } \gamma_0$ (Moon 1940, Robinson 1966). Simple expressions for solar radiation can be derived in terms of $\sin \gamma_0$ which represents the air mass

instead of cosec γ_0 . The actual form of these expressions may be derived for every locality from available meteorological data. These then give the direct and diffuse irradiance and the illuminance as a simple function of the sun's geometry.*

$$I_{DN}, I_{dh} = f(\gamma_0) \quad \dots 2.3(a)$$

$$E_{DN}, E_{dh} = f(\gamma_0) \quad \dots 2.3(b)$$

3.3.7 The intensity of the direct solar radiation falling on a surface is influenced by the obliquity of the solar rays relative to the plane of the surface. The diffuse radiation depends on the area of the sky seen by the surface and the intensity distribution of that area. The irradiance of a surface is then a function of :

- (i) the solar altitude γ_0 ,
- (ii) the solar azimuth α_0 ,
- (iii) surface orientation α_s , and
- (iv) surface inclination, tilt, γ_s .

The direct, diffuse and global radiation may then be expressed as

foot note : * Detailed analysis of this is given in Chapter III which deals with the development of standard methods for predicting the irradiance and illuminance for clear tropical skies.

$$I_{DS}, I_{ds}, I_{GS} = I_0 f(\gamma_0, \alpha_0, \gamma_S, \alpha_S) \quad \dots 2.4(a)$$

$$E_{DS}, E_{ds}, E_{GS} = E_0 f(\gamma_0, \alpha_0, \gamma_S, \alpha_S) \quad \dots 2.4(b)$$

4. PARAMETERS OF THE PHYSICAL SYSTEM, THE PHYSICAL STRUCTURE

4.0.1 The world may be described as a three-dimensional euclidean space with the ground as its horizontal plane. Buildings within this space are spatial arrangements of pieces of building materials (Wilson 1972). Accordingly, the elements required to define the physical structure here fall into two classes :

(i) geometrical, and

(ii) physical.

4.1 Geometrical Parameters

4.1.1 These are dimensional and angular which specify :

(i) The dimensions of the surfaces, lengths L , and heights h .

(ii) Position or the location of a surface or points on the surface from a specified point (x, y, z) .

(iii) Distance between surfaces or points on the surfaces d , ie, the street width separating two vertical facades.

(iv) Orientations of the surfaces from a fixed direction, ie, from the north point α_s .

(v) Inclinations of surfaces above the horizon, tilt, γ_s .

The geometrical parameters are explained by the diagram of Figure 2.9.

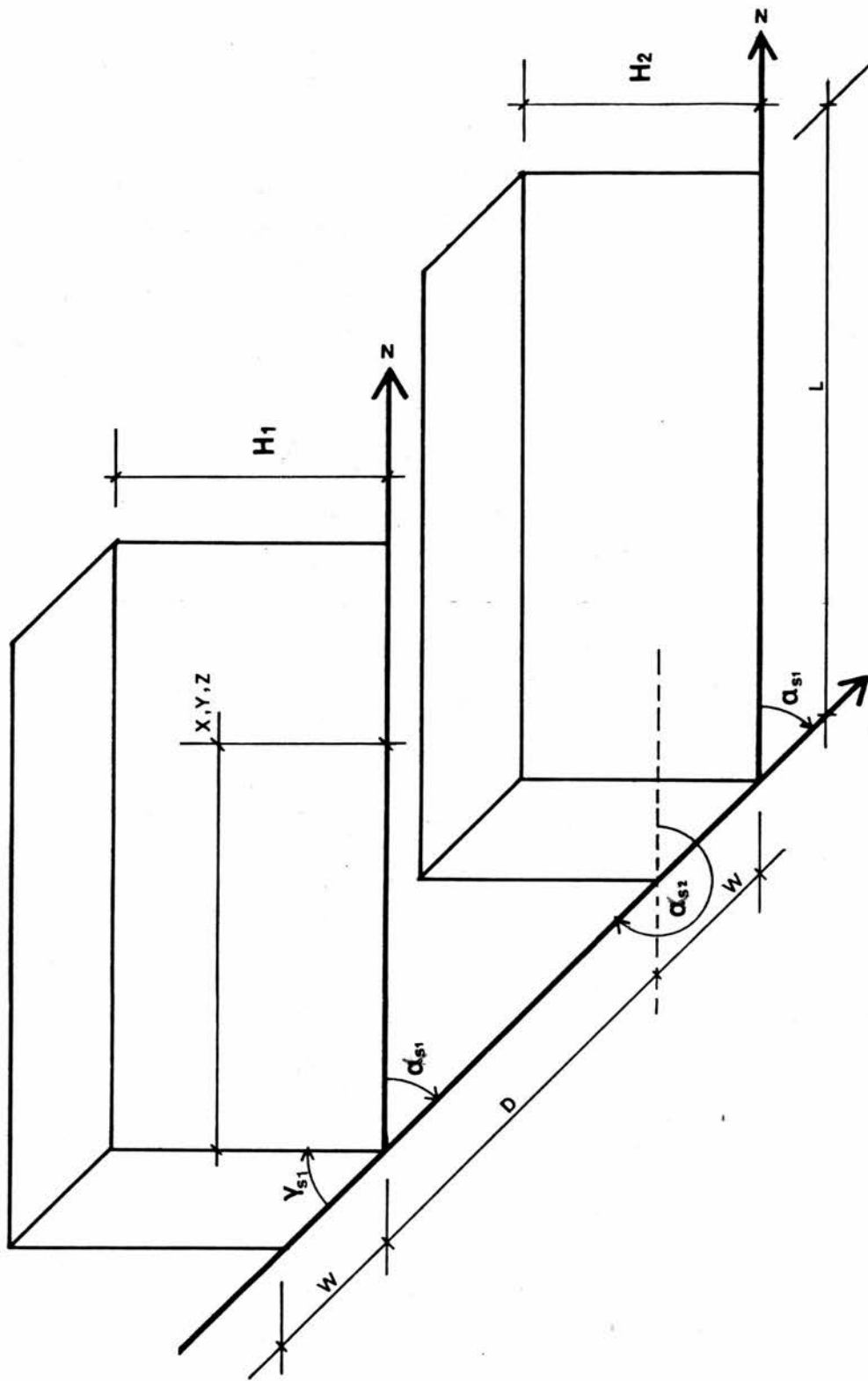


Figure 2.9 Geometrical Parameters of Form

4.1.2 Such parameters are commonly used to describe, to model and measure, and to perform mathematical operations relating the buildings and their physical environment, no matter how complex the geometrical form and the spatial arrangement of the numerous building materials employed, whether considering an individual building or group of buildings at an urban scale.

4.2 Physical Parameters : Reflectivity for Solar Radiation

4.2.1 When radiant energy impinges on an opaque surface, a fraction of the energy is absorbed and a fraction is reflected. For transparent surfaces a further fraction will be transmitted. The sum of all these quantities is equal to the total incident radiation. Accordingly, reflectivity is defined as a fraction of the incident radiation which is reflected by the surface.

4.2.2 We should distinguish between two types of reflectivities usually referred to in radiation transfer literature as monochromatic and total reflectivity (Giedt 1957, Wiebelt 1966).

- (i) Monochromatic reflectivity ρ_λ is defined as the fraction of the radiant energy incident on a surface for a wavelength interval λ to $\lambda + d\lambda$, which is reflected. It is a function of the nature of the surface and the wavelength.
- (ii) Total reflectivity ρ is similarly defined as the fraction of total radiant energy incident on the surface, over the entire spectrum of the incoming radiation, which is reflected. It may be obtained from the measurements of

the total incident and total reflected radiation, or by integrating the monochromatic reflected energy over the entire spectrum by the expression

$$\rho = 1/E \int_a^b \rho_\lambda \cdot E_\lambda \cdot d\lambda \quad \dots 2.5$$

where a and b are the wavelength limits of the incident radiation, E the total incident energy, E_λ the spectral energy distribution of the incident radiation.

Hence, the total reflectivity of a surface is determined by the spectral distribution of the incoming radiation.

4.2.3 Regarding the solar spectrum, two reflectivity values may be presented :

- (i) The total reflectivity of a surface for solar radiation; it is usually referred to as the reflectivity for solar radiation (Beckett 1931, Billington 1952, Van Straaten 1967), which determines the fraction of the solar radiant energy, coming in the wavelengths between 0.28 μ to 3.0 μ , which is reflected by the surface. It may be expressed by the function

$$\rho = \frac{\int_{0.28\mu}^{3.0\mu} \rho_\lambda \cdot E_\lambda \cdot d\lambda}{\int_{0.28\mu}^{3.0\mu} E_\lambda \cdot d\lambda} \quad \dots 2.6(a)$$

- (ii) The reflectivity of a surface for the visible band of the spectrum, in the wavelength region between 0.35 μ to

0.75 μ , is similarly defined as the total reflectivity and given by the function

$$\rho_V = \frac{\int_{0.35\mu}^{0.75\mu} \rho_\lambda \cdot E_\lambda \cdot d\lambda}{\int_{0.35\mu}^{0.75\mu} E_\lambda \cdot d\lambda} \quad \dots 2.6(b)$$

4.2.4 The spectral distribution of the reflectivities of a representative collection of building materials and finishes, over the solar spectrum range, are shown by the diagram of Figure 2.10. As seen from this diagram and equation 2.6(a), variations may be expected between the total reflectivity values of the surfaces for the direct solar, the diffuse sky and the global radiation and with the time of day and year, following the variations of the spectral distributions of the direct, diffuse and global radiation. However, such variations seem to be very small and they have been ignored by research workers (Billington 1952, ASHRAE 1963, Hopkinson 1966, Van Straaten 1967 and Tappuni 1973), who usually quote a constant value for the reflectivity of a surface for solar radiation, direct, diffuse sky and global radiation. From these sources, the reflectivity values for solar radiation for the building materials and finishes commonly used in the tropics have been collected and are presented in the form of a reflectivity chart, Figure 2.11. From these values, an average value for each surface is established to represent its reflectivity for solar radiation.

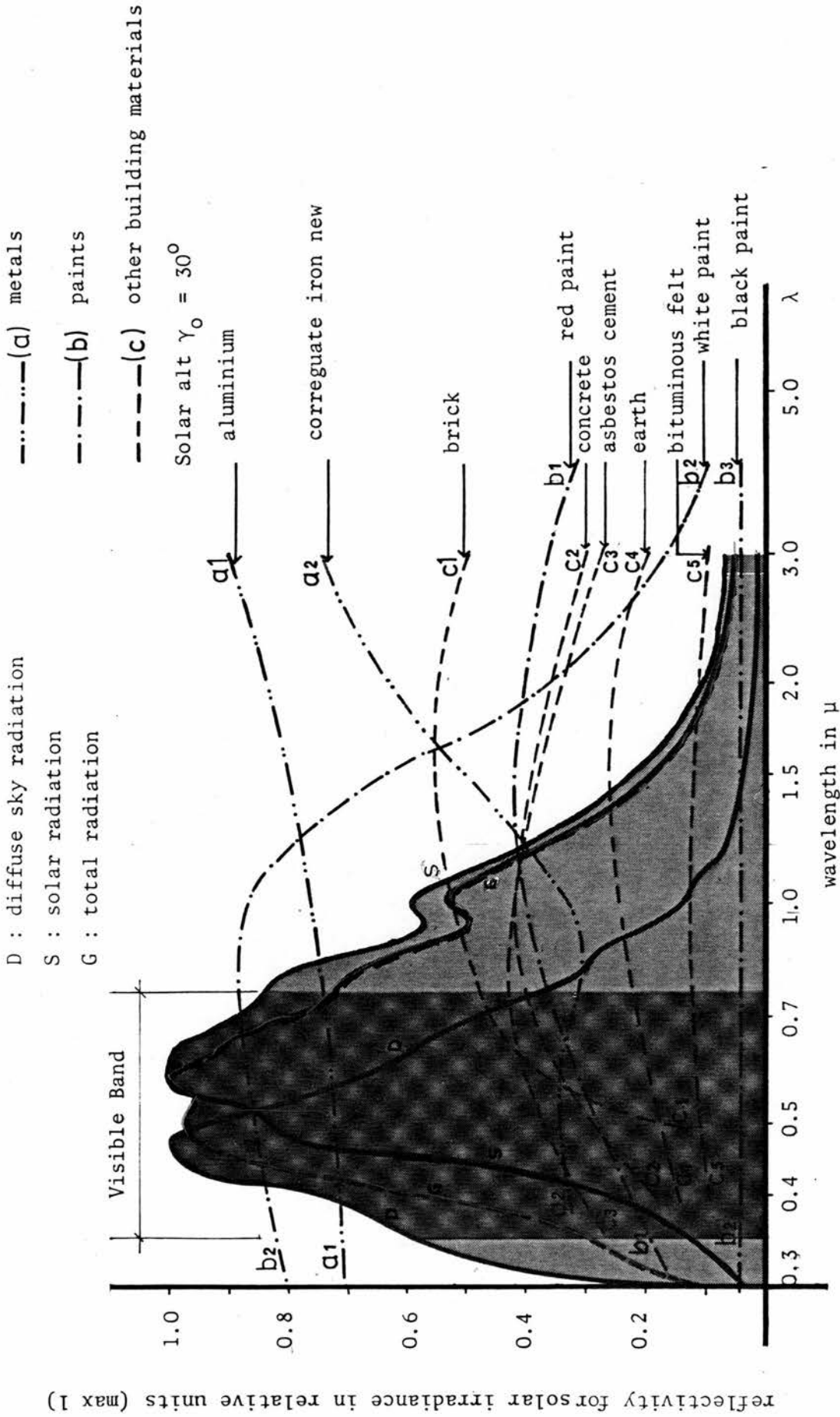


Figure 2.10 Spectral Distribution of Reflectivity of Building Materials Imposed on the Spectral Distribution of Solar Radiation

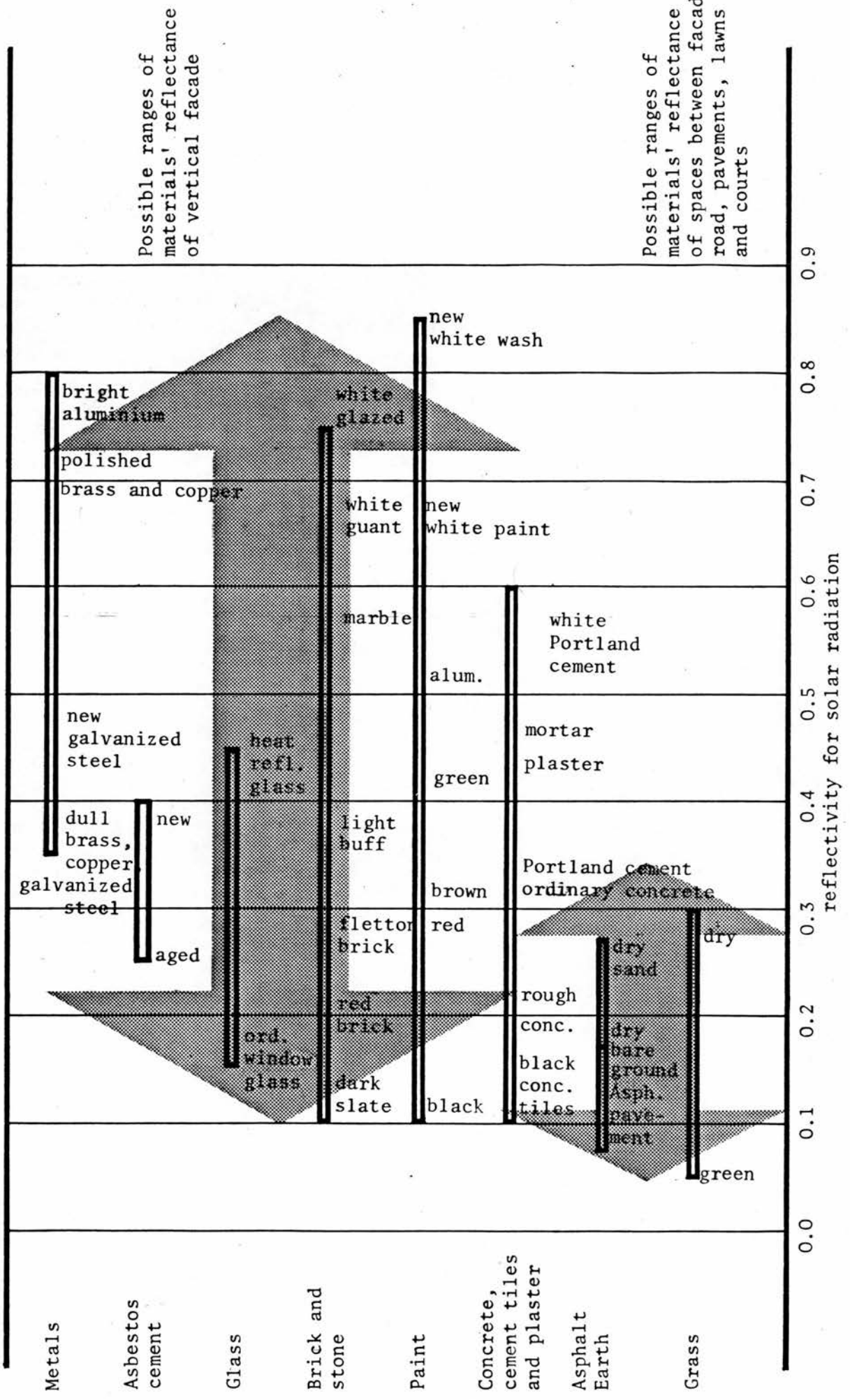


Figure 2.11 Reflectivity Chart : Reflectivity for Solar Radiation of Common Building Materials and Finishes

4.2.5 The following assumptions are implied in using these average values in the present study :

- (i) Surfaces are perfect diffusers .✓
- (ii) Surfaces are of uniform nature and the reflectivity is constant over the entire surface .✓
- (iii) Reflectivity of a surface for the direct solar, diffuse sky and global radiation is a constant value.✓

4.2.6 Some of the building materials and finishes, eg, white paint, may show a marked difference between their reflectivity values for the visible band, equation 2.6(b), and the invisible band, in the wavelength region between 0.75μ to 3.0μ , or the entire solar spectrum, equation 2.6(a). For a system of multiple surfaces having such reflection characteristics, it may be necessary to use the reflectivities of the surfaces for the visible band ρ_v to obtain a separate and accurate assessment of the inter-reflected light energy, while the total reflectivities would give the total interreflected solar radiant energy. /

4.2.7 As the initial irradiance of the surfaces of the system considered in this study is mainly short wavelength, solar radiation, the reflectivity of the surfaces for solar radiation is needed to evaluate the interreflected irradiance. It should be noted that a small portion of the interreflected radiation

is longwave radiation, with wavelengths greater than 3.0μ . This is mainly due to the low temperature radiation emitted by the sky, the ground and the building surfaces. The reflectivity values of most of the building materials and finishes for the shortwave and the longwave radiation differ greatly (Billington 1952, Van Straaten 1967). Hence, the reflectivity values of a surface for longwave radiation are required to calculate interreflected longwave radiation. However, as this study ignores the longwave radiation for the practical reasons which were stated in part 7.2 of this Chapter, the reflectivity of the surfaces for longwave radiation will not be considered. ✓



THE STRUCTURE OF THE MODEL, FORMULATION OF THE FACTORS AND
THE IRRADIANCE TRANSFER FUNCTIONS

5. TRANSFER FUNCTION

5.0.1 The quantitative relationship between the excitation and the response of the physical system is termed the transfer function (O'Brien 1959). This is a mathematical representation of the response in terms of the system's parameters. To derive a representative, practical and as accurate as possible function, it is necessary to define the actual physical processes involved and to take into account the most significant factors. The procedures to evaluate these factors which will serve as a base for the model need to be established.

5.0.2 The physics of the transfer function may be divided into two stages to simplify the study of the problem.

- (i) The first stage deals with the determination of the initial flux input to the system, the initial irradiance received by the surfaces before interreflection. This takes into account the direct and diffuse radiation and the shadow and diffusion effects.
- (ii) The second stage deals with the system's response, the final irradiances and their distribution over the surfaces after interreflection.

6. INITIAL IRRADIANCE FUNCTION

6.0.1 Three factors determine the magnitude of the initial flux received by each surface, the direct solar irradiance, the diffuse sky irradiance and the shading and obstruction of these irradiance components.

6.1 The Direct Radiation

6.1.1 The direct normal irradiance, or illuminance, is expressed as a function of the solar constant, the atmospheric ^{Turbidity} extinction and the solar altitude. For a particular locality, the direct normal irradiance may be taken as the function of the sine of the solar altitude

$$I_{DN} = f(\sin \gamma_0) \quad \checkmark \quad \dots 2.7$$

6.1.2 The magnitude of the direct incident irradiance impinging on a surface may be calculated from the direct normal irradiance and the angle of incidence, θ , which is the angle the direct solar beam makes with the normal to the surface. It may be defined in terms of the surface-solar azimuth, surface ^{α_s} inclination and the solar ^{γ_0} altitude and is given by the functions

$$\cos \theta = \sin \gamma_0 \cdot \cos \gamma_s + \cos \gamma_0 \cdot \sin \gamma_s \cdot \cos(\alpha_s - \alpha_0) \quad \dots 2.8(a)$$

where γ_0 is the solar altitude

α_0 is the solar azimuth from the north point

γ_s is the inclination angle of a surface, above the horizon

α_s is the orientation, azimuth, of a surface from the north point ✓

$\beta = \alpha_s - \alpha_0$ is the surface-solar azimuth

For a vertical surface where $\gamma_s = 90^\circ$,

$$\cos \theta = \cos \gamma_0 \cdot \cos(\alpha_s^{\beta} - \alpha_0) \quad \dots 2.8(b)$$

For a horizontal surface where $\gamma_s = 0^\circ$,

$$\cos \theta = \sin \gamma_0 \quad \dots 2.8(c)$$

The relations between the various angles are illustrated in Figures 2.12(a) and (b). Accordingly, the direct incident irradiance is given by the function

$$I_{DS} = I_{DN} \cdot \cos \theta \quad \dots 2.9$$

A surface will only receive direct solar irradiance if it is facing the sun, that is for a surface-solar azimuth within the range

$$-90^\circ < \beta < 90^\circ.$$

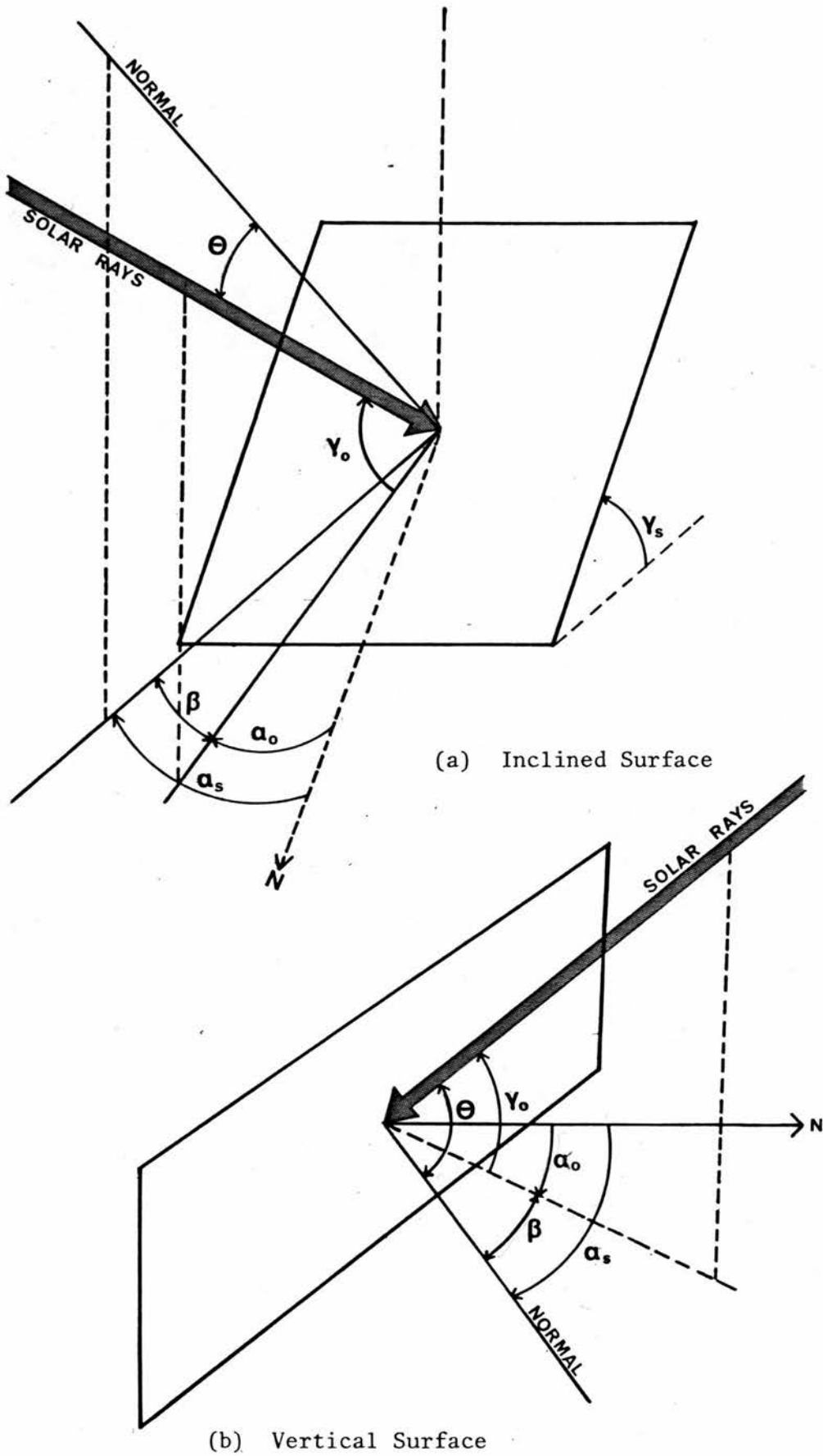


Figure 2.12 The Angle of Incidence of Solar Rays on a Surface

6.2 The Diffuse Sky Radiation

6.2.1 Experimental measurements of the luminance and radiant intensity distribution of clear skies have been conducted by various workers (Robertson 1965, Kittler 1965 and 1969, Rennhachkamp 1967, Narasimhan and Saxena 1967 and 1972), which show that clear skies are characterised by a non-uniform distribution. The sky luminance distribution in warm arid regions is similar to that of the C.I.E. clear sky. It was also suggested (Pleijel 1954, Krochmann 1969) that the radiant intensity distribution of the clear sky is similar to its luminance distribution. The C.I.E. (1973) recommended acceptance of the functional relationships presented by Kittler (1965, 1969) for the clear sky luminance distribution. These express the relative luminance distribution by the ratio of the luminance of an arbitrary sky element L_p , to the luminance at the zenith L_Z

$$L_p/L_Z = I_p/I_Z = \frac{f(\delta_p) \cdot f(\epsilon_p)}{f(\epsilon_0) \cdot f(0)} \quad \dots 2.10(a)$$

where the position of the sky element P is given by its angular distance from the zenith ϵ_p and its azimuthal angle from the north α_p , as shown in Figure 2.13(a). The functions $f(\epsilon_p)$, $f(\delta_p)$, $f(\epsilon_0)$, $f(0)$ are quoted in Chapter III.

6.2.2 Diffuse irradiance on a horizontal surface with an unobstructed view of the sky comes from all parts of the sky. It is a function of the direct normal irradiance and the solar altitude as given earlier in this Chapter by equations 2.2 and 2.3.

6.2.3 For vertical and other inclined surfaces the diffuse irradiance depends on the area of the sky viewed by the surface and its intensity distribution.

- (i) The relative luminance and radiant intensity distribution over the clear sky is a function of the solar altitude.
- (ii) The angular limits of the sky area viewed by the surface are dependent on the geometry of the surface. They may be taken to define the sky area as made of two parts, a and b, as shown in Figures 2.13(b) and 2.13(c).

Part a : This defines the sky shallow dome at an altitude γ_S , where the irradiance is coming from the whole sky dome circumference. The angular limits of this sky area are

1. altitude limits $\gamma_S < \gamma_p < \pi/2$
2. azimuth limits $0 < \alpha_p < 2\pi$

where γ_p is the altitude angle of an arbitrary sky element and α_p is the azimuth angle of an arbitrary sky element.

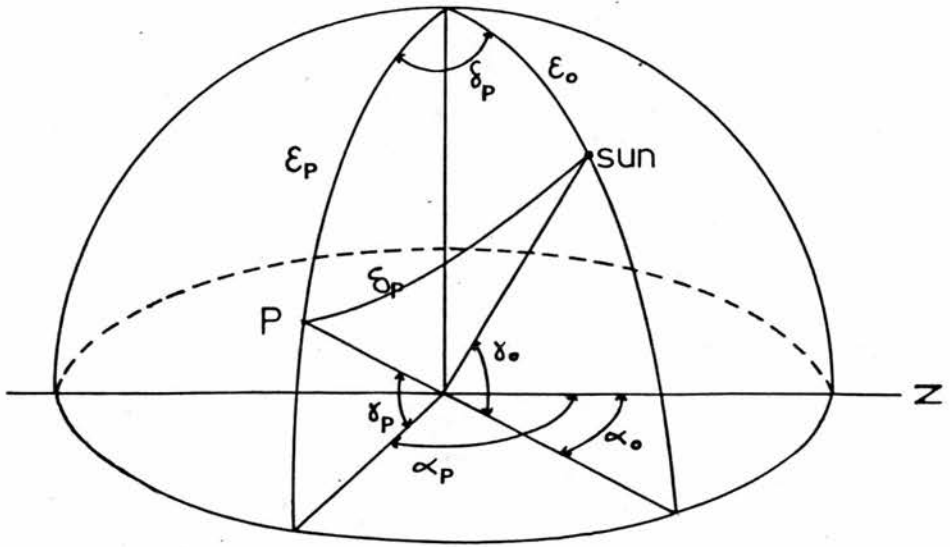


Figure 2.13(a) Angular Relation between the Sun and a Sky Element P

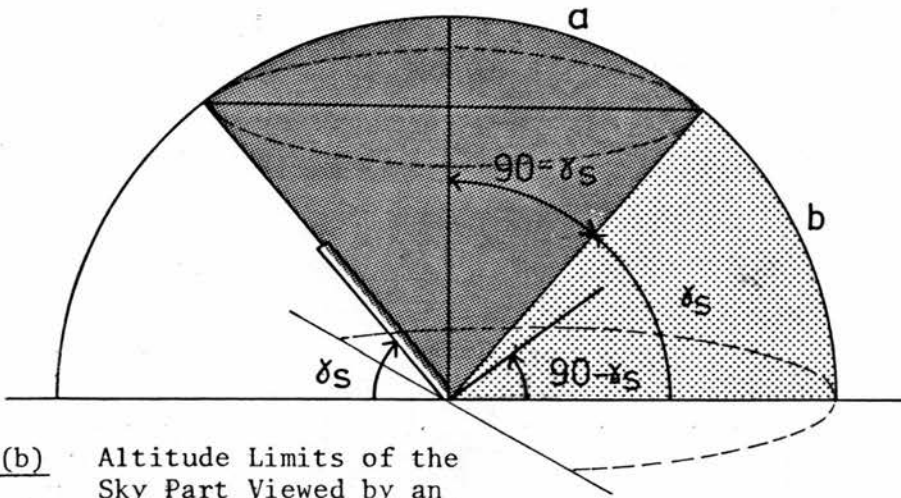


Figure 2.13(b) Altitude Limits of the Sky Part Viewed by an Inclined Surface

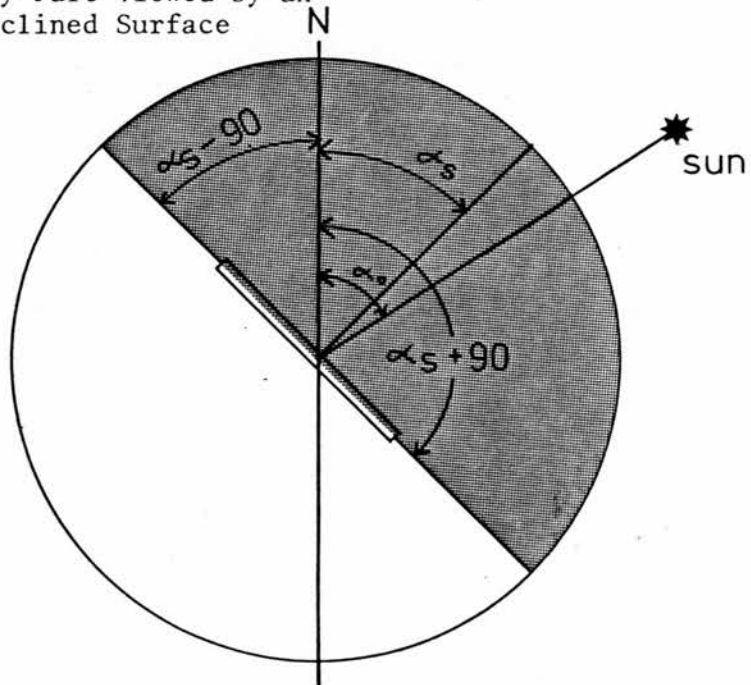


Figure 2.13(c) Azimuth Limits of the Sky Part Viewed by an Inclined Surface

Part b : This defines that part of the sky facing the surface where the irradiance is only coming from half the sky dome circumference.

1. altitude limits $0 < \gamma_p < \gamma_s$
2. azimuth limits $\alpha_s - 90 < \alpha_p < \alpha_s + 90$

6.2.4 The sky luminance distribution functions provide a theoretical means of evaluating the diffuse irradiance on an inclined surface by integrating the functions over the angular limits for the surface. This will give the diffuse irradiance on the surface as a proportion of the zenith intensity

$$I_{ds}/I_z = f(\delta_p) \cdot f(\epsilon_p) / f(\epsilon_0) \cdot f(0) \quad \dots 2.10(b)$$

A similar ratio may also be found for a horizontal unobstructed surface as I_{dh}/I_z . Dividing the ratio for the inclined surface by that of the horizontal surface will give the diffuse irradiance of the inclined surface as a proportion of the diffuse horizontal irradiance

$$R = I_{ds}/I_{dh} \quad \dots 2.11$$

6.2.5 R may be termed the sky component of the unobstructed inclined surface. This term is used here in a similar manner to the sky component of the daylight factor. The

values of R obtained by integration of the luminance distribution function are dependent on the angular parameters of the surface and the sun, sun's altitude and azimuth, surface's altitude and azimuth. These parameters may be combined into a single factor, the angle of incidence. Experimental measurements of R , for vertical surfaces, carried out by Van Deventer and others (1966, 1971) suggested the dependency of R on the angle of incidence. The calculated values of R confirmed that R is a function of $\cos \theta$ for every surface inclination and solar altitude as will be shown in Chapter III. $\cos \theta$ is given by equation 2.8(b).

$$R = f(\cos \theta) \quad \dots 2.12(a)$$

$$= f(\theta, \gamma_0, \gamma_s) \quad \dots 2.12(b)$$

6.2.6 The diffuse irradiance of an inclined surface is given as a function of the diffuse horizontal irradiance

$$I_{ds} = I_{dh} \cdot R \quad \dots 2.13(a)$$

$$= f(I_{DN}, \theta, \gamma_0, \gamma_s) \quad \dots 2.13(b)$$

The diffuse irradiance is uniformly distributed over the inclined surface.

6.3 The Global Irradiance

6.3.1 The global irradiance of an inclined surface is the sum of the direct and diffuse irradiances. It will be uniformly distributed over the surface. For a surface facing the sun, it is given by the function

$$I_{GS} = I_{DS} + I_{ds} \quad \dots 2.14(a)$$

$$= I_{DN} \cdot \cos \theta + I_{dh} \cdot R \quad \dots 2.14(b)$$

A surface oriented away from the sun receives diffuse irradiance only and the global irradiance is given by the function

$$I_{GS} = I_{ds} = I_{dh} \cdot R \quad \dots 2.14(c)$$

The total irradiance is a function of the surface's area where

$$I_{TS} = A \cdot I_{GS} \quad \dots 2.14(d)$$

6.4 Shadows and the Obstruction of the Direct Solar Rays

6.4.1 In the field of illuminating engineering, shadow is conceived of as a local reduction in the illuminance or the irradiance of a surface, or part of a surface, which makes that surface receive less radiant intensity than it would otherwise receive due to the full or partial obstruction of the irradiance source by an opaque object, termed shadow-

caster*. (Norden 1948, O'Brien 1968).

6.4.2 These authors classify shadows in three forms :

- (i) umbra or full shadow in which the irradiance source is completely obstructed from reaching the surface or part of it;
- (ii) penumbra or semi-shadow in which the irradiance source is partially obstructed and gradated illuminance or irradiance is received throughout the surface, or the shadowed area; and
- (iii) ultraumbra or no shadow when the surface is fully exposed to the irradiance source.

6.4.3 The formation of shadows on the surfaces of urban structures is due to the obstruction of the direct solar rays, coming as parallel beams, and the diffuse sky radiation by adjacent buildings, trees and other topological features (Sun 1968, Datta). The possible shadow features on building surfaces may be established from the manner in which either each or both of the direct and diffuse sky irradiance are obstructed.

foot note : *Norden (1948) presented an exhaustive treatment of the subject in his book "Shadow and Diffusion in Illuminating Engineering". His definitions and "Glossary of Special Terms used in Shadow Engineering" which are considered to be clear and precise are used here.

- (i) Roof surfaces of urban structures are the most likely to be free from shadow and fully exposed to both the direct and diffuse sky radiation, in ultraumbra.
- (ii) A vertical surface oriented away from the sun will receive only a portion of the diffuse sky radiation due to the partial obstruction of the sky by adjacent buildings. Gradated irradiance is received throughout the surface which is under semi-shadow, penumbra.
- (iii) A surface facing the sun where part of it is completely obstructed from receiving the direct solar rays is in penumbra with a nucleus of umbra, ie, the lower part of a vertical surface, which is partially shaded by an adjacent vertical surface, is in umbra while its upper part is in penumbra. The shadowed area in penumbra receives the direct and a portion of the diffuse radiation. The shadowed area in umbra receives only a portion of the diffuse sky radiation.
- (iv) A surface facing the sun is in full shadow if it is completely obstructed by adjacent buildings from receiving direct solar radiation. A small portion of the diffuse radiation is received throughout the surface. The full shadow may be regarded as uniform

throughout the shadowed area since the variation of the diffuse sky radiation received over the surface is practically imperceptible.

6.4.4 The shadowed area of a surface in umbra represents a silhouette of the shadow-caster projected onto the surface by the direct solar rays. The silhouette's form, total area and location on the shaded surface are dependent on the geometry of the sun, the receiving surface, the shadow-caster and the distance between the two surfaces, and will be continuously varying with the sun's movement. The result of this is that the shadow cast may have a more complex shape than the surfaces casting them. Sun (1968) has shown that there are more than twenty-three possible shadow shapes which a simple rectangular vertical surface may cast on an adjacent vertical surface. The different shadow shapes obtained here, using the shadow program developed with this study, for two simple rectangular vertical planes are shown in Appendix A.4.

6.4.5 Once the shadow profile (profile of full shadow or umbra) is known, its area A_S is easily calculated. The shadow area may be taken as a function of the geometrical parameters of the form and the sun as

$$A_S = f(\alpha_0, \gamma_0, \alpha_{S1}, \alpha_{S2}, \gamma_{S1}, \gamma_{S2}, L_1, L_2, h_1, h_2, d) \dots 2.15$$

The significance of the area lies in the fact that it is directly related to the amount of irradiance being obstructed from reaching the surface. This fact may be exploited, as has been done by the vernacular builders in tropical sunny climates, to reduce the irradiance load on surfaces by selecting forms which lead to maximum shading. With the mathematical formulation of shadow it is possible to manipulate the geometrical parameters of the form to produce the maximum shading or exposure of a surface or part of it for specific periods, ie, summer time or winter, or throughout the year (Roux 1973).

6.4.6 The total shadowed direct irradiance of a surface is a function of the surface area in full shadow A_S . It may be taken as

$$I_{DD} = A_S \cdot I_{DS} \quad \dots 2.16$$

6.5 Diffusion and the Obstruction of the Diffuse Sky Radiation

6.5.1 The clear tropical sky with its non-uniform luminance and radiant intensity distribution may be regarded as a fully extended irradiance source. The diffuse sky radiation received on a surface which is fully exposed to the sky is practically free from shadow and uniformly distributed over the surface. However, very few surfaces of the urban structures may have the full view of the sky which is usually partially obstructed by

adjacent buildings. Due to this obstruction different points on a surface will view different sky areas, as shown in Figures 2.14 (a) and (b) and the diffuse irradiance received will vary gradually across the surface resulting also in a gradual transition of the semi-shadow.

6.5.2 Similar to the diffuse sky irradiance received on a fully exposed surface, the diffuse sky irradiance which is obstructed from reaching an elemental area of a surface will depend on :

- (i) The sky area being obstructed from the elemental area. This is defined by the angular limits of the obstructing surface projected from the elemental area. The angular limits may be determined from the geometry of the caster, or the obstructing surface, its distance from the obstructed surface and the location of the elemental area on the surface as shown in Figures 2.14 (a) and (b). The angular limits of the obstructed sky area are :
1. the altitude limits of obstruction, $0 < \gamma_p < \gamma_{ob2}$
 2. the azimuth limits of obstruction, $\alpha_{ob1} < \alpha_p < \alpha_{ob2}$
- (ii) The radiant intensity distribution of the obstructed sky part which is represented by the relative luminance distribution function of the clear sky, given by Kittler (1964, 1969) and presented in equation 2.10(a) above. Integrating this function over the angular limits of the obstructed sky part will give the ratio of

the obstructed diffuse irradiance of the elemental area I_{ob} to the zenith intensity I_Z

$$I_{ob}/I_Z = \int_{\alpha_{ob1}}^{\alpha_{ob2}} \int_0^{\gamma_{ob2}} f(\delta_p) \cdot f(\epsilon_p) / f(\epsilon_0) \cdot f(0) d\gamma_p \cdot d\alpha_p \quad \dots 2.17$$

6.5.3 Similar ratios of the diffuse irradiance received on an elemental area of a surface, from the unobstructed sky part, to the zenith intensity may be obtained. A surface may be divided into small subelements and since the diffuse irradiance may not vary significantly across a small area, the diffuse irradiance or the ratio of the diffuse irradiance to the zenith intensity is evaluated at the centre of the subelement (Stibbs 1971). However, in dealing with the diffuse irradiance on a surface, from the unobstructed sky part, it is regarded as most practical to take an average value from the local values varying from point to point across the surface (Norden 1948). To overcome the difficulties in performing the computation several times in order to obtain the local values and evaluate the average a simple approximate procedure may be used which is based on :

- (i) The assumption that the diffuse irradiance received on a surface, from the unobstructed sky part, does not vary significantly across the surface, that it is taken as being uniformly distributed and that it is evaluated at the centre of the surface.

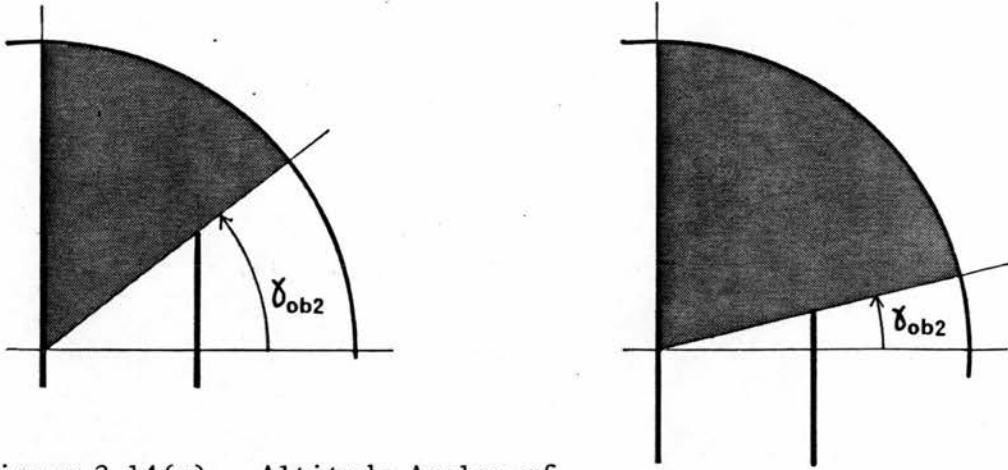


Figure 2.14(a) Altitude Angles of Obstruction from Different Points on the Surface

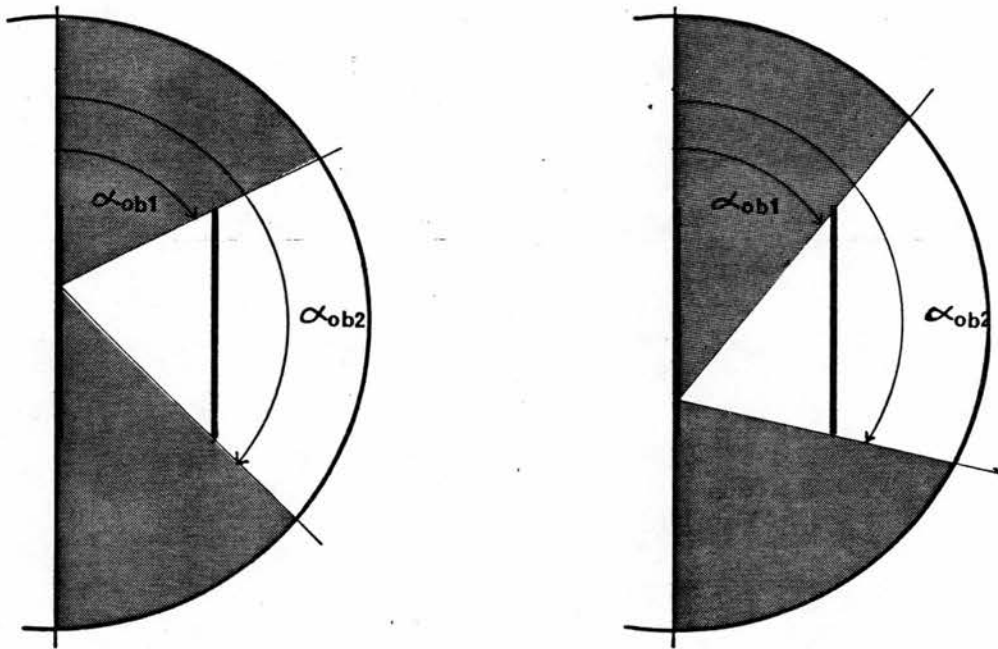


Figure 2.14(b) Azimuth Angles of Obstruction from Different Points on a Surface

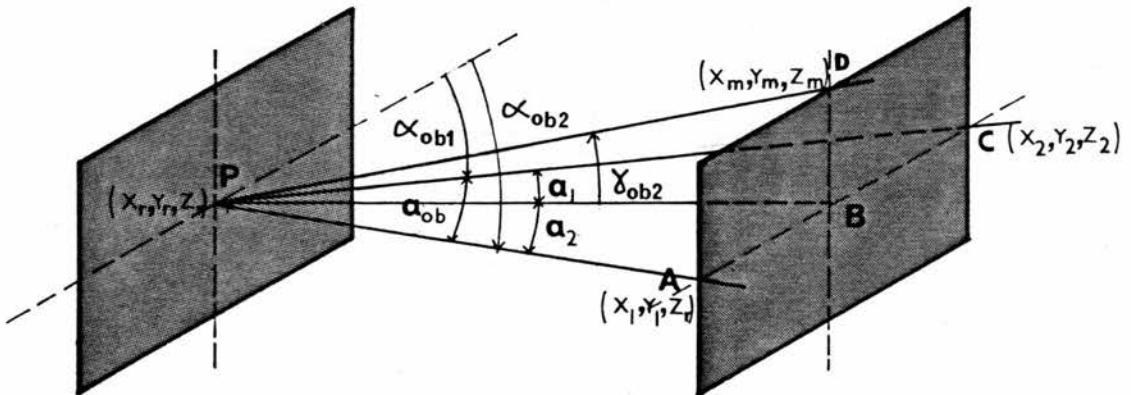


Figure 2.14(c) Angular Limits of Obstruction from the Centre of a Surface

- (ii) The angular limits of the obstructed sky area are taken from the centre of the surface to the boundary of the obstructing surface, as shown in Figure 2.14(c).

6.5.4 Integrating the sky luminance distribution function over the angular limits of obstruction and dividing the integral value I_{ob}/I_Z , by the ratio of the horizontal irradiance, from the whole sky, to zenith intensity I_{dh}/I_Z , gives the ratio R_{ob} , where

$$R_{ob} = I_{ob}/I_{dh} \quad \dots 2.18$$

R_{ob} then expresses the average diffuse irradiance being obstructed from reaching the surface as a proportion of the diffuse horizontal irradiance. R_{ob} is similar to the sky component R , and may be termed here as the obstructed sky component of a surface. The exposed sky component of a surface R_S is readily obtained by subtracting the obstructed component from the sky component of the fully exposed surface

$$R_S = R - R_{ob} \quad \dots 2.19$$

R_S is the ratio of the average diffuse irradiance/unit area received on the surface from the partially obstructed sky to the horizontal diffuse irradiance/unit area.

6.5.5 Once R_{ob} or R_S are found the average diffuse irradiance

on a surface is readily obtained from the value of the horizontal diffuse irradiance. The average obstructed and residual diffuse irradiance is given by the functions

$$I_{ds} = R_{ob} \cdot I_{dh} \quad \dots 2.20$$

$$I_{dr} = R_S \cdot I_{dh} \quad \dots 2.21$$

6.6 Shadow and Diffusion Factors

6.6.1 In order to treat shadows and diffusion as factors

influencing the initial irradiance function, it is essential to define them by measurable quantities, namely flux units. This is advantageous in presenting simple functions for evaluating the initial irradiance of surfaces expressed in terms of simple factors which are functions of the system's parameters, and deriving measures which express the shading and diffusion effects under varying conditions of the systems' parameters.

6.6.2 The definitions presented by Norden (1948) are regarded (O'Brien 1968) as clear and precisely phrased, although they are related to illumination they are taken here as equally applicable over the entire radiation spectrum.

(i) Shadow factor SF

Norden defined the SF as "A quotient characterizing the

the intensity of a shadow by the ratio of the shadowed illumination to the full unshadowed illumination prevailing before an umbration occurred".

The total unshadowed illuminance or irradiance will comprise the direct and diffuse components for a surface facing the sun and the diffuse component only for a surface away from the sun, given earlier by equations 2.14(a), (b) and (c). When a surface is in full shadow the residual irradiance is expressed by the average diffuse irradiance, given by equation 2.21 above, the shadow factor being given by the function

$$SF = \frac{I_{GS} - I_{dr}}{I_{GS}} \quad 2.22$$

(ii) Diffusion factor DF

The diffusion factor expresses the average diffuse irradiance received on a surface as a fraction of the total irradiance

$$DF = I_{ds}/I_{GS} \quad 2.23$$

SF and DF are interconnected where generally

$$DF = 1 - SF \quad 2.24$$

6.6.3 The shadow factor describes the condition of the shadow prevailing over a surface's area which is experiencing one of the three basic shadow forms. A surface which is partially obstructed from both the direct and diffuse sky irradiance is partly in umbra and partly in penumbra. Such combination of shadow forms are most commonly formed on surfaces of urban structures. The shadow factors for both parts of the surface in umbra and penumbra may then be evaluated separately.

- (a) the surface's part in full shadow which has an area A_S , will receive diffuse irradiance only.

$$SF_1 = \frac{I_{DS} + R_{ob} \cdot I_{dh}}{I_{DS} + R \cdot I_{dh}} \quad \dots 2.25$$

- (b) the surface's part in semi-shadow will receive both the direct and a portion of the diffuse sky radiation.

$$SF_2 = \frac{R_{ob} \cdot I_{dh}}{I_{DS} + R \cdot I_{dh}} \quad \dots 2.26$$

However, in order to determine the total shadowed irradiance or the total initial irradiance load on the surface it is necessary to take into account the size of the shadowed area together with its shadow factor for the two shaded parts of the surface. The shadow condition of the surface may then be expressed by the area weighted shadow factor SF_{av}

$$SF_{av} = \frac{A_S \cdot SF_{(1)} + (A - A_S) \cdot SF_{(2)}}{A} \quad \dots 2.27(a)$$

$$= \frac{A_S \cdot I_{DS} + A \cdot R_{ob} \cdot I_{dh}}{A(I_{DS} + R \cdot I_{dh})} \quad \dots 2.27(b)$$

$$= \frac{A_S \cdot I_{DS}}{A(I_{DS} + R \cdot I_{dh})} + \frac{R \cdot I_{dh}}{I_{DS} + R \cdot I_{dh}} - \frac{R_S \cdot I_{dh}}{I_{DS} + R \cdot I_{dh}} \quad \dots 2.27(c)$$

The last term of the equation 2.27(c) above is the DF.

This general equation may be used to calculate the SF for all the possible shadow forms on a surface which are described earlier in this chapter. In the situation where many patches of umbra, which are of different sizes, are formed on a surface, SF_{av} is given by the expression

$$SF_{av} = \frac{\sum_{i=1}^n SF_i \cdot A_{Si}}{A} \quad \dots 2.28$$

6.7 Initial Irradiance Functions of Surfaces

6.7.1 The initial irradiance expresses the total irradiance received on all the surface or the average irradiance received/unit area of the surface as

$$I_I = I_{GS}(1 - SF_{av}) \quad \dots 2.29$$

7. INTERREFLECTED IRRADIANCE

7.0.1 The second stage of the irradiance transfer functions define the final irradiance of the surfaces including reflected irradiance. Essentially, all opaque surfaces reflect a fraction of the energy incident on them. Of this only a fraction is intercepted by adjacent surfaces in view and in turn gets reflected between the various surfaces in a process of multiple reflection. The final irradiance of a surface comprises the initial input and the reflected component.

7.0.2 To evaluate the magnitude of the reflected irradiance and to derive final irradiance transfer functions of surfaces it requires a knowledge of the radiant energy reflected by one surface that is falling on another surface.

7.1 Configuration and Form Factors

7.1.1 The fraction of the radiant energy leaving one surface that is directly incident on another surface, to the total energy leaving the surface is identified by several names, ie, interchange factor, angle factor, shape factor, geometrical factor, configuration and form factors (Hamilton and Morgan 1952, McGuire 1962, Sparrow 1963, Toup 1965, and O'Brien 1967). To avoid confusion, the terms most commonly used and adequately descriptive which are used here to designate these fractions are :

- (i) configuration factor defines the radiant energy interchange between infinitesimal surfaces or an infinitesimal and finite surfaces; and
- (ii) form factor defines the energy interchange between finite surfaces.

The fraction of energy from surface A_1 to surface A_2 is usually written as, F_{A_1, A_2} . For simplicity, it may be written as $F_{1,2}$. One basic assumption postulated in defining these factors is that surfaces reflect the radiant energy diffusely following Lambert Cosine Law (Hamilton and Morgan 1952).

7.1.2 The mathematical description of the configuration factor begins with the radiant energy interchange between two infinitesimal surface elements dA_1 and dA_2 separated by a distance r as shown in Figure 2.15.

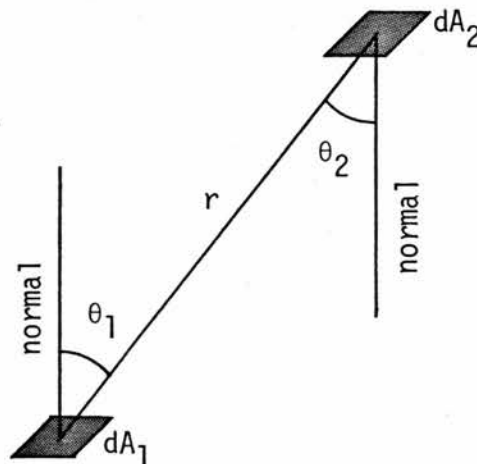


Figure 2.15 Radiation Interchange Between Two Elemental Areas

The total reflected irradiance by the surface element dA_1 is given by

$$I' = I_{I1} \cdot \rho_1 \cdot dA_1 \quad \dots 2.31$$

and the normal intensity by

$$I'_n = I'/\pi = I_{I1} \cdot \rho_1 \cdot dA_1/\pi \quad \dots 2.32$$

The intensity in direction θ_1 , which is falling on dA_2 is

$$I_{1,2} = I_{I1} \cdot \rho_1 \cdot \cos \theta_1 \cdot \cos \theta_2 \cdot dA_1 \cdot dA_2/\pi r^2 \quad \dots 2.33$$

θ_1 and θ_2 are shown in Figure 2.15 above.

From the definition of the configuration factor, the fraction of the energy leaving dA_1 which is incident on dA_2 is

$$F_{dA_1, dA_2} = \cos \theta_1 \cdot \cos \theta_2 \cdot dA_2/\pi r^2 \quad \dots 2.34$$

The configuration factor between an infinitesimal area and a finite area is obtained by integrating equation 2.33 over the whole receiving area. This gives

$$F_{dA_1, A_2} = \int_{A_2} \cos \theta_1 \cdot \cos \theta_2 \cdot dA_2/\pi r^2 \quad \dots 2.35$$

The form factor is similarly obtained by integrating the above

function over the two areas as follows

$$F_{A_1, A_2} = \frac{1}{A_1} \int_{A_1} \int_{A_2} \cos \theta_1 \cdot \cos \theta_2 \cdot dA_1 \cdot dA_2 / \pi r^2 \quad \dots 2.36$$

The configuration and form factors are dimensionless ratios. They are functions of the geometry of the surfaces and may be expressed in terms of their length, width, relative orientation and distance apart.

The main established characteristics of these factors which may greatly simplify the evaluation of the form factors between complex geometrical form and the calculation of the interreflected irradiance are (Hamilton and Morgan 1952, Weibelt 1966 and Billington 1967).

(i) reciprocity relationship which may be expressed by

$$A_1 \cdot F_{1,2} = A_2 \cdot F_{2,1} \quad \dots 2.37$$

(ii) additive property, where the form factor between a surface A_1 and another surface made of a number of unit elements A_{21}, A_{22} , as illustrated by the diagram of Figure 2.16, may be expressed by

$$F_{1,2} = F_{1,21} + F_{1,22} \quad \dots 2.38$$

These two equations are the basis for the laws of flux algebra, which describe the form factors for a system of surfaces that constitutes an enclosure. The geometric flux is given by

$$G_{i,k} = A_i \cdot F_{i,k} \quad \dots 2.39(a)$$

Equation 2.38 for the form factors of Figure 2.16 may be expressed by the geometric flux as

$$G_{1,2} = G_{(11,12),(21,22)} = G_{11,21} + G_{11,22} + G_{12,21} + G_{12,22} \quad \dots 2.39(b)$$

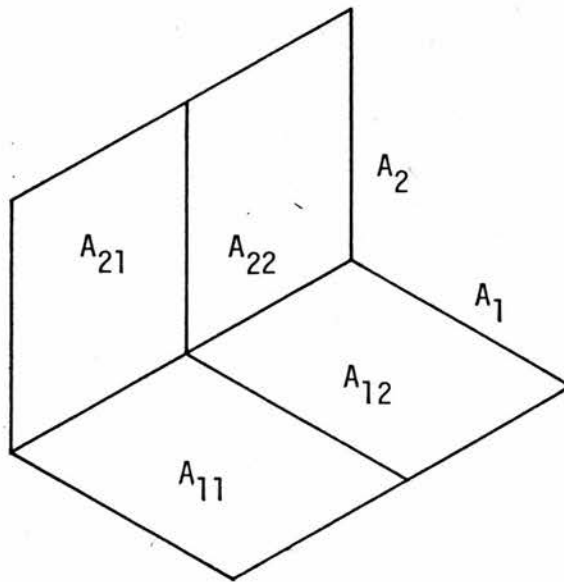


Figure 2.16 Example for Flux Algebra

7.2 Longwave Radiation Exchange Between Building Surfaces

7.2.1 The longwave radiation emitted by the sun in the wavelength region $3.0\mu < \lambda < \infty$ amount to less than two percent of the total solar energy. Practically it is all filtered out by atmospheric absorption (Moon 1940, Robinson 1966).

7.2.2 The main sources of longwave low temperature radiation are the sky, the ground and building surfaces. This sky radiation is emitted mainly by cloud and water vapour. Holden (1961) stated that the magnitude of the sky radiation is directly related to the absolute humidity of the atmosphere. Building surfaces and the ground continuously emit longwave low temperature radiation as they absorb solar radiation during the daylight hours and heat up. The magnitude of the radiation emitted by a surface is directly related to its temperature and emissive power.

7.2.3 The evaluation of the longwave radiation exchange between building surfaces presents practical difficulties because of the complex calculation involved and the extra knowledge about the humidity and surface temperature, which is not readily obtainable. Since the magnitude of the longwave radiation exchange between surfaces is relatively small compared to the interreflected shortwave radiation, it may be practical to ignore it on the assumptions that :

- (i) Longwave solar radiation is completely absorbed by the atmosphere;
- (ii) Humidity is very low in tropical arid regions, hence the magnitude of sky longwave radiation is small;
- (iii) Most building materials are nearly black in the long-wave region and there is little interreflection ; and
- (iv) During the day building surfaces receive nearly as much as they emit and hence no significant radiation is gained.

8. FINAL IRRADIANCE TRANSFER FUNCTION

8.1.1 The derivation of the final irradiance functions of the physical system's surfaces are expressions of radiant flux conservation which include both the initial input and reflected irradiance. These may be presented in a similar manner to those in other problems of radiation transfer, eg, illuminating engineering (O'Brien 1959, 1960, 1963 and 1967, Wiebelt 1966, Navasimhan 1968, 1969). The final irradiance is the sum of the initial and reflected irradiance. It is represented by the expression

$$I_F = I_I + I_R \quad \dots 2.40$$

The reflected irradiance received on a surface part of the physical system, comes from the other parts or surfaces of the system. This may be written as

$$I_R = 1/A_1 \cdot \pi \int_{A_1} \int_{A_2} I_{F_i} \cdot \rho_i \cdot \cos \theta_{1,i} \cdot \cos \theta_{i,1} \cdot dA_1 \cdot dA_i \quad \dots 2.41$$

where $1 < i < n$, as the system is made of n parts or surfaces. For the final irradiance received on surface A_1 due to reflection the n^{th} surface only, A_n , the function may be written as

$$I_{F_1} = I_{I_1} + 1/A_1 \cdot \pi (I_{F_n} \cdot \rho_n \cdot \int_{A_1} \int_{A_n} \cos \theta_{1,n} \cdot \cos \theta_{n,1} \cdot dA_1 \cdot dA_n \quad \dots 2.42$$

This function is of the Fredholm integral form of the second kind which is integrable only for limited simple geometries and known values of the final irradiance of the surfaces. However, O'Brien in his papers of 1959, 1960, 1963 and 1967 has shown that when this equation is thrown into a finite difference form, a solution of sufficient accuracy can be obtained using analogue or digital computers. It has since found wide application by research workers (Narasimhan 1968, 1969, Plant 1971 and Mirza 1973) in problems of radiation transfer where the solution of the finite difference equations is rapidly obtained using analogue or digital computers.

8.1.2 The finite difference function may be derived in the following manner :

The reflected irradiance from a surface S_n to a surface S_1 is given by the function

$$I_{R_{n,1}} = A_n \cdot \rho_n \cdot I_{F_n} \cdot F_{n,1} \quad \dots 2.43$$

Accordingly, we may derive an expression for the total final irradiance of surface S_1 in a system of n surfaces as

$$A_1 \cdot I_{F_1} = A_1 \cdot I_{I_1} + A_2 \cdot \rho_2 \cdot I_{F_2} \cdot F_{2,1} + A_3 \cdot \rho_3 \cdot I_{F_3} \cdot F_{3,1} + \dots + A_n \cdot \rho_n \cdot I_{F_n} \cdot F_{n,1}$$

... 2.44

Utilizing the reciprocity theorem and rearranging the terms, the above function may be written as

$$I_{I_1} = I_{F_1} - \rho_2 \cdot I_{F_2} \cdot F_{1,2} - \rho_3 \cdot I_{F_3} \cdot F_{1,3} \cdots - \rho_n \cdot I_{F_n} \cdot F_{1,n} \quad \dots \quad 2.45$$

In a similar manner a set of finite difference equations may be derived for all the surface which may be expressed by the following matrix :

$$\begin{vmatrix} 1 & -\rho_2 \cdot F_{1,2} & -\rho_3 \cdot F_{1,3} & \cdots & -\rho_n \cdot F_{1,n} \\ -\rho_1 \cdot F_{2,1} + 1 & & -\rho_3 \cdot F_{2,3} & \cdots & -\rho_n \cdot F_{2,n} \\ -\rho_1 \cdot F_{3,1} & -\rho_2 \cdot F_{3,2} + 1 & & \cdots & -\rho_n \cdot F_{3,n} \\ -\rho_1 \cdot F_{n,1} & -\rho_2 \cdot F_{n,2} & -\rho_3 \cdot F_{n,3} & \cdots & +1 \end{vmatrix} \times \begin{vmatrix} I_{F_1} \\ I_{F_2} \\ I_{F_3} \\ I_{F_n} \end{vmatrix} = \begin{vmatrix} I_{I_1} \\ I_{I_2} \\ I_{I_3} \\ I_{I_n} \end{vmatrix}$$

8.1.3 The solution of this unity diagonal matrix is readily obtainable by various numerical methods (IBM 1970, Dorn and McCracken 1972). Using the digital computer for the solution of this matrix, the choice of the numerical technique is chosen with respect to the minimum use of machine time and memory area.

8.1.4 The solution of the matrix gives the final irradiance received per unit area of the surfaces. The final irradiance is assumed to be uniformly distributed over the whole of that area of the surface. Dividing each of the surfaces into small units provides a picture of the final irradiance distribution over the surfaces. The accuracy is governed by the number of surface units taken. However, this should be weighed against the fact that the greater the number of surface units, the greater the number of simultaneous equations to be solved and hence the greater the machine time needed to solve each problem. Exploratory tests must first be carried out to decide on the optimum number of surface units.

9. THEORETICAL ANALYSIS OF IRRADIANCE TRANSFER FUNCTION

9.0.1 With the initial and final irradiance transfer function expressed mathematically, it is possible to deduce theoretically the form of the relationships between the system response, the final or reflected irradiance, and the physical system's parameters. This may indicate the significance of any of the parameters involved or the range at which they are more significant in influencing any of the factors of the transfer function. This serves as a guide in carrying the investigation with the mathematical model to provide the needed data. It is also helpful in suggesting the manner in which the data should be analysed and presented for practical application.

9.1 Analysis of Initial Irradiance Function

9.1.1 From equation 2.29 the initial irradiance is a linear function of both the total irradiance and the unobstructed surface I_{GS} and the area weighted average shadow factor SF_{av} . I_I is directly proportional to I_{GS} .

$$I_I \propto I_{GS} \quad \dots 2.47(a)$$

This also means

$$I_I \propto I_{DS} \quad \dots 2.47(b)$$

$$I_I \propto I_{ds} \quad \dots 2.47(c)$$

where I_{DS} and I_{ds} are non-linear functions of the angle of incidence $\cos \theta$ and linear function of I_{DN} . I_{DN} is also a non-linear function of the solar altitude angle, $\sin \gamma_0$, which increases with the increase of γ_0 , while $\cos \theta$ decreases with the increase both of γ_0 and the sun-surface azimuth β . This suggests a critical angle of γ_0 where the direct, diffuse and total radiation reach a maximum magnitude. For a vertical surface and a clear tropical sky this angle is about 30° . $\cos \theta$ has its maximum value at $\beta = 0$, for all solar altitudes. For a vertical surface I_{GS} decreases as the surface is orientated away from the sun. With regard to the total irradiance of unobstructed surfaces it seems that the orientation angle of a surface is the most effective parameter to achieve any reduction in the irradiance magnitude. This is by no means a new fact and has been the focus of many studies in the past to select the optimum orientation of surfaces (Olgyay 1967, 1969, Kuba 1969, Valko 1970, 1972, Tappuni 1973).

9.1.2 The initial irradiance of a surface is also a linear function of the total shadow factor where I_{GS} decreases with the increase of the shadow factor. The same is true for SF_{av} ; it will be seen from equations 2.15, 2.27 and 2.29, that the initial irradiance of a surface is a non-linear function of the geometrical parameters of the sun and the form. The form's geometrical parameters are most significant as they

directly influence the magnitude of the total shadow factor for any sun position and they are the ones that can be controlled and manipulated by the designer. These are :

- (i) The size and shape of the obstruction where the bigger the obstruction the greater is SF_{av} .
- (ii) The distance between surfaces or location of the obstruction in relation to the receiver. The nearer the surfaces to each other the greater the shadow area and SF_{av} .
- (iii) Orientation of the shaded surface, the smaller the surface-sun azimuth the greater the SF_{av} . However, this contradicts the other fact where the total irradiance increases with the decrease of β .

9.1.3 By taking the shading effect into consideration the initial irradiance may be used to provide a simple guide for the derivation of the optimum orientation of geometrical forms. By calculating the initial irradiance on the different surfaces of various geometrical configurations of form, either throughout the year or for specific periods, the optimum orientation may be defined by maximising the shadow factor and minimising the total irradiance. The performances of the forms may be considered with respect to the shadow factor and initial irradiance received on the surfaces of the form, eg, the vertical surfaces or the grounds,

or on all parts of the form. The geometrical forms may then be selected with regard to their performances.

9.1.4 However, it should be pointed out that only by taking into account the reflected irradiance can accurate assessments of form orientations and performances be made.

9.2.0 Analysis of the Final Irradiance Transfer Functions

9.2.1 Theoretical analysis of the final irradiance transfer functions is possible when the formulation of the governing equation is known. The integral equation of the irradiance transfer function of the physical system is not directly amenable for analysis. However, the basic forms of interrelations between the system's parameters may be deduced from the approximate mathematical formulation which may be given in two forms :

- (i) By the integrated sphere method which will give an average final irradiance for all the surfaces of the physical system by the expression (Dresler 1954, Hopkinson 1966)

$$I_{av} = \frac{I_{I_1} \cdot \rho_1 + I_{I_2} \cdot \rho_2 + \dots + I_{I_n} \cdot \rho_n}{A - (\rho_1 \cdot A_1 + \rho_2 \cdot A_2 + \dots + \rho_n \cdot A_n)} \quad \dots 2.48$$

- (ii) By taking the finite difference equations, equations

2.45 and 2.46, in a series of algebraic substitutions other formulations of the surface's final irradiance, or reflected irradiance, may be derived which are directly amenable for analysis. For a system of three surfaces such expressions may be given as

$$I_{F_1} = I_{R_1} + I_{I_1} \quad \dots 2.49$$

$$\begin{aligned} I_{R_1} = & (\rho_1 \cdot \rho_2 \cdot F_{2,1} \cdot F_{1,2} \cdot I_{I_1} \\ & + \rho_1 \cdot \rho_3 \cdot F_{3,1} \cdot F_{1,3} \cdot I_{I_1} \\ & + \rho_1 \cdot \rho_2 \cdot \rho_3 \cdot F_{1,3} \cdot F_{3,2} \cdot F_{2,1} \cdot I_{I_1} \\ & + \rho_1 \cdot \rho_2 \cdot \rho_3 \cdot F_{1,2} \cdot F_{2,3} \cdot F_{3,1} \cdot I_{I_1} \\ & + \rho_2 \cdot F_{1,2} \cdot I_{I_2} + \rho_2 \cdot \rho_3 \cdot F_{1,3} \cdot F_{3,2} \cdot I_{I_2} \\ & + \rho_3 \cdot F_{1,3} \cdot I_{I_3} + \rho_2 \cdot \rho_3 \cdot F_{1,2} \cdot F_{2,3} \cdot I_{I_3}) / \\ & (1 - \rho_1 \cdot \rho_2 \cdot F_{1,2} \cdot F_{2,1} - \rho_1 \cdot \rho_3 \cdot F_{1,3} \cdot F_{3,1} \\ & + \rho_2 \cdot \rho_3 \cdot F_{3,2} \cdot F_{2,3} - \rho_1 \cdot \rho_2 \cdot \rho_3 \cdot F_{1,3} \cdot F_{3,2} \cdot F_{2,1} \\ & - \rho_1 \cdot \rho_2 \cdot \rho_3 \cdot F_{1,2} \cdot F_{2,3} \cdot F_{3,1}) \end{aligned} \quad \dots 2.50$$

In this case I_I will be the initial irradiance/unit area of the surface.

9.2.2 In a similar manner expressions for the other surfaces may be derived. The denominator will remain the same for each given number of surfaces. It is possible to carry the above substitution for any number of surfaces, but the number of terms in the function increases rapidly with the increase in the number of surfaces, ie, a system of four surfaces will have 36 terms in the numerator and 21 in the denominator. The above function reveals the general form of the interrelation, making it unnecessary to present different functions for different combinations of surfaces of the physical system. Both formulations of the final irradiance, equations 2.48 and 2.50, show the same features of the system's parameters interrelations, however, the finite difference functions is more revealing in showing the variations of the final irradiance for each surface and the ways the different parameters and factors interact.

9.2.3 The following conclusion may be drawn from the above functions :

- (a) There are distinct patterns in which the parameters are arranged in the different combinations. The general form of the pattern may not be easily established unless a greater number of surfaces in the physical system are considered.
- (b) The reflected irradiance of a surface is a linear function

of the initial irradiance of the surfaces of the system and is directly proportional to them. This suggests that the initial irradiance of the surfaces may be used in deciding the optimum orientation of the geometrical form. It is not necessary then to select such orientation with regard to the final irradiance.

$$I_{R_1} = \alpha I_{I_n}$$

where I_{I_n} is the initial irradiance of any of the surfaces. The proportionality coefficient is dependent on the geometry and the reflectances of the form.

- (c) The reflected irradiance is a non-linear function with respect to the form's geometry and its physical properties. This is clear from the appearance of the configuration factors and reflectances parameters in the denominators of the irradiance functions.
- (d) The geometrical and physical parameters of the system interact in a complex form. This suggests that, within certain ranges of these parameters, the final irradiance may be represented by a simple linear function. It also suggests that, within certain ranges of these parameters, variations in them may result in significant variation of the final irradiance.

9.2.4 These ranges may be decided on by analysis of data of final irradiance for a wide range of system's parameters. It is possible to derive simple and approximate formulations - to evaluate the interreflected or final irradiance of surfaces of a physical system, for practical application. Such functions may be derived for a certain geometrical form, taken as a reference standard form. The irradiances and performances of other physical systems are evaluated and measured from the standard system by some simple relationship.

CHAPTER III

THE MATHEMATICAL MODEL AND ITS
COMPUTER APPLICATION

THE MATHEMATICAL MODEL AND ITS COMPUTER APPLICATION

1.0 INTRODUCTION

1.0.1 The physics of the problem and the quantitative relationships between the output and the system's parameters are defined. With the availability of high speed digital computers, with their capacity for rapid and repetitive calculations, the argument is very much in favour of conducting this study with a mathematical model programmed for a digital computer, as against other forms of model studies, eg, physical model or analogue computer.

1.0.2 The usefulness, accuracy and practicability of a digital computer model study are governed by such model features as :

- (i) the numerical methods and the procedures used;
- (ii) the considerations which influence the programming techniques with regard to the machine limitations, simplicity of input and output and low computing costs; and
- (iii) the lay-out of the model program and its various routines, which evaluate the different factors involved, and the way they are interrelated and

the possibility of using each routine individually.

1.0.3 The discussion which follows in this Chapter presents those numerical methods and procedures used to develop the mathematical model and to compile the computer programs which calculate the input, the factors involved and the output.

1.0.4 The lack of standard methods to predict the irradiance and illuminance and the very complex calculations required to evaluate the diffuse irradiance on illuminance on surfaces of different orientations and inclinations in dry sunny climates have always presented difficulties in evaluating the initial radiant flux on building surfaces. The expressions developed for the direct and diffuse radiation and the tables prepared for the sky component and the obstructed sky component surmount these difficulties and provide the base for a mathematical model for predicting the initial irradiance or illuminance on building surfaces.

2. THE CHOICE OF A MATHEMATICAL MODEL

2.0.1 Three types of models have frequently been used by research workers in studying similar physical systems (O'Brien 1959, Hopkinson 1963, Cowan 1968, Echenique 1968, Narasimhan 1968, Hawkes 1970 and Plant 1965, 1969 and 1973). These are :

- (i) physical models and analogues;
- (ii) mathematical models and analogue computer; and
- (iii) mathematical models and digital computers.

The choice of the most advantageous form of model to study a problem is made with regard to the nature of the problem itself, the objectives of the study and the resources which are available.

2.1 Physical Models

2.1.1 These are most suitable in situations where the governing equation of the system is wholly or partially unknown or, though known, not amenable to analytical solution. The physical model constructed should have the same governing equation and similar behaviour as the prototype. There are two forms of the physical model :

- (i) Full scale model : used in the case of constructing a full size structure or making use of an existing building exposed to actual climatic conditions.
- (ii) Scale model : used to study behaviour under natural climatical conditions, exposed to direct and diffuse radiation, or in controlled laboratory conditions using artificial skies, heliodons and solar scopes.

2.1.2 In a study with a physical model the irradiance output and its distribution over the surfaces is easily recorded and observed throughout the day. The effect of external colour, orientation and shading may be evaluated readily.

2.1.3 The main disadvantages of physical models are :

- (i) the greater cost involved in preparing the model and the photometric and other radiation measuring equipments.
- (ii) the considerable time and effort needed in setting up the equipment and taking the measurements.
- (iii) the observations are restricted and do not cover a wide range of combinations of variables.
- (iv) the effect of one parameter on the output cannot be

easily isolated and evaluated separately due to the cumulative effects of all the factors involved.

2.2 Analogue Computers

2.2.1 Analogues duplicate the network of irradiance transfer paths in a physical system with different forms of energy, (electrical energy) and different materials from those of the physical system, (electrical components, ie, resistances, capacitors, switches, voltmeters, and so on).

2.2.2 Analogues demand a precise knowledge of the physics of the problem and a mathematical formulation of the governing equation which can be transformed to a set of expressions of a similar form to Kirchhoff's node equation, Kirchhoff's current law. The physical system may then be interpreted as an electrical network and an analogue may be constructed to simulate the Kirchhoff node form of the equation.

2.2.3 Analogues are then another artifice of numerical analysis. They were particularly successful for studying irradiance transfer problems, being capable of both analysis and synthesis. O'Brien in his paper of 1959 described an electrical analogue he used, constructed in the Department of Engineering at the University of California in Los Angeles, which is capable of solving ten simultaneous

equations. Narasimhan and Maitreya (1968), at the Central Building Research Institute of India, used another analogue for six equations. Both analogues were used in studying daylighting problems. However, it is always possible to extend the number of equations for the analogue.

2.2.4 The finite difference equation, equations 2.45 and 2.46 may be transformed by algebraic operations to a set of expressions of the form of Kirchhoff's node equations. This is achieved by balancing the total radiant energy reflected by a surface towards its surrounding and the total radiant energy received by the surface from its surrounding. It is necessary here to take into consideration the radiant energy reflected by the surface back to the sky. This may be evaluated by the form factor between the surface and the sky area, in view, which is given by the expression

$$F_{1,s} = 1 - \sum_i^n F_{1,i} \quad \dots \quad 3.1$$

where n is the number of surfaces of the physical system. The finite difference equation may then be written as

$$\frac{(\rho_1 \cdot I_{F_1} - \rho_2 \cdot I_{F_2})}{1/A_1 \cdot F_{1,2}} + \frac{(\rho_1 \cdot I_{F_1} - \rho_3 \cdot I_{F_3})}{1/A_1 \cdot F_{1,3}} + \dots + \frac{(\rho_1 \cdot I_{F_1} - \rho_n \cdot I_{F_n})}{1/A_1 \cdot F_{1,n}} = \frac{[(I_{I_1} / (1 - \rho_1 + \rho_1 \cdot F_{1,s})) - I_{F_1}]}{1/A_1 (1 - \rho_1 + \rho_1 \cdot F_{1,s})}$$

$$\frac{(\rho_2 \cdot I_{F_2} - \rho_1 \cdot I_{F_1})}{1/A_2 \cdot F_{2,1}} + \dots + \frac{(\rho_2 \cdot I_{F_2} - \rho_n \cdot I_{F_n})}{1/A_2 \cdot F_{2,n}} = \frac{[(I_{I_2} / (1 - \rho_2 + \rho_2 \cdot F_{2,s})) - I_{F_2}]}{1/A_2 (1 - \rho_2 + \rho_2 \cdot F_{2,s})}$$

$$\frac{(\rho_n \cdot I_{F_n} - \rho_1 \cdot I_{F_1})}{1/A_n \cdot F_{n,1}} + \dots + \frac{(\rho_n \cdot I_{F_n} - \rho_{n-1} \cdot I_{F_{n-1}})}{1/A_n \cdot F_{n,n-1}} = \frac{[(I_{I_n} / (1 - \rho_n + \rho_n \cdot F_{n,s})) - I_{F_n}]}{1/A_n (1 - \rho_n + \rho_n \cdot F_{n,s})}$$

... 3.2(a)

substituting for the radiosity J , where

$$\text{initial radiosity } J_I = \rho \cdot I_I$$

$$\text{final radiosity } J_F = \rho \cdot I_F$$

the above equation will take the form

$$\frac{(J_{F_1} - J_{F_2})}{1/A_1 \cdot F_{1,2}} + \frac{(J_{F_1} - J_{F_3})}{1/A_1 \cdot F_{1,3}} + \dots + \frac{(J_{F_1} - J_{F_n})}{1/A_1 \cdot F_{1,n}} = \frac{[(J_{I_1} / (1 - \rho_1 + \rho_1 \cdot F_{1,s})) - J_{F_1}]}{\rho_1 / A_1 (1 - \rho_1 + \rho_1 \cdot F_{1,s})}$$

... 3.2(b)

In each term the numerators, eg, $J_{F_1} - J_{F_2}$, may be regarded as potentials and the denominators, $1/A_1 \cdot F_{1,2}$ as resistances. An electrical network interpretation of the finite difference approximation is readily achieved. A network representation for a system of four surfaces is shown here in Figure 3.1.

2.2.5 The analogue is more advantageous than the physical model because it is easier to vary the system parameters, greater numbers of combinations of parameters can be investigated and an instantaneous output is available. Synthesis is easily accomplished with the analogue,

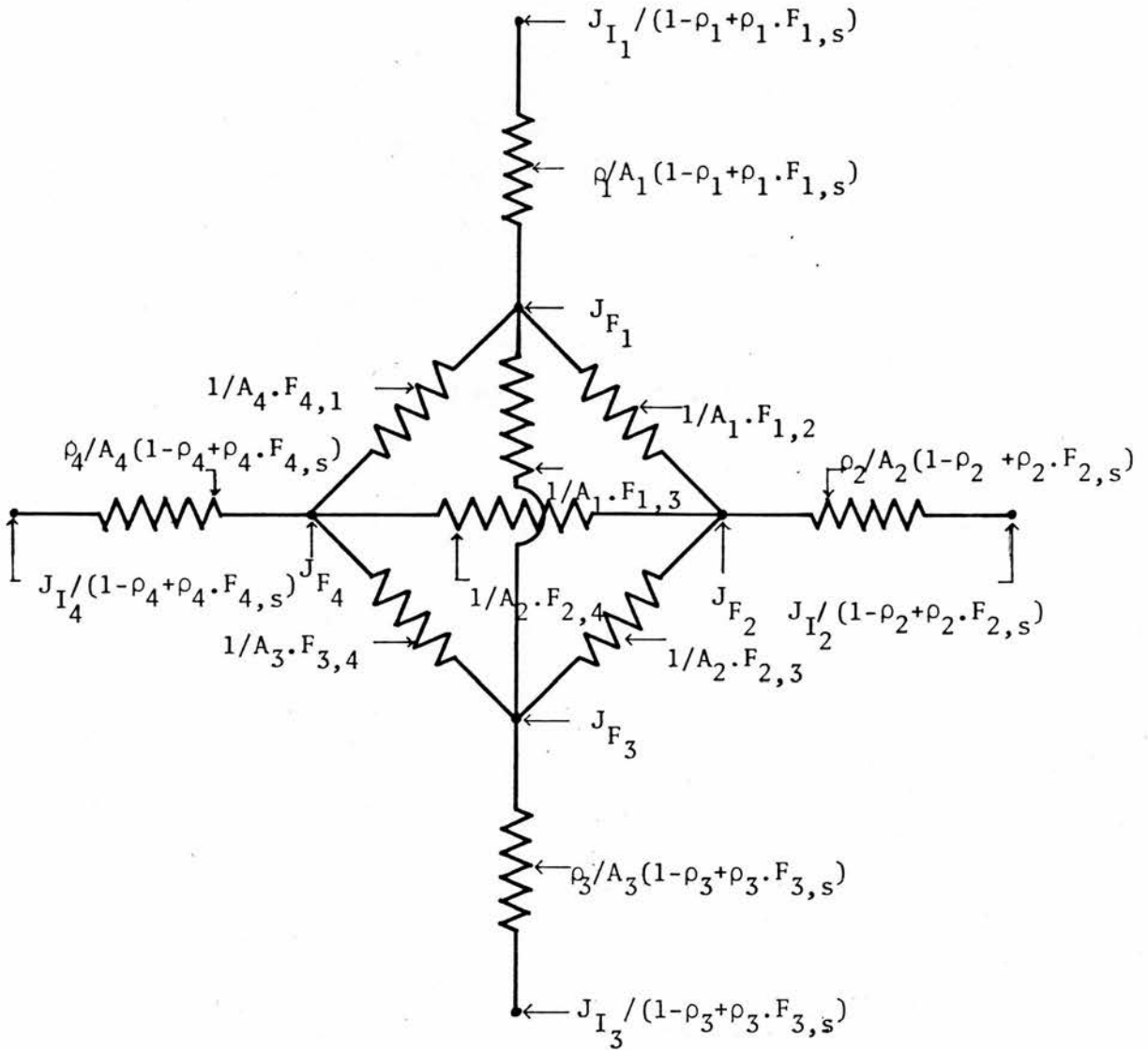


Figure 3.1 A Network Representation of Irradiance Transfer for a System of Four Surfaces

particularly in terms of the surfaces' reflectances.

2.2.6 The main disadvantages of the analogue are :

- (i) its use is limited to the problem it is designed for.
- (ii) it is expensive to construct, although the cost of individual components may not be very high and its construction requires specialised technical skills.
- (iii) it is necessary to compute such parameters as the initial irradiance of the surfaces, which depend on the shading and diffusion effects, and the form factors before setting the excitation potential at the network nodes and the resistances connecting them. This may be a very complex calculation in many cases and may itself require the aid of a digital computer.
- (iv) it does not allow direct study of the shading effect.
- (v) the synthesis of the output in terms of the geometrical parameters is difficult.

These, along with the advantage of solving the same problem with a digital computer, render the analogue computer obsolete.

2.3 THE DIGITAL COMPUTER MATHEMATICAL MODEL

2.3.1 As the analogue computer basically solves the finite difference equations, the initial irradiances and the form factors have to be predetermined before evaluating and setting the analogue's parameters; the excitation potential and the resistances. The prediction of a surface's initial irradiance is quite involved and requires a great deal of computation with complex functions, or interpolation from tables, expressing :

- (i) the position of the sun in the sky,
- (ii) the sky luminance distribution,
- (iii) the direct solar irradiance, and
- (iv) shadow and diffusion.

Similarly, the form factors are expressed by a more complex function which, when not available from tables, requires laborious numerical techniques even for simple geometries.

2.3.2 Nowadays, high speed electronic digital computers are available in most institutions. With their capacity for rapid and repetitive calculation they offer a better alternative to the analogue for studying such physical systems in an integrated way, determining the initial irradiance and the

the form factors, and solving the finite difference equations.

2.3.3 Computer programs may be developed to simulate the movement of the sun, the sky luminance and radiant energy distribution, direct irradiance, shading, diffusion and interreflection. Subsequently, the position of the sun, the initial irradiances, the total shadow factors, the boundaries of the shadow profiles, the form factors and the final irradiance are predicted with considerable accuracy and ease.

2.3.4 Computer model studies overcome the limitations of the analogue and physical models in the following ways :

- (i) the investigation may be carried out in an integrated way;
- (ii) there is no need for elaborate model mock-ups or measuring equipment;
- (iii) they provide speedy calculation and low computing cost;
- (iv) only simple data preparation is needed, the input is easy and the output is readily available;
- (v) they give flexibility in studying a greater number of combinations of the system's parameters;

- (vi) a wider variety of geometrical form, with greater numbers of surfaces, wider ranges of physical properties and different positions of the sun can be studied;
- (vii) the significance of any of the parameters and its effect on the various factors and the output may be readily established;
- (viii) the shading effect is readily evaluated;
- (ix) programs may be used in parts to evaluate certain factors, such as shading, initial irradiance, form factors, or in an integrated whole model to evaluate and output the final irradiance; and
- (x) the computer model is applicable in both analysis and synthesis of output with regard to any of the system parameters.

2.3.5 Although the development and compilation of computer programs may be quite complicated and may require a good knowledge of programming and numerical analysis techniques, expert advice about problems in these areas may be obtained. The Edinburgh Regional Computing Centre, servicing Edinburgh University, provides an advisory service and a comprehensive Program Library Unit supporting many packages of applications routines and programs available for users.

2.3.6 From previous studies (O'Brien and Howard 1959 a and b, Narasimhan and others 1968, 1969, Mirza 1973, Plant 1971, Plant and Archer 1973) which used computer models for similar problems and from the comparison which was made above, it may be concluded that, without doubt the use of a digital computer is the most advantageous way of conducting this study. The choice and development of the numerical methods to evaluate the various parameters and factors, the procedures used to compile the different routines and the layout of the model are described below.

3. SUN GEOMETRY

3.0.1 Knowledge of the altitude and azimuth angles of the sun is often needed in architectural design or research. Such information may be required for different times of the day and year and at different locations when studying the shading of buildings, the duration of insolation, irradiance and cooling loads, sky luminance and surface illuminance.

3.0.2 The basic geometry of the sun's movement is well known and different numerical and graphical techniques are available to provide such information (Smart 1962, Bussat and Jorgen 1972, Kuba 1972, Van Deventer 1972). These are usually provided in the form of tables and charts which are impractical to use in computer model studies since they require a large machine core store and may involve many interpolation processes of data and hence reduce the efficiency of the program.

3.0.3 A mathematical model can easily be developed and programmed for the computer which simulates the apparent movement of the sun. This model may be incorporated into models dealing with problems related to the sun. It may also be used to output tabulated information of the sun angles for any location on the earth's surface.

3.1 Fundamental Solar Angles

3.1.1 The apparent movement of the sun consists of a daily movement imposed on a yearly movement. The yearly movement is viewed when taking a celestial sphere with the earth at its centre. The sun will appear then to travel along the ecliptic with a varying angular velocity. For time keeping purposes a fictitious mean sun is assumed to travel along the celestial equator, which itself is in motion, with a constant angular velocity, equal to the mean angular orbital velocity of the sun, ω given by the expression

$$\omega = 360/365.24 \text{ degree/day} \quad \dots 3.3$$

The position of the sun on the celestial sphere, at any date, is defined by three fundamental angles as shown in Figure 3.2 :

(i) Longitude L

The sun's longitude, at any time, may be measured from a reference meridian which passes through the intersection of the ecliptic and the celestial equator, the vernal equinox, and the pole of the ecliptic. The mean longitude of the sun L_m would give the angle included between the reference meridian and the meridian through the corresponding location of the mean sun on the ecliptic. The mean sun will be on the reference meridian at the reference date t_0 , when the

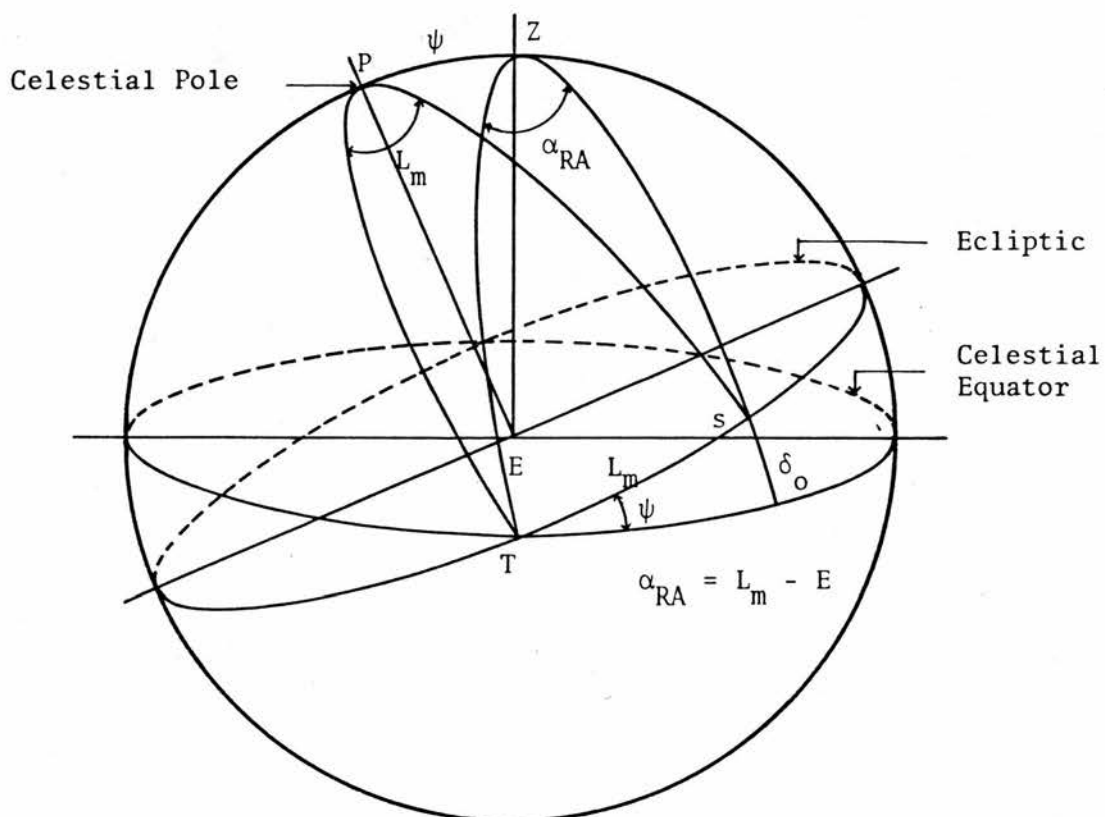


Figure 3.2 The Celestial Sphere

mean longitude $L_m = 0$. The mean longitude at any date t_1 is then given by the function (Smart 1962)

$$L_m = \omega(T_1 - t_0) \text{ degree} \quad \dots 3.4$$

(ii) Equation of time E

The difference between apparent and mean solar time is termed 'the equation of time'. This is due to the variation of the earth's angular velocity because of the eccentricity of the orbit and the obliquity of the ecliptic. Smart (1962) defined E as the difference between the right ascension of the mean sun α_{RAM} , and the right ascension of the true sun α_{RA} . The right ascension of the mean sun is defined as the angular distance from the vernal equinox to the mean sun's position on the celestial equator, taken in an eastward direction along the equator. It is equal to the sun's mean longitude. The right ascension of the true sun similarly measures the angular distance to the corresponding position of the true sun on the celestial equator. The equation of time is then given by the expressions

$$E = \alpha_{RAM} - \alpha_{RA} \text{ degrees} \quad \dots 3.5(a)$$

$$= L_m - \alpha_{RA} \text{ degrees} \quad \dots 3.5(b)$$

$$\alpha_{RA} = L_m - E \text{ degrees} \quad \dots 3.5(c)$$

E may be obtained from tables in the Nautical Almanac, but it is advantageous to evaluate it by a mathematical expression for computer application (Van Deventer 1972). A simple expression was given by Smart (1962), in Fourier Series, which expresses E as a function of the sun's mean longitude, as

$$\begin{aligned}
 E = & -97.8 \cdot \sin (L_m) - 431.3 \cdot \cos (L_m) \\
 & +596.6 \cdot \sin (2 \cdot L_m) - 1.9 \cdot \cos (2 \cdot L_m) \\
 & +4.0 \cdot \sin (3 \cdot L_m) + 19.3 \cdot \cos (3 \cdot L_m) \\
 & -12.7 \cdot \sin (4 \cdot L_m) \\
 & \text{seconds} \quad \dots 3.6
 \end{aligned}$$

On the 21st March, the true sun is at the vernal equinox, α_{RA} is equal to zero and $E = L_m$. Using this and equations 3.4 and 3.6, it can be proven that the reference date t_0 is about 82 days from the beginning of the year (taking February as 28.25 days) or on the 23rd of March. Equation 3.4 may be written as

$$L_m = \omega(t_1 - 82) \text{ degrees} \quad \dots 3.7$$

By this equation the mean longitude and the equation of time may be evaluated for any date.

(iii) Solar declination δ_0

This is the angular distance of the sun measured north or south of the equator. The solar declination may be obtained from tables provided in the Nautical Almanac (1964) or by mathematical expressions (Morris and Lawrence 1969, Van Deventer 1972). A simple expression for the solar declination may be derived, from the spherical triangle on the celestial sphere shown in Figure 3.2, as

$$\tan \delta_0 = \tan \psi \cdot \sin (L_m - E) \quad \dots 3.8$$

where ψ is the inclination of the axis and is equal to 23.45 degrees. δ_0 is taken positive when the sun is north of the equator and negative when south of the equator.

(iv) Hour angle H

The hour angle of the sun defines the angular distance between a meridian of a location on the earth's surface and another meridian on which the sun is overhead. It is calculated by the expression

$$H = H' - E + L_T - L_0 \quad \dots 3.9$$

where H' is the mean hour angle which is conventionally measured from 12 noon,

L_T is the longitude of standard time, and

L_0 is the longitude of the location.

3.2 THE ANGULAR PARAMETERS OF THE SUN

3.2.1 The position of the sun in the sky relative to a location on the earth's surface, at any time, may be described by two angles as shown in Figure 3.3 :

(i) Altitude γ_0

This is the angular distance of the sun above the horizon in the great circle containing the sun and the zenith. The solar altitude is evaluated by the following expression, derived from the spherical triangle shown in Figure 3.4

$$\sin \gamma_0 = \sin \phi \cdot \sin \delta_0 + \cos \phi \cdot \cos \delta_0 \cdot \cos H$$

... 3.10

(ii) Solar azimuth α_0

This is the angular distance between the vertical circle containing the zenith and the sun and the geographical north. Similarly, from Figure 3.4, the expression for the solar azimuth may be derived as

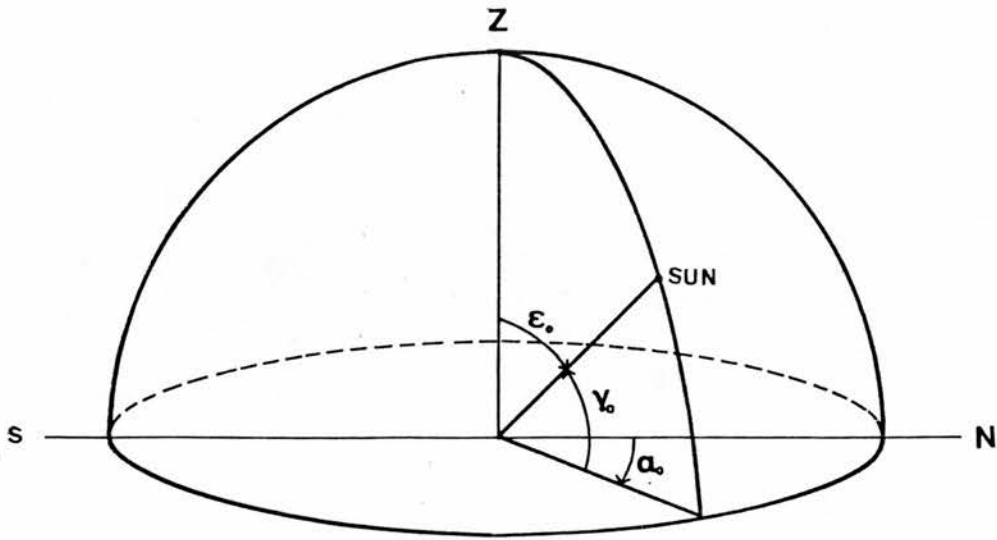


Figure 3.3 The Horizontal Co-ordinate System Defining the Sun's Position

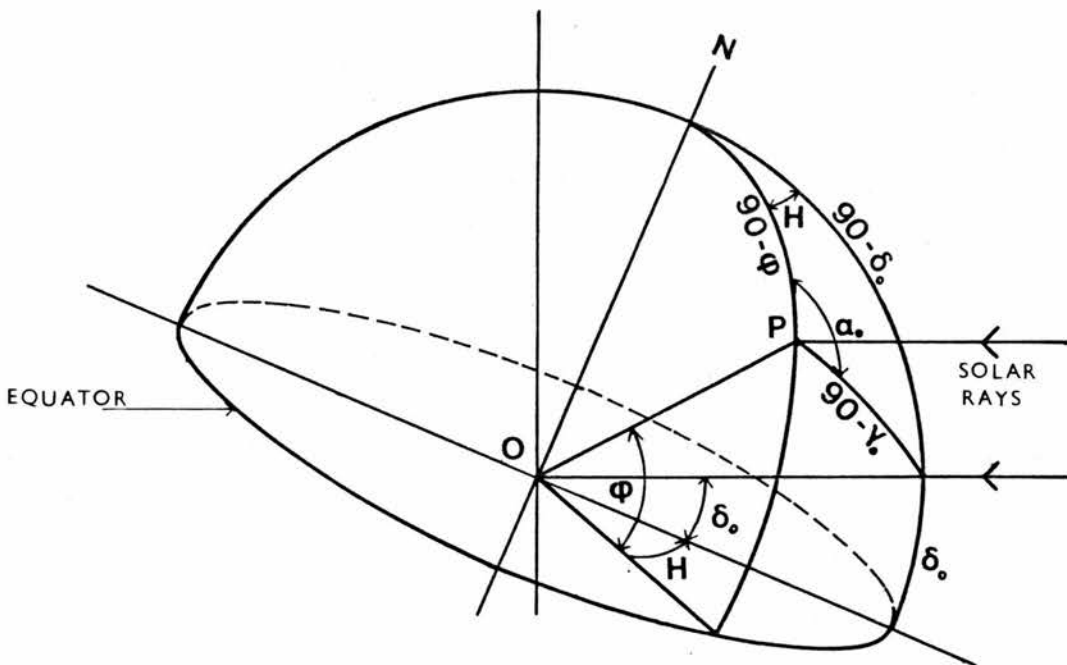


Figure 3.4 The Sun's Position Relative to a Location on the Earth's Surface

$$\sin \alpha_0 = \cos \delta_0 \cdot \sin H / \cos \gamma_0 \quad \dots 3.11(a)$$

$$\text{or } \cos \alpha_0 = \frac{\sin \delta_0 \cdot \cos \phi - \cos \delta_0 \cdot \sin \phi \cdot \cos H}{\cos \gamma_0} \quad \dots 3.11(b)$$

The azimuth is given from the north or south, to the east or west, but it is simpler to take it from the north and in a clockwise direction. When the hour angle is negative, past 12 noon, and the azimuth is to the west, the clockwise direction from the north is maintained by subtracting the azimuth from 360^0 .

3.2.2 Based on the above expressions a computer program was compiled for a model which simulates the apparent sun movement and evaluates the solar altitude and azimuth. The program will output these solar angles for any given location and any specified date and time. These angles are needed by the designer, especially in hot arid regions, when considering the shading of buildings, the irradiance load and interior illumination by daylighting. Tables of hourly values for the solar altitude and azimuth have been prepared for Khartoum. They are given for the 1st. and of the 15th. of each month of the year. These tables are presented here in Appendix A.1.

4. STANDARDISATION AND PREDICTION OF IRRADIANCE AND
ILLUMINANCE OF SURFACES OF DIFFERENT INCLINATIONS
AND ORIENTATIONS IN TROPICAL REGIONS *

4.0.1 Standard techniques to evaluate quantities of irradiance and illuminance would simplify the prediction of the radiant flux received on building surfaces. However, no standard techniques have yet been developed for tropical arid regions of clear skies. They pose a completely different problem from the overcast sky and the methods developed for the overcast sky cannot therefore be applied. Several analytical and empirical expressions have been proposed for predicting the irradiance and the illuminance (eg, Parmelee 1954, Pleijel 1954, Liu and Jordan 1960, Ballantyne 1965, Loudon 1965, Sharma and Pal 1965, Kittler 1972 and Krochmann 1969, 1973). By correlating these expressions, standard techniques for predicting the irradiance and illuminance in tropical arid regions may be developed.

footnote : * This part forms the main body of a paper presented to :

COMPLES RENCONTRE INTERNATIONALE 1974
LE SOLEIL CONSIDERE COMME SOURCE
ENERGETIQUE DE REMPLACEMENT
MADRID 23/28 SEPTEMBRE

It is also published in ,

COMPLES REVUE INTERNATIONALE D'HELIOTECHNIQUE
1 er SEMESTRE 1975 pp 9-18

4.0.2 This study utilises the existing knowledge in an attempt to define a standard tropical atmosphere in terms of :

- the different components of the solar radiant energy coming through and from such an atmosphere and received on a horizontal surface and a surface normal to the direct solar beam ;
- the interrelations between the different components of the solar energy ;
- the interrelations between radiant energy and turbidity for other tropical atmospheres and the standard one ; and
- the correlations between the diffuse sky radiation received on inclined surfaces of different orientations and that received on a horizontal surface.

4.0.3 These interrelations may be represented by a set of mathematical expressions that directly yield quantities for both illuminance and irradiance given as functions of the sun's geometry for the standard tropical atmosphere. For other tropical atmospheres, available information, ie, direct horizontal irradiance, may be used to derive the

different components of the radiant energy on the basis of the expressions for the different interrelations.

4.0.4 It is therefore the intention of this study to present a simple model for evaluating the irradiance and illuminance of surfaces of different orientations and inclinations in tropical regions. Such a model may be easily applied at two levels:

- (a) for computer application, the derived expressions are most advantageously used; and
- (b) for paper and pencil techniques, the tables provided are easily used with some interpolation, if required.

4.1 Standard Tropical Atmosphere

4.1.1 Threlkeld and Jordan (1957) developed expressions for the atmospheric transmission factors. These are the ratio of available direct solar radiation incident on a surface at sea level to that on a similarly oriented surface above the earth's atmosphere. Based on these, Rao and Sheshadri (1961) computed and presented curves connecting the direct normal solar energy with solar altitude for different precipitable vapour and dust proportions. They defined a standard tropical atmosphere

as one containing "15 mm precipitable water vapour, 300 dust particles/cm³, 2.5 mm ozone at 760 mm atmospheric pressure". This was shown to suit the general conditions prevailing in the tropics. The assumption was that the overall depletion of the atmosphere for solar energy is nearly constant. A mathematical expression giving the direct normal solar irradiance for the standard tropical atmosphere, which assumes a value of $I_0 = 2.0 \text{ cal cm}^{-2} \text{ m}^{-1}$, was derived by Sharma and Pal (1965). This expression is modified to account for $I_0 = 1.94 \text{ cal cm}^{-2} \text{ m}^{-1}$ and presented as

$$I_{cn} = 1247 \cdot \sin(\gamma_0) / (0.3135 + \sin(\gamma_0)) \quad \text{W/m}^2 \quad \dots 3.12(a)$$

or

$$I_{cn} = 0.92 \cdot I_0 \cdot \sin(\gamma_0) / (0.3135 + \sin(\gamma_0)) \quad \text{W/m}^2 \quad \dots 3.12(b)$$

$$I_{ch} = I_{cn} \cdot \sin(\gamma_0) \quad \text{W/m}^2 \quad \dots 3.13$$

4.1.2 Clearness Number

Radiation analyses should express the effect of the turbidity of the atmosphere and its relation to the available radiation. Parmelee (1954) related his observed direct normal intensities to the direct normal radiation values from Moon's work (1940), by the clearness

ratio. Sharma and Pal (1965) defined the clearness number, "The ratio of the measured direct radiation on a horizontal surface, to a similarly oriented surface under standard tropical atmosphere." This relates actual atmospheric conditions to the standard tropical atmosphere. It expresses the cumulative influence of the atmospheric variables.

4.1.3 The standard tropical atmosphere concept offers a base on which a set of standard mathematical expressions may be derived to evaluate the different components of the solar radiation, on the basis of the following considerations :

- (a) The atmospheric conditions were verified to be more representative of the actual tropical climates. Kittler (1972) suggests an f value, a measure of atmospheric conditions, of 0.33 - 0.43 for urban arid regions where for the standard tropical atmosphere $f \approx 0.36$.
- (b) The agreement between measured and calculated values was good. The relation between direct and diffuse radiation was in good correlation with data collected in US and India (Sharma and Pal 1965).
- (c) It offers simple mathematical expressions, which are functions of the solar altitude, to evaluate the

different components of solar radiation.

- (d) When atmospheric conditions are different from the standard, this effect may be expressed using the clearness number of modify the expressions. Another procedure was adopted by Ballantyne (1965), where he related data from Melbourne to the appropriate curve of Rao and Sheshadri (1961). It will be noticed that Melbourne has a clearness number of 1.02 - 1.15.

For any clearness number, the direct normal radiation is

$$I_{DN} = I_{cn} \cdot CN \quad W/m^2 \quad \dots 3.14$$

4.2 Direct Incident Irradiance

The direct incident irradiance on a surface facing the sun is evaluated by the expression given by equation 2.9 in Chapter II

$$I_{DS} = I_{DN} \cdot \cos \theta$$

where θ is the angle of incidence the direct solar beam makes with the normal to the surface.

4.3 Direct Solar, Diffuse Sky and Global Irradiance on a Horizontal Surface

4.3.1 Two points may be concluded from the empirical expressions derived by research workers for the horizontal direct, diffuse and global irradiance (Parmelee 1954, Liu and Jordan 1960, Sharma and Pal 1965, Ballantyne 1965, and Kittler 1972).

- (i) The horizontal direct and diffuse irradiance may be expressed as a function of the solar altitude, as shown by equation 2.3 given earlier in Chapter II

$$I_{Dh} = f(\gamma_0)$$

$$I_{dh} = f(\gamma_0)$$

- (ii) Linear relations exist between the direct and the diffuse and global radiation, on a horizontal surface, for every solar altitude. These relations may be expressed as

$$I_{dh} = A' + C' \cdot I_{Dh} \quad \dots 3.15(a)$$

$$I_{Gh} = A' + B \cdot I_{Dh} \quad \dots 3.15(b)$$

The constants A' , B' and C' are thus functions of the solar altitude. The relations may be expressed alternatively in such a form

$$I_{Gh} = A \cdot \sin \gamma_0 + B \cdot I_{Dh} \quad \dots 3.16(a)$$

$$I_{dh} = A \cdot \sin \gamma_0 + C \cdot I_{Dh} \quad \dots 3.16(b)$$

Accordingly, any set of data may be analysed to provide a set of mathematical expressions for calculating the radiation. This does not explicitly include the turbidity of the atmosphere nor does it help to predict the radiation in other localities where no data is available.

4.3.2 Equations 3.14 and 3.16(a) and 3.16(b) seem to indicate a similar relationship for all forms of atmospheres, suggesting that the constants A, B and C are functions of CN. These relations were investigated using values from Sharma and Pal (1965). The following functions were derived

$$A = 0.09 + 0.264 \cdot CN \quad \dots 3.17(a)$$

$$B = 0.122 \cdot \exp(1.08 \cdot CN) + 3.39 \cdot \exp(-2.57 \cdot CN) \quad \dots 3.17(b)$$

$$C = B - 1.0 \quad \dots 3.17(c)$$

4.3.3 For the standard tropical sky, the global and the diffuse horizontal irradiance are given by the functions

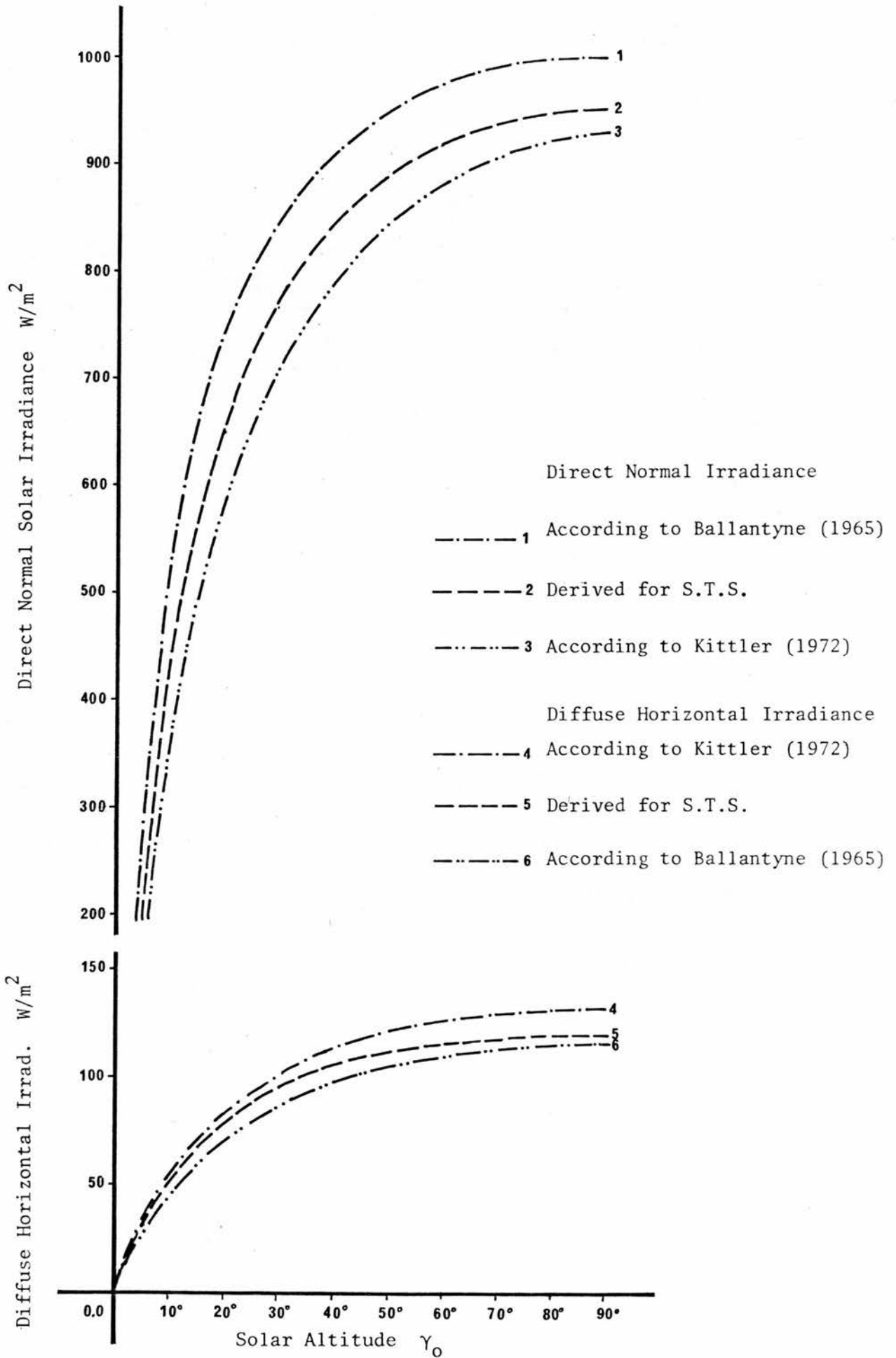


Figure 3.5 The Direct Normal and the Diffuse Horizontal Irradiance

$$I_{Gh} = 494.0 \cdot \sin \gamma_0 + 0.62 \cdot I_{ch} \quad \text{W/m}^2 \quad \dots 3.18(a)$$

$$I_{dh} = 494.0 \cdot \sin \gamma_0 - 0.38 \cdot I_{ch} \quad \text{W/m}^2 \quad \dots 3.18(b)$$

Figure 3.5 shows values for the direct normal and diffuse horizontal irradiance for the standard tropical sky, S.T.S., as compared with values suggested by other research workers (Lin and Jordan 1960, Ballantyne 1965, and Kittler 1972).

4.4 Solar and Sky Illuminances

4.4.1 This information is of greater importance for the calculation of day lighting in building design and town planning purposes. In tropical arid regions such data is always scarce. Most of the measurements conducted are confined to heat radiation only. It is possible to obtain the illuminance information from irradiance measurements by the use of the luminous efficacy factor (Pleijel 1954, Hopkinson 1966 and Krochmann 1969).

4.4.2 Luminous Efficacy

It is defined as units of the visible radiation per unit of the total irradiance. It depends on the way in which the radiant energy is shared between the visible and invisible parts of the solar spectrum. There are different suggestions about the luminous efficacy for sun, sky and global irradiance for clear

conditions which may be classified into two categories :

- (a) K_s , K_d and K_g have the same value. It is implied that they have a value = 100 Lm/W, according to Kittler (1972). Chroscicki (1971) suggested that they are dependent on the solar altitude and gave the expression

$$K_s = K_d = K_g = 59.3 \cdot \gamma_0^{0.1252} \quad \text{Lm/W} \quad \dots \quad 3.19$$

- (b) They do not have the same value (Pleijel 1954, Hopkinson 1966 and Krochmann 1969).

For K_s , most of the work showed that it depends on the solar altitude and the sky condition. The higher the content of the water vapour in the atmosphere, the greater the absorption of the radiant energy in the infra-red region, hence, the higher the value of K_s . The tropical arid regions are characterised by the low humidity, hence, a low value of K_s may be expected. Chroscicki's function is favoured here for evaluating K_s . As for K_d , there are strong indications that, it varies only a little with solar altitude. A value of $K_d = 132$ Lm/W was selected here. It is a mean value and out of those suggested by Krochmann, it seems to be an average between the two extremes suggested for K_d . Uncertainty cannot be eliminated until enough measurements, taken in hot arid regions, are available. The only check will be to correlate derived

illuminance values with available information.

4.4.3 Direct Solar Illuminance

Values for the direct normal solar illuminance of the standard tropical atmosphere are computed from the direct normal irradiance and K_s as given by Chroscicki's function, equation 3.19,

$$E_{Dn} = I_{Dn} \cdot K_s \quad \text{Lx} \quad \dots 3.20(a)$$

These values are expressed as a function of the solar altitude

$$E_{Dn} = 157.94 \cdot \sin \gamma_0 / (0.59 + \sin \gamma_0) \quad \text{KLx} \quad \dots 3.20(b)$$

$$E_{Dh} = E_{Dn} \cdot \sin \gamma_0 \quad \text{KLx} \quad \dots 3.20(c)$$

4.4.4 Horizontal Sky Illuminance

These values are derived from the horizontal irradiance values of the S.T.S. and taking a constant value for $K_d = 132 \text{ Lm/W}$

$$E_{dh} = 132 \cdot I_{dh} \quad \text{Lx} \quad \dots 3.21$$

It should be noted that the lack of adequate information made it difficult to include in the study the illuminance from other tropical skies where CN is $\neq 1.0$. However, as for the global illuminance it seems reasonable to adopt Kittler's suggestion (1972) that the illuminance in KLx = 0.1 the numerical values of the irradiance in W/m^2 , for the tropical non-standard skies.

My investigation showed that the interrelations between the global and sky and direct illuminance are similar to that of the irradiance. The following expressions are derived for the global horizontal and the horizontal sky illuminance, as a function of the direct horizontal illuminance and the solar altitude for the S.T.S.

$$E_{Gh} = 55.68 \cdot \sin \gamma_0 + 0.6 \cdot E_{Dh} \quad \text{KLx} \quad \dots 3.22$$

$$E_{dh} = 55.68 \cdot \sin \gamma_0 - 0.4 \cdot E_{Dh} \quad \text{KLx} \quad \dots 3.23(a)$$

E_{dh} may be expressed as a function of the solar altitude

$$E_{dh} = 21.15 \cdot \sin \gamma_0 / (0.33 + \sin \gamma_0) \quad \text{KLx} \quad \dots 3.23(b)$$

Direct normal and horizontal sky illuminance values derived for the standard tropical sky using the above equations 3.22 and 3.23(a) are compared with values given by other workers

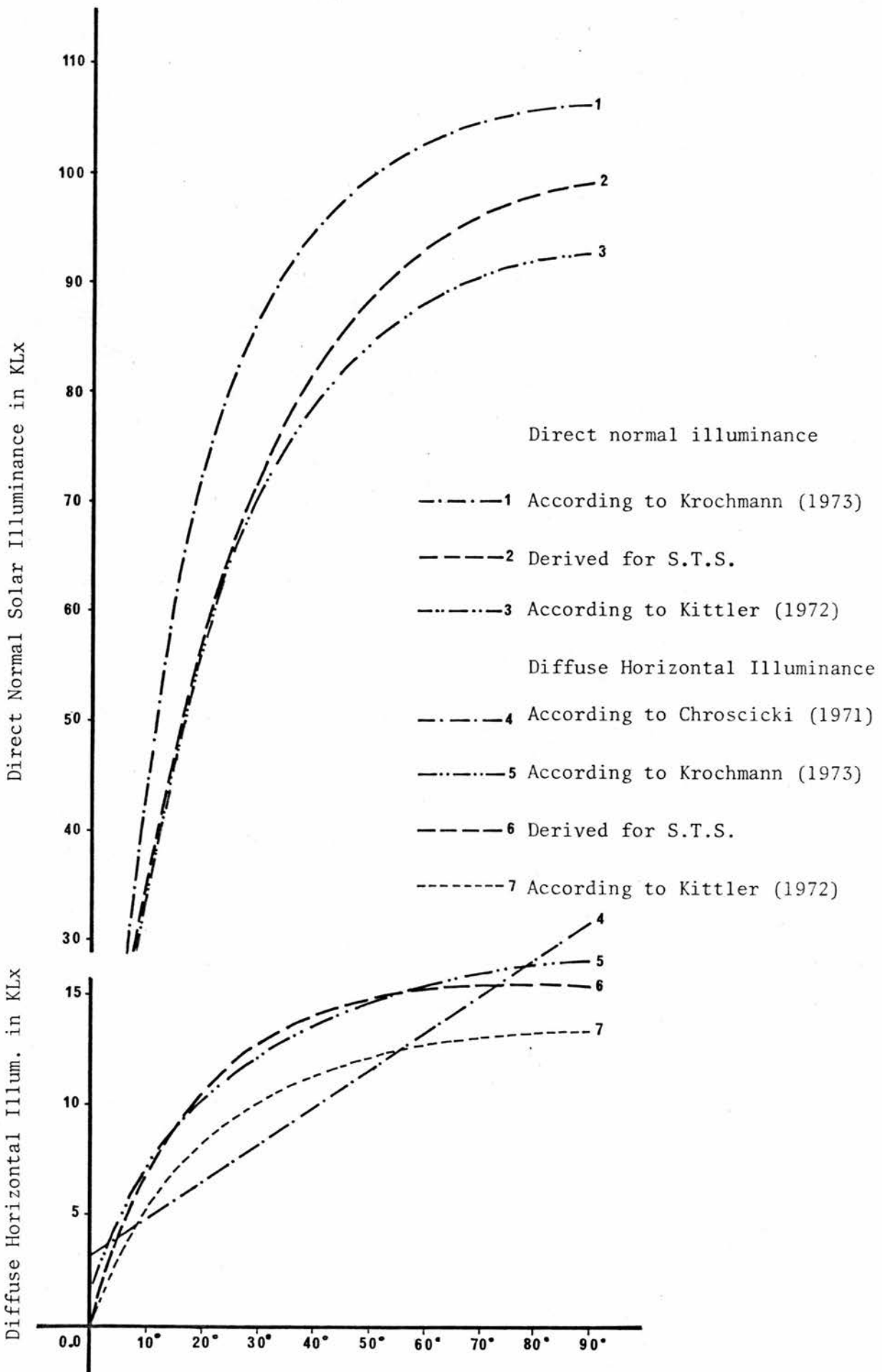


Figure 3.6 The Direct Normal and Diffuse Horizontal Illuminance

(Kittler 1972 and Krochmann 1973). See Figure 3.6.

Derived values for the direct, diffuse and global irradiance and illuminance for the S.T.S., for various solar altitudes are presented in Appendix A.2.

4.5 Diffuse Irradiance and Illuminance of Vertical and Inclined Surfaces

4.5.1 Previous studies have shown that diffuse irradiance on vertical surfaces is a function of the solar altitude, surface-solar azimuth and atmospheric turbidity (Parmelee 1954, Van Deventer and others 1966, 1971 and Valko 1970 and 1972). The measurements of the diffuse irradiance was limited to vertical surfaces because of the practical and experimental limitations which hinder a comprehensive study and the derivation of empirical expressions to evaluate the diffuse irradiance and illuminance on surfaces of different orientations and inclinations. Such limitations may be seen to arise from the following :

- (i) The limited range of the sun movement in every locality.
- (ii) The limited number of cases which are practically feasible to study, with regard to the ranges of orientations and inclinations of surfaces, where such study may require an elaborate experimental set-up, a considerable number of measuring equipments and an immense amount of data to be recorded and analysed.

- (iii) Diffuse radiation reflected by ground and adjacent surfaces which is difficult to isolate or evaluate as separate from the diffuse sky radiation.

4.5.2 It may be argued that the theoretical computation method using the luminance distribution functions would overcome the experimental limitation in determining the diffuse irradiance on any surface. These functions may be used to generate data and derive simple expressions to evaluate the diffuse irradiance and illuminance on surfaces of different orientations and inclinations.

4.5.3 It is necessary to establish first if the S.T.S. luminance distribution may be represented by the functional relationships of the luminance distribution of the clear sky. Accordingly, the turbidity of the S.T.S., linke turbidity factor T , was calculated for different solar altitudes, following the method given by Robinson (1966) and in the Annuals of the International Geophysical Year (1958). T was found to be between 2.8 and 3.6, with an average value $T = 3.3$. As $T < 5$, it seems reasonable then to adopt the relative luminance distribution of the clear sky for the S.T.S. which is represented by the following functions given by Kittler (1965, 1969), and recommended by the C.I.E. (1975).

$$L_p/L_z = f(\delta_p) \cdot f(\epsilon_p)/f(\epsilon_0) \cdot f(0)$$

For sky turbidity $T < 5$.

$$f(\delta_p) = 0.91 + 10.0 \cdot \exp(-3.0 \cdot \delta_p) + 0.45 \cdot \cos^2 \delta_p \quad \dots 3.24(a)$$

$$f(\epsilon_0) = 0.91 + 10.0 \cdot \exp(-3.0 \cdot \epsilon_0) + 0.45 \cdot \cos^2 \epsilon_0 \quad \dots 3.24(b)$$

$$f(\epsilon_p) = 1.0 - \exp(-0.32 \cdot \sec \epsilon_p) \quad \dots 3.24(c)$$

$$f(0) = 0.27385 \quad \dots 3.24(d)$$

4.5.4 Sky Component

The diffuse sky radiant energy received on surfaces with different orientations and inclinations is expressed as a proportion of the energy received on a horizontal surface from the whole unobstructed sky. It is presented as

$$R = I_{ds}/I_{dh} = E_{ds}/E_{dh}$$

To evaluate the proportion R over a wide range of a surface's orientations, inclinations, solar altitudes and azimuths, a computer program has been developed to double integrate the luminance distribution functions. The

limits of integration in every case are derived from the angular parameters of the surface shown earlier in Chapter II.

The ratio is expressed by the function of the form

$$E_{ds}/L_z = I_{ds}/I_z = \int_0^{2\pi} \int_{\gamma_s}^{\pi/2} [f(\delta_p) \cdot f(\epsilon_p)/f(\epsilon_0) \cdot f(0)] \cdot \cos \gamma_p \cdot \cos \theta_p \cdot d\gamma_p \cdot d\alpha_p + \int_{\alpha_s-90}^{90+\alpha_s} \int_0^{\alpha_s} [f(\delta_p) \cdot f(\epsilon_p)/f(\epsilon_0) \cdot f(0)] \cdot \cos \gamma_p \cdot \cos \theta_p \cdot d\gamma_p \cdot d\alpha_p \dots 3.25$$

The angle of incidence θ_p is evaluated from the geometry of the surface and an arbitrary sky element by the expression

$$\cos \theta_p = \sin \gamma_p \cdot \cos \gamma_s + \cos \gamma_p \cdot \sin \gamma_s \cdot \cos(\alpha_s - \alpha_p) \dots 3.26 (a)$$

δ_p is the angular distance between the sun and an elemental sky area and is given by the expression

$$\cos \delta_p = \sin \gamma_o \cdot \sin \gamma_p + \cos \gamma_o \cdot \cos \gamma_p \cdot \cos(\alpha_o - \alpha_p)$$

... 3.26(b)

The program gives the ratio E_{ds}/L_z for any surface with any orientation or inclination as well as for a horizontal surface. Accordingly, dividing the ratio for an inclined surface E_{ds}/L_z , by the ratio obtained for a horizontal surface E_{dh}/L_z , for the same solar altitude, the zenith luminance will disappear and the proportion R is obtained.

4.5.5 Values of R were calculated for a wide range of angular parameters :

- (i) Solar altitude from 5° to 90° at intervals of 15° .
- (ii) The inclination of a surface taken from 0° , for a horizontal surface, to 90° for a vertical surface, at intervals of 15° .
- (iii) The surface-solar azimuth taken from 0° , a surface directly facing the sun, to 180° , the sun behind the surface, at intervals of 15° .

4.5.6 The values of R calculated here are in good agreement

with values presented by Krochmann (1974)*.

Tables showing the calculated R values have been prepared for surfaces of different orientations and inclinations and various sun's location and are given in Appendix A.3.

4.5.7 Previous investigations by Van Deventer and others (1966, 1971) suggested that R varies with the cosine of the angle of incidence θ , for vertical surfaces. The investigation is extended here over a wide range of a surface's inclinations. When R is plotted against $\cos \theta$, the curves obtained reveal that every surface inclination gives a family of curves. Each curve in each family corresponds to a particular solar altitude where R varies with $\cos \theta$. These curves are shown here in Figures 3.7 to 3.12. For

* Krochmann, J. 'Personal correspondence'. Institut Fur Lichttechnik Der Technischen Universitat, Berlin : 1974.

The values of R were first prepared for this study prior to those presented by Krochmann. He used a different method. This was a step by step angle approach where the sky hemisphere is divided into angular cells. A similar method was used by Plant (1973). The difference between the two sets of R values, though insignificant is due mainly to the different numerical methods used. However, the computer program developed here is faster and more flexible in evaluating the sky component for any given sky area. This proved to be useful in evaluating the obstructed sky component for any obstructed sky area.

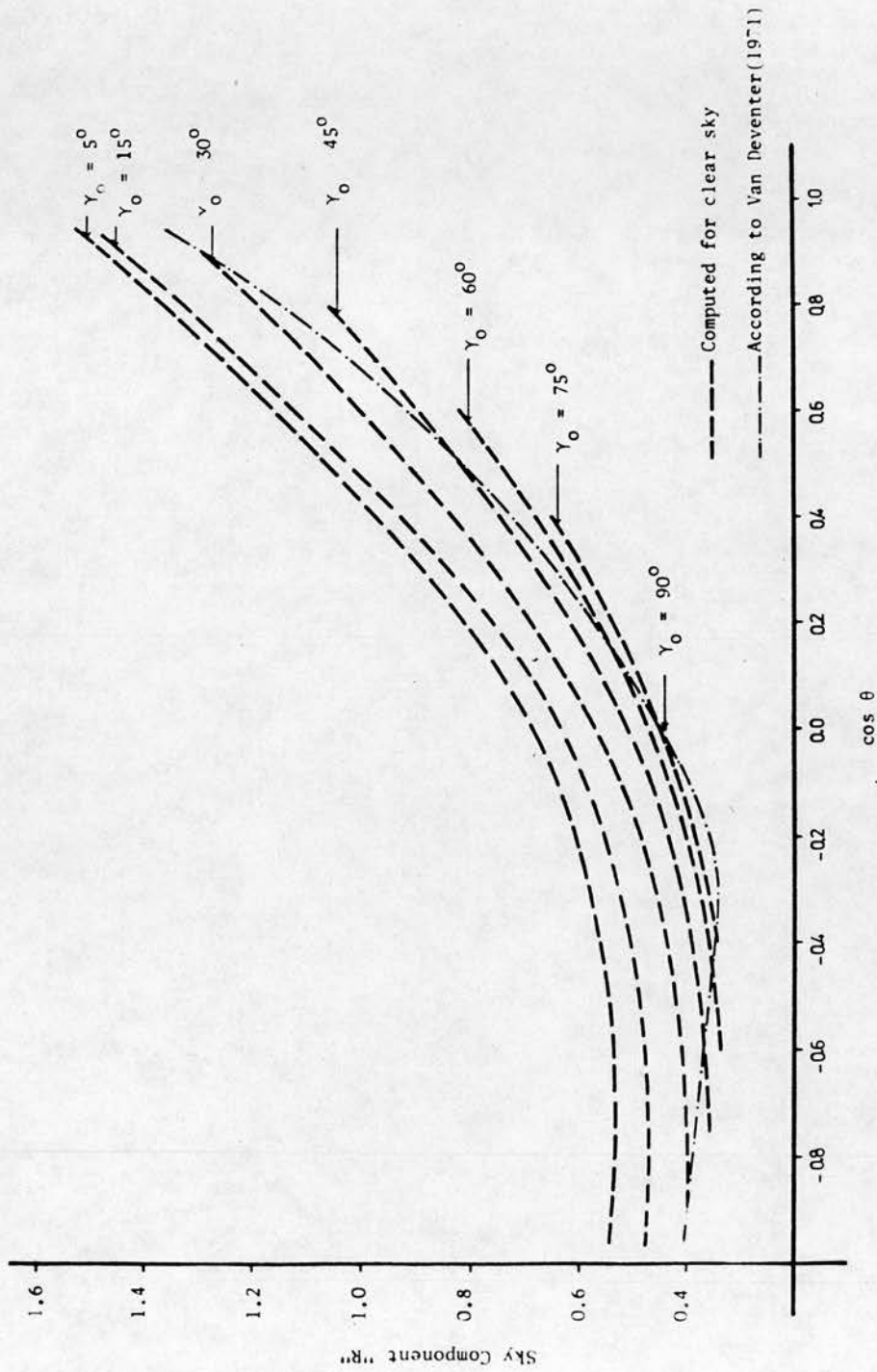


Figure 3.7 Variation of the Sky Component "R" with $\cos \theta$ for an Inclined Surface
 $\gamma_s = 90^\circ$ (Vertical Surface)

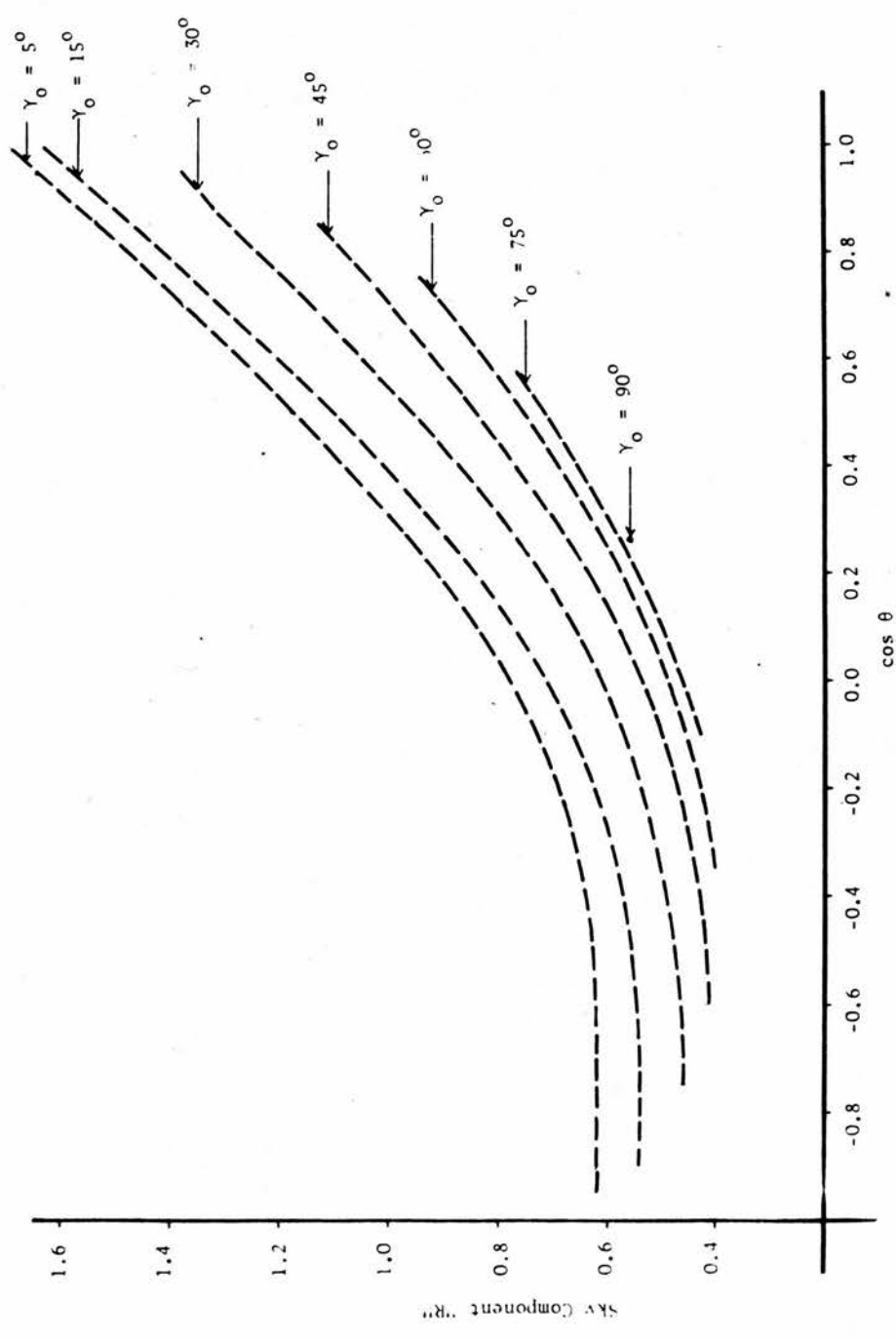


Figure 3.8 Variation of the Sky Component "R" with $\cos \theta$ for an Inclined Surface $\gamma_s = 75^\circ$

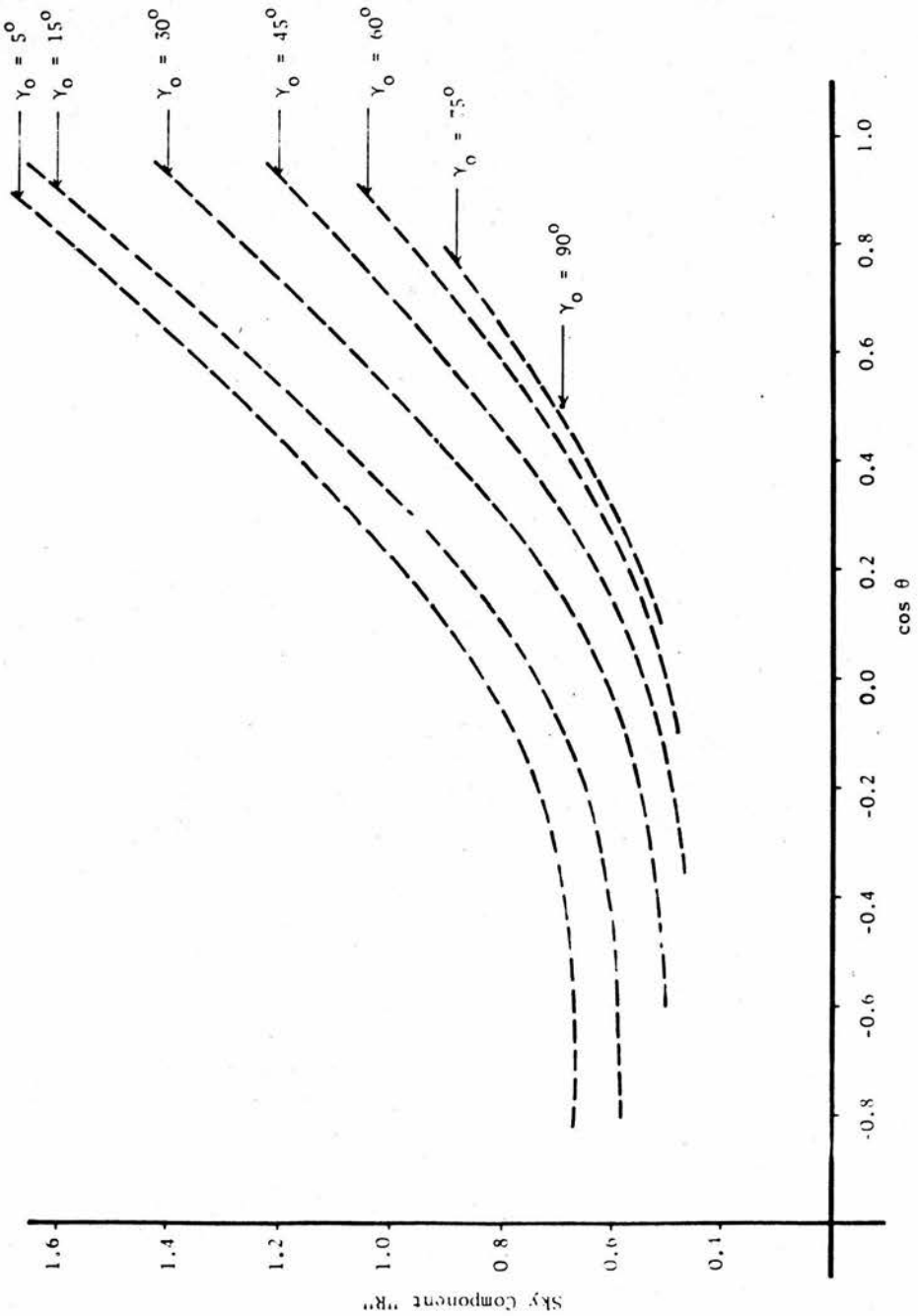


Figure 3.9 Variation of the Sky Component "R" with $\cos \theta$ for an Inclined Surface $\gamma_s = 60^\circ$

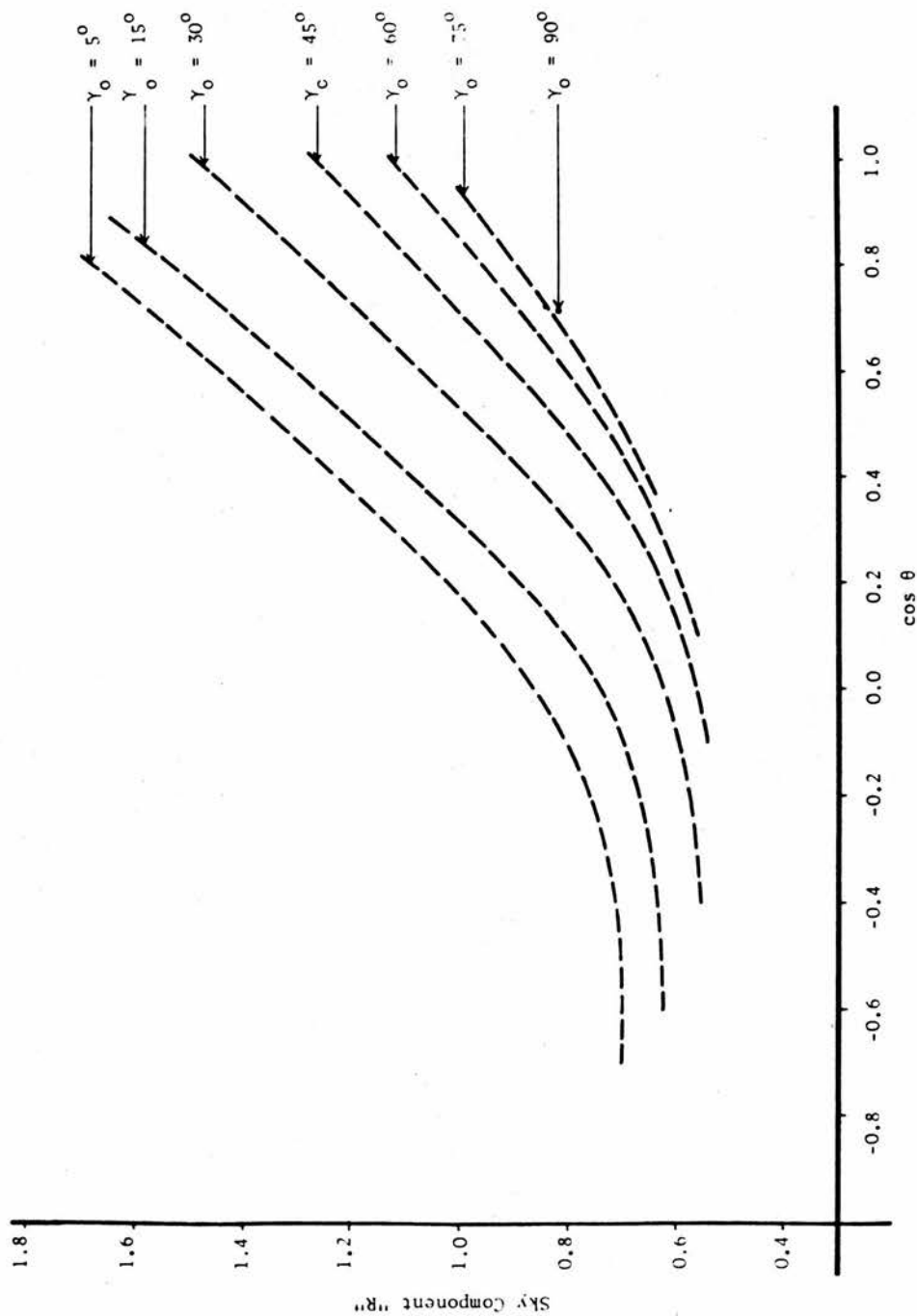


Figure 3.10 Variation of the Sky Component "R" with $\cos \theta$ for an Inclined Surface $\gamma_s = 45^\circ$

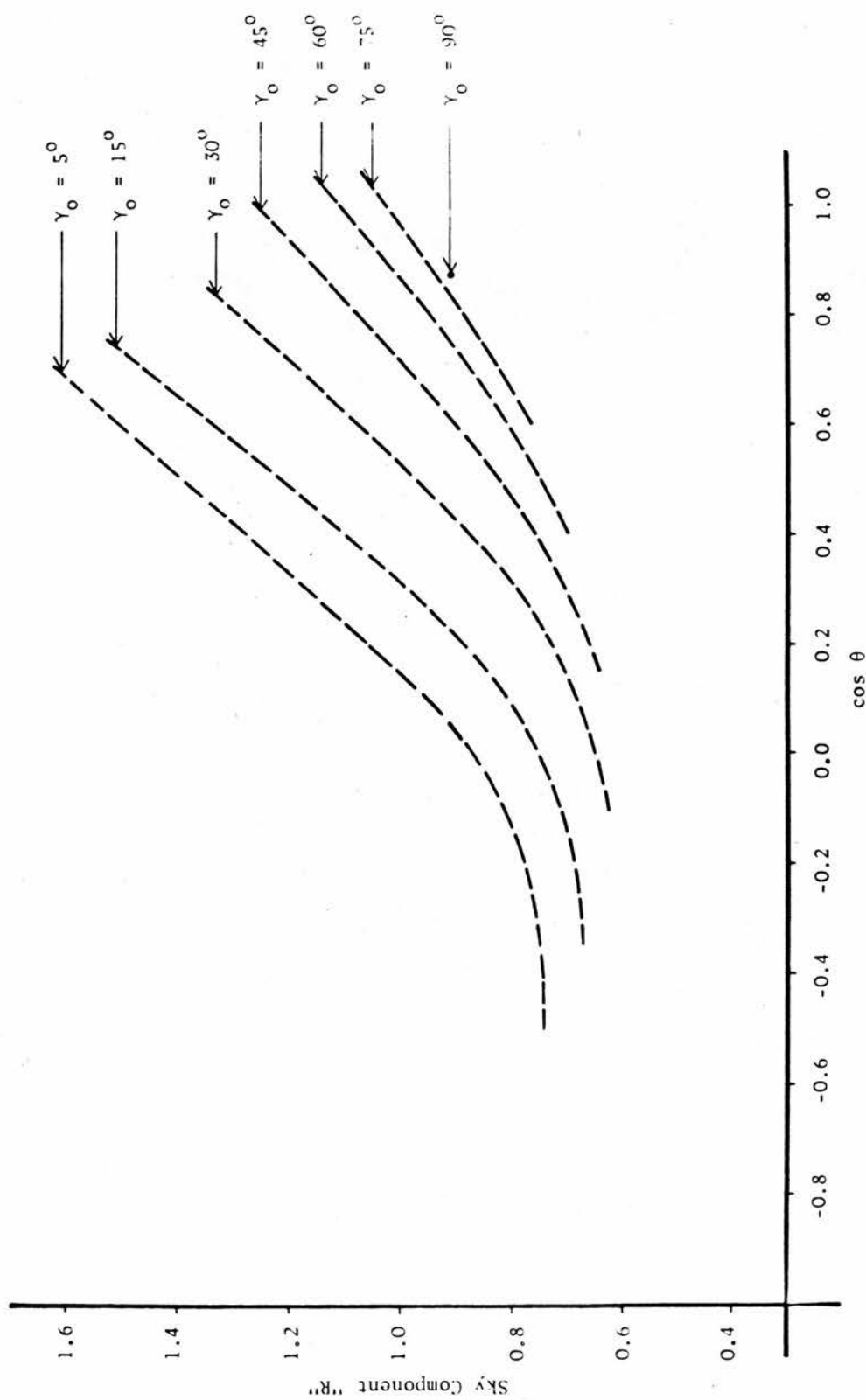


Figure 3.11 Variation of the Sky Component Ratio "R" with $\cos \theta$ for an Exposed Inclined Surface $\gamma_s = 30^\circ$

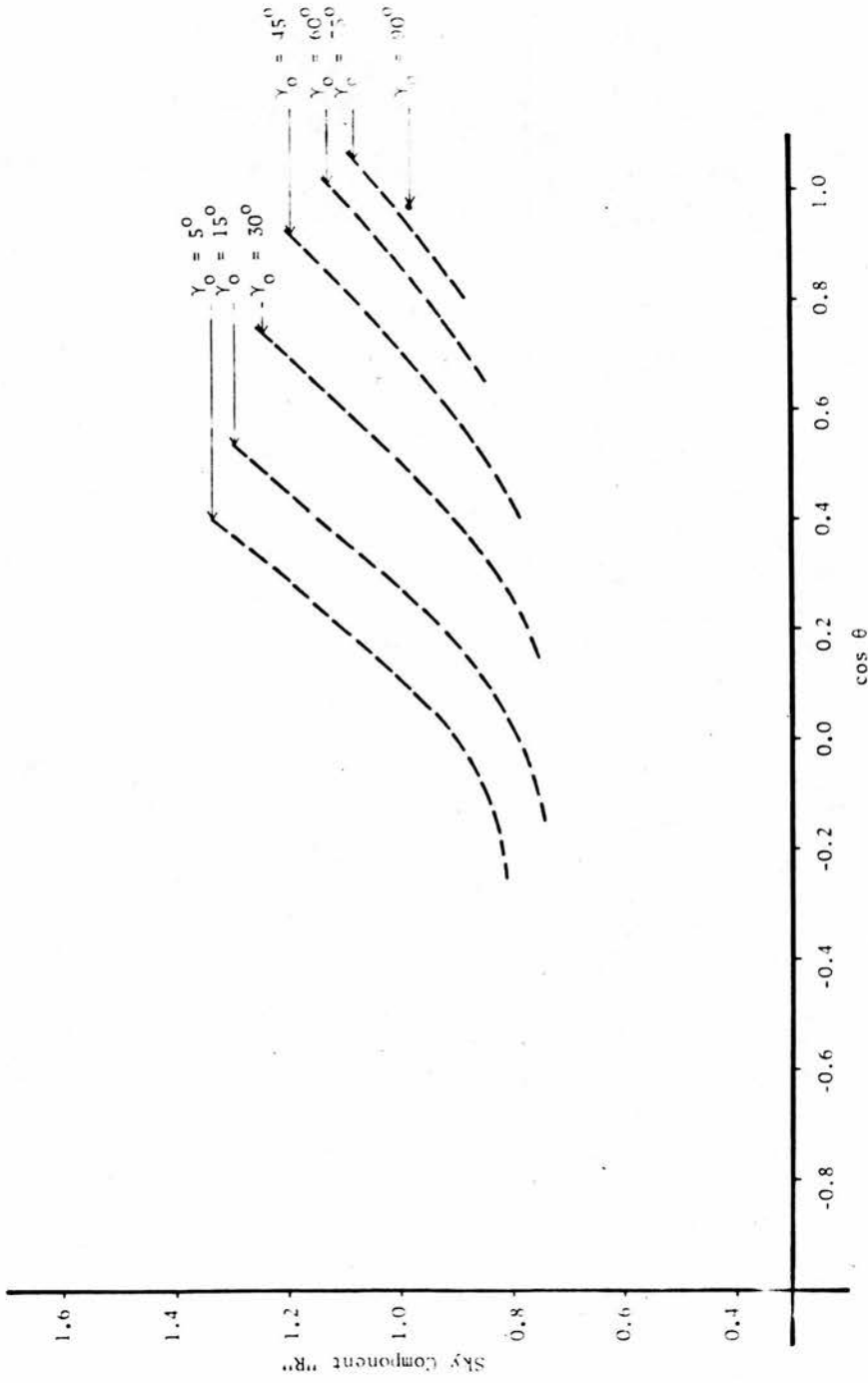


Figure 3.12 Variation of the Sky Component Ratio "R" with $\cos \theta$ for an Exposed Inclined Surface $\gamma_s = 15^\circ$

comparison, a curve for R, for a vertical surface, presented by Van Deventer et al in their papers of 1971 is also shown in Figure 3.7.

The curves in each family appear to be nearly parabolic functions of the form

$$R = A + B \cdot \cos \theta + C \cdot \cos^2 \theta \quad \dots 3.27$$

The constants A, B and C are functions of the solar altitude and surface inclination. This suggested that mathematical expressions may be derived to evaluate these constants A, B and C as functions of the solar altitude for every surface inclination. The expressions are derived here for a vertical surface $\gamma_s = 90^\circ$

$$A = 0.44 \cdot \exp(0.12 \cdot \cos \gamma_0) + 0.00023 \cdot \exp(6.8 \cdot \cos \gamma_0) \quad \dots 3.28(a)$$

$$B = 0.32 \cdot \exp(0.48 \cdot \cos \gamma_0) + 0.0074 \cdot \exp(-11.9 \cdot \cos \gamma_0) \quad \dots 3.28(b)$$

$$C = 0.18 \cdot \exp(0.73 \cdot \cos \gamma_0) + 0.028 \cdot \exp(-7.8 \cdot \cos \gamma_0) \quad \dots 3.28(c)$$

4.5.8 These functions are derived only for a vertical surface as the one most relevant in architectural investigations. It may be possible to derive similar expressions for inclined surfaces or perhaps general expressions which will take into account the angle of inclination. However, it does not seem that the general expressions would be simple or easy to use. From the tables presented for R an interpolation may be used to find the R value for any inclined surface.

4.5 Zenith Luminance and Intensity

4.5.1 The ratio of horizontal illuminance to zenith luminance may be obtained by integrating the luminance distribution function over the whole sky dome, for any solar altitude. It is presented as

$$E_{dh}/L_z = I_{dh}/I_z = \int_0^{2\pi} \int_0^{\pi/2} [f(\delta_p) \cdot f(\epsilon_p)/f(\epsilon_0) \cdot f(0)] \cdot \cos \gamma_p \cdot \cos \theta_p \cdot d\gamma_p \cdot d\alpha_p \quad \dots 3.29$$

These ratios were obtained for a number of solar altitudes, $5^\circ - 90^\circ$, with the computer program. A mathematical expression is derived which gives the ratio of the zenith luminance to the horizontal illuminance as a function of the solar altitude as

$$I_z/I_{dh} = L_z/E_{dh} = 0.01 \cdot \exp(2.90 \cdot \gamma_0) + 0.13 \cdot \exp(-0.23 \cdot \gamma_0) \quad \dots 3.30(a)$$

where γ_0 is in radians.

An alternative expression for the ratio I_{dh}/I_z was derived as

$$I_{dh}/I_z = 6.8 + 4.2 \cdot \sin \gamma_0 - 9.8 \cdot \sin^2 \gamma_0 \quad \dots 3.30(b)$$

The above function may also be used with equation 3.25 to evaluate the sky component R or the obstructed sky component R_{ob} . The zenith intensity or luminance are readily obtained then from horizontal values of illuminance and irradiance. Values for the zenith luminance were calculated for the S.T.S. and presented in Appendix A.2.

5. THE EVALUATION OF THE SHADED DIRECTED AND THE OBSTRUCTED DIFFUSE SKY RADIATION

5.1 Formulation of Shadow Geometry

5.1.1 The basic formulation of shadow geometry may be presented by an equation of a line joining a point P in space, whose coordinates are (X_p, Y_p, Z_p) , and its point image P_s , whose coordinates are (X_s, Y_s, Z_s) , which is projected along the solar rays as illustrated in Figure 3.13. It can be proven that any two coordinates of the shadow point may be expressed by functions in terms of the third coordinate, the coordinates of the point caster and the sun geometry. An example of this may be given by expressing the X_s and Y_s coordinates of the shadow point in terms of its Z_s coordinate, with the orientation angles expressed with reference to the y-axis.

$$X_s = X_p - [(Z_p - Z_s) \cdot \sin(\alpha_s - \alpha_0) / \tan \gamma_0] \quad \dots \quad 3.31(a)$$

$$Y_s = Y_p - [(Z_p - Z_s) \cdot \cos(\alpha_s - \alpha_0) / \tan \gamma_0] \quad \dots \quad 3.31(b)$$

For a horizontal surface α_s is taken as 90° .

Similar expressions can be derived for functions in terms of X_s and Y_s . The expressions for the coordinates of the shadow point are then derived from the plane equation of a surface on which the shadow is cast. The shaded surface may be a planar or a non-planar surface. Taking a planar surface having an equation of the form

$$A \cdot X + B \cdot Y + C \cdot Z + D = 0 \quad \dots 3.32$$

the following equations are derived.

$$X_S = \frac{[X_p(B \cdot \cos(\alpha_S - \alpha_0) + C \cdot \tan \gamma_0) - \sin(\alpha_S - \alpha_0)(B \cdot Y_p + C \cdot Z + D)]}{[A \cdot \sin(\alpha_S - \alpha_0) + B \cdot \cos(\alpha_S - \alpha_0) + C \cdot \tan \gamma_0]} \quad \dots 3.33(a)$$

$$Y_S = \frac{[Y_p(A \cdot \sin(\alpha_S - \alpha_0) + C \cdot \tan \gamma_0) - \cos(\alpha_S - \alpha_0)(A \cdot X_p + C \cdot Z + D)]}{[A \cdot \sin(\alpha_S - \alpha_0) + B \cdot \cos(\alpha_S - \alpha_0) + C \cdot \tan \gamma_0]} \quad \dots 3.33(b)$$

$$Z_S = \frac{[Z_p(A \cdot \sin(\alpha_S - \alpha_0) + B \cdot \cos(\alpha_S - \alpha_0) - \tan \gamma_0(A \cdot X_p + B \cdot Y_p + D)]}{[A \cdot \sin(\alpha_S - \alpha_0) + B \cdot \cos(\alpha_S - \alpha_0) + C \cdot \tan \gamma_0]} \quad \dots 3.33(c)$$

A, B, C and D are the coefficients of the plane equation.

For non-planar surfaces similar expressions can be derived by substituting equations 3.31 (a) and (b) in the equation of the plane.

5.1.2 An equation for a planar surface, the coordinates of whose

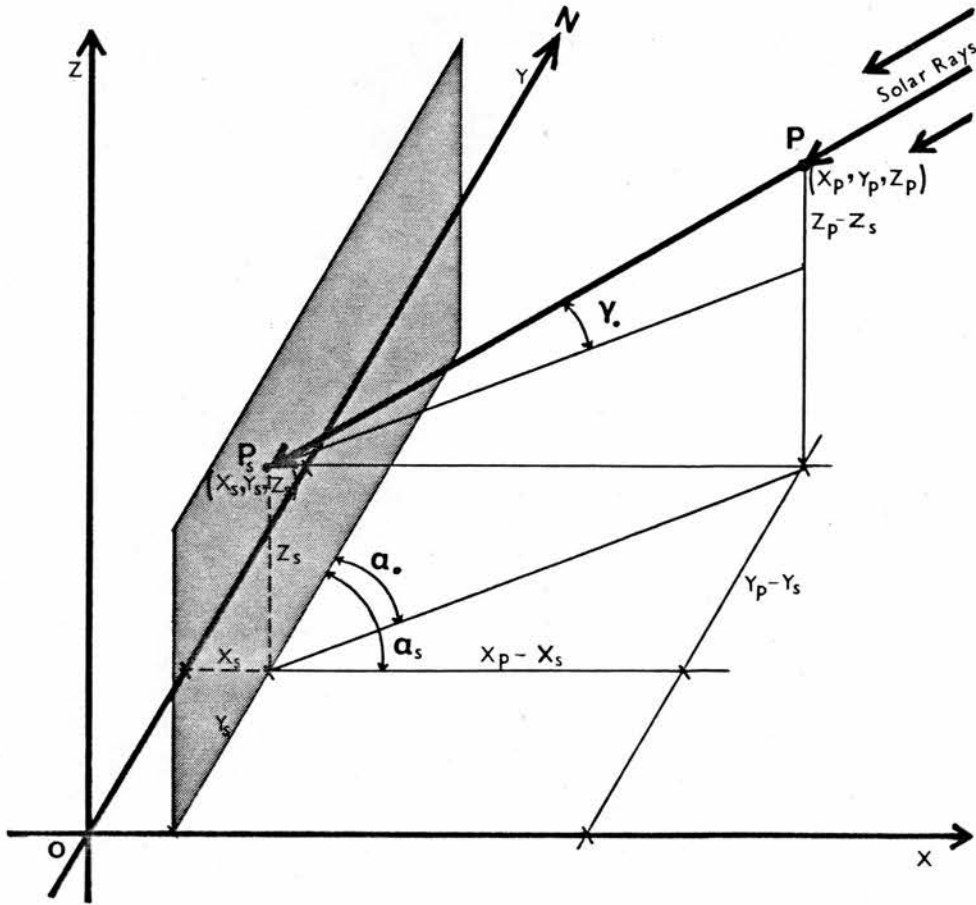


Figure 3.13 The Geometry of the Point Shadow

contour points are known, is easily derived by the point plane formulae. Three contour points are used to give the determinant :

$$\begin{vmatrix} X & Y & Z & 1 \\ X_1 & Y_1 & Z_1 & 1 \\ X_2 & Y_2 & Z_2 & 1 \\ X_3 & Y_3 & Z_3 & 1 \end{vmatrix} = 0$$

The coefficients of the plane equation are obtained by solving the minors,

$$A = \begin{vmatrix} Y_1 & Z_1 & 1 \\ Y_2 & Z_2 & 1 \\ Y_3 & Z_3 & 1 \end{vmatrix} \quad B = - \begin{vmatrix} X_1 & Z_1 & 1 \\ X_2 & Z_2 & 1 \\ X_3 & Z_3 & 1 \end{vmatrix}$$

$$C = \begin{vmatrix} X_1 & Y_1 & 1 \\ X_2 & Y_2 & 1 \\ X_3 & Y_3 & 1 \end{vmatrix} \quad \text{and} \quad D = - \begin{vmatrix} X_1 & Y_1 & Z_1 \\ X_2 & Y_2 & Z_2 \\ X_3 & Y_3 & Z_3 \end{vmatrix}$$

5.1.3 The shadow cast on a given finite surface is established by projecting onto its plane the contour points of a casting surface using the above equations. The contour points and coordinates of the shadow profile formed on the surface may then be defined and its area easily evaluated.

When the shadow on a surface is cast by more than one surface two forms of shadow profiles may be expected. These are :

- (i) The shadows are overlapping. In this case the most outer boundary of the shadow silhouette defines its profile.
- (ii) The shadows are not overlapping and hence they appear as individual patches on different parts of the surface.

5.1.4 Utilizing the expressions presented above a computer program has been developed to define the profile of the shadow cast on any planar surface by any object, which has a continuous contour formed by a series of straight line segments, obstructing the direct solar rays. The program is also capable of evaluating the shadow on non-planar surfaces whose plane equations are specified. The program defines the coordinates of the shadow contour points and evaluates its area. The shadow factor is established in order to determine the magnitude of total direct irradiance being obstructed.

5.1.5 The shadow height cast on a vertical facade of infinite length by its opposing may be determined by the expression

$$h_s = h_2 - D \cdot \tan \gamma_0 / \cos(\alpha_0 - \alpha_s) \quad \dots 3.34(a)$$

The shadow factor may then be expressed as

$$SF = [h_2 - D \cdot \tan \gamma_0 / \cos(\alpha_0 - \alpha_s)] / h_1 \quad \dots 3.34(b)$$

where h_1 and h_2 are the heights of the vertical and opposing facades respectively and D their distance apart.

5.2 The Obstructed Sky Component and Radiation

5.2.1 The portion of the sky radiation being obstructed or received on a surface from a partially obstructed sky is not uniformly distributed over the surface. However, mean values for the diffuse irradiance being obstructed or received and averaged throughout the surface may be used (Norden 1948). This will simplify the calculations dealing with the diffuse radiation. The average diffuse irradiance being obstructed and received may then be expressed as fractions of the horizontal diffuse irradiance, from the whole sky dome, by the obstructed sky component and exposed sky component respectively. These components are evaluated in a similar manner to the sky component of a surface fully exposed to the sky, using the relative luminance distribution function. The interrelations between these components is shown by equation 2.19, given earlier in Chapter II,

$$R = R_{ob} + R_s$$

5.2.2 To establish the average for the obstructed sky component requires a lengthy procedure which may involve a substantial amount of computation. This computation involves integrating the sky luminance distribution function to obtain the ratios of the obstructed irradiance to the zenith intensity for the individual points across the surface. A simple procedure may be adopted by selecting an appropriate reference point on the surface at which the obstructed component may be regarded as a typical average value (Hopkinson 1966). This

is illustrated by the diagram of Figure 3.14.

- (i) The reference point is located at the centre point of a vertical facade when its opposing facade is higher. When the opposing facade is shorter, the reference point is located at a height h_r which is below the level of the opposing facade. The height is determined by the expression

$$h_r = h_1 \cdot h_2 / h_2 + h_1 \quad \dots 3.35(a)$$

- (ii) On ground the reference point is taken at the centre when the two vertical facades are of equal height. When the two facades are not of equal height, it is located at a distance D_r from the higher facade which is determined by the expression

$$D_r = D \cdot h_2 / h_2 + h_1 \quad \dots 3.35(b)$$

Hence, one set of calculations may then be performed to obtain the obstructed and exposed sky components for the reference point.

5.2.3 The obstruction may have an irregular sky line as it may be caused by a number of neighbouring buildings or sloped, curved and irregular surfaces. It is suggested here that these obstructions are aggregated and treated as a

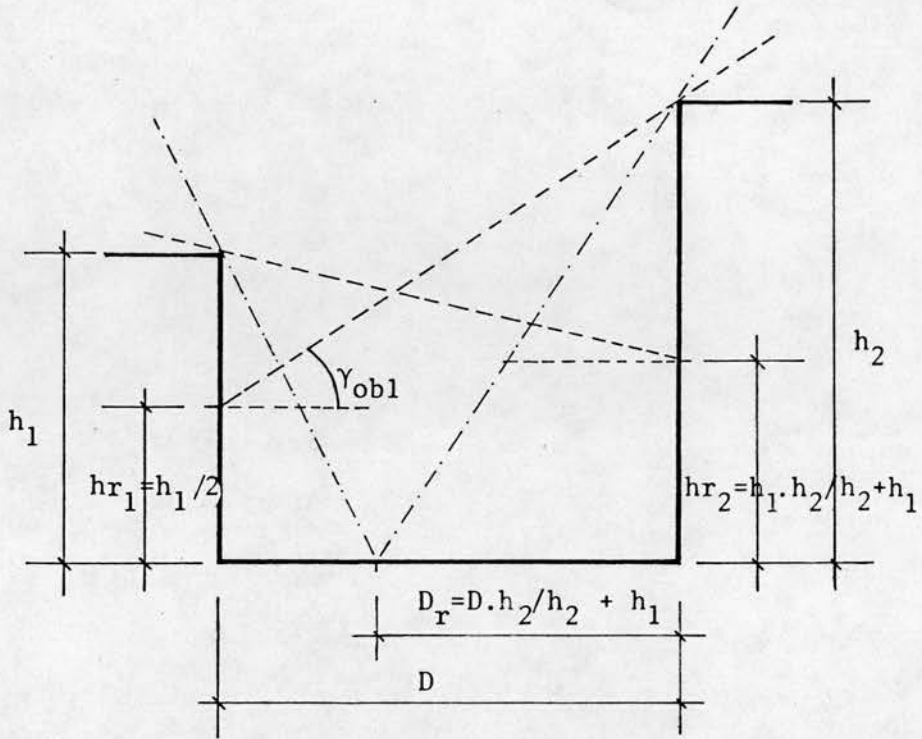


Figure 3.14 Location of Reference Point for the Calculation of the Sky Component

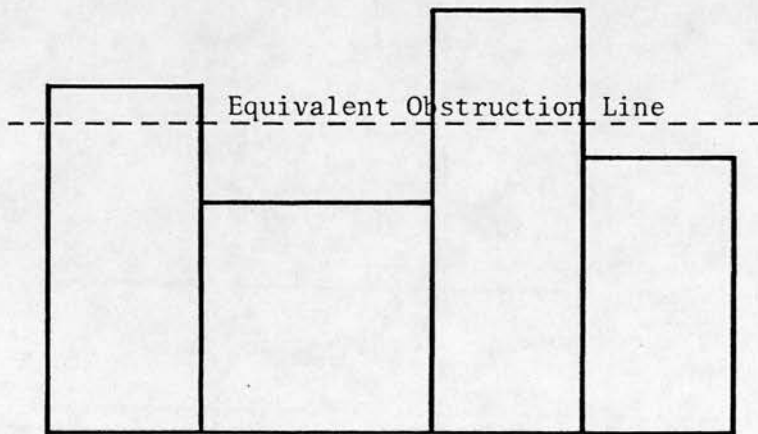


Figure 3.15 Equivalent Obstruction Line (Hopkinson 1966)

single obstruction. This is an established procedure employed in the calculation of the externally reflected component of the day light factor, where an equivalent obstruction line is used as a means of representing the irregular sky line as shown in Figure 3.15 (Hopkinson 1966). Since the luminance distributions of the overcast and clear skies are very much different one had to be very careful in adopting such procedures employed in the calculation with the overcast skies. However, the use of the 'equivalent obstruction line' with clear skies may be justified for practical reasons as follows :

- (i) The luminance distribution of the clear sky may not vary significantly across a small patch of the sky area.
- (ii) It greatly simplifies the complex calculations of the obstructed or received diffuse irradiance and avoids unnecessary difficulties in evaluating them.

5.2.4 Alternatively, the obstructed sky components may be evaluated separately for each of the different patches of obstruction.

5.2.5 The program compiled to double integrate the sky luminance distribution function is also used to evaluate the obstructed sky component. The limits of integration specified define

the obstructed sky area as viewed from the reference point. The azimuthal and elevation angles are determined from the geometry of the obstruction, the location of the reference point and the distance apart. To evaluate these angles it may be simpler in some cases to project the obstructing surface onto a plane parallel to the obstructed surface. The angles are to be determined prior to the input stage for the program. As explained in Figure 2.8(c) in Chapter II, these angles are determined in the following manner:

(a) The elevation angles of obstruction

The horizon is taken to be on the same horizontal level with the reference point and hence the lower elevation angle limit is equal to zero. The upper elevation angle limit is formed between the line joining the reference point and the equivalent obstruction line PD and the normal passing through the reference point PB. The elevation angle is then given by the expression

$$\gamma_{ob} = \text{Arc tan } (Z_m - Z_r) / (X_m - X_r) \quad \dots 3.36(a)$$

(b) The azimuthal angles of obstruction

The angular width of the obstruction, on the horizontal plane passing through the reference point, is given by the angle α_{ob} subtended at the reference point by the lines

PA and PC, joining the reference point to the boundary of the obstruction. α_{ob} may be evaluated from the angles α_1 and α_2 which are measured to one side of the normal to the obstruction which is passing through the reference point.

$$\alpha_{ob} = \alpha_2 - \alpha_1 \quad \dots 3.36(b)$$

where α_1 and α_2 are evaluated by the expression

$$\alpha_1 = \text{Arc tan } (Y_r - Y_1)/(X_1 - X_r) \quad \dots 3.37(a)$$

$$\alpha_2 = \text{Arc tan } (Y_r - Y_2)/(X_2 - X_r) \quad \dots 3.37(b)$$

To simplify the calculation and utilize the symmetry of the sky luminance pattern with regard to the sun's meridian, the azimuthal angles of the obstruction may be expressed relative to :

- (i) The sun's position, when evaluating R_{ob} for a horizontal surface, in terms of the angular width and orientation of the obstruction by

$$\alpha_{ob1} = \alpha_{s2} + \alpha_1 - \alpha_0 - 180^\circ \quad \dots 3.38(a)$$

$$\alpha_{ob2} = \alpha_{s2} + \alpha_2 - \alpha_0 - 180^\circ \quad \dots 3.38(b)$$

- (ii) The plane of the obstructed surface, when evaluating R_{ob} for a vertical or an inclined surface, in terms of the orientation of the obstructed and obstructing surfaces α_{s1} and α_{s2} ,

$$\alpha_{ob1} = \alpha_{s2} - \alpha_{s1} + \alpha_1 - 90^\circ \quad \dots 3.39(a)$$

$$\alpha_{ob2} = \alpha_{s2} - \alpha_{s1} + \alpha_2 - 90^\circ \quad \dots 3.39(b)$$

5.2.6 The program first evaluates the integral function for the given limits, azimuthal and elevation angles of the obstructed sky area, giving the ratio of the obstructed diffuse irradiance to the zenith intensity I_{ob}/I_z . The obstructed sky component, the ratio of average diffuse irradiance being obstructed to the horizontal diffuse irradiance, is then easily obtained. Simplified tables for the obstructed sky component for vertical and horizontal surfaces are prepared here for various combinations of angular parameters of the sun, the surface and the obstructed sky areas. These are presented in Appendix A.3.

5.3 The Initial Irradiance Model

5.3.1 It is possible to construct a mathematical model which evaluates the initial irradiance on horizontal and inclined surfaces from the expressions of the direct, normal, diffuse horizontal irradiance, the sky component, obstructed sky component, and the shadow area. A flow diagram of the model is shown in Figure 3.16.

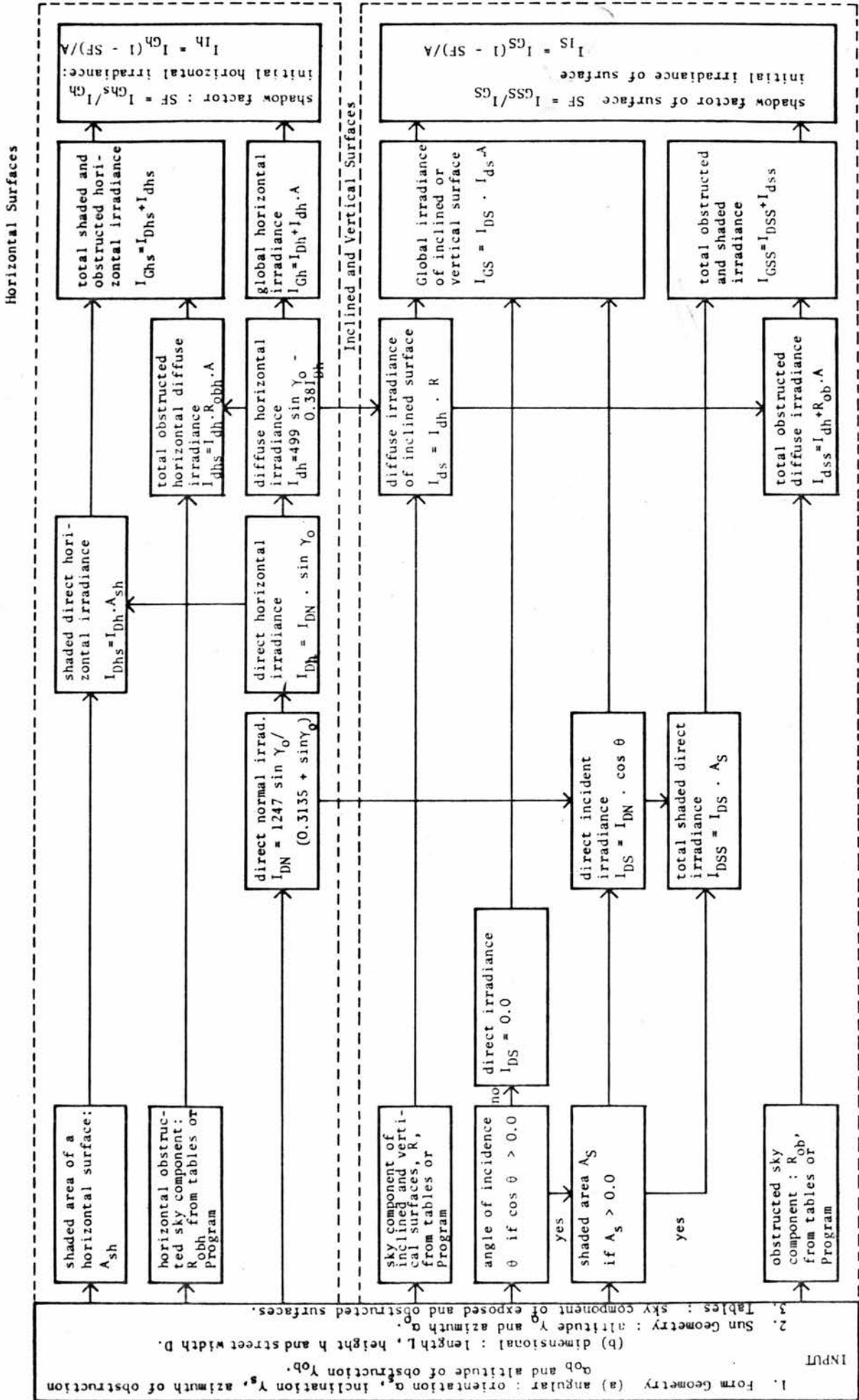


Figure 3.16 Flow diagram for a model to evaluate the initial irradiance of a surface

6. THE BUILDING DESCRIPTION

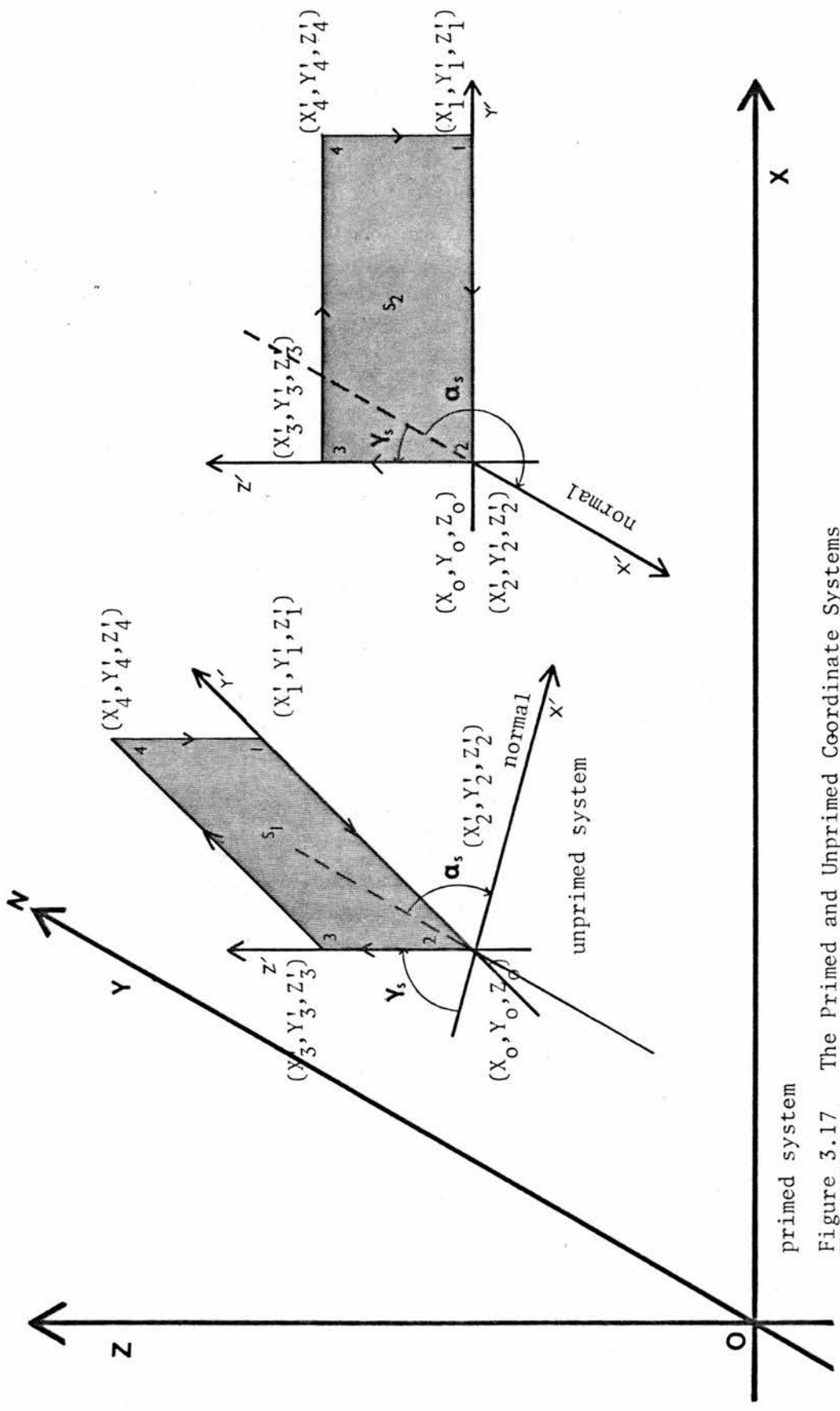
6.0.1 It is of primary importance in constructing a computer mathematical model for the interactions of solar radiation and buildings to devise the means by which the building description is translated to the 'working core' of the model in order to perform the necessary mathematical operations. Such means should also provide easy collection and entry of the building data.

6.1 Geometrical Description of the Built Form

6.1.1 The three-dimensional coordinate system has always been conveniently used for the basic geometrical description of buildings (Toups 1965, O'Brien 1967, Hawkes and Stibbs 1970). This allows the form to be defined by units of planar surfaces, which may be rectangular or polygonal, or perhaps non-planar surfaces. The model of the geometrical form is then defined in terms of the rectangular coordinate system. Each surface of the form is defined by its contour points and their coordinates specified by the (X,Y,Z) format. To simplify the entry of data when the surfaces may appear in skewed relative positions a prime and unprimed coordinate system may be used as illustrated by the diagram in Figure 3.17.

- (i) In the unprimed system each surface is defined in terms of a local rectangular coordinate system with a convenient local origin. The surface is located in the $Y'-Z'$ plane with its normal parallel to the X' -axis, as shown by Figure 3.17. Although the surfaces may be specified by their lengths and heights or in terms of the ratios of length to height, the coordinates (X',Y',Z') of their unprimed points may be easily established.
- (ii) The prime coordinate system refers to the basic rectangular coordinate system reference to which the coordinates of all the points of the surfaces are finally expressed. The north point is chosen arbitrary along its Y -axis. Each surface is defined by, as shown by Figure 3.17,
- (a) a local origin with respect to the prime system (X_0, Y_0, Z_0) ;
 - (b) its azimuth angle α_s , which its normal makes with the north direction; and
 - (c) its altitude angle ϵ_s , which its normal makes with the horizon. The inclination angle of the surface $\gamma_s = 90 - \epsilon_s$.

6.1.2 By a primary transformation the unprimed coordinates of



primed system

Figure 3.17 The Primed and Unprimed Coordinate Systems

points of the surfaces are transformed to prime coordinates using the angular parameters of the surfaces. The directional cosines for the unprimed axes of a surface relative to the axes of the prime system are given by the matrix

	X	Y	Z
X'	$\sin \alpha_S \cdot \sin \gamma_S$	$\cos \alpha_S \cdot \sin \gamma_S$	$\cos \gamma_S$
Y'	$-\cos \alpha_S$	$\sin \alpha_S$	0
Z'	$-\sin \alpha_S \cdot \cos \gamma_S$	$-\cos \gamma_S \cdot \cos \alpha_S$	$\sin \gamma_S$

From this the primed coordinates of a point on the surface are derived by the expressions

$$X = X_0 + X' \cdot \sin \alpha_S \cdot \sin \gamma_S - Y' \cdot \cos \alpha_S - Z' \sin \alpha_S \cdot \cos \gamma_S \quad \dots 3.40(a)$$

$$Y = Y_0 + X' \cdot \cos \alpha_S \cdot \sin \gamma_S + Y' \cdot \sin \alpha_S - Z' \cdot \cos \alpha_S \cdot \cos \gamma_S \quad \dots 3.40(b)$$

$$Z = Z_0 + X' \cdot \cos \gamma_S + Z' \cdot \sin \gamma_S \quad \dots 3.40(c)$$

6.1.3 To decide on the geometrical parameters of the surfaces defining the form, the boundary of each of the surfaces has to be established. The part of the geometrical form which may be regarded as a separate surface element is distinguished by the following characteristics :

- (i) all parts of the surface being on the same plane;
- (ii) all parts of the surface having the same physical properties, especially the reflectivity for solar radiation;
- (iii) the surface having a continuously connector contour;
and
- (iv) the surface having a regular shape.

These points are illustrated in Figure 3.18.

6.1.4 This method is used to develop a computer program which carries the transformation of the coordinates of the contour points of the surface, entered in the unprimed format, to the required primed format. The data prepared for each surface should specify its azimuth angle, inclination angle, coordinates of local origin, number of contour points and their unprimed coordinates.

6.2 The Physical Parameters of the Built Form

6.2.1 The only physical property required for each surface of the form is its reflectivity for solar radiation. Each surface is represented by a distinct value of reflectivity which is entered together with its geometrical data.

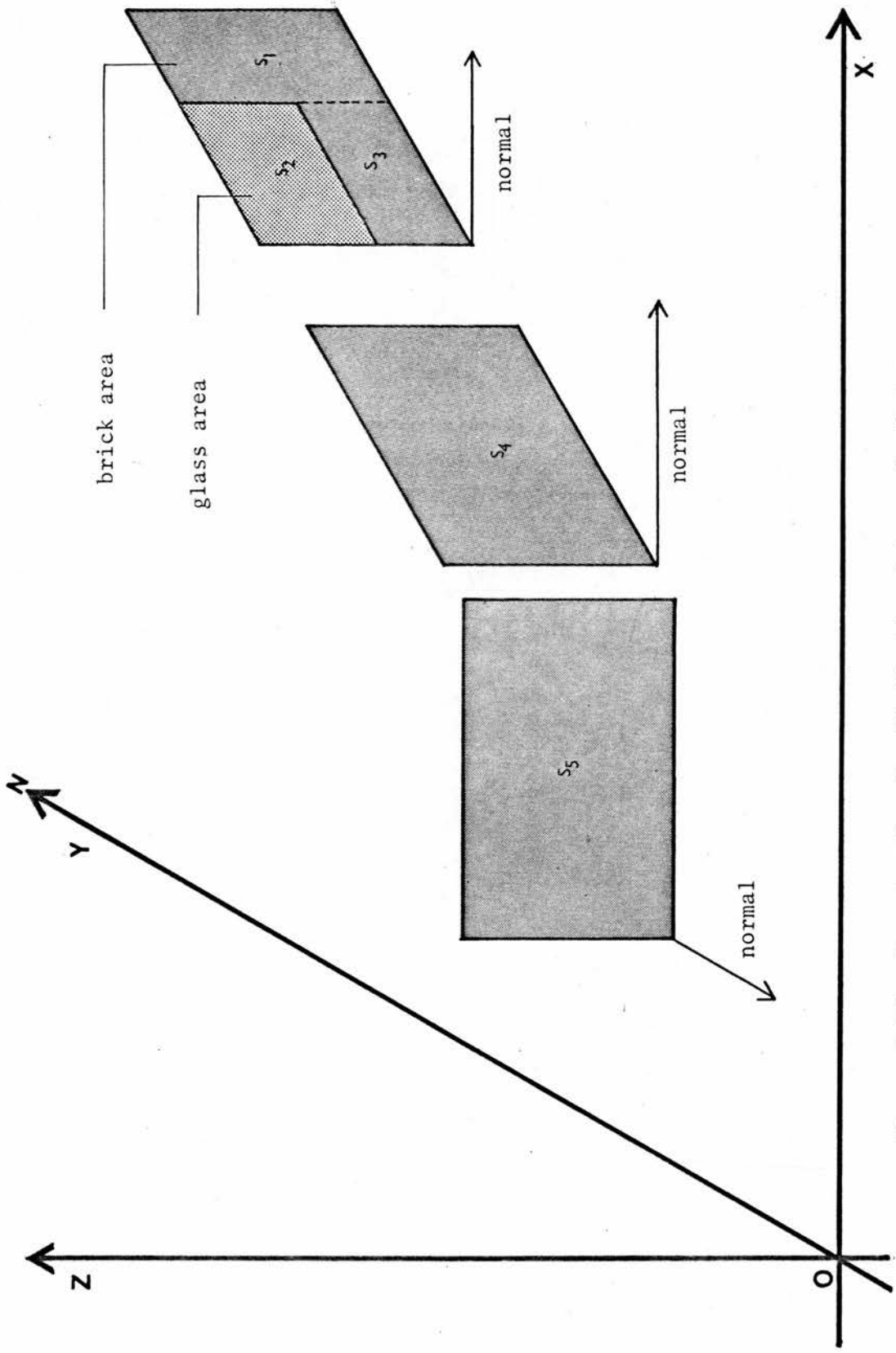


Figure 3.18 Geometry for the Distinction Between Surfaces

7. THE EVALUATION OF THE FORM FACTORS

7.0.1 The calculation of the configuration and form factors involves the evaluation of area integrals which may require double and quadruple integration. In practice this was found to be quite difficult even for simple geometries. Different techniques have previously been employed to obtain solutions and to prepare tables and charts for the configuration and form factors for a restricted geometrical configuration of surfaces and thus serve a limited purpose (Hamilton and Morgan 1952, McGuire 1962, Weibelt 1966, Billington 1967 and O'Brien 1967).

7.0.2 The use of vector analysis and Stokes' theorem have been shown to provide a simple representation for the configuration and the form factors (Moon 1961, Sparrow 1963, Toups 1965 and Hottel 1967). This simplifies the numerical evaluation of the integrals and is ideally suited to digital computer application.

7.1 Formulation of the Configuration and Form Factors for Finite Surfaces

7.1.1 In his paper of 1963, Sparrow was able to derive simple formulations for the configuration and the form factors using the contour integration method which

involves the use of Stokes' theorem to reduce the order of the integrands. He formulated a single line integral for the configuration factor which may be written as

$$\begin{aligned}
 F_{dA_1, A_2} = L_1 \oint_C & \frac{(Z_2 - Z_1)dy_2 - (Y_2 - Y_1)dZ_2}{2\pi r^2} \\
 & + m_1 \oint_C \frac{(X_2 - X_1)dZ_2 - (Z_2 - Z_1)dX_2}{2\pi r^2} \\
 & + n_1 \oint_C \frac{(Y_2 - Y_1)dX_2 - (X_2 - X_1)dY_2}{2\pi r^2}
 \end{aligned}$$

... 3.41

where the coordinates X_1 , Y_1 and Z_1 represent the location of an infinitesimal area dA_1 and L_1 , m_1 and n_1 are its directional cosines. r is the line connecting dA_1 and any point (X_2, Y_2, Z_2) on the contour of a finite surface A_2 . It is given by the function

$$r^2 = (X_2 - X_1)^2 + (Y_2 - Y_1)^2 + (Z_2 - Z_1)^2 \quad \dots 3.42$$

7.1.2 On the basis of his configuration factor

formulation, Sparrow was also able to derive a new representation for the form factor which reduces the

four-dimensional area integral to a two-dimensional contour integration. This is given by the expression

$$F_{A1,A2} = \frac{1}{2\pi A_1} \oint_{c1} \oint_{c2} \ln r \, dX_1 \cdot dX_2 + \ln r \, dY_1 \cdot dY_2 \\ + \ln r \, dZ_1 \cdot dZ_2$$

... 3.43

The simplicity and repetitive form of this function, with regard to its three terms, where each relates to a coordinate axis, makes the numerical solution of it practicable with the computer.

7.1.3 Based on this method a computer program has been developed which evaluates the form factor of two finite surfaces.

7.1.4 A difficulty with the numerical evaluation of the form factor function, equation 3.43, arises when the two surfaces have a common edge as shown by Figure 3.19.

From equation 3.43, r takes the value of zero along the side AD and $\log r$ tends to ∞ thus giving serious difficulties with the computer calculation. However, such difficulties can be avoided by separating the two

surfaces by a small distance dL as shown by Figure 3.19. A good approximation of the form factor is established when dL is about 1.0 percent of length of the side L of A_1 . Alternatively, r may be taken as equal to dW , the interval width of the common side AD , at the points where r is equal to zero.

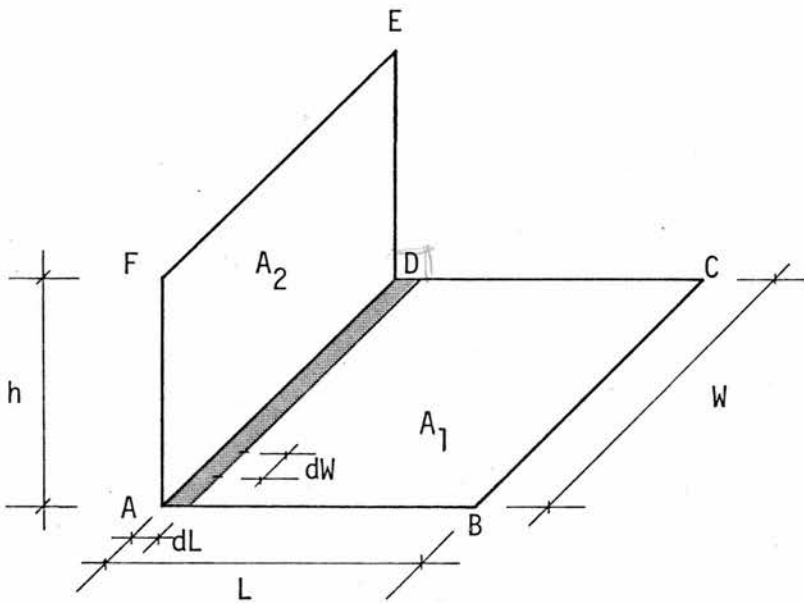


Figure 3.19 Two Surfaces with Common Edge

7.1.5 An alternative solution was established with the assistance of Dr. T. Gilbert of the Department of Applied Mathematics of Edinburgh University. In this approach the analytical solution of the contour integration along the common line AD was established as

$$\frac{1}{2\pi A_1} \oint_{c1} \oint_{c2} \ln r dx_1 \cdot dx_2 = \frac{3/2 W^2 - W^2 \ln W}{2\pi A_1} \dots 3.44$$

where W is the length of the common side.

7.1.6 The form factor program offers the advantages of simplicity of data entry, speed and economy of operation. It is also flexible in that it can be used either as an integrated part of a computer model to study the irradiance transfer problems conducted in this study or separately to compile and tabulate form factors for geometrical forms not yet tabulated. As an example of this, tables of form factors for a number of geometrical forms, which have been determined during this study, are presented in Appendix A.5.

7.1.7 Using flux algebra the form factors for complex geometrical forms, eg, the form factor from a plane polygon to a polyhedron, may be obtained from the form factors of simple finite planes as shown in Appendix A.5.

7.1.8 It should be noted here that a general purpose computer program for the numerical evaluation of the configuration and the form factors was developed by Toups (1965). The program calculates the configuration factor by a numerical method based on the double projection principle for a unit sphere and vector algebra. A surface A_1 is taken on the X-Y plane and divided into small subelements. The configuration factor is then established between the subelement and a finite surface A_2 projected to the base of a unit sphere and the projected area established by contour integration.

However, this work by Toups was not easily obtainable and before a copy was obtained, the form factor program described above was already developed and successfully used. It should also be said that the program by Toups was meant for more complex problems of irradiance transfer involving more complex geometrical forms.

7.1.9 Within the range of architectural forms usually studied the program developed in this study is more advantageous because of its practicability, speed and simplicity of data entry.

7.2 The Form Factors of Infinitely Long Surfaces

7.2.1 The form factors for two surfaces that extend infinitely long in one direction are obtained by the crossed string method (Hottel 1967). From Figure 3.20, the form factor from A_1 to A_2 is given by the function

$$F_{A_1, A_2} = \frac{(ad + bc) - (ac + bd)}{2cd} \quad \dots 3.45$$

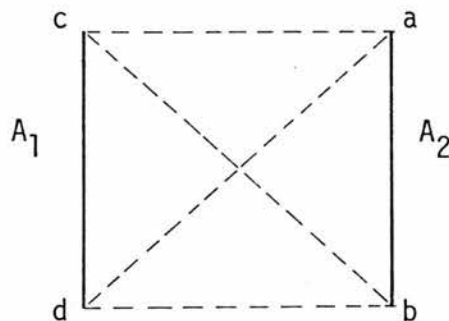


Figure 3.20 The Crossed String Method

8. THE NUMERICAL EVALUATION OF DOUBLE INTEGRAL FUNCTIONS

8.1.1 Double integration is required to determine the form factors, the sky component and the obstructed sky component. The numerical method used to evaluate double integral functions involves two successive integrations performed in two stages.

- (i) In the first stage the integration range, for one of the variables of the integral function, eg, X , which is between the two limits X_a and X_b is divided into pairs of elemental strips of equal intervals. The interval width h is determined by the expression

$$h = \frac{X_b - X_a}{n} \quad \dots 3.46$$

where n is the number of intervals.

The value of X_i at the end of each interval i is then established. Substituting for X_i , the function is reduced to a single variable function, function of Y . Integrating the function over the limits Y_a and Y_b gives the value of the integrand $A(X_i)$ at the point X_i , such as

$$A(X_i) = \int_{Y_a}^{Y_b} f(Y) dY \quad \dots 3.47$$

The integration of (Y) is performed by an IBM routine available in the program support Library of Edinburgh Regional Computing Centre. The program uses the method of the Trapezoidal rule with Romberg's extrapolation (IBM-SSP 1970).

- (ii) In the second stage the total integral value of the function is determined by integrating $A(X_i)$ over the limits X_a and X_b by Simpson's rule as given by the expression

$$V = \int_{X_a}^{X_b} A(X) dX = h/3 [A(X_a) + A(X_b) + 4(A(X_1) + A(X_3) + \dots + A(X_{n-1})) + 2(A(X_2) + A(X_4) + \dots + A(X_{n-2}))]$$

... 3.48

CHAPTER IV

TECHNICAL SPECIFICATION OF THE COMPUTER PROGRAMS PACKAGE

TECHNICAL SPECIFICATION OF THE COMPUTER PROGRAMS PACKAGE

1. INTRODUCTION

1.1.1 A description of the physical and mathematical basis of the model which evaluates the irradiance at the external surfaces of buildings and the numerical methods used to compute the different factors involved has been presented in the last two chapters.

1.1.2 Prior to making investigations with the model, it is necessary to implement it on a computer as a set of programs. A description of the logical structure of the processes performed by the programs, the manner in which they are assembled to form an integrated computer model of the physical system, the computing techniques and machine features which constrained or contributed to the efficiency of the model are presented in this Chapter. The logical structure of the programs is explained by a series of high level flow charts.

1.1.3 It is anticipated that certain routines which were developed in this study and coded in FORTRAN IV language could be employed in similar studies or be used to generate and tabulate useful data. Descriptive summaries which detail their logical processes are therefore given. The listing of these routines is presented in Appendix A6.

2. THE OPERATION AND ORGANISATION OF THE MODEL PROGRAM PACKAGE

2.1 Hardware and Software Background

2.1.1 The compilation and the running of the program package have been carried out at Edinburgh Regional Computing Centre (ERCC). It was possible to utilize the Edinburgh Multi Access System (EMAS) and the Operating System (OS) computing services available at the centre.

2.1.2 EMAS runs on the ICL system 4/75. It provides an interactive service useful for editing, compiling and making short test runs of programs. This provides a practical means of preparing and testing the individual subroutines.

2.1.3 An OS service was provided by the ERCC IBM 370/158 computer until September 1975. It is currently provided by Northumbrian Universities Multiple Access Computer (NUMAC) which uses IBM 360/65 and 370/168 computers. It offers a wide range of compilers including three FORTRAN IV compilers. The service is capable of handling both patch jobs and with longer running times. The integrated model is run on the OS service as it provides a powerful and rapid means for generating and analysing the model data.

2.1.4 ERCC computing facilities support many packages of application routines and programs available for users. These are directly accessible from both the EMAS and the OS

services. A number of these routines have been employed in the model package and in the analysis of data.

2.2 The Programming Language

2.2.1 The FORTRAN IV language was used to code the programs and routines used in this study. The main virtues of using FORTRAN IV are :

(i) Its world-wide adoption as a standard language for scientific problems allows programs to be transferred from one machine to another with the minimum of modification;

(ii) It allows new subroutines or functions to be developed and tested independently before being incorporated in the program package; and

(iii) It allows the program package to make use of routines from existing program libraries, many of which are only coded in FORTRAN. Equally, it offers the possibility of incorporating programs written by other research workers in the field.

2.3 The Data Structure

2.3.1 An important part of the programs is the data structure which is used to store the input and the computed data and to transfer the intermediate information between the different subroutines. The essential features of a good data structure

are the ease of access, creation and extension of data and the efficient use of the core storage.

2.3.2 The basic information specifying the geographical location of the site, the time of day and date of year to be considered, the geometrical and physical parameters of the form to be studied are collected and entered in a simple format. The programs then translate the information into a form suitable for computation. To provide for the direct access to the information, the data is organised into series of simple lists in form of multi-dimensional arrays. The dimensions of the arrays are directly related to the number of variables describing the items to be considered (for example, the number of surfaces needed to describe the form and the number of contour points which define the boundary of a surface) and, because of this, it may sometimes be necessary to enlarge the arrays. In order to accomplish this with the minimum of alteration, the dimensions of the arrays in the sub-programs have been specified using dummy arguments. A change may thus be made by simply altering the array sizes in the main program and the values assigned to the dummy arguments. The information which is accessed by the different sub-programs are stored in a "Common block". The use of tables, which take considerable storing space and involve interpolation, has been avoided except where they may provide significant savings in computation time.

2.3.3 It is possible to investigate a number of cases during each run of the program (for example, the irradiance on the surfaces of a particular form may be calculated for several times of the day or for a number of days). In such situations, the information prepared for each case overwrites the data of the previous case, in order to make efficient use of storage.

2.4 The Layout and Organisation of the Program Package and its Output

2.4.1 The flow of computation is controlled by a monitor program which reads the initial input, calls the sub-routines to execute the various instructions, organises and passes intermediate information between subroutines and evaluates the output. Output may be obtained at three levels of detail :

(i) At the most basic level, output which relates to the specialist activities of the various sub-programs may be produced. For example, detailed information concerning the form factors, the sun's position, the sky component or the obstructed sky component may be printed. This facility enables the program to provide data which may be of use in different but related studies to the present one.

(ii) At the intermediate level, information concerning such topics as the initial irradiance or the shadow factors

of the surfaces may be obtained. Such information enables the user to investigate the effects of orientation and form on the minimum irradiance load or the maximum degree of shadow.

(iii) The highest level of output provides the final results of calculation, namely the final irradiance on the various surfaces of the form. This data may be generated for different combinations of form parameters and it is analysed to establish the significance of each parameter.

3. DESCRIPTION OF THE MAIN SUBROUTINES

3.1 The Shadow Subroutine SHGT

3.1.1 This routine determines the contour points of the shadow silhouette cast on any finite planar surface by an adjacent finite planar or non-planar surface. It is also capable of evaluating the shadow profile cast on a curved surface whose equation is known, providing some minor adjustments are made to account for the surface's equation. The two surfaces are defined by the co-ordinates of the contour points which define their boundaries. The program demands that the co-ordinates of the contour points are presented in such a way that the two surfaces have the same contour direction. The contour direction specifies the direction of travel along the boundary contour of the surface.

3.1.2 The operations executed by the program may be viewed as taking place at two main stages :

(i) In the first stage, the program used the subroutine PLEQ to establish the equation of the surface. It then projects the contour points of the shadow cast onto the plane in which the surface lies. It determines the contour points of the shaded area using the subroutine PSHP.

(ii) In the second stage, the program ensures that the projected shaded area has the same contour direction as the surface. It then uses the subroutine POLINT to check

if the shaded area lies wholly outside, wholly inside or partially within the boundary of the surface. It also defines the profile of the shadow cast on the surface and establishes its contour points and their co-ordinates. The program uses a code (NCD) which is assigned integer values to describe the form of the shadow cast on the surface. The values used are :

- NCD = 0 when no shadow is formed on the surface;
- NCD = 1 for a point shadow;
- NCD = 2 for a line shadow; and
- NCD = 3 for a shadow having more than three contour points.

3.1.3 The programs employ a number of subroutines, the most important of which are described below.

3.1.4 Subroutine PLEQ : This routine is used to derive the general equation of a given planar surface in the form

$$A . X + B . Y + C . Z + D = 0 \quad \dots (4.1)$$

The subroutine utilizes the co-ordinates of three contour points of the surface to evaluate the coefficients of the equation (A, B, C and D). Even if the surface has an equation different to that given above, it should still be coded in subroutine PLEQ, although it may be necessary to

make modifications to subroutine PSHP.

3.1.5 Subroutine PSHP : This routine determines the co-ordinates at which the shadow due to a point in space intersects with a given plane. It substitutes for the solar angles, the co-ordinates of the point and the coefficients of the plane's equation to determine the shadow point's co-ordinates.

3.1.6 Subroutine POLINT : The routine establishes the common area of two finite surfaces (S_1 and S_2) which lie within the same plane. The two surfaces are defined by their contour points and the program demands that they should have the same contour direction. It investigates three possibilities :

(a) The two surfaces are located far apart and hence share no common area.

(b) Surface S_1 lies wholly within the boundary of S_2 or vice versa. The program then defines the boundary of the common area - that is, the boundary of the surface which is enclosed within the other one.

(c) The two surfaces are partially overlapped. The program then determines which parts of the boundary contours of the two surfaces define the common area as illustrated in Figure 4.1. This is carried by the following procedures :

(i) The program moves along the contour of S_2 , following its direction, until it reaches an intersection point with the contour of S_1 . This point is taken as a reference intersection point.

(ii) It uses the contour point of S_2 which lies prior to the reference intersection point to select one of two possible routes to follow until it reaches the next intersection point. The first route is indicated by the contour point lying outside the boundary of S_1 and the program then proceeds along the contour of S_2 . The second route is indicated by the contour point lying within the boundary of S_1 and in this case the program moves along the contour of S_1 . That part of the contour which is between the two intersection points and which forms the route of the program is assigned as part of the boundary contour of the common area.

(iii) The program then picks the contour line of S_2 at the last intersection and repeats the above processes until it reaches the reference intersection point.

(iv) It ensures that none of the contour points of the common area coincide with one another.

(v) It assigns integer values using a code, similar to that used for the shadow area, to distinguish between the different forms of the common area (eg, a point, a line

or more than three contour points). The program returns the value of the code, the number of contour points of the common area and their co-ordinates.

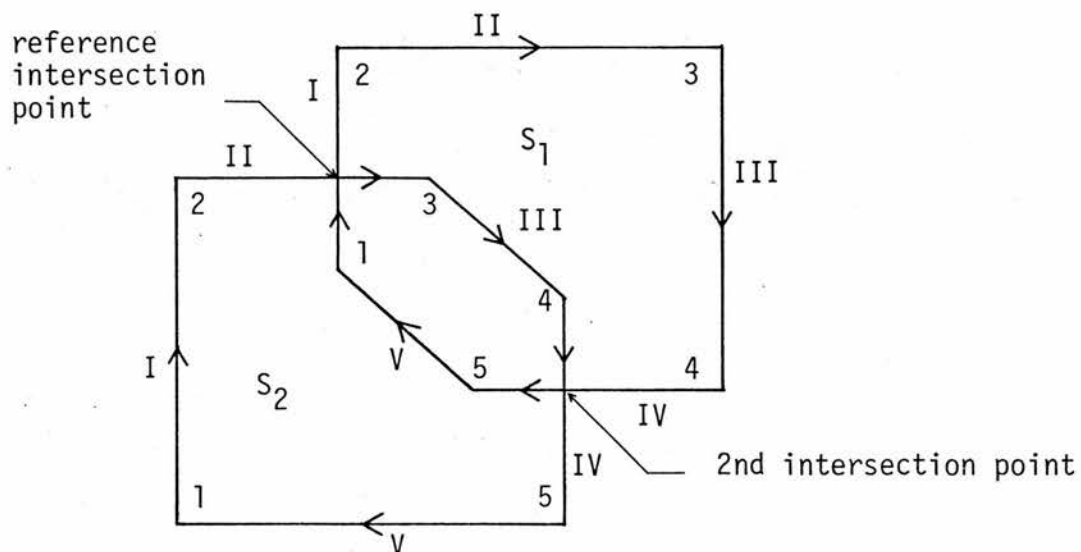


Figure 4.1(a)

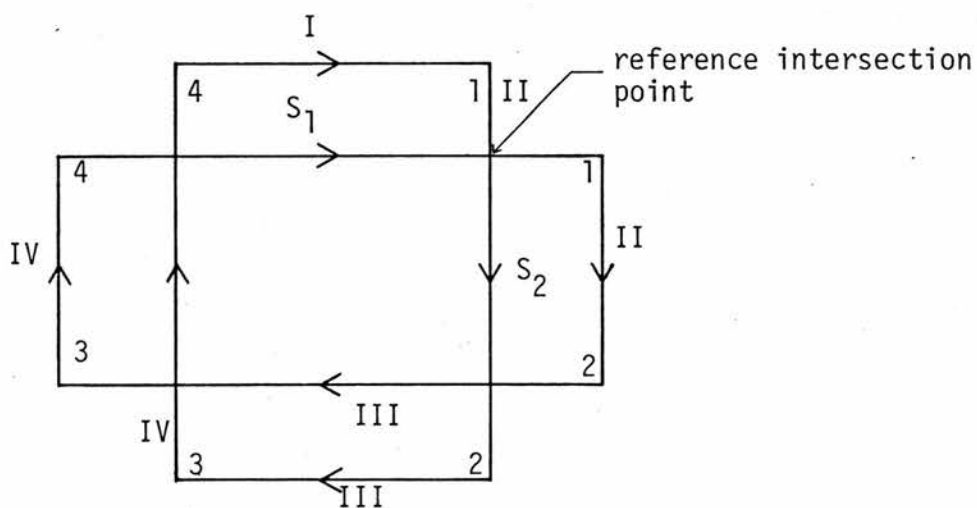


Figure 4.1(b) Geometry of Contour Movement by the Program to Define the Common Area for the Two Surfaces

3.2 The Sky Component Subroutine SKYCOM

3.2.1 Essentially, the routine evaluates the ratio of the diffuse sky radiation, being obstructed or received on a surface of any orientation and inclination from a given sky area to the zenith intensity, as explained in Chapter III, part 4.4.

3.2.2 The program first establishes if the profile of the sky area being considered forms a single unit in the shape of a lune or a circular ring, or a shallow dome or a combination of two units forming a lune with either a circular ring or a shallow dome. It then sets the altitude and azimuthal angular limits of the units accordingly.

3.2.3 The program expresses the integrand, which is composed of the relative luminance progression from the zenith to the horizon function and the diffusion indicatrix function (given earlier in Chapter III by equations 3.24(c) and 3.24(a) respectively), in terms of two variables, the altitude and azimuth angles of an elemental sky area. This is achieved by substituting in the integrand for the angular parameters of the sun and the surface, which are stored in the common data block. The integrand is coded in the function subroutine FCT.

3.2.4 The routine performs the double integration by first taking the altitude angular distance, dividing it into pairs of elemental sky strips of equal intervals and determining the

altitude angles of the strips at the interval points, the limits of the altitude and azimuth angles being specified. In some cases, when the altitude angle of the elemental sky strip is very small and when its lower limit is the horizon, there is a danger that the program will attempt to calculate a number which is too large to be stored and which, therefore, will cause calculation to be aborted. In order to avoid this, the horizon is set at an altitude angle of 0.5° . The error resulting from this approximation is negligible. The program then takes the altitude angle at each strip and substitutes it in the integral function in order to express it in terms of the azimuth angle only. It integrates the function over the azimuthal limits using the subroutine QATR, which is a routine in the IBM SSP library. The total ratio of the diffuse sky radiation to zenith intensity is obtained by summing the integral values calculated for all the elemental sky strips using Simpson's rule.

3.2.5 The value of the sky component or the obstructed component is then obtained by dividing the total integral value, for the ratio of the sky radiation to the zenith intensity, by the ratio of horizontal diffuse irradiance to the zenith intensity.

3.3 The Form Factor Subroutine FOFAC

3.3.1 This routine calculates the form factors for a finite planar polygon and a planar or non-planar polygon at any spatial locations.

It is also capable of calculating the form factors for surfaces with curved boundary lines if these are approximated by series of straight line segments or whose equations are given. The program assumes that the two surface view and exchange radiation with every part of each other.

3.3.2 The polygons are described in terms of a three-dimensional co-ordinate system. The geometrical description of the two surfaces is prepared and entered in a simple format by defining the contour points and their co-ordinates as illustrated in Figure 4.2. The program does not make any restriction on the direction of the contours. The absolute value of the form factor integral function is the same regardless of the directions of the two contours. The program generates the necessary data in a format acceptable for computation.

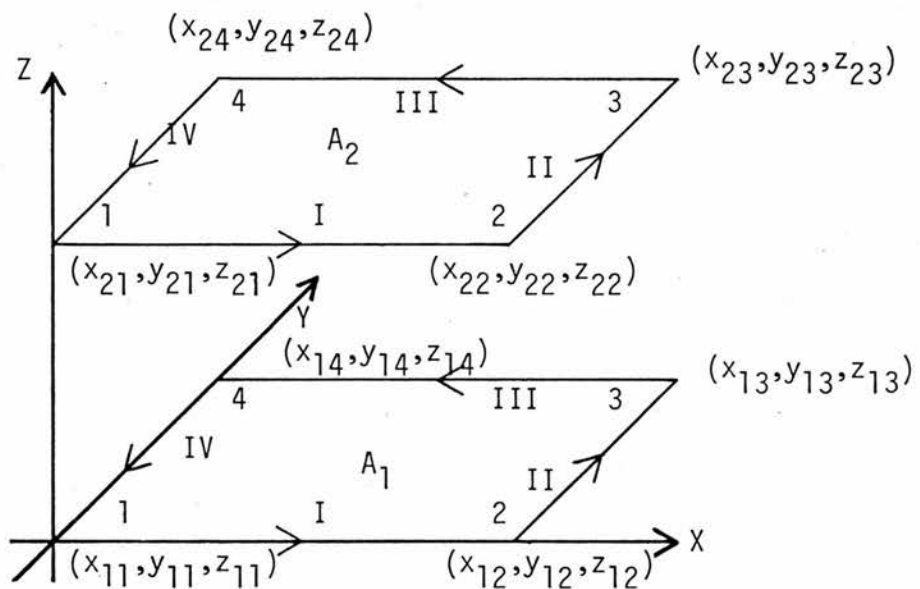


Figure 4.2 The Geometrical Description of Two Surfaces for Contour Integration

3.3.3 The accuracy and speed of the program are determined by the number of intervals used to perform the calculation. The program can calculate the form factors for two rectilinear surfaces using ten intervals in a fraction of a second with less than 1% error.

3.3.4 Contents of the Program

The main operations performed by the program are as follows :

(i) The program treats the contour of the surfaces as series of straight lines. It generates the necessary geometrical information describing the lines, for example the co-ordinates of the line's end points and the lengths along each axis. The derivatives of the functions of the lines are not required, instead the program assigns a zero or one value for the differentials to distinguish whether the x, y and z co-ordinates are either constant or varying along each line. For example, when the x co-ordinate is varying along a line dx is taken = 1.0 and when y is constant, $dy = 0$.

(ii) The program picks a set of two lines at a time, one from each surface, for the contour integration. It goes through all the combinations of line pairs by means of two nested "DO" loops.

(iii) It evaluates the integral values for the X, Y and Z axes separately, for each set of lines. The integration is

only performed when the co-ordinates of both lines along the respective axis are varying. For example, when x_1 and x_2 are variables, that is both dx_1 and $dx_2 = 1$, the integral value for the X-axis is evaluated. When the co-ordinate for either of the two lines is constant, eg, dx_1 and $dx_2 = 0$, the integral value for the axis is set equal to zero.

(iv) The program expresses the integral function in terms of two variables pertaining to the co-ordinates of the two lines for the axis considered. For example, the integral function for the X-axis is expressed in terms of X_1 and X_2 , for the Y-axis in terms of Y_1 and Y_2 and for the Z-axis in terms of Z_1 and Z_2 . The program uses the subroutine EQAT to derive equation for the lines such as

$$Y_1 = f_1(X_1) \quad \dots (4.2a)$$

$$Z_1 = f_2(X_1) \quad \dots (4.2b)$$

$$Y_2 = f_3(X_2) \quad \dots (4.2c)$$

$$Z_2 = f_4(X_2) \quad \dots (4.2d)$$

The coefficients of the functions are stored in the common data block. This allows access for the integration routine DOBINT and external function FCT in order to substitute for Y_1 , Y_2 , Z_1 and Z_2 in the integral function and to express it in terms of X_1 and X_2 .

(v) The evaluation of the integral function is performed

by the routine DOBINT. The form factor is obtained by summing the integral values obtained for the three axes and for all the sets of the two lines combinations of the two surfaces.

3.3.5 Supplementary Subroutines

The most important subroutines employed by FOFACT are :

(i) DOBINT, which performs the double integration of a given function which is coded in the routine FCT. The form factor function given in this routine relates to one co-ordinate axis and the integration is evaluated for a set of two lines. For the X-axis, the function is given as

$$f(\text{FCT}) = \int_{a_1}^{b_1} \int_{a_2}^{b_2} \text{Inr } dx_1 \cdot dx_2 \quad \dots \quad 4.3$$

The limits of integration for the two lines (a_1, b_1 and a_2, b_2) along the respective axis are specified by the main subroutine together with the number of intervals needed to carry the integration. The program divides the first line into pairs of equal intervals. It establishes the co-ordinates (x_1, y_1 and z_1) of each interval point and substitutes for them in the integral function to reduce it to a single variable function in terms of x_2 only. The values of the integral function at the interval points are evaluated by the routine QATR for which the integration limits of the second line are specified. The program then determines the value of the contour integral function for the two lines by adding integral values, evaluated

at the interval points of the first line, using Simpson's rule.

(ii) The subroutine QATR is available in the IBM Scientific Subroutines Packages and performs integration of a single variable function by the Trapezoidal rule with Romberg's extrapolation. The accuracy of the computation is determined by specifying the magnitude of the error to be tolerated.

(iii) EQAT : This routine uses the co-ordinates of a line's end-points to derive its equation in the form

$$A_1 \cdot X + B_1 \cdot Y + D_1 = 0 \quad \dots \quad 4.4(a)$$

$$A_2 \cdot X + C_2 \cdot Z + D_2 = 0 \quad \dots \quad 4.4(b)$$

$$B_3 \cdot Y + C_3 \cdot Z + D_3 = 0 \quad \dots \quad 4.4(c)$$

By means of this, it is possible to express any two of the co-ordinates for a line in terms of the third co-ordinate as shown by equations 4.2. The coefficients of the expressions are stored in the common data block and are used to evaluate the integrand. When the equation of the line is known, it should be coded in this routine, along with the necessary modification to the main subroutine to account for the form of the line equation.

3.3.6 Subroutine INFMFT

This routine was used to evaluate the form factors in the case where the surfaces were regarded of infinite length. It is based on the crossed string method described earlier in

Part 7.2 of Chapter III. The routine demands that the coordinates of the end points of the lines defining the cross-section of the form to be specified.

3.3.7 Alternative short routines which calculate the form factors for specific geometrical configuration of surfaces may also be compiled. These can utilize the available mathematical expressions and the flux algebra relations as in the case of perpendicular rectangular planes with a common edge. This example will be illustrated in Appendix A.5.

3.4 The Initial Irradiance Subroutine IRRILL

3.4.1 This routine evaluates the initial irradiance or illuminance on the surfaces of a building, on any site and at any time of day and date of year. The solar angles are either given or may be evaluated by the routine SUNGT.

3.4.2 The program takes into consideration the shadow cast on the surface by adjacent buildings and uses the routine SHGT to evaluate the profile and area of shadow. It then calculates the total direct incident irradiance received on the exposed area of the surface. It uses the routine SKYCOM to determine the sky component and calculates the total diffuse irradiance received on the surface. The initial irradiance is taken as the weighted average of the direct and diffuse irradiance received.

3.5 The Sun Geometry Subroutine SUNGT

3.5.1 This routine was coded for a model which simulates the apparent movement of the sun. It calculates the solar declination, altitude and azimuth angles by the equations given earlier in Part 3 of Chapter III. The program demands that the latitude, longitude and the local standard time longitude of a location to be specified together with the date and time at which the solar angles are required. It will output the altitude and azimuth angles of the sun with reference to the local standard time. These angles are defined only when the sun is above the horizon. The azimuth angle is measured from the north point in a clockwise direction.

3.6 The Assembly and Solution of the Final Irradiance Transfer Functions, The Subroutine MATRIX

3.6.1 This routine assembles the final irradiance transfer functions of a system of N surfaces. The functions are represented by a set of simultaneous linear equations (see Chapter II, equation 2.46) in the form of two matrices :

(i) The coefficient matrix. An $N \times N$ array, the elements of which are the product of the form factors and reflectivities. It is assembled by means of two nested "DO" loops which pick two surfaces at a time and determines their form factors using FOFAC.

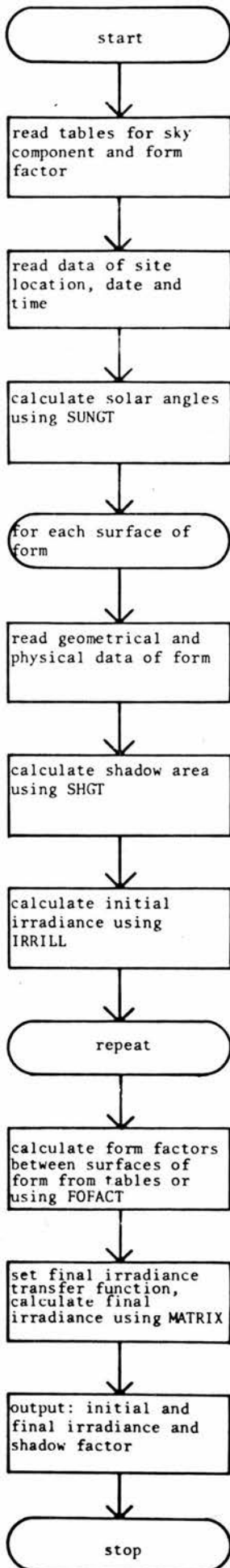
(ii) A corresponding identity vector matrix of dimension N, where the elements of the matrix are the initial irradiance of the surfaces which are obtained by means of routine IRRILL.

3.6.2 The final irradiance of the surfaces are obtained by solving the matrices equation by use of Subroutine GELG, which is a routine in the IBM SSP Library.

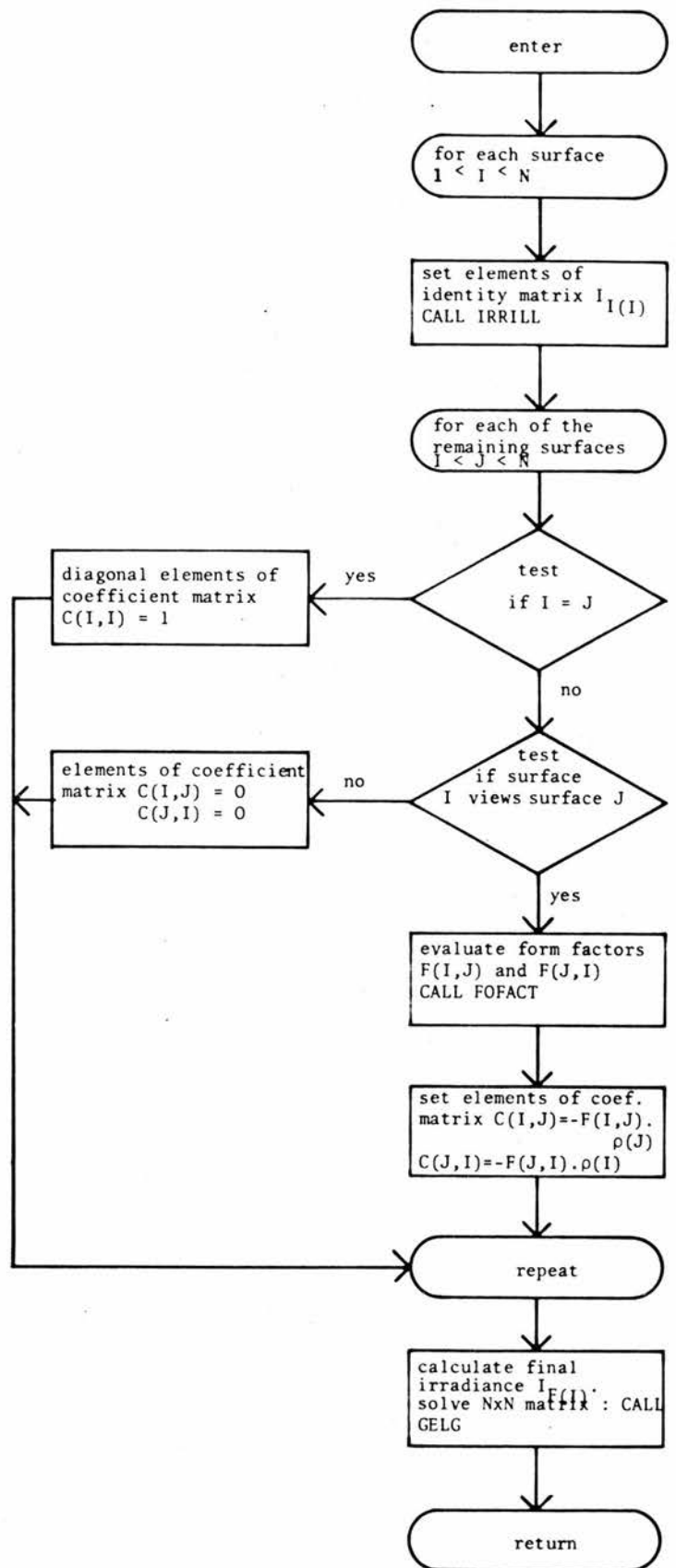
4. THE FLOW CHARTS

4.1.1 Flow charts are usually regarded as the best possible means of explaining the logical structure of computer programs (Hawkes and Stibbs 1970, Dorn and McCracken 1972). It is usually difficult to understand the logic of a computer program due to the programming language's inherent characteristics and the individual way in which the program is compiled and coded. The flow chart format presents the logic in a simple and clear way. The shapes used in the charts are those most commonly used to signify the different operations. Ellipses are used for start, entry, return and stop statements. Rectangulars are used for instructions, eg, reading, calculation and so on. Diamonds are used for tests. Two ellipses are used for loops with the start containing a 'for' statement and the end containing a 'repeat' statement. Small circles with figures indicate the continuation of the charts. Subroutines are referred to by their names which are written in the upper case. The flow charts of programs package are given in the following diagrams.

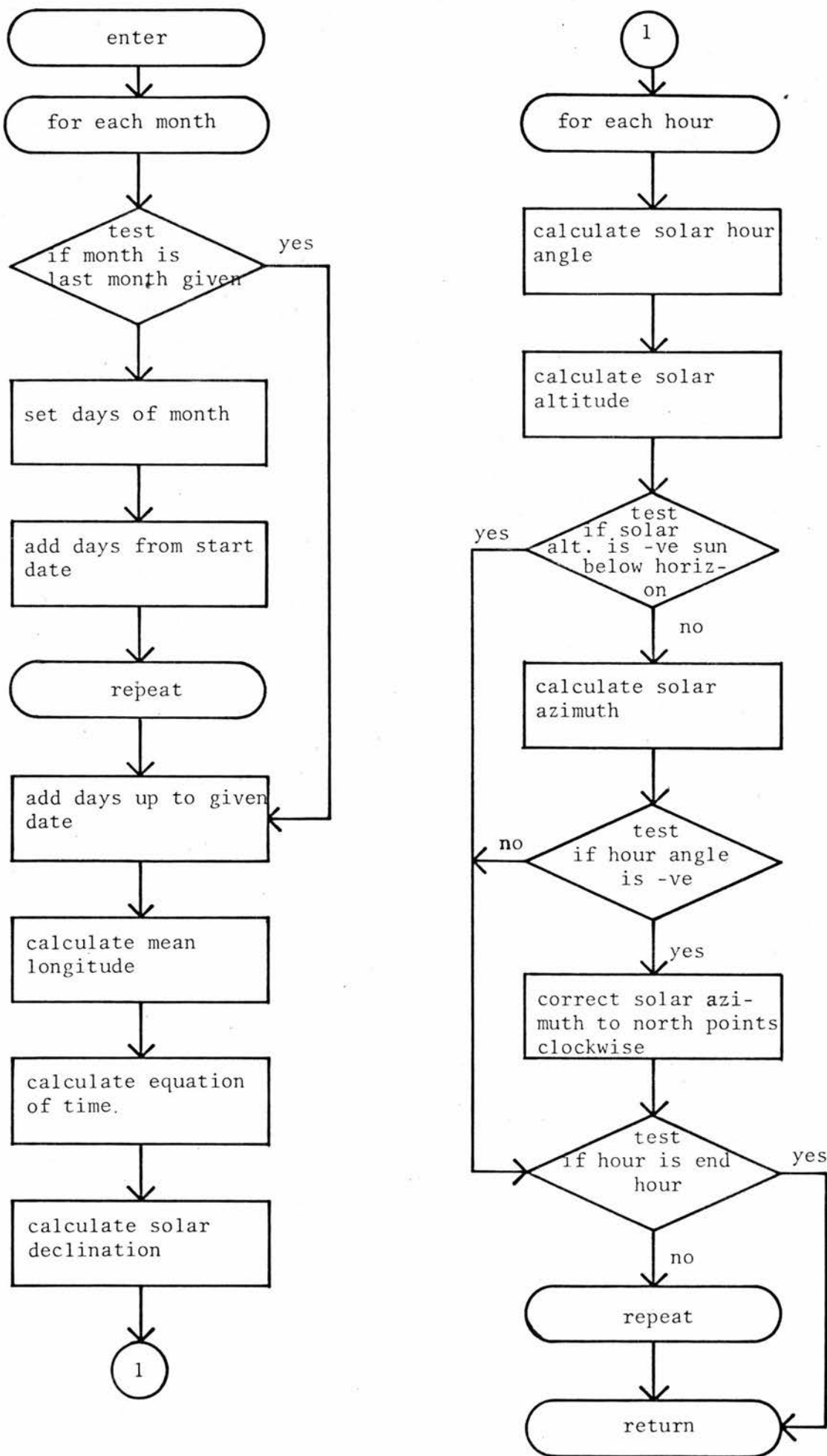
Main Program for an Evaluative Model



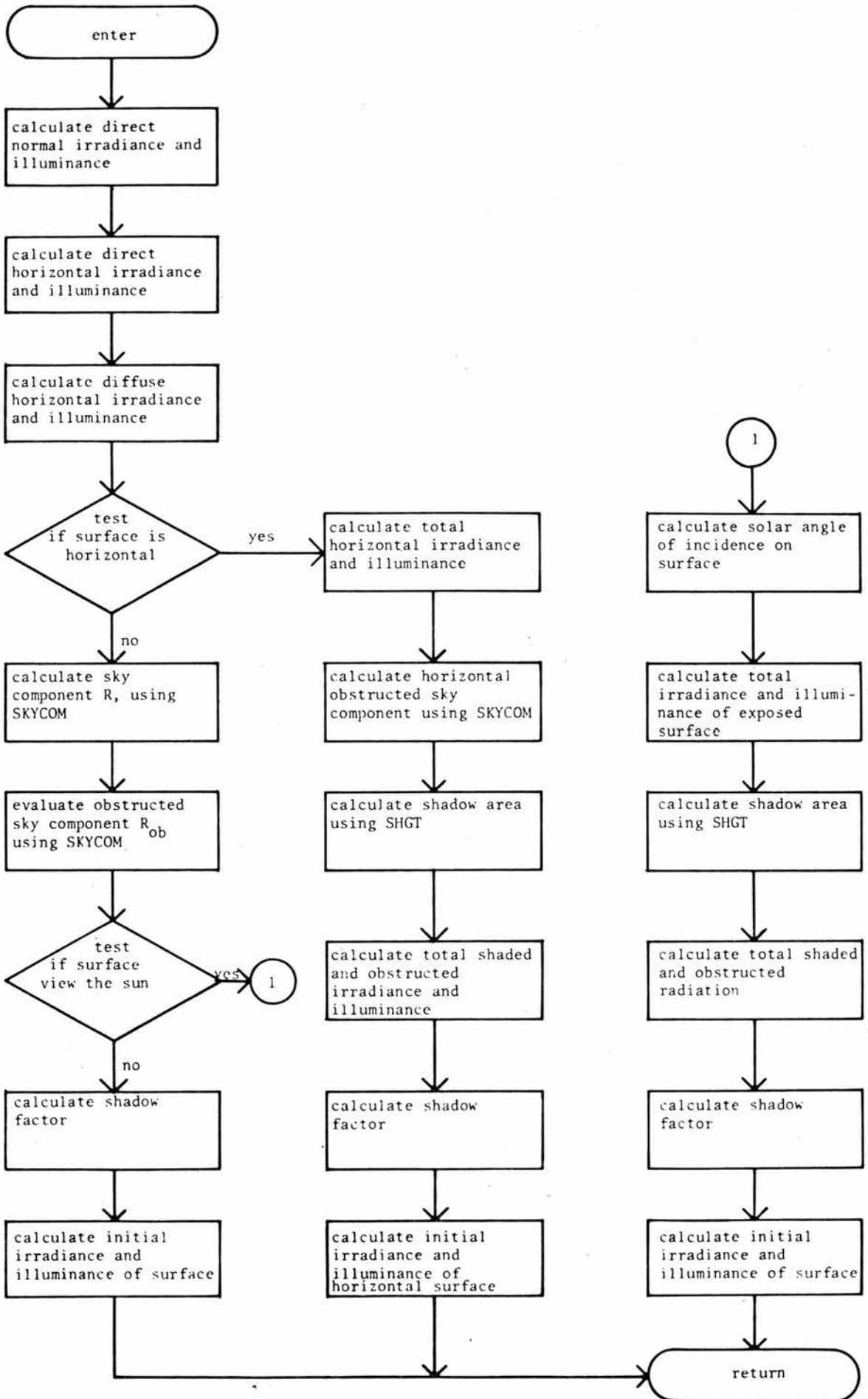
Subroutine MATRIX

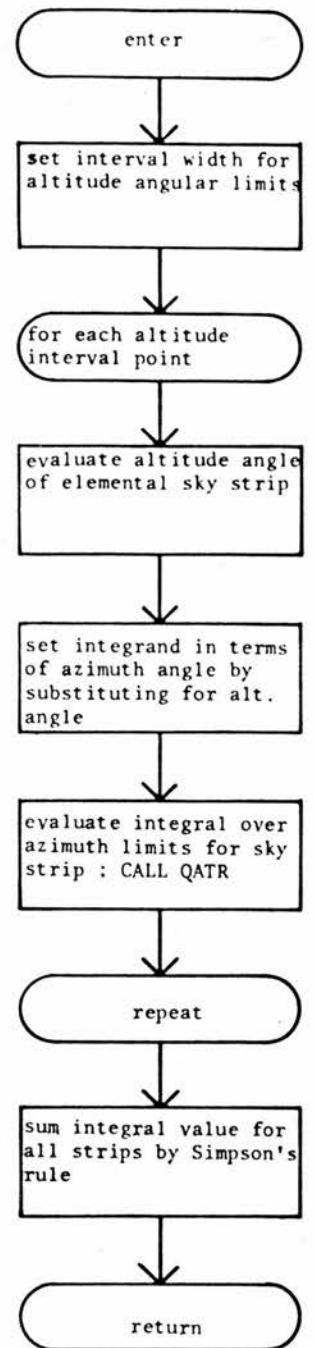
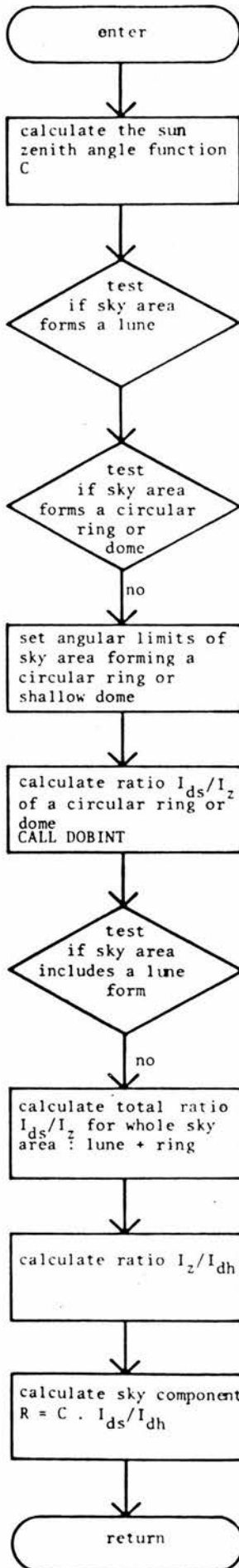


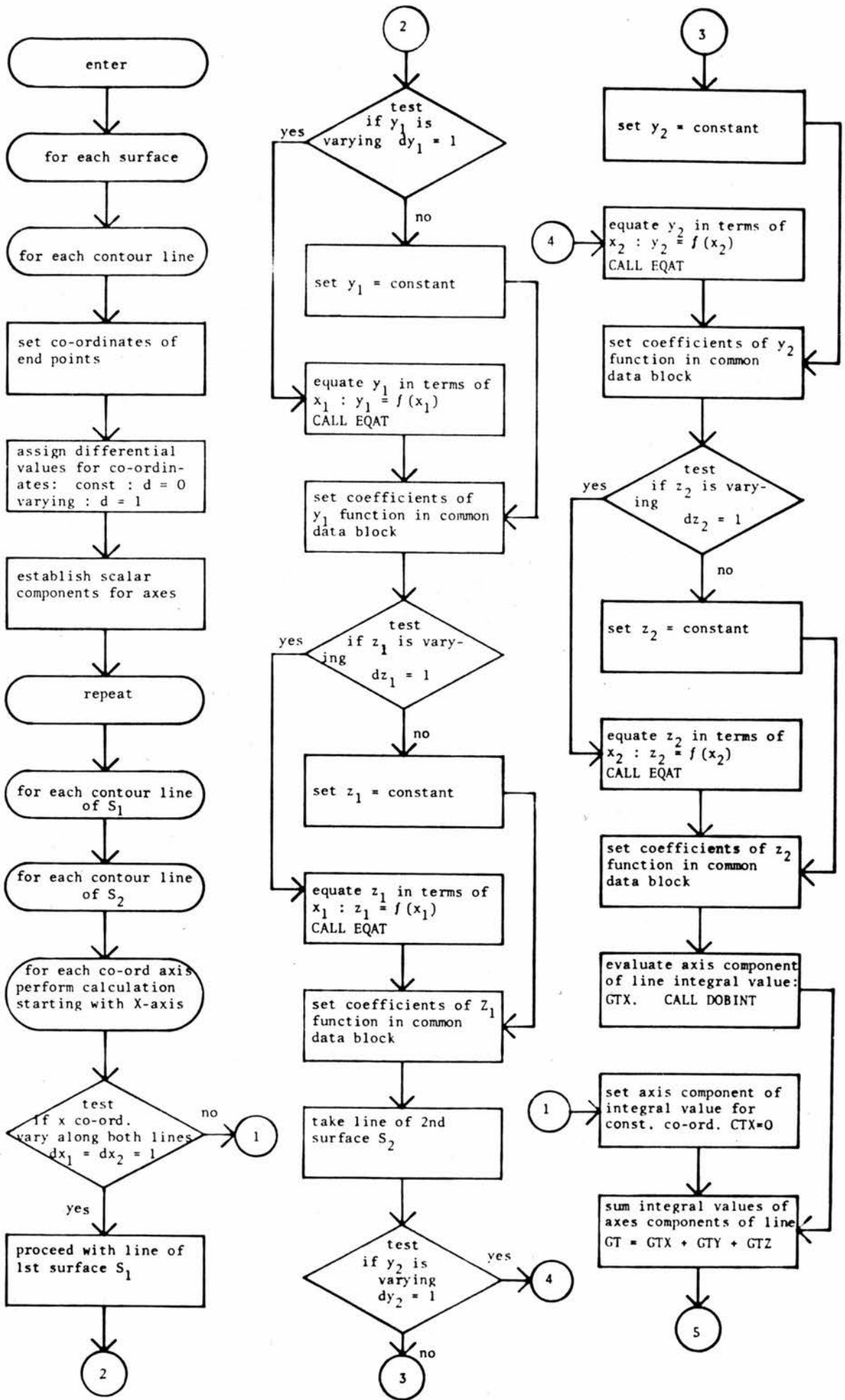
Subroutine SUNGT

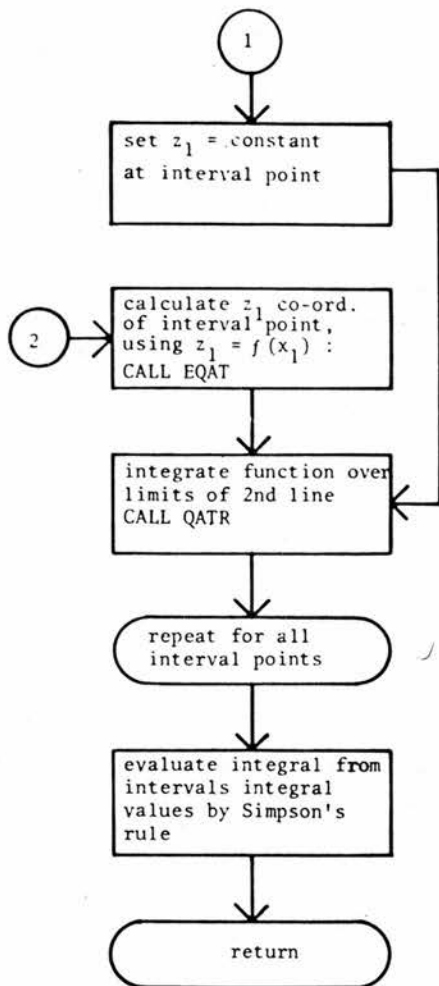
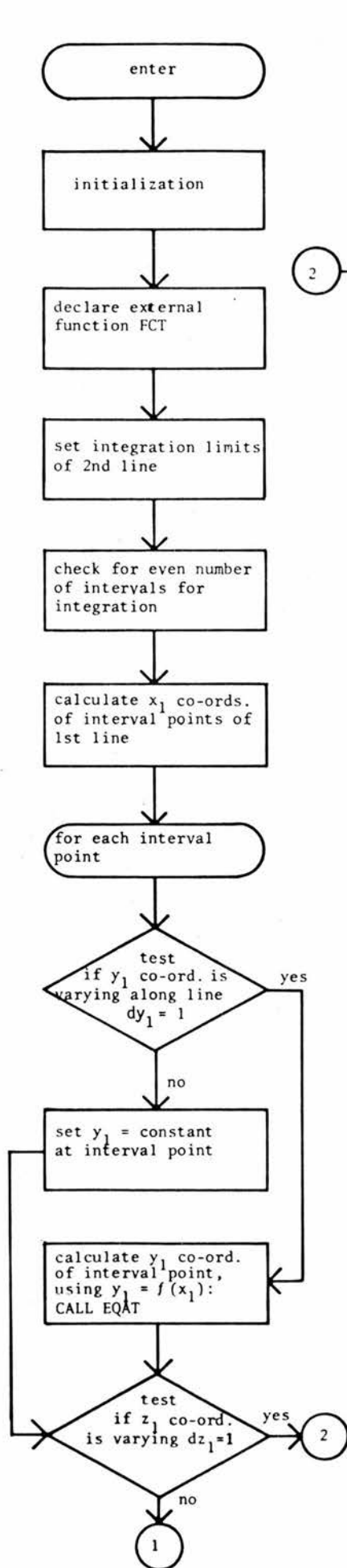
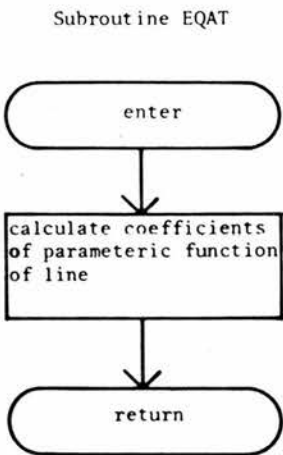
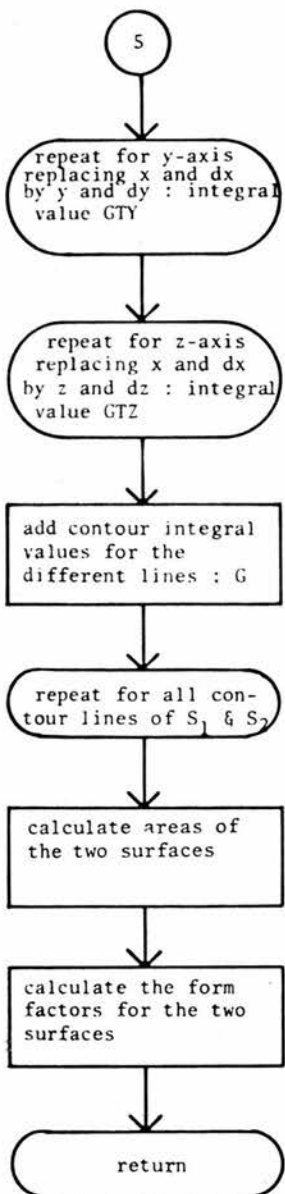


Subroutine IRRILL

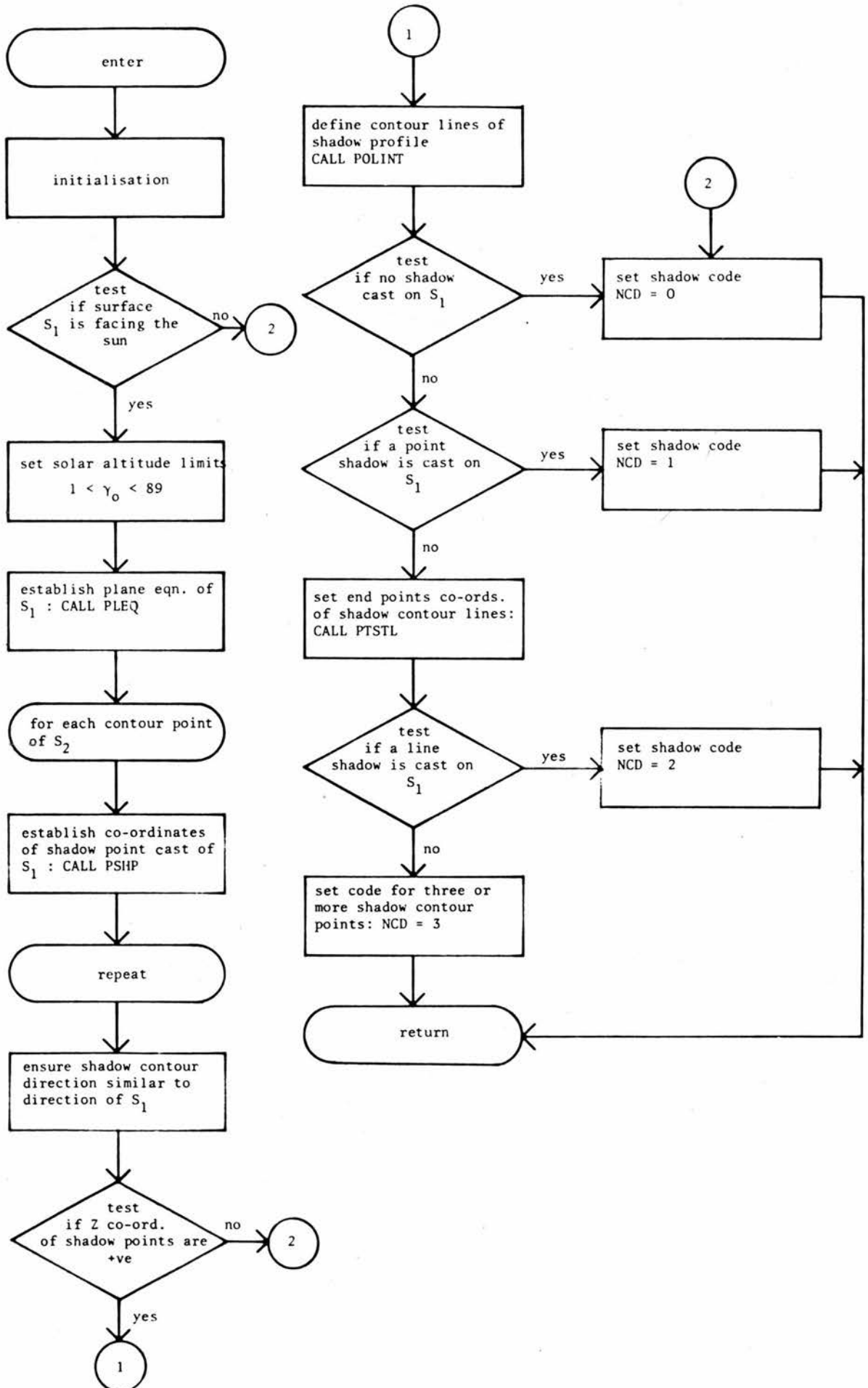




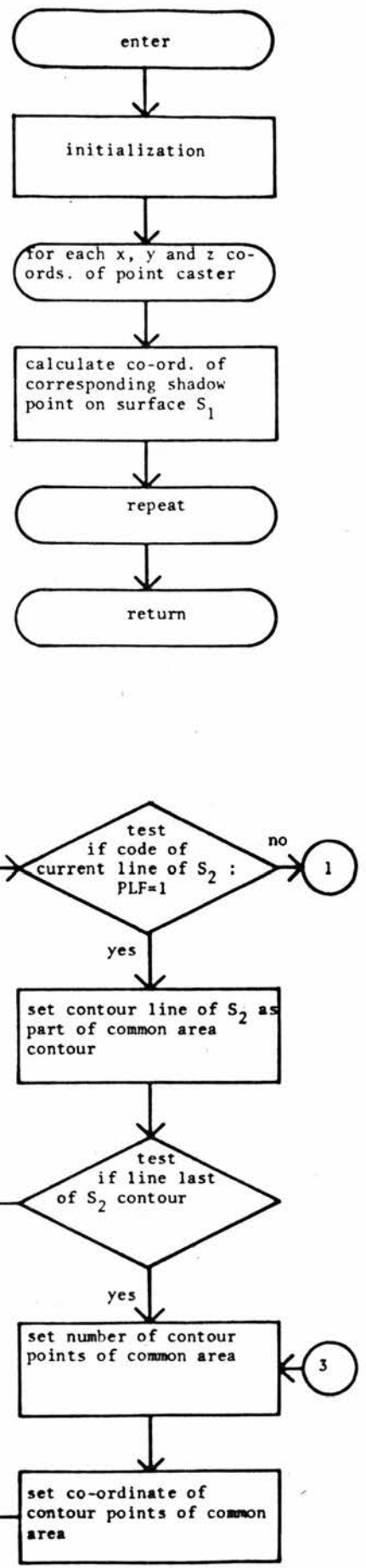
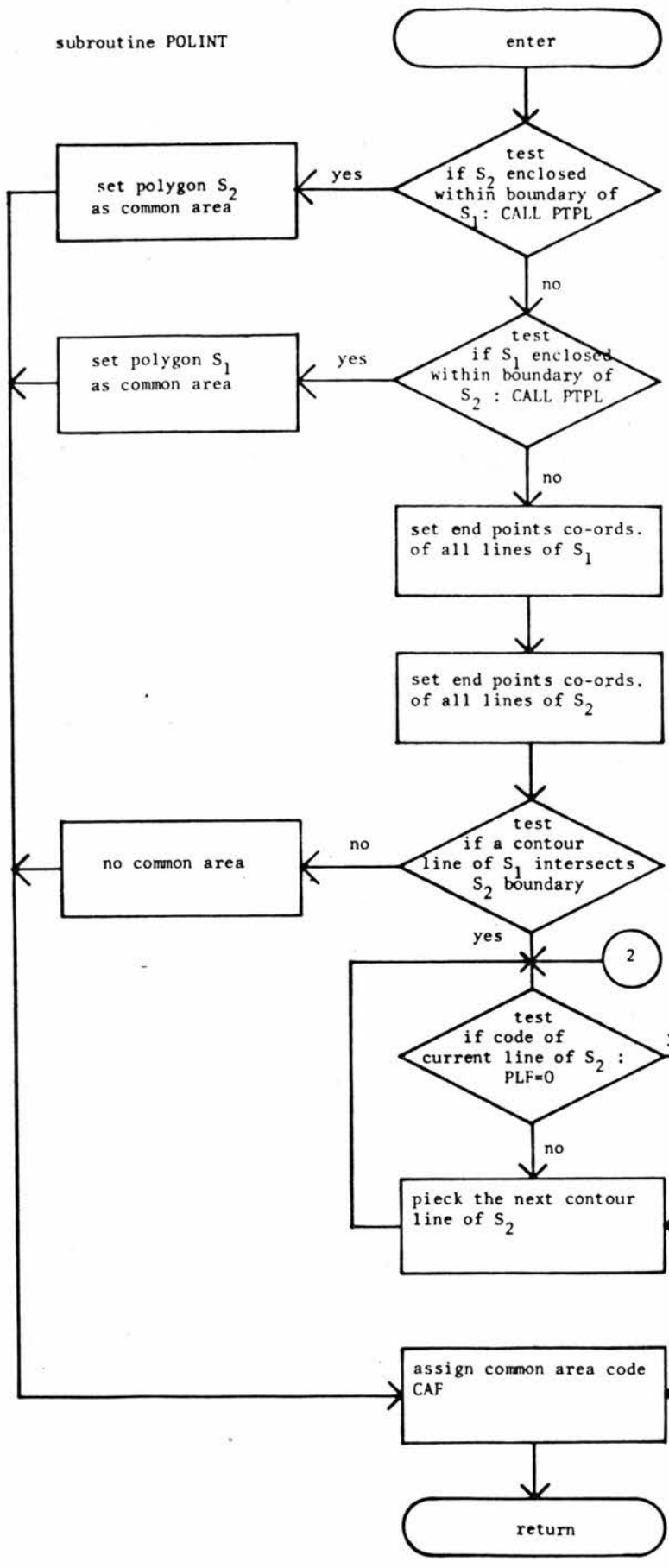


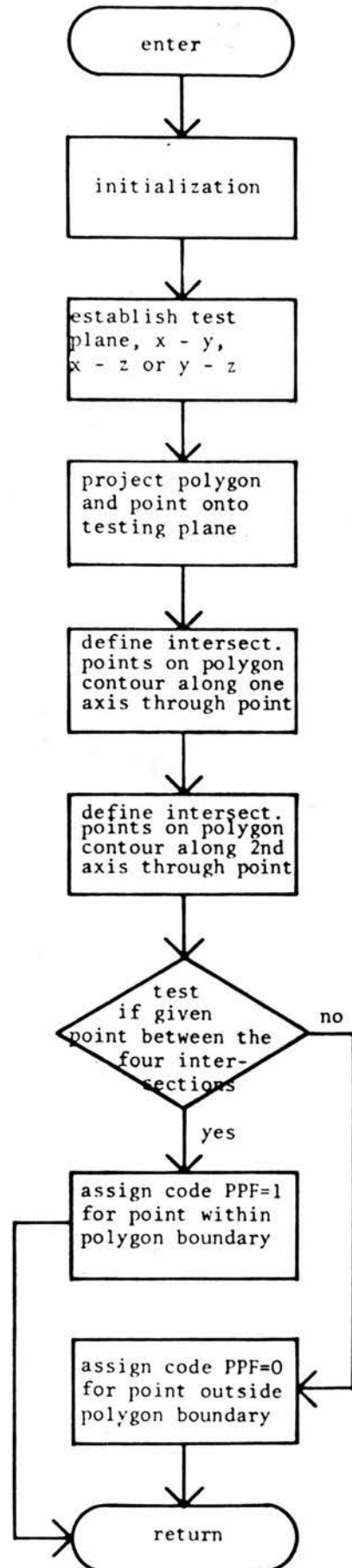
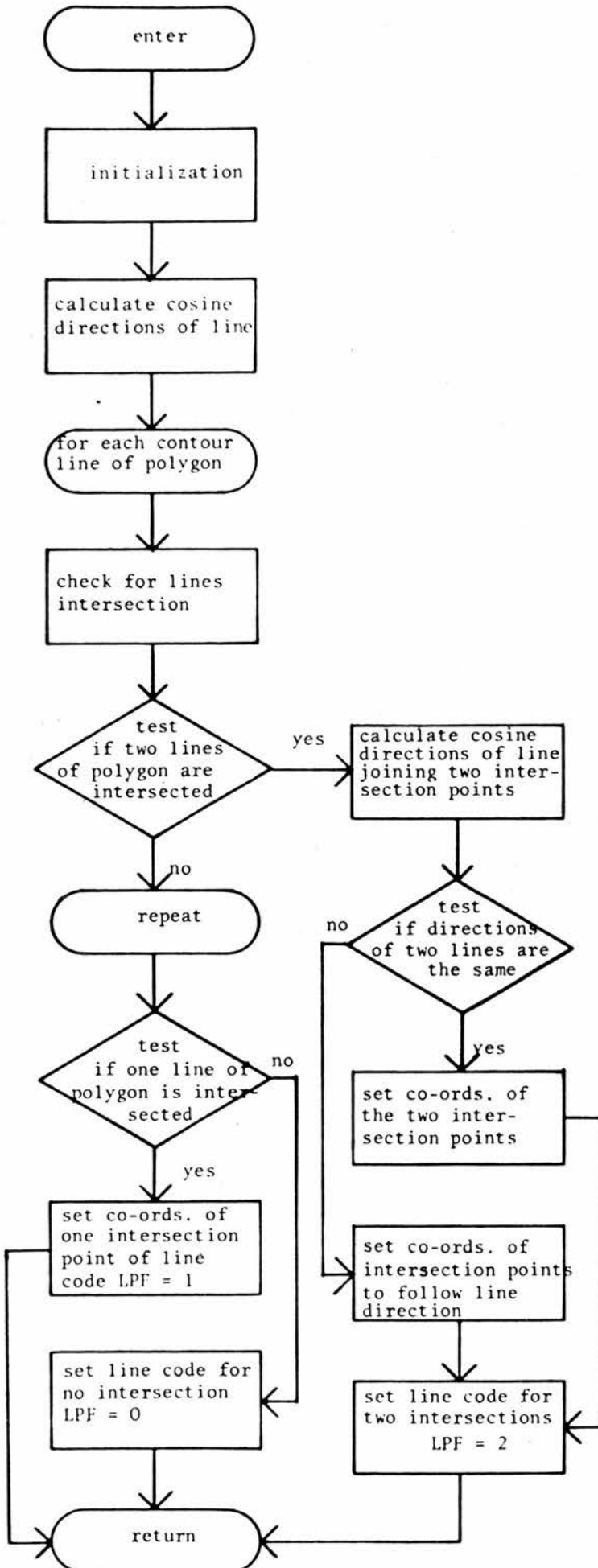


Subroutine SHGT



subroutine POLINT





CHAPTER V

EXPLORATORY INVESTIGATIONS

EXPLORATORY INVESTIGATIONS

1. INTRODUCTION

1.1.1 The results obtained in this study are derived from the solutions of the mathematical model for the different combinations of the parameters of the form and the sun, using the digital computer. Errors may be introduced in the computed values for the different factors involved and the final output of the model for a number of reasons :

(i) The mathematical model is formulated with postulations which describe an idealised situation. The model performance may differ from the real physical irradiance system.

(ii) Practical reasons necessitate the use of simplified and approximate procedures to evaluate the complex factors.

(iii) The input to the model is based on estimates.

(iv) The numerical processes carried out by the computer introduce computational errors.

1.1.2 Prior to generating systematic and detailed data for the study using the model program package, exploratory investigations have been carried out in order to establish the accuracy and overall performance of the model. These investigations estimate and analyse the errors encountered with regard to the following points :

(i) The significance of the computational errors involved.

(ii) The choice of the optimum interval widths with regard to the level of accuracy to be accepted and the minimisation of the computational time for the numerical evaluation of the factors and the final output.

(iii) The verification of the assumption used to simplify the calculation of the output of the model.

2. THE COMPUTATIONAL ERRORS

2.0.1 Inherent, truncation and roundoff are the three basic types of error in a numerical computation.

2.1 Roundoff Error

2.1.1 Roundoff error is inherent in floating point arithmetical operations, in particular additions and subtractions performed by the computer. This is due to the machine characteristics of interpreting real numbers by a finite number of significant decimal digits and the procedures by which it handles arithmetical operations. Real (floating point) constants, expressed by up to seven significant decimal digits, are used for the calculation. Simple procedures are employed to minimise error propagation during the course of a computation. It is impractical to present figures of more than three significant decimal digits. Hence the results obtained are accurate enough for the purpose of this study and the overall roundoff error is insignificant.

2.2 Truncation Error

2.2.1 This refers to the error introduced by truncating an infinite mathematical process.

Truncation errors are introduced by the numerical integration method and the finite difference representation of integral function due to the fact that differential areas are represented by finite areas. The truncation error is the difference between

the solution obtained with finite area representation and the exact solution of integral function. Generally the magnitude of the truncation error is determined by the size and number of intervals into which a surface is divided for the computation. The greater the number of intervals the smaller the size of the surface element and hence the smaller the truncation error. Inevitably, increasing the number of intervals increases the amount of computation. Hence by estimating and analysing the truncation error the optimum number and size of intervals, with regard to the magnitude of the error and computation time, may be established.

2.2.2 The truncation error introduced by the numerical method used to evaluate the sky component and the form factor is analysed using a procedure presented by Dorn and McCracken (1972). The true integral is estimated from values obtained for two runs of the program using, for example, N and $2N$ intervals by the expression

$$I = I_h + \frac{I_h - I_k}{k^4/h^4 - 1} \quad \dots 5.1$$

where I is the estimated true integral, I_h and I_k the computed integrals for N and $2N$ intervals and h and k the corresponding interval widths.

From the size of the difference between the two computed values it is possible to determine the number of intervals to use routinely. An estimate of the truncation error is easily obtained.

2.2.3 The truncation error in the form factor was investigated using values calculated for two equal rectangular opposing surfaces for different combinations of length, width and distance apart. The following points were concluded :

(i) The increase of intervals, irrespective of the interval widths, does not reduce significantly the magnitude of the truncation error. For example, doubling the number of intervals from 10 to 20 reduces the error by 0.1 percent while quadrupling the computation time. 10 intervals were found to represent an optimum number for the numerical evaluation of the form factors of rectilinear surfaces.

(ii) The magnitude of the truncation error is directly proportional to the distance r , separating the two surfaces. This may be explained by the fact that the form factor is a function of $\log r$, given earlier by equation 3.4.3 in Chapter III. As illustrated by the digram in Figure 5.1, the contribution to the form factor value at any of the elemental contours of the two surfaces may be given by the expression

$$df = \int \int \frac{1}{dL} + \int \int \log r \, dr_1 \cdot dr_2 \quad \dots 5.2$$

This requires the evaluation of quantities like, $\log r_2 - \log r_1$. As the separation increases, r_1 and r_2 both tend to be nearly equal large values.

Thus $\log r_2 - \log r_1$ equals the difference of two nearly equal large numbers. Any errors in these large numbers cause a disproportionately large error in the difference quantity and hence in the value of the form factor. For example, in the case of the two rectangles, varying r from 10 to 20 units was found to increase the error by 2 percent.

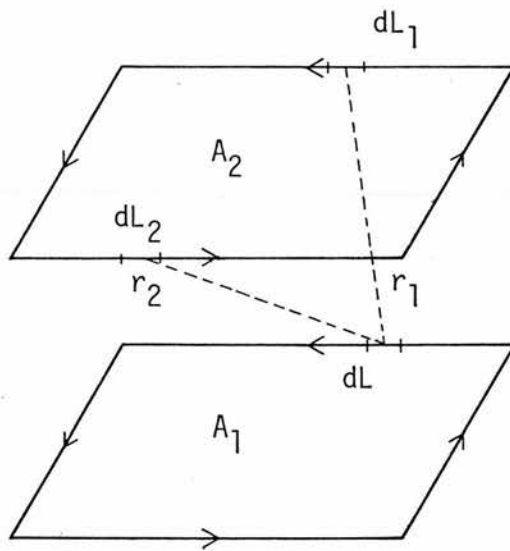


Figure 5.1 Contribution of elemental section of the contour to form factor value

Form factor values calculated for different proportions of r were compared with similar tabulated values given by Hamilton (1952). This indicated that the error does not exceed 1 percent when ' r ' is taken as less than 10 units. ' r ' may be represented by the perpendicular distances for two parallel surfaces or

the distance joining the furthestmost points of two perpendicular or obliquely located surfaces.

(iii) In the case of two surfaces with a common edge another form of truncation error may be introduced by taking the two surfaces apart by a small distance d_L to avoid r equals zero, as explained in Chapter III part 7.1.4. The truncation error is less than 3 percent when d_L is taken as 1.0 percent of the length of the common side. The magnitude of the truncation error can be further reduced by taking r equal to the interval width of the common side at the points where r is equal to zero. Alternatively, r may be set as equal to nearest number to zero that the computer can handle.

2.2.4 The truncation error of the sky component values was investigated in a similar manner to the form factor. The computed values were also compared with values provided by Krochmann (1974).

The relative truncation error introduced by using 10 intervals for the numerical integration, which was taken as the optimum number, is about -0.3 percent. Using 20 intervals increases the accuracy of the computation by less than 0.1 percent.

2.2.5 The truncation error in the finite differences representation of irradiance transfer functions has been investigated by O'Brien (1959). He estimated the error in the luminous

emittance of the surfaces of an infinitely long hallway with luminous ceiling for one, two and four equal wall sections. The relative error was within the range of ± 5 , ± 1.4 and -2 percent for the one, two and four wall sections respectively. A similar investigation of the error in the final irradiance of the physical system was carried out. A simple model of infinitely long street facades was taken for the physical system. As the form factors are accurately determined, the errors in the calculation due to them are eliminated. The final irradiance was calculated with the vertical surface facing the sun divided into one, two, four, eight and sixteen equal sections. As no accurate solution of the final irradiance is available, an estimate of the error for the one, two, four and eight sections surface was obtained by relating the corresponding irradiance values to the values obtained for the sixteen section surface. The results are shown in Table 5.1. These show that the accuracy of the calculation does not significantly increase by increasing the number of surfaces sections. This confirms the suggestions made by Phillips, in a discussion of the paper presented by O'Brien (1959), that the finite difference method when used for a system with a limited number of surfaces with true values of the form factors can give fairly accurate results. Hence it seems practical to use a one section surface for the solution of the finite difference method since this will greatly reduce the computation involved.

Table 5.1 Initial and final irradiance distribution of a physical system of infinitely long vertical parallel surfaces and the ground separating them. $\rho_1 = \rho_3 = 0.6$, $\rho_2 = 0.2$.

No. of Surface Sections	Distance of Mid-Point of Section from ground (units)	Initial Irrad. per unit area	Final Irradiance/Unit Area		Truncation Error percent
			Solution for 16 Sections Wall	Approximate Solution	
S ₁		26.2	231.4	230.9	-0.65
S ₂		32.2	208.6	208.9	+0.14
S ₃ - 1	1.0	704.8	778.4	774.4	-0.57
weighted average irradiance of S ₃		704.8	776.2	774.4	-0.23
S ₁		26.2	231.4	231.2	-0.009
S ₂		32.2	208.6	208.7	+0.005
S ₃ - 2	0.5	692.6	766.9	766.0	-0.12
S ₃ - 2	1.5	719.6	786.4	785.6	-0.10
weighted average irradiance of S ₃		706.3	776.2	775.8	-0.005
S ₁		26.2	231.4	231.3	-0.004
S ₂		32.2	208.6	208.6	0.0
S ₃ - 4	0.25	687.5	760.1	759.9	-0.003
S ₃ - 4	0.75	698.4	773.0	772.8	-0.003
S ₃ - 4	1.25	711.9	782.9	782.6	-0.004
S ₃ - 4	1.75	727.8	789.2	789.1	-0.001
weighted average irradiance of S ₃		706.4	776.2	776.1	-0.001

2.3 Inherent Error

2.3.1 This is the error in the values of the input data caused by estimating of input. With the integrated mathematical model, the initial irradiance input is obtained by calculating the direct and diffuse irradiance. However, this form of error is of no significance since the output of the model would be viewed with reference to its calculated input.

3. VERIFICATION OF THE APPROXIMATE TECHNIQUES USED TO SIMPLIFY THE EVALUATION OF MODEL OUTPUT

3.0.1 The calculation of the output of the physical system should take into account two main points :

(i) That a building facade is normally a combination of pieces of building materials with varying geometrical, physical and spatial properties.

(ii) That variation of the initial irradiance on the different parts of the facade may be expected. This is due to the different patches of shadow, of varying areas, which are formed on the facade.

3.0.2 The consideration of the different parts of a facade, as characterised by their physical and geometrical properties (outlined in part 6.1.1 of Chapter III) and of the prevailing initial irradiance and shadow conditions as separate surface elements would inevitably increase the amount of the computation involved. However, considerable simplification of computation and saving of time can be achieved by the use of appropriate weighting which allows for the different initial irradiance, reflectance and areas of the facade parts. The following discussion considers the accuracy of using the area weighted average reflectance and the initial irradiance of facades in evaluating the output.

3.1 The Weighted Average Reflectance of Facade

3.1.1 The area weighted average reflectance of surfaces has been used in daylighting studies to account for the different reflectance and the different areas of the materials of building's facades and internal surfaces (Dresler 1954, Hopkinson 1966, Plant 1969).

It is calculated by the expression

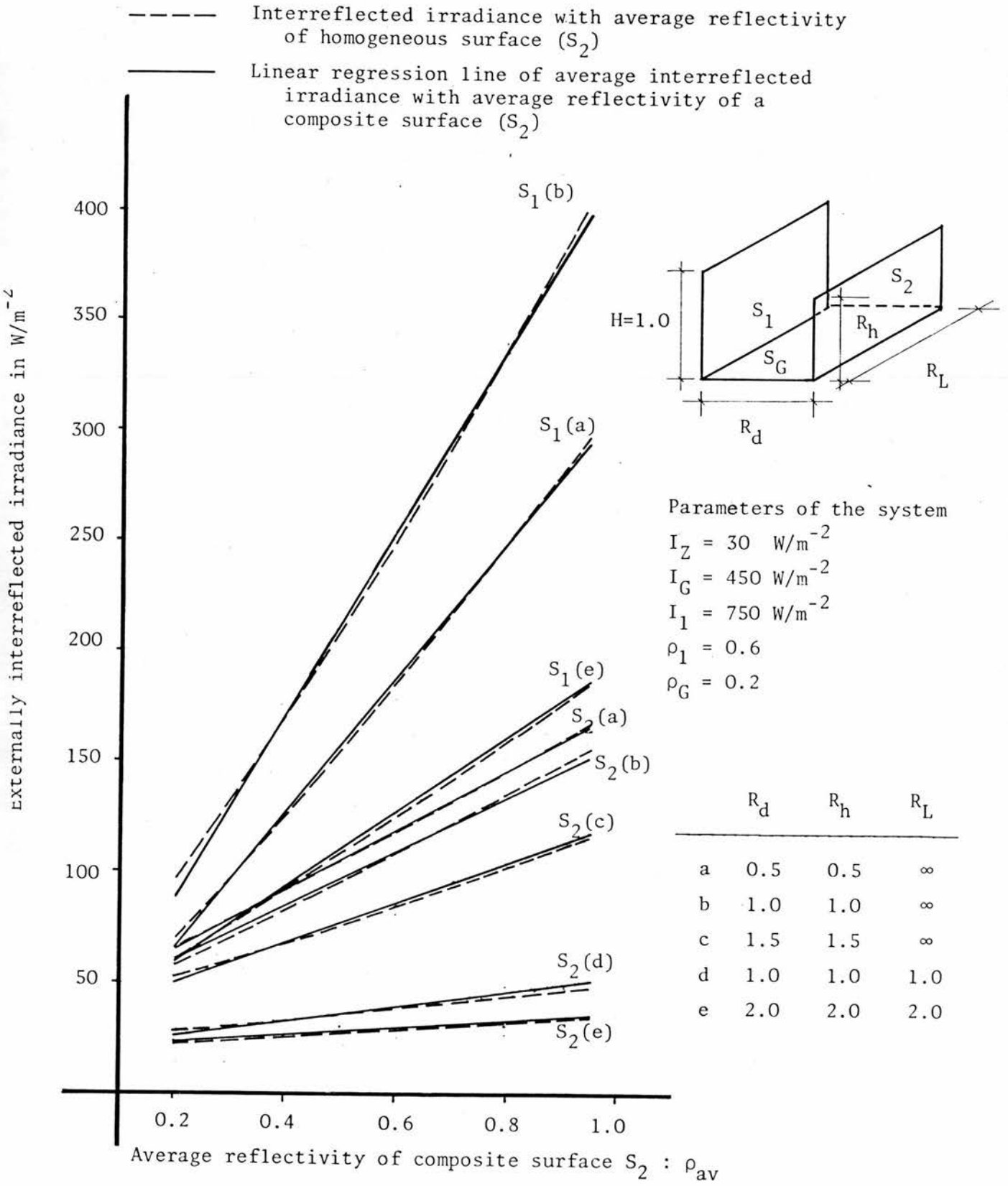
$$\rho_{av} = \frac{\sum_{i=1}^n \rho_i \cdot A_i}{\sum A_i} \quad \dots 5.3$$

where A_i is the area of a material used on the facade and ρ_i its reflectance.

3.1.2 The model was used to verify the use of the average reflectance for the calculation of the interreflected irradiance of the external surfaces. Systems of finitely and infinitely long parallel opposing facades of different proportions of height and width apart were investigated. A composite facade was taken to be represented by a number of elements of different area proportions and reflectance. The interreflected irradiance on the surfaces of the system was calculated with both the average reflectance and the facade taken as one unit and then with the set of reflectance and the facade as made of different elements. The two sets of data obtained for the vertical surfaces are shown by the diagram of Figure 5.2. The interreflected irradiance is taken as the average per unit area of the surface.

Figure 5.2

Comparison between the variation of the externally interreflected irradiance with average and homogeneous reflectivity of vertical facade.



3.1.3 Linear regression was used for simple representation of the relation between the interreflected irradiance and the average reflectance of the composite facade as it is difficult to establish the non-linear regression relation from the scattered data. It was found that, for the range of geometrical proportions used for the form, the relation is nearly linear.

3.1.4 As seen from the graphs in Figure 5.2, it was found that the two sets of data, for the average reflected irradiance per unit area of facade, were in good agreement. The reflected irradiance calculated with the weighted average reflectance appears to represent the regression line for the average reflected irradiance data derived from the inter-reflection of the different elements of the composite facade. The variation of the data is within the range ± 4 percent. Hence, in case of the composite facade its weighted average reflectance will be used for the calculation of the inter-reflected irradiance.

3.2 The Weighted Average Initial Irradiance of Facade

3.2.1 The following equations, which were presented earlier in Chapter II by equation 2.28 and 2.29, express the weighted average initial irradiance of a surface with different patches of shadow cast on it.

$$SF_{av} = \frac{\sum_{i=1}^n S F_i \cdot A_{si}}{A}$$

$$I_I = I_{GS} (1 - SF_{av})$$

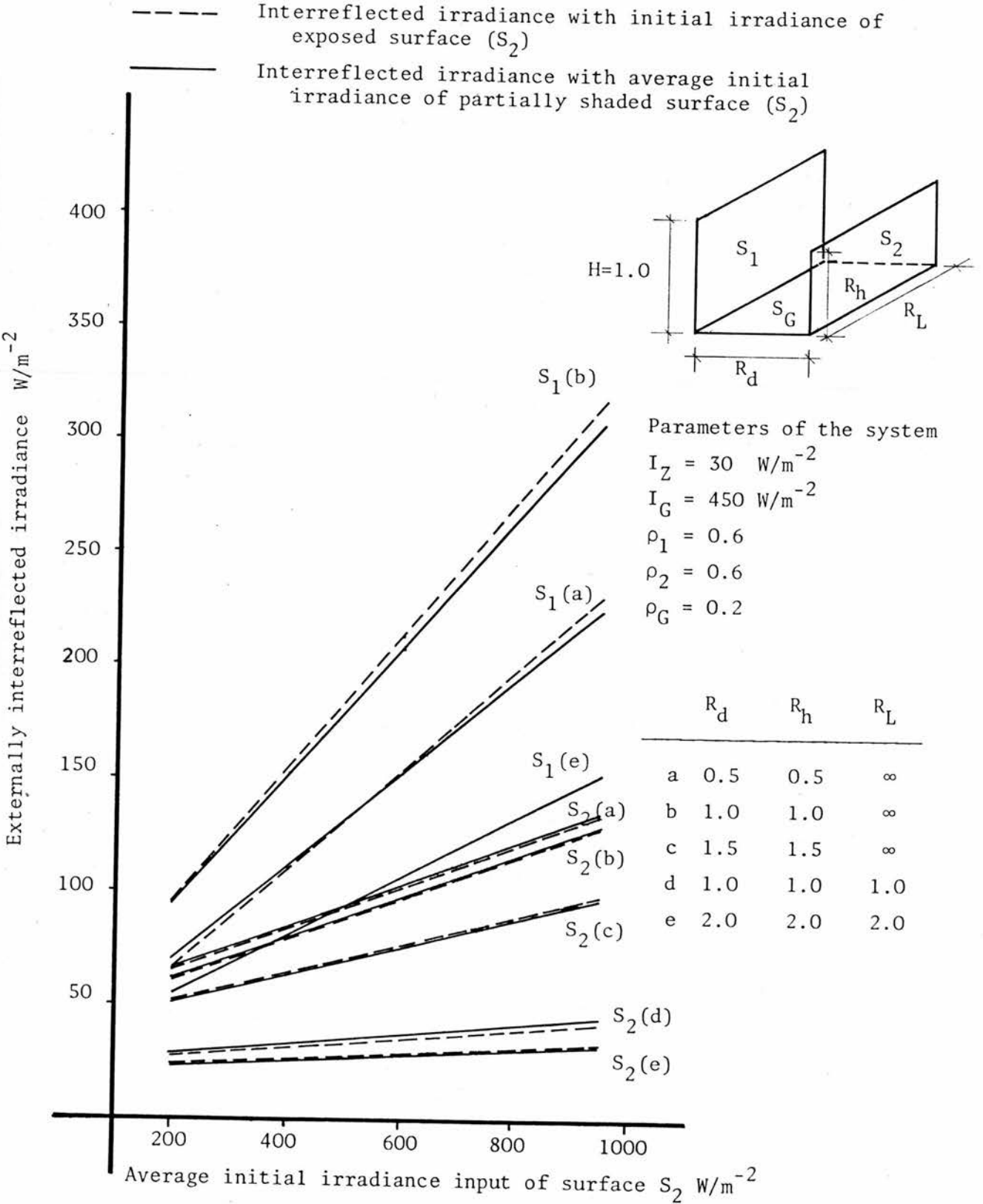
The output of the model was evaluated with a vertical facade taken to experience different patches of shadow of varying intensity and area proportions. Two sets of data for the interreflected irradiance of the vertical facades were obtained.

- (i) The average reflected irradiance per unit area of the facade was first calculated with the different patches of shadow taken as separate units with separate initial irradiance .
- (ii) The second set was obtained using the area weighted average initial irradiance with the facade regarded as one unit.

3.2.2 The relation between the reflected and initial irradiance is expressed by the linear regression lines shown in Figure 5.3. The graphs clearly show that there is no significant difference between the average reflected irradiance per unit area calculated with either the weighted average initial irradiance or with the initial irradiance of the different patches of the facade.

Figure 5.3

Comparison between the variations of the externally interreflected irradiance with average initial irradiance of fully exposed and partially shaded vertical facade.



3.2.3 Values of the obstructed sky component R_{ob} are required for the calculation of the diffuse and initial irradiance received on the different parts of the building facades and the ground between them. The calculation is greatly simplified by taking a single value for R_{ob} , for each part of the facades. R_{ob} is determined at an appropriate reference point on the surface and is regarded as a typical average value for the corresponding part of the surface. This procedure was verified to be sufficiently accurate as illustrated by the example shown in Figure 5.4. The diffuse, initial and final irradiances were calculated at different points over the height of a vertical facade, which is being partially obstructed by an opposing facade. From these, average values for the diffuse, initial and final irradiances were obtained for the unobstructed part of the surface. These were found to be in good agreement with the values calculated at the reference point, as shown in Figure 5.4.

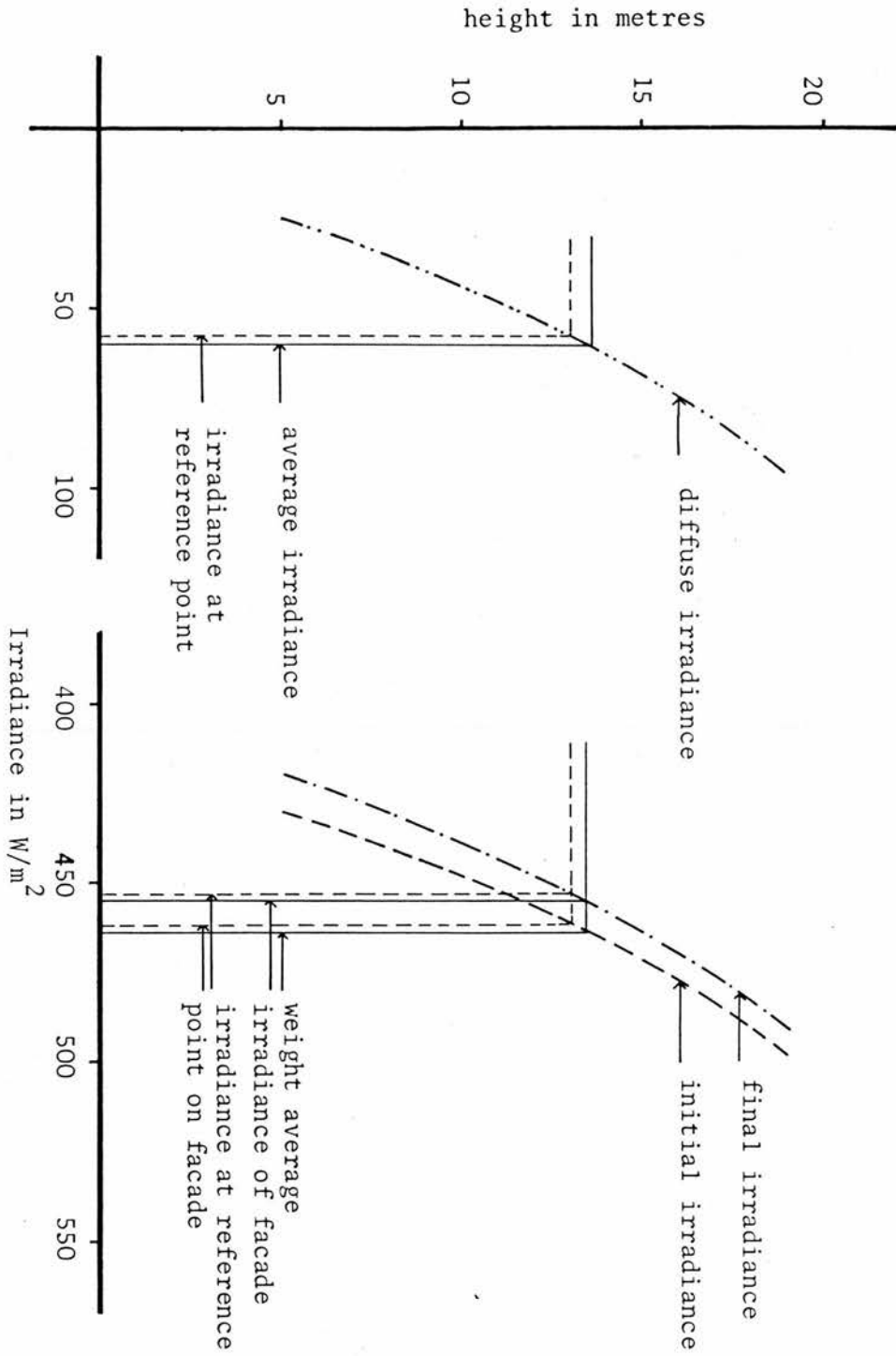
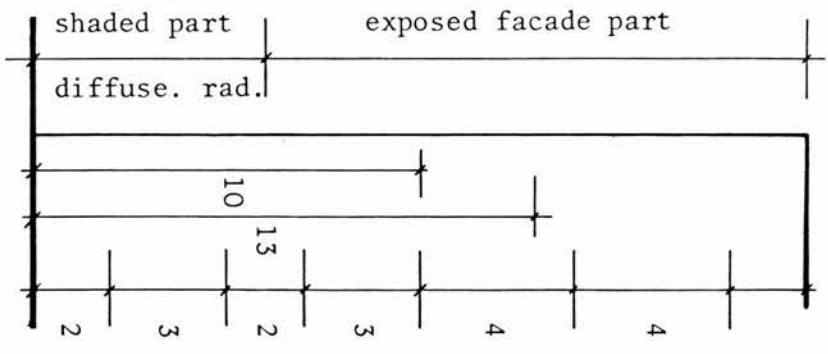


Figure 5.4 Variation of irradiance with height of facade and the comparison between the average irradiance and the irradiance at a reference point



Location of reference points on the facade

4. THE OVERALL PERFORMANCE AND ACCURACY OF THE MODEL

4.1.1 With the different postulations adopted in the formulation of the mathematical model and the approximate procedures used in evaluating its output, it remains to verify that the overall performance and accuracy of the model correlate closely with those of a real physical system. This determines the usefulness and reliability of the model. This can be achieved by evaluating the output of the model and noting its variation, with the variation of the system's parameters, in situations where the pattern of variation is known accurately at the limits.

4.1.2 This may be demonstrated by following the variation of the obstruction angle. Two main forms of variation can be expected in the initial and final irradiance patterns of the surfaces of a system, which is composed of two vertically opposing facades and the ground separating them, due to the variation of the obstruction angle, γ_{om} .

(i) The first case deals with the decrease in the obstruction angle as it approaches its lower limit (zero). Such situations are encountered when the opposing facade is either being drawn further away or its height is being reduced. The initial irradiances of the vertical facade and ground approach their maximum values which correspond to those of fully exposed surfaces.

The form factors between the vertical surface and the ground and the opposing facade decrease with the decrease of the

obstruction angle. Hence, the interreflection component from the opposing facade decreases accordingly. At a zero degree obstruction angle the interreflection is restricted to the irradiance exchange between the ground and the vertical facade.

(ii) The second case follows the variation of the irradiance with the increase of the obstruction angle as it approaches its upper limit of 90° . This represents the situation where the obstructing surface is drawn near or its height is increased. The initial irradiance of the vertical facade and the ground approaches zero. The interreflected irradiance is dominated by the reflected irradiance from the vertical facade.

4.1.3 These situations were simulated by the model. The initial and final irradiances of the surfaces were evaluated for different obstruction angles. The results obtained are presented in the diagram in Figure 5.5. It is evident from the graphs shown that the computed initial and final irradiance of the vertical surface approach their corresponding maximum and minimum values asymptotically towards the two limits of the obstruction angle. Similarly, the initial and final irradiance of the ground surface, for the range of the obstruction angle considered, appear to follow the same pattern with no indication to suggest otherwise. It may be concluded then that the performance of the mathematical model follows accurately that of the real physical system.

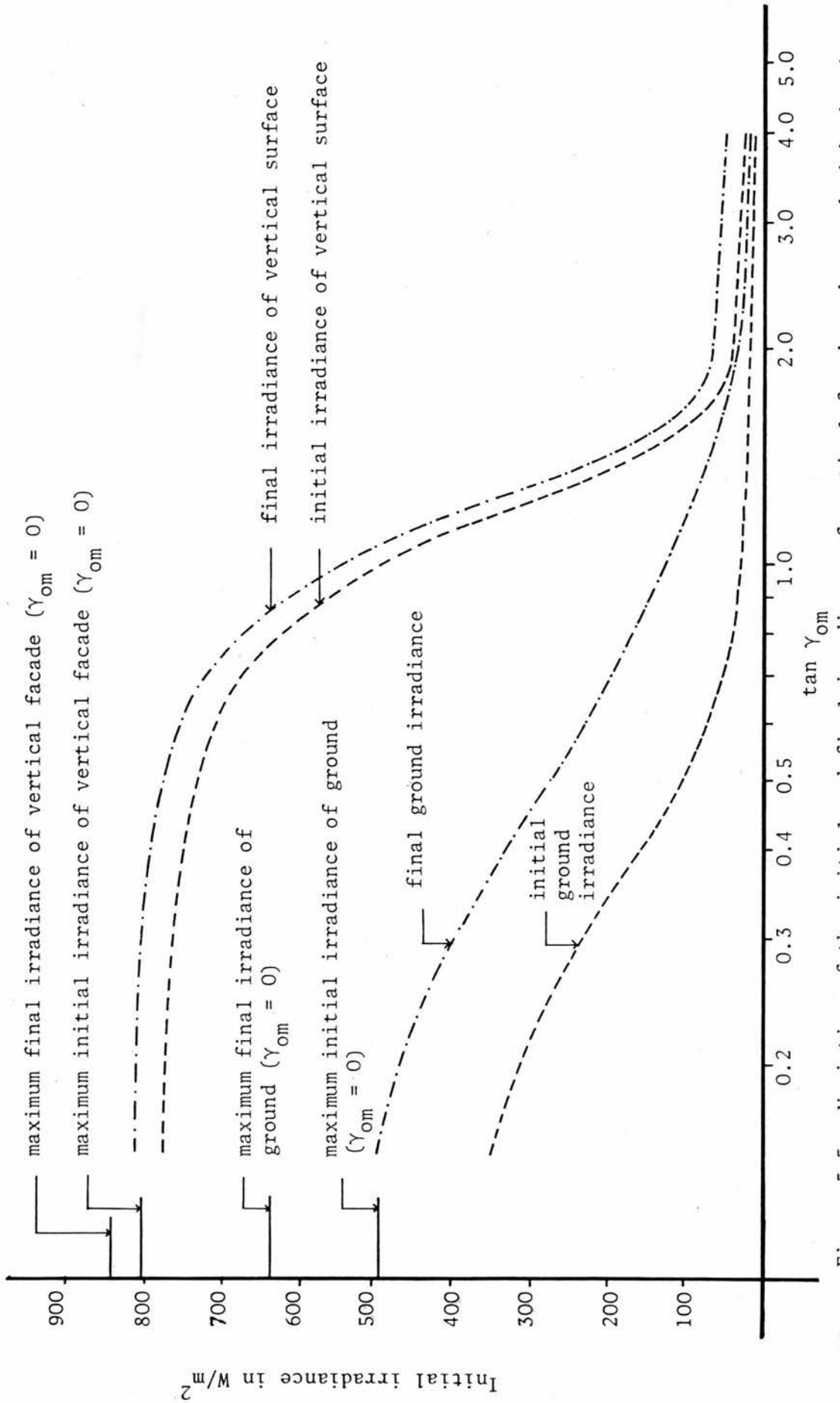


Figure 5.5 Variation of the initial and final irradiance of vertical facade and ground with the obstruction angle

CHAPTER VI

INVESTIGATION WITH THE MODEL :
THE EFFECTS OF ORIENTATION, PLAN PROPORTION AND
CONFIGURATION OF FORM AND SURROUNDINGS ON
THE INITIAL IRRADIANCE LOAD

INVESTIGATION WITH THE MODEL : THE EFFECTS OF ORIENTATION, PLAN PROPORTION AND CONFIGURATION OF FORM AND SURROUNDINGS ON THE INITIAL IRRADIANCE LOAD

1. INTRODUCTION

1.1.1 A primary objective for constructing the model was to carry out systematic and detailed investigations.

These reveal facts pertaining to the model's output at any level of detail. They also provide simplified and readily available information for practical application by the designer. This task may be conveniently simplified by evaluating and analysing the output at two main levels of detail with regard to the initial and final irradiance.

1.1.2 The theoretical analysis discussed earlier, in part 9 of Chapter II, showed the direct proportionality of the final irradiance to the initial irradiance. This indicated the possibility of analysing and defining orientation, plan proportion and form configuration in terms of the initial irradiance load on the surfaces of buildings. Therefore, the discussion which follows in this chapter is mainly concerned with the initial irradiance level of the output of the model.

1.1.3 Prior to generating the output data it was essential to define two main points :

- (i) The hourly, daily and seasonal variability of the initial irradiance load and its distribution over the surfaces necessitate a yard-stick for measuring the overall initial irradiance load and verifying the performances of forms. The yearly and daily total were found to lend themselves as useful measures for hot sunny regions.
- (ii) Within the time of this study, it was only practical to study a limited number of cases of possible combinations of form configurations and arrangements of building blocks. It was therefore decided to tackle the most common. However limited an objective this may achieve, nonetheless it illustrates the application of the model in such studies and derives general conclusions for the common cases. Any further investigations for specific cases may then be carried out along similar lines.

1.1.4 On this basis the initial irradiance data was generated for a wide range and combinations of form parameters. This was carried out in two stages. The first stage dealt with the individual surfaces of the form, mainly vertical and horizontal surfaces. The analysis of the data was mainly concerned with the following :

- (i) illustrating the patterns of distribution of the output with the variation of the parameters of the form,
- (ii) defining the ranges of parameters within which they significantly influence the output,
- (iii) formulating the interrelationships between the output and the form's parameters, and
- (iv) deriving measures, indices and performance specifications of building surfaces and forms.

1.1.5 One main advantage that can be drawn from such information and findings is their direct utilization to simplify the formulation and the calculation procedures of the model and the estimation of the initial irradiance load on buildings. In addition to this they also provide the means for the development of building regulations, design aids and indicators for planning control. This was illustrated by the development of irradiance indices and shadow factor indicators.

1.1.6 The second stage of the initial irradiance load investigations dealt with the yearly total load received on the external surfaces of buildings. Rectangular building blocks mainly were studied. The model was

used to generate a wide variety of building blocks for alternative configurations of surroundings and evaluate their total initial irradiance load. Minimum irradiance load and maximum shadow factor were used as criteria for defining the form's geometry. On this basis the proportions of the block sides at the different orientations, configuration of surroundings and street widths were investigated.

2. EVALUATION OF THE SURFACES INITIAL IRRADIANCE LOAD

2.1 Measures of the Surface's Irradiance Input

2.1.1 Different irradiance quantities have been used previously in the evaluation of orientation, plan proportion and the thermal form's performance. These resulted from the different methods and concepts adopted for the computation and the adaption of the irradiance data for the various climatic conditions which were studied.

2.1.2 In climates that are characterised by hot summers and cold winters, it is desirable to minimise the irradiance input during the summer months and to maximise it during the winter. The numerous studies related to these conditions may be classified into three main categories :

- (i) The studies of Valko (1969) estimated the instantaneous irradiance load per unit area of the form for various solar positions.
- (ii) The investigations by Buchburgh and Naruishi (1966, 1967) and by Valko (1972) were based on the daily total irradiance energy received per unit area. The daily total irradiance was calculated for different times of the year.

(iii) Olgyay (1967, 1969) used the direct solar irradiance as the yard-stick. He calculated the total yearly direct average irradiance per unit area for the overheated and underheated periods. These periods were defined by the air temperature above or below 21°C respectively. Tappuni (1973) used the same concept, but included the diffuse sky and ground reflected irradiance.

2.1.3 In hot arid regions such as Khartoum the intensity and duration of the solar irradiance is characteristically high throughout the year. The air temperature is generally above 21°C , which is regarded as the upper comfort limit, apart from the early hours of winter days. Accordingly, the studies in these regions were justifiably concerned with minimising the yearly total irradiance load on the surfaces of buildings. This may be illustrated by the investigations by Kuba (1969) to establish a minimum thermal axis. He used the yearly total irradiance per unit area as the yard-stick and this has also been adopted for the present study.

2.2 The Average Daily Total as a Measure of Irradiance Input of Surfaces

2.2:1 The main shortcoming of the studies discussed above is that the buildings were treated as free-standing

isolated units. They did not take into consideration the shading and obstruction of the direct and diffuse irradiance by surrounding buildings and external inter-reflections. Therefore, for an accurate assessment of the irradiance input of the surfaces, the calculation in this study has been based on the initial irradiance. This takes into consideration those factors which determine the initial irradiance input. The yearly total was evaluated for the initial irradiance input. This was calculated from the hourly initial irradiance for all hours of sunshine (from sunrise to sunset) for each day throughout the year. It is expressed by the function

$$I_{yt} = \sum_{\text{sunrise}}^{\text{sunset}} \sum_{\text{1st Jan.}}^{\text{31st Dec.}} I_I \quad \dots 6.1$$

As this yields large figures of many digits the presentation and handling of the initial irradiance data has been simplified by using the daily total average irradiance input. This is obtained by the expression

$$I_{dt} = I_{yt}/365 \quad \dots 6.2$$

The average hourly distribution of the initial irradiance of a surface is similarly obtained from the total hourly values calculated over the year.

2.2.2 The irradiance calculations were performed by the subroutine IRRILL which was described earlier in Chapter IV. These were carried out for Khartoum as an example of a typical hot arid site. Khartoum is located at Latitude 16°N and Longitude 32°E . The latitude and longitude were specified to the programme together with the parameters defining the configuration of the geometrical form and its surfaces. As seen from appendix A.1, the sunshine hours for Khartoum are mainly between 6.00 and 18.00 hours. The daily total is calculated between these two units at hourly intervals. This was carried out for two days in the month, towards the end of the first and third weeks. This allows the calculation to be performed at 15-day intervals from the beginning of the year. This gives more accurate and representative data for the average monthly total than does taking one day for each month as in previous work (Buchburgh 1966, 1967, Olgyay 1967, 1969, Tappuni 1973).

3. INITIAL IRRADIANCE AND THE GEOMETRICAL PARAMETERS OF FORM

3.1 Configuration and Ranges of Form Parameters

3.1.1 The magnitude of the initial irradiance is determined by the geometrical configurations of the form. Prior to evaluation of the initial irradiance input it is necessary to define the form and layout of building blocks and the representation of their geometrical parameters. The most common form and arrangement of buildings was considered. These represented rectangular blocks arranged in parallel rows. The streets separating the blocks were taken to be of equal width. This rectilinear layout is illustrated by Figure 6.1.

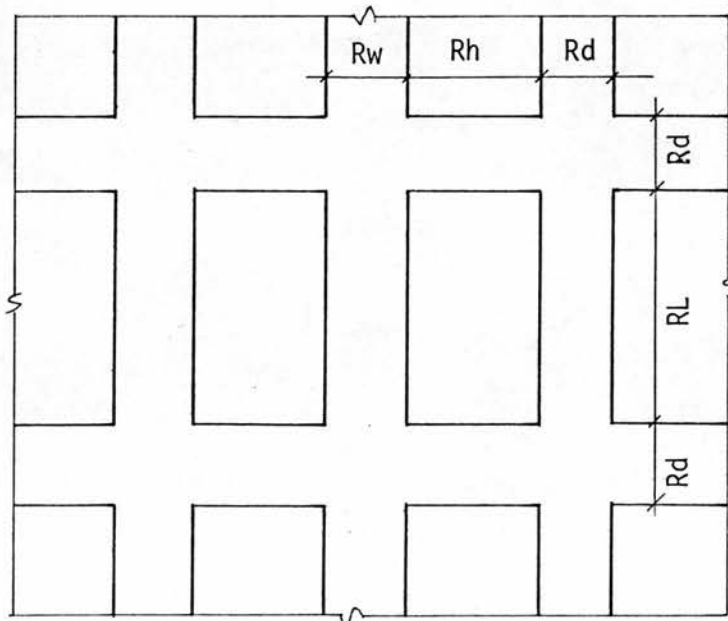


Figure 6.1 Arrangement of Building Blocks

3.1.2 The dimensional parameters of the form may be expressed in a simple format in terms of the height of the block. The block length and width are then specified by the proportions RL , Rw . These are obtained by the functions

$$RL = L/H \quad \dots 6.3(a)$$

$$Rw = W/H \quad \dots 6.3(b)$$

L and w are the length and width of the block. The street width is similarly expressed

$$Rd = D/H \quad \dots 6.3(c)$$

3.1.3 The obstruction to a vertical facade or ground is determined by the height and the separating distance of the opposing facade. A simple measure of the obstruction may be expressed by the maximum obstruction angle of the vertical surface γ_{om} rather than defining it in terms of the obstruction height. It is the angle subtended by the ground and the line joining the bottom of the vertical facade and top level of its opposing facade as illustrated by the diagram of Figure 6.2. The advantage of this procedure is that it easily allows the definition of the limits of the obstruction. The vertical and ground surfaces are completely obstructed when γ_{om} is equal to 90° and fully exposed at γ_{om} equal to zero. The height proportion of

the opposing facade is then determined by the street width and the obstruction angle γ_{om} by the expression

$$R_h = R_d \cdot \tan \cdot \gamma_{om} \quad \dots \quad 6.4$$

The appropriate reference points on the vertical and the horizontal surfaces and the corresponding elevation angles of obstruction γ_{ob} needed for the evaluation of the obstructed sky component are then determined by the equations and the procedure outlined earlier in part 5.2 of Chapter III.

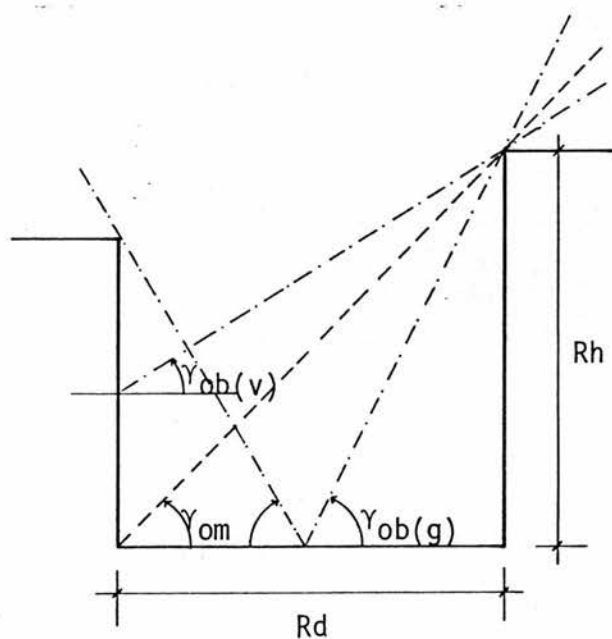


Figure 6.2 The Altitude Obstruction Angle of the Vertical Facade

3.1.4 The geometrical configuration of the form was then defined by the orientation angle α_s , the obstruction angle γ_{om} , the proportion of facade length RL and the proportion of

the street width R_d . The initial irradiance of the vertical and ground surface was evaluated for the different combinations of these parameters. The parameters were considered for the following ranges :

- (i) R_d and R_L were taken from 0.25 to 8 at 0.25 intervals. The limits of the range were taken to comply with the most common practical situation.
- (ii) γ_{om} was taken from 0 to 90° at 15° intervals.
- (iii) α_s was taken from 0 to 180° at 15° intervals. It was not necessary to consider the orientation within the range from 180° to 360° because of the symmetry of the irradiance distribution of the vertical and ground surfaces along the N-S axis.

3.2 The Evaluation of the Initial Irradiance of Vertical and Horizontal Surfaces

3.2.1 It can be shown that for the rectilinear arrangement of blocks that the vertical facades of the blocks of the same orientation will have similar shadow patterns at any time of the day. As the magnitude of the daily average initial irradiance is the same for those facades, it was only evaluated for one facade for the different combinations of the parameters. Accordingly, the irradiance of the

different facades of the block and their corresponding opposing facades may then be determined according to their orientation and obstruction angles.

3.2.2 Similarly, a regular pattern of shadow will be cast on the ground area separating the blocks. The horizontal daily average irradiance was then calculated for that part of the street in front of the facade and the adjoining intersections. This is illustrated by the diagram in Figure 6.3.

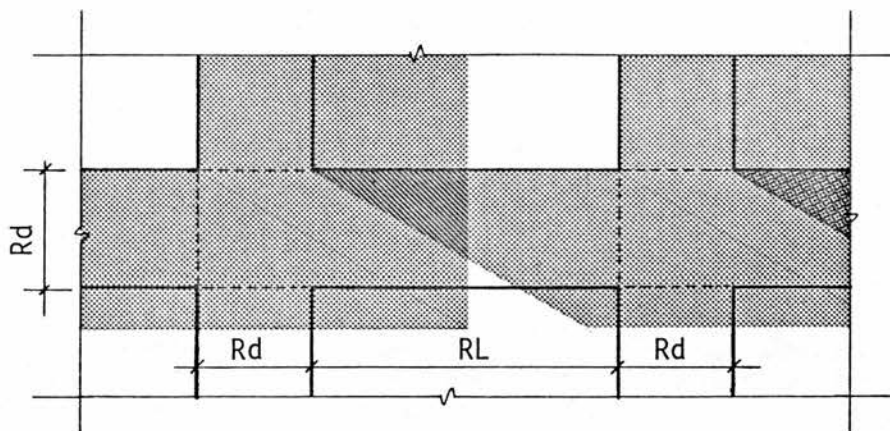


Figure 6.3 The Street Part Used for Calculating the Average Irradiance of Ground Area

This gives the average irradiance/unit area for the whole street.

3.2.3 Two sets of initial irradiance data were prepared for the vertical and horizontal surfaces for the different combination and range of the form parameters. The corresponding shadow factor data was prepared in a similar way.

4. ANALYSIS OF THE VARIATION AND DISTRIBUTION OF THE AVERAGE DAILY TOTAL INITIAL IRRADIANCE WITH THE GEOMETRICAL PARAMETERS OF FORM

4.1 The Distribution of the Initial Irradiance of the Vertical Surface

4.1.1 In the model studied, the height of an opposing facade at any obstruction angle γ_{om} , was determined by the street width, as expressed by equation 6.4 given above. Accordingly, it can be shown that the shadow factor of vertical surfaces is also determined by the street width proportion Rd . This may be illustrated by the case of infinitely long surfaces which was expressed by equation 3.34(b), given earlier in Chapter III. The equation may then be written in the form

$$SF = Rd [\tan \gamma_{om} - \tan \gamma_0 / \cos(\alpha_0 - \alpha_s)] \quad \dots 6.5$$

It was therefore expected that the average shadow factor of the vertical facade SF_{av} increases with the increase of Rd . The corresponding initial irradiance decreases accordingly.

4.1.2 However, building facades are of finite length. The intersecting streets therefore create gaps in the opposing facades. Obviously, these gaps will expose extra parts of the facade to the direct solar rays. They also admit extra amounts of the diffuse sky radiation. The form, location and area of this exposed part of the facade is determined by the

form of the shadow cast on it. This is governed by the geometrical parameters of the form and the sun. However, the wider the gap and the greater the surface-solar azimuth, the greater is the area of the exposed part of this facade. It can be argued that the width of the exposed part of a facade may remain constant beyond certain units of RL, with the maximum possible width equal to that of the street Rd at any particular time and date. This is illustrated by the diagram in Figure 6.4.

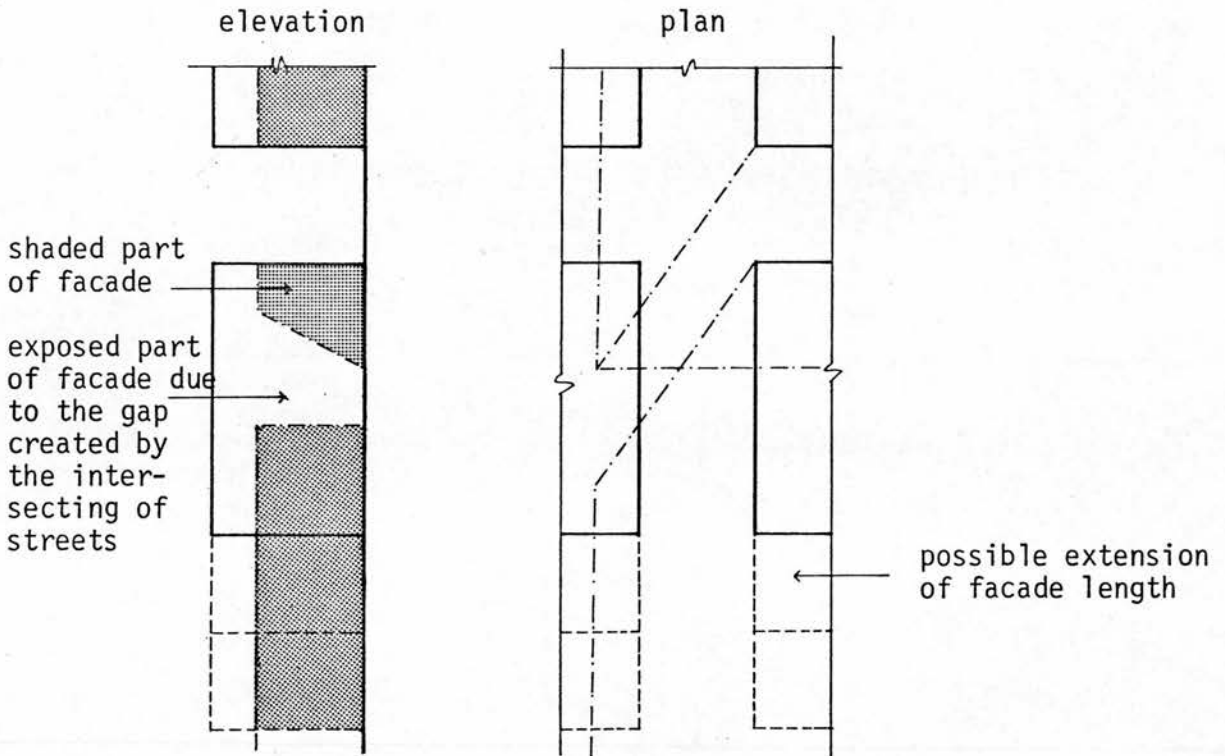


Figure 6.4 Example of the Geometry of the Shaded and Exposed Parts of a Vertical Facade

Therefore, the ratio of the exposed part of the facade to the total area approaches that of an infinitely long facade with the increase of RL.

4.1.3 The above discussion indicates that the initial irradiance of the vertical facade is governed by complex interrelationships between the geometrical parameters of the form. It may be argued therefore, that it is more practical to define the general form of these interrelationships and the ranges within which the different parameters of form may significantly influence the distribution of I_{dt} . This may be illustrated by considering the variations of I_{dt} and SF_{av} for a number of combinations of the form's parameters.

4.1.4 The distribution of I_{dt} with Rd : A general picture of this may be simply illustrated by considering the variation of the average I_{dt} and its corresponding SF_{av} with Rd . The averages were calculated from their individual values obtained for the different orientations of the vertical facade. The average SF_{av} was plotted against Rd for different obstruction angles and for RL equal to 1 and ∞ , as illustrated by the diagram in Figure 6.5. The graphs show that at a low obstruction angle, eg, γ_{om} up to 30° , SF_{av} increases gradually with Rd . The increase is more significant with Rd up to 4 than with Rd greater than that. At higher obstruction angles, eg, $\gamma_{om} > 30^{\circ}$, it may be possible to distinguish two ranges of Rd which show distinct patterns of variation of SF_{av} with Rd :

- (i) In the first range SF_{av} increases rapidly with Rd . It reaches its maximum at the upper limit of Rd

for this range. The upper limit of R_d decreases gradually with the increase of γ_{om} . For γ_{om} equal to 45° the R_d upper limit is about 2.5 and the corresponding maximum SF_{av} is about 30 percent. Similarly, for γ_{om} 60° and 75° the R_d limits are 1.5 and 1.0 with maximum SF_{av} about 50 percent and 75 percent respectively.

- (ii) In the second range, the SF_{av} decreases or increases gradually with R_d . The pattern of variation in this range is determined by the length proportion parameter. The SF_{av} of facades with greater length proportions, eg, $RL = \infty$, generally increases gradually with R_d . In the case of smaller length proportions such as $RL = 1$, SF_{av} decreases with the increase of R_d up to a point where $R_d \approx 4.0$. After that it increases gradually. The difference between the maximum SF_{av} values at the upper limit of the first range and those at $R_d \approx 4.0$ is also influenced by γ_{om} . This is more significant at higher obstruction angles, eg, $\gamma_{om} = 75^\circ$, than at intermediate angles, eg, $\gamma_{om} = 45^\circ$. The patterns of variation of SF_{av} with R_d within this range may be interpreted as caused by the extra irradiance of the vertical facade which was admitted through the gaps in the opposing facades. It indicates that the magnitude of this irradiance

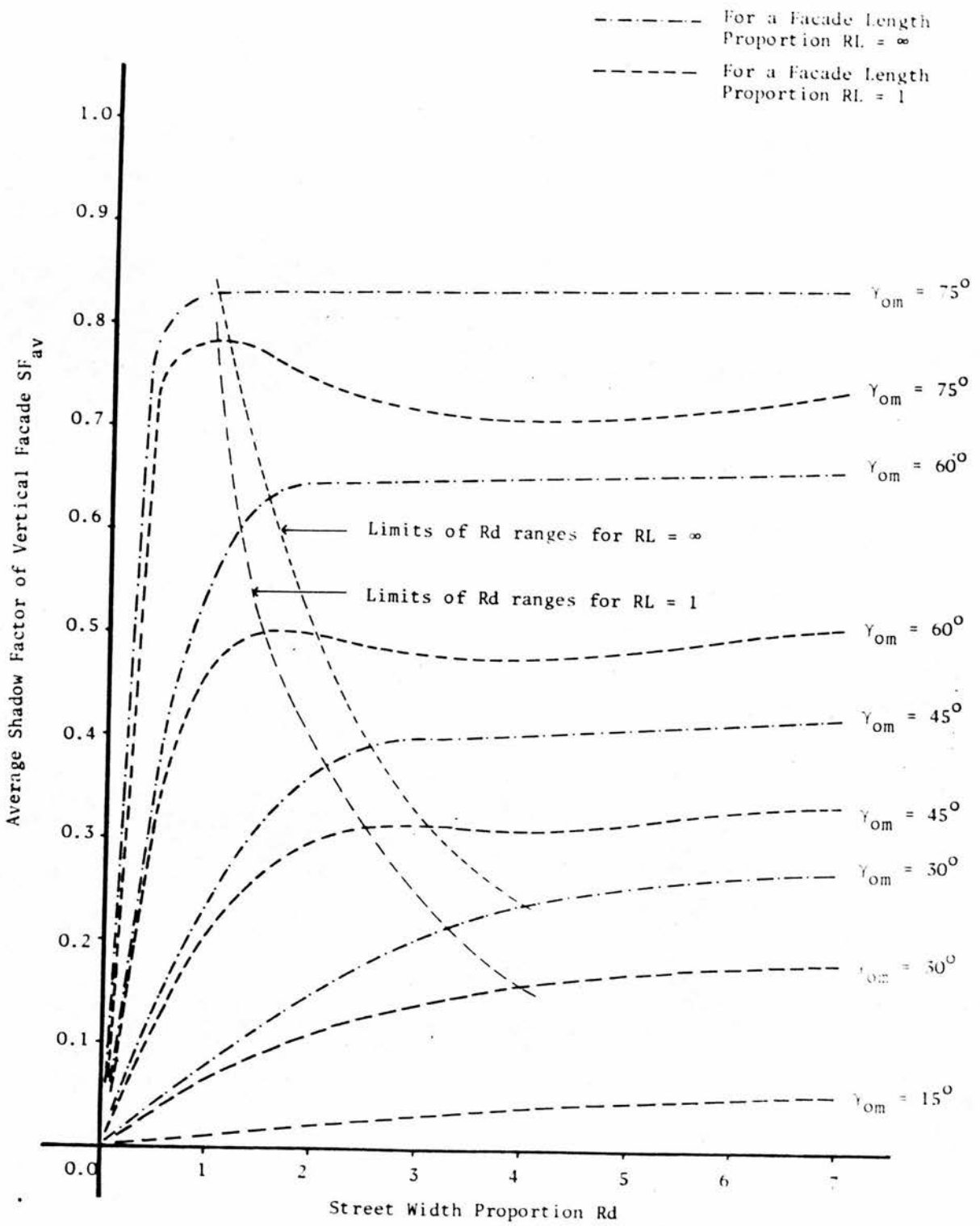


Figure 6.5 The Distribution of the Average Shadow Factor of the Vertical Facade with the Street Width Proportion R_d , for a Number of Obstruction Angles

is most significant at R_d about 4.0. From the patterns of distribution of SF_{av} with R_d which were defined above, it is therefore simple to deduce the distribution of the corresponding I_{dt} . In this sense I_{dt} behaves in an opposite manner to the SF_{av} . That is, if SF_{av} increases, I_{dt} will be decreasing and vice versa.

4.1.5 The distribution of I_{dt} with orientation

Apart from the general form of the distribution of I_{dt} with R_d which was presented above, the actual form of this distribution is determined by the orientation angle of the facade. The polar charts shown by the diagrams in Figures 6.6 to 6.9 illustrate the azimuthal distribution of I_{dt} of a vertical facade, for a number of combinations of the form's parameters. In the charts shown, RL was limited to 1 and ∞ and R_d to a range up to 4. This seemed sufficient to present the most critical situations without confusing the presentation of the charts. From these charts, it is possible to establish the following main points which illustrate the range and significance of orientation in influencing the distribution of I_{dt} of the vertical surface.

- (i) Generally, I_{dt} increases with the orientation away from the North point up to a maximum and then decreases for the different combinations of R_d , RL and γ_{om} . For $\gamma_{om} \leq 45^\circ$ the maximum I_{dt} is received

towards an orientation angle α_s at 110° from North. For $\gamma_{om} > 45^\circ$ the distribution of I_{dt} with α_s shows a number of peaks at different α_s . For example, at $\gamma_{om} 60^\circ$ one peak corresponds to $\alpha_s 60^\circ$ with the peak for maximum I_{dt} at $\alpha_s 140^\circ$ from North. Similarly, at $\gamma_{om} 75^\circ$ the maximum is at about 85° with a second peak at 150° from North.

- (ii) At low obstruction angles, eg, $\gamma_{om} \leq 30^\circ$, I_{dt} decreases as **Rd increases**, for all orientations. However, at higher obstruction angles, eg, $\gamma_{om} \geq 45^\circ$, I_{dt} increases with Rd within its second range, which was defined earlier and illustrated by the diagram of Figure 6.5. At the same time, this increase is confined to a certain range of α_s . The azimuthal angular limits of the range are governed by the obstruction angles. For example, at $\gamma_{om} 45^\circ$ the range is between 60° and 135° from North. Similarly, the ranges for $\gamma_{om} 60^\circ$ and 75° are between 45° to 165° and between 45° to 180° from North respectively.

4.1.6 The distribution of I_{dt} with RL

The distribution of I_{dt} with RL at the different orientation angles showed the same patterns. Accordingly, the average I_{dt} was used to illustrate the typical pattern of distribution of I_{dt} with RL. The data for average I_{dt} was plotted against

Figure 6.6 Variation of the Daily Total Initial Irradiance of Vertical Facade with the Parameters of the Form : $RL = 1$

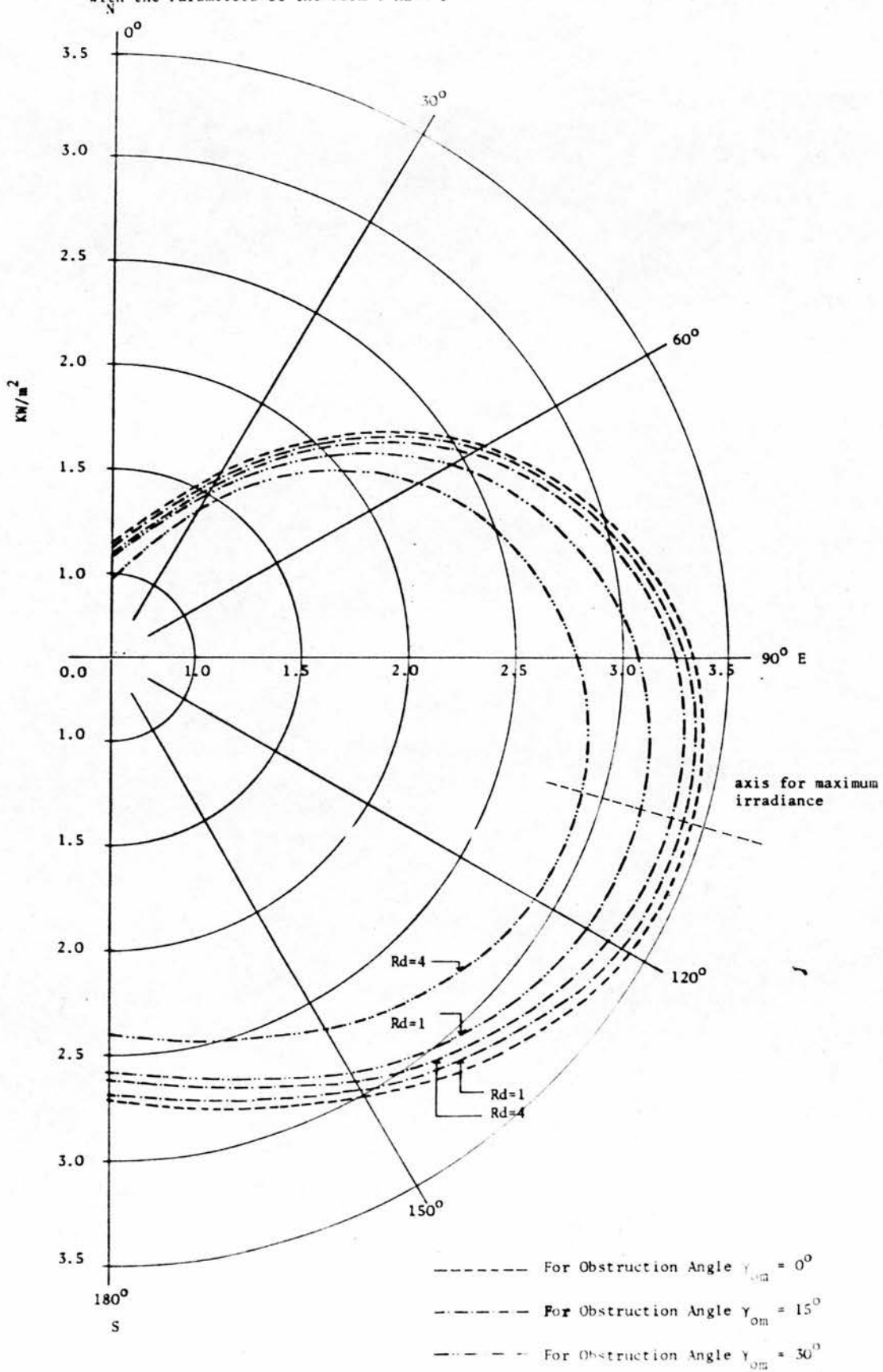


Figure 6.7 Variation of the Daily Total Initial Irradiance of Vertical Facade with the Parameters of the Form : $\gamma_{om} = 45^\circ$

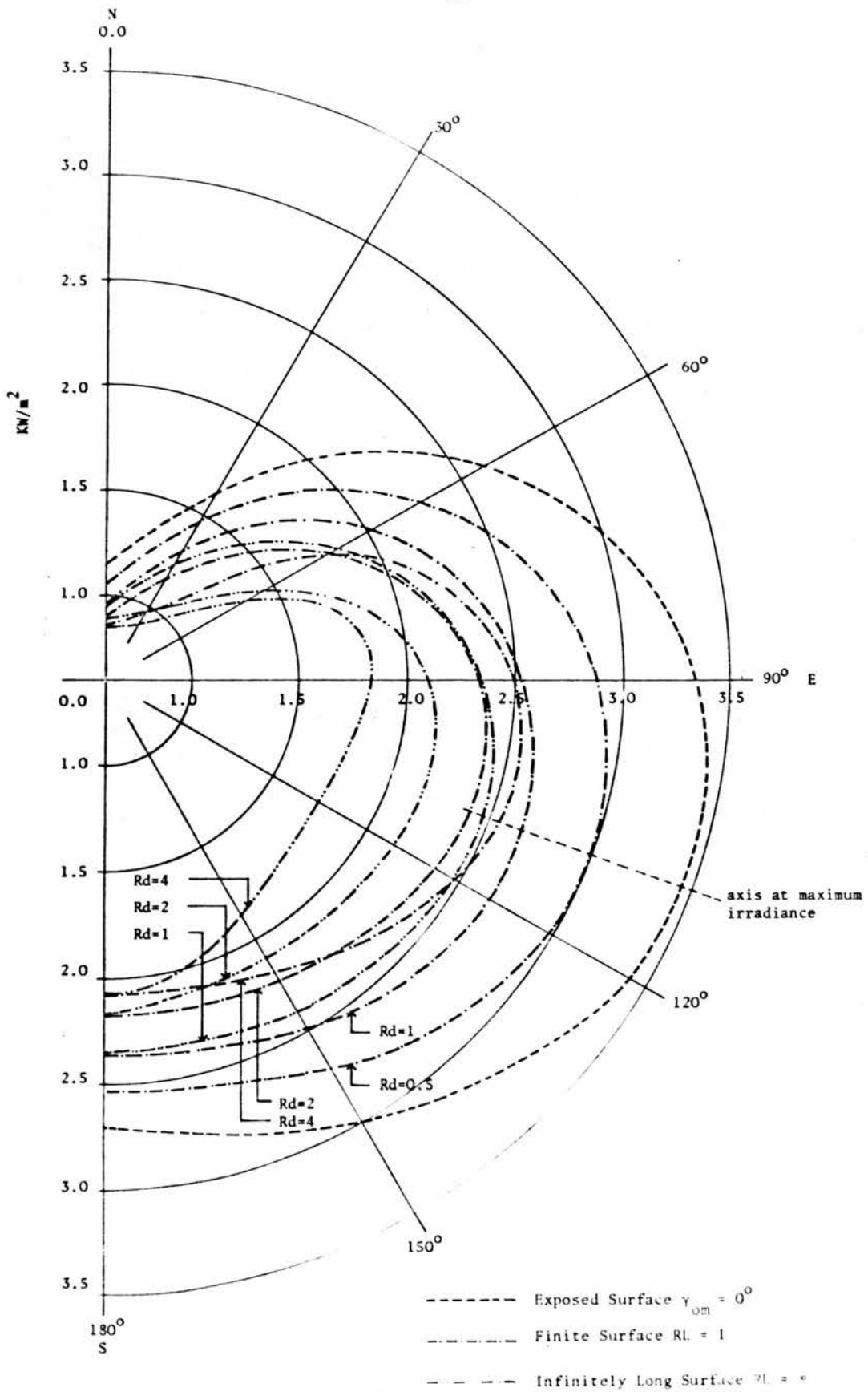


Figure 6.8 Variation of Daily Total Initial Irradiance of Vertical Facade with the Parameters of the Form : $\gamma_{om} = 60^\circ$

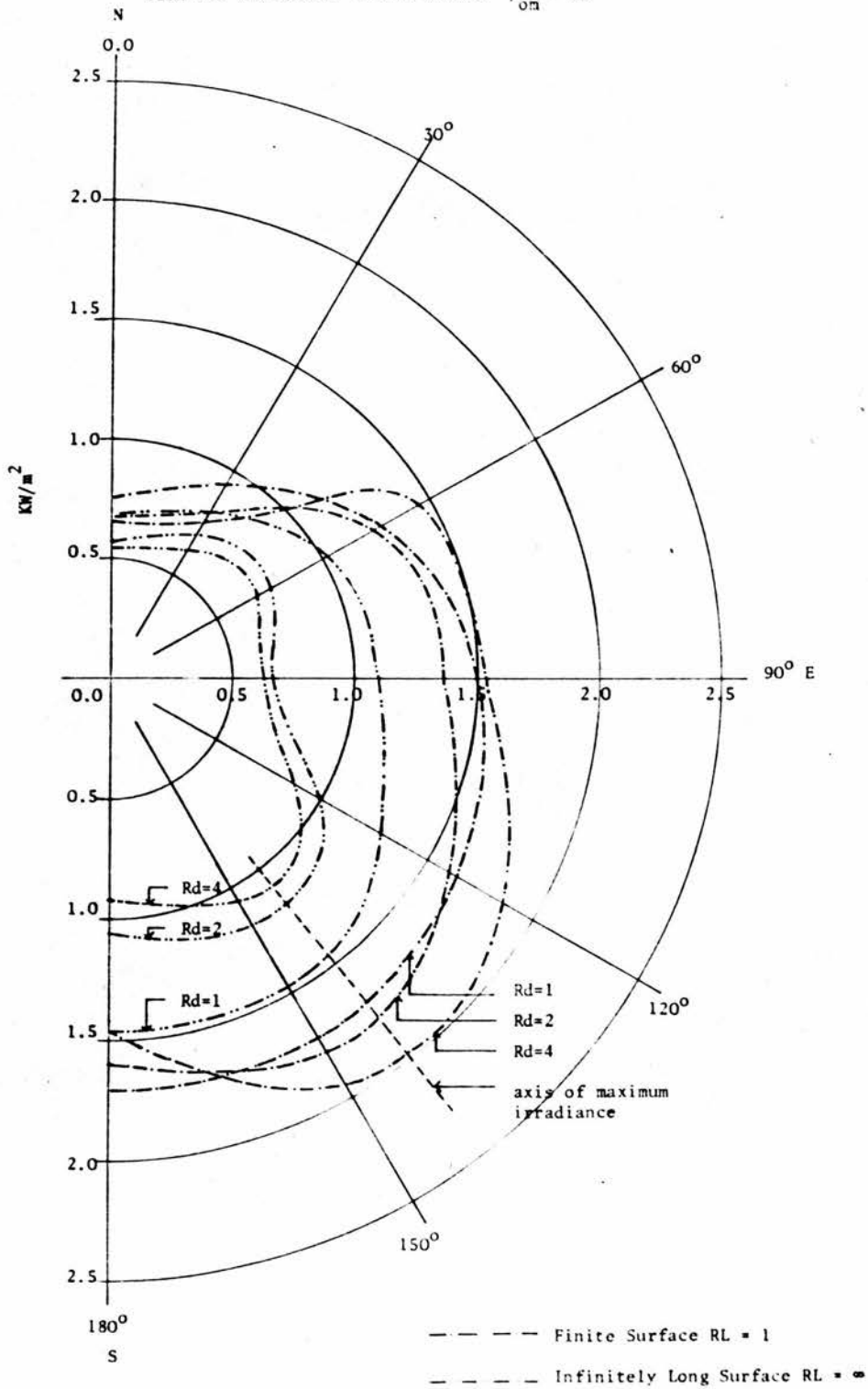
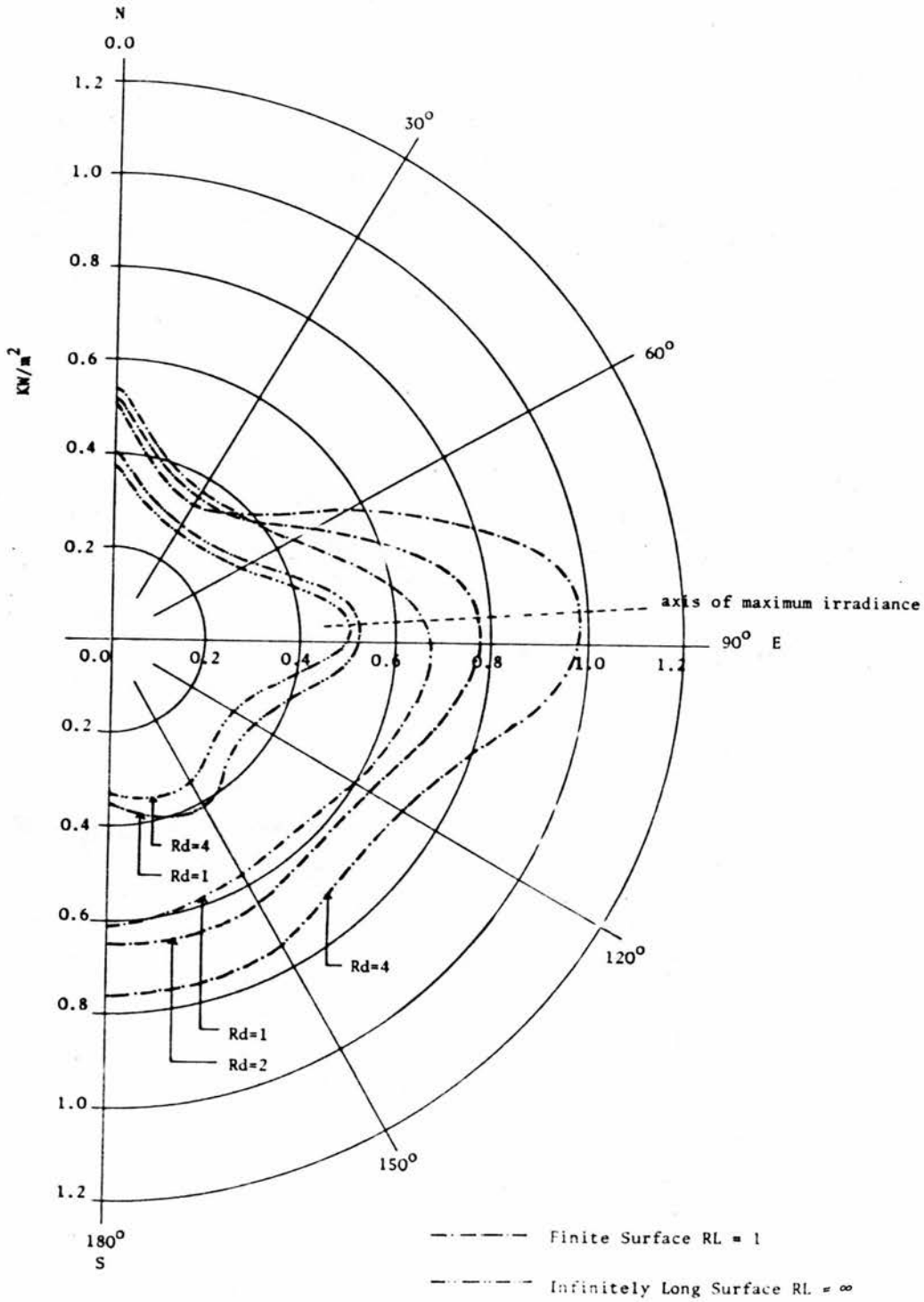


Figure 6.9 Variation of the Daily Total Initial Irradiance with the Parameters of the Form : $\gamma_{\text{um}} = 75^\circ$



RL for a number of combinations of R_d and γ_{om} . This is shown by the diagram in Figure 6.10. The graphs indicate the following main points :

- (i) At the lower range of RL, eg, $RL < 0.5$, I_{dt} generally increases with RL. The maximum of I_{dt} occurs at RL about 0.5. Beyond this range of RL, I_{dt} then decreases gradually with the increase of RL, approaching the value of I_{dt} when RL is infinitely long asymptotically. This pattern of distribution may be interpreted as due mainly to the varying proportion of the exposed part of the facade, caused by the gaps in the opposing facade, to the total area of the facade with the increase of RL.
- (ii) The range of RL within which the extra irradiance, coming through the gaps of the opposing facade, is most significant, is determined by proportion R_d and the obstruction angle γ_{om} . For $R_d = 1$, the significant range of RL is between 0.1 and 1.25. The range gets bigger with the increase of proportion R_d and γ_{om} . For example, in the case of $\gamma_{om} = 60^\circ$ the amount of I_{dt} received at RL equals 1 when R_d is 1 will be received at RL equals 2 when R_d is 4. Similarly, at $\gamma_{om} = 75^\circ$, I_{dt} received at RL and R_d equals 1 will be received at RL equals 3 when R_d is 4.

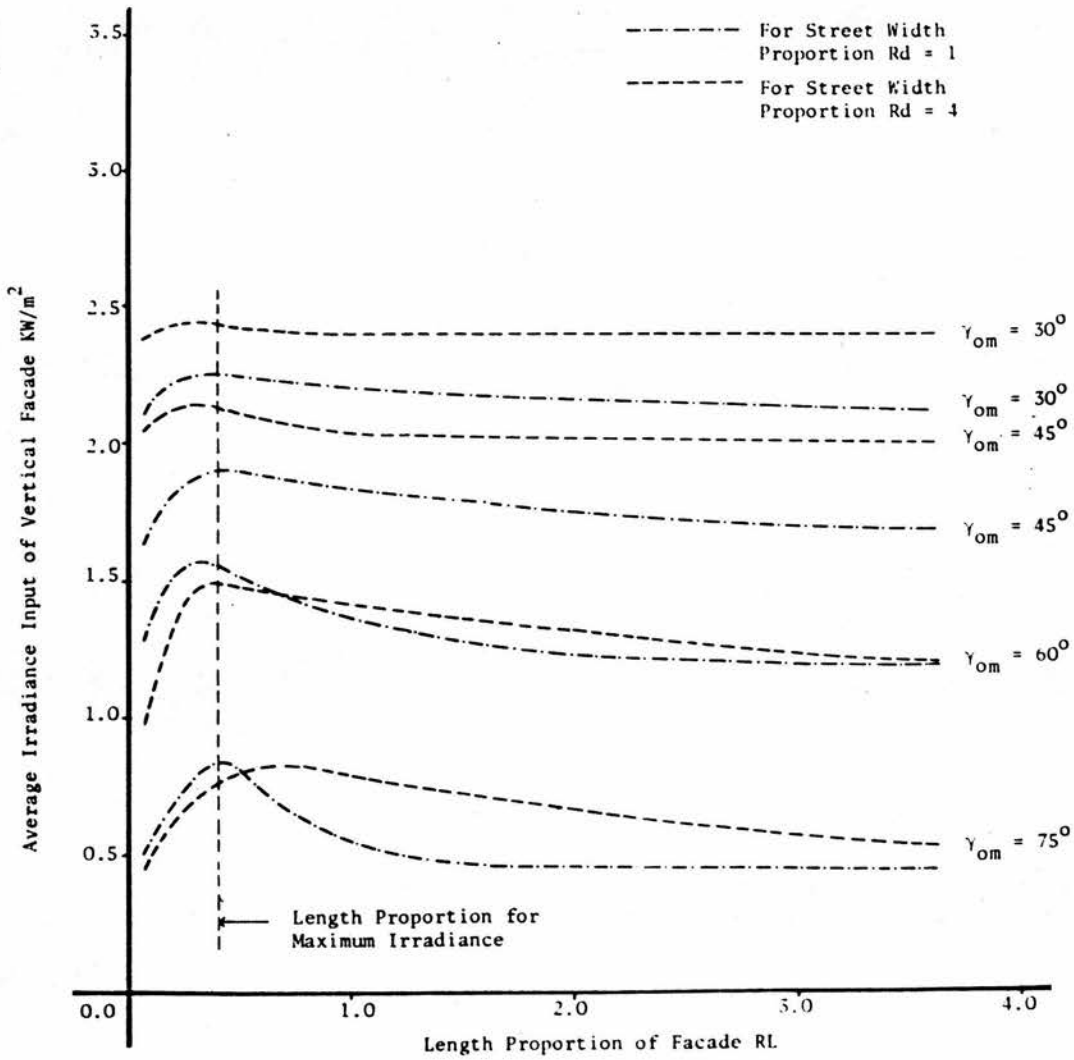


Figure 6.10 The Variation of the Average Daily Total Irradiance of Vertical Facade I_{dt} with the Length Proportion RL for Various Obstruction Angles

4.1.7 The distribution of I_{dt} with γ_{om} for different orientations and combinations of Rd and RL showed similar patterns. An example of a typical pattern is illustrated by the diagram in Figure 6.11. Generally, I_{dt} decreases rapidly when γ_{om} is increased beyond 30° . The magnitude of the shadow factor or the total irradiance being obstructed and shaded is more significant at $\gamma_{om} > 30^\circ$. However, the obstruction angle which may provide a particular level of shading and reduction of the total irradiance of the vertical facade will be determined by the proportions Rd and RL. The smaller these proportions, the greater the obstruction angle required to provide the desirable irradiance reduction. For example, an obstruction angle of 47° provides a 50 percent irradiance reduction when Rd and RL are equal to 4, but only about 12 percent when they are equal to 0.5. To obtain a 50 percent reduction for the latter combination of Rd and RL the obstruction angle would be about 68° .

4.2 The Distribution of the Initial Irradiance of the Ground Surface Separating the Vertical Facades

4.2.1 The analysis of the distribution of I_{dth} , the daily total initial irradiance on the ground separating the two vertical facades, with the form's parameters was conducted in a similar manner to that of I_{dt} . The data used for I_{dth} was generated for a number of combinations of the parameters. The patterns of distribution of I_{dt} and I_{dth} with RL and γ_{om}

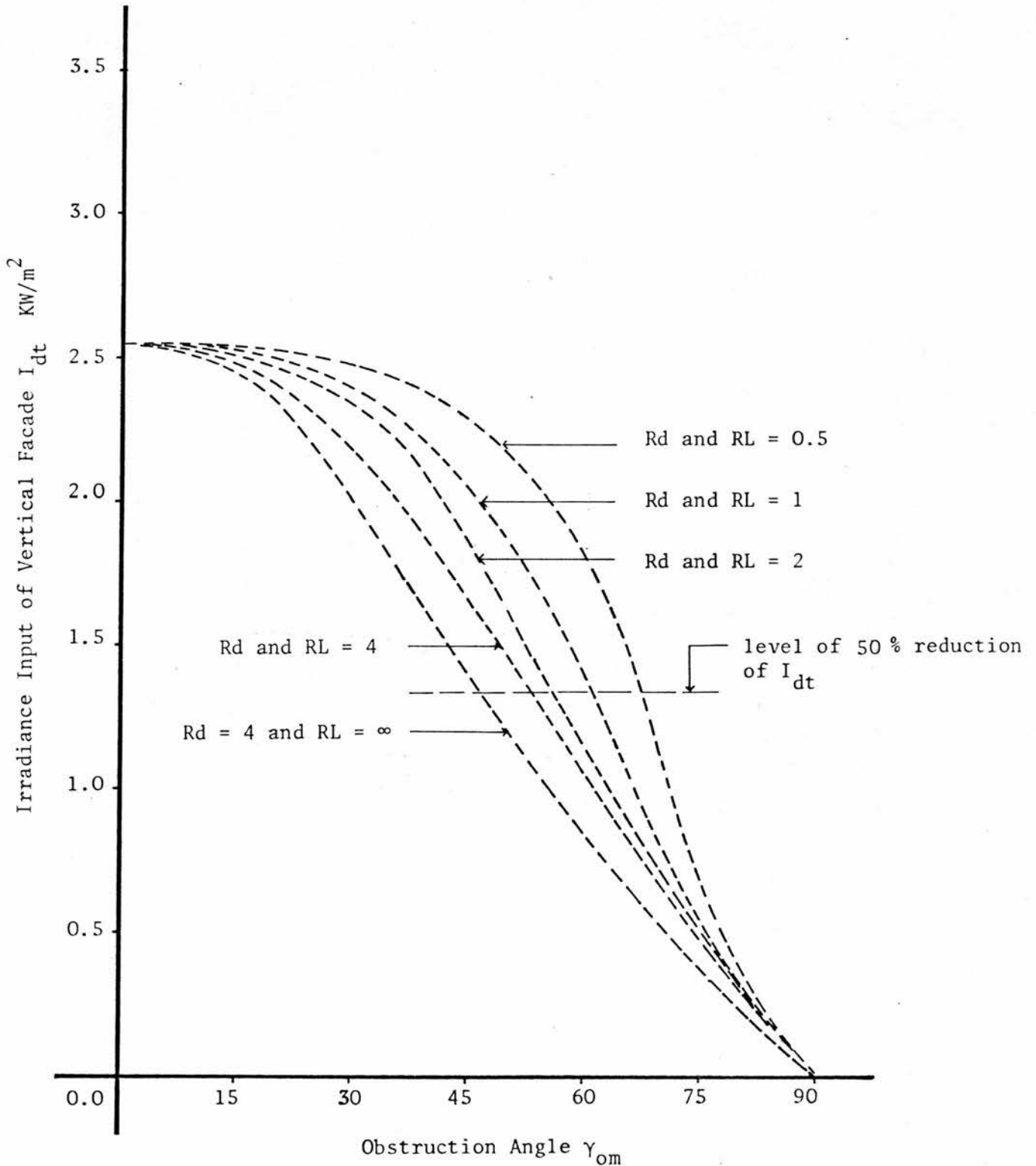


Figure 6.11 Variation of the Daily Average Irradiance of Vertical Facade I_{dt} with Obstruction Angle γ_{om} for a Number of Combinations for R_L and R_d

showed strong similarities, but they were different with regard to R_d and α_s . The following discussion illustrates the patterns of the distribution of I_{dth} , the manner in which they differ from that of I_{dt} and the range of the form's parameters within which they significantly influence I_{dth} .

4.2.2 The distribution of I_{dth} with R_d

I_{dth} generally increases with R_d . The increase is sharper and more significant within the range of R_d less than 4, and more gradual above this. I_{dth} approaches its maximum value when the ground is fully exposed to the direct and the diffuse irradiance, asymptotically. Such a pattern of distribution is typical for all combinations of RL , γ_{om} and α_s . An example of this is illustrated by the diagram in Figure 6.12. The distribution of I_{dth} may be explained as due to two main factors :

- (i) the part of the ground area exposed to the direct and diffuse irradiance due to the gaps in the opposing facade, increases with R_d , and
- (ii) as the street width is increased a greater part of the sky is viewed from the ground, as illustrated by the following diagram, Figure 6.13.

4.2.3 The distribution of I_{dth} with α_s

The graphs shown in the diagram of Figure 6.14 are presented as examples illustrating the distribution of I_{dth} with α_s for a number of combinations of a form's parameters. These show that I_{dth} generally decreases with α_s to a minimum value and then increases after that. Such a pattern is opposite to that of I_{dt} .

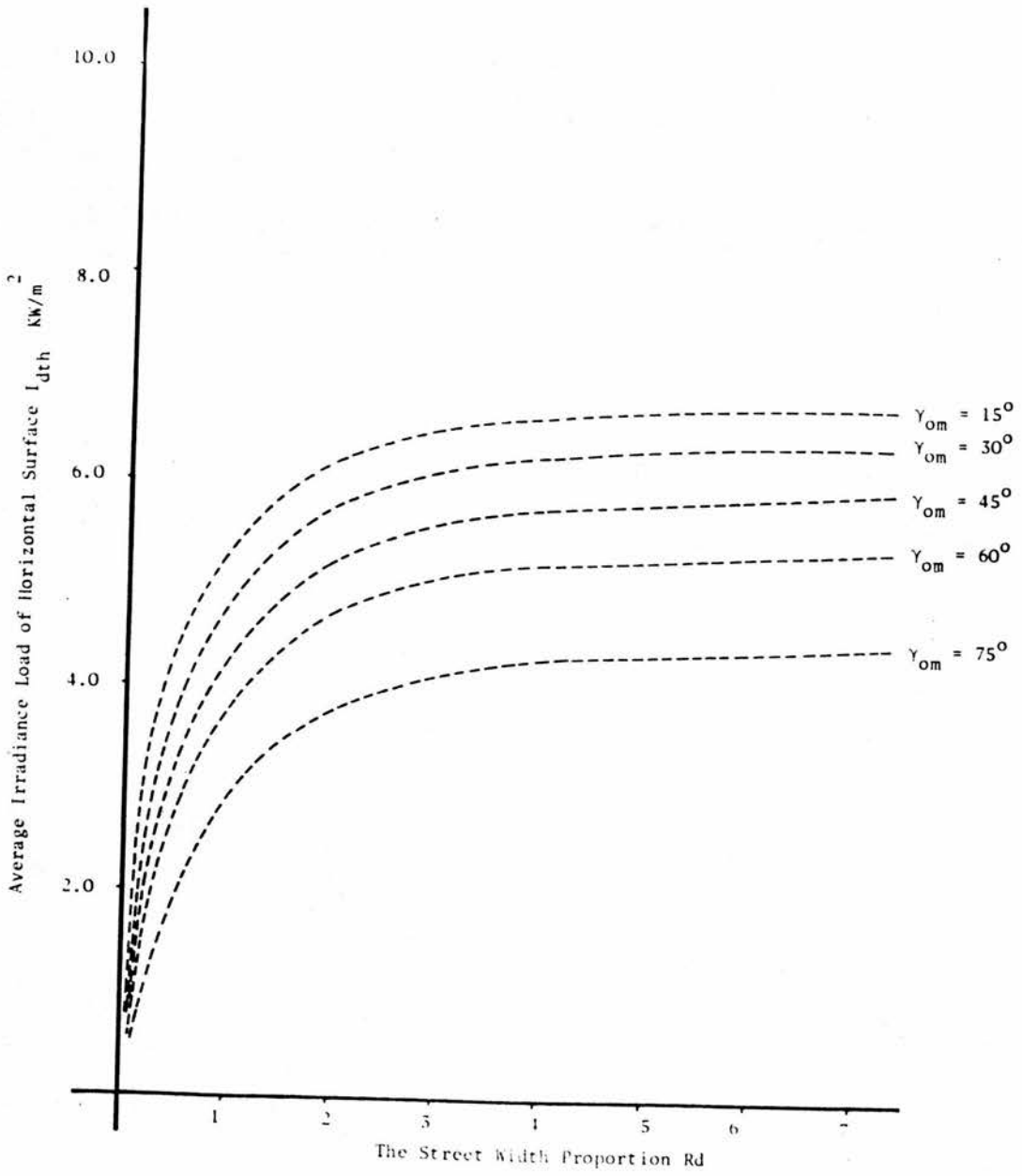


Figure 6.12 The Variation of the Average Irradiance Load of Ground I_{dth} with the Street Width Proportion R_d for an Orientation angle α_s equals 90°

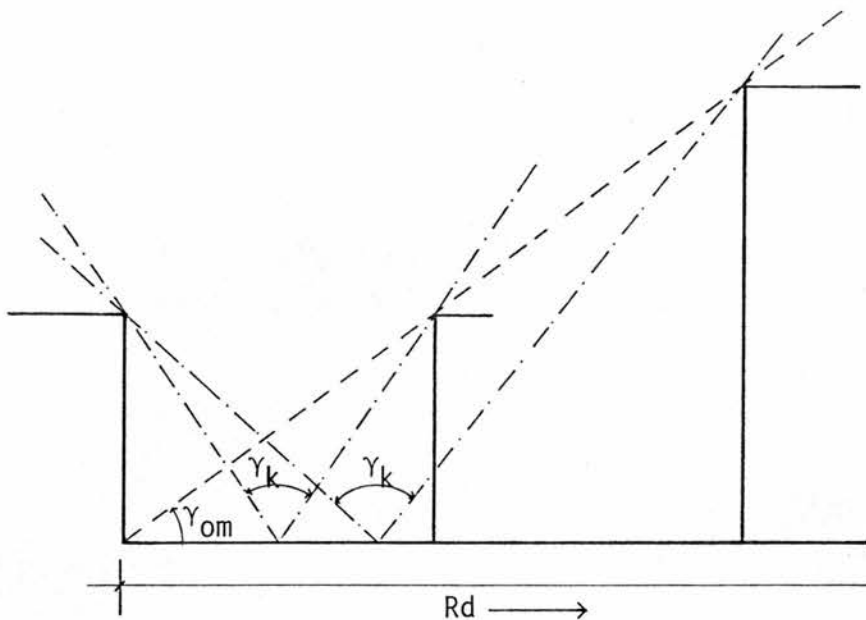


Figure 6.13 The Increase of the Sky Area Viewed by the Ground, As Indicated by the Angle γ_k , with the Increase of the Street Width

The obstruction angle determines the orientation of the axis of minimum irradiance as well as the rate of variation. The greater the obstruction angle the greater the azimuth angle of the axis of minimum irradiance and the greater the rate of variation. For example, where both parameters R_d and R_L have a value of 1, the minimum irradiance axis is oriented at 60° and 135° from North when γ_{om} equals 15° and 75° respectively. At the same time, the orientation of the axis is also determined by R_d and R_L . For example, where R_d and R_L are increased to 2, the axis will be oriented at 80° and 150° from North for γ_{om} 15° and 75° respectively. These orientations will be shifted to 90° and 160° where R_d and R_L are increased to 4.

4.2.4 The distribution of I_{dth} with R_L follows the same pattern as that of I_{dt} , an example of which is illustrated by the diagram in Figure 6.15. In the lower ranges of R_L , eg, $R_L < 0.25$, I_{dth} increases with R_L , from the value at R_L equals zero which is

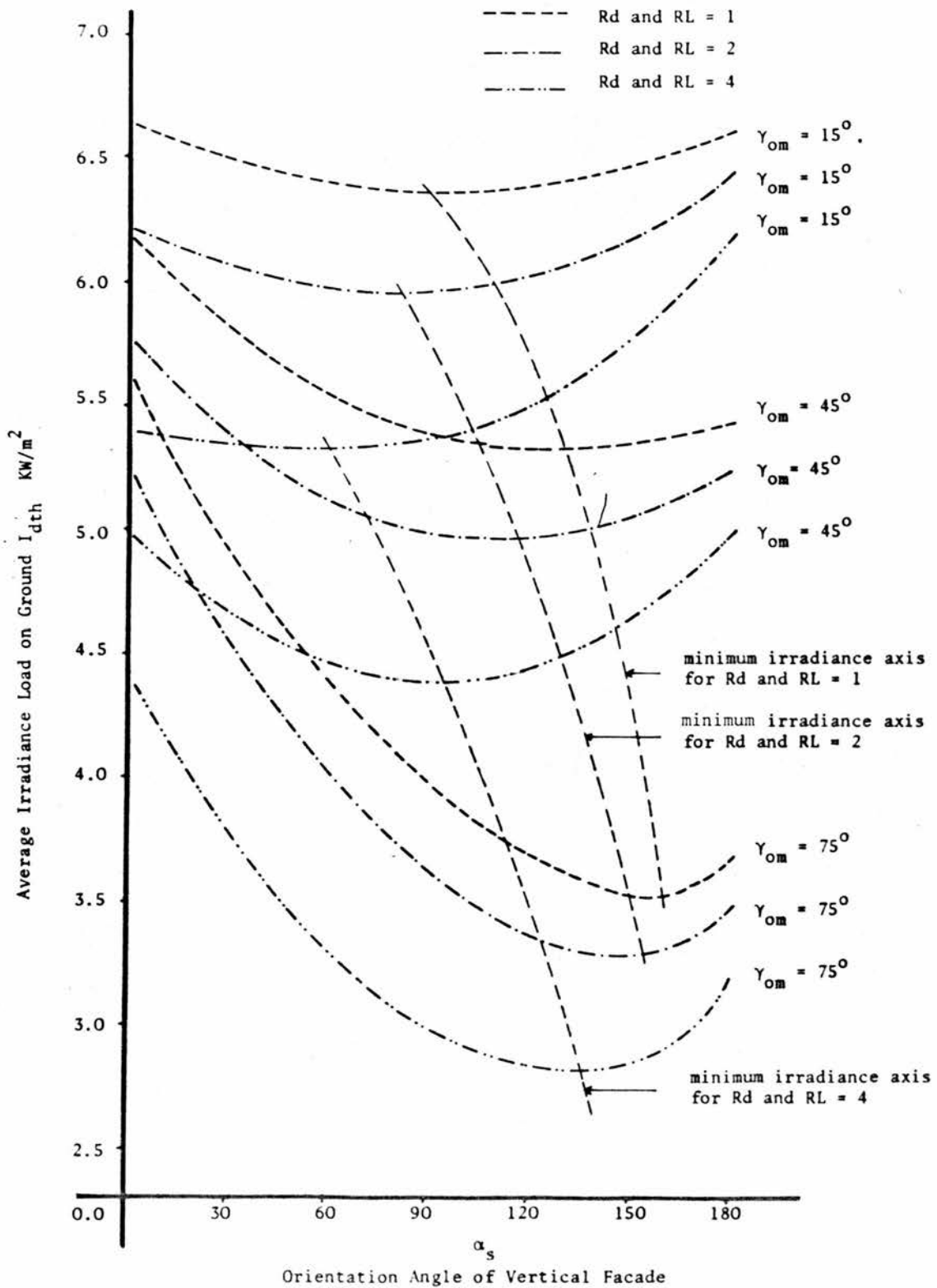


Figure 6.14 The Variation of Irradiance Load on the Ground with Orientation of Vertical Facade

assumed equals the corresponding value when RL is infinitely long. It reaches a maximum when RL equals 0.25 and then decreases with RL. It approaches the value of I_{dth} for $RL \infty$ asymptotically. The reasons for this are the same as those of I_{dt} .

4.2.5 The distribution of I_{dth} with γ_{om} is illustrated by Figure 6.16. The pattern is similar to that of I_{dt} . However, at the extreme limits of γ_{om} , eg, at 0° and 90° , the amount of the irradiance received on the ground is determined by the length and width proportion of the street, Rd and RL. This is due to the fact that the variation of the obstruction angle only influences the direct and diffuse irradiance on one half of the sky dome which is behind the opposing facade. The height of the vertical facade on the other half of the sky dome remains constant. Hence direct irradiance will be received on the ground as the solar altitude is greater than the obstruction angle of the facade. Similarly, diffuse irradiance will be received on the ground from that side of the sky dome as it is only partially obstructed.

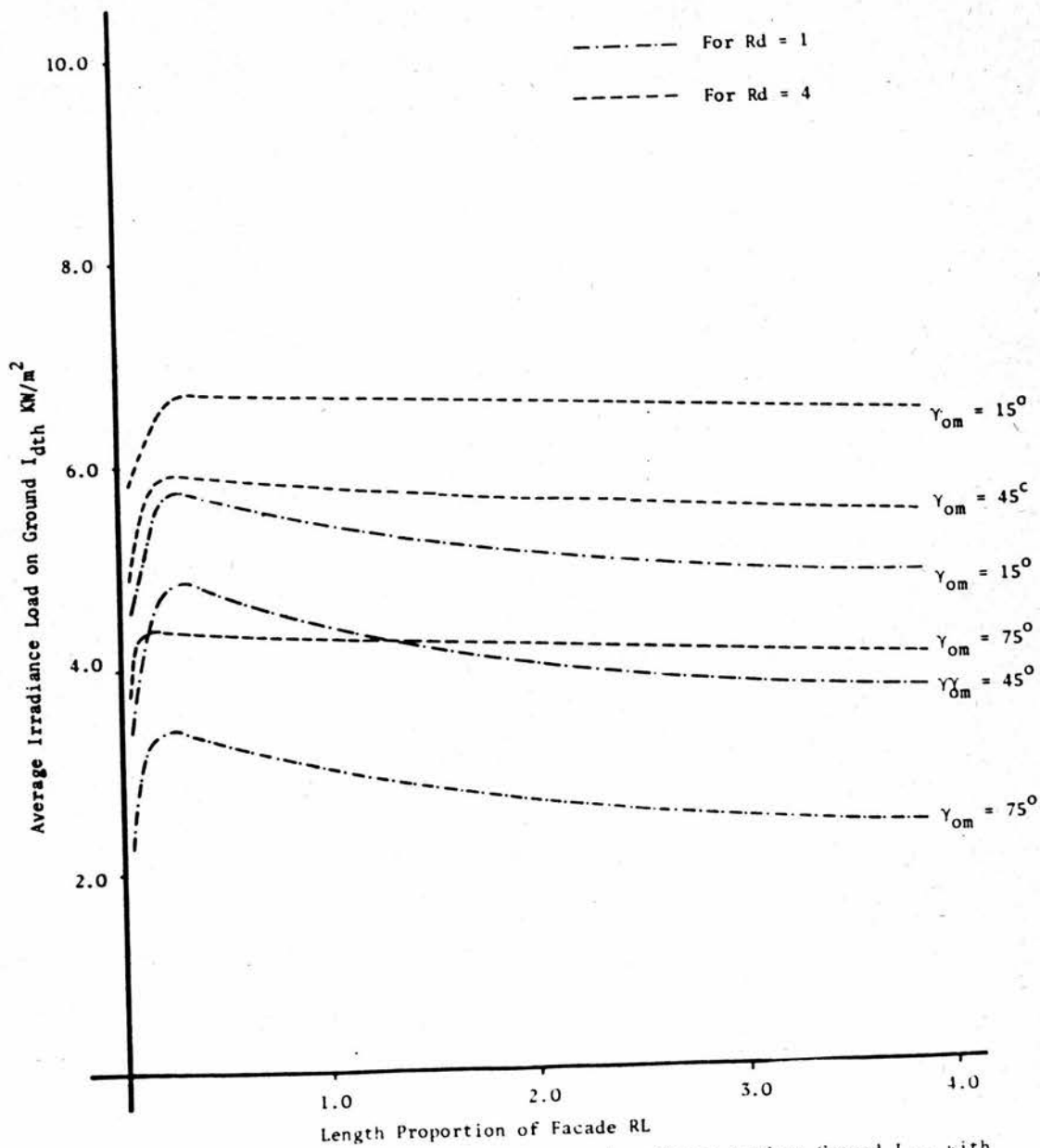


Figure 6.15 The Variation of the Average Irradiance Load on Ground I_{dth} with the Length Proportion of Facade RL , for an Orientation Angle α_s of 90°

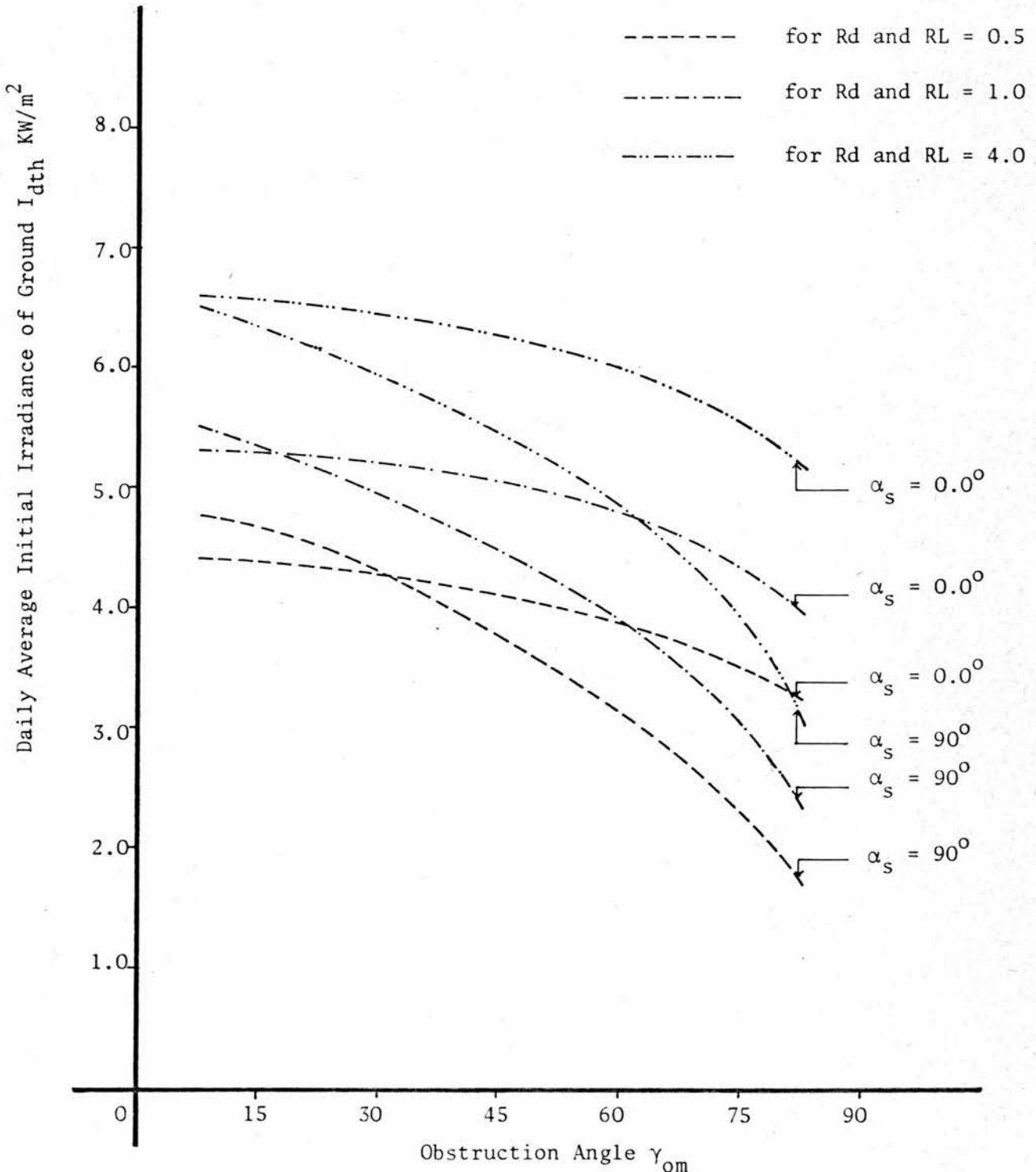


Figure 6.16 Variation of the Daily Average Initial Irradiance on Ground I_{dth} with the Obstruction Angle

5. IRRADIANCE AND SHADOW FACTOR INDICES

5.0.1 Values of daily total initial irradiance of vertical and horizontal surfaces are required by the designer. These are needed for the estimation of the total initial and final irradiance load on buildings, whether daily or yearly. For example, the initial daily irradiance load is directly obtainable by multiplying the areas of the various surfaces of a building by their corresponding I_{dt} and adding the total. The irradiance load I_{dL} may then be expressed mathematically by the function

$$I_{dL} = \sum_i^n I_{dt_i} \cdot A_i \quad \dots 6.6$$

where n is the number of building surfaces and A_i their corresponding areas. This enables the designer to analyse and evaluate the performance of various geometrical forms and building arrangements, in terms of the initial or final irradiance load, and to synthesise an architectural solution for thermal and visual comfort. Apart from calculating the irradiance values using the computer model, coded in the subroutine IRRILL, it is more useful to have them readily available and presented in a simple format for practical application. To this end, initial irradiance indices for vertical and horizontal surfaces were developed. These simplify the calculations and directly yield values of

average daily total initial irradiance received on the surfaces, I_{dt} and I_{dth} . The indices were based on the data generated using the model for various combinations of the parameters of the form.

5.1 Initial Irradiance Index of the Vertical Surface

5.1.1 Standard Irradiance Index

The amount of I_{dt} data generated was very large because of the wide ranges and combinations of the parameters considered. Accordingly, a standard irradiance index was constructed to simplify the presentation of the data. The standard index is represented by a series of concentric rings indicating the obstruction angles. They ranged from zero degrees at the outermost ring to 90° at the innermost, spaced at 15° intervals. The rings are radially divided to indicate the orientation angles as measured from the North point. The standard irradiance index shows the I_{dt} values of a unit surface and a unit street width, that is both Rd and RL equals 1, for the corresponding obstruction and azimuthal angular divisions. For differentiation, these values are referred to by the term I_{xv} . The standard irradiance index of the vertical surface is shown by the diagram in Figure 6.17.

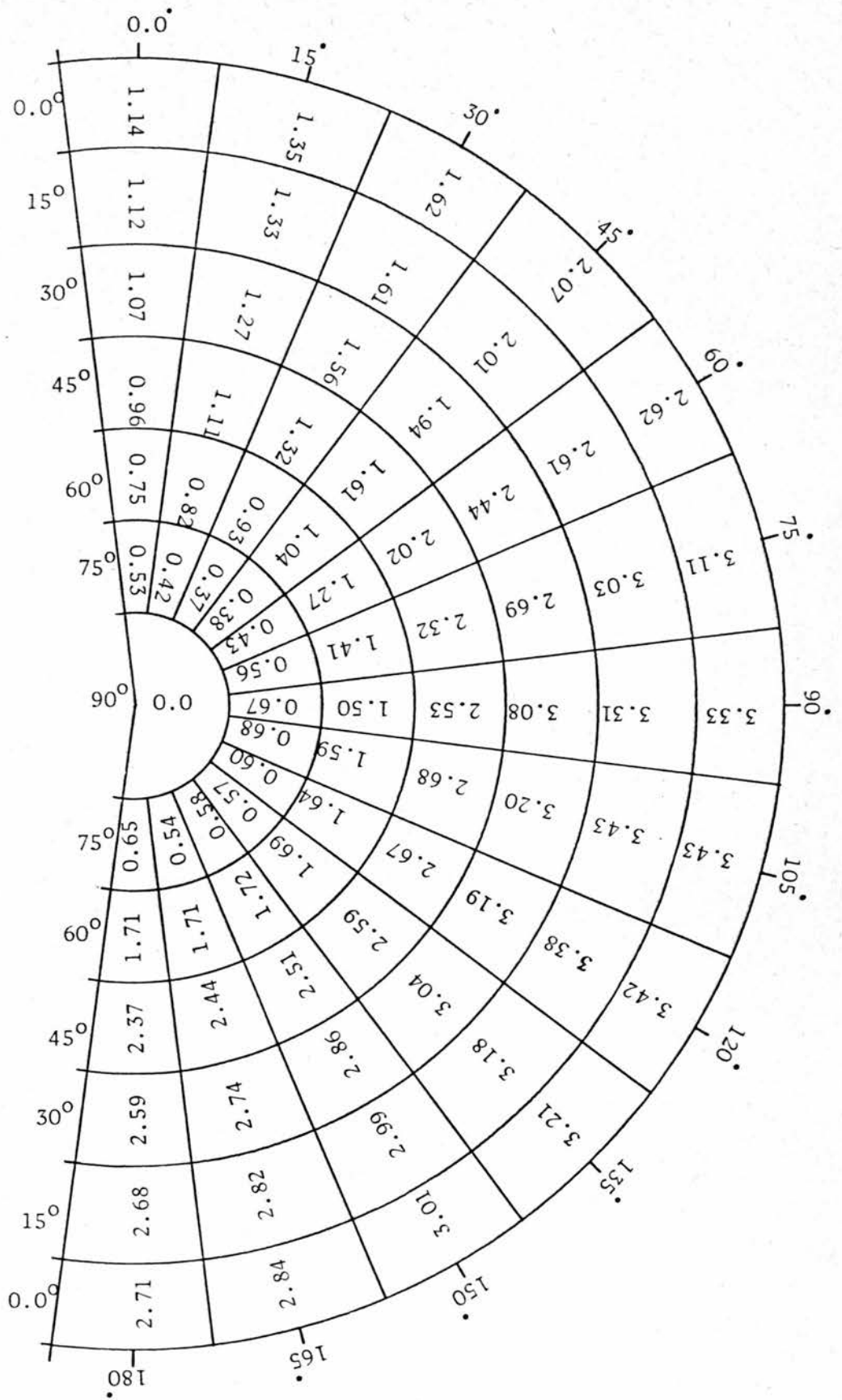


Figure 6.17 The Standard Irradiance Index of the Vertical Facade. This shows the Average Irradiance of a Unit Facade with $R_d = 1$, in KW/m^2 .

5.1.2 Correction Factor

This expresses the variation of I_{dt} of a surface for any combination of R_d and R_L from the standard irradiance index I_{xv} , for the corresponding orientation and obstruction angles. The cumulative correction factor C_f is given by the function

$$C_f = I_{dt}/I_{xv} \quad \dots 6.7(a)$$

The irradiance index of a surface may then easily be determined from the standard irradiance index and the correction factor as

$$I_{dt} = C_f \cdot I_{xv} \quad \dots 6.7(b)$$

An expression for the correction factor was derived as

$$C_f = P_v(1 - q_v/100) \quad \dots 6.8$$

P_v and q_v express the variation of the correction factor with R_d and R_L respectively. They are functions of α_s and γ_{om} .

5.1.3 Correction functions for R_d

P_v is expressed by the interrelationships

$$Pv = (a_1 + b_1 \cdot \alpha_t + c_1 \cdot \alpha_t^2) / (A_1 + B_1 \cdot Rd + C_1 \cdot Rd^2) \quad \dots 6.9$$

α_t represents the orientation angle as a multiple of 30° such as

$$\alpha_t = \alpha_s / 30 \quad \dots 6.10$$

The coefficients a_1 , b_1 and c_1 are functions of Rd . These were derived and shown in Table 6.1 below.

	$Rd < 1.0$	$Rd = 1.0$	$Rd > 1.0$
a_1	0.92	1.0	0.86
b_1	0.07	0.0	0.12
c_1	-0.01	0.0	-0.017

Table 6.1 Coefficients of Correction Function for Rd and α_s

The coefficients A_1 , B_1 and C_1 are similarly functions of Rd and γ_{om} . Their values were derived and presented in Table 6.2.

γ_{om}	Rd < 1.0			Rd > 1.0		
	A_1	B_1	C_1	A_1	B_1	C_1
0.0	1.00	0.0	0.0	1.0	0.0	0.0
15	0.989	0.012	-0.001	0.99	0.011	-0.001
30	0.943	0.064	-0.007	0.962	0.042	-0.003
45	0.781	0.277	-0.058	0.954	0.05	-0.004
60	0.526	0.684	-0.210	1.008	-0.009	0.001
75	0.21	2.13	-1.34	1.081	-0.087	0.006

Table 6.2 Coefficients of Correction Function for Rd and γ_{om}

5.1.3 Correction functions for RL

q_v are expressed by a similar relationship to P_v as

$$q_v = (0.134 + 0.913 \alpha_t - 0.133 \alpha_t^2)(A_2 + 0.6^{RL} B_2)(1.12 Rd - 0.12 Rd^2) \quad \dots 6.11$$

The coefficients A_2 and B_2 were derived for various γ_{om} .

These are given in Table 6.3.

γ_{om}	A_2	B_2
0.0	0.0	0.0
15	0.0	0.0
30	1.4	-2.2
45	3.7	-6.2
60	17.2	-28.7
75	20.0	-33.3

Table 6.3 Coefficient of Correction Function for RL and γ_{om}

5.1.4 Although the correction functions may appear complex, the evaluation of the correction factor is a simple procedure. Once the parameters of the form are defined, the corresponding standard irradiance index and the correction functions for R_d and R_L are easily determined. When the average of the irradiance index values of the various orientations only is required, the correction functions of α_s for both R_d and R_L may be ignored.

5.2 Initial Irradiance Index of the Ground

5.2.1 The initial irradiance index of the ground between the two vertical facades was constructed in a similar manner to that of the vertical surface. The standard irradiance index of the ground of a unit width and length, referred to here by the term I_{xg} , is shown by Figure 6.18. Correction functions were also derived to account for the variation of the ground irradiance index I_{dth} with R_L and R_d , from the standard index. The correction factor expresses the relationships.

$$C_g = I_{dth}/I_{xg} \quad \dots 6.12(a)$$

$$I_{dth} = C_g \cdot I_{xg} \quad \dots 6.12(b)$$

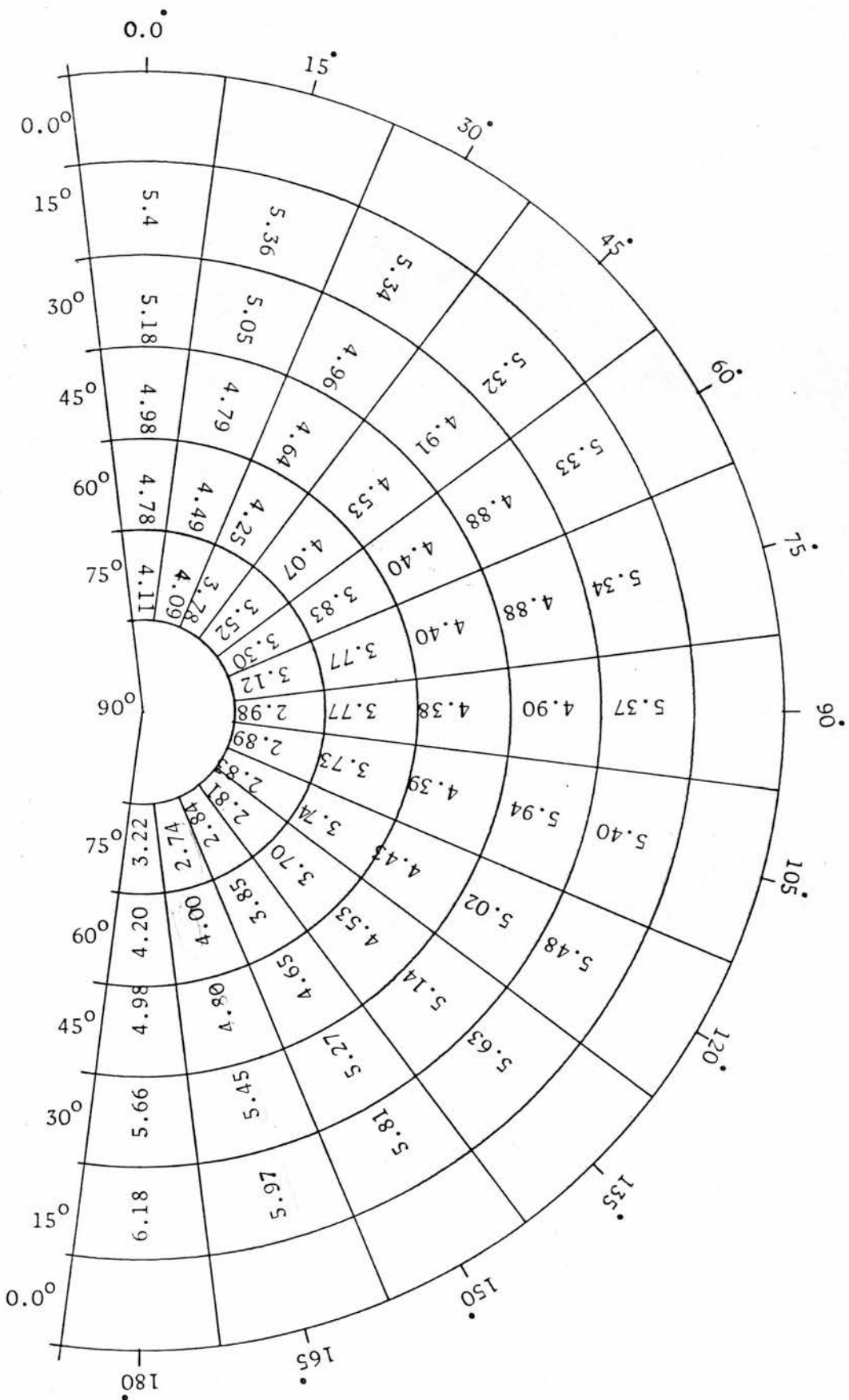


Figure 6.18 The Standard Irradiance Index of Ground. This Shows the Average Irradiance on Ground of Unit Length and Width in KW/m².

5.2.2 Expressions for the correction factor were also derived as

$$C_g = P_g(1 - q_g/100) \quad \dots 6.13$$

where P_g and q_g determine the variation of the correction factor with R_d and RL . P_g was expressed by the relationship

$$P_g = (a_3 + b_3 \alpha_t + c_3 \alpha_t^2)(A_3 + B_3 \cdot C_3^{R_d}) \quad \dots 6.14$$

The coefficients a_3 , b_3 and c_3 were derived as functions of R_d . These are shown in Table 6.4 below.

	a_3	b_3	c_3
$R_d < 1$	0.98	-0.094	0.024
$R_d = 1$	1.0	0.0	0.0
$R_d > 1$	1.003	0.044	-0.01

Table 6.4 Coefficients of Correction Function for R_d and α_s

Similarly, the coefficients A_3 , B_3 and C_3 were derived for the various obstruction angles. These are also shown in Table 6.5.

γ_{om}	A_3	B_3	C_3
15	1.22	-1.22	0.18
30	1.25	-1.25	0.20
45	1.299	-1.299	0.23
60	1.316	-1.316	0.24
75	1.389	-1.389	0.28

Table 6.5 Coefficient for Correction Function for Rd and γ_{om}

5.2.6 Similar expressions for the variation of the correction factor q_g with RL were derived.

$$q_g = (0.674 + 0.472 \cdot \alpha_t - 0.08 \alpha_t^2)(A_4 + 0.8^{RL} \cdot B_4)/Rd$$

... 6.15

The coefficients A_4 and B_4 were derived and presented in Table 6.6.

γ_{om}	A_4	B_4
15	14.24	-17.80
30	18.72	-23.40
45	23.04	-28.75
60	27.04	-33.80
75	29.04	-36.30

Table 6.6 Coefficient for the Correction Factor Function q_g for RL

5.2.7 One apparent advantage that can be drawn from the development of total irradiance indices is their direct utilization to simplify the formulation of the model and the calculation procedures in evaluating the yearly total initial or final irradiance load of buildings. The initial irradiance load of the different individual surfaces of a building is directly obtained from the index value for the corresponding parameters and area of the facades. The total irradiance load is the sum of the total irradiance received on the various surfaces of a building.

5.2.8 Further information regarding the SF, final irradiance and so on, may therefore be derived with the aid of the model. On this basis building regulation criteria and indicators for planning controls may then be developed.

5.3 Development of a Simplified Shadow Factor Index for Block-Spacing Criteria

5.3.1 On the basis of the principles of the shadow factor, a daily shadow factor may be defined. It represents the ratio of the daily total initial irradiance which is obstructed from the surfaces of a building block or facade, to the daily total which may be received on the surfaces when fully exposed. It is referred to here by the term SF_d . The SF_d value is easily determined from the I_{dt} values for the facades and the corresponding ones when γ_{om} is regarded as equal to zero. It is

apparent that SF_d provides a simple measure characterising the performances of various configurations of facades or forms and provides an alternative to I_{dt} . The need for and importance of shading buildings is obvious in tropical sunny regions. Therefore, the shadow factor SF_d may serve as a useful criterion for the definition of values of the forms' parameters, in particular in terms of street width and the obstruction angle of the opposing facade.

5.3.2 It may be argued that in planning for shading, as well as for other planning aims such as daylighting, sunlight, traffic, privacy and so on, block spacing is a critical factor. For this purpose a simplified shadow factor index was prepared to facilitate the derivation of R_d for various combinations of parameters of the form with reasonable accuracy. The index shows the R_d values which may yield the same shadow factor SF_d for a vertical surface of a unit area with various combinations of orientation and obstruction angles. The index is presented here in Table 6.7 with the SF_d ranging from 0.1 to 0.8 at 0.1 intervals. Values of R_d within the range $0.25 < R_d < 10$ only are shown here. In cases where the specified SF_d are only obtainable with $R_d > 10$, these are indicated by the sign (-). Similarly values for $R_d < 0.25$ are indicated by (*). As seen from the table, higher shadow factors can only be obtained with higher obstruction angles.

For example, an SF_d of 0.5 is obtained at $\gamma_{om} \geq 60^\circ$. SF_d greater than 0.5 are only possible with $\gamma_{om} \geq 75^\circ$.

5.3.3 To account for the variation of the facade length proportion RL from 1, a correction factor cf_s was derived. This enables the actual value of Rd for any facade length proportion to be determined from the index, by multiplying the index value by the correction factor. The correction factor is expressed by the function

$$cf_s = 1/[1.3 - (0.54 * 0.56^{RL})] \quad \dots 6.16$$

SF _d	Y _{om}	α_s						
		0.0	30	60	90	120	150	180
0.1	15	-	-	-	-	-	-	-
	30	1.30	1.42	1.54	1.65	1.77	1.88	2.0
	45	0.46	0.39	0.35	0.36	0.40	0.49	0.61
	60	*	*	*	*	*	*	*
0.2	30	3.75	7.0	10.0	-	-	-	-
	45	0.89	0.79	0.76	0.81	0.92	1.11	1.37
	60	0.24	0.26	0.25	0.26	0.28	0.31	0.35
	75	*	*	*	*	*	*	*
0.3	30	-	-	-	-	-	-	-
	45	2.16	1.26	1.11	1.72	3.09	5.21	8.10
	60	0.51	0.42	0.37	0.37	0.42	0.51	0.65
	75	*	*	*	*	*	*	*
0.4	45	-	-	-	-	-	-	-
	60	1.22	0.53	0.22	0.31	0.78	1.65	2.90
	75	*	*	*	*	*	*	*
0.5	45	-	-	-	-	-	-	-
	60	2.01	1.47	1.16	1.06	1.19	1.54	2.11
	75	0.25	0.23	0.21	0.20	0.21	0.23	0.26
0.6	60	-	-	-	-	-	-	-
	75	0.30	0.27	0.25	0.25	0.26	0.28	0.31
0.7	75	0.40	0.34	0.31	0.30	0.32	0.36	0.42
0.8	75	1.05	0.68	0.46	0.39	0.47	0.70	1.08

Table 6.7 Shadow Factor Indicator for the Street Width Proportion Rd

6. THE EVALUATION OF FORM GEOMETRY, PLAN PROPORTION AND ORIENTATION IN TERMS OF TOTAL INITIAL IRRADIANCE LOAD

6.0.1 The total irradiance load received on the external surfaces of buildings is particularly important for the assessment of the thermal response and planning of buildings. On this basis, previous studies were able to investigate the influence of the geometric shape and orientation (Buchberg and Naruishi, 1967, Olgyay, 1969, Valko, 1969, 1970 and 1972, Tappuni, 1973). They derived the optimum orientation and plan proportions with regard to total irradiance load criteria. These criteria generally represented the maximum irradiance load in winter and minimum load in summer. However, as these studies were based on different methods and concepts in the evaluation of the total irradiance load they lead to different solutions. In addition to this they generally ignored the shading and obstruction of the direct and diffuse radiation caused by surrounding buildings and the subsequent reduction of total irradiance load.

6.0.2 Therefore the need arose for a quantitative treatment of the total irradiance load which takes into consideration the additional shading effect. The variation of the irradiance load with the geometric configurations and orientations of the block may then be investigated. The proportions of the block side, orientation and configuration of surroundings may

be defined with regard to the total initial irradiance load received on the block. This was verified by the theoretical investigation discussed in part 9 of Chapter II. For this purpose the computer model was utilized to generate a wide variety of rectangular blocks with varying side proportions and configurations of surroundings and to calculate their total initial irradiance load at different orientation angles. The optimum block geometry and the configuration of the surrounding buildings were then determined in terms of the total minimum irradiance load of the block.

6.1 Generation of Geometric Configuration of Block and Surroundings and the Evaluation of the Total Initial Irradiance Load

6.1.1 The first task of the model was to generate systematically a wide variety of block shapes and configurations of surroundings. Those principally considered were rectangular blocks arranged in parallel rows. The block was taken to be of a unit volume. In this way immediate comparison of the effects of shape and orientation and the general applicability of the results may be achieved.

6.1.2 Three main geometric configurations of block and surroundings were considered. These were classified in terms of the block's height as illustrated by the three diagrams in Figures 6.19(a), (b) and (c). They represent the following cases :

- (i) The building block and its surrounding blocks were taken to be of equal height which was kept constant (Figure 6.19a).
- (ii) The blocks on each of the parallel rows were taken to be of equal height, the height of the block and its adjacent blocks on the same row being kept constant, while the height of the opposing parallel blocks were varied (Figure 6.19b).
- (iii) The surrounding blocks on the four sides of a block were taken to have equal heights which was varied while the height of the block was kept constant (Figure 6.19c).

6.1.3 The model generated various geometric configurations of form and surroundings by a major progression for each of the three main cases considered. The progression was defined by five primary descriptors representing the geometrical parameters of the form. The remaining, secondary, descriptors were then expressed in terms of the primary ones. The primary descriptors were varied at two main stages of the progression :

- (i) The first stage of the progression solely defined the block geometry. It was determined by the variations of two primary descriptors, which were the same for the three cases considered. The two descriptors

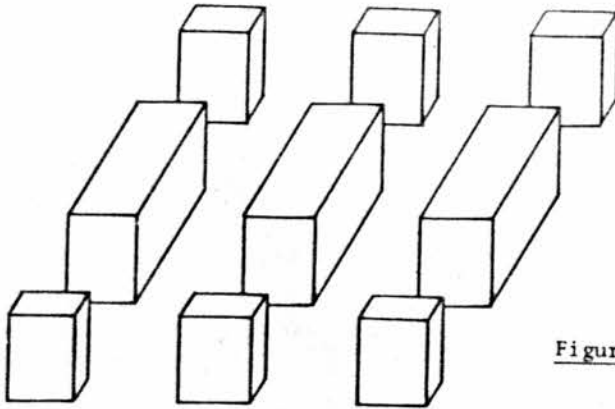


Figure 6.19(a) Equal Height Blocks

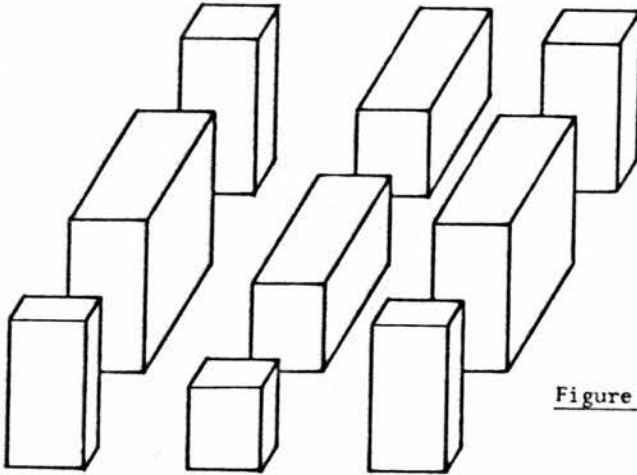


Figure 6.19(b) Blocks on Each Row Are of Equal Height

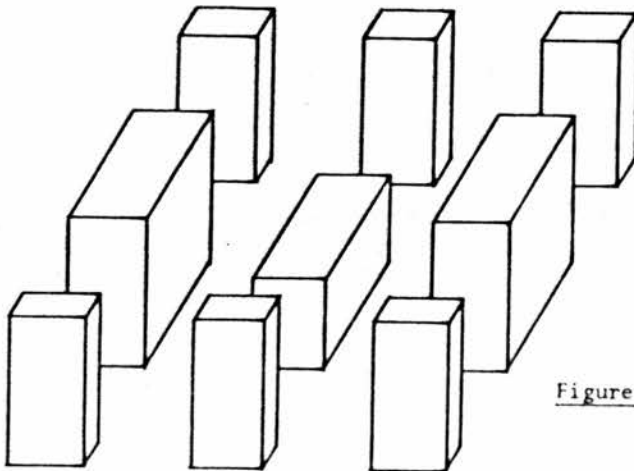


Figure 6.19(c) Surrounding Block of Equal Height which is Different from That of the Block

Figure 6.19 The Three Types of the Geometric Configuration of Block and Surrounding Investigated by the Three Progressions

involved represented the base area of the block A and its plan proportion of width to length P. From these, the secondary descriptors defining the remaining geometrical parameters of the block, eg, H, RL, Rw and total area of facades A_f , were directly determined by the relations expressed in Tables 6.8(a) and (b).

- (ii) The second stage of the progression defined the geometric configuration of the surrounding blocks. It involved three primary descriptors. These specified the two obstruction angles γ_{om1} and γ_{om2} of two perpendicular facades of the block and the street width proportion Rd. One and two descriptors were varied independently for the first and second cases respectively. In the first case only the street width proportion was varied in terms of which the two obstruction angles are expressed. In the second case the obstruction angle is varied in addition to the street width. In the third case all the descriptors were varied independently. The secondary descriptors defining the height proportions of surrounding blocks were similarly determined from the primary descriptors, for this stage of the progression, by the relations expressed in Table 6.8(a).

Primary Descriptor		Secondary Descriptor					
A	P	H	L	RL = L/H	W	Rw = W/H	Total Area of Facades
0.25 - 2.0	0.2 - 5.0	1/A	$\sqrt{A/P}$	A $\sqrt{A/P}$	$\sqrt{A \cdot P}$	A $\sqrt{A \cdot P}$	$(2P + 2)/\sqrt{A \cdot P}$

Table 6.8(a) The Ranges of the Primary Descriptors and the Relations of the Secondary Descriptors for the First Stage of the Progression

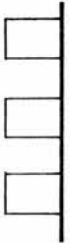
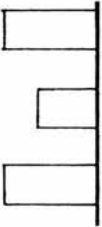
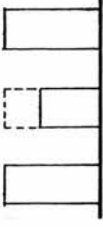
Progression	Primary Descriptor				Secondary Descriptor	
	Rd = D/H	γ_{om1}	γ_{om2}	$Rh_1 = H_1/H$	$Rh_2 = H_2/H$	
1. 	0.25 - 4.0	Arc Cot Rd	Arc Cot Rd	1	1	
2. 	0.25 - 4.0	15° - 75°	Arc Cot Rd	Rd · tan γ_{om1}	1	
3. 	0.25 - 4.0	15° - 75°	15° - 75°	Rd · tan γ_{om1}	Rd · tan γ_{om2}	

Table 6.8(b) The Ranges of the Primary Descriptors and the Relations of the Secondary Descriptors for the Three Cases Considered at Second Stage of the Progression

6.1.4 The size of the progression and the number of the alternative forms generated by the model for each of the three cases studied, were determined by the combinations and ranges of the variable parameters considered. These are shown in Tables 6.8(a) and (b). Examples of the geometric configuration of form are illustrated by the diagrams in Figures 6.20 and 6.21 for the first and second stages of the progression respectively.

6.2 Evaluation of the Total Irradiance Load of a Building Block

6.2.1 The model computed the total irradiance load for each of the rectangular blocks generated in the progression. The total irradiance load was calculated for the vertical facades only. This is a practical procedure which has been previously used in a number of similar studies, eg, Buchburgh and Naruishi, 1967. The assumption was made here that roofs are totally shaded. This was prompted by the fact that various shading structures are generally used in tropical sunny regions for roof protection.

6.2.2 The calculation of the initial irradiance load of the block was carried out at seven different positions of orientation. The block orientation was arbitrarily represented by the orientation of one of its vertical facades. The block was then rotated from the north point in a clockwise direction in steps of 15° within the range of the first quadrant ($0^{\circ} < \alpha_s < 90^{\circ}$). It was not necessary to consider the block's orientation beyond this range as the azimuthal distributions of the irradiance load of the block within the ranges of the different quadrants are symmetrical.

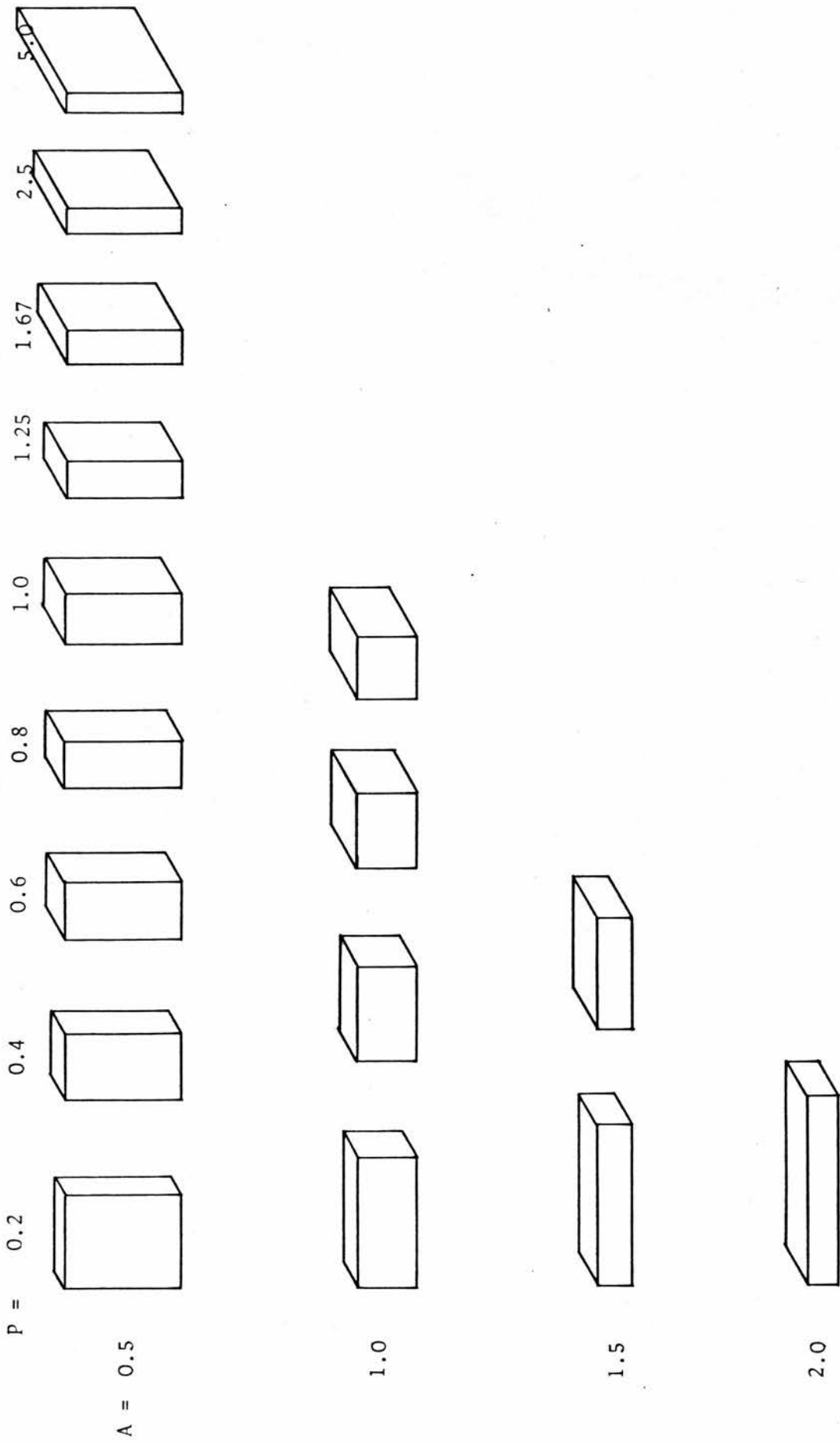


Figure 6.20 Phases of Change of Block Geometry in the First Stage of the Progression

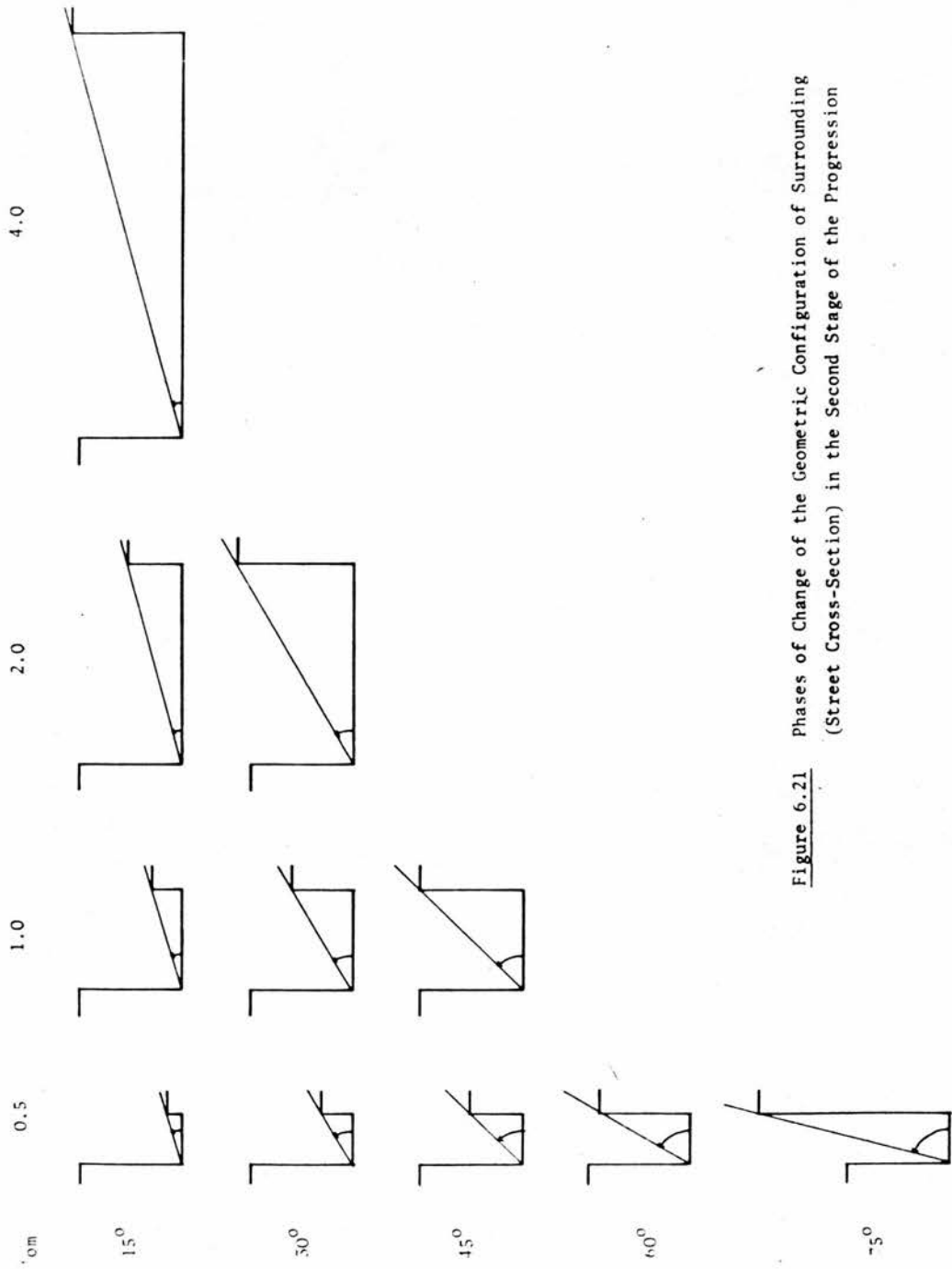


Figure 6.21 Phases of Change of the Geometric Configuration of Surrounding (Street Cross-Section) in the Second Stage of the Progression

6.2.3 The minimum irradiance load and the maximum shadow factor were used as criteria for defining the optimum proportions of the building block sides. On this basis, the model was then instructed to determine the optimum plan proportions for the various combinations of descriptors in the major progression and at the different orientation positions. The model then outputs the optimum plan proportion, surface area, irradiance load and shadow factor of the block for the two criteria.

6.3 Analysis of the Results : The Relations Between Optimum Plan Proportion of Block, Orientation and Geometric Configuration of Urban Form

6.3.1 The minimum total irradiance load on building blocks was conveniently achieved with the model by minimising the length of its facades receiving a relatively higher irradiance load. The model was used to prepare data for the optimum plan proportion of the block P , which satisfies the minimum irradiance load criterion, for the different combinations of cases in the three major progressions studied. The proportion P expresses the ratio of the length of one side of the block to its perpendicular side at which the orientation of the block was defined. The following discussion analyses the effects of orientation and the geometric considerations on the optimum plan proportion.

6.3.2 The effect of orientation on the optimum plan proportion P
The cases of the three major progressions studied showed that

P generally increases with the rotation of the block away from the north point in the first quadrant. Two main forms of patterns and ranges for the variation of P with α_s were identified. These were directly related to the heights of the obstructions of the surrounding blocks as determined by Rd and γ_{om} .

- (i) The first form of patterns characterised the cases of the first and third progressions which were represented by equal height of obstruction on all sides of the block. These cases showed similar patterns for the variation of P with α_s for the different combinations of the parameters A, Rd and γ_{om} . The patterns were mainly influenced by the obstruction angle γ_{om} . Typical examples of these are illustrated by the diagrams in Figures 6.22 and 6.23. These indicate that P mainly varies within the range $0.5 < P < 2.0$, but with a distinctive value of 1 at $\alpha_s = 45^\circ$. They also show that P increases with γ_{om} , but at a decreasing rate as α_s increases from 0° to 45° , where it assumes a constant value of 1 for all obstruction angles. This pattern is reversed as α_s varies from 45° to 90° . It may be concluded then that the optimum form favoured a rectangular shape plan tending towards a square shape with α_s varying from 0° to 45° or with the increase of the obstruction angle. Subsequently, the change in the

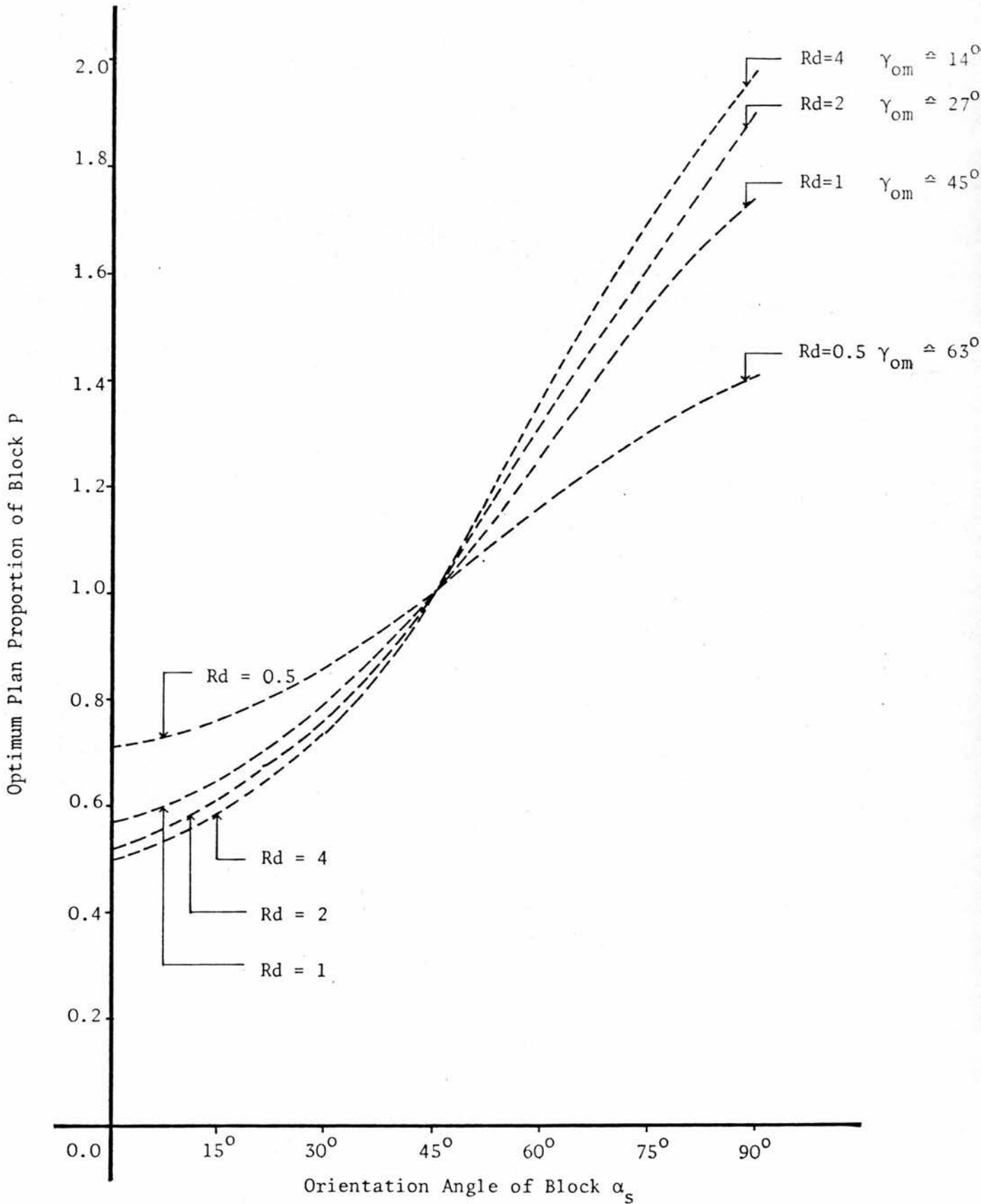


Figure 6.22 Variation of Plan Proportion of Block with α_s for the Cases of the First Major Progression with Base Area $A=1.0$

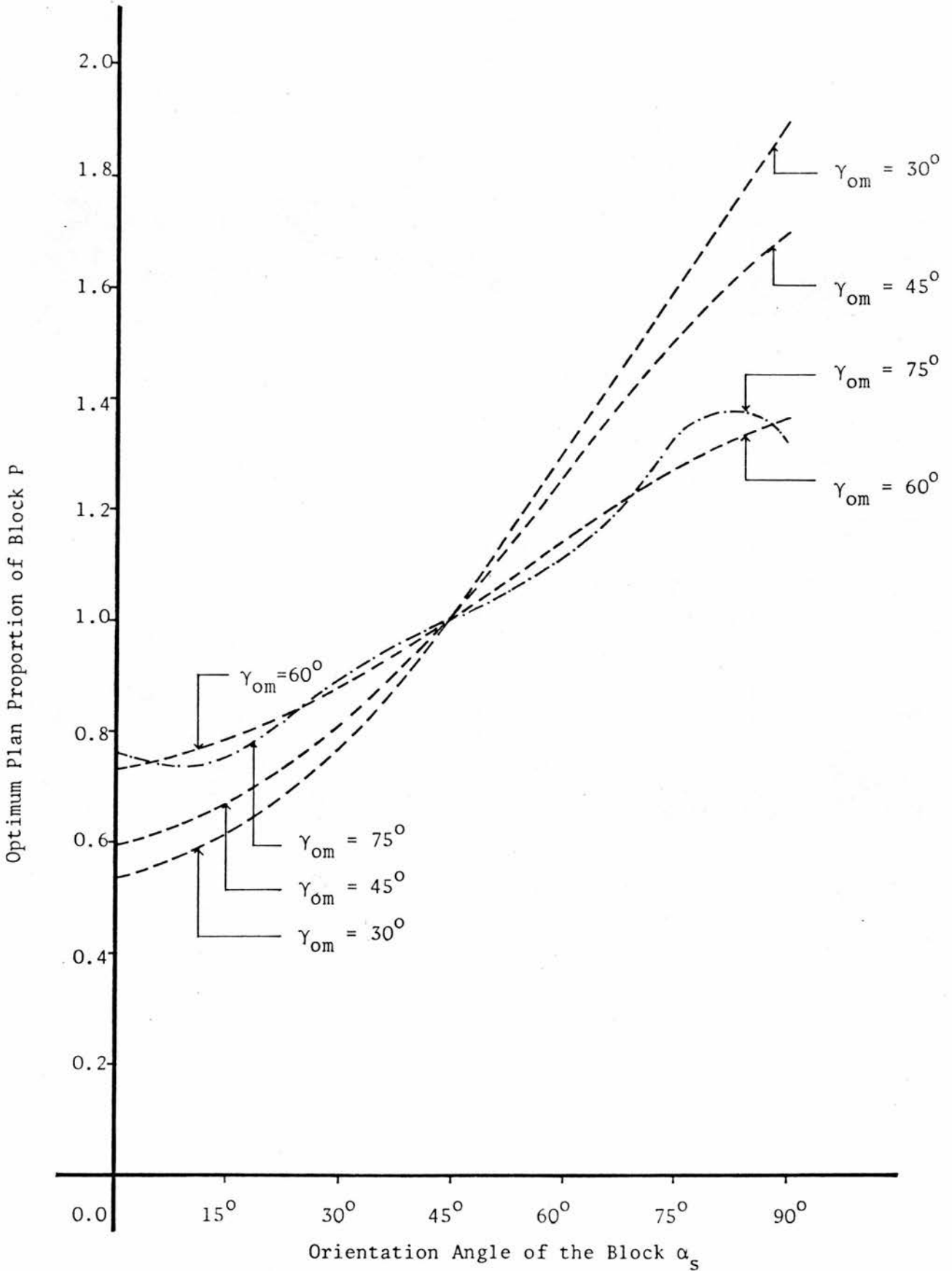


Figure 6.23 Variation of Plan Proportion of Block with Orientation for Cases of the Third Major Progression with Base Area $A = 1.0$ and $R_d = 1.0$

plan shape is similarly reversed as α_s increases from 45° to 90° . This cycle is also repeated with further rotation of the block within the ranges of the subsequent quadrants. It is apparent that the length of a side of an optimum block is related to the angular displacement of its orientation axis from the N-S axis where the length of side decreases as its orientation angle increases.

- (ii) The second form of patterns mainly represented the cases of the second progression. Typical examples of these are illustrated by the graphs shown in Figure 6.24. These show that P similarly increases with the rotation of α_s away from the north point, in the first quadrant, for the different combinations of Rd and γ_{om} . They also indicate that the values of P at the different orientation angles are determined by the proportion of the height of obstruction Rh, expressed here in terms of Rd and γ_{om} and was varied on one side of the block only. P was found to decrease with the increase of Rh. For example, at $\alpha_s = 0.0^\circ$ and $\gamma_{om} = 45^\circ$, P decreased from about 1 to about 0.6 as Rh increased from about 0.3 to 1. The rate of decrease of P is more rapid for Rh within the range ≤ 1.0 . It is more gradual as $Rh > 1.0$, where the height of obstruction is above the level of the block. For example, when Rh was increased from 1 to 4, P decreased from about 0.6 to 0.4. Thus the variation

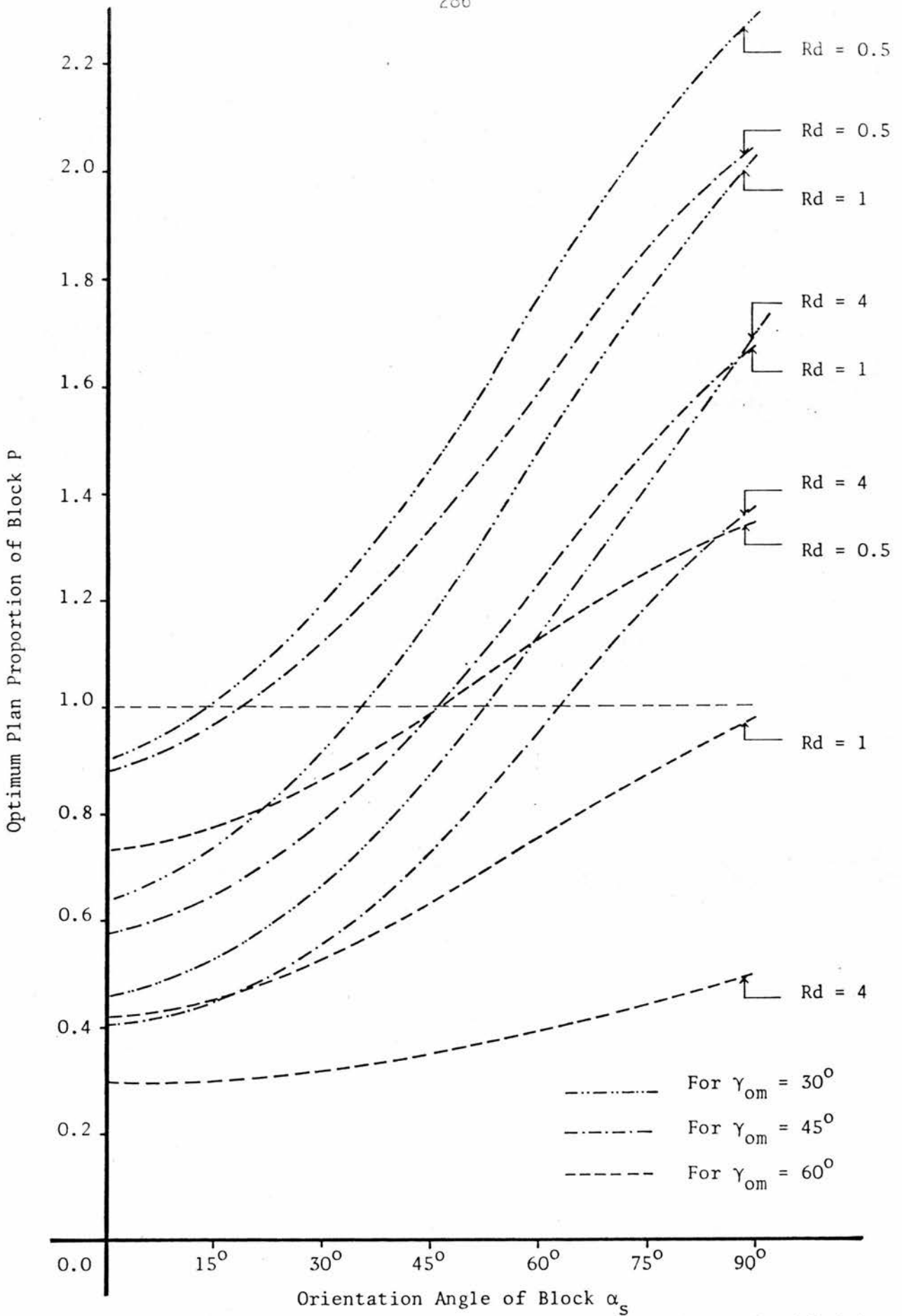


Figure 6.24

Variation of the Plan Proportion of the Block with Orientation for the Cases of the Second Major Progression for Base Area A=1

of P is inversely proportional to that of R_h . This may be interpreted by the fact that the facade of the block tends to receive relatively more irradiance load as the height of its obstruction is shortened. Hence the tendency is to reduce its length for the optimum form. Accordingly, as the height of the obstruction is increased the corresponding sides of the block are increased while the perpendicular sides decreased. Thus P decreases accordingly. It is evident then that the shape of the optimum plan of the block varies from a deeper rectangular form, with the longer side parallel to the higher obstruction, to square form as the height of the shorter obstruction is increased. The pattern is reversed with the further increase of the height of the obstruction on one side of the block. The height of the variable obstruction on one side of the block which may produce square form ($P=1$) increases with orientation. For example, the variable obstruction R_h varies from about 0.3 at $\alpha_s = 0^\circ$ to about 1 at $\alpha_s = 45^\circ$. For $\alpha_s > 45^\circ$ R_h is generally greater than 1.

6.3.3 The effect of the obstruction height on the optimum plan proportion P

In the first progression, the fact that the obstruction height was taken as constant and R_d was the only variable parameter means that the obstruction angle decreases with the increase of R_d . The optimum plan proportion may then be regarded as varying with γ_{om} . The pattern of variation appeared to be dependent on the value of P , as determined by the orientation angle α_s . When the value of P was less than 1, that is when

$\alpha_s > 45^\circ$, it was found to increase with γ_{om} . This pattern was reversed as $P > 1$ and $\alpha_s > 45^\circ$. P remained constant and equal to 1 at $\alpha_s = 45^\circ$. The cases of the third progression showed identical patterns to those of the first progression. Examples of these are illustrated by the diagram in Figure 6.25. In these cases the effect of Rd on P was less significant. P varied only slightly with Rd . For example, doubling Rd caused P to vary within the range of ± 1 percent. P increased with Rd when $\alpha_s < 45^\circ$ and decreased when $\alpha_s > 45^\circ$. It is evident that the plan shape tends towards a square form with the increase of obstruction height. Obviously as the height of the surroundings was increased, all sides of the block become equally shaded and tend to receive small and nearly equal amounts of direct and diffuse irradiance. In the cases of the second progression, P generally decreased with the increase of γ_{om} ; see Figure 6.25. The effect of Rd on P was more significant. P , similarly, decreased with the increase of Rd , as illustrated by the diagram in Figure 6.26. The effect of Rd on P was less significant for $Rd > 2.0$. This may be explained by the fact that as the increase of the obstruction height with Rd and γ_{om} was restricted to one pair of parallel facades of the block, the tendency was to maximise their lengths with the increase of the obstruction.

6.3.4 The effect of the base area and the block's height on the optimum plan proportion

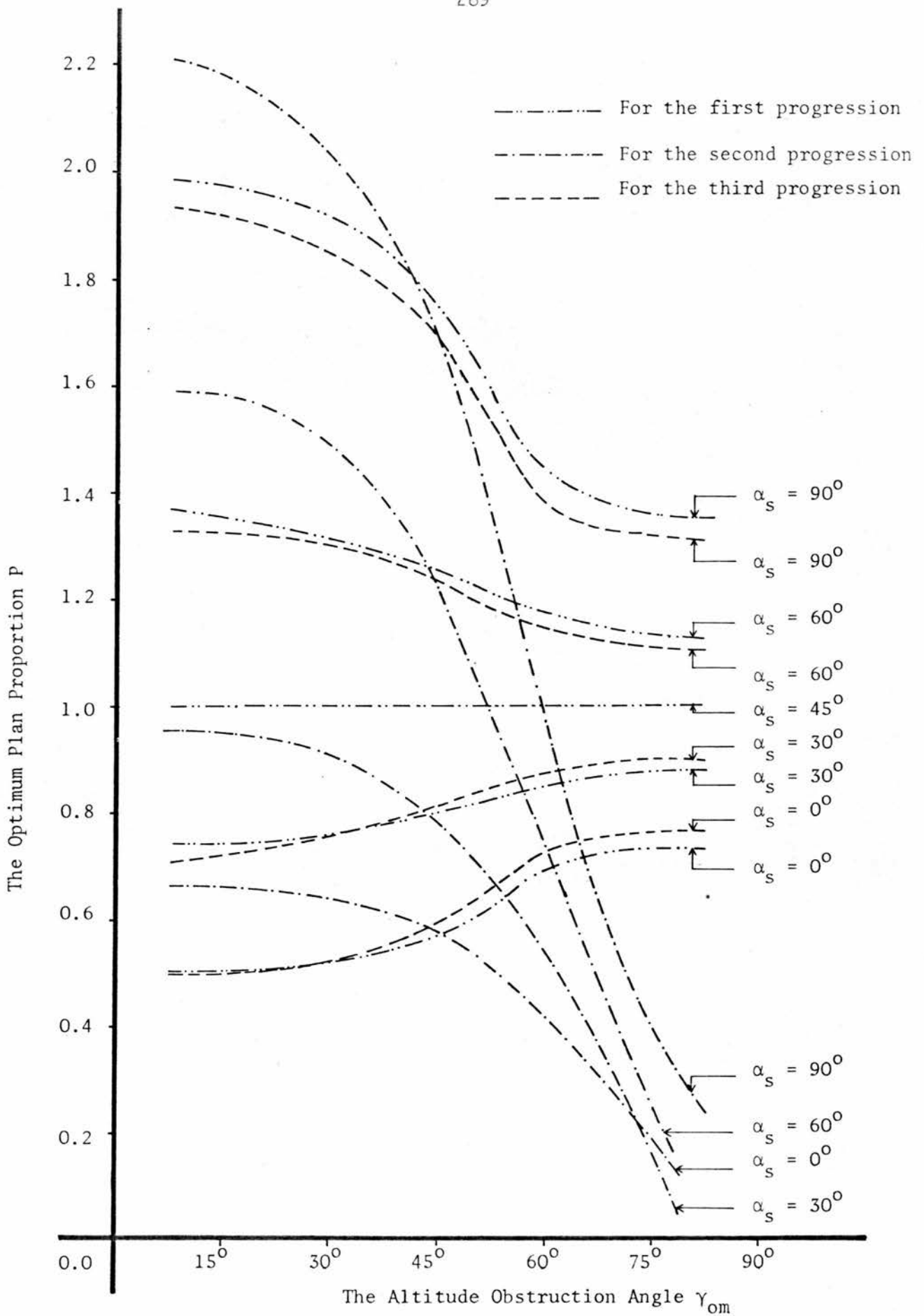


Figure 6.25 Variation of the Optimum Plan Proportion with the Altitude Obstruction Angle for the Three Major Progressions for a Base Area A and Street Width Proportion R_d equals 1

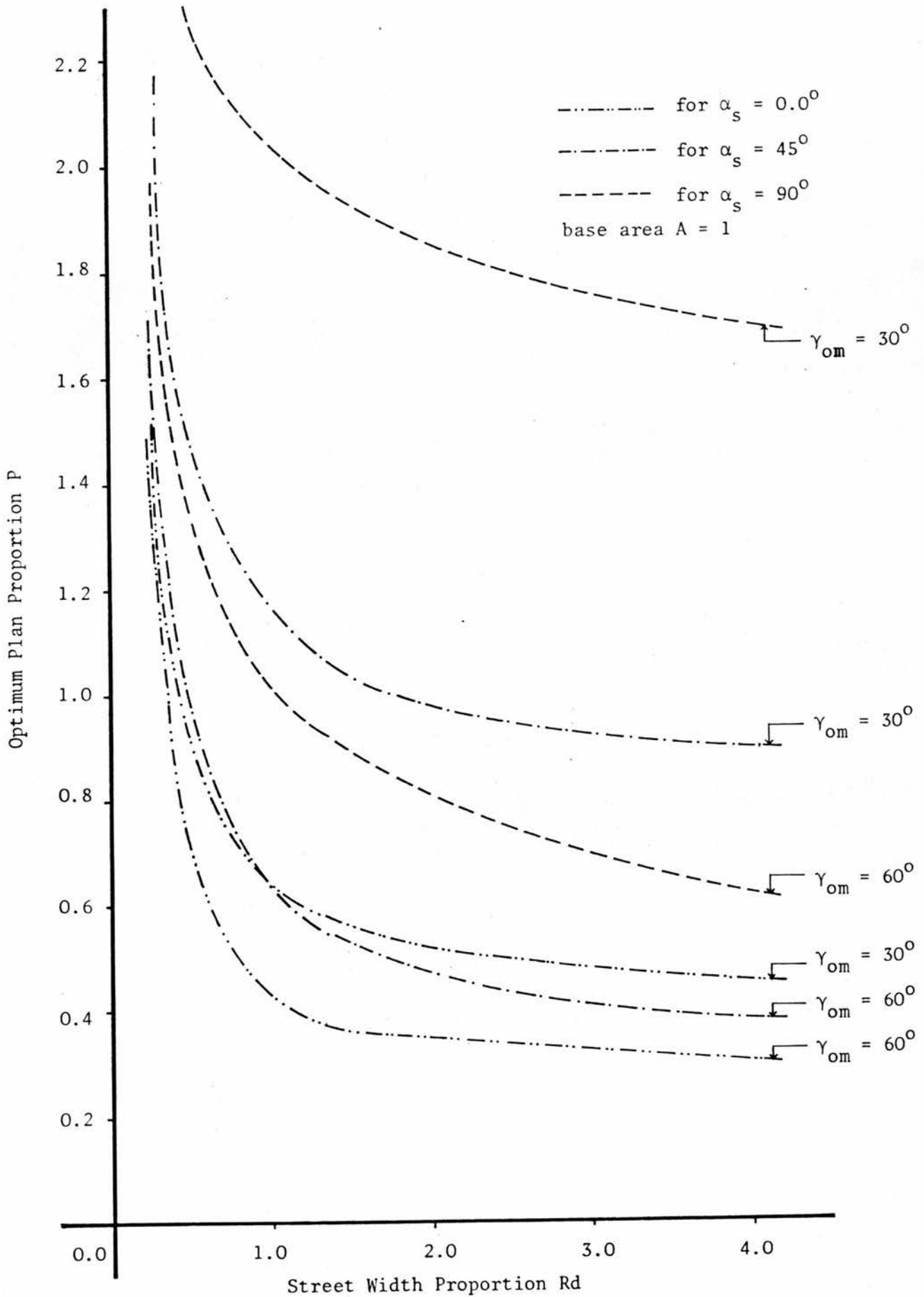


Figure 6.26 The Effect of the Street Width Proportion R_d on the Optimum Plan Proportion for Cases of the Second Progression

The cases of the three major progressions showed that the variation of the base area of the block, and the corresponding variation of the block's height, had no significant effect on the optimum plan proportion. For example, P was found to vary within the range of ± 2 percent by doubling the base area. However, the variation of P with A was found to be influenced by the height of the obstruction and the orientation angle of the block. In the first and third progressions P was found to increase only slightly with the increase of the base area, and the corresponding decrease of the block's height, for $\alpha_s < 45^\circ$. This process was reversed when α_s was greater than 45° . In the second progression P increased with A when the obstruction height was small, ie, less than 1, it decreased as the obstruction height was greater than 1. As the obstruction height approached 1, that is the obstruction height nearly equal that of the block, the variation pattern of P with A was similar to those of the first and third progressions.

6.3.5 The estimation of the optimum plan Proportion P

The estimation of the optimum plan proportion of rectilinear forms, for any orientation and configuration of surrounding, may be achieved from the knowledge of the initial irradiance loads of the facades. The relation between the optimum plan proportion and the irradiance load of the facades has been derived theoretically using the differential calculus. This was achieved by differentiating the function for the irradiance load. The function was derived from the expressions for correction factors, given earlier by equations 6.7 - 6.11.

The differential was then equated to zero to establish the function for minimum irradiance load. The analysis involved was too lengthy and complex to be included and there is room only to state the conclusions and the interpretations of the optimum irradiance function arrived at. These indicated that the ratio of the two dimensions of the optimum plan, that is, the plan proportion P , is inversely proportional to the ratio of the total irradiance load of their respective facades. This closely agreed with the findings of Tappuni (1973), regarding free standing blocks. On this basis, a simplified procedure for estimating the optimum plan proportion has been developed for practical application. In this the initial irradiance load of the facades was approximated by their standard irradiance index, corrected for the variation of the street width proportion. This eliminates the need for correcting the irradiance index with respect to the lengths of the facades, presumably unknown. This procedure was verified and found to agree closely with calculated results obtained from the model. The error involved was within the range of $\pm 5\%$. The procedure may be illustrated clearly by the following example. Taking a case of a building block in the third progression let :

A be the base area equal to 1

R_d the street width proportion equal to 2

α_s the orientation angle of the block at 30° from north

γ_{om} the obstruction angle of the surrounding block at 45°

RL the length proportion of the block

Rw the width proportion of the block

I_{x1}, I_{x2} the standard irradiance index of the facades with the length proportion RL

P_{x1} , P_{x2} the corresponding correction factors of the facades for the street proportion R_d

I_{y1} , I_{y2} the standard irradiance index of the facades with the length proportion R_w

P_{y1} , P_{y2} the corresponding correction factors for R_d

x_1 , x_2 , y_1 , y_2 the irradiance index of the facades corrected for R_d . These are determined according to the expression

$$x_1 = I_{x1} \cdot P_{x1} \quad \dots 6.17(a)$$

$$y_1 = I_{y1} \cdot P_{y1} \quad \dots 6.17(b)$$

x_2 and y_2 are similarly determined.

P is then expressed by the relation

$$P = R_w/RL = (x_1 + x_2)/(y_1 + y_2) \quad \dots 6.18$$

The standard irradiance indices I_{x1} and I_{x2} were obtained from the diagram in Figure 6.17 for the respective orientation angles of the facades of 30° and 120° from north and for $\gamma_{om} = 45^\circ$. They were equivalent to 1.32 and 2.67 KW/m^2 respectively. The corresponding correction factors were calculated according to equation 6.9, P_{x1} and $P_{x2} = 0.928$ and 0.997 respectively, therefore, x_1 and x_2 were equivalent to 1.225 and 2.662 KW/m^2 . Similarly, I_{y1} and I_{y2} were determined as equal to 2.51 and 2.02 KW/m^2 . The correction factors P_{y1} and P_{y2} were 1.029 and 0.994 respectively, y_1 and y_2 were equal to 2.583 and 2.008 KW/m^2 , $P = R_w/RL = 3.887/4.591 = 0.847$.

This estimation of P varies from the true value obtained by the model by about 3 percent. It may be concluded then that the optimum plan proportion is inversely proportional to the ratio of the total standard irradiance indices of their corresponding facades, corrected for the street proportion R_d .

6.3.6 Once the optimum plan proportion was established, the length proportion of the sides of the block, ie, RL and Rw are directly derived according to the base area of the block. These are calculated by the relations given in Table 6.8(a).

$$RL = A\sqrt{A/P} \quad \dots 6.19(a)$$

$$Rw = A\sqrt{A \cdot P} \quad \dots 6.19(b)$$

However, in practical application buildings can be expected to contain volumes, different from the unit volume used in this study. It is also necessary for the designer to interpret the optimum plan and the length proportions of the sides into actual dimensions. This can be achieved by multiplying the final proportions obtained for the sides of the optimum block by a correction factor. It can be proved that the correction factor is a function of the volume of the block. Expression for the correction factor C_p has been derived as

$$C_p = \sqrt[3]{V_n} \quad \dots 6.20$$

where V_n is the required volume of the block.

6.3.7 Variation of the facade area of the optimum form

The total facade area of the optimum block fluctuates only slightly

with orientation. It was found to vary within the range of ± 3 percent. It generally decreases with α_s up to 45° and then increases. The variation of the parameters R_d and γ_{om} showed no significant effect on the optimum facade area. The most significant effect was due to the variation of the base area and height of the block. This is illustrated by the diagram in Figure 6.27.

6.3.7 These patterns were nearly coincidental for all the cases of the three major progressions. It may be concluded that the optimum facade area remains nearly constant regardless of the optimum plan proportion, orientation of the block and the configuration of the surroundings. The length and width proportions of the facades of the optimum form are therefore adjusted in such a way as to maintain the constant facade area.

6.4 THE VARIATION OF THE OPTIMUM IRRADIANCE LOAD WITH THE PARAMETERS OF THE FORM

6.4.1 The effect of orientation on the optimum irradiance load
The optimum irradiance load represented the minimum amount of irradiance which was received on all facades of the optimum block. The effect of orientation on the optimum irradiance load was not significant. Generally, the optimum irradiance increases with α_s up to 45° and then decreases. This explains the tendency for the optimum facade area to decrease with α_s up to 45° and thereafter increase. Such a pattern of variation was typical for the three progressions. The maximum difference of the optimum irradiance

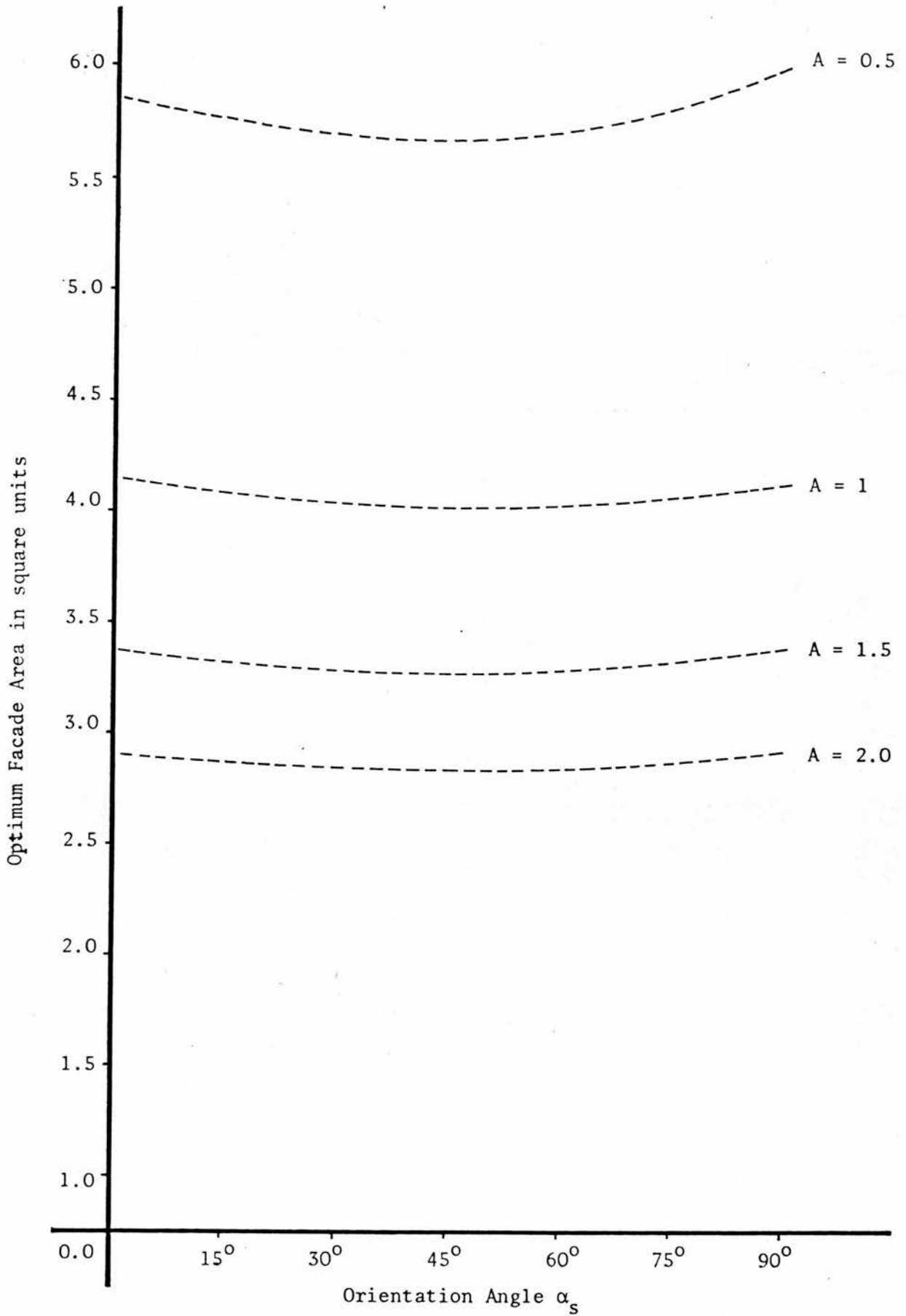


Figure 6.27 Variation of the Optimum Facade Area of the Building Block with Base Area and Orientation

at the different orientations, ie, 0° and 45° , ranged from 5 to 8 percent. The corresponding optimum irradiance of square plan form was slightly greater than that of a rectangular shape. The least amount of optimum irradiance load corresponded to a rectangular plan shape block with its longer facades oriented towards a north-south axis.

6.4.2 The effect of the height of the surrounding obstructions on the optimum irradiance load

In the cases of the first and second progressions the optimum irradiance load increased with the proportion R_d . This was attributed to the fact that the obstruction angles, for the blocks' sides whose opposing obstructions were kept at a constant height, decreased with the increase in R_d . The irradiance load on those facades increased accordingly. However, in the third progression the optimum irradiance load decreased with the increase of R_d . This was due to the corresponding increase of the obstruction height of the surroundings with R_d . The diagram in Figure 6.28 illustrates the variation of the optimum irradiance with R_d . It may be noted that the effect of R_d on the optimum irradiance is most significant for $R_d < 1$. The most significant effect on the optimum irradiance load was due to the variation of the obstruction angle γ_{om} . Obviously, the optimum irradiance decreased with the increase of γ_{om} . An example illustrating this is shown in Figure 6.29. From the graphs shown, a comparison between the performances of the three geometric configuration of the surroundings, in terms of the optimum initial irradiance load of the block, may be drawn. It was evident that the first

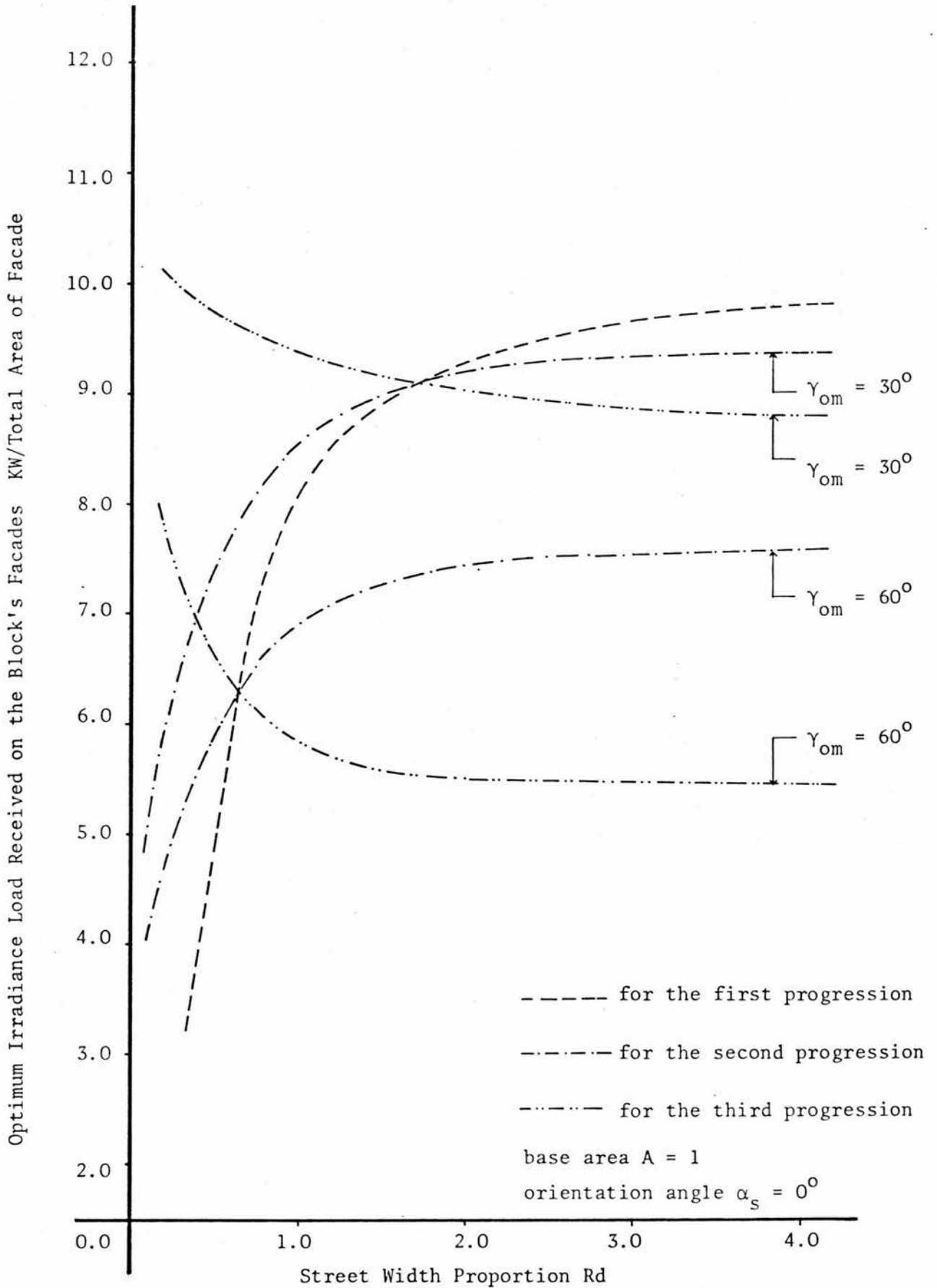


Figure 6.28 Variation of the Optimum Initial Irradiance Load on the Block with Street Width Proportion Rd

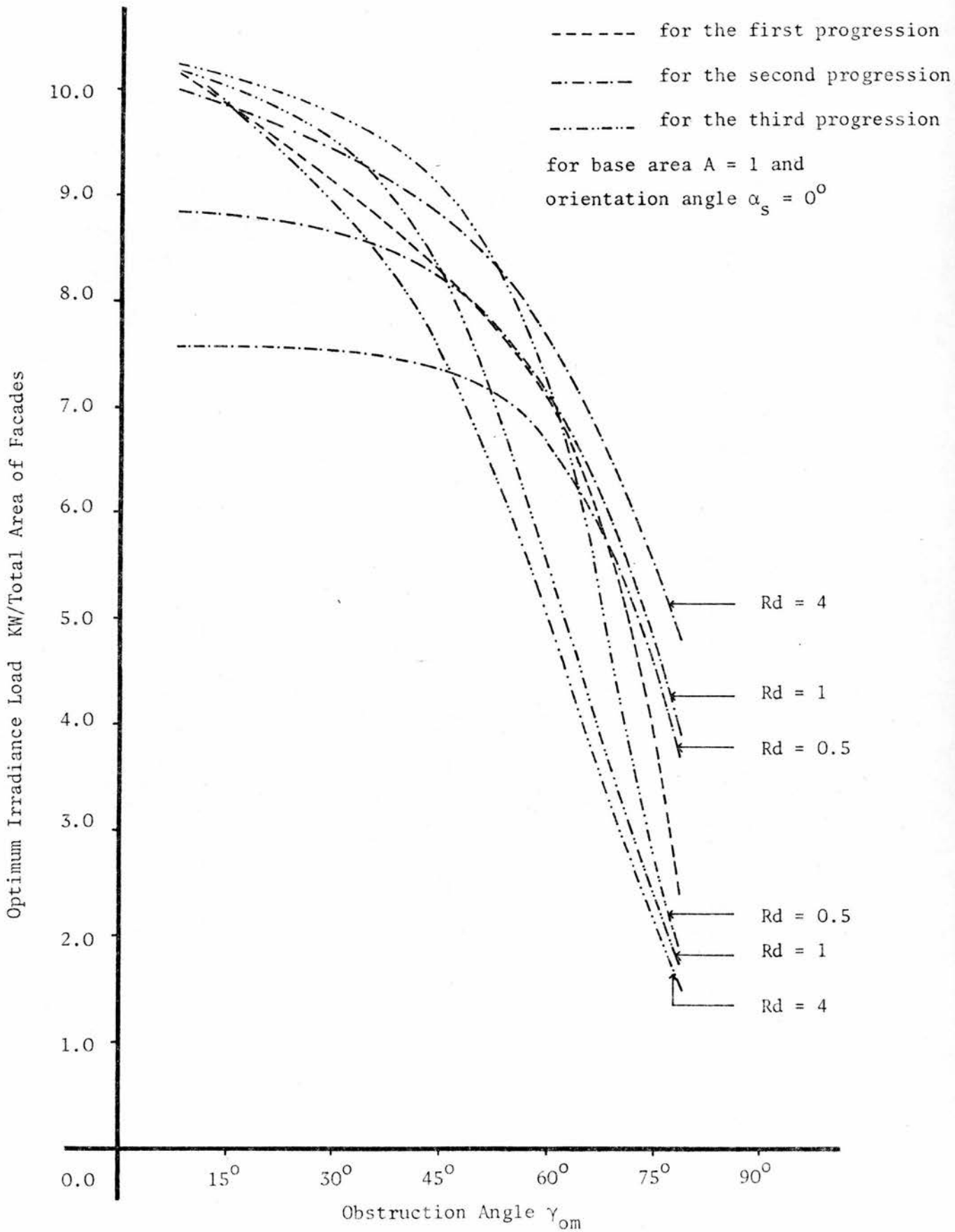


Figure 6.29 Variation of Optimum Initial Irradiance Load of the Block with the Obstruction Angle γ_{om}

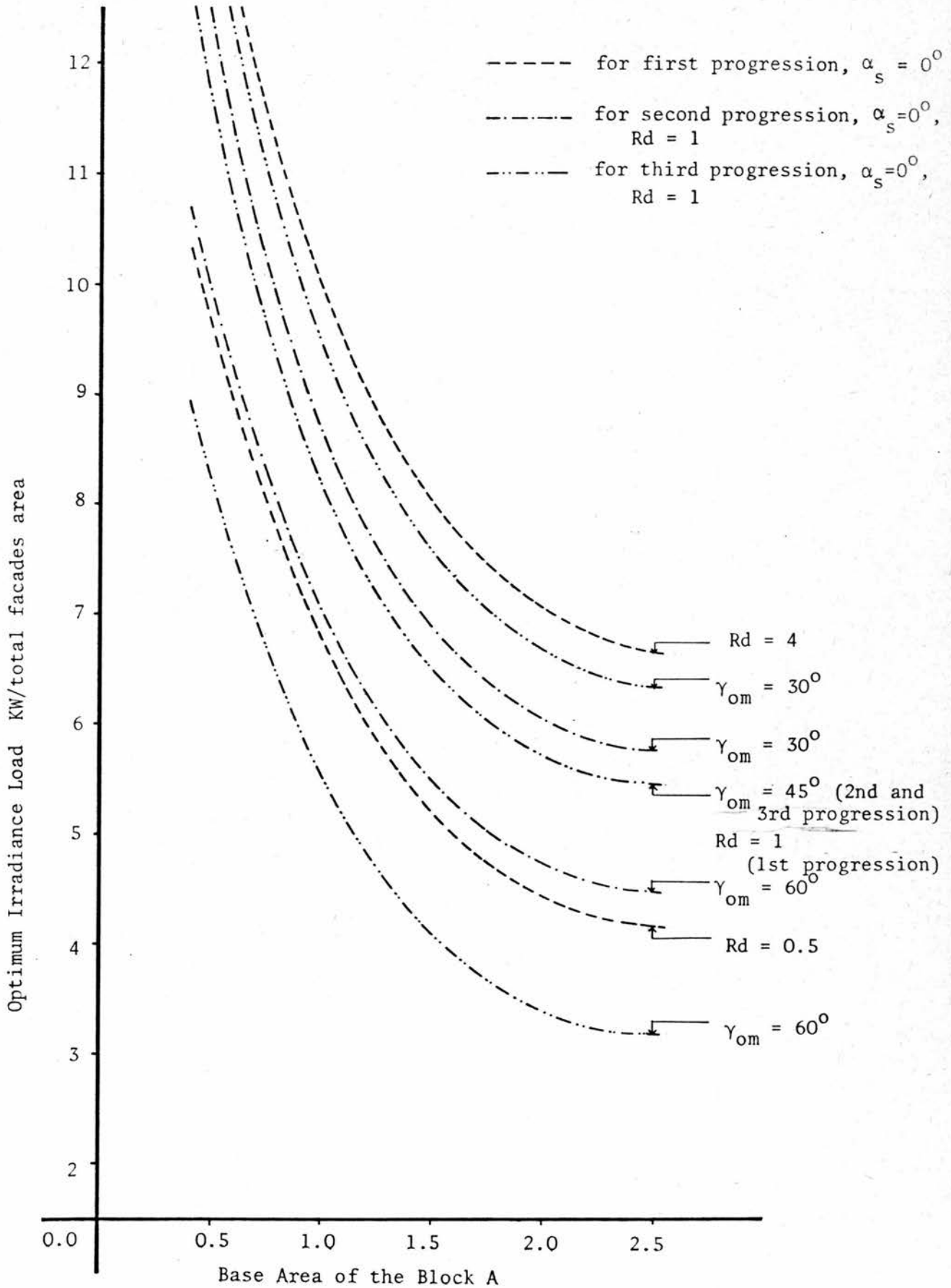


Figure 6.30 Variation of the Optimum Initial Irradiance Load of the Optimum Block with Base Area

progression would provide the least amount of optimum irradiance load in the cases where variable obstruction height of the second and third progressions was less than that of the block. At the same time, the second progression would be better than the third. This order would be reversed as the variable obstruction height is greater than that of the block. In such cases the third progression would serve best followed by the second progression.

6.4.3 The effect of base area and height of block on the optimum irradiance load

The variation of the optimum irradiance load with the base area is illustrated by the diagram in Figure 6.30. This shows that optimum irradiance falls rapidly with the increase of base area. It may be concluded that the shorter the block, the less will be the amount of the optimum irradiance load received. Extrapolation of the curves reveals that the increase of the base area within the range $A > 2.0$ does not significantly affect the magnitude of the optimum irradiance load.

6.5 Consideration of the Optimum Plan Proportion and the Initial Irradiance Load for Maximum Shadow Factor

6.5.1 The model was also used to generate data for the optimum plan proportions of blocks and their total initial irradiance load with respect to the maximum SF criterion. The results indicated that the magnitude of the optimum SF, that is the maximum SF corresponding to the optimum form, generally decreases as the orientation angle α_s approaches 90° . The maximum degree of obstruction to the initial irradiance load corresponds to block

oriented towards the north point.

6.5.2 It appeared that the optimum form favoured a deeper rectangular shape plan. The plan proportion P generally showed constant values and two ranges for the orientation angle, for $\alpha_s < 45^0$ and $\alpha_s > 45^0$. However, the variation of P with the height of the obstruction was similar to that for the minimum irradiance load criterion.

6.5.3 The corresponding optimum irradiance load for the maximum SF was found to be very much greater than the one obtained for the minimum irradiance criterion. This meant that the optimum form determined in terms of the SF criterion would receive more irradiance load even though the degree of obstruction is greater. This may be explained by the fact that the SF only indicates the proportion of the irradiance being obstructed to the total which may be received. The maximisation of the SF involves the adjustment of the lengths of the block's side, by increasing the length of the sides with the highest SF as then it increases with the length. This in turn would result in the increase of the total irradiance load received on the block's facades.

6.5.4 It may be advantageous then to decide on the optimum form in terms of the minimum irradiance rather than in terms of the maximum shadow factor.

7. CONCLUDING REMARKS

7.1.1 On the basis of the analysis of the variation of the optimum irradiance with the geometrical parameters of the form, general geometrical recommendations may be presented for the configuration of form and surroundings for minimum initial irradiance load on buildings.

7.1.2 It has been established that the optimum form may be advantageously defined in terms of the minimum irradiance load rather than on the maximum shadow factor criterion.

7.1.3 Comparison of the optimum irradiance data, representing the minimum irradiance load received on the block's faces, for the different combinations in the three progressions indicates that the optimum irradiance is significantly reduced by increasing the height of the surrounding blocks above the level of the block concerned. The obstruction to all four sides of the block appear to produce twice as much effect than if it was limited to two parallel sides. For example, the optimum irradiance load is decreased by about one percent with the increase of each degree of obstruction on two parallel sides of the block only, while it decreased by 2 percent when the obstruction is on all sides. However, the height obstruction increases rapidly with obstruction angle, proportionally to the tangent of the obstruction angle and R_d . This meant that the increase of the height of obstruction with γ_{om} is disproportionately large with regard to the corresponding decrease of the initial irradiance load which it causes. For example, in a case of the second progression where R_d equals 1, the increase of the obstruction angle from 45° to 50° increases the obstruction height

by 20 percent while reducing the optimum irradiance load by 5 percent. Similarly, at γ_{om} equals to 60° the increase of the obstruction height was about 70 percent while the irradiance load was only reduced by about 15 percent. It may be recommended that γ_{om} should not exceed 60° . This may give a SF_d , on any of the block's facades, by up to 0.5 for the street width proportion within the range $1 < Rd < 4.0$.

7.1.4 Two ranges for the variation of the street width proportion which showed different effects on the optimum irradiance load were identified. The optimum irradiance load was significantly affected by the variation of the street width proportion within the first range where $Rd < 1.0$. For example, the cases of the second progression showed an average increase of the optimum irradiance of about 100 percent with Rd increased from 0 to 1. The variation of the street width proportion within the second range where $Rd > 1$, did not significantly affect the optimum irradiance load. For example, the optimum irradiance load increased by about 6 and 3 percent with each unit of Rd for the cases of the first and second progression respectively. It decreased by about 2 percent for the cases of the third progression.

7.1.5 The optimum irradiance load was found to decrease significantly with the increase in the base area of the block and the subsequent reduction of its height. It decreases by about 50 percent with the increase of each unit of base area, within the range $A < 2.0$. However, the results obtained appear to indicate no significant reduction of irradiance for a base area of $A > 2.5$. The base area should then be decided according to the level of irradiance

load required. It may be recommended that the maximum limit for the base area is $A \approx 2.5$.

7.1.6 It was evident that the optimum form receiving the minimum initial irradiance load favours a rectangular shape with its longer sides oriented towards a north-south axis. In the cases where the surrounding obstruction on sides of the block are of equal height, the optimum plan proportion of the rectangular block may be taken as about 0.55. This is an average value for the different obstruction angles, $\gamma_{om} \leq 60$. To maintain the same level of initial irradiance load, the block may be oriented away from the north-south axis, but with slight modification to the plan proportions, tending to a square shape at 45° . This requires the shortening of the longer sides, that is increasing P by about 1.5 percent, with each degree of displacement from the orientation axes at the 15° intervals. At $\alpha_s = 45^\circ$ from the north point a square shape is favoured. The following values may be recommended for P at the different orientations, for the cases where the height of obstruction on all sides equals that of the block.

α_s	0.0°	15°	30°	45°	60°	75°	90°
P	0.55	0.67	0.82	1.00	1.22	1.49	1.82

7.1.7 A square plan form may be maintained at all orientations by adjusting the height of the obstruction to the facades at which the orientation axis is defined. This may roughly be estimated by taking the height of the obstruction below the level of the block by about 1.5 percent for each angle of displacement from 45°

orientation of the block within the range $0.0 < \alpha_s < 45^\circ$.

Similarly, for the orientation angle within the range $45^\circ < \alpha_s < 90^\circ$ the height of the obstruction is increased above the level of the block by 1.5 percent for each angle of displacement from the 45° orientation axis.

7.1.8 On this basis, the following estimates for the height of obstruction which may produce a square plan, ie, $P = 1$, at the different orientations may be presented.

α_s	0.0	15°	30°	45°	60°	75°	90°
Rh	0.3	0.6	0.8	1.0	1.2	1.5	1.7

7.1.9 A similar procedure may also be followed to decide on the height of the obstruction at the various orientations for specific plan proportion where $P \neq 1$. This first requires the definition of the orientation axis at which the given proportion is achieved when the height of obstruction on all sides equals that of the block. For example, taking a $P = 0.8$ to be maintained at all orientations, the orientation angle for the axis where $P = 0.8$ and $Rh = 1$, is determined from Figure 6.23 or 6.24, it is equivalent to $\alpha_s \approx 30^\circ$. The same procedure as above was then used to estimate the height of obstruction. The values obtained are tabulated below.

α_s	0.0	15°	30°	45°	60°	75°	90°
Rh	0.6	0.8	1.0	1.2	1.5	1.7	1.9

7.1.10 Similarly, the optimum plan proportion at any orientation may be modified by adjusting the height of the obstruction along the orientation axis. This may also roughly be estimated by increasing the optimum proportion for the reduction of the height of obstruction below the level of the block. The optimum plan proportion may be decreased by about 1 percent for every 5 percent increase of the obstruction height above the level of the block. The length proportions of the sides of the optimum block are directly determined from its plan proportion and base area as given by the relations in equations 6.19(a) and 6.19(b).

CHAPTER VII

INVESTIGATION WITH THE MODEL :
THE EFFECTS OF THE GEOMETRICAL AND PHYSICAL PARAMETERS
OF THE FORM ON THE INTERREFLECTED AND FINAL IRRADIANCE

INVESTIGATION WITH THE MODEL : THE EFFECTS OF THE GEOMETRICAL AND PHYSICAL PARAMETERS OF THE FORM ON THE INTERREFLECTED AND FINAL IRRADIANCE

1. INTRODUCTION

1.1.1 The second stage of the investigation with the model being discussed in this chapter deals mainly with the externally interreflected and final irradiance output level of the model. It involves the use of the model in an integrated simulation of the physical processes involved by taking into account the effects of the parameters on both the initial irradiance input of the surfaces of the model and subsequently the interreflected and final irradiance output. The mathematical formulation of the model's interreflected irradiance transfer function was presented in finite difference form by a set of simultaneous equations as discussed earlier in Chapter II. The interreflected irradiance of the surfaces of the model is evaluated by solving the finite difference equations with the computer.

1.1.2 Prior to generating output data for the interreflected irradiance for the vertical facades of the model, two main practical procedures were established. These further simplify the evaluation of the interreflected irradiance and minimise the computation time while retaining sufficient accuracy.

(i) It is verified that a practical geometrical representation for the numerous finite surfaces of the model, which are involved in the multiple interreflection, is conveniently

achieved by taking the vertical facades of the block and the ground between them to be of infinite length.

(ii) It is also verified that the daily average inter-reflected irradiance may be evaluated directly from the values of the daily average initial irradiance of the surfaces of the model.

1.1.3 The analysis of the effects of the geometrical and physical parameters of the form and the ranges within which they significantly influence the interreflected and final irradiance output of the model is conveniently conducted at three main stages in this chapter. The first two stages deal mainly with the effects of the parameters on the interreflected irradiance of a vertical facade of the model. The first assesses the variations of the coefficients of the functions defining the interreflected irradiance components contributed by the different surfaces of the model and finally received on the vertical facade. The coefficients are determined by the geometric configuration of the form and the reflectances of its surfaces. Following this, the second stage of the analysis considers the effects of the parameters on both the initial irradiance input of the surfaces and subsequently on their interreflected irradiance components. These effects are illustrated by the cases where each component is at its maximum with its respective surfaces alternatively facing the sun and receiving maximum irradiance input. The effects of the

parameters on the significance of the contribution of the different interreflected irradiance components to the total interreflected and final irradiance load on a vertical facade are illustrated by their hourly distribution and daily average. It should be noted that a huge amount of data was generated with the model as wide ranges and combinations of parameters were considered. The results presented illustrate typical patterns of distribution of the interreflected irradiance.

1.1.4 The third stage of the investigation deals with the yearly total final irradiance load received on the vertical facade of buildings. As previously done with the initial irradiance, rectangular building blocks are studied. The final irradiance load is evaluated for a wide range geometric configuration of surroundings and facade reflectances. The minimum final irradiance is used as a criterion for defining optimum plan proportions for the block. On this basis the effects of orientation, configuration of surrounding, street width and facade's reflectances on the optimum plan proportion and optimum final irradiance load are investigated and compared with the data previously prepared for the minimum initial irradiance load.

2. EVALUATION OF THE INTERREFLECTED AND FINAL IRRADIANCE LOAD OF THE FACADES

2.1 Geometrical Representation of Block's Finite Facades by a Model of Infinitely Long Surfaces

2.1.1 The interreflection irradiance exchange involves numerous surfaces of the system. In reality, only some of the surfaces may be in direct view of each other. The evaluation of the interreflected and final irradiance which may be received on a surface requires the solution of the finite difference matrix representation of the interreflected irradiance transfer function, which were discussed earlier in parts 7 and 8 of Chapter II. This involves the evaluation of the form factors between the different surfaces of the system, which are in direct view of each other, as well as their initial irradiance. Accordingly, the greater the number of surfaces considered for the model, the greater the computation time and machine capacity required to obtain a solution. The need, therefore, arises for a practical geometrical representation of the numerous finite surfaces of the system which simplifies the calculation of the form factors and the interreflected irradiance while retaining sufficient accuracy.

2.1.2 A number of previous studies considered the numerous finite surfaces involved as extended surfaces of infinite length (O'Brien 1959, 1963, Narasimhan 1969, Plant et al 1969, Mirza 1973). The merits of this procedure in simplifying the

complex calculation of the form factor are evident. However, its accuracy has not been clearly stated. The model was therefore used to verify the accuracy of this procedure.

2.1.3 An alternative model was established. In this model, the numerous surfaces of the system were defined by few finite elements. The definition of the geometrical boundary of the elements of the model was based on the analysis of the form factors between the surfaces of the system. The diagram shown in Figure 7.1 illustrated the hypothetical boundary of the surroundings which was used to simulate the interreflection irradiance exchange between a finite facade, the facades of the surrounding blocks and the ground between them.

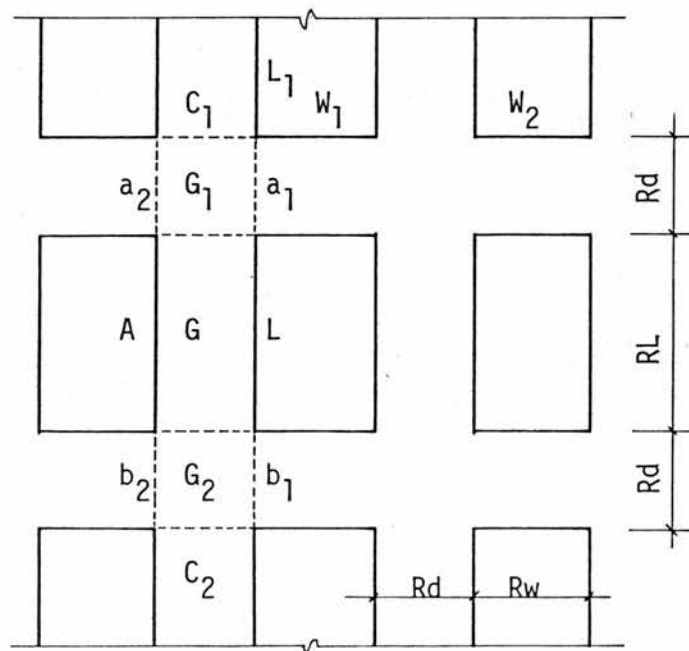


Figure 7.1 The Hypothetical Geometrical Boundary of a Model for the Evaluation Interreflection Irradiance Exchange Between the Surfaces of the System

As seen from the diagram the reflected irradiance from the facade A, which is exchanged with the blocks' facades on the side street W_1 and W_2 , is assumed to be received on a hypothetical side a_1 . This may be justified on the basis of the form factor cosine law (McGuire 1953). It was verified that the form factor between A and the opposing distant facade (L_1) represented less than 10 percent of the form factor value between A and L. This was compensated by considering the irradiance to the distance opposing facades as being received on a hypothetical vertical facade C_1 . Thus, the form factor between A and the opposing open rectangular surrounding of the sides C_1 , a_1 , L, b_1 and C_2 was found to give a form factor value equivalent to that of an opposing extended facade of more than 8 times the facade's length, L.

2.1.4 It was also verified that about 97 percent of the form factor value between the vertical facade and the ground area is due to the ground area (G_1 , G and G_2) contained between the sides of the hypothetical open rectangle shape of the vertical surrounding facade. Doubling this area will only increase the form factor value by 1 percent. However, the irradiance from the ground to the vertical facade was found to be mainly contributed by the immediate ground area G, in front of the vertical facade. The contribution from the ground area G_1 and G_2 was found to be less than 5 percent of the value from G.

2.1.5 On this basis, a model of the finite elements was constructed for the evaluation of the interreflected irradiance. The irradiance from the vertical facade was regarded as being received on the vertical sides and the base of an opposing open rectangular shape as shown in the diagram. The irradiance from vertical opposing facade was similarly determined. The irradiance from the ground was taken as coming from the immediate ground area G only.

2.1.6 The interreflected irradiance of the vertical facade was then calculated for different combinations of facades' reflectance, length and street width proportion. The vertical facades were taken to be of equal height. The ground reflectance was taken to have a constant value of 0.2. The daily average irradiance data, with the vertical facades oriented towards the North-South axis were used for the initial irradiance input to the surfaces. A second set of data for the interreflected irradiance was also prepared on the basis that the vertical facades and the ground between were of infinite length.

2.1.7 Comparison between the two sets of data showed that the interreflected irradiance values calculated for the vertical facade with the finite elements model were slightly higher than those calculated with the model elements of infinite length. The difference between the two values was found to narrow as the facade length and the street width proportions increased.

The figures shown in Table 7.1 illustrate the difference between the values of the finite elements model and that of infinite length. It is given here for a number of combinations of RL and Rd and for a reflectance of the vertical facades (ρ_1 and ρ_2) equal to 0.6.

Rd	RL				
	0.5	1.0	2.0	4.0	8.0
0.5	5.6%	4.6%	3.6%	3.3%	1.8%
1.0	4.6	4.1	3.3	2.7	3.0
2.0	1.9	2.1	1.9	1.4	0.8
4.0	-0.4	0.0	0.2	0.0	-0.4

Table 7.1 Percentage of the Difference Between the Inter-Reflected Irradiance Values Calculated for the Vertical Facade with a Model of Finite and Infinite Length Elements.

2.1.8 It is evident that the difference between the two values is not significant. It may be argued that the difference of the calculated values for the finite model is within the margin of error brought about by the approximate definition of the geometrical boundary of the numerous surface elements of the system. It seems practical then to utilise the model with the infinite length elements for the evaluation of the inter-reflected irradiance. Its accuracy is sufficient for the purpose of this study and it provides greater simplification in the calculation of the form factor values. The effect of facade's

length may be taken into consideration when determining the initial irradiances of the surfaces of the model.

2.1.9 The external subsystem would be represented then by three surfaces only of infinite length, that is the vertical facade, its opposing facade and the ground between them. For this case an expression for the direct evaluation interreflected irradiance of the vertical facade was derived. This was achieved by taking the finite difference equations in a series of algebraic substitutions as shown earlier by equation 2.50 in part 9 of Chapter II, which is given below.

$$\begin{aligned}
 I_{R1} = & [\rho_1 \cdot \rho_2 \cdot F_{21} \cdot F_{12} \cdot I_{11} + \rho_1 \cdot \rho_3 \cdot F_{13} \cdot F_{31} \cdot I_{11} + \rho_1 \cdot \rho_2 \cdot \rho_3 \cdot F_{13} \cdot F_{32} \cdot F_{21} \cdot I_{11} \\
 & + \rho_1 \cdot \rho_2 \cdot \rho_3 \cdot F_{12} \cdot F_{23} \cdot F_{31} \cdot I_{11} + \rho_2 \cdot F_{12} \cdot I_{12} + \rho_2 \cdot \rho_3 \cdot F_{13} \cdot F_{32} \cdot I_{12} \\
 & + \rho_3 \cdot F_{13} \cdot I_{13} + \rho_2 \cdot \rho_3 \cdot F_{12} \cdot F_{23} \cdot I_{13}] / \\
 & [1.0 - \rho_1 \cdot \rho_2 \cdot F_{12} \cdot F_{21} - \rho_1 \cdot \rho_3 \cdot F_{13} \cdot F_{31} - \rho_2 \cdot \rho_3 \cdot F_{32} \cdot F_{23} \\
 & - \rho_1 \cdot \rho_2 \cdot \rho_3 \cdot F_{13} \cdot F_{32} \cdot F_{21} - \rho_1 \cdot \rho_2 \cdot \rho_3 \cdot F_{12} \cdot F_{23} \cdot F_{31}] \quad (7.1)
 \end{aligned}$$

Similar expressions can easily be derived for the other two surfaces of the system. This equation was incorporated into the model for the evaluation of the interreflected irradiance. The form factors for the surfaces were then determined with the crossed-string method.

2.2 Evaluation of the Daily Average Interreflected Irradiance Load

2.2.1 The yearly total and daily average may also be taken as measures for the final and the externally interreflected irradiance load on a similar basis to the initial irradiance load. The calculation of the daily average interreflected irradiance I_{rd} , may then be carried out on a similar basis to the initial irradiance load as expressed by equations 6.1 and 6.2 given earlier in part 2.2 of Chapter VI. However, it was evident that such a procedure would require a greater amount of computation and time since it involves the evaluation of hourly initial irradiance values for all the surfaces of the system considered.

2.2.2 An exploratory investigation was therefore carried out to establish a simplified procedure for the evaluation of I_{rd} . The model was used to generate data for I_{rd} using hourly values for the initial irradiance input to the surfaces of the system for a number of combinations of the geometrical and physical parameters. These were compared with a second set of data generated by the model using the daily average for the initial irradiance input to the surfaces. The two sets of data were found to be in good agreement. Hence, it was concluded that the daily average interreflected irradiance I_{rd} can be determined with reasonable accuracy from the daily average initial irradiance values of the surfaces, which are directly obtainable with the initial irradiance indices and their associated correction factors described earlier in part 5 of Chapter VI.

3. THE EFFECTS OF THE GEOMETRICAL AND PHYSICAL PARAMETERS ON THE INTERREFLECTED IRRADIANCE

3.1 Components of the Interreflected Irradiance

3.1.1 As seen from equation 7.1 given above, the externally interreflected irradiance which may be received on a surface of the system may be regarded as composed of three components. Thus, the following components are taken to comprise the total interreflected irradiance received on a vertical facade :

- (i) Facade component I_{rf} , which defines that part of the interreflected irradiance received on the facade due to its own initial irradiance after multiple interreflection between the surfaces of the system;
- (ii) Ground component I_{rg} , which similarly defines the part of the interreflected irradiance received on the facade due to multiple interreflection of the initial ground irradiance; and
- (iii) Surrounding component I_{rs} , similarly defining the part of the interreflected irradiance caused by the multiple interreflection of the initial irradiance of the surrounding vertical surfaces.

The total interreflected irradiance I_R is then given by the function

$$I_R = I_{rf} + I_{rg} + I_{rs} \quad (7.2)$$

The magnitude of each component is, therefore, determined by the magnitude of its initial irradiance, geometrical and reflectance characteristics of the surfaces of the system.

3.1.2 The theoretical analysis of the interreflected irradiance transfer function, which was discussed earlier in part 9 of Chapter II, has indicated that the components of the interreflected irradiance are directly proportional to their initial irradiance I_I . Hence, an interreflected irradiance component I_{rc} may be expressed by a function of the form :

$$I_{rc} \propto I_I \quad 7.3(a)$$

$$I_{rc} = a \cdot I_I \quad 7.3(b)$$

The coefficient a expresses the effect of the geometrical and reflectance characteristics of the surfaces. Therefore, it directly determines the magnitude of the interreflected component.

3.1.3 The variation of the geometrical parameters of the form was shown to have significant effect on the magnitude of the initial irradiance load of the surfaces, as discussed earlier in part 4 of Chapter VI. Accordingly, the effects of varying the parameters of the system on the components of the interreflected irradiance may be clearly established by isolating their effects on the initial irradiance. This may be conveniently achieved by expressing the components of the interreflected irradiance as proportions of their initial

irradiance inputs. The proportions are then functions of the geometrical and reflectance properties of the surfaces. They may be expressed by a function of the form

$$a = I_{rc}/I_I \quad 7.4$$

3.2 Coefficients of the Interreflected Irradiance Components and their Variations with the Parameters of the System

3.2.1 The following terms are used, for convenience, to express the coefficients of the functions defining the components of the interreflected irradiance received on a vertical facade.

(i) Coefficient of facade component a_{cf} : It expresses the proportion of the facade component of the interreflected irradiance, which is initiated by its own irradiance input and is finally received on the facade after multiple inter-reflection I_{rf} , to its initial irradiance input I_{If} .

$$a_{cf} = I_{rf}/I_{If} \quad 7.5(a)$$

(ii) Coefficient of ground component a_{cg} which similarly expresses the proportion of the ground component of the interreflected irradiance received on the vertical facade I_{rg} to the ground initial irradiance input I_{Ig} .

$$a_{cg} = I_{rg}/I_{Ig} \quad 7.5(b)$$

(iii) Coefficient of surrounding component a_{cs} , similarly gives the proportion of the surrounding component of the interreflected irradiance I_{rs} , to its initial irradiance I_{Is} .

$$a_{cs} = I_{rs}/I_{Is} \quad 7.5(c)$$

Expressions for the coefficients of the three components are directly derived from equation 7.1. They are expressed in terms of the reflectance of the surfaces and the form factors between them.

$$\begin{aligned} a_{cf} = & (\rho_f \cdot \rho_g \cdot F_{fg} \cdot F_{gf} + \rho_f \cdot \rho_s \cdot F_{fs} \cdot F_{sf} + \rho_f \cdot \rho_g \cdot \rho_s \cdot F_{fs} \cdot F_{sg} \cdot F_{gf} \cdot \\ & + \rho_f \cdot \rho_g \cdot \rho_s \cdot F_{fg} \cdot F_{gs} \cdot F_{sf}) / (1 - \rho_f \cdot \rho_g \cdot F_{fg} \cdot F_{gf} - \rho_f \cdot \rho_s \cdot F_{fs} \cdot F_{sf} \cdot \\ & - \rho_g \cdot \rho_s \cdot F_{gs} \cdot F_{sg} - \rho_f \cdot \rho_g \cdot \rho_s \cdot F_{fs} \cdot F_{sg} \cdot F_{gf} \cdot \\ & - \rho_f \cdot \rho_g \cdot \rho_s \cdot F_{fg} \cdot F_{gs} \cdot F_{sf}) \end{aligned} \quad 7.6(a)$$

$$\begin{aligned} a_{cg} = & (\rho_g \cdot F_{fg} + \rho_g \cdot \rho_s \cdot F_{fs} \cdot F_{sg}) / (1 - \rho_f \cdot \rho_g \cdot F_{fg} \cdot F_{gf} - \rho_f \cdot \rho_s \cdot F_{fs} \cdot F_{sf} \cdot \\ & - \rho_g \cdot \rho_s \cdot F_{gs} \cdot F_{sg} - \rho_f \cdot \rho_g \cdot \rho_s \cdot F_{fs} \cdot F_{sg} \cdot F_{gf} - \rho_f \cdot \rho_g \cdot \rho_s \cdot F_{fg} \cdot F_{gs} \cdot F_{sf}) \end{aligned} \quad 7.6(b)$$

$$\begin{aligned} a_{cs} = & (\rho_s \cdot F_{fs} + \rho_g \cdot \rho_s \cdot F_{fg} \cdot F_{gs}) / (1 - \rho_f \cdot \rho_g \cdot F_{fg} \cdot F_{gf} - \rho_f \cdot \rho_s \cdot F_{fs} \cdot F_{sf} \cdot \\ & - \rho_g \cdot \rho_s \cdot F_{gs} \cdot F_{sg} - \rho_f \cdot \rho_g \cdot \rho_s \cdot F_{fs} \cdot F_{sg} \cdot F_{gf} - \rho_f \cdot \rho_g \cdot \rho_s \cdot F_{fg} \cdot F_{gs} \cdot F_{sf}) \end{aligned} \quad 7.6(c)$$

3.2.2 Thus the coefficients of the interreflected irradiance components may be evaluated and their variation with the parameters of the system analysed. A model of two infinitely

long opposing facades with a ground space separating them was then used to generate data for the coefficients of the inter-reflected irradiance components for a vertical surface and for a wide range and combination of parameters.

3.2.3 Variation of the interreflected irradiance components' coefficients with the street width proportion R_d : The data obtained indicated that values of the coefficient of the surrounding component were appreciably greater than the corresponding coefficient of the facade component for different geometric configurations of form. However, the variation of the two coefficients with R_d showed similar patterns. Typical patterns of distribution are illustrated by the diagram in Figure 7.2. As seen from the diagram, the two coefficients decrease with the increase of R_d . The decrease is more rapid for the street width proportion within the range $R_d < 2.0$, but more gradual for $R_d > 2.0$. The coefficient of the ground component a_{cg} was found to vary in an opposite manner to a_{cs} and a_{cf} . Typical patterns of variation of a_{cg} with R_d are also shown in Figure 7.2. The ground coefficient increases with R_d . The increase is more rapid within the range $R_d < 2.0$. It is less significant for $R_d > 2.0$ where a_{cg} increases by about 3 percent with each unit of R_d .

3.2.4 Variation of the interreflected irradiance components' coefficients with the obstruction height proportion R_h : The variation patterns of the coefficients of the three

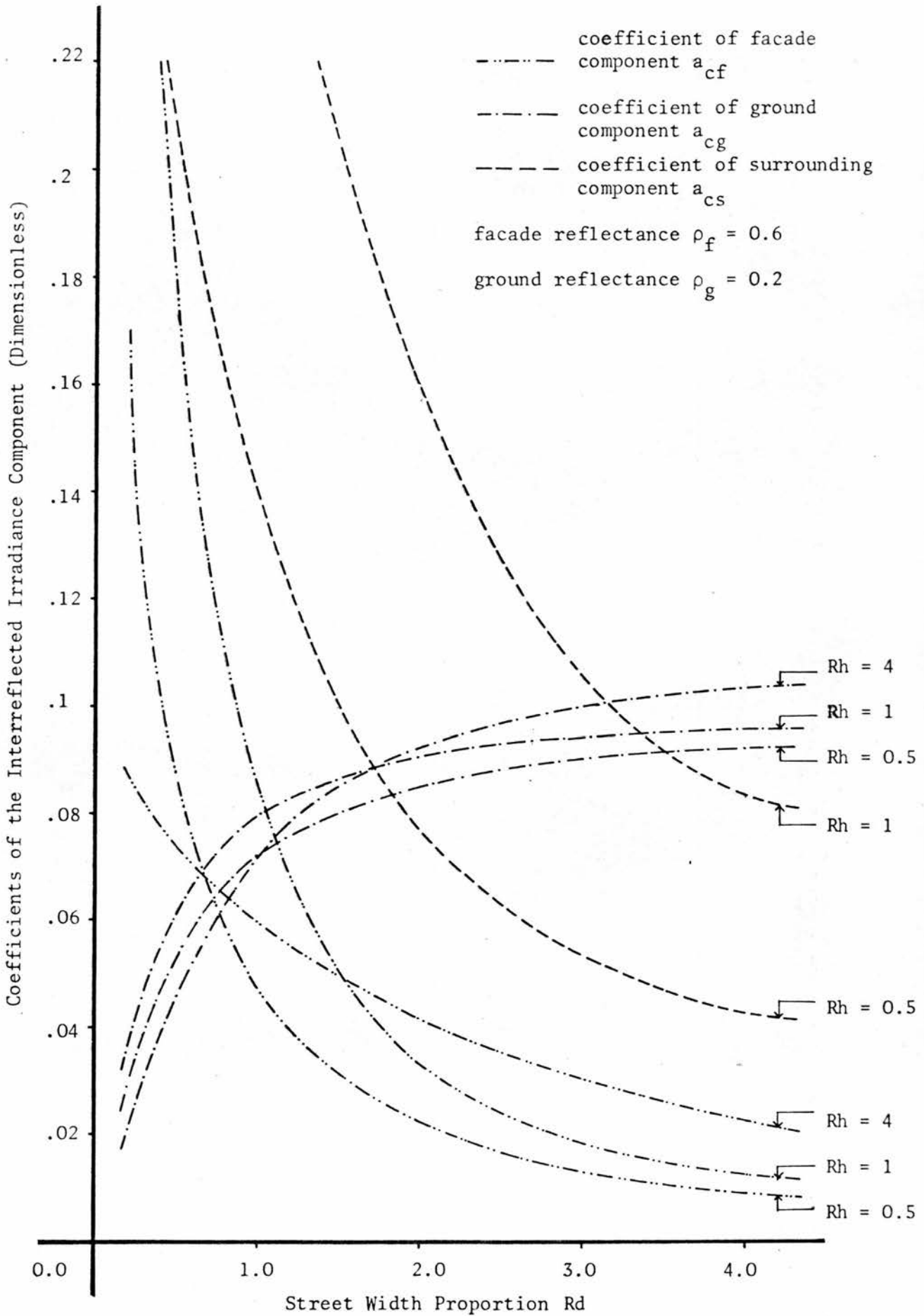


Figure 7.2 Variation of the Coefficients of the Interreflected Irradiance Components of a Vertical Facade with the Geometrical Parameters

components of the interreflected irradiance of the vertical facade with the proportion of the height of obstruction are illustrated by the example shown in Figure 7.3. From the diagram shown it may be possible to define two ranges for R_h which indicate different patterns of variation for the coefficients of the facade and ground with R_d . In the first range the coefficients increase with R_h . The rate of increase is particularly rapid for the facade coefficient, but decreases with the increase of R_d . Thus, the smaller value of R_d , the smaller the value of R_h which defines the upper limit of the first range. For example, in the case of the coefficient of the facade component, the upper limit varies from R_h about 1 for R_d equals 0.5, to R_h about 1.7 when R_d equals 4. In the second range both ground and facade coefficients decrease with further increase in R_h . The rate of decrease is reduced with the increase of R_d . It is evident that the coefficients a_{cg} and a_{cf} are less significantly affected with the increase of R_h beyond certain limits in the second range. For example, the coefficient of the ground component a_{cg} is not reduced significantly with $R_h > 2.0$, for different street width proportions. The coefficient of the facade component, similarly, is not reduced significantly with $R_h > 4$ when $R_d \geq 1$. As R_d is increased to be greater than 2, a_{cf} is not significantly affected by the variation of R_h within the range greater than 2.0. As for the coefficient of the surrounding component the indications are that it

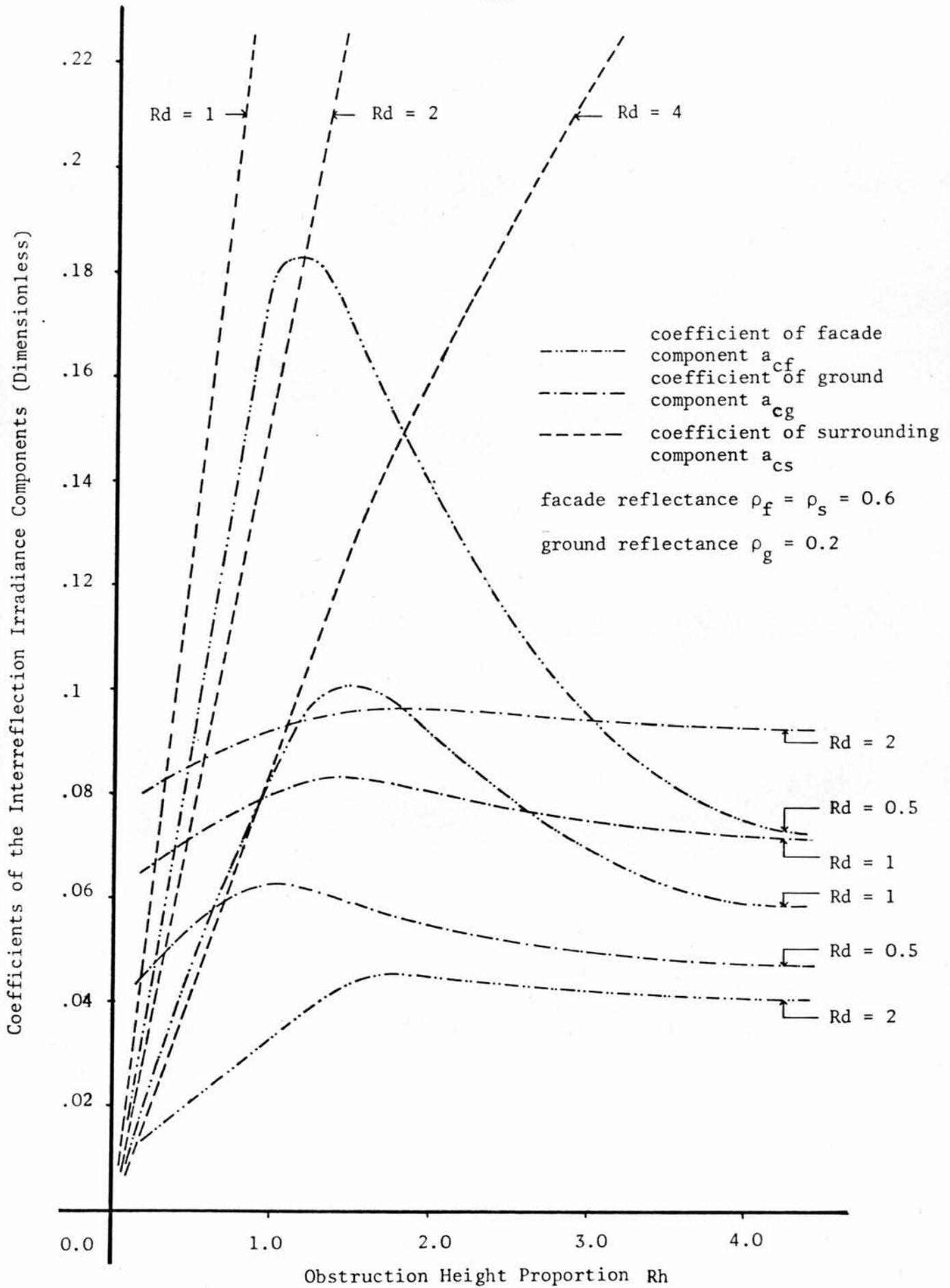


Figure 7.3 Variation of the Coefficients of the Interreflected Irradiance Components of a Vertical Facade with the Geometrical Parameters

increases rapidly with the increase of R_h . The rate of increase is slightly reduced with the increase of R_h and R_d .

3.2.5 Variation of the coefficients of the interreflected irradiance components with the simultaneous variation of the street width and the obstruction height proportions

Since the height of obstruction R_h was expressed in terms of the street width and obstruction angle, R_h therefore varies with the variation of R_d for any given obstruction angle. The combined effect due to the simultaneous variation of R_d and R_h on the interreflected components' coefficients is illustrated in Figure 7.4. The diagram shows that the facade coefficient generally increases with γ_{om} . It also increases with R_d , reaches a maximum value, and then decreases. Hence, two ranges of R_d may be identified which define the variation pattern of a_{cf} with R_d . In the first range a_{cf} increases rapidly from zero to its maximum value with the increase of R_d . The greater the obstruction angle, that is the obstruction height, the greater the rate of increase. The upper limit of R_d for this range is governed by γ_{om} . The greater the value of γ_{om} , the smaller the value of R_d . For example, when γ_{om} equals 30° R_d is about 0.8 and when γ_{om} equals 60° R_d is about 0.4. The increase of a_{cf} with R_d in the first range may be attributed mainly to the corresponding increase of R_h .

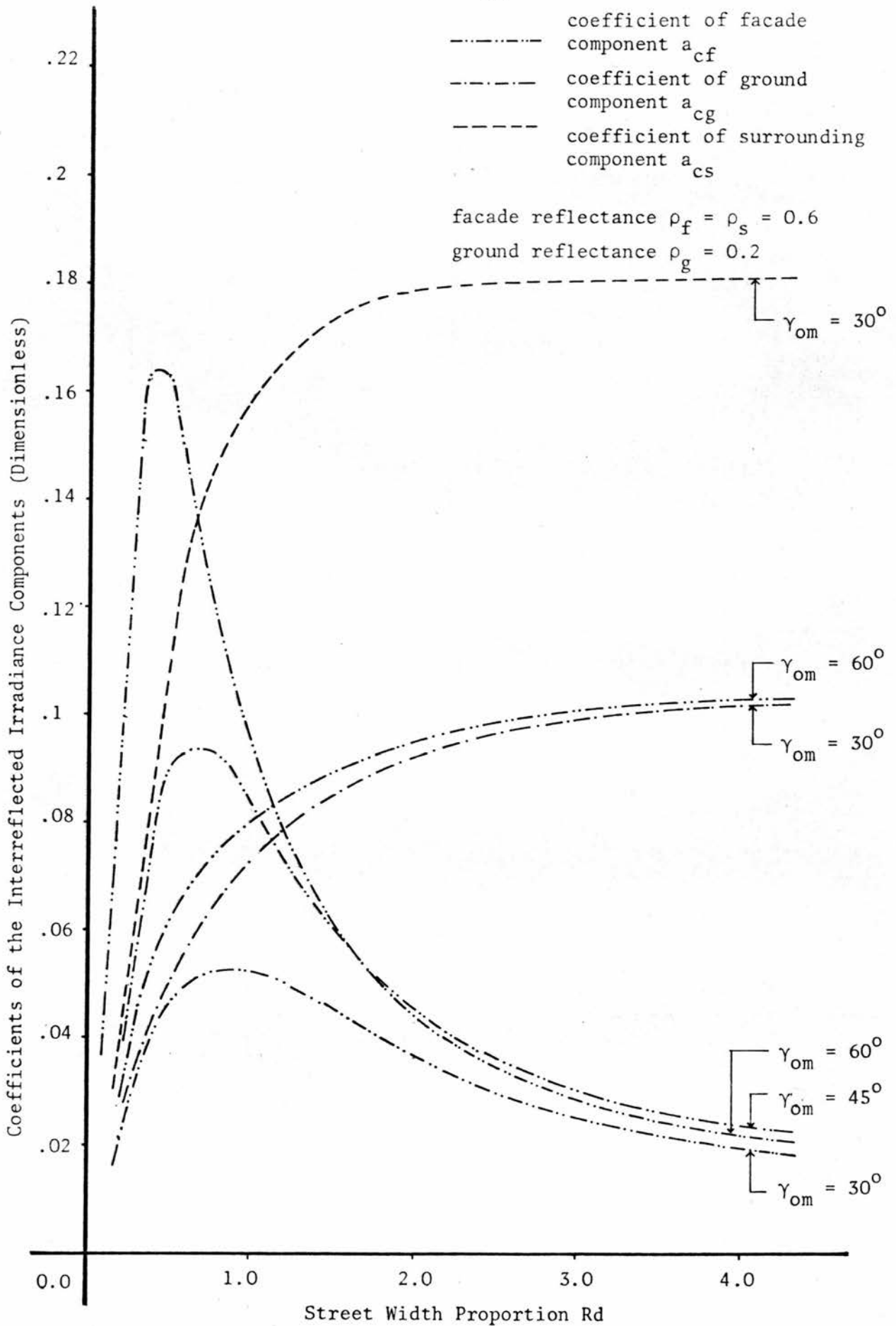


Figure 7.4 Variation of the Coefficients of the Interreflected Irradiance Components of a Vertical Facade with the Simultaneous Variation of the Street Width and Obstruction Angle

In the second range of R_d , a_{cf} generally decreases with the increase of R_d . The rate of decrease is reduced with the increase of the facades' reflectance and also with R_d . However, for $R_d > 2.0$, a_{cf} does not vary significantly with γ_{om} . It is evident that the variation of R_h for the second range of R_d does not significantly affect the general pattern of variation of a_{cf} with R_d . The ground coefficient a_{cg} increases with R_d . The rate of increase is rapid for $R_d < 2.0$ but more gradual beyond this point. It is evident that the general pattern of variation of a_{cg} with R_d is not significantly affected by the variation of γ_{om} and the corresponding variation of R_h , particularly when $R_d > 2.0$. The variation patterns of the surrounding coefficient a_{cs} with R_d are similar to those of the facade component. a_{cs} increases rapidly with R_d in the first range, the upper limit of which is governed by γ_{om} . The upper limit values of the first range of R_d for a_{cs} are slightly greater than the corresponding ones for a_{cf} . The increase of a_{cs} in this range may also be attributed to the increase of R_h . a_{cs} also decreases with the increase of R_d in its second range. The rate of decrease is slightly increased with the increase of γ_{om} , but a_{cs} does not vary significantly with $R_d > 2.0$. However, the increase of R_h in the second range increases the value of a_{cs} appreciably.

3.2.6 The effects of surfaces' reflectances on the interreflected irradiance components' coefficients

The variation of the reflectances of the model's surfaces

showed similar effects on the interreflected irradiance components of the vertical facade. The components showed varying degrees of increase with the increase of the different reflectances of the surfaces. Typical patterns for the distribution of the interreflected components' coefficients with the surfaces' reflectances are illustrated in Figure 7.5 for a form configuration of R_d and R_h equals 1. The graphs shown indicate an almost linear relationship between the components' coefficients and the reflectances. Each coefficient appears to be directly proportional to the reflectance of its corresponding surface. For example, the ground coefficient is directly proportional to the ground reflectance. However, the rates of increase for the different coefficients of the interreflected irradiance components with the reflectances of the surfaces are determined by the geometrical configuration of the form. It is evident from the data obtained that the rates of increase for the facade coefficient with the surfaces' reflectances; in other words, the slopes of the curves shown in Figure 7.5, generally decrease with the increase of R_d and R_h , particularly for $R_h > 1$. The rates of increase for the ground and surrounding coefficients with the reflectances of the surfaces, however, increase with the increase of R_h and R_d , particularly within the range $R_d < 2$. Thus, the indications are that the effects of reflectances on the coefficients of the ground and surrounding components are enhanced by the increase in the form parameters while retarded in the case of the facade component. An illustration of the effects of the

reflectances on the coefficients of the interreflected components may be drawn from the graphs shown in Figure 7.5 for a form configuration of R_h and R_h equals 1. The increase in the facade reflectance ρ_f does not seem to have significant effect on the ground and the surrounding coefficients. For example, the increase of ρ_f from 0.2 to 0.4 increases both the ground and the surrounding coefficients by about 8 percent. Variation of the ground reflectance ρ_g have a marked effect on the facade coefficient, but less significant effect on the surrounding coefficient. For example, when ρ_g was increased from 0.2 to 0.4 the facade and surrounding coefficients increased by about 23 and 5 percent respectively, whereas the ground coefficient is doubled. The variation of the surrounding reflectance ρ_s also showed a marked effect on the facade coefficient, but a less significant effect on the ground one. For example, when ρ_s is increased from 0.2 to 0.8 the facade coefficient is tripled while the ground coefficient is increased by 32 percent. At the same time the value of the surrounding coefficient is quadrupled. It may be concluded then that each of the interreflected irradiance components' coefficients of the vertical facade is mainly influenced by the reflectance of its respective surface. The facades coefficient is additionally influenced to a great extent by the reflectance of the ground ρ_g and surrounding ρ_s .

----- Variation with the reflectance of facade ρ_f
 for $\rho_s = 0.6$ and $\rho_g = 0.2$

----- Variation with the reflectance of ground ρ_g ,
 for ρ_s and $\rho_f = 0.6$

----- Variation with the reflectance of the surrounding
 ρ_s , for $\rho_f = 0.6$ and $\rho_g = 0.2$

Proportion of form parameters, R_d and $R_h = 1$

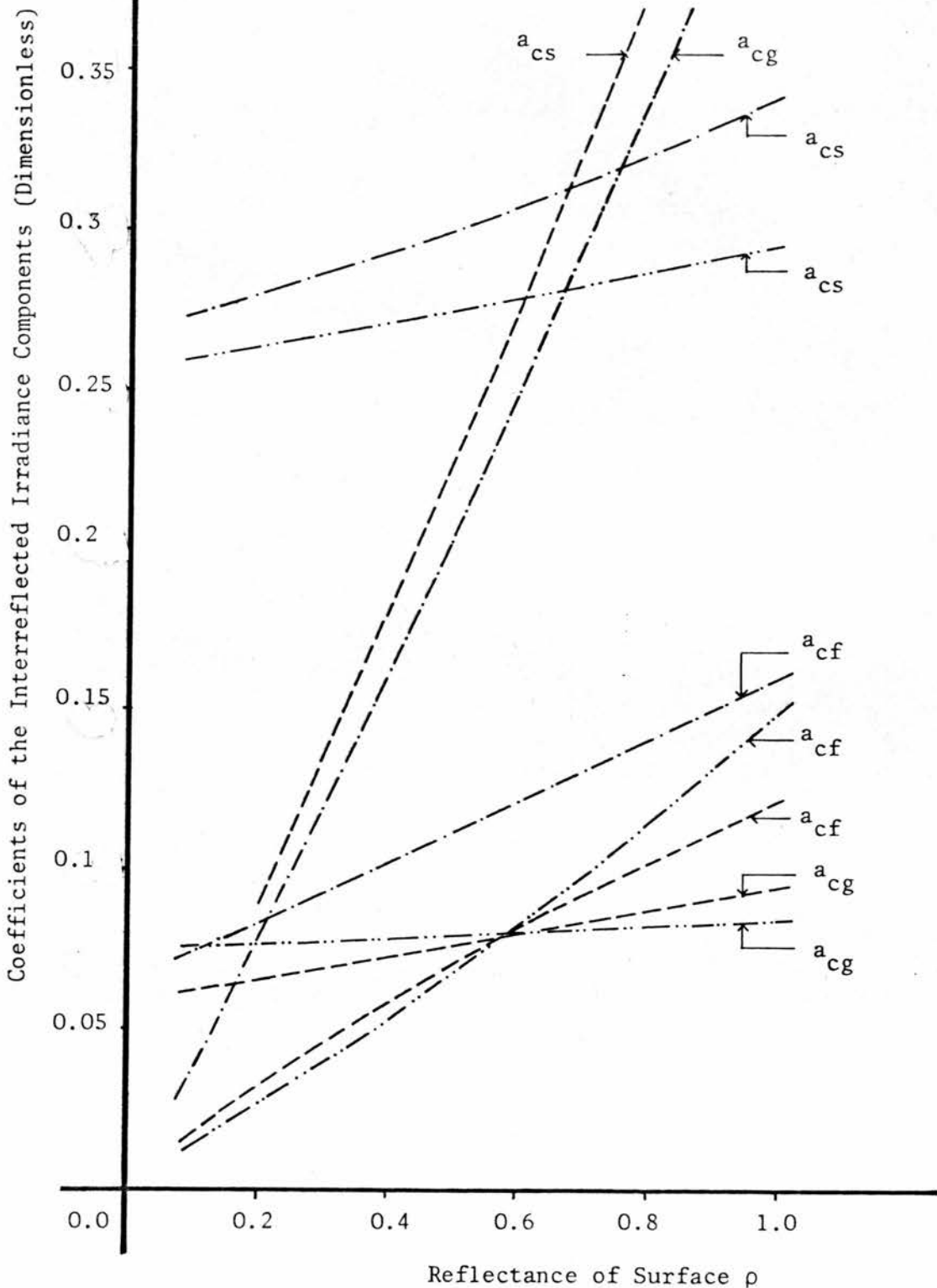


Figure 7.5 Variation of the Coefficients of the Interreflected Irradiance Components of a Vertical Facade with the Reflectances of the Surfaces of the Model

3.3 The Effect of the Geometrical and Physical Parameters of the Form on the Instantaneous Initial Irradiance and Interreflected Irradiance and its Components

3.3.1 The magnitude of the total interreflected irradiances and their constitutive components which are finally received on the surfaces of the model are determined by the relative position of the sun in the sky and the geometrical configuration of the form with respect to the shading and obstruction of the direct solar and diffuse sky radiation by the adjacent buildings. Therefore, any accurate assessment of the effects of varying the geometrical parameters of the form on the interreflected irradiance has to take into account their effects on the initial irradiance inputs of the system's surfaces.

3.3.2 On this basis the model of the infinitely vertical facades and the ground separating them was used to investigate the cumulative effects of varying the geometrical parameters of the forms on the interreflected irradiance and its components. The vertical facades of the model were oriented towards an east west axis. Data for the interreflected irradiance for a vertical facade of the model was prepared for a wide range and combinations of parameters. This was calculated at different times of day on August 8th, where the declination of the sun coincides with the latitude of Khartoum.

3.3.3 To illustrate and assess the effects of the variation of the parameters of the form on the total interreflected irradiance and its components, three cases are chosen indicating different positions of the sun at 8.00, 12.00 and 16.00 hours. They represent the situations where the sun has an altitude of about 33° and directly opposite the vertical facade, for which the interreflected irradiance is being evaluated, vertically overhead the ground and directly opposite the vertical surrounding with an altitude of 32° respectively. Thus, each surface of the model alternatively faces the sun and receives the maximum initial irradiance input.

3.3.4 The magnitudes of the initial irradiances of the surfaces of the model are determined by the values of their shadow factors and the relative position of the sun. The initial irradiance of a vertical facade facing the sun is mainly composed of direct solar irradiance which is generally of a much higher order compared to the diffuse sky radiation. The initial irradiance of the vertical facade, facing the sun, increases rapidly with the decrease of the height of the shadow cast on it by surrounding buildings, following the increase of the street width or the decrease of the obstruction height. When the facade is fully exposed to the direct solar rays and free from shadow its initial irradiance varies only slightly with the variation of R_d or R_h following the variation of the diffuse sky radiation received. Thus, the vertical facade receives its greatest initial irradiance when it is directly opposite the sun and the least when the sun is behind it, where it receives diffuse sky

radiation only. When the solar altitude is low, such as in the first and third cases at 8.00 and 16.00 hours, where γ_0 is about 33° , the magnitude of the initial ground irradiance is relatively smaller than that of the vertical facade facing the sun. However, it similarly increases with the decrease of its shadow factor following the increase of R_d or the decrease of R_h . The ground receives its greatest initial irradiance when the sun is overhead, such as in the second case at 12.00 hours. Its initial irradiance then varies only slightly with the variation of R_d and R_h . The diagrams shown in Figures 7.6 and 7.7 illustrate typical patterns of variation of the initial irradiances of the surfaces of the model with the geometrical parameters as the sun is facing the vertical facades and overhead the ground.

3.3.5 It has been shown earlier by equation 7.3 that the inter-reflected irradiance components are directly proportional to the coefficients and initial irradiances of their respective surfaces. The variation patterns of the total interreflected irradiance and its constitutive components which may be received on a vertical facade of the model, with the parameters of the form are, therefore, determined by the corresponding variation of the coefficients and initial irradiances of the surfaces of the model. The inter-reflected irradiance components then reach their highest values in the situations where both the initial irradiances and coefficients of their respective surfaces are highest and vice versa for their lowest values.

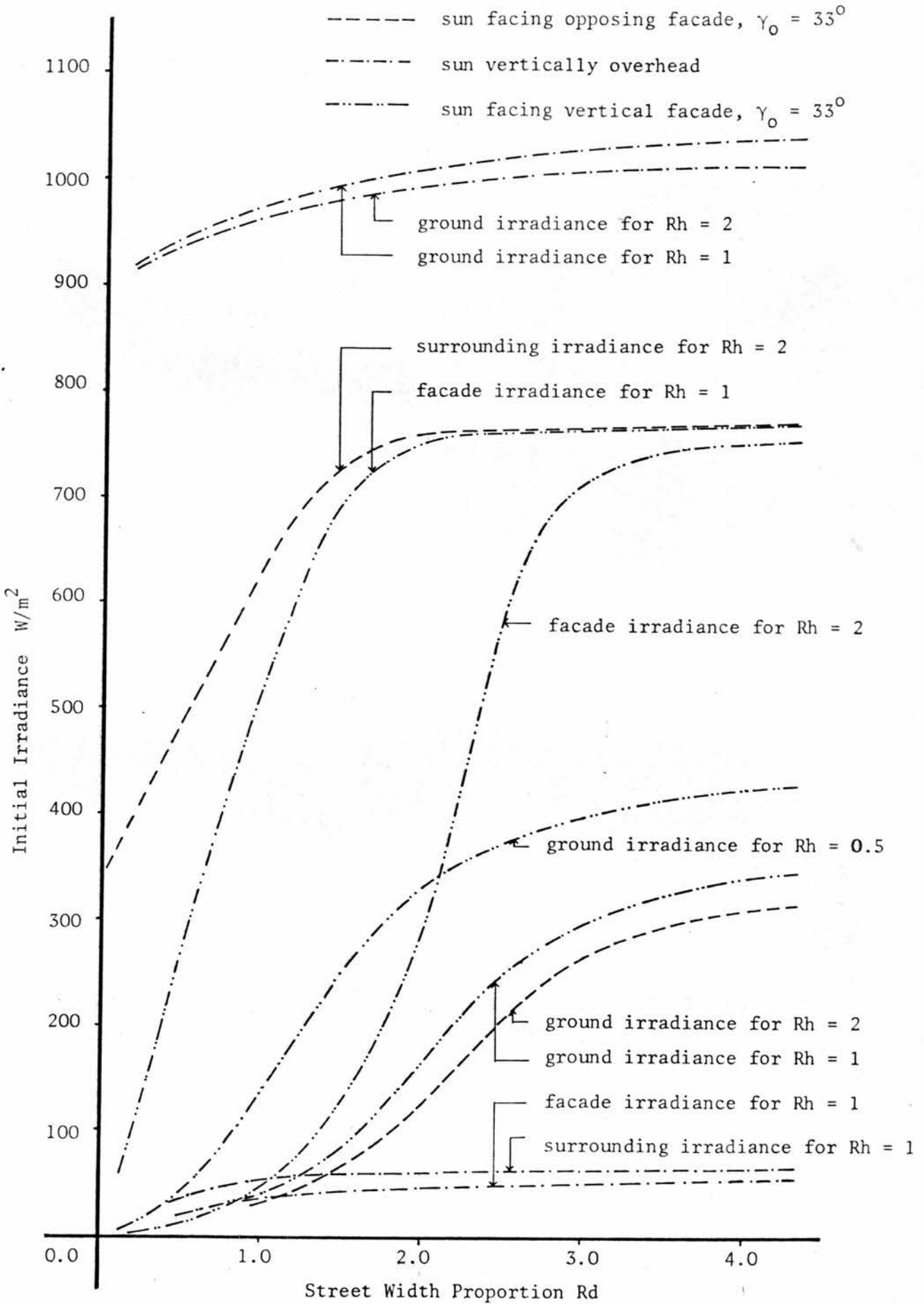


Figure 7.6 Variation of the Initial Irradiance of the Surfaces of the Model with R_d for Different Sun's Positions

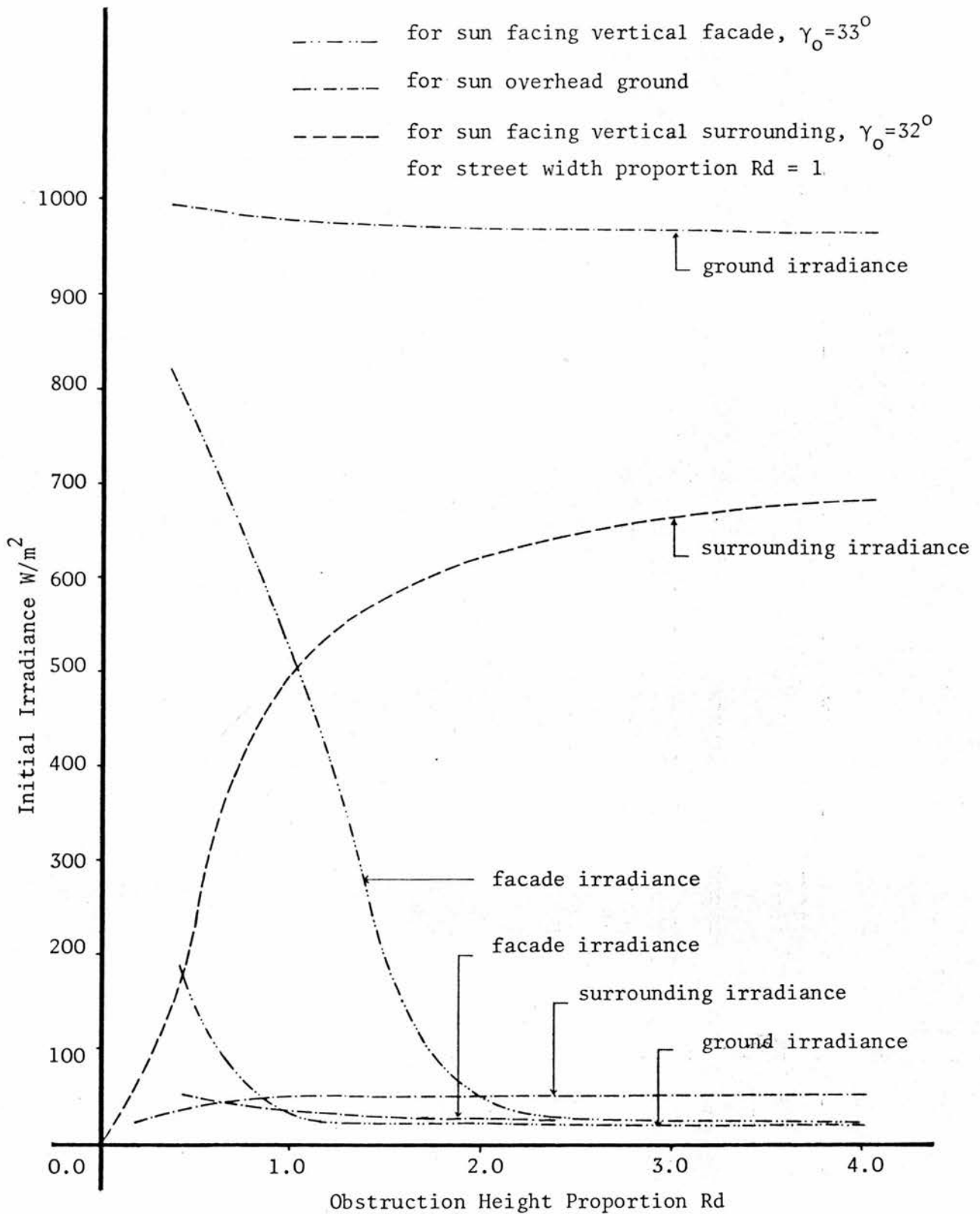


Figure 7.7 Variation of the Initial Irradiance of the Surfaces of the Model with R_d for Different Sun's Positions

3.3.6 The variation of the facade component with the street width and obstruction height proportions R_d and R_h , showed similar patterns for the different combinations of facades' reflectances and initial irradiances. A typical example of this is illustrated by the diagram in Figure 7.8, for the case where the sun is facing the facade of the block. The diagram shows that for any obstruction height the facade component increases with the increase of R_d reaching a maximum and then decreases. The height of the obstruction appears to determine the R_d values for the maximum facade component which varies proportionally to the height of the obstruction. Therefore, the shorter the height of the obstruction, the smaller the R_d value for maximum facade component. For example, R_d for maximum facade component is about 0.5 and 2.5 when R_h is 1 and 2 respectively. Two ranges of R_d may then be defined to distinguish the variation patterns of the facade component with R_d . The rapid increase of the facade component with R_d in the first range is mainly due to influence of the initial irradiance of the facade. In the second range of R_d , the facade component is mainly affected by the facade coefficient and hence varies with R_d accordingly. The variation of the facade component with R_h showed similar patterns as with R_d . It first increases with R_h reaching a maximum value, mainly due to the increase of the facade coefficient and then decreases with further increase in R_h as both the coefficient and initial irradiance decrease. The value of R_h for maximum facade component is also determined

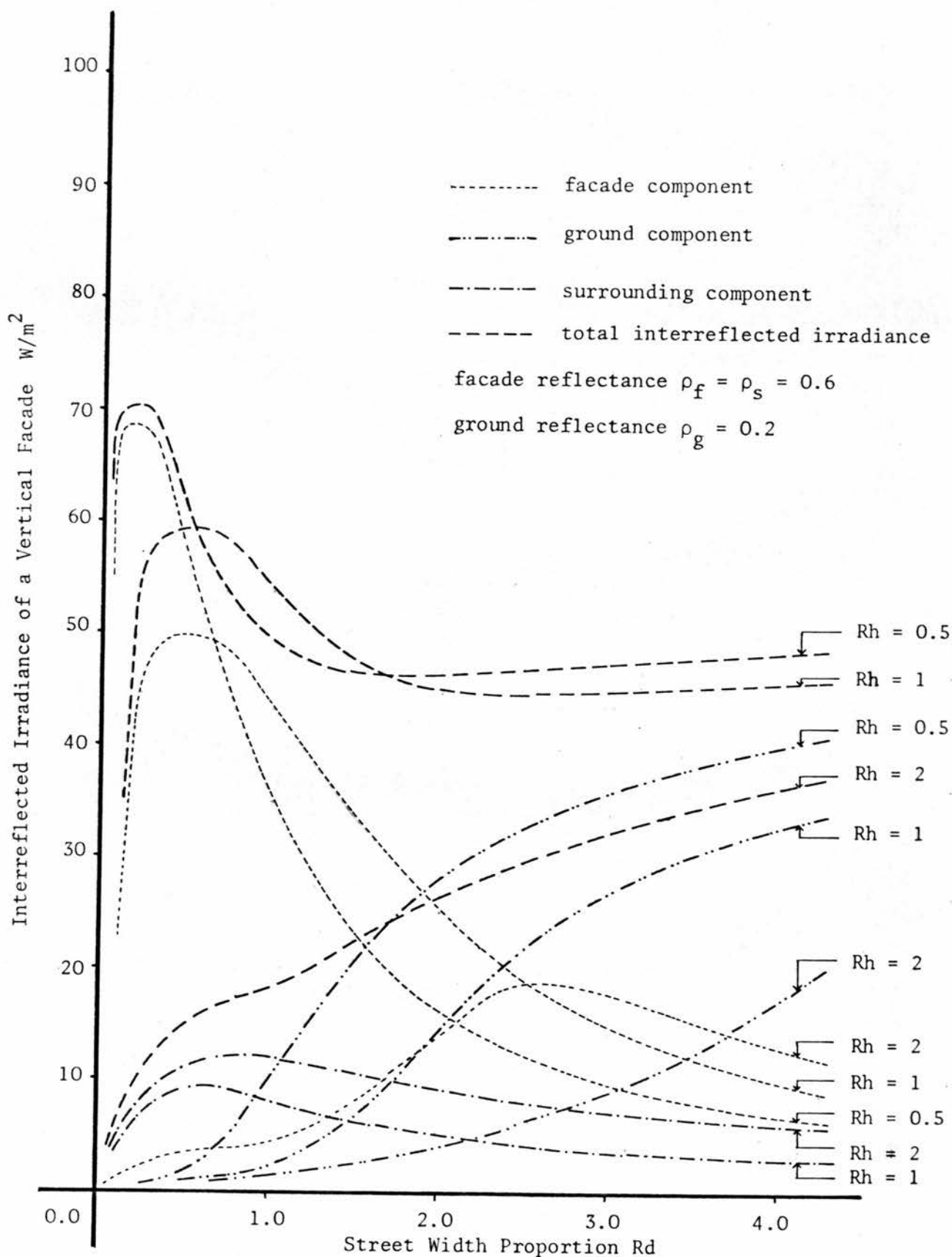


Figure 7.8 Variation of the Interreflected Irradiance Components of a Vertical Facade with R_d , for the Sun Facing the Facade with $\gamma_0 = 33^\circ$

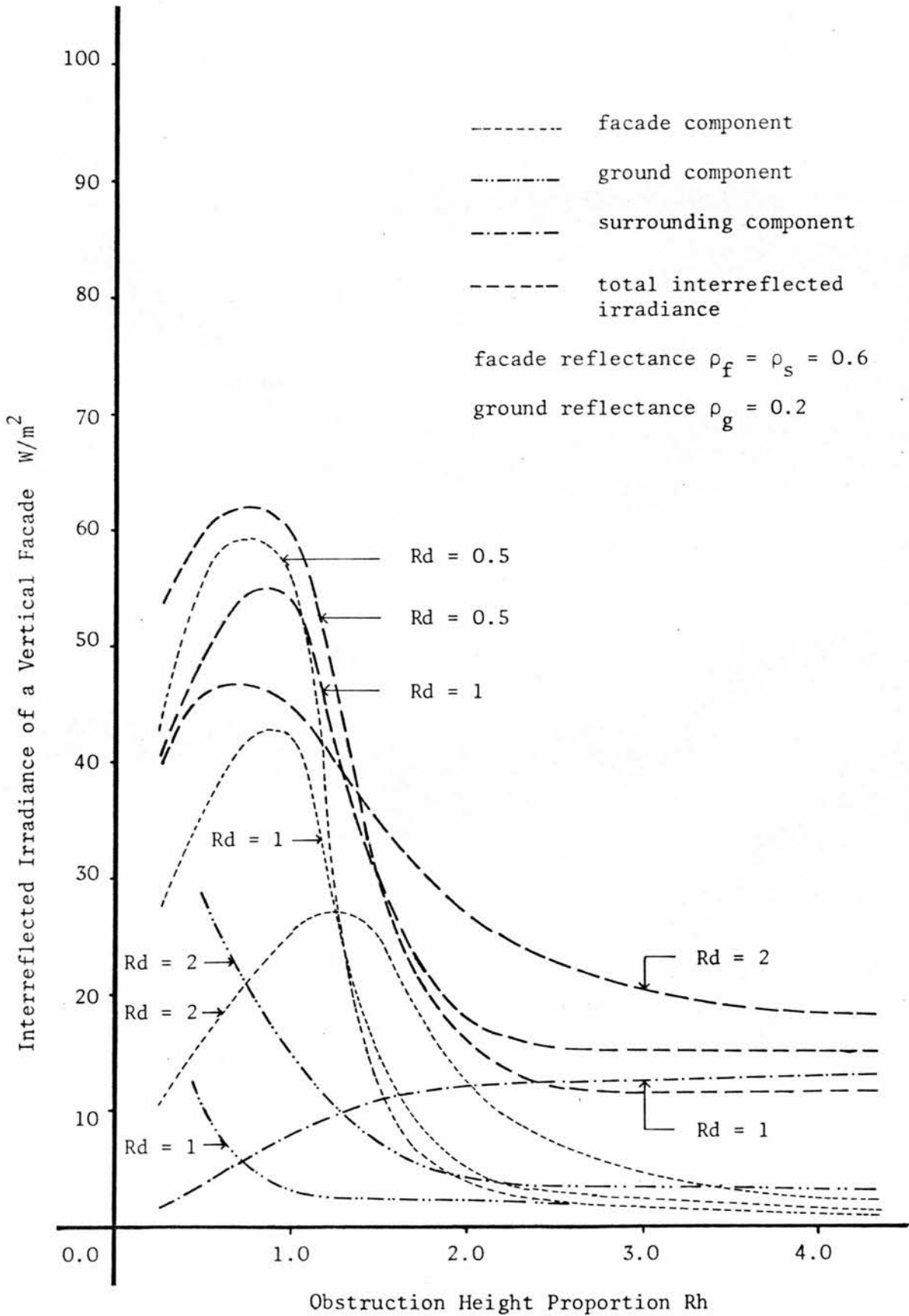


Figure 7.9 Variation of the Interreflected Irradiance Components of a Vertical Facade with R_h , for the Sun Facing the Facade with $\gamma_o = 33^\circ$

by R_d . An illustration of this is given by the diagram in Figure 7.9. It is evident from the graphs shown that the facade component does not vary significantly with the variation of either R_d or R_h within the range greater than 2.5.

3.3.7 The variation of the ground component with R_d follows similar patterns to those of its initial irradiance and coefficient, see figures 7.2 and 7.6. The ground component generally increases with R_d . As the rate of increase for the ground coefficient is high for $R_d < 2$, the rate of increase of the ground component within this range of R_d is similarly high, when the ground also has high initial irradiance. The ground component generally increases gradually with $R_d > 2$. The ground component varies only slightly with R_h in a similar manner to its coefficient except in the cases where the variation of R_h significantly effects the ground initial irradiance and in particular the direct solar irradiance. Then it decreases rapidly with the increase of R_h where $\gamma_{om} < \gamma_o$. An illustration of the variation of the ground component with the geometrical parameters of the form is shown in Figures 7.10 and 7.11 for the case where the sun is overhead at mid-day. At low solar altitude the ground component increases gradually with the decrease of the obstruction and the subsequent decrease in the shadow factor.

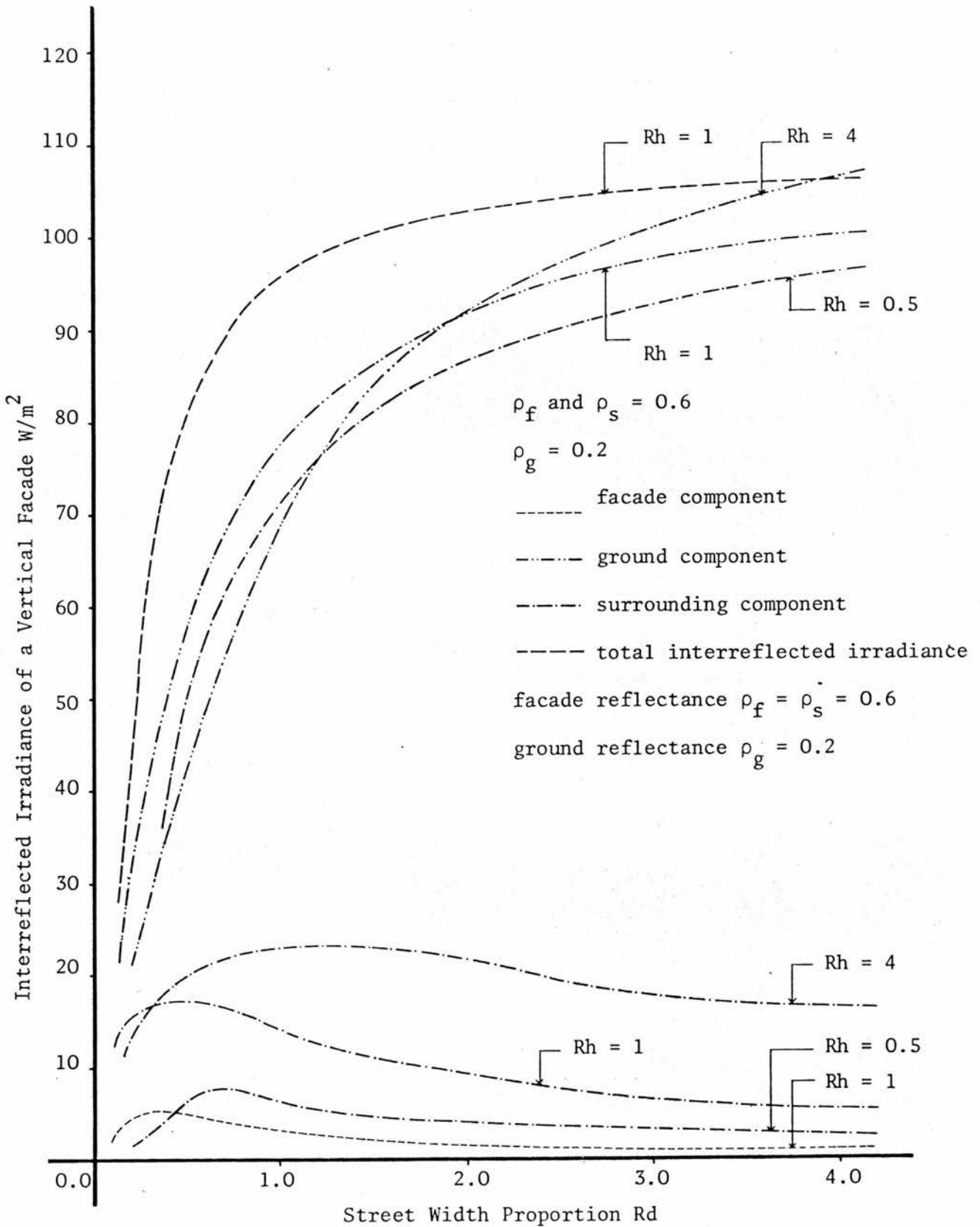


Figure 7.10 Variation of the Interreflected Irradiance Components of a Vertical Facade with R_d for the Sun Overhead the Ground

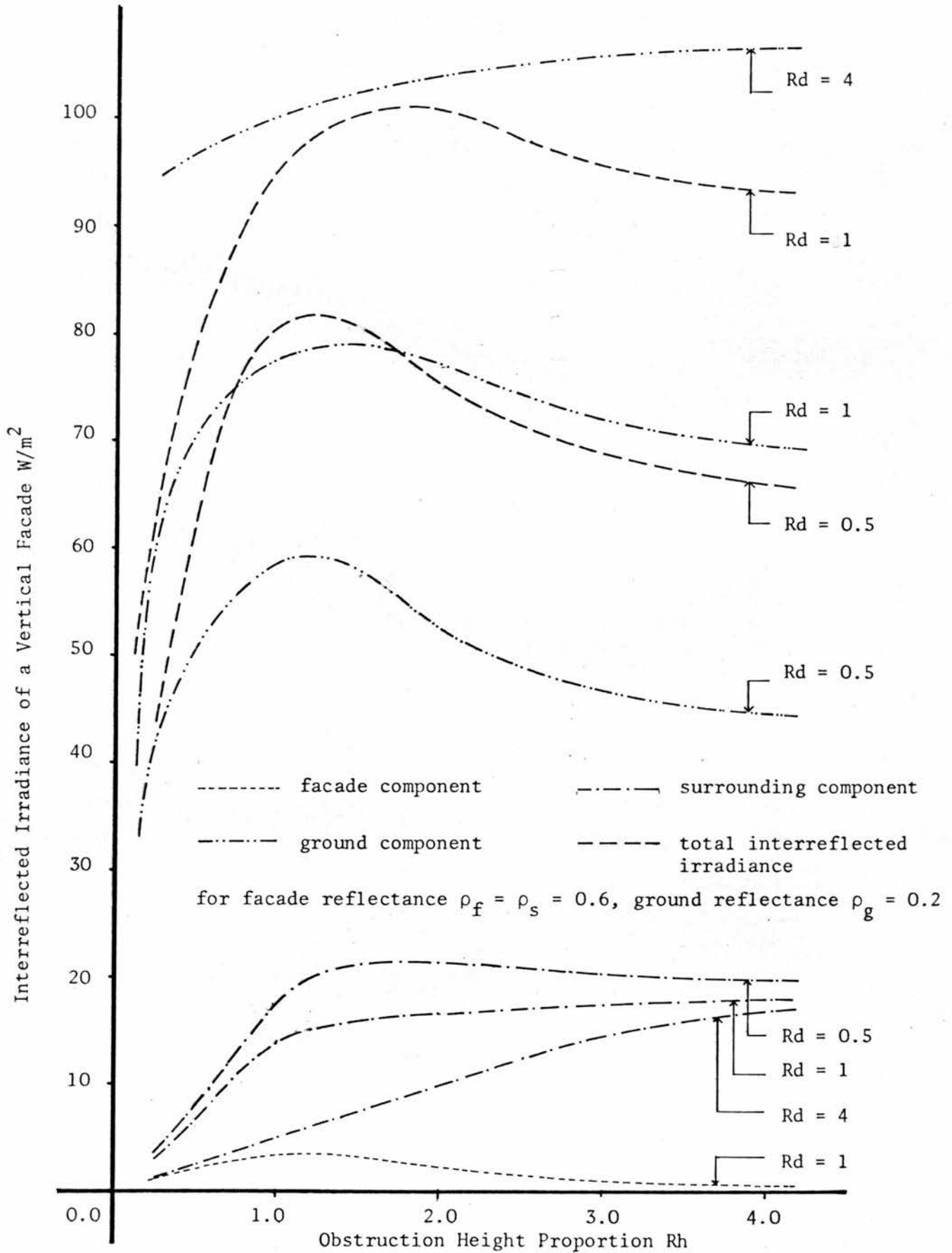


Figure 7.11 Variation of the Interreflected Irradiance Components of a Vertical Facade with R_h , for the Sun Overhead the Ground

3.3.8 The variation of the surrounding component with the geometrical parameters of the forms follows similar patterns to those of the facade component where it increases with the increase of R_d reaching a maximum value and then decreases. This may also be explained by the fact that while the initial irradiance of the surroundings increases with R_d , its coefficient decreases. Thus, the increase in the surrounding component in the first range of R_d is due mainly to increase of its initial irradiance while it decreases in the second range of R_d following the decrease of its coefficient. The R_d values at which maximum surrounding component is achieved is also determined by the obstruction height. The smaller the proportion of the height of the facade to that of its vertical surrounding, as the height of the vertical surrounding is increased, the smaller the value of R_d for maximum surrounding component. This may be explained for both the surrounding and facade components by the fact that both the initial irradiances and coefficients of the vertical facade increase with R_h for any street width proportion R_d . The rate of increase is particularly rapid as R_d is decreased. Hence, the higher the obstruction to the facade the smaller the value of R_d for maximum component. As the surrounding coefficient is generally of a higher value than both the ground and facades coefficients, the surrounding components tend to have higher values particularly when the surrounding vertical facade receives the main initial irradiance input. The surrounding component appears to increase

with R_h . This may be explained by the fact that both initial irradiance and coefficient increase with R_h . The rate of increase is determined by R_d and is more gradual as the surrounding is exposed to the direct solar irradiance. An example illustrating the variation of the surrounding components with the geometrical parameters of the form is shown in Figure 7.12 for the case where the sun, with an altitude of 32° , is opposite the surrounding facades.

3.3.9 The effects of varying the reflectances of the surfaces of the model on the different interreflected irradiance components follow directly their corresponding effects on the different coefficients of the interreflected components (Figure 7.5). These indicate a linear relationship between the components and the reflectances of the various surfaces where the components increase with the increase of the reflectances. The effects of the reflectances of the different surfaces of the model on their respective components are particularly significant, but of smaller extent in relation to the other components. The rate of increase of the components with the reflectances is also a function of the geometric configuration of the form as similar to their coefficients. The diagram in Figure 7.13 illustrates the variation of the interreflected irradiance components with the reflectances of the surfaces of the model. It represents the situations where each component constitutes the major portion of the total interreflected irradiance as its

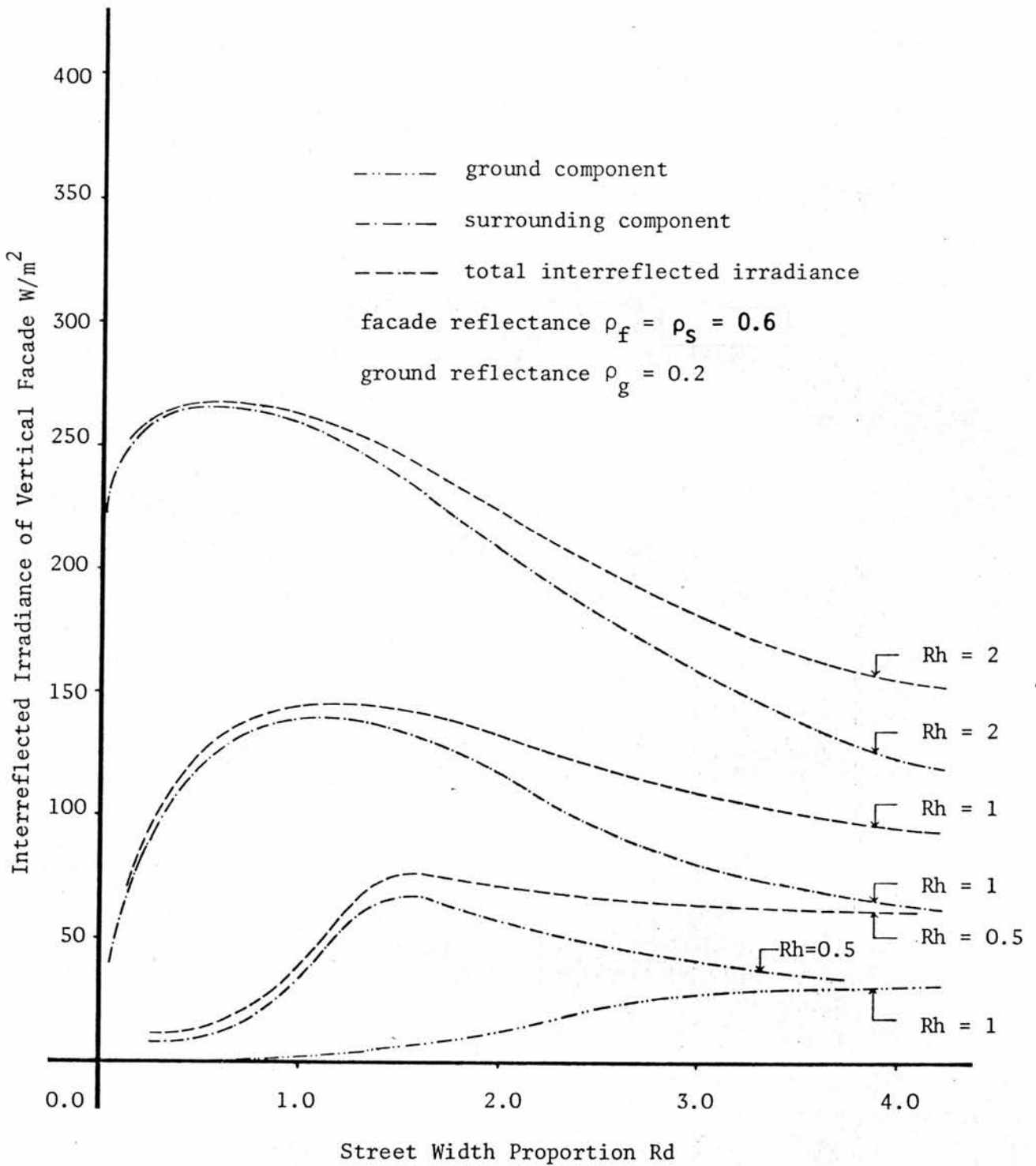


Figure 7.12 Variation of the Interreflected Irradiance Components with R_d for the Sun Facing the Opposite Facade at $\gamma_0 = 32^\circ$

1st case : sun facing facade

2nd case : sun overhead

3rd case : sun facing surrounding proportions
of form parameters $R_h, R_d = 1$

----- total interreflected irradiance

- · - · - facade component, 1st case

- · - · - ground component, 2nd case

- - - - - surrounding component, 3rd case

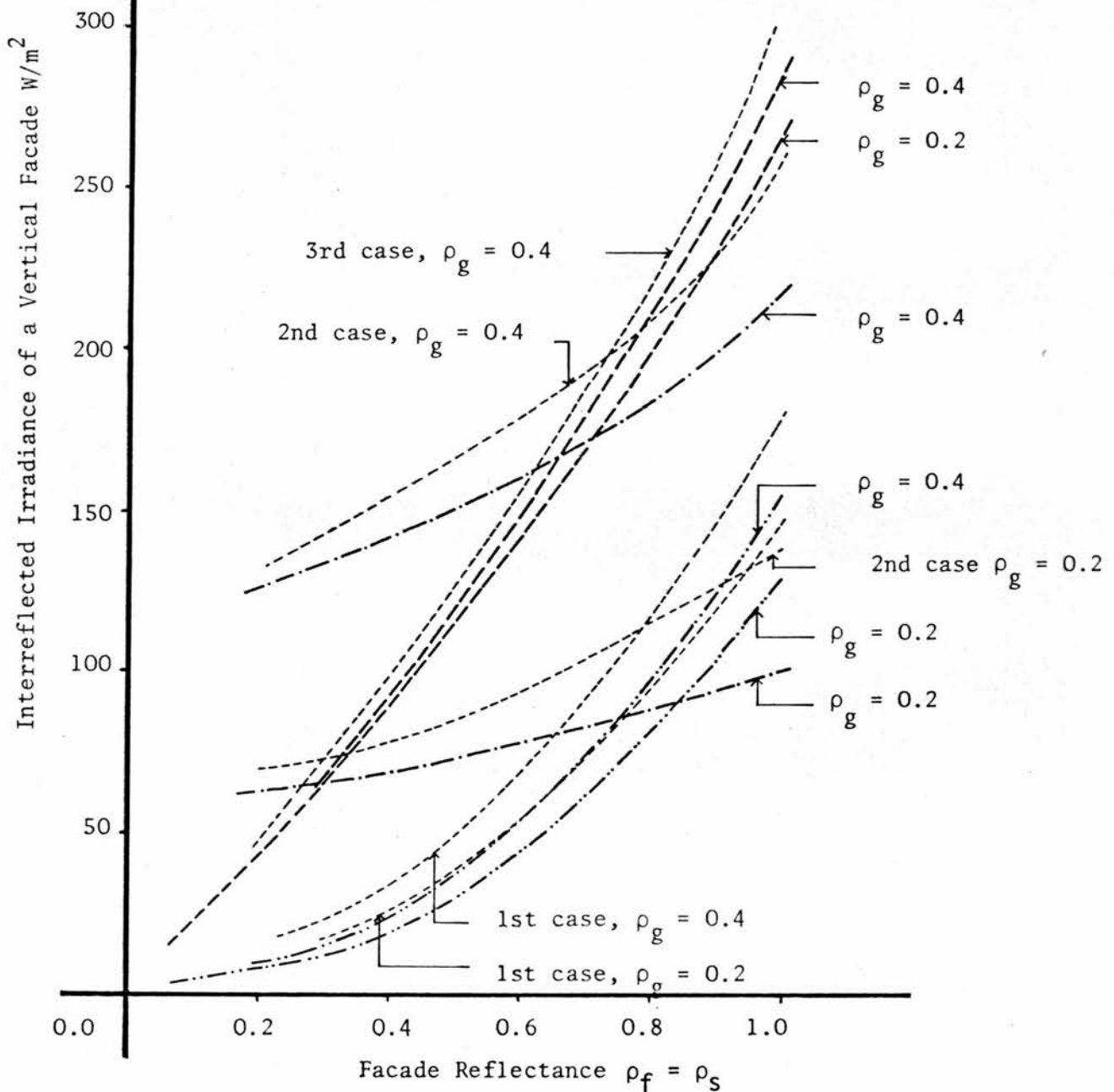


Figure 7.13

Variation of the Interreflected Irradiance Components with the Facade Reflectance

corresponding input. The non-linear relationship shown emphasises the cumulative effects brought about by the simultaneous variation of the facades' reflectances.

3.3.10 The magnitude of the total interreflected irradiance received on a facade is the sum of its different components for any combination of form configuration, facades' reflectances and initial irradiances. Hence, the variation patterns of the total interreflected irradiance with the parameters of the form follow those of its components in the situations where they constitute its major portions. It is evident then that the significance of the different parameters on them, with regard to the total interreflected irradiance, is only emphasised in the situations where the components are of high values, corresponding to their high initial irradiances. These effects may then be illustrated by the three cases considered, where each component in turn constitutes the main part of the interreflected irradiance.

3.3.11 In the first case representing the sun at a low altitude ($\gamma_0 \approx 33^\circ$) the vertical facade directly facing the sun receives its maximum initial irradiance. The total interreflected irradiance is mainly composed of facade component when the obstruction angle to the vertical facade γ_{om} is greater than the solar altitude, and the ground is fully shaded. The variation patterns of the total interreflected irradiance with

the parameters of the form then follow those of its facade component. However, the most significant contribution of the facade component to total interreflected is mainly within the range of R_d and $R_h < 2.5$. As the obstruction angle falls below the solar altitude, with the increase of R_d or the decrease of R_h , the ground irradiance increases with the subsequent increase of its component. The ground component then constitutes the main portion of the total interreflected irradiance which will then vary with the parameters of the form in a similar manner to the ground component, ie, increasing with R_d and decreasing with the increase of R_h . As the height of obstruction is increased and both the facade and ground are fully shaded, the magnitude of the total interreflected irradiance falls rapidly and will be mainly composed of surrounding component. A typical pattern for the variation of the total interreflected irradiance with the parameters of the form for this case is illustrated by the diagrams of Figure 7.8 and 7.9. It is evident from the diagrams shown that the interreflected irradiance is not significantly affected by the variation of R_d and R_h within the range >2.5 . It is affected by the facade and ground reflectance when their respective components are dominant. With low facades' reflectance, ie $\rho_f \leq 0.3$, the values of the facade component are small and hence the variation pattern of the total interreflected irradiance with R_d follows that of its more dominant ground component.

3.3.12 The initial irradiances of the vertical facades decrease while the initial ground irradiance increases rapidly with the increase of the solar altitude reaching its maximum when the sun is vertically overhead. Then it would constitute the main initial irradiance input to the model as represented in the second case (Figure 7.10 and 7.11). Evidently the total interreflected irradiance of the vertical facade would be mainly composed of ground component and varies with the parameters of the form in accordance with it. This indicates that the total interreflected irradiance increases with R_d . The rate of increase is more rapid in the range $0 < R_d < 2$ and less significant beyond that where the total interreflected irradiance is increased by less than 2 percent with every extra unit of R_d . Within the range of $R_d < 2$, the interreflected irradiance increases with R_h reaching a maximum at R_h about 1.5 and then decreases. It also increases gradually with R_h where $R_d > 2.0$. The surrounding component tends to contribute slightly to the total interreflected at higher obstruction. The total interreflected irradiance is also greatly affected by the variation of the ground reflectance, subsequent to its affect on the ground component, and to a smaller degree by the facade reflectance particularly at higher obstruction.

3.3.13 When the total interreflected irradiance is mainly composed of surrounding components as represented in the third case shown in Figure 7.12, obviously it would vary with the

parameters of the form in accordance with the variation of the surrounding component. In this context, it is evident that it increases with R_d and R_h reaching a maximum and then decreases. The higher the value of R_h , the smaller the value of R_d for maximum interreflected irradiance. For example, the R_d values for maximum interreflected irradiance for R_h 1 and 2 is about 1 and 0.5 respectively. It should be noted that the magnitude of the surrounding component is appreciably higher than the facade or the ground components; hence their contribution to the total interreflected irradiance is only significant at wider street widths $R_d > 4$ and shorter obstructions $R_h < 1$. The variation of reflectance of the surrounding facade effects the interreflected irradiance as similar to the surrounding component.

3.4 The Effects of Form Parameters on the Hourly Distribution of the Interreflected and Final Irradiance

3.4.1 With the movement of the sun across the sky the magnitude of the different interreflected irradiance components continuously change following the variation of the initial irradiances of their respective surfaces. Therefore, the significance of the contribution of the different components to the total interreflected irradiance and the effects of the form parameters on them also vary continuously during the day. It may be useful then to analyse the cumulative effects of the form parameters on the hourly distribution for the total

interreflected and final irradiances. Evidently, this will indicate the possibilities for manipulating the form parameters in order to achieve an interreflected and final irradiance load which may satisfy the thermal load and interior illumination criteria at different times of the day.

3.4.2 The hourly distributions of the different interreflected irradiance components indicate that they generally increase to a maximum value at different times of the day, and subsequently decrease. These maximums occur at morning, mid-day and afternoon for the facade, ground and surrounding components respectively. The parameters of the form determine the magnitude of the hourly values of the different components. They subsequently determine the hourly values and distribution of the interreflected irradiance which generally increases during the day to a maximum value and then decreases as similar to its components. The time at which it may reach its maximum value corresponds to that of its component with the highest maximum value usually that of its surrounding component.

3.4.3 The effect of the form parameters on the distribution of the interreflected irradiance may be conveniently illustrated within two main time intervals of the day, before and after noon. This is because the surrounding component generally

has a relatively higher value than those of the facade and ground components. Illustrations for typical hourly distribution for different parameters of form are shown in Figures 7.14 and 7.15. In the morning interval the total interreflected was found to decrease with the increase in obstruction height proportion R_h , particularly for $R_h > 1$. The increase of R_d did not significantly effect the total interreflected irradiance. The interreflected irradiance for this time interval is mainly composed of facade and ground components which generally have small values and so their subsequent variations with R_d and R_h affect the interreflected irradiance only slightly. In the second interval the interreflected irradiance increases with the increase of R_h but decreases with the increase of R_d . The fact that the interreflected irradiance within this time interval is mainly composed of surrounding component explains its variations with R_d and R_h .

3.4.4 It is apparent that the reflectances of the surfaces affect the hourly distribution of the total interreflected irradiance, particularly at the time when the components of their respective surfaces constitute the main part of the interreflected irradiance (see Figure 7.15). The increase of the ground reflectance ρ_g tends to cause an overall increase of the total interreflected irradiance but more distinctly at mid-day. For example, the increase of ρ_g from 0.2 to 0.4

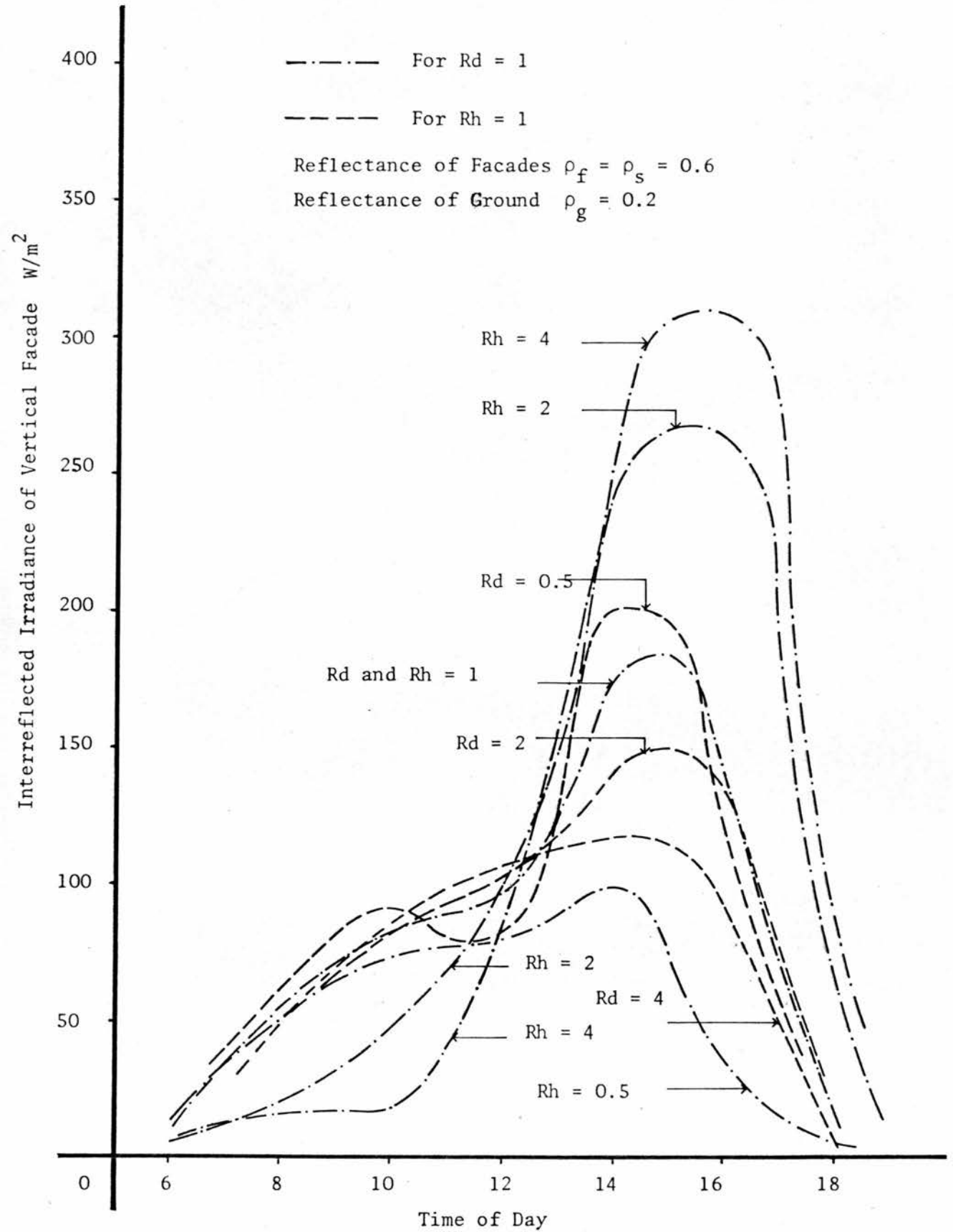


Figure 7.14 The Effects of the Geometric Parameters of Form on the Hourly Distribution of the Interreflected Irradiance on a Vertical Facade

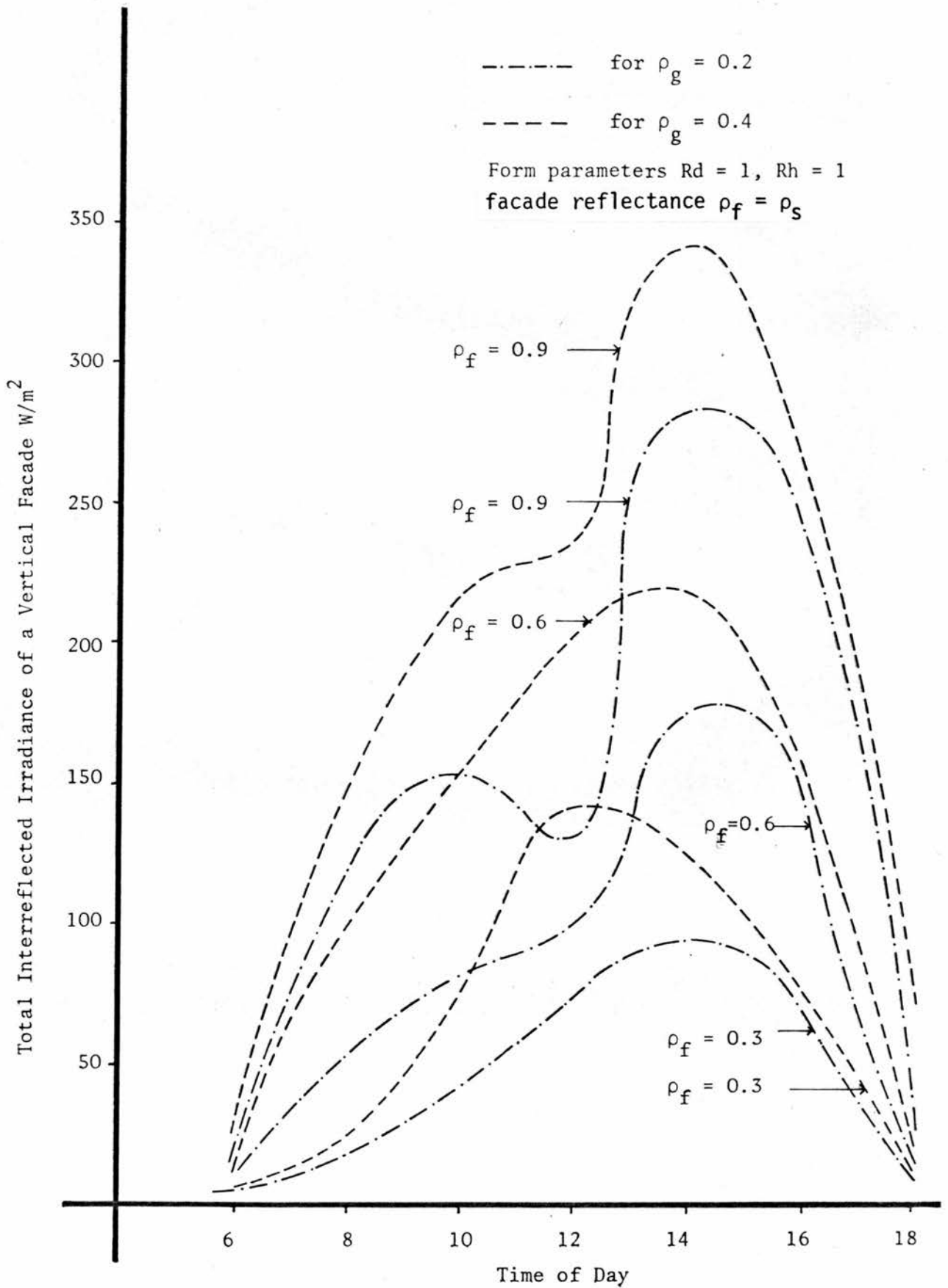


Figure 7.15 Affect of the Surfaces' Reflectances on the Hourly Distribution of the Total Interreflected Irradiance for R_h and $R_d = 1$

may cause an increase of the total interreflected irradiance in the afternoon equivalent to that caused by doubling the height of the obstruction. Similarly, the total interreflected irradiance increases markedly in the morning and in the afternoon with the increase of the facades' reflectances. For example, the increase of ρ_f from 0.6 to 0.9 increases the total interreflected irradiance in the afternoon by more than 50 percent. This is equivalent to the increase caused by tripling the height of the obstruction. Similarly, the decrease of ρ_f from 0.6 to 0.3 causes a decrease in the total interreflected equivalent to that caused by the quadrupling of R_d .

3.4.5 The ultimate effects of the parameters of the form on the final irradiance load of a surface of the model are evidently determined by their effects on its initial and total interreflected irradiances that constitute the final irradiance load. It is apparent that the effects of the parameters on the initial and interreflected irradiances can be exploited to manipulate the parameters of the form for the control of the final irradiance which may be received on the surfaces at different times of day. An example of typical hourly distributions of the final irradiance load of a vertical facade, for different geometric configurations, is shown in Figure 7.16. As seen from the diagram the increase of R_h and the decrease of R_d causes the decrease

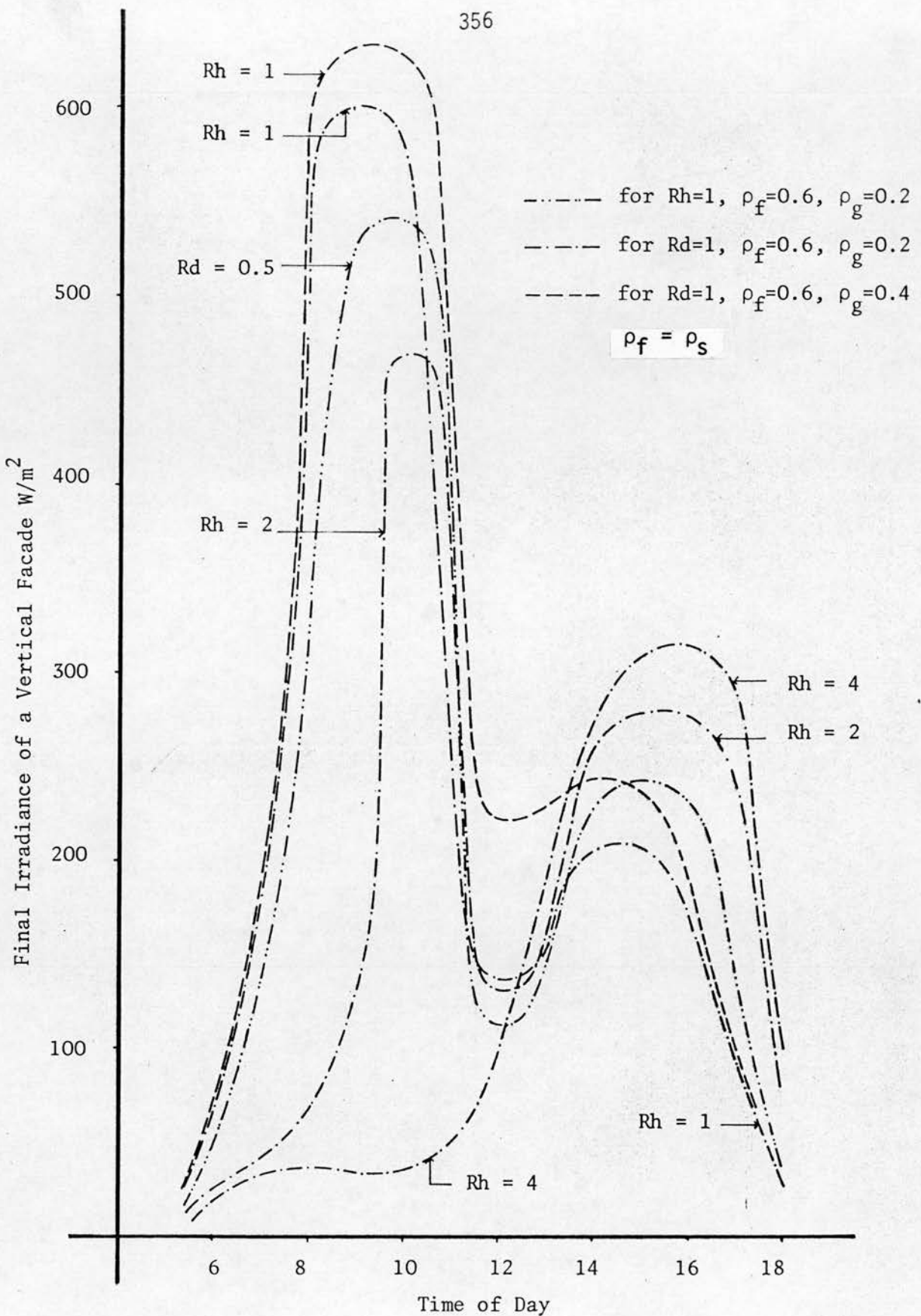


Figure 7.16 The Effects of the Form Parameters on the Hourly Distribution of the Final Irradiance Load of a Vertical Facade

of the final irradiance in the morning and its increase in the afternoon. It is apparent here that the increase of the obstruction to the vertical facade with the increase of R_h and decrease of R_d caused the decrease of the initial irradiance at the time when it is facing the sun, before noon. The magnitude of its interreflected irradiance then being mainly composed of facade and ground component and decreasing with the increase of the obstruction, is too small to compensate for the obstructed initial irradiance. In the afternoon, however, the magnitude of the initial irradiance of the facade is small and its interreflected irradiance is then mainly composed of surrounding component which increases with the increase of the obstruction. Thus the opposing vertical surrounding may be used for the double purpose of reducing the initial irradiance at the time when its higher and providing interreflected irradiance at the time when the initial irradiance is small. Furthermore, the ground reflectance may also be used to increase the magnitude of the interreflected and final irradiance, particularly at mid-day.

3.5 Effects of the Parameters of the Form on the Daily Average Interreflected Irradiance

3.5.1 The model representing the vertical opposing facades and the ground between them by a system of infinitely long surfaces, which was earlier verified to give reasonably

accurate results for the purpose of this study, was also used for the evaluation of the daily average interreflected irradiance. The calculation of the daily average interreflected irradiance components and final irradiance was carried out with the daily average initial irradiance as input to the surfaces of the model. The initial irradiances of the surfaces were determined using the initial irradiance indices with the vertical facades oriented on a North-South axis. The interreflected irradiance was computed for a vertical facade for wide ranges and combinations of reflectances and geometric configuration of form. The following analysis illustrates the main effects on the interreflected irradiance due to the variation of the reflectance, street width and obstruction height proportions, as these determine the coefficients of the interreflected irradiance components.

3.5.2 The variation of the parameters of the form showed similar effects on the daily average interreflected irradiance components as on the hourly values. The diagrams shown in Figure 7.17 and 7.18 illustrate such typical patterns of variations of the components with the parameters. These show that the facade and surrounding components also increase with R_d to maximum values and then decrease. The R_d value for maximum facade and surrounding component appears to be influenced by facade's reflectances. It decreases

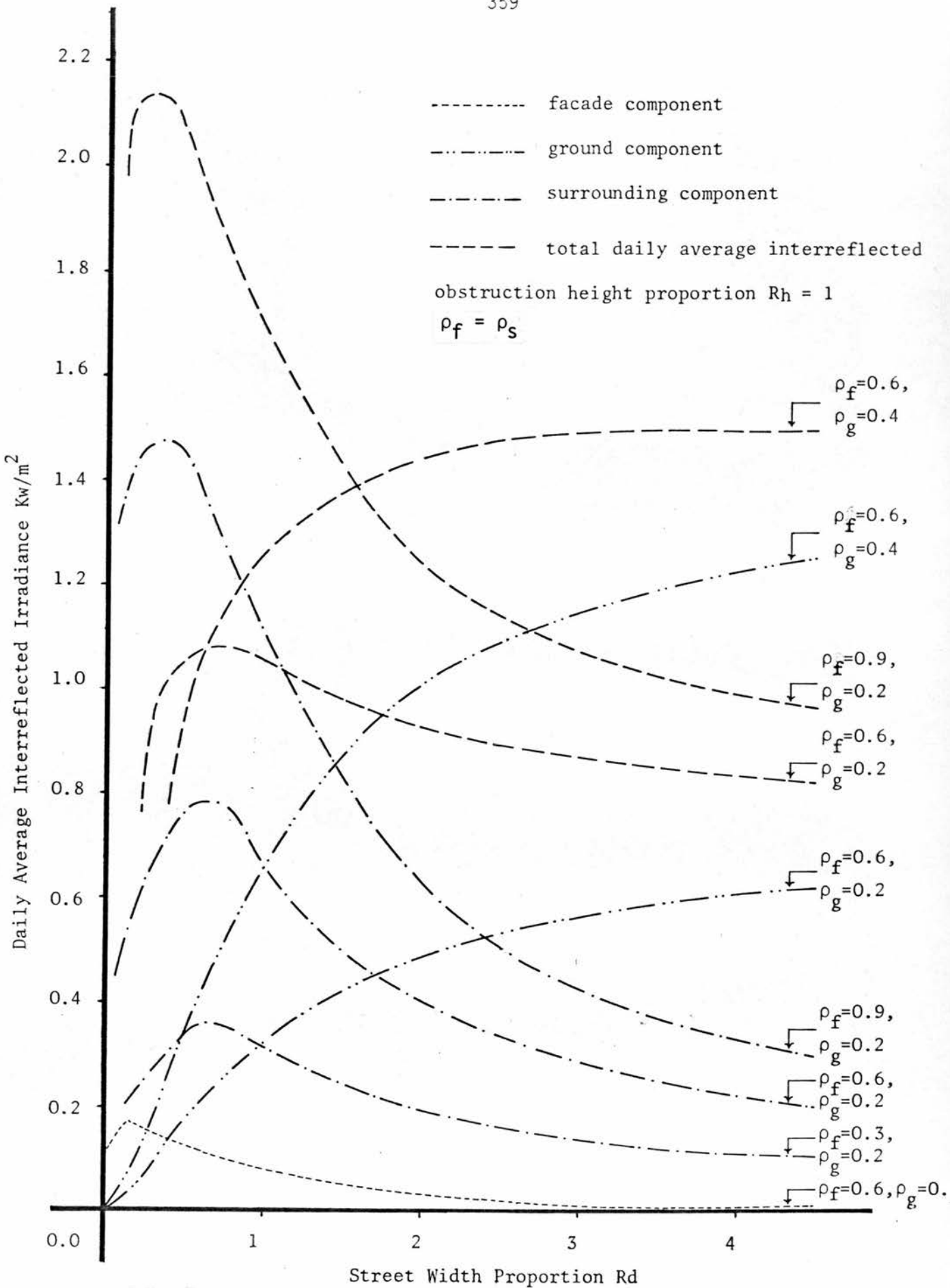


Figure 7.17 Variation of the Daily Average Interreflected Irradiance of a Vertical Facade with R_d

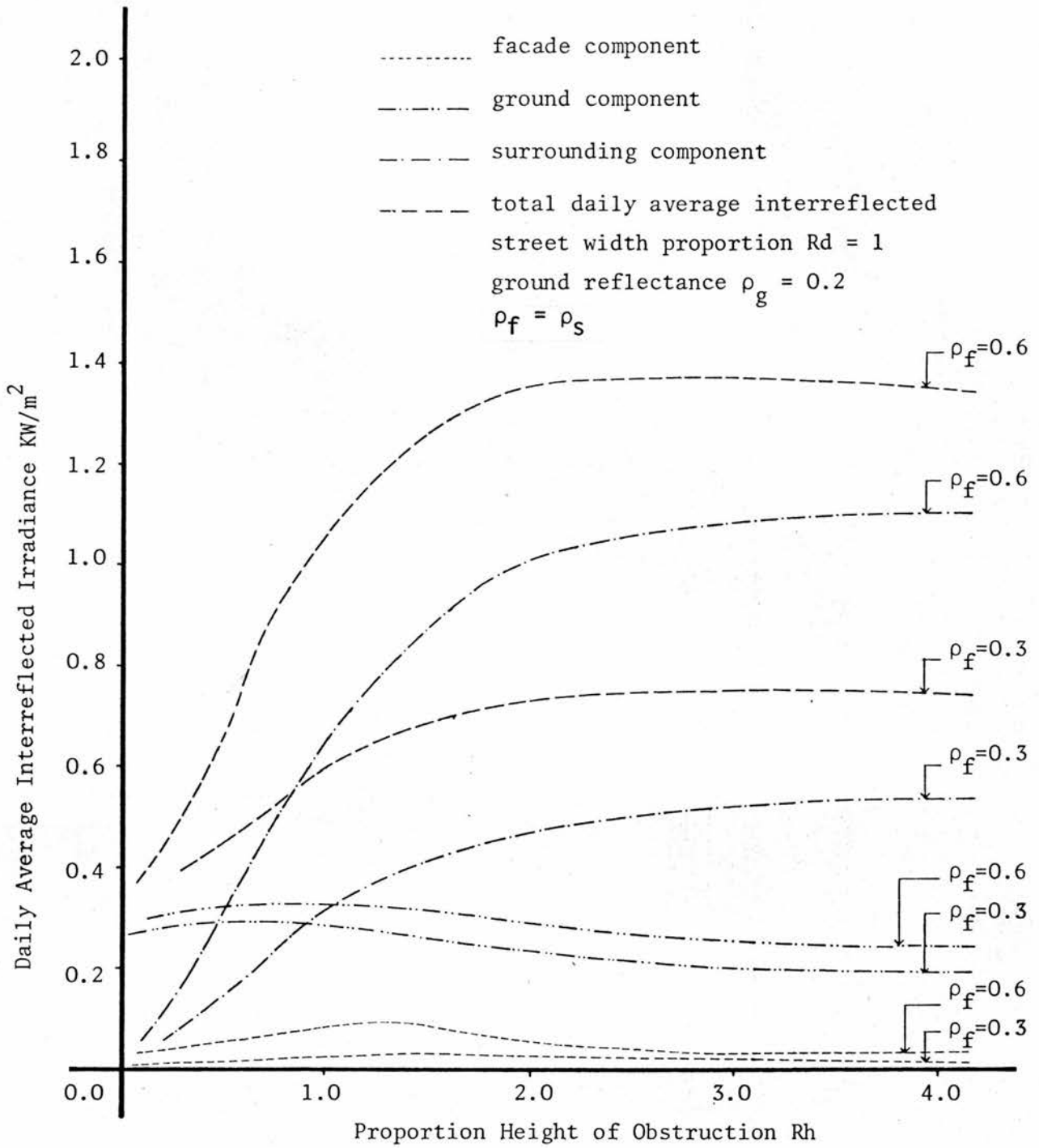


Figure 7.18 Variation of the Daily Average Interreflected Irradiance and Vertical Facade with R_h

slightly as ρ_f is increased. The increase in the first range of R_d is thus due mainly to the rapid increase of the daily average initial irradiance inputs. As the increase in their daily initial irradiances becomes more gradual the effects of their coefficients become dominant and the values of their components decrease accordingly with further increase of R_d . The daily average ground component increases with R_d following the increase of its coefficient and initial irradiance. The variation of R_h mainly affects the surrounding component causing it to increase rapidly within the range $R_h < 2$. It does not vary significantly with $R_h > 2.0$. The facade and ground components vary only slightly with R_h . The variations of the reflectances of the surface also seem mainly to influence the components of their corresponding surfaces.

3.5.3 It is apparent from the diagrams shown above that the surrounding and ground components constitute the main portions of the daily average interreflected irradiance of a vertical facade at different ranges of the geometrical parameters. This is because they generally showed significantly higher values than the facade components. It is evident that this is generally the case. It is expected then that the variations of the daily average interreflected irradiance with the parameters of the form will follow either its surrounding or ground components within the different ranges of the parameters. The ground component tends to dominate

daily average interreflected irradiance, which then varies in a similar manner to it, in the cases where the reflectance and height of obstruction are small (when $\rho_s < 0.3$ and $R_h > 1$) and particularly when its reflectance $\rho_g > 0.2$. At higher reflectance and height of opposing obstruction the daily average interreflected irradiance varies with R_d following its surrounding component, mainly with R_d within the range $R_d < 2$, where it increases to a maximum and then decreases. Following that, $R_d > 2$, the ground component contributes markedly to the daily interreflected irradiance. However, the increase of the ground component with R_d does not compensate for the decrease of the corresponding surrounding component. The daily interreflected irradiance then decreases gradually with the increase of R_d . This remains the general pattern even though the surrounding component may increase rapidly with the reflectance and height of obstruction. The daily average increases with R_h within the range $R_h < 2$ as similar to surrounding component, but it varies only slightly with $R_h > 2$.

3.5.4 The daily average interreflected irradiance generally constitutes a significant proportion of the daily average final irradiance load of a vertical facade. It may amount to many times the amount of the daily average initial irradiance load. The effects of the different parameters on the final irradiance is similarly determined by their combined effects on the daily average initial and interreflected

irradiance. Generally, the final daily average varies with R_d in a similar manner to its interreflected irradiance. This is mainly due to the fact that both the initial and interreflected irradiance increase with R_d in the first range ($R_d < 1$). While the interreflected irradiance decreases with further increase in R_d at its upper range, the initial irradiance varies only slightly. An example of this is illustrated by Figure 7.19. The increase in the height of the obstruction causes the initial irradiance to decrease while increasing the interreflected irradiance. Thus, the final daily average appears to increase first with R_h reaching a maximum value, mainly due to the increase of the interreflected irradiance. It subsequently decreases with the further increase of R_h as the slight increase of the interreflected irradiance does not compensate for the fall of the initial irradiance. The diagram in Figure 7.20 illustrates the variation of the final irradiance with R_h for different reflectances of the surfaces. It is evident from the diagram shown above that the final daily average irradiance does not vary significantly with R_d and R_h within the ranges >2 . The effects of the reflectances of the surfaces on the final daily average varied within the different ranges of the geometrical parameters due to the fact that the effects of the reflectances of the different surfaces on the total interreflected irradiances is emphasised within certain ranges of the geometrical parameters where the

interreflected irradiance components of their respective surfaces constitute the main portion of the total interreflected irradiance and hence the final irradiance.

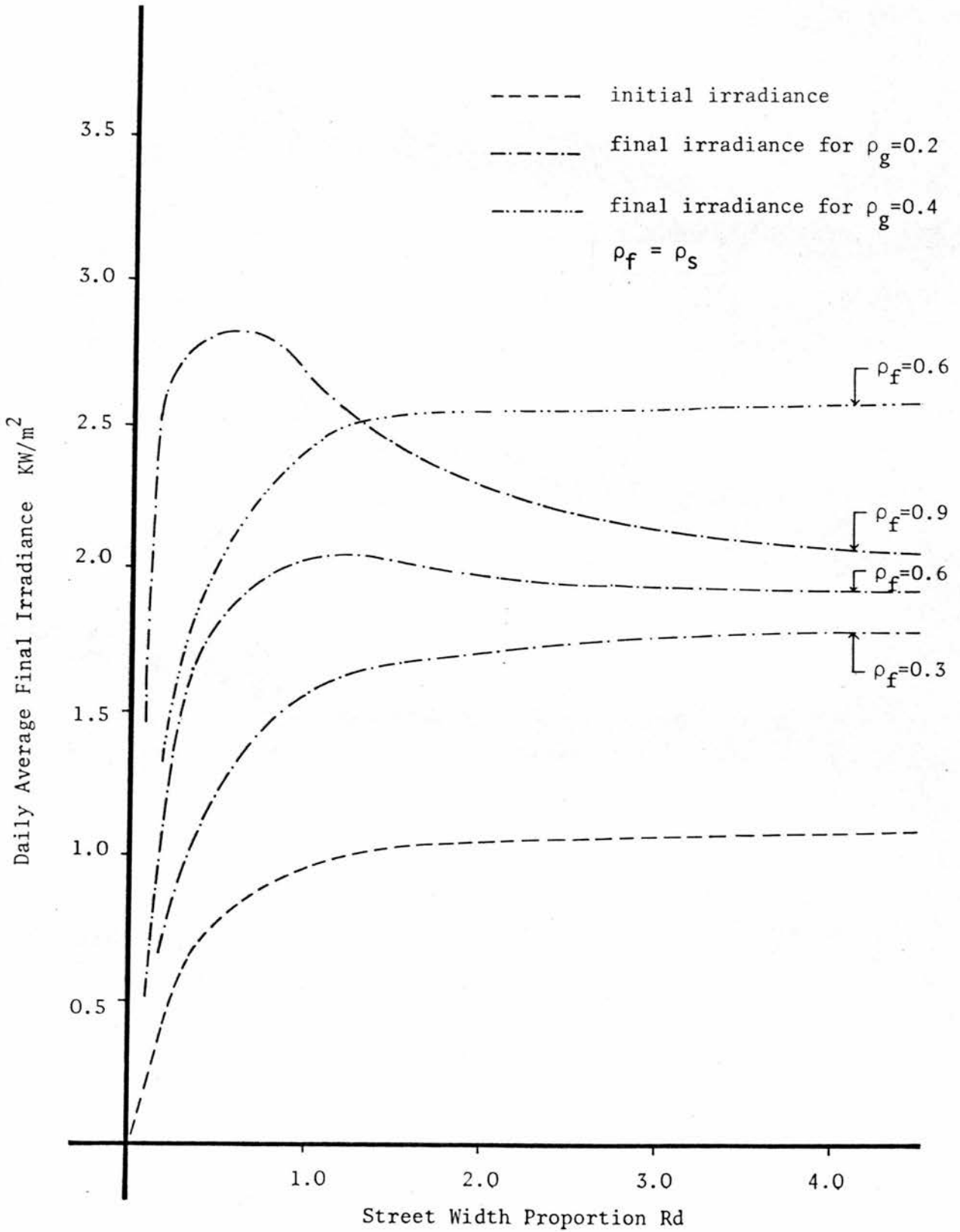


Figure 7.19 Variation of the Daily Average Final Irradiance of a Vertical Facade with Rd, for $R_h = 1$

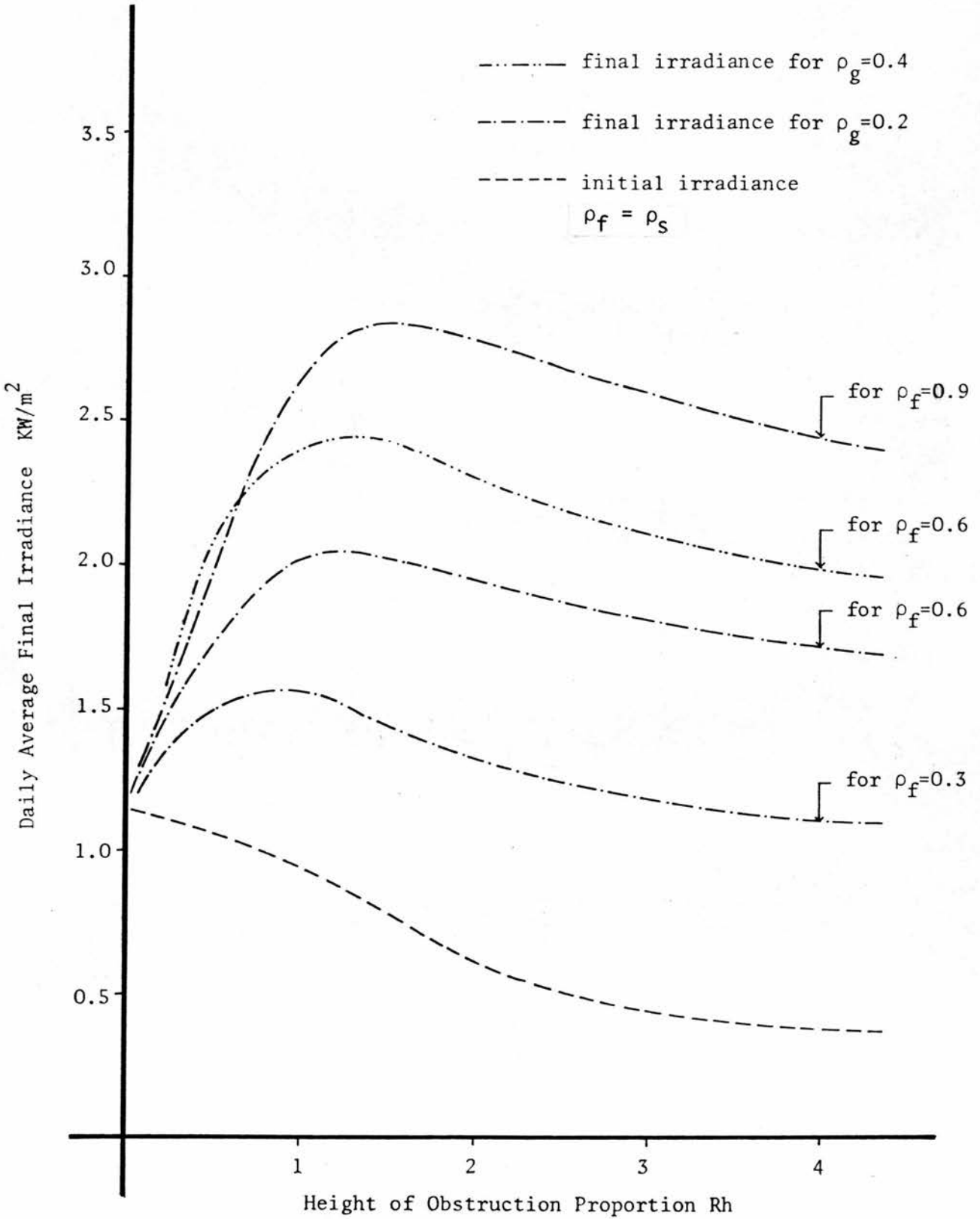


Figure 7.20

Variation of the Daily Average Final Irradiance of a Vertical Facade with Rh, for $R_d = 1$

4. DEVELOPMENT OF FORM PERFORMANCES INDEX FOR THE INTERREFLECTED IRRADIANCE

4.1.1 It is apparent that economical solution procedures which define the performances of the different geometrical configurations of form and facilitate immediate comparison between them in terms of the interreflected irradiance of their surfaces, provide many advantages in practical applications. For this purpose an attempt was made to develop an index which may define the performance of the geometric configuration of the model in terms of the interreflected irradiance on its vertical facade.

4.1.2 Because of the complex interrelationships between the parameters of the model and the interreflected irradiance the index was devised to be least sensitive to the variations of the initial irradiances and reflectances of the surfaces. It expresses solely the effects of the geometrical parameters on the interreflected irradiance of the vertical facade. After trying several procedures this was conveniently achieved by adopting a standard form of a fixed geometrical configuration as a basis for measuring the interreflected irradiance of any other geometrical configurations of form. The assumption was that the surfaces of any given form have the same initial irradiance and reflectance characteristics as those of the standard form. The two forms, therefore, differ only in their geometric configuration. The difference between the interreflected irradiance of a given form from that of the

standard form, therefore, presents a direct measure of the variation of the geometry of the given form from that of the standard one. The form performance index I_{P_x} was then defined by the proportion of the difference between the interreflected irradiance of a given form and that of the standard form to the interreflected irradiance of the standard form. It is expressed by the function

$$I_{P_x} = (I_R - I_{RS}) \cdot 100/I_{RS} \quad 7.7$$

where I_{P_x} is the performance index, I_{RS} the interreflected irradiance of the standard form and I_R the interreflected irradiance of a given form. The index therefore presents a direct measure for the variation interreflected irradiance for a given geometrical configuration from that of the standard form.

4.1.3 It was not possible to use one standard form for the index to ensure its insensitivity to the variation of the reflectance and irradiance of the surfaces of the form. Instead, it was found that the effects of the reflectances and irradiance can be greatly minimised by limiting the variation of the geometrical parameters for the variable form configuration to its height proportion only, while keeping its street width proportion equal to that of the standard form. This may be explained by the fact that the

variation of each coefficient of the interreflected irradiance components of a vertical facade with R_h showed similar patterns at different R_d , but with varying rate of variations. The facade and ground coefficients also showed two different rates of variation within two ranges of R_h . The boundary between the two ranges may be conveniently set at $R_h \approx 1$. It was evident that the variation pattern of the total interreflected irradiance with R_h would be similar to those of its ground and facade coefficients when its surrounding component is of small value.

4.1.4 A set of standard forms was therefore adopted. They represented equal height opposing facades, giving a height proportion for the obstruction $R_h = 1$, but with different street width proportions taken to range from 0.25 to 4. The form performance index was then evaluated for each of the standard form. In each case the height proportion of the variable form was varied within the range $0.25 < R_h < 4$, while its proportion R_d was kept constant and equals that of the standard form. Data for the index in each case, ie, the difference between the interreflected irradiance of the standard form and the variable form, was prepared for a wide range of initial irradiances and reflectances of the surfaces of the model which showed only slight variation mainly at $R_h < 0.75$. The average of the data, for the different initial irradiances and reflectances was obtained and assigned to represent the performance index, I_{p_x} . It was

verified that more than 80 percent of the values obtained varied within ± 10 percent from the average values. It may therefore be argued that the suggested index may give a reasonable measure of the form performance from that of the standard form irrespective of the irradiance and reflectances of the surfaces. It will directly indicate if a given form will receive more interreflected irradiance than the standard form or vice versa.

4.1.5 As expected the values of the form performance index for the different sets of the standard forms varied with R_h . They generally showed that a variable form will receive more interreflected irradiance than the standard form as its height is increased above that of the standard form and vice versa. The rate of increase decreases rapidly as the street width proportion is increased. The diagram shown in Figure 7.21 illustrates the variation of the performance index with the geometrical parameters. It also serves as a chart for defining the performance index of different geometrical configurations. It can also be used for approximate estimation of the interreflected irradiance of a vertical facade of a variable form using the interreflected irradiance of the standard form as expressed in equation 7.7.

4.1.6 The evaluation of the interreflected irradiance of a facade for any geometric configuration of the model may be further simplified by approximation of the irradiance transfer

function given earlier by equation 7.1. The terms in the denominator may be ignored on the assumption that their values are generally too small to have any significant effect on the interreflected irradiance value. This may be justified by the general cases in reality where the street width proportion R_d is generally greater than 1, thus giving small form factor values. Also, the value of the reflectances of the surfaces are not exceptionally high, particularly that of the ground. Similarly the last two terms of the numerator of the facade coefficient may be ignored. The equation for the interreflected irradiance of a vertical facade may then be given in the form

$$I_R = \rho_f \cdot \rho_g \cdot F_{fg} \cdot F_{gf} \cdot I_f + \rho_f \cdot \rho_s \cdot F_{fs} \cdot F_{sf} \cdot I_f + \rho_g \cdot F_{fg} \cdot I_g + \rho_g \cdot \rho_s \cdot F_{fs} \cdot I_{sg} \cdot I_g$$

$$+ \rho_s \cdot F_{fs} \cdot I_s + \rho_s \cdot F_{fg} \cdot F_{gs} \cdot I_s \quad 7.8$$

The above equation suggests that any interreflected irradiance after the second reflection is of no practical significance and may be ignored.

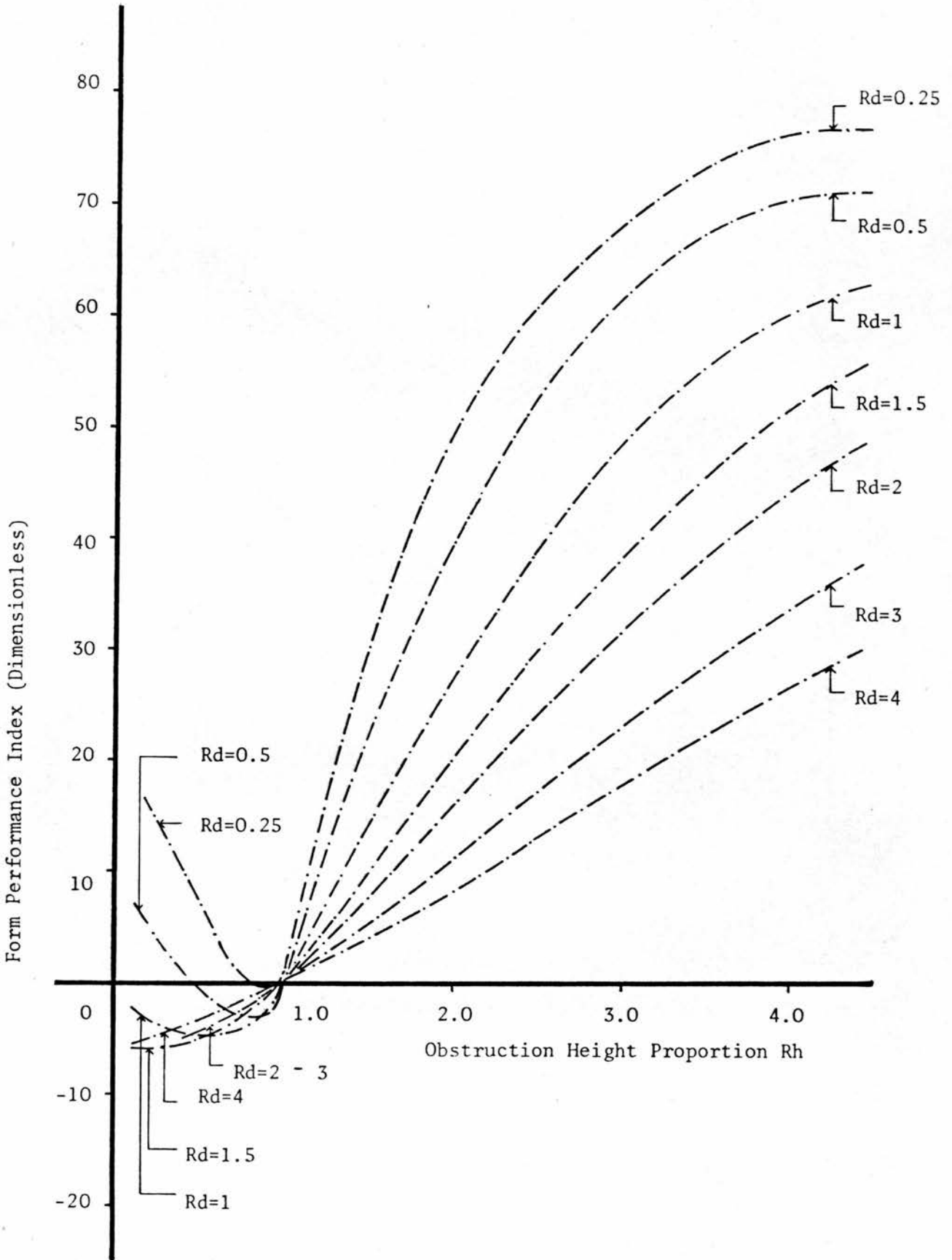


Figure 7.21 Variation of Form Performance Index with the Geometrical Parameters R_d , R_h

5. THE EFFECTS OF ORIENTATION, GEOMETRIC CONFIGURATION OF SURROUNDINGS AND REFLECTANCES OF SURFACES ON THE OPTIMUM PLAN PROPORTION AND FINAL IRRADIANCE LOAD OF THE BLOCK

5.1 Evaluation of Optimum Form of Block for Minimum Irradiance Load

5.1.1 The above discussion illustrated that generally a significant proportion of the final irradiance load received on a vertical facade of a block is contributed by the inter-reflected irradiance from its opposing facades and the ground space between them. Thus any accurate assessment of the irradiance load which may be received on the external surfaces of a building has to take into account the contribution of the interreflected irradiance. The fact that the final irradiance load on a building block accounts for both the initial irradiance and the interreflected irradiance, provides a practical measure for a criterion for the evaluation of the optimum form, its orientation or the reflectance characteristics of the surfaces. In this respect, the levels of the final irradiance load may be practically set with respect to the required levels of interior illumination which eventually takes into account the window area.

5.1.2 Consequent on the analysis of the optimum form discussed in the previous chapter, the minimum daily average final irradiance load was adopted as the criterion for the evaluation of the optimum plan proportion of the block for

different orientations, geometric configuration of surrounding and facades' reflectances. This may be justified by the fact that the interreflected irradiance evidently increases the thermal load on the external surfaces of buildings. On this basis, it may be possible to illustrate the full potential of the model in an integrated and quantitative evaluation of the final irradiance load on buildings at a higher level of detail.

5.1.3 The model was therefore used to generate wide ranges of geometric configurations of buildings and surroundings by the three progressions explained in the last chapter. In addition three descriptors representing the reflectance properties of the surfaces of the block, the ground and the surfaces of the surrounding blocks were included. These were varied independently within ranges which were taken to comply with practical situations. The daily total final irradiance load received on all the facades of the block for the different cases of the progressions was then evaluated from the daily average initial irradiance on the different facades of the block, the surrounding blocks and the ground space between them using the initial irradiance indices described earlier in the last chapter. The optimum plan proportion of the block was then evaluated in terms of the minimum final irradiance load received on its facades. This was carried out for the different combinations of geometric configuration of form and reflectance of the

surfaces generated by the three progressions and for different orientation angle α_s within the first quadrant at 15° intervals. The optimum plan proportion for final irradiance load is referred to here by the symbol P_f to differentiate it from the optimum plan proportion for initial irradiance referred to earlier by P . The following discussion analyses the effects of the geometrical and physical parameters of the form on the optimum plan proportion P_f and the optimum irradiance load. It compares the results with those obtained earlier for minimum initial irradiance load.

5.2 Variation of the Optimum Plan Proportion with Orientation and Parameters of the Form

5.2.1 The three progressions studied showed that the optimum plan proportion P_f , derived for the minimum final irradiance load criterion, increases with the rotation of the block as the orientation angle α_s varies within the range of the first quadrant. The patterns for the variation of P_f with α_s for the different combinations of the geometrical parameters are similar to those of P which were obtained earlier for minimum initial irradiance. However, the values of P_f at the different orientations for the different cases of the progressions differ from the corresponding values for P . This evidently is a response to the added effect of the interreflected irradiance.

5.2.2 The cases of the first and third progressions generally showed that P_f varies within the range $0.55 < P_f < 1.85$

and with a distinctive value of 1 at $\alpha_s = 45^\circ$, for the different combinations of form parameters. Its values at $\alpha_s < 45^\circ$ were higher than the corresponding values for P and lower for $\alpha_s > 45^\circ$. The effects of the parameters A, Rd and γ_{om} on P_f and its patterns of variations with α_s for the cases of these two progressions were identical to those shown for P, see Figures 6.22 and 6.23.

P_f was mainly affected by the variation of γ_{om} , which in the case of the first progression was determined by the variation of Rd. It increases with γ_{om} , but at a decreasing rate as α_s varies from 0° to 45° and vice versa for α_s varying 45° to 90° . The variation of Rd showed a slight effect on P_f for the cases of the third progression. This indicates that, for $\alpha_s < 45^\circ$, P_f increases with Rd up to 1 and decreases with further increase of Rd and vice versa for $\alpha_s > 45^\circ$. The rate of variation with Rd evidently varies with α_s as P_f assumes a constant value of 1 at $\alpha_s = 45^\circ$.

The variation of the reflectance of the facades showed no significant effect on P_f , particularly for the cases of the first progression. This may be explained by the fact that the interreflected irradiance received on the different facades of the block is directly proportional to the reflectance of the facades. Hence, as the surrounding blocks on all sides of the block were of equal height, the proportion of the final irradiance on each pair of parallel facades of

the block remained constant for the different reflectance values of the facades. P_f on the other hand, was found to increase with the increase of ground reflectance, ρ_g , but at a decreasing rate as α_s increases from 0° to 45° and vice versa for α_s varying from 45° to 90° . This effect is particularly evident for $R_d > 1$. It is evident therefore, that the ground reflectance was mainly responsible for the variation of the values of P_f from the corresponding values of P . For example, the values of P_f varied from those of P by an average of ± 10 percent for a ground reflectance $\rho_g = 0.2$ and by twice as much for $\rho_g = 0.4$. Figure 7.22 illustrates typical examples for the variations of P_f with α_s , γ_{om} and ρ_g for the cases of the first and third progressions.

5.2.3 The second progression showed that the variation of the values for the optimum plan proportion P_f from the corresponding values for P was mainly determined by the obstruction height of the opposing facades which was varied on one side of the block. The values of P_f were found to be less than the corresponding values of P when the height of the variable obstruction, to one side of the block, was less than that of the block, with the obstruction height to the other side of the block being kept equal to that of the block. In the cases when $R_h > 1$, P_f was greater than P . When $R_h = 1$, the variation pattern of the values of P_f from those of P was similar to those of the first and third progressions

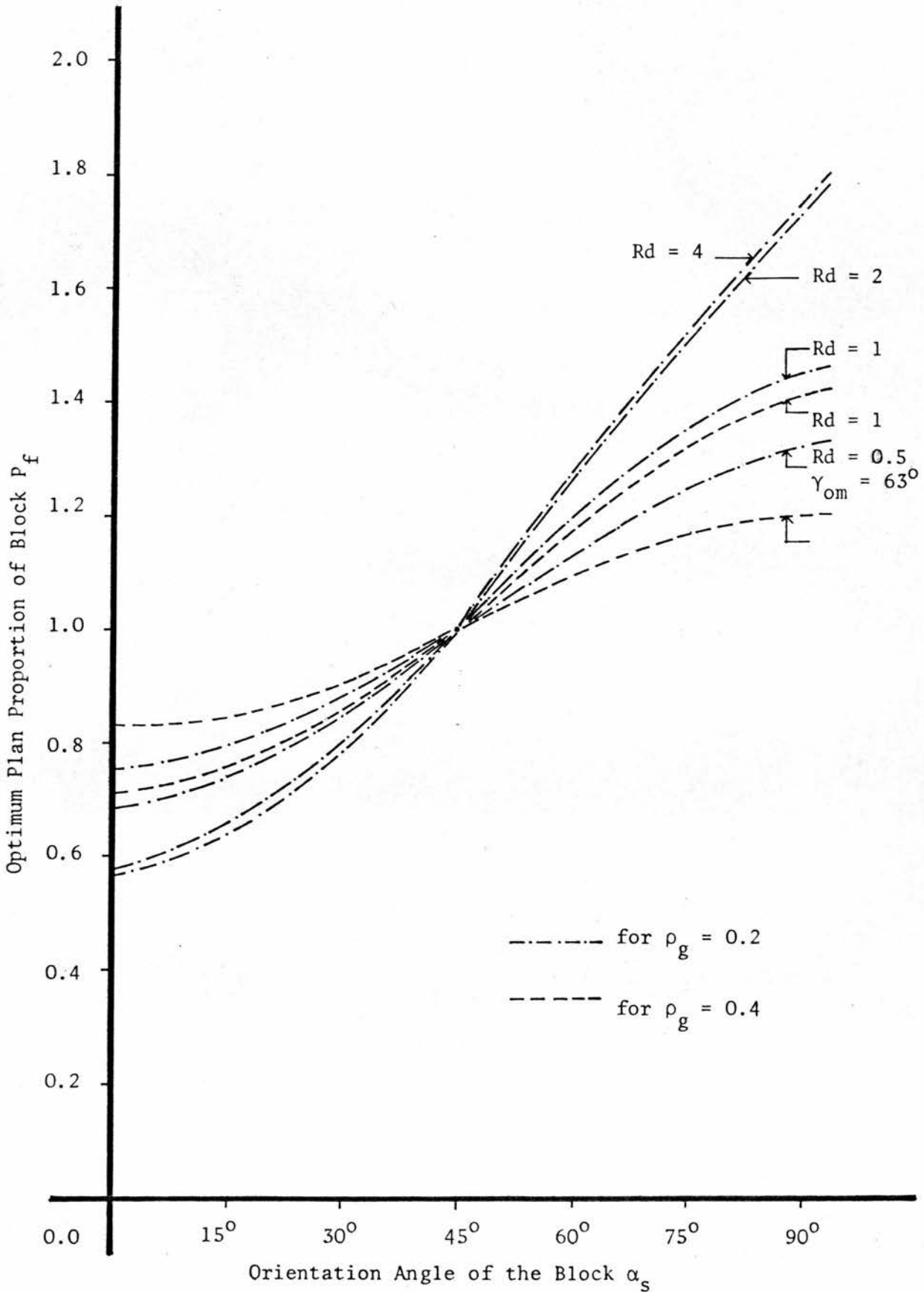


Figure 7.22 Variation of the Optimum Plan Proportion of the Block with Orientation for the Cases of the First Progression for Base Area $A = 1$

where $P_f > P$ for $\alpha_s < 45^\circ$ and $P_f < P$ when $\alpha_s > 45^\circ$. This is explained by the fact that the magnitude of the inter-reflected irradiance of a facade of the block increases with the increase of the height of its opposing facade. The interreflected irradiance on the block side with the variable obstruction height is therefore less than that with the constant obstruction height when $R_h < 1$ and greater when $R_h > 1$. It is evident, however, that the proportion of the interreflected irradiance on the two sides of the block is less than the corresponding proportion of their initial irradiances, which was also defined by P , when $R_h < 1$ and greater when $R_h > 1$.

5.2.4 The height of the obstruction being varied on one side of the block, was determined by the parameters R_d and γ_{om} . P_f was found to decrease with the increase of R_d , for any obstruction angle. The rate of decrease, however, was more gradual and less significant for $R_d > 1$. This is also explained by the fact that the final irradiance on the block side with the constant obstruction increases with the increase of R_d . At the same time the final irradiance on the block side with the variable obstruction height may vary only slightly with the increase of $R_d > 2$. As the tendency for the optimum form was to increase the length of the block side with the least amount of irradiance load, P_f therefore decreases with the increase of R_d .

P_f was found to increase slightly with the increase of the obstruction angle γ_{om} where $R_h < 1$, but at a decreasing rate with α_s varying from 0° to 45° . For $\alpha_s > 45^\circ$, P_f generally decreases with the increase of γ_{om} . When $R_h > 1$, P_f was found to decrease with the increase of γ_{om} , but at a decreasing rate as α_s increases. The variation of P_f with the form parameters is explained by the fact that the final irradiance on block side with the variable obstruction increases with γ_{om} for $R_h < 1$ due to the high increase of the interreflected irradiance. Thus P_f tends to increase with γ_{om} at first, for $R_h < 1$. As the initial irradiance on the block side with the variable obstruction falls rapidly with the increase of $R_h > 1$ while the interreflected irradiance increases only slightly, its final irradiance generally decreases with the increase of γ_{om} leading to the increase of the length for this block side for the optimum form.

The rotation of the block from the north point evidently increases the final irradiance on the block side with the variable obstruction, but also emphasises the effect of the obstruction. The increase of α_s increases the rate of increase for obstructed initial irradiance with γ_{om} and decreases the rate of increase of the interreflected irradiance. Thus the first range of γ_{om} , where P_f increases with γ_{om} , gets smaller with the increase of α_s . This explains the effect of α_s on the variation patterns of P_f with γ_{om} . The diagram shown in Figure 7.23 illustrates the effects of the form

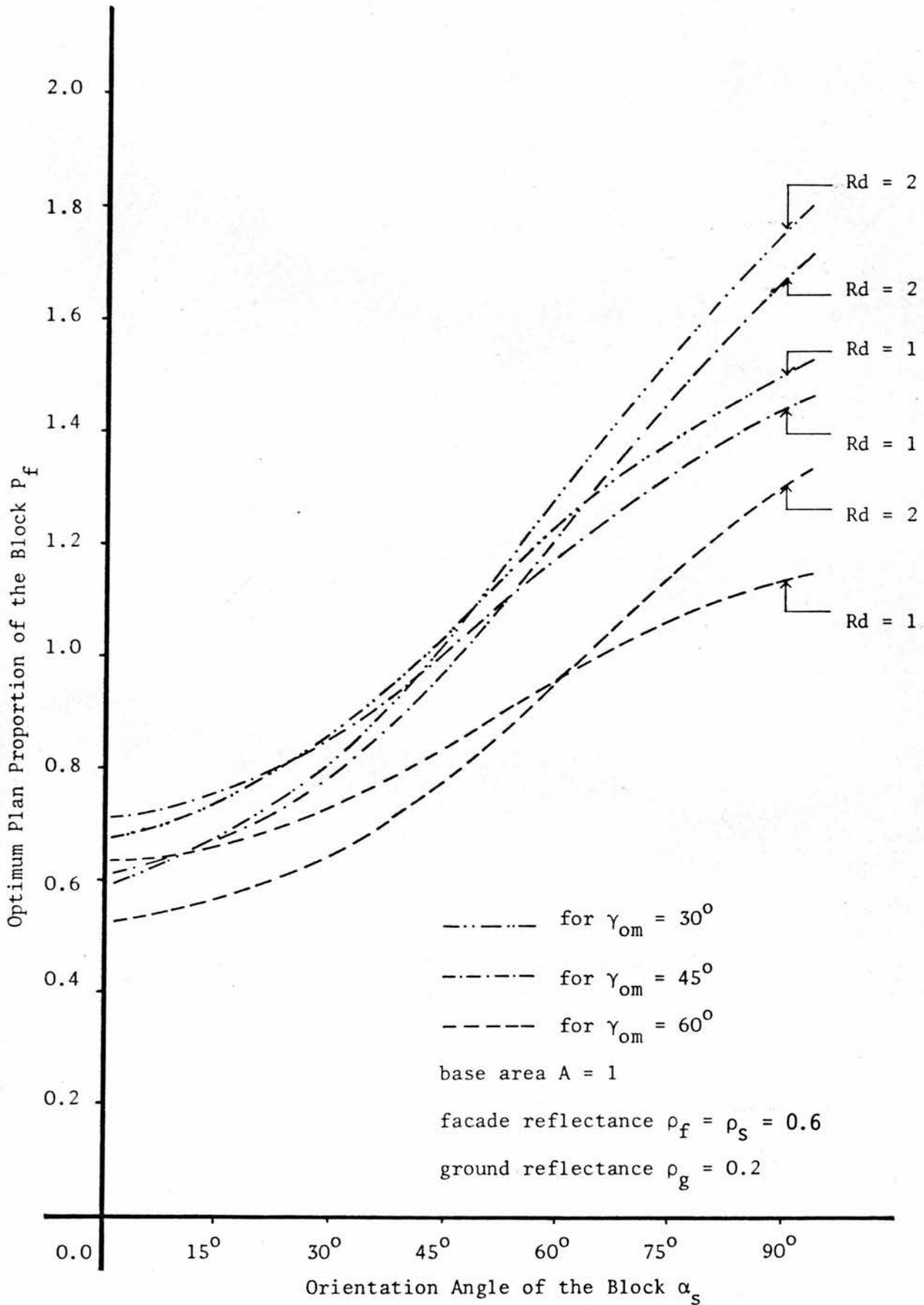


Figure 7.23 Variation of the Optimum Plan Proportion with the Form Parameters for the Cases of the Second Progression

parameters on P_f for the cases of the second progression.

5.2.5 The variation of the base area A also showed slight variation on P_f within the range of ± 10 percent for the cases of the second progression. P_f was found to increase with the increase of A for $R_h < 1$ and decrease for $R_h > 1$. This is also explained by the fact that the length proportions of the block's sides increase with A . Thus the shadow factors of the facades of the block increase as well as those of the surrounding blocks and subsequently decrease their initial irradiance load. This eventually decreases the final irradiance load on the block side with the relatively higher obstruction. Thus when $R_h < 1$, P_f increases with A and similarly decreases when $R_h > 1$.

5.2.6 The effect of the facades' reflectance on the optimum plan proportion P_f was also determined by the variable height of the obstruction to the block for the cases of the second progression. It is apparent that the increase of the facade reflectance increases the magnitude of the interreflected and subsequently the final irradiance which may be received on a facade of the block. The rate of increase for the interreflected irradiance with facade reflectance evidently increases with the increase of the height of obstruction following the increase of the surrounding component of the interreflected irradiance. Thus the interreflected and final irradiance load on the block side with relatively higher

obstruction tends to increase more rapidly with ρ_f than the final irradiance load on the side with the shorter obstruction. This evidently explains the reasons for the variation patterns of the optimum plan proportion P_f with the facade reflectance ρ_f . Thus P_f decreases with the increase of ρ_f where $R_h < 1$, though only slightly. It decreased by an average of 2 percent for every 0.1 increase of ρ_f . When $R_h > 1$, P_f was found to increase with the increase of ρ_f by an average of 5 percent for every 0.1 increase of ρ_f .

Ground reflectance ρ_g on the other hand had little effect on P_f , though P_f was found to increase with the increase of ρ_g for $\alpha_s < 45^\circ$ and decreases as $\alpha_s > 45^\circ$. For example, the increase of ρ_g from 0.2 to 0.4 was found to cause P_f to vary within the range of ± 5 percent. The effect of α_s on the variation pattern of P_f with ρ_g is mainly attributed to the ground reflection which increases with α_s on the street side with the variable obstruction but decreases on the other side as the block is rotated.

5.3 Variation of the Optimum Final Irradiance Load on Building Blocks with its Form Parameters and Orientation

5.3.1 The optimum final irradiance load represents the minimum amount of the daily average irradiance load, comprising initial and interreflected irradiance, which is received on the block's facades. The variation of the optimum final irradiance load

with the variation of the block's orientation angle α_s within the ranges of the first quadrant also showed similar patterns to those established earlier for the optimum initial irradiance for the different cases of the three progressions. These indicated that the optimum final irradiance generally increases slightly with the increase of α_s up to 45° and subsequently decreases with further increase of α_s . The least amount of optimum irradiance is received at $\alpha_s = 0^\circ$. The optimum final irradiance values at the different orientations generally vary within the range ± 8 percent. They are higher than the corresponding values derived for initial irradiance. This is obviously due to the added effect of the interreflected irradiance. The interreflected component of the optimum final irradiance also showed similar variation patterns with orientation for the different cases of the three progressions.

5.3.2 The cases of the first and second progressions indicated that the optimum final irradiance increases at a decreasing rate with the increase of R_d . The increase is less significant for $R_d > 1$ where it amounts to less than 5 percent with each unit of R_d . This increase is mainly due to the increase of the initial irradiance and the ground component of the interreflected irradiance, particularly on the block's sides with the constant obstruction height. In the cases of the third progression, the optimum final irradiance was found to increase with the increase of R_d when $R_h < 1$, but decreases when $R_h > 1$.

This is also explained by the fact that at low obstruction height the increase of the interreflected irradiance, particularly its ground component with the increase of R_d , compensates for the decrease of the initial irradiance, due to the resulting increase of R_h , with a net increase to the final irradiance, whereas at higher obstruction, the decrease of the initial irradiance outweighs the increase of the interreflected irradiance. The rate of variation, however, is also less significant for $R_d > 1$. The effects of varying the height of obstruction on the optimum final irradiance are illustrated by the variation of the obstruction angle in the second and third progressions. These show that the optimum irradiance increases with γ_{om} mainly when $R_h < 1$. It subsequently decreases with further increase of γ_{om} leading to the increase of $R_h > 1$. This is similarly explained by the effects of the height of obstruction on the initial and interreflected components of the final irradiance as explained above. The diagram shown in Figure 7.24 illustrates the effects of the obstruction angle and height on the optimum final irradiance.

5.3.3 The variation of the base area, on the other hand, produced a similar effect on the optimum final irradiance as in the case of the initial irradiance. Similarly the decrease of the optimum irradiance with the increase of the base area was less significant for $A > 2.0$.

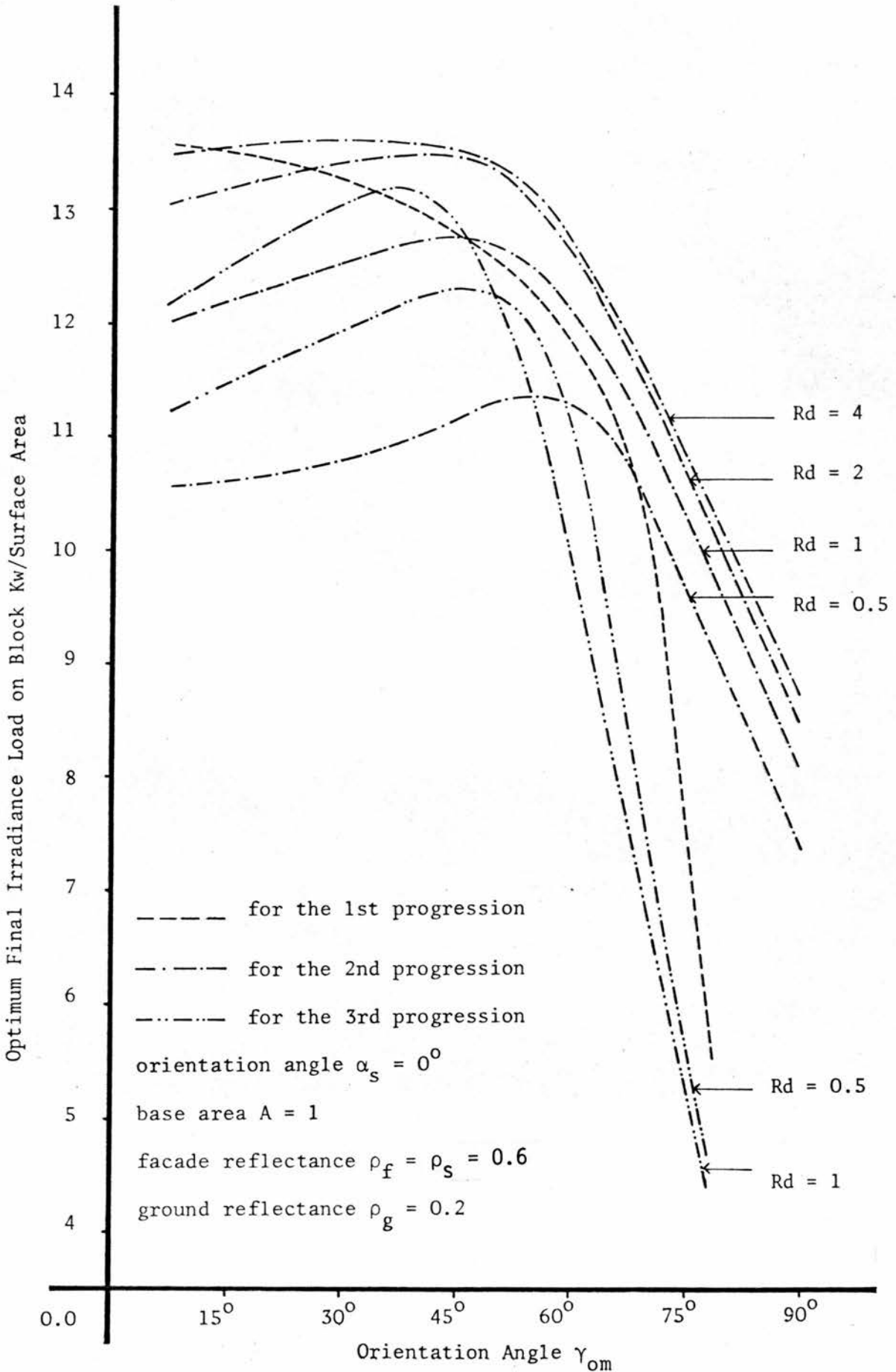


Figure 7.24 Variation of Optimum Final Irradiance with Obstruction Angle γ_{om}

5.3.4 It was apparent that the optimum final irradiance of the block in the three progressions tends to increase with the increase of facade and ground reflectances due to the increase of its interreflected irradiance component. The rate of increase was evidently determined by the street width and the height obstruction. The rate of increase for optimum final irradiance with the reflectance of facade was most significant for $R_d < 2$ and $R_h > 1$. The effect of ground reflectance on the other hand is most evident for $R_d > 1$. The combined effects of the reflectances and the geometrical parameters are illustrated by the diagram in Figure 7.25.

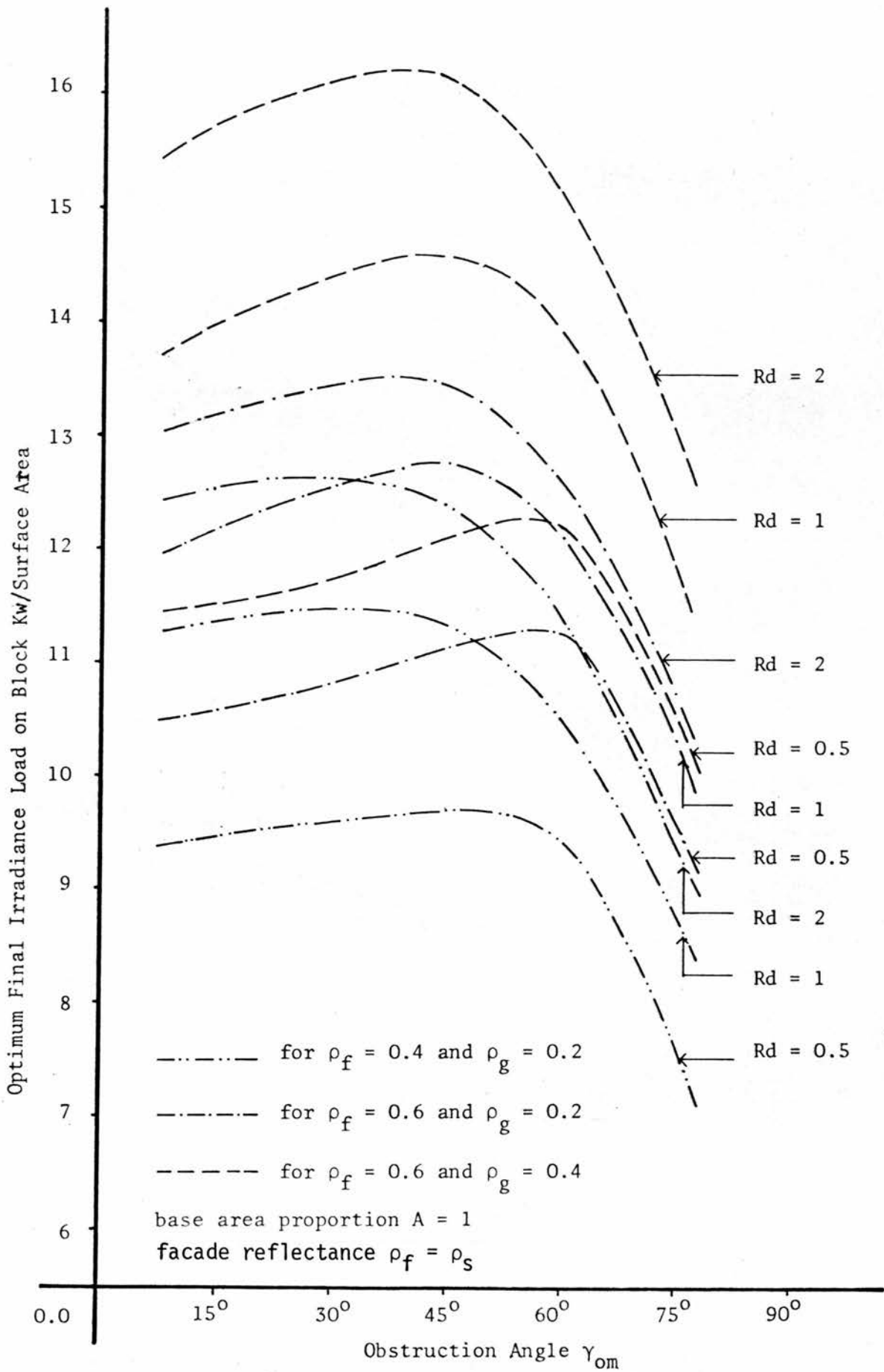


Figure 7.25 Variation of the Optimum Final Irradiance Due to the Combined Effects of the Reflectance and Geometrical Parameters of Form for the Cases of the Second Progression

6. CONCLUDING REMARKS

6.1.1 On the basis of the above analysis, it may be possible to present general conclusions on the cumulative effects of the geometrical and physical parameters of buildings on the initial and interreflected irradiance components constituting the final irradiance load which may be received on the facades of buildings. These may serve as guide lines for manipulating the parameters of buildings and the geometric configuration of the surrounding blocks to utilize the interreflected irradiance and ultimately control the final irradiance load on buildings.

6.1.2 The most important components of the interreflected irradiance to a vertical facade are those initiated by the surrounding and ground surfaces. They generally contribute significantly to the final irradiance load of the facade and constitute major portions of it, particularly at times when the initial irradiance of the facade is low, while the initial irradiances of the ground and the surrounding opposing facades are high. The interreflected facade component is of no practical significance as it generally constitutes a minute portion of its final irradiance load. The magnitudes of these components are determined by the geometrical configuration of the form and its surrounding, the reflectances and the initial irradiance of their respective surfaces. For any given geometric configuration, the interreflected irradiance

components vary proportionally to the variation of the reflectances of their respective surfaces as well as to their initial irradiances which are also determined by the geometrical configuration of the surrounding. The surrounding component increases rapidly with the increase of the obstruction height. Its rate of increase escalates with the increase of its reflectance, but decreases with the increase of street width proportion R_d . This also indicates that the surrounding component generally decreases with the increase of R_d . The ground component on the other hand increases with the increase of R_d , but at a decreasing rate. It does not vary significantly with $R_d > 2$. It also increases gradually with $R_h < R_d$, but decreases slightly with further increase of R_h . Both components are most significantly affected by the variation of the reflectances of their respective surfaces.

6.1.3 The effects of the geometrical parameters on the initial and interreflected irradiance components are of direct benefit in controlling the final irradiance load on a building facade at different times of the day. For example, the effect of the obstruction height may be utilized to shade the facade and reduce its initial irradiance when it is facing the sun while providing it with interreflected surrounding component as the sun moves away from it.

6.1.4 The effects of the form parameters on the final irradiance load of a vertical facade represent their combined effects on

its initial and interreflected irradiance components. The final irradiance of a facade therefore increases at a decreasing rate with the increase of obstruction height and street width proportion mainly within the range R_d and $R_h < 2$. It generally tends to fall slightly with further increase of R_h as the increase of the surrounding component of the interreflected irradiance does not compensate for the decrease of the initial irradiance. Further increase of $R_d > 2$ may also produce similar results as the increase of the initial irradiance and the interreflected irradiance ground component may not compensate for the decrease of the interreflected surrounding component.

6.1.5 The selection of the geometric form of building and the configuration of its surrounding is practically considered in terms of the final irradiance load on the building. This takes into account the effects of the form parameters on both the initial and interreflected irradiance components. The minimum final irradiance data derived for the optimum form for the different cases of the three progressions indicated that it is generally of a higher magnitude than the optimum initial irradiance data derived earlier. This is obviously due to the added contribution of the interreflected irradiance. However, the magnitudes of the initial irradiance component of the optimum final irradiance ^{for most cases,} remain nearly the same as when derived separately for the optimum form in terms of the

minimum initial irradiance for the different cases of the three progressions. The optimum final irradiance also varies only slightly with orientation, with the least amount received on the block oriented towards the N-S axis.

6.1.6 The optimum final irradiance is reduced by increasing the height of obstruction on either side of the block above its level. This results from the decrease of the initial irradiance and the ground component of the interreflected irradiance which is not being compensated by an equivalent increase in the interreflected irradiance of the surroundings component. It may be regarded as decreasing by about 1 percent with the increase of the obstruction height on one side of the block above its level for each degree of the obstruction angle to the block side. The optimum final irradiance is reduced by twice as much when the obstruction height is increased on both sides of the block. The optimum final irradiance is also reduced when the obstruction height is decreased below the level of the block. This is mainly due to the decrease of the interreflected irradiance ground and surrounding components which is not compensated by the increase of the initial irradiance. However, this variation is of no practical significance as the optimum final irradiance load varies by less than 0.2 percent with each degree for the obstruction angle.

6.1.7 The optimum final irradiance increases rapidly with the increase of street width within the range $R_d < 2$ for different

geometric configuration of surrounding. Further increase of $R_d > 2$ is of no practical significance as the optimum final irradiance tends to vary only slightly.

6.1.8 The effects of the facade reflectance on the optimum interreflected and final irradiance are most significant for $R_h > 1$. The interreflected irradiance changes by an average of 30 percent for each change of 0.1 of facade reflectance while the final irradiance changes by an average of 10 percent. The ground reflectance produces similar effects on the interreflected and final irradiances particularly for the street width within the range $R_d > 1$. The variation of facade and ground reflectance generally produces less than half as much effect where $R_d < 1$ and $R_h < 1$.

6.1.9 It is apparent that the optimum form of a block for the minimum final irradiance load favours a rectangular shape plan with its longer side oriented towards a N-S axis. The proportions of the plan sides derived for the minimum final irradiance differed slightly from those derived earlier for minimum initial irradiance for the different cases of the progressions studied. This variation accounts for the differing proportions of the interreflected irradiance received on the different sides of the block for the different cases. A number of practical recommendations may be presented for the optimum plan proportions of a

rectangular block for different geometric configurations of surroundings' and surfaces' reflectances. A ground reflectance value $\rho_g = 0.2$ is taken to represent the typical ground condition.

6.1.10 In cases where the obstruction height on all sides of the block is equal to its height, the rectangular shape of the block plan may be taken to have sides proportion $P_f = 0.66$ for an N-S orientation of the block and for all street width proportions $R_d > 1$. This plan proportion may be modified with the rotation of the block from the N-S axis in order to maintain the same level of final irradiance load. It is to be increased by an average of 1 percent for each degree of angular displacement from the orientation axis at the 15° intervals. The following values are recommended for P_f at the different orientations within the ranges of the first quadrant. These are average values for different street width proportions. The values of P_f at various orientations in the subsequent quadrant are easily defined from the symmetry of the azimuthal distribution of P_f within the ranges of the first and subsequent quadrants.

α_s	0.0°	15°	30°	45°	60°	75°	90°
P_f	0.66	0.76	0.87	1.0	1.15	1.32	1.52

More accurate values of P_f for specific street width proportion are easily determined from the graphs shown in Figure 7.22.

The variation of the facade reflectance is of no practical significance. The variation of ground reflectance from 0.2, which is generally small, may also be considered of no practical significance.

6.1.11 The optimum plan proportion P_f may also be varied by changing the height of obstruction on either side of the block. When the obstruction height on any side of the block is reduced below the level of the block, P_f does not vary significantly, particularly for $\alpha_s \leq 45^\circ$. Hence, the values presented above may be taken for the cases where $R_h \leq 1$, on any side of the block. When the obstruction height is increased above the level of block on the side defining its orientation, P_f is to be reduced by 2 percent for every degree of obstruction angle by which the obstruction height is increased above the level of the block at the different orientation angle, assuming that the block's facades are non-reflective. However, P_f should also be altered to account for the variation of the facade reflectance. It is to be varied proportionally to the variation of the facade reflectance. Thus the rate for the variation of P_f with γ_{om} is to be reduced by an average of 5 percent for every 0.1 of facade reflectance. The decrease of P_f with the decrease of γ_{om} in the cases where $R_h < 1$ and $\alpha_s > 45^\circ$ may be accounted for by assuming half of the above rate for the variation of P_f with γ_{om} and ρ_f . Recommended values for the rate of variation of P_f with the variation of the

obstruction height for every degree of obstruction angle above or below the level of the block are given in the following table for different reflectances of facade.

Reflectance of Facade	Rate of Variation of P_f for Every Degree of γ_{om}	
	Rh < 1	Rh > 1
0.0	- 1%	-2%
0.2	- 0.9	-1.8
0.4	- 0.8	-1.6
0.6	- 0.7	-1.4
0.8	- 0.6	-1.2

6.1.12 When the obstruction is increased simultaneously on all sides of the block, P_f is increased at a decreasing rate for α_s varying from 45° to 90° . It is to be increased by 1 percent per degree of obstruction angle where $Rh > 1$, but with this rate being decreased by 2 percent with every degree of angular displacement from the N-S axis. The rate for the variation of P_f with γ_{om} is to be reversed for α_s varying between 45° and 90° . The effect of varying the facade reflectance on P_f is of no practical significance for these cases. For this case, the following table gives recommended values for the rate of variation of P_f with each degree of γ_{om} at the different orientation angles.

Orientation Angle α_s	0	15 ⁰	30 ⁰	45 ⁰	60 ⁰	75 ⁰	90 ⁰
Variation Rate of P_f with γ_{om}	1%	0.7%	0.4%	0.0	-0.4%	-0.7%	-1%

6.1.13 A fixed optimum final irradiance load and plan proportion for the rectangular block may be maintained at the different orientations by varying the obstruction height or the facade reflectance on either side of the block. This is practically achieved by utilizing the effects of the facade reflectance and the height of the obstruction on the final irradiance load on the block's facades. Thus the final irradiance load on the facade with the relatively higher irradiance may be reduced by either increasing the height of the obstruction or reducing the facade reflectance. The facade length may then be increased in an inverse proportion to the decrease of the final irradiance.

6.1.14 The procedure for manipulating the height of obstruction and reflectance in order to maintain a fixed plan proportion at all orientations is best illustrated by the case for square plan shape. For such a case the obstruction height to side parallel to the orientation axis of the block is increased at an increasing rate for α_s varying from 0⁰ to 45⁰. When α_s is varied from 45⁰ to 90⁰ the obstruction height to the block's

perpendicular to its orientation axis is increased. The facade reflectance determines the rate of increase for the obstruction. It is apparent that the greater the facade reflectances, the greater is the final irradiance on the block and the greater is the obstruction height needed to reduce it. For example, for a typical situation of white-washed buildings, with a facade reflectance ρ_f of about 0.8, the obstruction height is to be increased by about 1.2 percent for every degree of angular displacement from the 45° orientation axis. This rate is to be varied proportionally to the variation of the facade reflectances. For example, for an old white-wash of a reflectance ρ_f of about 0.4, the rate of increase is reduced to about 0.9 percent for every degree of angular displacement. Similar procedures may also be developed for specific optimum plan proportions where $P_f \neq 1$. It is evident, however, that any given plan proportion may be defined by alternative combinations of form parameters.

6.1.15 A practical procedure may also be suggested for the evaluation of the optimum plan proportion for a rectangular block for any given geometric configuration of surroundings and combination of facades' reflectances. The ratio of the two dimensions for an optimum rectangular shape plan may be taken as inversely proportional to the ratio of the total final irradiance load of their respective facades. The initial irradiance load on the block's facades, the surrounding

facades and the ground between them are easily derived by the procedure utilizing the initial irradiance indices described earlier in the last chapter. The final irradiance load on the different facades are then evaluated by the procedure described earlier in this chapter. These are then used to determine the plan proportion in a similar manner as described in the last chapter for the initial irradiance. The length proportions and the dimensions of the block's sides are then determined by the relations expressed by equations 6.19 and 6.20 shown in the last chapter.

6.1.16 Examples are given in Appendix A.7 illustrating alternative practical interpretations of the proportions and the dimensions of the sides of the blocks and the configuration of the surroundings for minimum irradiance load.

CHAPTER VIII
GENERAL CONCLUSION

GENERAL CONCLUSION

1. PRACTICAL INTERPRETATION OF THE RESULTS

1.1.1 Control of the thermal and visual performance of buildings in relation to solar radiation is an important aspect of the design of buildings in tropical arid regions. It is most practically achieved if all possible steps are taken to make the best use of passive control by natural means through the manipulation of the geometrical and physical parameters of buildings. However, this evidently requires precise understanding of the radiation from the sky and the sun, the interactions between the radiation and the urban form, identification of the physical processes involved and definition of the interrelationships between the initial irradiance input, the final irradiance output of buildings and their geometrical and physical characteristics. Aspects of these tasks have been attempted in this thesis which dealt particularly with the solar irradiance load on the external surfaces of buildings as an external subsystem of a physical system. As a result a computerised mathematical model was developed for the systematic generation of alternative geometrical forms of buildings and configurations of surroundings and for the rapid evaluation of the initial, interreflected and final irradiance load on the building's external surfaces.

1.1.2 The underlying objectives for developing the computer model were twofold :

- (i) To establish a practical research tool for investigating the problem of solar irradiance and buildings which would be capable of providing information for practical application at any level of detail and defining the effects of the geometrical and physical parameters of buildings and the ranges within which they significantly influence the initial and final irradiance loads on their surfaces.
- (ii) To provide a versatile design tool for the systematic generation of wide ranges of alternative building forms and the rational evaluation of alternative forms for any specified irradiance load criteria.

1.1.3 The model can also be directly integrated into a comprehensive model for the analysis and synthesis of alternative architectural solutions for the relevant and determining performance criteria. The aim of this is to maximise the designer's ability to manipulate the geometrical and physical parameters in the synthesis of a balanced and total architectural solution. The need for maximum efficiency and economy in operating the model was emphasised by the development and the incorporation into the model of economical solution procedures of sufficient accuracy. These simplified

the formulation of the model and the evaluation of the initial and interreflected irradiance, and reduced the computation time.

1.1.4 The model allowed detailed and intensive investigations into the effects of the various form parameters on the initial irradiance input and final irradiance output of the facades of buildings to be carried out. Wide ranges and combinations of form parameters were studied at different dates and times of the year. On this basis, the interrelationships between the initial irradiance load, the final irradiance load and the parameters of form were analysed. The ranges within which the form parameters significantly influenced the initial and final irradiance load on building facades were identified.

1.1.5 The generative potential of the model was illustrated by the series of investigations for the definition of the optimum plan proportions for a rectangular building block. This was achieved by generating wide ranges of alternative combinations for the side proportions of a block and subsequently selecting the ones which satisfied the irradiance load criterion. On this basis, using Khartoum as an example of a typical arid region, and with the irradiance load criteria appropriately expressed by the minimum daily average initial and final irradiance load, it was possible to define alternative optimum proportions for the block's sides for different orientations and configurations of surroundings. While the results in the

were derived from the study of rectangular shaped building blocks in a rectilinear arrangement, it may be argued nevertheless that these results provide a general indication of the alternative possibilities for manipulating the geometrical parameters and reflectance characteristics of buildings for the control and the minimisation of the irradiance load on their facades.

1.1.6 The general recommendations presented in the previous two chapters, though they may not fully satisfy the designer's ultimate objective in specifying constructional elements, nonetheless clearly identify the significance of the different form parameters and their effects on the optimum final irradiance on building facades. They were intended to provide simple guidelines for the designer in the synthesis of a building form or in devising building regulations and planning control for minimum irradiance load on buildings. It is recognised that in any given situation the irradiance load criterion is applicable to all buildings in any given neighbourhood. It is essential, therefore, to extend the practical interpretation of the results to achieve the irradiance load criteria for all buildings. This will evidently present wider ranges of possible alternative combinations of building volumes, heights, proportions of sides, orientations, materials and street width. A few examples are therefore presented in Appendix A7 to illustrate alternative practical interpretations of the optimum form recommendations.

2. FURTHER DEVELOPMENT OF THE EVALUATIVE MODEL AND ITS GENERATIVE POTENTIALS

2.1.1 Recent trends in architectural research are justifiably directed towards the development of computerised mathematical models which simulate the building performance in a number of respects. This has expanded the capabilities of architectural research to carry out rigorous and intensive investigations into complex architectural problems and building configurations, thus overcoming the difficulties generally presented by the multiplicity of the factors and parameters involved and the complexity of their interrelationships which earlier deterred detailed investigations.

2.1.2 It is conceivable that these computerised models could ultimately build up into an integrated and comprehensive package, thus providing a powerful tool for the detailed and integrated analysis of building performance. In this manner a wide range of alternative building forms and configuration of surroundings can be tested and the interrelationships between the various performance criteria and the form parameters may be defined, so developing a clear understanding of the building as a total system and accumulating valuable information for practical application which expands the designers options and allows him to carry out a synthesis of a total architectural solution on rational and balanced basis.

2.1.3 The advantages of including the integrated evaluative model in the design process are evident. With it, it is possible to generate a wide range of building forms, evaluate their performances and define those forms which satisfy the demands and the constraints imposed. It is equally conceivable that the integrated model package would eventually build up into an interactive system. This would not only allow the designer to generate the building form for any set of determinants, but also allow him to change his decisions and observe almost immediately the effects of value-based judgements.

2.1.4 The development of the computerised mathematical model in conjunction with this study stemmed from these recent approaches in architectural research. Although the model only dealt with a limited aspect of the evaluation of the environmental performance of building, its main contribution may be seen in providing the tool for the systematic generation of building configurations and the evaluation of their performances with respect to solar irradiance which is the major environmental physical field in the tropical arid regions. It provides the basic framework for the development and extension of other environmental models. The investigations carried out, though limited in scope, provided valuable information which has not been readily available before. Further investigations can be carried out with the model as a degree of flexibility is incorporated in the description of the building form and the

configuration of its surroundings. Other complex conventional forms, such as courtyard shapes, cruciform shapes and so on, as well as other non-conventional forms may be studied for wide ranges and combinations of parameters. For example, the street width and the obstruction height on all sides of the block may be taken to have varying proportions.

2.1.5 It is recognised, however, that the response of a building ^{for} to solar irradiance is ultimately measured by the thermal and visual performance of its internal enclosures. The immediate next step in development of the model is therefore seen to be the inclusion of the internal subsystem, complementing the external subsystem considered in this thesis, in an integrated model for the physical system. On this basis, accurate assessment of the building performance for solar irradiance may be achieved with regard to the thermal and visual demands of the internal spaces. In this respect, the development of the model to simulate the irradiance transfer through the structure and the thermal performance of the building is easily achieved on the basis of the large body of knowledge and thermal evaluative procedures available. Alternatively, existing thermal models, eg, Tappuni 1973, may be adapted and directly integrated into the model.

2.1.6 The main difficulties that may be seen to arise here are in the simulation of interior illumination due to the direct solar and externally ~~ly~~ interreflected irradiance.

This is because of the lack of adequate evaluative procedures for interior illumination and glare for the tropical arid regions. Further work is evidently needed to overcome these difficulties prior to developing an integrated model for the physical system. The alternative would be the development of a complex model which may turn out to be inefficient. It is essential for the research work which may be further pursued in this area to develop a basic modification to the standard procedures developed for temperate regions with overcast skies. A number of suggestions have previously been outlined (Hopkinson et al 1966, Plant et al 1969, 1973, Van Breman 1969). Once such procedures are developed and incorporated into the model, detailed analysis may be conducted into the effects of window size and location on interior illumination. With the further inclusion of other sub-models or models which simulate the building performances in a number of respects a powerful tool may ultimately be built up for intensive architectural research into the production of balanced designs for buildings in tropical arid regions.

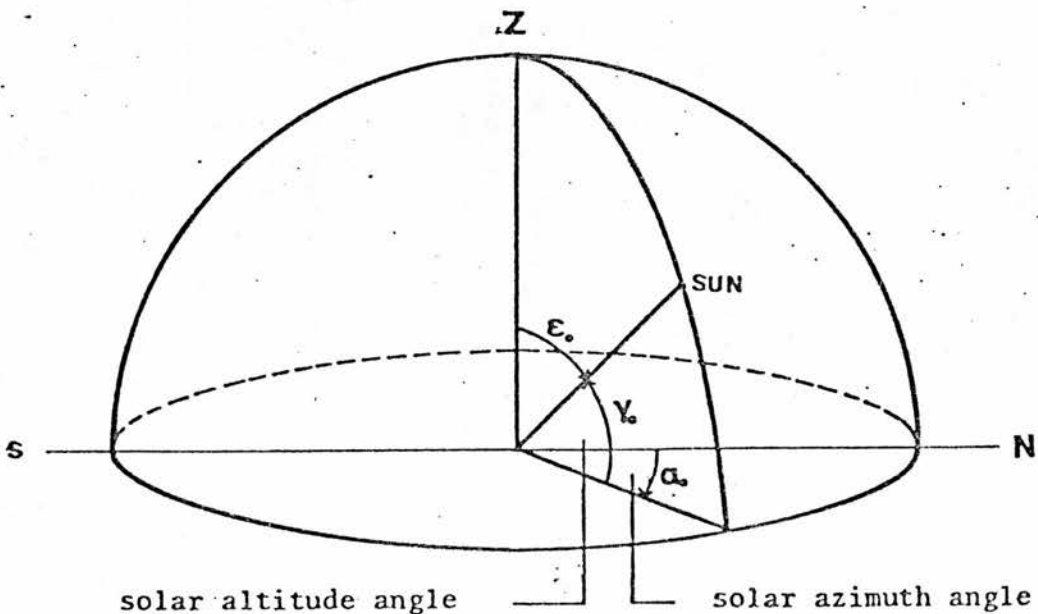
APPENDICES

LIST OF APPENDICES

- APPENDIX A.1 Tables for Altitude and Azimuth Angles
of the Sun for Khartoum
- APPENDIX A.2 Irradiance and Illuminance Data for the
Standard Tropical Sky at Different
Solar Altitudes
- APPENDIX A.3 Tables for the Sky Component for Surfaces
of Different Orientations, Inclinations
and Obstructions, at Different Positions
of the Sun and Clear Tropical Skies
- APPENDIX A.4 Possible Shapes and Locations of Shadow
which may be cast on a Rectangular Vertical
Surface by an Adjacent Rectangular Vertical
Surface with Varying Sizes and Relative
Positions
- APPENDIX A.5 Form Factor Tables for Surfaces of
Different Geometric Configurations
- APPENDIX A.6 Listing of the Main Routines
- APPENDIX A.7 Example for Alternate Practical Interpretation
of the Dimensions and Proportions of the Sides
of the Blocks and the Configuration of the
Surrounding for Minimum Final Irradiance
Load on the Blocks

APPENDIX A.1 TABLES FOR ALTITUDE AND AZIMUTH ANGLES OF THE
SUN FOR KHARTOUM

Knowledge of the altitude and azimuth angles of the sun is essential for architectural studies and design in the tropical arid regions when dealing with such building's problems as related to orientation, daylighting, sunlight and shade control and the evaluation of the irradiance load. Such information can be tabulated in more detail, for minimum interpolation, for different times of the day and the year and for any location on the earth's surface with the routine SUNGT. This routine was used to prepare tables for the solar angles for Khartoum (latitude 16°N , longitude 32°E). These are presented here for the first and fifteenth of every month at hourly intervals. The program can also be instructed to tabulate further relevant data such as shadow angles, times of sunrise and sunset and so on.



TABLES FOR SUN POSITIONS
 KHARTOUM 1, LATITUDE = 16.0 DEG, N. LONGITUDE = 32.0 DEG, E. S. T. LONGITUDE = 36.0 DEG, S. E

MONTH	DAY	ANGLE	TIME OF DAY												
			6	7	8	9	10	11	12	13	14	15	16	17	18
1	1	ALT.	****	7.9	20.0	32.0	41.8	48.7	50.9	47.9	40.4	30.3	18.0	5.9	*****
		AZ.	****	116.0	122.8	131.3	143.5	160.5	181.7	202.4	218.7	230.2	236.2	243.9	*****
15	15	ALT.	****	7.3	20.1	32.0	42.3	49.8	52.7	50.1	42.7	32.5	20.0	7.9	*****
		AZ.	****	114.6	120.4	128.6	140.5	157.6	179.5	201.6	218.9	231.0	239.3	245.1	*****
2	1	ALT.	****	7.7	20.9	33.4	44.5	53.3	56.7	54.1	46.4	35.7	23.4	10.2	*****
		AZ.	****	110.5	116.2	124.0	135.7	153.4	177.5	202.5	221.5	234.1	242.0	248.0	*****
15	15	ALT.	****	9.0	22.0	35.0	47.4	56.8	61.0	58.2	49.7	38.2	25.4	11.9	*****
		AZ.	****	106.3	111.8	119.4	131.0	149.5	170.8	205.4	225.6	238.5	246.0	252.7	*****
3	1	ALT.	****	11.0	24.9	38.5	51.0	61.3	66.1	62.5	52.8	40.5	27.1	13.1	*****
		AZ.	****	101.5	106.9	114.1	125.4	145.0	177.2	210.9	232.2	244.4	252.2	257.7	*****
15	15	ALT.	****	13.4	27.6	41.6	54.8	66.2	71.6	66.6	55.4	42.2	28.2	14.0	*****
		AZ.	****	96.5	101.5	108.2	118.9	139.2	179.0	219.5	240.0	251.4	258.2	263.3	*****
4	1	ALT.	2.1	16.5	30.9	45.2	59.2	71.9	78.2	78.4	67.4	45.4	29.1	14.7	0.3
		AZ.	86.2	90.2	94.7	100.3	109.2	120.9	164.7	234.9	252.3	260.5	265.9	270.3	274.4
15	15	ALT.	4.5	18.0	33.2	47.6	61.9	75.7	83.2	72.3	58.2	43.9	29.4	15.1	0.8
		AZ.	01.4	85.2	89.0	93.4	99.9	115.4	196.5	250.0	262.2	267.9	272.9	275.8	279.7
5	1	ALT.	6.6	20.7	34.9	49.3	63.7	76.1	87.1	72.9	58.5	44.1	29.0	15.0	1.0
		AZ.	76.4	79.8	82.8	85.6	88.7	93.8	240.9	260.6	272.5	275.4	270.2	261.4	255.9
15	15	ALT.	7.8	21.6	35.7	49.9	64.1	78.2	86.1	72.7	58.5	44.3	30.2	16.2	2.4
		AZ.	72.7	75.0	78.2	79.8	80.0	75.0	314.3	281.0	279.8	260.7	262.7	265.3	268.3
6	1	ALT.	5.3	21.9	35.7	49.0	63.5	76.9	83.0	72.3	58.0	44.5	30.9	17.1	3.0
		AZ.	69.4	72.3	74.2	74.7	72.7	61.1	337.9	292.4	280.1	285.3	280.4	268.6	291.0
15	15	ALT.	6.0	21.5	35.2	49.0	62.7	75.7	82.5	72.4	59.1	45.3	31.0	17.9	4.0
		AZ.	68.0	70.8	72.5	72.7	70.1	57.2	340.8	297.2	288.8	287.2	287.8	269.8	293.0

***** INDICATES THAT THE SUN IS BELOW THE HORIZON, ANGLES ARE IN DEGREES & DECIMALS
 AZIMUTH MEASURED FROM NORTH POINT CLOCKWISE.
 LONG. & TIME LONG. ARE +VE WHEN EAST, -VE WEST. LAT. & DEC. ARE +VE NORTH, -VE SOUTH.

Table Al.1 Altitude and Azimuth Angles of the Sun for Khartoum

TABLES FOR SUN POSITIONS KHARTOUM : LATITUDE = 16.0 DEG, N ; LONGITUDE = 32.0 DEG, S ; S, T, LONGITUDE = 30.0 DEG, E

TIME OF DAY

MONTH DAY	ANGLE	6	7	8	9	10	11	12	13	14	15	16	17	18
7	ALT.	7.2	20.7	34.4	48.2	61.9	75.1	82.8	73.2	59.9	46.1	32.4	18.7	5.2
	AZ.	67.9	70.8	72.6	72.9	70.6	59.1	351.7	297.8	288.7	287.0	287.6	289.6	292.6
15	ALT.	6.4	20.0	33.8	47.7	61.6	75.2	84.3	74.2	60.6	46.6	32.7	18.9	5.3
	AZ.	69.3	72.3	74.3	75.2	73.9	65.3	354.6	293.4	285.8	284.8	285.8	287.9	291.0
8	ALT.	5.3	19.2	33.3	47.5	61.7	75.9	87.7	75.1	60.9	46.6	32.4	18.4	4.5
	AZ.	72.6	75.9	78.4	80.3	81.2	78.9	349.2	280.7	278.8	279.8	281.7	284.3	287.7
15	ALT.	4.7	18.8	33.1	47.4	61.8	76.3	88.1	74.6	60.2	45.8	31.4	17.2	3.1
	AZ.	76.5	80.0	83.1	86.1	89.5	95.3	206.1	265.7	270.9	274.2	277.2	280.4	284.0
9	ALT.	4.2	18.5	33.0	47.4	61.6	75.2	82.3	71.9	57.9	43.6	29.2	14.8	0.5
	AZ.	82.3	86.2	90.1	94.8	101.9	118.8	194.5	247.8	260.4	266.6	271.0	274.8	278.7
15	ALT.	3.9	18.3	32.7	46.9	60.7	72.7	76.9	68.1	55.0	41.0	26.7	12.3	****
	AZ.	87.7	91.8	96.5	102.6	112.8	136.2	193.9	236.4	252.2	260.2	265.6	269.9	****
10	ALT.	3.5	17.9	32.0	45.7	58.5	68.4	70.6	63.0	51.0	37.5	23.5	9.3	****
	AZ.	94.0	98.5	104.0	111.7	124.7	150.4	193.7	227.2	244.0	253.3	259.5	264.2	****
15	ALT.	3.0	17.1	30.9	44.0	55.7	64.0	65.1	58.4	47.3	34.4	20.0	6.7	****
	AZ.	99.5	104.1	110.2	119.0	133.3	158.1	193.0	221.4	237.9	247.8	254.4	259.4	****
11	ALT.	1.8	15.5	28.8	41.1	51.7	58.5	59.2	53.3	43.3	31.2	18.1	4.4	****
	AZ.	105.3	110.2	116.7	126.1	140.7	163.3	191.6	215.7	231.6	241.8	248.8	253.9	****
15	ALT.	0.4	13.8	26.6	38.4	48.3	54.5	55.2	50.0	40.8	29.3	16.0	3.3	****
	AZ.	109.2	114.0	120.6	130.1	144.3	165.0	189.8	211.8	227.3	237.6	244.7	249.9	****
12	ALT.	****	11.6	24.1	35.5	44.9	51.0	52.0	47.6	39.2	28.3	16.2	3.2	****
	AZ.	****	116.8	123.3	132.6	146.0	164.8	187.2	207.8	223.1	233.7	241.1	246.3	****
15	ALT.	****	9.7	22.1	33.4	42.9	49.1	50.6	46.9	39.0	28.6	16.8	4.1	****
	AZ.	****	117.7	124.0	132.9	145.7	163.4	184.8	204.9	220.5	231.4	239.0	244.4	****

**** INDICATES THAT THE SUN IS BELOW THE HORIZON, ANGLES ARE IN DEGREES & DECIMALS
 AZIMUTH MEASURED FROM NORTH POINT CLOCKWISE, LAT. & DEC. ARE +VE NORTH, -VE SOUTH
 LONG. & TIME LONG. ARE +VE WHEN EAST, -VE WEST.

Table A1.2 Altitude and Azimuth Angles of the Sun for Khartoum

γ_0 Solar Alt.	Irradiance in W/m^2				Illuminance in KLx				Kcd/m ² LZ Zenith Luminance
	I_{Dn} Direct Solar Normal	I_{Dh} Direct Solar Horizontal	I_{dh} Diffuse Sky Horizontal	I_{Gh} Global Horizontal	E_{Dn} Direct Solar Normal	E_{Dh} Direct Solar Horizontal	E_{dh} Diffuse Sky Horizontal	E_{Gh} Global Horizontal	
10°	444.5	77.2	56.4	132.7	35.9	6.2	7.1	13.4	1.06
20°	650.5	222.5	84.1	304.0	58.0	19.8	11.0	30.8	1.29
30°	767.3	383.7	100.7	480.5	72.5	36.2	13.2	49.4	1.65
40°	839.1	539.4	111.9	645.5	82.4	52.9	14.35	67.3	2.25
50°	885.6	678.4	119.8	789.7	89.2	68.4	14.96	83.3	3.14
60°	915.5	792.9	125.5	909.0	93.9	81.4	15.26	96.6	4.57
70°	935.0	878.6	129.2	995.4	97.0	91.2	15.39	106.6	6.84
80°	946.8	932.4	131.0	1061.8	98.8	92.3	15.43	112.7	10.63
90°	949.2	949.2	134.8	1070.1	99.3	99.3	15.44	114.8	16.64

Appendix A.2 Irradiance and Illuminance Data for the Standard Tropical Sky at Different Solar Altitudes

APPENDIX A.3 TABLES FOR THE SKY COMPONENT FOR SURFACES OF DIFFERENT ORIENTATIONS, INCLINATIONS AND OBSTRUCTIONS, AT DIFFERENT POSITIONS OF THE SUN AND CLEAR TROPICAL SKIES

The sky component concept was discussed earlier in parts 6.2 and 4.5 of Chapter II and III respectively. The sky component is defined here as the ratio of the diffuse radiant energy which is received at a point of a given surface from a clear sky to the diffuse radiant energy received on a horizontal surface from the whole unobstructed sky. The luminance and radiant intensity distribution of the clear sky was represented by the functional relationships of the C.I.E. (1973) standard clear sky. These functions, given by Kittler (1969), were shown earlier in Chapter II and III by equations 2.10, 3.24, (a), (b), (c) and (d). These functions were also assumed to represent the relative luminance distribution of the standard tropical sky.

Tables for the sky components of fully and partially exposed surfaces were produced using the subroutine SKYCOM, which basically carries out double integration for Kittler's relative luminance distribution functions over the sky area viewed from a reference point on a surface as explained in parts 6.2 and 4.5 of Chapters II and III. These tables enable a quick evaluation of the sky component of surfaces of different orientations, inclinations and obstructions and for different solar positions. They can be advantageously used in evaluating the diffuse sky irradiance and illuminance on any surface.

The sky components for fully exposed surfaces were prepared with regard to the whole sky areas viewed from the reference points on the surfaces as illustrated in Figures 2.13 (b) and (c) shown earlier in Chapter II. These are presented in Tables A3.1 to A3.6 for the following ranges of angular parameters and at 15° intervals :

- (i) solar altitude γ_0 from 5° to 90° ;
- (ii) surface-solar azimuth ($\alpha_s - \alpha_0$) from 0° to 180° ; and
- (iii) surface inclination γ_s , from 0° (horizontal) to 90° (vertical).

The sky component is directly read from the tables for any given combination of angular parameters for the surface and the sun. Interpolation can be used to define the sky component for any angular parameters not tabulated.

Partial sky components for partially exposed sky areas were produced for vertical and horizontal surfaces. This was achieved by dividing half the sky dome facing the surfaces into units of modular grid along the latitude and meridian circles. Wide ranges of sky patches were then orderly generated as multiples of grid units as illustrated by Figure A3.3. The partial sky components for the vertical and horizontal surfaces were then evaluated for the different sky patches generated. For a vertical surface, the meridians for the sky patches were defined with reference to the meridian at the intersection of the plane of the vertical surface and the sky dome as illustrated by Figure A3.1. Thus the azimuth

angle of the sky patch is measured with reference to the plane of the vertical surface. For a horizontal surface, the azimuth angle of the sky patch was defined with reference to the sun's meridian as illustrated in Figure A3.2. The altitude angles of the sky patches were similarly defined by the angles of the latitude circles above the horizon.

Partial sky components for a vertical surface are presented in Tables A3.7 to A3.12. These were prepared for the following ranges of angular parameters :

- (i) solar altitude from 15° to 90° , at 15° intervals;
- (ii) surface-solar azimuth from 0° to 180° , at 20° intervals;
- (iii) altitude of sky patch from 15° to 75° , at 15° intervals; and
- (iv) azimuth of sky patch from 20° to 180° , at 20° intervals.

The tables can be used to determine the obstructed or exposed sky component for any sky patch facing the vertical surface. As interpolation may be cumbersome, it is suggested that the angular parameters are rounded to the nearest corresponding values shown in the tables. The following procedure is also suggested for using the tables :

- (i) Select the table with the nearest value to the solar altitude given. Table A3.7 is to be used for solar altitude angles $\gamma_0 \leq 15^{\circ}$.
- (ii) Evaluate the surface-solar azimuth $(\alpha_s - \alpha_0)$ and select the corresponding section of the table.

- (iii) Evaluate the altitude angle of the sky patch or the altitude angle of obstruction as given by equation 3.31(a) and select the corresponding row for the table's section.
- (iv) Evaluate the azimuthal limits of the sky patch or the obstruction as given by equations 3.35(a) and (b). Define the partial sky components for the two azimuthal angles as R_{ob1} and R_{ob2} respectively. The partial sky component of the sky patch R_{ob} is taken as the difference between the two values

$$R_{ob} = R_{ob2} - R_{ob1}$$

This procedure is illustrated by the following example.

Example :

Let a vertical facade oriented at 40° from N is obstructed by an adjacent building. The altitude angle of obstruction with reference to a point on the surface is taken as $\gamma_{ob} = 45^{\circ}$ and the azimuth angles of obstruction are taken as 60° and 120° respectively. The solar altitude and azimuth are taken 60° and 120° respectively.

Solution :

- (i) For $\gamma_0 = 60^{\circ}$, use table A3.10.
- (ii) Surface-solar azimuth $\alpha_s - \alpha_0 : 40 - 120 = -80^{\circ}$.
- (iii) The sky component for $\gamma_{ob} = 45^{\circ}$ and $\alpha_{ob1} = 60^{\circ}$:
 $R_{ob1} = 0.15$.

(iv) The sky component for $\gamma_{ob} = 45^{\circ}$ and $\alpha_{ob2} = 120^{\circ}$:

$$R_{ob2} = 0.34.$$

(v) The obstructed sky component : $R_{ob} = R_{ob2} - R_{ob1} = 0.19.$

Partial sky components for the horizontal surface are given in Table A3.13. These were also prepared for the following ranges of angular parameters :

- (i) solar altitude from 15° to 90° , at 15° intervals;
- (ii) altitude of obstruction from 15° to 75° , at 15° intervals; and
- (iii) azimuth of obstruction from 20° to 180° , at 20° intervals.

The tables can be used to the partial sky component for any given sky patch following the procedure described above for the vertical surface. In addition the following considerations account for the angular spread of the sky patch relative to the position of the sun.

(i) When the sky patch lies solely within the quadrants to one side of the sun's meridian, as shown by Figure A3.4(a), the partial sky component of the sky patch is the difference between the sky components obtained for the two azimuthal angles defining the sky patch R_{ob1} , R_{ob2}

$$R_{ob} = R_{ob2} - R_{ob1}$$

(ii) When the sky patch includes the quadrant containing the sun as illustrated by Figure A3.4(b), its sky component is taken as the sum for the partial sky components obtained for the two

azimuthal angles defining it.

$$R_{ob} = R_{ob2} + R_{ob1}$$

(iii) When the sky patch includes the quadrant opposite the sun as illustrated by Figure A3.4(c), the sky components are obtained for the two azimuthal angles defining the sky patch R_{ob1} and R_{ob2} as well as for an azimuth angle of 180° and an equivalent altitude of obstruction R_{obF} . The partial sky component of the sky patch is then determined by the function

$$R_{ob} = 2 \cdot R_{obF} - R_{ob1} - R_{ob2}$$

The following example illustrates the procedure for use with the partial sky component table for a horizontal surface.

Let the sun altitude and azimuth angles correspond to 30° and 90° respectively. Take an obstructing surface with an altitude angle $\gamma_{ob} = 45^{\circ}$ and azimuth angles as 70° and 130° respectively.

Solution :

- (i) The two azimuth angles of the obstruction with reference to the sun's meridian are :

$$\alpha_{ob1} = -20^{\circ}, \quad \alpha_{ob2} = 40^{\circ}.$$

- (ii) The partial sky components for the two azimuthal angles of the obstruction are :

$$R_{ob1} = 0.11, \quad R_{ob2} = 0.18.$$

- (iii) The sky patch includes the quadrant containing the sun, the partial sky component : $R_{ob} = R_{ob1} + R_{ob2} = 0.39$.

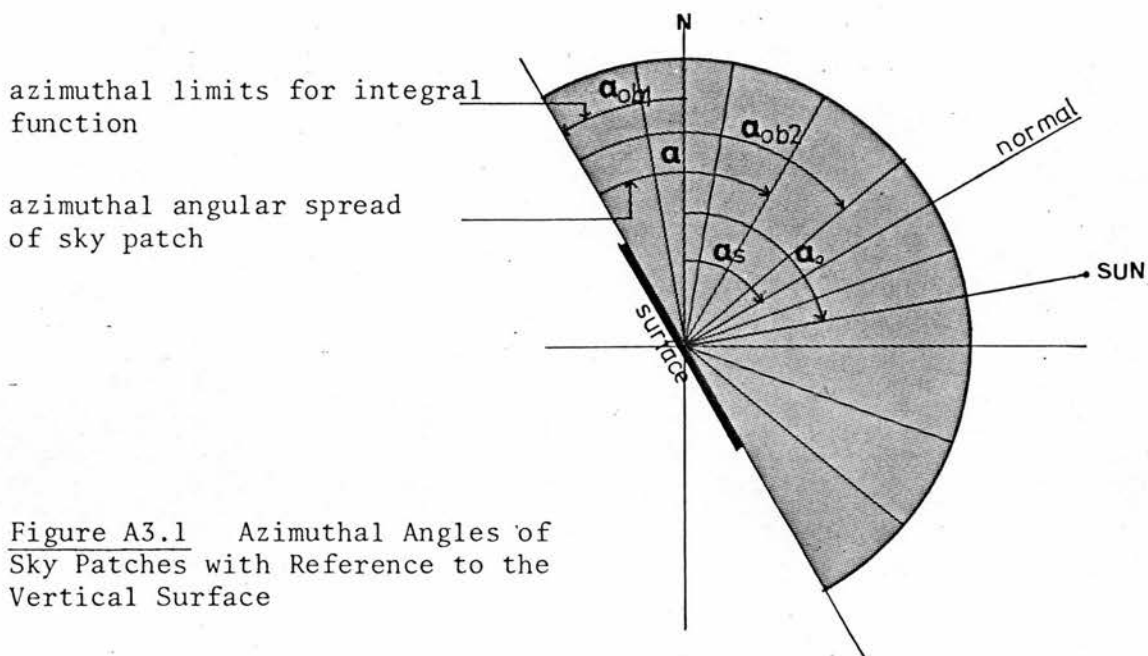


Figure A3.1 Azimuthal Angles of Sky Patches with Reference to the Vertical Surface

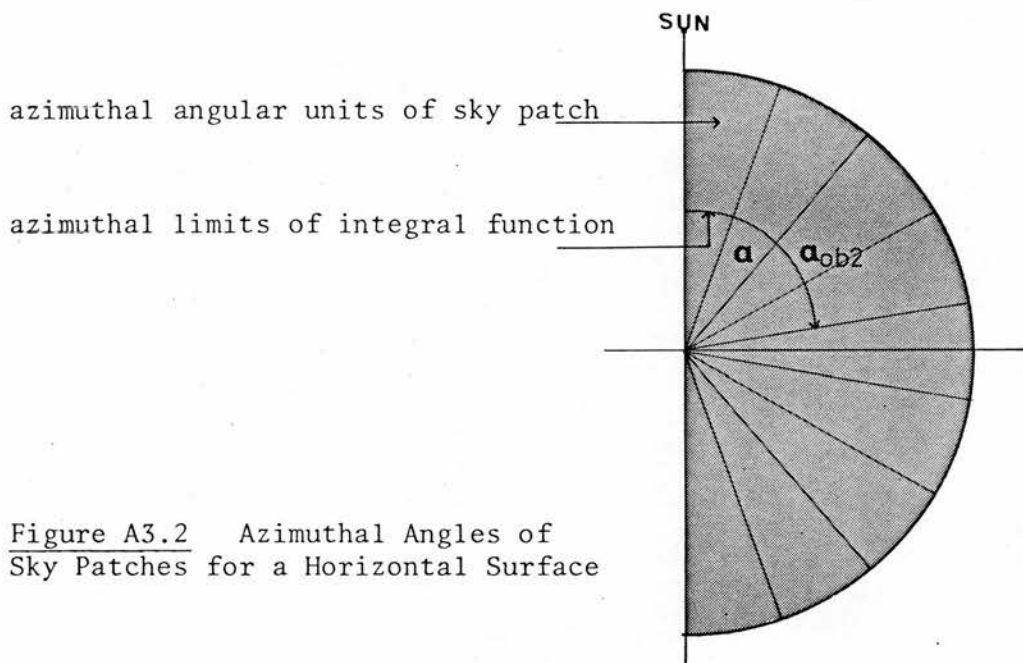


Figure A3.2 Azimuthal Angles of Sky Patches for a Horizontal Surface

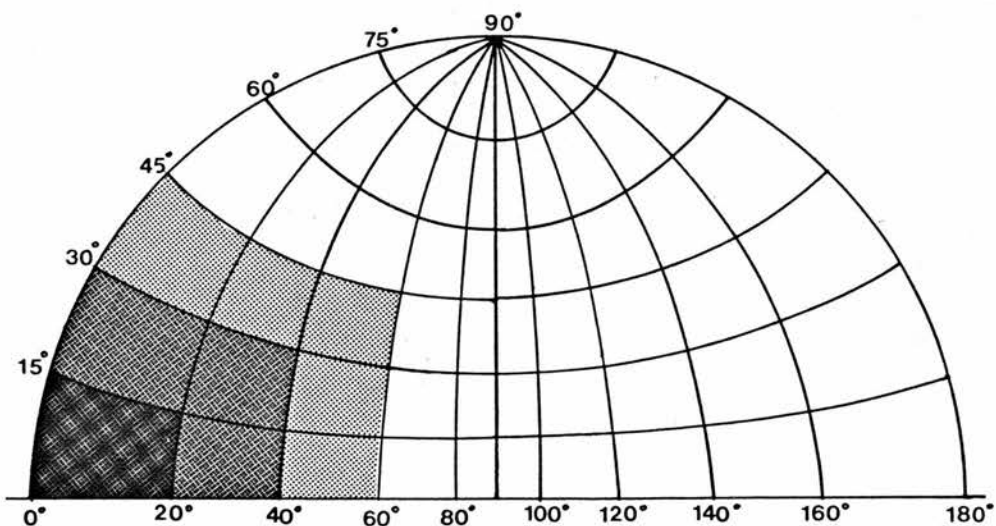


Figure A3.3 Modular Grid of the Sky Dome

Figure A3.4(a)

The Sky Patch within the Quadrants to One Side of the Sun's Meridian

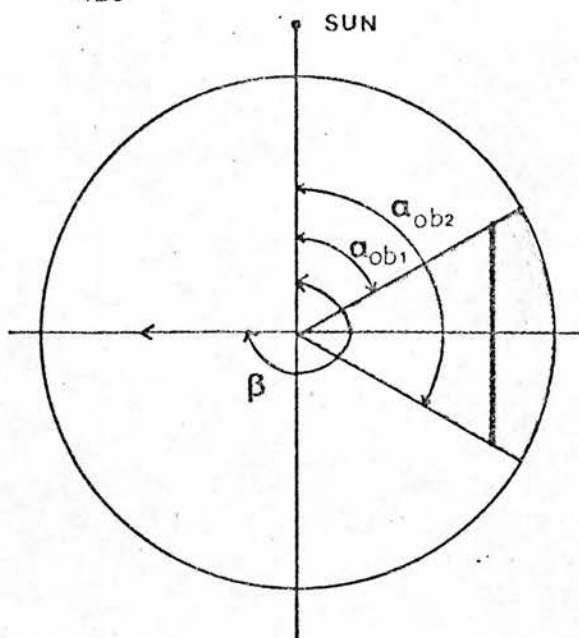


Figure A3.4(b)

The Sky Patch includes the Quadrant Containing the Sun

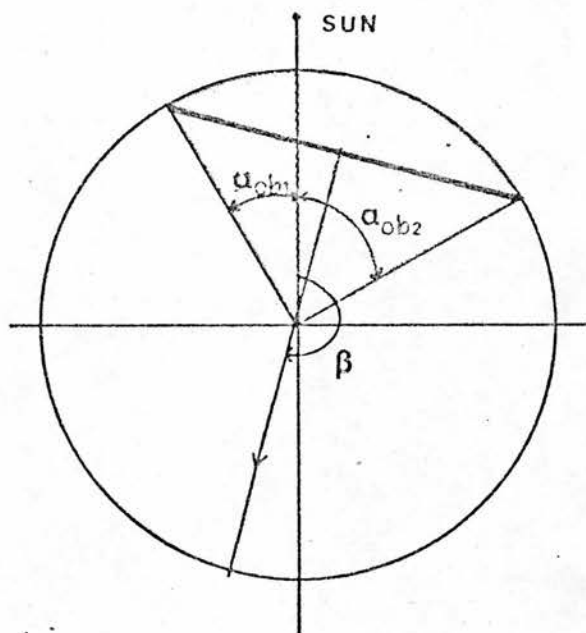


Figure A3.4(c)

The Sky Patch Includes the Quadrant Opposite to the Sun

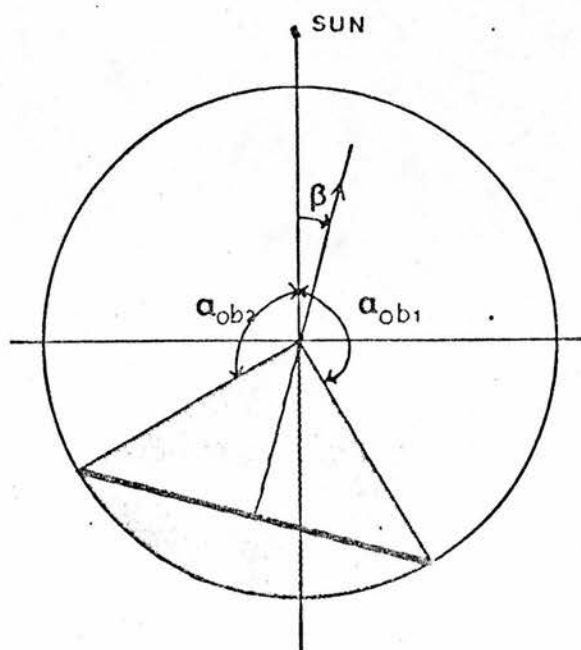


Table A3.5 Sky Component of an Inclined Surface $\gamma_s = 30^\circ$

Solar Altitude γ_0	surface - solar azimuth ($\alpha_s - \alpha_0$)												
	0°	15°	30°	45°	60°	75°	90°	105°	120°	135°	150°	165°	180°
5°	1.47	1.45	1.40	1.31	1.20	1.07	0.94	0.84	0.79	0.76	0.75	0.74	0.74
15°	1.45	1.44	1.38	1.30	1.18	1.05	0.91	0.81	0.75	0.71	0.69	0.68	0.68
30°	1.36	1.34	1.30	1.23	1.13	1.02	0.91	0.81	0.74	0.70	0.67	0.66	0.65
45°	1.23	1.21	1.18	1.13	1.07	0.99	0.91	0.84	0.78	0.74	0.71	0.69	0.69
60°	1.11	1.10	1.08	1.05	1.01	0.96	0.91	0.86	0.82	0.79	0.77	0.76	0.75
75°	1.01	1.00	0.99	0.98	0.96	0.94	0.91	0.89	0.87	0.85	0.84	0.83	0.83
90°	0.91	0.91	0.91	0.91	0.91	0.91	0.91	0.91	0.91	0.91	0.91	0.91	0.91

Table A3.6 Sky Component of an Inclined Surface $\gamma_s = 15^\circ$

Solar Altitude γ_0	surface - solar azimuth ($\alpha_s - \alpha_0$)												
	0°	15°	30°	45°	60°	75°	90°	105°	120°	135°	150°	165°	180°
5°	1.25	1.24	1.21	1.17	1.11	1.04	0.97	0.91	0.87	0.85	0.83	0.82	0.82
15°	1.25	1.24	1.21	1.17	1.11	1.04	0.97	0.90	0.86	0.83	0.81	0.80	0.79
30°	1.20	1.20	1.17	1.14	1.09	1.03	0.97	0.92	0.88	0.85	0.82	0.81	0.80
45°	1.13	1.13	1.11	1.08	1.05	1.02	0.98	0.94	0.90	0.86	0.85	0.84	0.84
60°	1.08	1.07	1.06	1.05	1.03	1.00	0.98	0.95	0.93	0.91	0.89	0.89	0.88
75°	1.03	1.03	1.02	1.01	1.00	0.99	0.98	0.96	0.95	0.94	0.94	0.93	0.93
90°	0.98	0.98	0.98	0.98	0.98	0.98	0.98	0.98	0.98	0.98	0.98	0.98	0.98

Sky Component of a Horizontal Surface ($\gamma_s = 0^\circ$) $R = 1$ for all Solar Altitudes and Azimuths

Table A3.7 Partial Sky Component for a Vertical Surface
Solar Altitude $\gamma_0 = 15^\circ$

SURF.-SOLAR AZ.	ALT. OBST.	AZ. of Sky Patch from Surface Plane α_{ob}								
		20.0	40.0	60.0	80.0	100.0	120.0	140.0	160.0	180.0
+ - 0.0	15.0	0.01	0.03	0.10	0.26	0.52	0.68	0.75	0.77	0.78
	30.0	0.01	0.05	0.16	0.41	0.83	1.08	1.19	1.23	1.24
	45.0	0.01	0.06	0.19	0.48	0.94	1.23	1.36	1.41	1.42
	60.0	0.01	0.07	0.20	0.50	0.98	1.28	1.41	1.47	1.48
	75.0	0.01	0.07	0.21	0.51	0.99	1.29	1.43	1.48	1.50
+ - 20.0	15.0	0.01	0.05	0.18	0.43	0.60	0.68	0.72	0.74	0.75
	30.0	0.02	0.09	0.29	0.69	0.95	1.08	1.14	1.18	1.19
	45.0	0.02	0.10	0.34	0.78	1.08	1.23	1.31	1.35	1.36
	60.0	0.02	0.11	0.35	0.80	1.12	1.28	1.37	1.41	1.42
	75.0	0.02	0.11	0.36	0.81	1.13	1.29	1.38	1.42	1.43
+ - 40.0	15.0	0.02	0.10	0.30	0.46	0.55	0.60	0.63	0.64	0.65
	30.0	0.03	0.16	0.48	0.73	0.87	0.95	0.99	1.02	1.03
	45.0	0.03	0.19	0.54	0.83	0.99	1.08	1.14	1.17	1.19
	60.0	0.03	0.19	0.56	0.86	1.03	1.13	1.19	1.23	1.24
	75.0	0.03	0.20	0.57	0.86	1.04	1.14	1.21	1.24	1.26
+ - 60.0	15.0	0.03	0.16	0.29	0.37	0.42	0.46	0.49	0.51	0.51
	30.0	0.03	0.26	0.46	0.59	0.67	0.73	0.77	0.80	0.81
	45.0	0.06	0.29	0.52	0.67	0.77	0.84	0.89	0.93	0.94
	60.0	0.06	0.30	0.54	0.70	0.81	0.88	0.94	0.97	0.99
	75.0	0.06	0.30	0.54	0.70	0.82	0.89	0.95	0.99	1.00
+ - 80.0	15.0	0.05	0.13	0.19	0.24	0.28	0.32	0.34	0.36	0.37
	30.0	0.07	0.20	0.30	0.38	0.45	0.50	0.54	0.57	0.59
	45.0	0.08	0.23	0.35	0.45	0.52	0.58	0.64	0.67	0.69
	60.0	0.08	0.23	0.37	0.47	0.55	0.62	0.67	0.71	0.73
	75.0	0.08	0.24	0.37	0.48	0.56	0.63	0.68	0.72	0.74
+ - 100.0	15.0	0.05	0.07	0.11	0.14	0.18	0.21	0.25	0.27	0.28
	30.0	0.04	0.11	0.17	0.23	0.29	0.34	0.39	0.42	0.43
	45.0	0.05	0.13	0.20	0.27	0.34	0.40	0.46	0.50	0.51
	60.0	0.05	0.13	0.22	0.29	0.36	0.43	0.49	0.53	0.55
	75.0	0.05	0.13	0.22	0.30	0.37	0.44	0.50	0.54	0.56
+ - 120.0	15.0	0.01	0.04	0.07	0.10	0.14	0.18	0.21	0.23	0.24
	30.0	0.02	0.06	0.11	0.16	0.22	0.28	0.33	0.36	0.38
	45.0	0.03	0.08	0.13	0.19	0.26	0.33	0.39	0.43	0.45
	60.0	0.03	0.08	0.14	0.21	0.28	0.35	0.42	0.46	0.48
	75.0	0.03	0.08	0.15	0.21	0.29	0.36	0.43	0.47	0.49
+ - 140.0	15.0	0.01	0.03	0.05	0.09	0.13	0.17	0.21	0.23	0.24
	30.0	0.01	0.04	0.09	0.14	0.20	0.27	0.32	0.35	0.36
	45.0	0.02	0.05	0.10	0.17	0.24	0.31	0.38	0.42	0.43
	60.0	0.02	0.06	0.11	0.18	0.26	0.34	0.40	0.45	0.46
	75.0	0.02	0.06	0.11	0.18	0.26	0.35	0.41	0.46	0.47
+ - 160.0	15.0	0.01	0.02	0.05	0.09	0.13	0.18	0.21	0.23	0.24
	30.0	0.01	0.04	0.08	0.14	0.21	0.27	0.33	0.36	0.37
	45.0	0.01	0.04	0.10	0.17	0.25	0.32	0.38	0.42	0.43
	60.0	0.01	0.05	0.10	0.18	0.26	0.34	0.41	0.45	0.46
	75.0	0.01	0.05	0.11	0.18	0.27	0.35	0.42	0.46	0.47
+ - 180.0	15.0	0.01	0.02	0.06	0.10	0.14	0.19	0.22	0.24	0.24
	30.0	0.01	0.04	0.09	0.15	0.22	0.28	0.33	0.36	0.37
	45.0	0.01	0.04	0.10	0.18	0.26	0.33	0.39	0.42	0.43
	60.0	0.01	0.05	0.11	0.19	0.28	0.35	0.41	0.45	0.46
	75.0	0.01	0.05	0.11	0.19	0.28	0.36	0.42	0.46	0.47

Table A3.8 Partial Sky Component for a Vertical Surface
Solar Altitude $\gamma_0 = 30^\circ$

SURF. - SOLAR AZ.	ALT. OBST.	AZ. of Sky Patch from Surface Plane α_{ob}								
		20.0	40.0	60.0	80.0	100.0	120.0	140.0	160.0	180.0
+ - 0.0	15.0	0.01	0.03	0.08	0.18	0.32	0.42	0.47	0.49	0.50
	30.0	0.01	0.05	0.14	0.32	0.58	0.77	0.86	0.90	0.91
	45.0	0.01	0.06	0.17	0.40	0.74	0.97	1.08	1.13	1.14
	60.0	0.01	0.07	0.19	0.43	0.79	1.04	1.16	1.21	1.23
	75.0	0.01	0.07	0.19	0.44	0.81	1.05	1.18	1.23	1.25
+ - 20.0	15.0	0.01	0.04	0.13	0.25	0.36	0.42	0.46	0.48	0.48
	30.0	0.01	0.07	0.22	0.47	0.67	0.78	0.83	0.86	0.87
	45.0	0.02	0.09	0.28	0.60	0.84	0.98	1.05	1.08	1.10
	60.0	0.02	0.10	0.30	0.64	0.90	1.05	1.13	1.17	1.18
	75.0	0.02	0.10	0.31	0.65	0.91	1.06	1.14	1.18	1.20
+ - 40.0	15.0	0.01	0.07	0.17	0.27	0.34	0.38	0.41	0.42	0.43
	30.0	0.02	0.12	0.32	0.51	0.62	0.69	0.74	0.76	0.77
	45.0	0.03	0.15	0.41	0.64	0.78	0.87	0.92	0.95	0.96
	60.0	0.03	0.16	0.44	0.68	0.84	0.94	0.99	1.02	1.04
	75.0	0.03	0.17	0.44	0.69	0.85	0.95	1.01	1.04	1.05
+ - 60.0	15.0	0.02	0.09	0.17	0.23	0.28	0.31	0.33	0.35	0.36
	30.0	0.04	0.17	0.32	0.42	0.50	0.55	0.59	0.62	0.62
	45.0	0.05	0.22	0.40	0.53	0.63	0.69	0.74	0.77	0.78
	60.0	0.05	0.23	0.43	0.57	0.67	0.75	0.80	0.83	0.84
	75.0	0.05	0.23	0.43	0.58	0.69	0.76	0.81	0.84	0.85
+ - 80.0	15.0	0.02	0.08	0.13	0.17	0.21	0.24	0.26	0.28	0.28
	30.0	0.03	0.14	0.23	0.30	0.36	0.40	0.44	0.47	0.48
	45.0	0.06	0.18	0.29	0.37	0.44	0.50	0.54	0.58	0.59
	60.0	0.06	0.19	0.31	0.40	0.48	0.54	0.59	0.62	0.64
	75.0	0.06	0.19	0.31	0.41	0.49	0.55	0.60	0.64	0.65
+ -100.0	15.0	0.02	0.05	0.09	0.12	0.15	0.18	0.21	0.22	0.23
	30.0	0.03	0.09	0.15	0.20	0.25	0.29	0.33	0.36	0.37
	45.0	0.04	0.11	0.18	0.24	0.30	0.36	0.41	0.44	0.45
	60.0	0.04	0.12	0.20	0.27	0.33	0.39	0.44	0.48	0.49
	75.0	0.04	0.12	0.20	0.27	0.34	0.40	0.45	0.49	0.50
+ -120.0	15.0	0.01	0.03	0.06	0.09	0.12	0.15	0.18	0.20	0.21
	30.0	0.02	0.06	0.10	0.15	0.19	0.24	0.29	0.32	0.32
	45.0	0.02	0.07	0.12	0.18	0.24	0.29	0.34	0.38	0.39
	60.0	0.03	0.08	0.13	0.19	0.26	0.32	0.37	0.41	0.42
	75.0	0.03	0.08	0.14	0.20	0.26	0.33	0.38	0.42	0.43
+ -140.0	15.0	0.01	0.03	0.05	0.08	0.11	0.15	0.18	0.20	0.20
	30.0	0.01	0.04	0.08	0.12	0.18	0.23	0.27	0.30	0.31
	45.0	0.02	0.05	0.10	0.15	0.21	0.27	0.32	0.36	0.37
	60.0	0.02	0.05	0.10	0.16	0.23	0.30	0.35	0.38	0.40
	75.0	0.02	0.06	0.11	0.17	0.24	0.30	0.36	0.39	0.41
+ -160.0	15.0	0.01	0.02	0.05	0.08	0.12	0.15	0.18	0.20	0.20
	30.0	0.01	0.03	0.07	0.12	0.18	0.23	0.27	0.30	0.31
	45.0	0.01	0.04	0.09	0.14	0.21	0.27	0.32	0.35	0.36
	60.0	0.01	0.05	0.09	0.16	0.23	0.29	0.35	0.38	0.39
	75.0	0.01	0.05	0.10	0.16	0.23	0.30	0.35	0.39	0.40
+ -180.0	15.0	0.01	0.02	0.05	0.08	0.12	0.16	0.18	0.20	0.20
	30.0	0.01	0.03	0.07	0.13	0.18	0.24	0.28	0.30	0.31
	45.0	0.01	0.04	0.09	0.15	0.22	0.28	0.32	0.35	0.36
	60.0	0.01	0.04	0.09	0.16	0.23	0.30	0.35	0.38	0.39
	75.0	0.01	0.04	0.10	0.16	0.24	0.30	0.36	0.39	0.40

Table A3.9 Partial Sky Component for a Vertical Surface
Solar Altitude $\gamma_0 = 45^\circ$

SURF. SOLAR AZ.	ALT. OBST.	AZ. of Sky Patch from Surface Plane α_{ob}								
		20.0	40.0	60.0	80.0	100.0	120.0	140.0	160.0	180.0
+ - 0.0	15.0	0.01	0.03	0.07	0.13	0.20	0.26	0.30	0.32	0.33
	30.0	0.01	0.04	0.11	0.23	0.37	0.49	0.56	0.59	0.60
	45.0	0.01	0.06	0.15	0.31	0.52	0.68	0.77	0.81	0.82
	60.0	0.01	0.06	0.17	0.35	0.59	0.78	0.88	0.93	0.94
	75.0	0.01	0.06	0.17	0.36	0.61	0.80	0.91	0.96	0.97
+ - 20.0	15.0	0.01	0.03	0.08	0.15	0.22	0.27	0.30	0.32	0.32
	30.0	0.01	0.06	0.15	0.29	0.41	0.50	0.55	0.58	0.58
	45.0	0.02	0.08	0.21	0.40	0.57	0.69	0.75	0.78	0.79
	60.0	0.02	0.09	0.24	0.46	0.66	0.79	0.86	0.90	0.91
	75.0	0.02	0.09	0.24	0.48	0.68	0.81	0.89	0.92	0.94
+ - 40.0	15.0	0.01	0.04	0.10	0.16	0.21	0.25	0.27	0.29	0.29
	30.0	0.02	0.08	0.19	0.31	0.40	0.46	0.50	0.52	0.53
	45.0	0.02	0.11	0.27	0.43	0.55	0.63	0.68	0.71	0.72
	60.0	0.03	0.12	0.31	0.49	0.63	0.72	0.77	0.80	0.81
	75.0	0.03	0.13	0.32	0.51	0.65	0.74	0.80	0.83	0.84
+ - 60.0	15.0	0.01	0.05	0.10	0.15	0.19	0.22	0.24	0.25	0.26
	30.0	0.02	0.09	0.19	0.27	0.34	0.39	0.43	0.45	0.46
	45.0	0.03	0.14	0.27	0.38	0.46	0.52	0.57	0.59	0.60
	60.0	0.04	0.16	0.31	0.43	0.53	0.60	0.64	0.67	0.68
	75.0	0.04	0.16	0.31	0.44	0.54	0.62	0.66	0.70	0.71
+ - 80.0	15.0	0.01	0.05	0.08	0.12	0.15	0.18	0.20	0.22	0.22
	30.0	0.03	0.09	0.16	0.22	0.27	0.31	0.35	0.37	0.38
	45.0	0.04	0.12	0.21	0.29	0.36	0.41	0.45	0.48	0.49
	60.0	0.04	0.14	0.24	0.33	0.40	0.46	0.51	0.54	0.55
	75.0	0.04	0.14	0.25	0.34	0.42	0.48	0.52	0.56	0.57
+ - 100.0	15.0	0.01	0.04	0.07	0.10	0.13	0.15	0.17	0.19	0.20
	30.0	0.02	0.07	0.12	0.16	0.21	0.25	0.29	0.31	0.32
	45.0	0.03	0.09	0.15	0.21	0.27	0.32	0.36	0.39	0.40
	60.0	0.03	0.10	0.17	0.24	0.30	0.36	0.40	0.43	0.44
	75.0	0.03	0.10	0.18	0.25	0.31	0.37	0.42	0.45	0.46
+ - 120.0	15.0	0.01	0.03	0.05	0.08	0.11	0.14	0.16	0.18	0.18
	30.0	0.02	0.05	0.09	0.13	0.18	0.22	0.26	0.28	0.29
	45.0	0.02	0.06	0.11	0.17	0.22	0.27	0.31	0.34	0.35
	60.0	0.02	0.07	0.13	0.18	0.24	0.30	0.34	0.37	0.38
	75.0	0.02	0.07	0.13	0.19	0.25	0.31	0.36	0.39	0.40
+ - 140.0	15.0	0.01	0.02	0.05	0.07	0.10	0.13	0.15	0.17	0.18
	30.0	0.01	0.04	0.07	0.12	0.16	0.21	0.24	0.27	0.27
	45.0	0.01	0.05	0.09	0.14	0.20	0.25	0.29	0.32	0.33
	60.0	0.02	0.05	0.10	0.16	0.21	0.27	0.32	0.35	0.36
	75.0	0.02	0.05	0.10	0.16	0.22	0.28	0.33	0.36	0.37
+ - 160.0	15.0	0.01	0.02	0.04	0.07	0.10	0.13	0.15	0.17	0.17
	30.0	0.01	0.03	0.07	0.11	0.16	0.20	0.24	0.26	0.27
	45.0	0.01	0.04	0.08	0.13	0.19	0.24	0.28	0.31	0.32
	60.0	0.01	0.04	0.09	0.14	0.20	0.26	0.31	0.34	0.35
	75.0	0.01	0.05	0.09	0.15	0.21	0.27	0.32	0.35	0.36
+ - 180.0	15.0	0.01	0.02	0.04	0.07	0.10	0.13	0.15	0.17	0.17
	30.0	0.01	0.03	0.07	0.11	0.16	0.20	0.24	0.26	0.27
	45.0	0.01	0.04	0.09	0.13	0.19	0.24	0.28	0.31	0.32
	60.0	0.01	0.04	0.09	0.14	0.20	0.26	0.30	0.33	0.34
	75.0	0.01	0.04	0.09	0.15	0.21	0.27	0.31	0.34	0.36

Table A3.10 Partial Sky Component for a Vertical Surface
Solar Altitude $\gamma_0 = 60^\circ$

SURF.-SOLAR AZ.	ALT.OBST.	AZ. of Sky Patch from Surface Plane α_{ob}								
		20.0	40.0	60.0	80.0	100.0	120.0	140.0	160.0	180.0
+ - 0.0	15.0	0.01	0.02	0.05	0.09	0.14	0.18	0.21	0.23	0.24
	30.0	0.01	0.04	0.09	0.17	0.25	0.33	0.38	0.41	0.42
	45.0	0.01	0.05	0.12	0.23	0.35	0.45	0.53	0.56	0.58
	60.0	0.01	0.06	0.14	0.27	0.42	0.55	0.63	0.68	0.69
	75.0	0.01	0.06	0.15	0.29	0.45	0.59	0.68	0.73	0.74
+ - 20.0	15.0	0.01	0.03	0.06	0.10	0.15	0.19	0.21	0.23	0.23
	30.0	0.01	0.05	0.11	0.19	0.27	0.34	0.38	0.41	0.41
	45.0	0.01	0.06	0.15	0.26	0.37	0.46	0.52	0.55	0.56
	60.0	0.02	0.07	0.18	0.32	0.45	0.56	0.63	0.66	0.67
	75.0	0.02	0.08	0.18	0.34	0.49	0.60	0.67	0.71	0.72
+ - 40.0	15.0	0.01	0.03	0.07	0.11	0.15	0.18	0.20	0.22	0.22
	30.0	0.01	0.05	0.12	0.20	0.26	0.32	0.36	0.38	0.39
	45.0	0.02	0.07	0.17	0.27	0.36	0.44	0.49	0.51	0.52
	60.0	0.02	0.09	0.20	0.33	0.44	0.52	0.58	0.61	0.62
	75.0	0.02	0.09	0.22	0.36	0.47	0.56	0.62	0.65	0.66
+ - 60.0	15.0	0.01	0.03	0.07	0.10	0.14	0.16	0.19	0.20	0.20
	30.0	0.01	0.06	0.12	0.18	0.24	0.29	0.33	0.35	0.35
	45.0	0.02	0.08	0.17	0.25	0.33	0.39	0.43	0.46	0.47
	60.0	0.02	0.10	0.20	0.31	0.39	0.46	0.51	0.54	0.55
	75.0	0.03	0.11	0.22	0.33	0.42	0.49	0.54	0.58	0.59
+ - 80.0	15.0	0.01	0.03	0.06	0.09	0.12	0.15	0.17	0.18	0.19
	30.0	0.01	0.06	0.11	0.16	0.21	0.26	0.29	0.31	0.32
	45.0	0.02	0.08	0.15	0.22	0.28	0.34	0.38	0.40	0.41
	60.0	0.03	0.09	0.18	0.26	0.33	0.39	0.44	0.47	0.48
	75.0	0.03	0.10	0.19	0.28	0.35	0.42	0.46	0.49	0.50
+ -100.0	15.0	0.01	0.03	0.05	0.08	0.11	0.13	0.16	0.17	0.17
	30.0	0.01	0.05	0.09	0.14	0.19	0.23	0.26	0.28	0.29
	45.0	0.02	0.07	0.12	0.18	0.24	0.29	0.33	0.35	0.36
	60.0	0.02	0.08	0.14	0.21	0.28	0.33	0.37	0.40	0.41
	75.0	0.02	0.08	0.15	0.22	0.29	0.35	0.40	0.42	0.43
+ -120.0	15.0	0.01	0.02	0.05	0.07	0.10	0.12	0.15	0.16	0.16
	30.0	0.01	0.04	0.08	0.12	0.16	0.20	0.24	0.26	0.27
	45.0	0.02	0.05	0.10	0.15	0.21	0.26	0.30	0.32	0.33
	60.0	0.02	0.06	0.12	0.18	0.24	0.29	0.33	0.36	0.37
	75.0	0.02	0.07	0.12	0.19	0.25	0.30	0.35	0.38	0.39
+ -140.0	15.0	0.01	0.02	0.04	0.07	0.09	0.12	0.14	0.16	0.16
	30.0	0.01	0.03	0.07	0.11	0.15	0.19	0.23	0.25	0.25
	45.0	0.01	0.04	0.09	0.14	0.19	0.24	0.28	0.30	0.31
	60.0	0.01	0.05	0.10	0.15	0.21	0.26	0.31	0.34	0.35
	75.0	0.02	0.05	0.10	0.16	0.22	0.28	0.32	0.35	0.36
+ -160.0	15.0	0.01	0.02	0.04	0.06	0.09	0.12	0.14	0.15	0.16
	30.0	0.01	0.03	0.06	0.10	0.15	0.19	0.22	0.24	0.25
	45.0	0.01	0.04	0.08	0.13	0.18	0.23	0.27	0.29	0.30
	60.0	0.01	0.04	0.09	0.14	0.20	0.25	0.30	0.32	0.33
	75.0	0.01	0.05	0.09	0.15	0.21	0.26	0.31	0.34	0.35
+ -180.0	15.0	0.00	0.02	0.04	0.06	0.09	0.12	0.14	0.15	0.16
	30.0	0.01	0.03	0.06	0.10	0.14	0.18	0.22	0.24	0.25
	45.0	0.01	0.04	0.08	0.12	0.18	0.22	0.26	0.29	0.30
	60.0	0.01	0.04	0.08	0.14	0.19	0.25	0.29	0.32	0.33
	75.0	0.01	0.04	0.09	0.14	0.20	0.26	0.30	0.33	0.34

Table A3.11 Partial Sky Component for a Vertical Surface
Solar Altitude $\gamma_0 = 75^\circ$

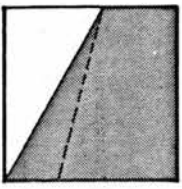
SURF. SOLAR AZ.	ALT. OBST.	AZ. of Sky Patch from Surface Plane α_{ob}								
		20.0	40.0	60.0	80.0	100.0	120.0	140.0	160.0	180.0
+ - 0.0	15.0	0.01	0.02	0.05	0.08	0.11	0.14	0.17	0.18	0.19
	30.0	0.01	0.03	0.08	0.13	0.19	0.25	0.29	0.31	0.32
	45.0	0.01	0.05	0.10	0.18	0.25	0.33	0.38	0.42	0.43
	60.0	0.01	0.05	0.12	0.21	0.30	0.39	0.46	0.50	0.51
	75.0	0.01	0.06	0.13	0.23	0.33	0.43	0.50	0.54	0.56
+ - 20.0	15.0	0.01	0.02	0.05	0.08	0.11	0.14	0.17	0.18	0.18
	30.0	0.01	0.04	0.08	0.14	0.20	0.25	0.29	0.31	0.32
	45.0	0.01	0.05	0.11	0.19	0.26	0.33	0.38	0.41	0.42
	60.0	0.01	0.06	0.13	0.22	0.31	0.39	0.45	0.49	0.50
	75.0	0.02	0.06	0.14	0.24	0.34	0.43	0.50	0.54	0.55
+ - 40.0	15.0	0.01	0.02	0.05	0.08	0.11	0.14	0.16	0.18	0.18
	30.0	0.01	0.04	0.08	0.14	0.19	0.24	0.28	0.30	0.31
	45.0	0.01	0.05	0.11	0.19	0.26	0.32	0.37	0.40	0.41
	60.0	0.02	0.06	0.14	0.22	0.31	0.38	0.44	0.47	0.48
	75.0	0.02	0.07	0.15	0.25	0.34	0.42	0.48	0.52	0.53
+ - 60.0	15.0	0.01	0.02	0.05	0.08	0.11	0.14	0.16	0.17	0.17
	30.0	0.01	0.04	0.08	0.14	0.19	0.23	0.27	0.29	0.30
	45.0	0.01	0.05	0.11	0.18	0.25	0.31	0.35	0.38	0.39
	60.0	0.02	0.06	0.14	0.22	0.30	0.36	0.41	0.45	0.46
	75.0	0.02	0.07	0.15	0.24	0.32	0.40	0.45	0.48	0.49
+ - 80.0	15.0	0.01	0.02	0.05	0.08	0.10	0.13	0.15	0.16	0.17
	30.0	0.01	0.04	0.08	0.13	0.18	0.22	0.25	0.28	0.28
	45.0	0.01	0.05	0.11	0.17	0.23	0.29	0.33	0.36	0.37
	60.0	0.02	0.06	0.13	0.20	0.28	0.34	0.39	0.42	0.43
	75.0	0.02	0.07	0.14	0.22	0.30	0.37	0.42	0.45	0.46
+ -100.0	15.0	0.01	0.02	0.05	0.07	0.10	0.12	0.14	0.16	0.16
	30.0	0.01	0.04	0.08	0.12	0.17	0.21	0.24	0.26	0.27
	45.0	0.01	0.05	0.10	0.16	0.22	0.27	0.31	0.34	0.35
	60.0	0.02	0.06	0.12	0.19	0.25	0.31	0.36	0.39	0.40
	75.0	0.02	0.07	0.13	0.20	0.27	0.34	0.38	0.42	0.43
+ -120.0	15.0	0.01	0.02	0.04	0.07	0.10	0.12	0.14	0.15	0.16
	30.0	0.01	0.04	0.07	0.12	0.16	0.20	0.23	0.25	0.26
	45.0	0.01	0.05	0.09	0.15	0.20	0.25	0.29	0.32	0.33
	60.0	0.02	0.05	0.11	0.17	0.23	0.29	0.34	0.36	0.38
	75.0	0.02	0.06	0.12	0.18	0.25	0.31	0.36	0.39	0.40
+ -140.0	15.0	0.01	0.02	0.04	0.07	0.09	0.12	0.14	0.15	0.16
	30.0	0.01	0.03	0.07	0.11	0.15	0.19	0.22	0.24	0.25
	45.0	0.01	0.04	0.09	0.14	0.19	0.24	0.28	0.31	0.32
	60.0	0.01	0.05	0.10	0.16	0.22	0.27	0.32	0.35	0.36
	75.0	0.02	0.05	0.11	0.17	0.23	0.29	0.34	0.37	0.38
+ -160.0	15.0	0.01	0.02	0.04	0.06	0.09	0.12	0.14	0.15	0.15
	30.0	0.01	0.03	0.06	0.10	0.15	0.19	0.22	0.24	0.25
	45.0	0.01	0.04	0.08	0.13	0.18	0.23	0.27	0.30	0.31
	60.0	0.01	0.05	0.09	0.15	0.21	0.26	0.31	0.34	0.35
	75.0	0.01	0.05	0.10	0.16	0.22	0.28	0.33	0.36	0.37
+ -180.0	15.0	0.01	0.02	0.04	0.06	0.09	0.11	0.13	0.15	0.15
	30.0	0.01	0.03	0.06	0.10	0.14	0.18	0.22	0.24	0.25
	45.0	0.01	0.04	0.08	0.13	0.18	0.23	0.27	0.30	0.31
	60.0	0.01	0.04	0.09	0.14	0.20	0.26	0.30	0.30	0.35
	75.0	0.01	0.05	0.09	0.15	0.21	0.27	0.32	0.36	0.37

Table A3.12 Partial Sky Component for a Vertical Surface
Solar Altitude $\gamma_0 = 90^\circ$

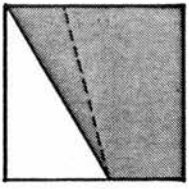
SURF.-SOLAR AZ.	ALT. ORST.	AZ. of Sky Patch from Surface Plane α_{ob}								
		20.0	40.0	60.0	80.0	100.0	120.0	140.0	160.0	180.0
+ - 0.0	15.0	0.01	0.02	0.04	0.07	0.09	0.12	0.14	0.16	0.16
	30.0	0.01	0.03	0.07	0.11	0.16	0.20	0.24	0.26	0.27
	45.0	0.01	0.04	0.09	0.15	0.20	0.26	0.31	0.34	0.35
	60.0	0.01	0.05	0.10	0.17	0.24	0.30	0.35	0.39	0.40
	75.0	0.01	0.05	0.11	0.18	0.25	0.33	0.38	0.42	0.43
+ - 20.0	15.0	0.01	0.02	0.04	0.07	0.09	0.12	0.14	0.16	0.16
	30.0	0.01	0.03	0.07	0.11	0.16	0.20	0.24	0.26	0.27
	45.0	0.01	0.04	0.09	0.15	0.20	0.26	0.31	0.34	0.35
	60.0	0.01	0.05	0.10	0.17	0.24	0.30	0.35	0.39	0.40
	75.0	0.01	0.05	0.11	0.18	0.25	0.33	0.38	0.42	0.43
+ - 40.0	15.0	0.01	0.02	0.04	0.07	0.09	0.12	0.14	0.16	0.16
	30.0	0.01	0.03	0.07	0.11	0.16	0.20	0.24	0.26	0.27
	45.0	0.01	0.04	0.09	0.15	0.20	0.26	0.31	0.34	0.35
	60.0	0.01	0.05	0.10	0.17	0.24	0.30	0.35	0.39	0.40
	75.0	0.01	0.05	0.11	0.18	0.25	0.33	0.38	0.42	0.43
+ - 60.0	15.0	0.01	0.02	0.04	0.07	0.09	0.12	0.14	0.16	0.16
	30.0	0.01	0.03	0.07	0.11	0.16	0.20	0.24	0.26	0.27
	45.0	0.01	0.04	0.09	0.15	0.20	0.26	0.31	0.34	0.35
	60.0	0.01	0.05	0.10	0.17	0.24	0.30	0.35	0.39	0.40
	75.0	0.01	0.05	0.11	0.18	0.25	0.33	0.38	0.42	0.43
+ - 80.0	15.0	0.01	0.02	0.04	0.07	0.09	0.12	0.14	0.16	0.16
	30.0	0.01	0.03	0.07	0.11	0.16	0.20	0.24	0.26	0.27
	45.0	0.01	0.04	0.09	0.15	0.20	0.26	0.31	0.34	0.35
	60.0	0.01	0.05	0.10	0.17	0.24	0.30	0.35	0.39	0.40
	75.0	0.01	0.05	0.11	0.18	0.25	0.33	0.38	0.42	0.43
+ -100.0	15.0	0.01	0.02	0.04	0.07	0.09	0.12	0.14	0.16	0.16
	30.0	0.01	0.03	0.07	0.11	0.16	0.20	0.24	0.26	0.27
	45.0	0.01	0.04	0.09	0.15	0.20	0.26	0.31	0.34	0.35
	60.0	0.01	0.05	0.10	0.17	0.24	0.30	0.35	0.39	0.40
	75.0	0.01	0.05	0.11	0.18	0.25	0.33	0.38	0.42	0.43
+ -120.0	15.0	0.01	0.02	0.04	0.07	0.09	0.12	0.14	0.16	0.16
	30.0	0.01	0.03	0.07	0.11	0.16	0.20	0.24	0.26	0.27
	45.0	0.01	0.04	0.09	0.15	0.20	0.26	0.31	0.34	0.35
	60.0	0.01	0.05	0.10	0.17	0.24	0.30	0.35	0.39	0.40
	75.0	0.01	0.05	0.11	0.18	0.25	0.33	0.38	0.42	0.43
+ -140.0	15.0	0.01	0.02	0.04	0.07	0.09	0.12	0.14	0.16	0.16
	30.0	0.01	0.03	0.07	0.11	0.16	0.20	0.24	0.26	0.27
	45.0	0.01	0.04	0.09	0.15	0.20	0.26	0.31	0.34	0.35
	60.0	0.01	0.05	0.10	0.17	0.24	0.30	0.35	0.39	0.40
	75.0	0.01	0.05	0.11	0.18	0.25	0.33	0.38	0.42	0.43
+ -160.0	15.0	0.01	0.02	0.04	0.07	0.09	0.12	0.14	0.16	0.16
	30.0	0.01	0.03	0.07	0.11	0.16	0.20	0.24	0.26	0.27
	45.0	0.01	0.04	0.09	0.15	0.20	0.26	0.31	0.34	0.35
	60.0	0.01	0.05	0.10	0.17	0.24	0.30	0.35	0.39	0.40
	75.0	0.01	0.05	0.11	0.18	0.25	0.33	0.38	0.42	0.43
+ -180.0	15.0	0.01	0.02	0.04	0.07	0.09	0.12	0.14	0.16	0.16
	30.0	0.01	0.03	0.07	0.11	0.16	0.20	0.24	0.26	0.27
	45.0	0.01	0.04	0.09	0.15	0.20	0.26	0.31	0.34	0.35
	60.0	0.01	0.05	0.10	0.17	0.24	0.30	0.35	0.39	0.40
	75.0	0.01	0.05	0.11	0.18	0.25	0.33	0.38	0.42	0.43

Table A3.13 Partial Sky Component for a Horizontal Surface

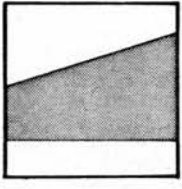
SOLAR ALT.	Patch Alt Y _{ob}	AZ. of Sky Patch from Sun Meridian ϕ_{ob}									
		± 20.0	± 40.0	± 60.0	± 80.0	± 100.0	± 120.0	± 140.0	± 160.0	± 180.0	
15.0	15.0	0.03	0.05	0.05	0.06	0.06	0.07	0.07	0.08	0.08	0.08
	30.0	0.08	0.15	0.15	0.17	0.18	0.19	0.21	0.22	0.22	0.23
	45.0	0.12	0.18	0.22	0.25	0.27	0.29	0.31	0.33	0.33	0.36
	60.0	0.13	0.21	0.26	0.30	0.33	0.35	0.38	0.41	0.41	0.44
	75.0	0.14	0.25	0.28	0.32	0.36	0.39	0.42	0.45	0.45	0.49
30.0	15.0	0.02	0.05	0.04	0.04	0.04	0.05	0.05	0.06	0.06	0.06
	30.0	0.07	0.10	0.12	0.14	0.15	0.16	0.17	0.19	0.19	0.20
	45.0	0.11	0.18	0.22	0.24	0.26	0.28	0.30	0.32	0.32	0.34
	60.0	0.14	0.22	0.27	0.31	0.34	0.36	0.39	0.41	0.41	0.44
	75.0	0.15	0.24	0.30	0.34	0.37	0.40	0.43	0.46	0.46	0.49
45.0	15.0	0.01	0.02	0.02	0.05	0.05	0.04	0.04	0.04	0.04	0.05
	30.0	0.04	0.06	0.08	0.10	0.11	0.12	0.13	0.14	0.14	0.15
	45.0	0.08	0.14	0.17	0.20	0.22	0.24	0.25	0.27	0.27	0.29
	60.0	0.12	0.20	0.25	0.29	0.32	0.34	0.37	0.39	0.39	0.41
	75.0	0.14	0.25	0.29	0.35	0.37	0.40	0.43	0.45	0.45	0.48
60.0	15.0	0.01	0.01	0.02	0.02	0.02	0.03	0.03	0.03	0.03	0.04
	30.0	0.02	0.04	0.06	0.07	0.08	0.09	0.10	0.11	0.11	0.12
	45.0	0.05	0.09	0.12	0.15	0.17	0.18	0.20	0.22	0.22	0.23
	60.0	0.09	0.15	0.20	0.24	0.27	0.30	0.32	0.34	0.34	0.37
	75.0	0.11	0.20	0.26	0.31	0.35	0.38	0.41	0.44	0.44	0.47
75.0	15.0	0.00	0.01	0.01	0.02	0.02	0.02	0.03	0.03	0.03	0.03
	30.0	0.02	0.03	0.04	0.05	0.07	0.08	0.09	0.10	0.10	0.11
	45.0	0.03	0.06	0.09	0.11	0.13	0.15	0.17	0.19	0.19	0.20
	60.0	0.05	0.10	0.14	0.18	0.21	0.24	0.27	0.30	0.30	0.32
	75.0	0.08	0.14	0.20	0.25	0.30	0.34	0.38	0.41	0.41	0.44
90.0	15.0	0.00	0.01	0.01	0.01	0.02	0.02	0.03	0.03	0.03	0.03
	30.0	0.01	0.02	0.03	0.05	0.06	0.07	0.08	0.09	0.10	0.10
	45.0	0.02	0.04	0.06	0.09	0.11	0.13	0.15	0.17	0.17	0.19
	60.0	0.03	0.07	0.10	0.14	0.18	0.21	0.24	0.27	0.30	0.31
	75.0	0.05	0.10	0.14	0.19	0.24	0.29	0.34	0.38	0.41	0.43



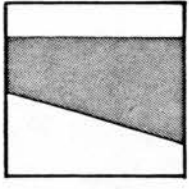
A8



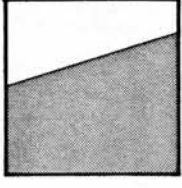
B8



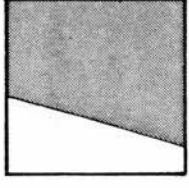
A7



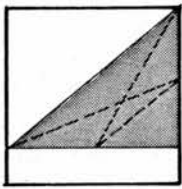
B7



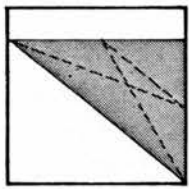
A6



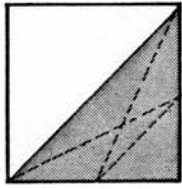
B6



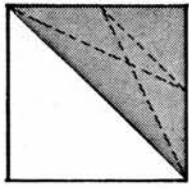
A5



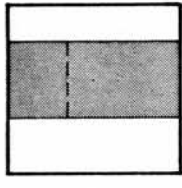
B5



A4



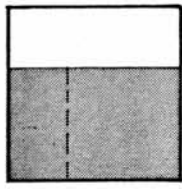
B4



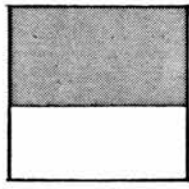
A3



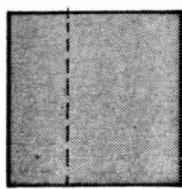
B3



A2



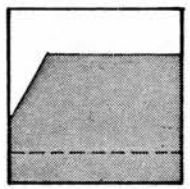
B2



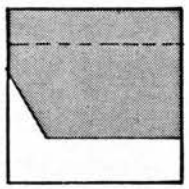
A1



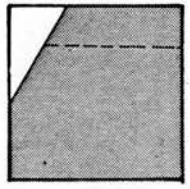
B1



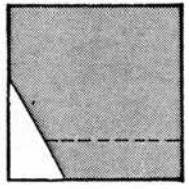
A13



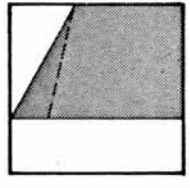
B13



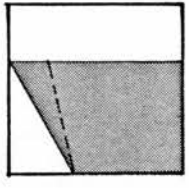
A12



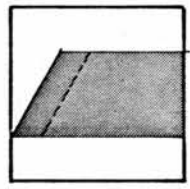
B12



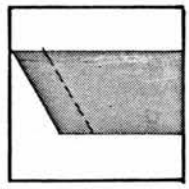
A11



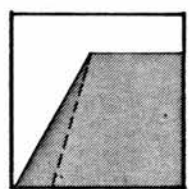
B11



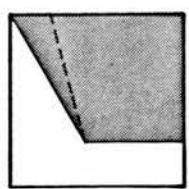
A10



B10



A9



B9

Appendix A.4 : Possible Shapes and Locations of Shadow which may be cast on a Rectangular Vertical Surface by an Adjacent Rectangular Vertical Surface with Varying Sizes and Relative Positions

APPENDIX A.5 FORM FACTOR TABLES FOR SURFACES OF DIFFERENT
GEOMETRIC CONFIGURATIONS

The calculation of radiant energy interchange and the inter-reflected irradiance on the surfaces of buildings requires knowledge of the form factors. These factors represent the fraction of the radiant energy leaving one surface which is incident upon an other.

Tabulated data for the form factor is limited. It generally covers restricted cases of geometric configuration of surfaces (Hamilton and Morgan 1952). This was mainly because the calculation of the form factor involves the evaluation of area integrals which may require double and quadruple integration, thus making the form factor equations too complex for analytical solution and involving extensive numerical calculation even for simple geometrical configuration of surfaces.

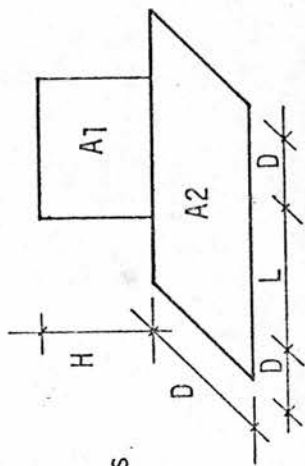
The form factors subroutines developed for this study which is based on Sparrow's formulation for the form factor (1963) and uses the contour integration method can be advantageously used together with the geometric flux algebra relations to tabulate form factor data for wide ranges and complex geometric configuration of surfaces not yet readily available. This will contribute in building up comprehensive and readily available data for the form factor which will greatly facilitate the evaluation of the inter-reflected irradiance.

Data for the form factor was prepared and tabulated for a number of different geometric configurations of surfaces. Examples are presented in the following tables, A5.1 to A5.3.

RATIO R/L

HORIZON, DIST, RATIO RD

	0,25	0,50	0,75	1,00	1,50	2,00	2,50	3,00	3,50	4,00
0,2500	0,096	0,171	0,230	0,274	0,332	0,368	0,392	0,409	0,421	0,431
0,5000	0,100	0,170	0,234	0,277	0,335	0,370	0,393	0,410	0,422	0,431
0,7500	0,102	0,179	0,236	0,279	0,336	0,371	0,394	0,410	0,422	0,432
1,0000	0,104	0,181	0,239	0,281	0,330	0,372	0,395	0,411	0,423	0,432
1,2500	0,105	0,183	0,240	0,283	0,339	0,373	0,396	0,412	0,423	0,432
1,5000	0,105	0,184	0,241	0,284	0,340	0,374	0,396	0,412	0,424	0,433
1,7500	0,106	0,185	0,242	0,285	0,341	0,374	0,397	0,413	0,424	0,433
2,0000	0,106	0,185	0,243	0,286	0,341	0,375	0,397	0,413	0,424	0,433
2,2500	0,107	0,186	0,244	0,286	0,342	0,376	0,398	0,413	0,425	0,434
2,5000	0,107	0,186	0,244	0,287	0,342	0,376	0,398	0,414	0,425	0,434
2,7500	0,107	0,187	0,245	0,287	0,343	0,376	0,398	0,414	0,425	0,434
3,0000	0,107	0,187	0,245	0,288	0,343	0,377	0,399	0,414	0,425	0,434
3,2500	0,108	0,187	0,245	0,288	0,343	0,377	0,399	0,414	0,426	0,434
3,5000	0,108	0,188	0,246	0,288	0,344	0,377	0,399	0,415	0,426	0,435
3,7500	0,108	0,188	0,246	0,289	0,344	0,377	0,399	0,415	0,426	0,435
4,0000	0,108	0,188	0,246	0,289	0,344	0,378	0,400	0,415	0,426	0,435



RD = L/H
 RD = D/H
 Form Factor : F_{A1,A2}

Table A5.1 Form Factors for two Rectangular Perpendicular Planes of Different Lengths and a Common Edge

HORIZON, DIST, RATIO : RD

RATIO : RL

	0,25	0,50	0,75	1,00	1,50	2,00	2,50	3,00	3,50	4,00
0,2500	0,672	0,520	0,419	0,346	0,252	0,196	0,160	0,134	0,116	0,102
0,5000	0,708	0,545	0,435	0,357	0,258	0,200	0,162	0,136	0,117	0,103
0,7500	0,727	0,560	0,446	0,365	0,263	0,203	0,165	0,138	0,119	0,104
1,0000	0,739	0,570	0,454	0,372	0,267	0,206	0,167	0,139	0,120	0,105
1,2500	0,746	0,578	0,460	0,377	0,271	0,208	0,168	0,141	0,121	0,106
1,5000	0,752	0,583	0,465	0,381	0,274	0,210	0,170	0,142	0,122	0,106
1,7500	0,756	0,588	0,469	0,384	0,276	0,212	0,171	0,143	0,123	0,107
2,0000	0,759	0,591	0,472	0,387	0,278	0,214	0,173	0,144	0,123	0,108
2,2500	0,761	0,594	0,475	0,390	0,280	0,215	0,174	0,145	0,124	0,108
2,5000	0,763	0,596	0,477	0,391	0,282	0,217	0,175	0,146	0,125	0,109
2,7500	0,764	0,598	0,479	0,393	0,283	0,218	0,176	0,147	0,126	0,110
3,0000	0,769	0,599	0,480	0,395	0,284	0,219	0,177	0,147	0,126	0,110
3,2500	0,767	0,602	0,482	0,396	0,285	0,220	0,177	0,148	0,127	0,111
3,5000	0,768	0,603	0,483	0,397	0,286	0,221	0,178	0,149	0,127	0,111
3,7500	0,769	0,604	0,484	0,398	0,287	0,221	0,179	0,149	0,128	0,111
4,0000	0,769	0,605	0,485	0,399	0,288	0,222	0,179	0,150	0,128	0,112

RL = L/H
RD = D/H

Form Factor : F_{A1,A2}

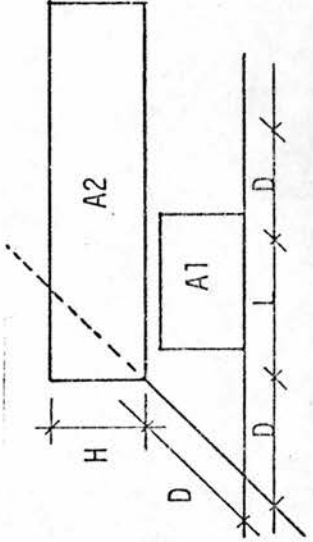


Table A5.2 Form Factors between Two Parallel Finite Planes of Different Lengths and Equal Heights

HORIZON, DIST, RATIO ; RD

RATIO ; RL

	0,25	0,50	0,75	1,00	1,50	2,00	2,50	3,00	3,50	4,00
0,2500	0,808	0,657	0,541	0,453	0,335	0,263	0,216	0,182	0,157	0,139
0,5000	0,800	0,648	0,533	0,446	0,331	0,260	0,213	0,180	0,155	0,138
0,7500	0,796	0,642	0,527	0,441	0,327	0,258	0,212	0,179	0,155	0,137
1,0000	0,793	0,638	0,523	0,438	0,328	0,256	0,210	0,178	0,154	0,136
1,2500	0,791	0,635	0,520	0,435	0,322	0,254	0,209	0,177	0,153	0,135
1,5000	0,789	0,633	0,517	0,432	0,320	0,252	0,207	0,176	0,152	0,135
1,7500	0,789	0,631	0,515	0,430	0,319	0,251	0,206	0,175	0,152	0,134
2,0000	0,788	0,630	0,514	0,429	0,317	0,250	0,205	0,174	0,151	0,133
2,2500	0,787	0,628	0,513	0,428	0,316	0,249	0,205	0,174	0,151	0,133
2,5000	0,786	0,627	0,511	0,427	0,315	0,248	0,204	0,173	0,150	0,132
2,7500	0,786	0,627	0,511	0,426	0,314	0,247	0,203	0,172	0,150	0,132
3,0000	0,788	0,626	0,510	0,425	0,314	0,247	0,203	0,172	0,149	0,132
3,2500	0,785	0,627	0,509	0,424	0,313	0,246	0,202	0,171	0,149	0,131
3,5000	0,785	0,626	0,508	0,423	0,312	0,246	0,202	0,171	0,148	0,131
3,7500	0,784	0,626	0,508	0,423	0,312	0,245	0,201	0,171	0,148	0,131
4,0000	0,784	0,626	0,508	0,422	0,311	0,245	0,201	0,170	0,148	0,130

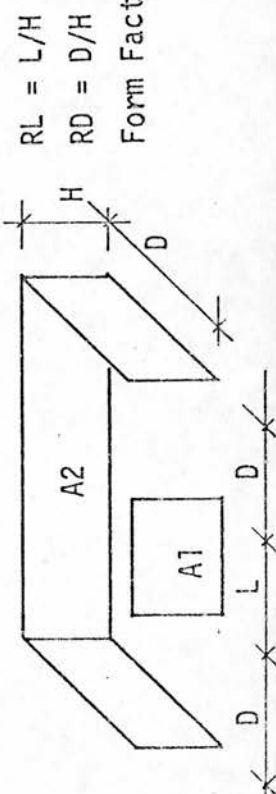


Table A5.3 Form Factors for a Vertical Block Side and Vertical Surroundings of Three Sides

Form Factor : $F_{A1,A2}$

RL = L/H

RD = D/H

APPENDIX A.6 LISTING OF THE MAIN ROUTINES

```

C *****
0001 SUBROUTINE SUNGT(OL1,OL2,OL3,M,ND,KHS,KHE,ALT,AZ)
0002 DIMENSION ALT(24),AZ(24)
C **ROUTINE TO EVALUATE THE SUN GEOMETRY
C SPECIFICATION :LATITUDE ,LONGITUDE ,TIME LONGITUDE OF A PLACE
C **SPECIFICATION :MONTH ,DAY ,STARTING HOUR ,NUMBER OF HOURS
C **OL1=LATITUDE OF A PLACE :OL2=LONGITUDE :OL3=TIME LONGITUDE
C **M=MONTH : ND=DAY : KHS=START HOUR : KHE=NUMBER OF HOURS
0003 CC=3.1415927/180.0
0004 FCT=6.2832/365.24
0005 NDT=0
0006 M1=M-1
0007 CONT=TAN(23.45*CC)
0008 IF(M1.EQ.0) GO TO 182
0009 DO 181 I=1,M1
0010 IF(I.LT.8) GO TO 11
0011 IF(I.GT.7) GO TO 15
0012 11 I1=MOD(I,2)
0013 IF(I1)12,12,13
0014 12 NDY=30
0015 GO TO 14
0016 13 NDY=31
0017 14 IF(I.EQ.2)NDY=28
0018 GO TO 18
0019 15 I1=MOD(I,2)
0020 IF(I1)17,17,16
0021 16 NDY=30
0022 GO TO 18
0023 17 NDY=31
0024 18 NDT=NDT+NDY
0025 181 CONTINUE
0026 182 NDT=NDT+ND
0027 DAYS=FLOAT(NDT)
0028 TR1=(DAYS-02.0)*FCT
0029 TR2=TR1*2.0
0030 TR3=TR1*3.0
0031 TR4=TR1*4.0
0032 TS1=SIN(TR1)
0033 TS2=SIN(TR2)
0034 TS3=SIN(TR3)
0035 TS4=SIN(TR4)
0036 TC1=COS(TR1)
0037 TC2=COS(TR2)
0038 TC3=COS(TR3)
C **EQUATION OF TIME ,FUNCTION OF SUN MEAN LONGITUDE
0039 A=(97.8*TS1)-(596.6*TS2)-(4.0*TS3)+(12.7*TS4)
0040 B=(431.3*TC1)+(1.9*TC2)-(19.3*TC3)
0041 E=(A+B)*15.0/3600.00
0042 ER=E*CC
0043 TLNG=TR1+ER
0044 SNTL=SIN(TLNG)
0045 SNDC=SNTL*CONT
0046 ASD=ATAN(SNDC)
0047 CDC=COS(ASD)
0048 DEC=ASD/CC
C **ASET THE ARCS OF THE SPHERICAL TRIANGLE,PLACE AND SUN POSITIONS
C **SUN AND PLACE SOUTH ,ARC > 90 :ALTAN=90+ALT ,DECAN =90+DEC
C **SUN AND PLACE NORTH ,ARC <90 :ALTAN =90-ALT ,DECAN =90-DEC
0049 ALTAN=90,0=OL1
0050 CLT=COS(ALTAN*CC)
0051 SLT=SIN(ALTAN*CC)
0052 DECAN=90,0=DEC
0053 CDCA=COS(DECAN*CC)
0054 SDCA=SIN(DECAN*CC)
0055 DO 23 K=KHS,KHE
0056 T=K
0057 TANG=(12.0-T)*15.0
0058 HANG=TANG+OL3-OL2+E
0059 HR=HANG*CC
0060 CHA=COS(HR)
0061 SHA=SIN(HR)
0062 SAL=CLT*CDCA+SLT*SDCA*CHA
0063 ALR=ARSIN(SAL)
0064 CAL=COS(ALR)
0065 CAZ=(CDCA*SLT-SDCA*CLT*CHA)/CAL
0066 AZR=ARCOS(CAZ)
C **ALTITUDE ABOVE HORIZON
C **AZIMUTH IS TAKEN FROM THE NORTH POINT
0067 ALT(K)=ALR/CC
0068 AZ(K)=AZR/CC
0069 IF(HANG.LT.0.0)AZ(K)=360.0-AZ(K)
0070 23 CONTINUE
0071 RETURN
0072 END

```

```

C*****
0001      SURROUTINE FOFACT(N1,XW1,YW1,ZW1,N2,XW2,YW2,ZW2,INT,NDIM,F12)
0002      DIMENSION XW1(N1),YW1(N1),ZW1(N1),XW2(N2),YW2(N2),ZW2(N2),
          1      XP1(10),YP1(10),ZP1(10),XP2(10),YP2(10),ZP2(10),
          2      XL1(10),YL1(10),ZL1(10),XL2(10),YL2(10),ZL2(10),
          3      DX1(10),DY1(10),DZ1(10),DX2(10),DY2(10),DZ2(10)
0003      COMMON X11,X12,X13,X22,X23,XW
0004      COMMON A12,F12,C12,D12,A13,B13,C13,D13,A22,B22,C22,D22
0005      COMMON A23,B23,C23,D23
C*****PROGRAM TO EVALUATE FORM FACTOR FOR TWO FINITE PLANES
C **THE FORM FACTOR (FF)HERE MEANS THAT POLYGON (1) IS RADIATING TO POL.(2)
C **DOUBLE AREAS INTEGRALS REDUCED TO DOUBLE INTEGRATION
C **USING CONTOUR INTEGRATION METHOD
C **AUXILIARY INFORMATION FOR COMPUTATION OF FORM FACTOR (LENGTH &
C **DERIVATIVES)ARE GENERATED BY THE ROUTINE,AN ARBITRARY NO.IS ASSUMED
C **FOR THE DIMENSION OF THE AUXILIARY INFORMATION .GE.N1 &N2
C*****INTEGRAL EQ.IS GIVEN IN 3 PARTS FOR X,Y,Z
C **TAKE TWO SIDES ONE OF EVERY SURF. IN TURN AND EVALUATE THE INTG.
C **FOR EVERY PART
C **ESTABLISH NO. OF INTEG.INTERVALS FOR EVERY SIDE TAKEN=10 HERE
0006      PI2=6.2831854
0007      GINT=0.00
C **AUXILIARY INFORMATION OF LINE (1)
0008      DO 50 I=1,N1
C **SET THE CO-ORD.S OF END POINTS OF EACH LINE
0009      II=I+1
0010      IF(II.GT.N1) II=II-N1
0011      XP1(I)=XW1(II)
0012      YP1(I)=YW1(II)
0013      ZP1(I)=ZW1(II)
C **SCALAR AXIAL COMPONENTS
0014      XL1(I)=ABS(XP1(I)-XW1(I))
0015      YL1(I)=ABS(YP1(I)-YW1(I))
0016      ZL1(I)=ABS(ZP1(I)-ZW1(I))
C **DERIVATIVES
0017      DX1(I)=1.0
0018      DY1(I)=1.0
0019      DZ1(I)=1.0
0020      IF(XL1(I).LT.0.001)DX1(I)=0.0
0021      IF(YL1(I).LT.0.001)DY1(I)=0.0
0022      IF(ZL1(I).LT.0.001)DZ1(I)=0.0
0023      IF(DX1(I).EQ.0.0)XL1(I)=XP1(I)
0024      IF(DY1(I).EQ.0.0)YL1(I)=YP1(I)
0025      IF(DZ1(I).EQ.0.0)ZL1(I)=ZP1(I)
0026      50 CONTINUE
C **LINE (2)
0027      DO 51 I=1,N2
C **SET THE CO-ORD.S OF END POINTS OF EACH LINE
0028      II=I+1
0029      IF(II.GT.N2) II=II-N2
0030      XP2(I)=XW2(II)
0031      YP2(I)=YW2(II)
0032      ZP2(I)=ZW2(II)
0033      XL2(I)=ABS(XP2(I)-XW2(I))
0034      YL2(I)=ABS(YP2(I)-YW2(I))
0035      ZL2(I)=ABS(ZP2(I)-ZW2(I))
0036      DX2(I)=1.0
0037      DY2(I)=1.0
0038      DZ2(I)=1.0
0039      IF(XL2(I).LT.0.001)DX2(I)=0.0
0040      IF(YL2(I).LT.0.001)DY2(I)=0.0
0041      IF(ZL2(I).LT.0.001)DZ2(I)=0.0
0042      IF(DX2(I).EQ.0.0)XL2(I)=XP2(I)
0043      IF(DY2(I).EQ.0.0)YL2(I)=YP2(I)
0044      IF(DZ2(I).EQ.0.0)ZL2(I)=ZP2(I)
0045      51 CONTINUE
0046      DO 110 I=1,N1
0047      DO 110 J=1,N2
C **X-AXIS
0048      IF(DX1(I).EQ.0.0.OR.DX2(J).EQ.0.0) GO TO 104
C **VARIABLES WITH Y1
0049      D12=DY1(I)
0050      IF(D12.EQ.1.0) GO TO 10
0051      X12=YL1(I)
0052      GO TO 11
0053      10 CALL EQAT(XW1(I),XP1(I),YW1(I),YP1(I),A12,B12,C12)
C **VARIABLES WITH Z1
0054      11 D13=DZ1(I)
0055      IF(D13.EQ.1.0) GO TO 12
0056      X13=ZL1(I)
0057      GO TO 13
0058      12 CALL EQAT(XW1(I),XP1(I),ZW1(I),ZP1(I),A13,B13,C13)
C **VARIABLES WITH Y2
0059      13 D22=DY2(J)
0060      IF(D22.EQ.1.0) GO TO 14
0061      X22=YL2(J)
0062      GO TO 15
0063      14 CALL EQAT(XW2(J),XP2(J),YW2(J),YP2(J),A22,B22,C22)

```

```

C   **VARIABLES WITH Z2
0064   15 D23=DZ2(J)
0065       IF(D23.EQ.1.0) GO TO 16
0066       X23=ZL2(J)
0067       GO TO 17
0068   16 CALL EGAT(XW2(J),XP2(J),ZW2(J),ZP2(J),A23,B23,C23)
0069   17 CALL DOBINT(XW1(I),XP1(I),INT,NDIM,XW2(J),XP2(J),GTJ)
0070       GO TO 105
0071   104 GTJ=0.0
C   **Y-AXIS
0072   105 IF(DY1(I).EQ.0.0.OR.DY2(J).EQ.0.0) GO TO 106
C   **VARIABLES WITH X1
0073       D12=DX1(I)
0074       IF(D12.EQ.1.0) GO TO 18
0075       X12=XL1(I)
0076       GO TO 19
0077   18 CALL EGAT(YW1(I),YP1(I),XW1(I),XP1(I),A12,B12,C12)
C   **VARIABLES WITH Z1
0078   19 D13=DZ1(I)
0079       IF(D13.EQ.1.0) GO TO 20
0080       X13=ZL1(I)
0081       GO TO 21
0082   20 CALL EGAT(YW1(I),YP1(I),ZW1(I),ZP1(I),A13,B13,C13)
C   **VARIABLES WITH X2
0083   21 D22=DX2(J)
0084       IF(D22.EQ.1.0) GO TO 22
0085       X22=XL2(J)
0086       GO TO 23
0087   22 CALL EGAT(YW2(J),YP2(J),XW2(J),XP2(J),A22,B22,C22)
C   **VARIABLES WITH Z2
0088   23 D23=DZ2(J)
0089       IF(D23.EQ.1.0) GO TO 24
0090       X23=ZL2(J)
0091       GO TO 25
0092   24 CALL EGAT(YW2(J),YP2(J),ZW2(J),ZP2(J),A23,B23,C23)
0093   25 CALL DOBINT(YW1(I),YP1(I),INT,NDIM,YW2(J),YP2(J),GTJ)
0094       GO TO 107
0095   106 GTJ=0.0
C*****Z-AXIS
0096   107 IF(DZ1(I).EQ.0.0.OR.DZ2(J).EQ.0.0) GO TO 108
C   **VARIABLES WITH X1
0097       D12=DX1(I)
0098       IF(D12.EQ.1.0) GO TO 26
0099       X12=XL1(I)
0100       GO TO 27
0101   26 CALL EGAT(ZW1(I),ZP1(I),XW1(I),XP1(I),A12,B12,C12)
C   **VARIABLES WITH Y1
0102   27 D13=DY1(I)
0103       IF(D13.EQ.1.0) GO TO 28
0104       X13=YL1(I)
0105       GO TO 29
0106   28 CALL EGAT(ZW1(I),ZP1(I),YW1(I),YP1(I),A13,B13,C13)
C   **VARIABLES WITH X2
0107   29 D22=DX2(J)
0108       IF(D22.EQ.1.0) GO TO 30
0109       X22=XL2(J)
0110       GO TO 31
0111   30 CALL EGAT(ZW2(J),ZP2(J),XW2(J),XP2(J),A22,B22,C22)
C   **VARIABLES WITH Y2
0112   31 D23=DY2(J)
0113       IF(D23.EQ.1.0) GO TO 32
0114       X23=YL2(J)
0115       GO TO 33
0116   32 CALL EGAT(ZW2(J),ZP2(J),YW2(J),YP2(J),A23,B23,C23)
0117   33 CALL DOBINT(ZW1(I),ZP1(I),INT,NDIM,ZW2(J),ZP2(J),GTZ)
0118       GO TO 109
0119   108 GTZ=0.0
0120   109 GT=GTJ+GTI+GTZ
0121       GINT=GINT+GT
0122   110 CONTINUE
C*****
0123   C   **THE AREA (A1) OF POLYGON (1) IS CALCULATED BY THE ROUTINE POLA
       CALL POLA(N1,XW1,YW1,ZW1,A1)
C   **A2 IS THE AREA OF POLY. (2)
0124       CALL POLA(N2,XW2,YW2,ZW2,A2)
0125       AP1=A1*PI2
0126       AP2=A2*PI2
0127       F12=ABS(GINT/AP1)
0128       F21=ABS(GINT/AP2)
0129       RETURN
0130       END

```



```

C*****
0001      SUBROUTINE DOBINT(A1,B1,NN,NDIM,A2,B2,GRAND)
C*****SUBROUTINE FOR DOUBLE INTEGRATION.FIRST AREA INTEGRAL WITH
C **ROMBERG PRINCIPLE,SECOND AREA INTEGRAL WITH SIMPSON'S RULE
C **A1,B1,A2,B2,ARE THE LIMITS OF THE TWO LINES IN ONE AXIS THE OTHER
C **CO-ORD.S ARE EITHER CONST.OR FUNCTION OF OF THE TWO VARIABLES
C **NN :NO.S OF INTERVALS USED FOR INTEGRATION ,SHOULD BE EVEN
0002      DIMENSION AUX(20)
0003      COMMON X11,X12,X13,X22,X23,XW
0004      COMMON A12,B12,C12,D12,A13,B13,C13,D13,A22,B22,C22,D22
0005      COMMON A23,B23,C23,D23
0006      EXTERNAL FCT
0007      EPS=1.0E-6
0008      EVN1=0.00
0009      ODD1=0.00
0010      M1=(NN/2)*2
0011      IF(M1.GE.2) GO TO 10
0012      GRAND=0.00
0013      GO TO 13
0014 10 MM1=M1-1
0015      MM2=M1-2
0016      FM1=M1
0017      H1=(B1-A1)/FM1
C **INTERVAL WIDTH OF X2
0018      XW=ABS(H1/100.0)
C **SET THE LIMITS OF X2:UPPER LIMIT XU=B2,LOWER LIMIT XL=A2
0019      XL=A2
0020      XU=B2
C **FIRST LIMIT OF X1:A1
0021      X11=A1
0022      IF(D12.EQ.0.0) GO TO 20
0023      X12=(-A12*X11-C12)/B12
0024 20 IF(D13.EQ.0.0) GO TO 21
0025      X13=(-A13*X11-C13)/B13
0026 21 CALL QATR(XL,XU,EPS,NDIM,FCT,VALA1,IER,AUX)
0027      X11=B1
0028      IF(D12.EQ.0.0) GO TO 30
0029      X12=(-A12*X11-C12)/B12
0030 30 IF(D13.EQ.0.0) GO TO 31
0031      X13=(-A13*X11-C13)/B13
0032 31 CALL QATR(XL,XU,EPS,NDIM,FCT,VALB1,IER,AUX)
0033      END1=VALA1+VALB1
C*****ODD VALUES
0034      DO 11 I=1,MM1,2
0035      X11=A1+H1*FLOAT(I)
0036      IF(D12.EQ.0.0) GO TO 40
0037      X12=(-A12*X11-C12)/B12
0038 40 IF(D13.EQ.0.0) GO TO 41
0039      X13=(-A13*X11-C13)/B13
0040 41 CALL QATR(XL,XU,EPS,NDIM,FCT,ODD1,IER,AUX)
0041      ODD1=ODD1+ODD11
0042 11 CONTINUE
C **EVEN VALUES
0043      DO 12 I=2,MM2,2
0044      X11=A1+H1*FLOAT(I)
0045      IF(D12.EQ.0.0) GO TO 50
0046      X12=(-A12*X11-C12)/B12
0047 50 IF(D13.EQ.0.0) GO TO 51
0048      X13=(-A13*X11-C13)/B13
0049 51 CALL QATR(XL,XU,EPS,NDIM,FCT,EVN1,IER,AUX)
0050      EVN1=EVN1+EVN11
0051 12 CONTINUE
0052      S1=H1/3.0
0053      S2=ODD1*4.0
0054      S3=EVN1*2.0
0055      S4=S2+S3+END1
0056      GRAND=S1*S4
0057 13 RETURN
0058      END

```

```

C*****
0001      SUBROUTINE EQAT(X1,X2,Y1,Y2,A,B,C)
C **EQ.OF A LINE IN THE FORM :A*X+B*Y+C=0.0
0002      A=Y2-Y1
0003      B=X1-X2
0004      C=Y1*X2-X1*Y2
0005      RETURN
0006      END

```

```

C*****
0001 REAL FUNCTION FCT(X21)
C*****FCT IS THE FUNCTION NAME WITH DUMMY ARGUMENTS X11--X23
0002 COMMON X11,X12,X13,X22,X23,XW
0003 COMMON A12,B12,C12,D12,A13,B13,C13,D13,A22,B22,C22,D22
0004 COMMON A23,B23,C23,D23
0005 DX=X21-X11
0006 DUMX=DX*DX
0007 IF(D22.EQ.0.0) GO TO 10
0008 X22=(-A22*X21-C22)/B22
0009 10 DYY=X22-X12
0010 DUMY=DYY*DYY
0011 IF(D23.EQ.0.0) GO TO 11
0012 X23=(-A23*X21-C23)/B23
0013 11 DZZ=X23-X13
0014 DUMZ=DZZ*DZZ
0015 DUM=SQRT(DUMX+DUMY+DUMZ)
0016 IF(DUM.EQ.0.0) DUM=0.1E-23
0017 FCT=ALOG(DUM)
0018 RETURN
0019 END

C*****
0001 SUBROUTINE POLA(NS,XR,YR,ZR,AP)
0002 DIMENSION XR(NS),YR(NS),ZR(NS)
C **ROUTINE TO EVALUATE AREA OF A POLYGON GIVEN ITS NO.OF SIDES & VERTICES
C **POLY.IS DIVIDED INTO UNITS OF TRIANGLES
C **MINIMUM NO.OF SIDES IS (3) OR AREA WILL BE GIVEN =0.0
0003 NU=NS-2
0004 AP=0.0
0005 IF(NS.LT.3) GO TO 12
C **DECIDE ON THE VERTICES OF EACH TRIANGLE (XU,YU,ZU)&EVALUATE ITS AREA (AP)
C **FIRST POINT OF UNITS : ALL UNITS HAS ONE COMMON VERTICE
0006 XU1=XR(1)
0007 YU1=YR(1)
0008 ZU1=ZR(1)
0009 DO 11 I=1,NU
0010 I1=I+1
0011 I2=I+2
C **SECOND POINT OF UNITS
0012 XU2=XR(I1)
0013 YU2=YR(I1)
0014 ZU2=ZR(I1)
C **THIRD POINT OF UNITS
0015 XU3=XR(I2)
0016 YU3=YR(I2)
0017 ZU3=ZR(I2)
0018 CALL TRIA(XU1,YU1,ZU1,XU2,YU2,ZU2,XU3,YU3,ZU3,AU)
0019 AP=AP+AU
0020 11 CONTINUE
0021 12 RETURN
0022 END

C*****
0001 SUBROUTINE TRIA(X1,Y1,Z1,X2,Y2,Z2,X3,Y3,Z3,A)
C **ROUTINE TO EVALUATE THE AREA OF A TRIANGLE GIVEN THE CO-ORD.S
C **OF ITS VERTICES
C **COMPONENTS OF TWO VECTORS ,STARTING EACH FROM COMMON POINT(X1,Y1,Z1)
C **EACH JOINING ONE OF THE OTHER TWO POINTS
C **VECT. (PQ) BETWEEN (X1,Y1,Z1) AND (X2,Y2,Z2)
0002 X11=X2-X1
0003 Y11=Y2-Y1
0004 Z11=Z2-Z1
C **VECT. (PR) BETWEEN (X1,Y1,Z1) AND (X3,Y3,Z3)
0005 X12=X3-X1
0006 Y12=Y3-Y1
0007 Z12=Z3-Z1
C **COMPONENTS OF CROSS PRODUCT OF TWO VECT.S
0008 A1=Y11*Z12-Y12*Z11
0009 A2=X12*Z11-X11*Z12
0010 A3=X11*Y12-X12*Y11
0011 AS2=A1*A1+A2*A2+A3*A3
0012 A2=SQRT(AS2)
0013 A=A2/2.0
0014 RETURN
0015 END

```

```

C*****
0001 SUBROUTINE IRRILL(Z0,AZ0,ZS,AZS,ZB1,AZB1,ZB2,AZB2,
      IHF,ASF,NDIM1,NDIM2,RII,RLI,SF)
C
C **THIS SUBROUTINE EVALUATES IRRADIANCE AND ILLUMINANCE ON SURFACES
C **OF DIFFERENT ORIENTATIONS AND INCLINATIONS FOR DIFFERENT SOLAR
C **POSITIONS FOR STANDARD TROPICAL SKY
C**
C **IHF:FACTOR INDICATING THAT THE RECEIVING SURFACE IS HORIZONTAL, FOR IHF=1
C **FOR IHF=0, NOT HORIZONTAL
C **ASF:SHADOW FACTOR, INDICATING SHADED AREA OF SURFACE/TOTAL AREA OF SURFACE
C **Z0 :SOLAR ALTITUDE
C **AZ0 :SOLAR AZIMUTH
C **AZS :SURFACE AZIMUTH
C **ZB1,ZB2, :ALTITUDE LIMITS FOR THE OBSTRUCTED SKY AREA
C **AZB1,AZB2 :AZIMUTH LIMITS FOR THE OBSTRUCTED SKY AREA
C **NDIM1,NDIM2 :UNITS FOR INTEGRATION
C **INITIALIZATIONS
      CC=3.1415927/180.0
0002 C **SURFACE SOLAR AZIMUTH:AZ
      AZ=AZS-AZ0
0003 C
0004 C CAZ=COS(AZ*CC)
0005 C CZ0=COS(Z0*CC)
0006 C SZ0=SIN(Z0*CC)
0007 C SZS=SIN(ZS*CC)
0008 C CZS=COS(ZS*CC)
C
0009 C **ANGLE OF INCIDENCE OF THE DIRECT BEAM
      CK=SZS*SZ0+CZS*CZ0*CAZ
C
C **IRRAD: IN W/M2 , ILLUM IN KLX
C **DIRECT NORMAL
0010 C RIN=(1285.4*SZ0)/(0.3135+SZ0)
0011 C RIN=(157.94*SZ0)/(0.59+SZ0)
C **DIRECT HORIZONTAL
0012 C RIH=RIN*SZ0
0013 C RLH=RLN*SZ0
C **DIFFUSE HORIZONTAL
0014 C RIDH=494.0*SZ0-0.3813*RIH
0015 C RLDH=55.68*SZ0-0.4*RLH
C
C **TEST IF SURFACE IS HORIZONTAL
0016 C IF(IHF.EQ.1) GO TO 11
C
C **INCLINED OR VERTICAL SURFACE
C **OBSTRUCTED SKY COMPONENT
0017 C CALL SKYCOM(Z0,AZ0,ZS,AZS,ZB1,ZB2,AZB1,AZB2,
      INDIN1,NDIM2,RR,A,ROB)
C **SET LIMITS FOR THE SKY AREA SEEN BY FULLY EXPOSED SURFACE
C **AZIMUTH LIMITS
0018 C AZB1=AZS-90.0
0019 C AZB2=AZS+90.0
C **ALTITUDE LIMITS
0020 C ZB1=0.0
0021 C ZB2=90.0
C **SKY COMPONENT FOR FULLY EXPOSED SURFACE
0022 C CALL SKYCOM(Z0,AZ0,ZS,AZS,ZB1,ZB2,AZB1,AZB2,
      INDIN1,NDIM2,RR,A,REX)
C **SKY COMPONENT FOR PARTIALLY EXPOSED SURFACE
0023 C RX=REX*ROB
C **DIFFUSE IRRAD. & ILLUM. OF INCLINED SURFACE
0024 C RIDDS=RX*RIDH
0025 C RLDDS=RX*RLDH
C
C **DIRECT IRRAD. & ILLUM.
0026 C RDS=ASF*RIN*CK
0027 C RLS=ASF*RLN*CK
C **TOTAL IRRAD & ILLUM.
0028 C RII=RDS+RIDDS
0029 C RLI=RLS+RLDDS
C
C **SHADOW FACTOR
0030 C SP=RII/((REX*RIDH)+(RIN*CK))
0031 C GO TO 12
C
C **HORIZONTAL SURFACE
C **OBSTRUCTED SKY COMPONENT
0032 C 11 CALL SKYCOM(Z0,AZ0,ZS,AZS,ZB1,ZB2,AZB1,AZB2,
      INDIN1,NDIM2,RR,A,ROB)
C **SKY COMPONENT FOR PARTIALLY EXPOSED SURFACE
0033 C RX=1.0*ROB
C **DIFFUSE IRRAD. & ILLUM. OF INCLINED SURFACE
0034 C RIDDS=RX*RIDH
0035 C RLDDS=RX*RLDH
C **DIRECT IRRAD. & ILLUM.
0036 C RDS=ASF*RIH
0037 C RLS=ASF*RLH
C **TOTAL IRRAD & ILLUM.
0038 C RII=RDS+RIDDS
0039 C RLI=RLS+RLDDS
C **SHADOW FACTOR
0040 C SP=RII/(RIH*RIDH)
0041 C 12 RETURN
0042 C END

```

```

C*****
0001      CUPROUTINE SKYCOM(AL0,AZ0,ALT,AZS,AL1,AL2,AZ1,AZ2,N,NDIM,RR,A,R)
0002      COMMON SYZ,CYZ,SCYZ,CZ,SZ,SGM,CGM,AZC,AZSC
C      **THIS ROUTINE EVALUATES THE RATIO OF THE DIFFUSE SKY RADIATION,
C      **BEING OBSTRUCTED OR RECEIVED ON A GIVEN SURFACE FROM A GIVEN
C      **A SKY AREA, TO THE ZENITH INTENSITY.
C      **THE SKY COMPONENT, OR OBSTRUCTED, MAY BE EVALUATED FROM THIS RATIO.
C      **SUN ANGLES : AZIMUTH =AZ0, ALTITUDE =ALT
C      **SURFACE ANGLES : AZIMUTH =AZS, ALTITUDE =ALT
C      **ANGULAR LIMITS OF SKY AREA : ALTITUDE , LOWER =AL0, UPPER =AL2
C      **AZIMUTH LOWER =AZ1, UPPER =AZ2
C      **ALL AZIMUTH ANGLES ARE MEASURED FROM THE NORTH POINT IN CLOCKWISE
C      **DIRECTION, AND ALTITUDE FROM THE HORIZON.
C      **INITIALS
0003      CC=3.1415927/180.0
0004      SYZ=0.0
0005      CYZ=0.0
0006      SCYZ=0.0
0007      AZC=AZ0*CC
0008      AZSC=AZS*CC
0009      SGM=SIN(ALT*CC)
0010      CGM=COS(ALT*CC)
C      **SUN ZENITH ANGLE FUNCTION
0011      ZR=AL0*CC
0012      CZ=COS(ZR)
0013      SZ=SIN(ZR)
0014      S2=SZ*SZ
0015      SNZ=1.5707964-ZR
0016      CSNZ=COS(SNZ)
0017      C1=0.45*CSNZ*CSNZ
0018      C2=EXP(3.0*SNZ)
0019      C3=10.0/C2
0020      C4=(0.91*C3+C1)*0.27385
0021      CON=1.0/C4
C      **CHECK IF THE SKY MAY BE DIVIDED INTO ONE UNIT, A LUNE, OR TWO UNITS.
C      **A LUNE AND A CIRCULAR RING OR SHALLOW DOME
C      **TEST FOR ALTITUDE LIMITS LT. OR GT. TILT ANGLE OF SURFACE
0022      IF(AL1.GE.ALT) GO TO 20
0023      IF(AL2.LE.ALT) GO TO 23
C
C      **THE UNIT OF THE SKY AREA FORMING A CIRCULAR RING OR DOME
C      **ALT. LIMITS
0024      Y1=ALT*CC
0025      GO TO 21
0026      20 Y1=AL1*CC
0027      21 Y2=AL2*CC
C      **AZIMUTH LIMITS
0028      X1=AZ1*CC
0029      X2=AZ2*CC
0030      IF(Y1.EQ.0.0) Y1=0.5*CC
0031      CALL DOBINT(Y1,Y2,N,NDIM,X1,X2,RRING)
C
0032      IF(AL1.LT.ALT) GO TO 22
0033      RLUNE=0.0
0034      GO TO 25
C      **THE SKY AREA FORMING A LUNE
0035      22 Y2=ALT*CC
0036      GO TO 24
0037      23 RRING=0.0
0038      Y2=AL2*CC
0039      24 IF(AL1.EQ.0.0) AL1=0.5
0040      Y1=AL1*CC
0041      AZS1=AZS-90.0
0042      AZS2=AZS+90.0
0043      IF(AZ1.LT.AZS1) AZ1=AZS1
0044      IF(AZ2.GT.AZS2) AZ2=AZS2
0045      X1=AZ1*CC
0046      X2=AZ2*CC
0047      CALL DOBINT(Y1,Y2,N,NDIM,X1,X2,RLUNE)
0048      25 RR=(RRING+RLUNE)*CON
C
C      **RATIO OF ZENITH INTENSITY TO HORIZONTAL RADIATION
0049      A1=0.01*(EXP(2.9*ZR))
0050      A2=0.13*(EXP(-0.23*ZR))
0051      A=A1+A2
C      **SKY COMPONENT
0052      R=A*RR
0053      RETURN
0054      END

```

```

C*****
0001 SURROUTINE DOPOINT(A1,P1,NN,NDIM,A2,AZC,GFAND)
0002 DIMENSION AUX(20)
0003 COMMON SYZ,CYZ,SCYZ,CZ,SZ,SGM,CGM,AZC,AZSC
0004 EXTERNAL FCT
0005 EPS=1.0E-6
0006 EVN1=0.0
0007 ODD1=0.0
0008 AB=ABS(B1-A1)
0009 IF(AB.LT.C.00001) GO TO 9
0010 P1=(NN/2)*2
0011 IF(M1.GE.2) GO TO 10
0012 9 GRAND=0.0
0013 GO TO 13
0014 10 MM1=M1-1
0015 MM2=M1-2
0016 FM1=M1
0017 H1=(P1-A1)/FM1
0018 YL=A2
0019 XU=B2

```

```

C*****Y IS ALTITUDE
0020 Y=A1
0021 SYZ=SIN(Y)
0022 CYZ=COS(Y)
0023 SCYZ=1.0/SYZ
0024 CALL GATR(XL,XU,EPS,NDIM,FCT,VALA1,IER,AUX)
0025 Y=B1
0026 SYZ=SIN(Y)
0027 CYZ=COS(Y)
0028 SCYZ=1.0/SYZ
0029 CALL GATR(XL,XU,EPS,NDIM,FCT,VALB1,IER,AUX)
0030 END1=VALA1+VALB1
0031 DO 11 I=1,MM1,2
0032 Y=A1+P1*FLOAT(I)
0033 SYZ=SIN(Y)
0034 CYZ=COS(Y)
0035 SCYZ=1.0/SYZ
0036 CALL GATR(XL,XU,EPS,NDIM,FCT,ODD1,IER,AUX)
0037 ODD1=ODD1+ODD1
0038 11 CONTINUE
0039 DO 12 I=2,MM2,2
0040 Y=A1+H1*FLOAT(I)
0041 SYZ=SIN(Y)
0042 CYZ=COS(Y)
0043 SCYZ=1.0/SYZ
0044 CALL GATR(XL,XU,EPS,NDIM,FCT,EVN1,IER,AUX)
0045 EVN1=EVN1+EVN1
0046 12 CONTINUE
0047 S1=H1/3.0
0048 S2=ODD1*4.0
0049 S3=EVN1*2.0
0050 S4=S2+S3+END1
0051 GRAND=S1*S4
0052 13 RETURN
0053 END

```

```

C*****
0001 REAL FUNCTION FCT(X)
0002 COMMON SYZ,CYZ,SCYZ,CZ,SZ,SGM,CGM,AZC,AZSC
0003 D1=0.32*SCYZ
0004 ABSD=ABS(D1)
0005 IF(ABSD.GT.36.0) GO TO 10
0006 D2=1.0/EXP(D1)
0007 GO TO 11
0008 10 D2=0.0
0009 11 D3=1.0-D2
C **ANGULAR DISTANCE BETWEEN THE SUN AND AN ELEMENTAL SKY AREA
0010 CX=COS(X-AZC)
0011 G1=SYZ*SZ
0012 G2=CYZ*CZ+CX
0013 CG=G1+G2
0014 GR=ARCOS(CG)
C **ANGLE OF INCIDENCE
0015 CA=COS(X-AZSC)
0016 E1=EXP(3.0*GR)
0017 E2=10.0/E1
0018 E3=0.45*CG*CG
0019 E4=0.91+E2+E3
0020 T1=SYZ*CGM
0021 T2=CYZ*SGM+CA
0022 T3=T1+T2
0023 E5=CYZ*T3
0024 FCT=D3+E4+E5
0025 RETURN
0026 END

```

```

1 C*****
2 SUBROUTINE CFINT(N,ALT,AZ,X11,Y11,X12,Y12,P)
3 DIMENSION ALT(20),AZ(20),X11(20),X12(20),Y11(20),Y12(20),A(20),
4 F(20,20)
5 INTEGER ALT,AZ
6 C **ROUTINE TO EVALUATE THE CON,FIG,FACTOR INTER=RELATIONS FOR A
7 C **GIVEN SET OF SURFACES
8 C **N=NO. OF UNITS IN THE SET
9 C **1=CHECK THAT EVERY TWO UNITS OF SURFACES ARE NOT HORIZONTAL ALT1
10 C **AND ALT2=90
11 C **CHECK THAT EVERY TWO UNITS OF SURFACES DO NOT HAVE THE SAME
12 C **AZIMUTH AZ1=AZ2 ,OTHER WISE THEIR CON,FACT.=0,0
13 NN=N+1
14 DO 11 I=1,NN
15 F(I,I)=0,0
16 II=I+1
17 DO 11 J=II,N
18 IF(ALT(I),EQ,90,AND,ALT(J),EQ,90) GO TO 12
19 IF(AZ(I),EQ,AZ(J)) GO TO 12
20 CALL INFMFY(X11(I),Y11(I),X12(I),Y12(I),
21 X11(J),Y11(J),X12(J),Y12(J),A(I),A(J),F(I,J))
22 F(J,I)=A(I)*F(I,J)/A(J)
23 GO TO 11
24 F(I,J)=0,0
25 F(J,I)=0,0
26 11 CONTINUE
27 F(N,N)=0,0
28 WRITE(6,22)
29 22 FORMAT(1H0,10X,'CONFIG,FACTORS!//)
30 DO 21 I=1,N
31 WRITE(6,20)(F(I,J),J=1,N)
32 20 FORMAT(6(3X,F10,4)/)
33 21 CONTINUE
34 RETURN
35 END

```

```

1 C*****
2 SUBROUTINE INFMFY(X11,Y11,X12,Y12,X21,Y21,X22,Y22,A1,A2,F12)
3 C
4 C **CONFIGURATION FACTOR BETWEEN TWO INFINITE PLANES OF CONSTANT CROSS=SECTION
5 C **RADIATION FROM PLANE (1) TO PLANE (2) IS EXPRESSED BY F12
6 C
7 C **1=THE DISTANCE BETWEEN THE TWO POINTS REPRESENTING PLANE (1)P11&P12
8 C
9 X1112=X12-X11
10 Y1112=Y12-Y11
11 P11P12=SQRT((X1112*X1112)+(Y1112*Y1112))
12 A1=P11P12
13 C
14 C **2=DISY, FROM BOTTOM PT, OF PLANE (1)=P11 TO TOP PT, OF PLANE (2)=P22P11P22
15 X1122=X22-X11
16 Y1122=Y22-Y11
17 P11P22=SQRT((X1122*X1122)+(Y1122*Y1122))
18 C
19 C **3=DISY, FROM BOTTOM PT, OF PLANE (1)=P11 TO BOTTOM PT, OF PLANE (2)=P21P11P21
20 X1121=X21-X11
21 Y1121=Y21-Y11
22 P11P21=SQRT((X1121*X1121)+(Y1121*Y1121))
23 C ** =DISY, FROM TOP PT, OF PLANE (1) TO TOP PT, OF PLANE (2)=P12&P22 P12P22
24 X1222=X22-X12
25 Y1222=Y22-Y12
26 P12P22=SQRT((X1222*X1222)+(Y1222*Y1222))
27 C
28 C **5=DISY, FROM TOP PT, OF PLANE (1) TO BOTTOM PT, OF PLANE (2)=P12&P21P12P21
29 X1221=X21-X12
30 Y1221=Y21-Y12
31 P12P21=SQRT((X1221*X1221)+(Y1221*Y1221))
32 C **DISTANCE BETWEEN THE TWO POINTS OF PLANE (2)
33 X2122=X22-X21
34 Y2122=Y22-Y21
35 P21P22=SQRT((X2122*X2122)+(Y2122*Y2122))
36 A2=P21P22
37 C
38 D=ABS(P11P22+P12P21-P11P21-P12P22)
39 C=P11P12+2,0
40 F12=D/C
41 RETURN
42 END

```

```

1 C*****
2 C
3 SUBROUTINE MATRIX(N,RO,RIT,F,C,RIF)
4 DIMENSION RO(20),RIT(20),RLT(20),RIF(20),RLF(20),
5 F(20,20),C(20,20),RI(20),RL(20),CC(100),SC(100)
6 EPS=10,OE=07
7 IER=0
8 DO 11 I=1,N
9 RIT(I)=RIT(I)
10 DO 11 J=1,N
11 C(I,J)=F(I,J)*RO(J)
12 IF(T,FO,J) C(I,J)=1,0
13 11 CONTINUE
14 KR=0
15 DO 23 I=1,N
16 DO 23 J=1,N
17 KR=K+1
18 CC(K)=C(J,I)
19 23 CONTINUE
20 CALL GELG(RI,CC,N,1,EPS,IER)
21 DO 20 I=1,N
22 RIF(I)=RI(I)
23 20 CONTINUE
24 RETURN
25 END

```

Subroutine GELG available
in IBM SSP library

```

C
0001 SUBROUTINE SHGM(ALT0,AZ0,AZ1,N1,X1,Y1,Z1,AZ2,N2,X2,Y2,Z2,
      1NS,XS,YS,ZS,NCD)
C
0002 DIMENSION X1(N1),Y1(N1),Z1(N1),X2(N2),Y2(N2),Z2(N2),
      1XSP(20),YSP(20),ZSP(20),XS(20),YS(20),ZS(20),X(20),Y(20),Z(20),
      2XT(20),YT(20),ZT(20)
C **THIS ROUTINE ESTABLISHES THE CONTOUR POINTS (NS) CO-ORD.S OF THE
C SHADOW CAST ON A PLANE SURFACE S1,WITH N1 CONTOUR POINTS AND
C CO-ORD.S(X1,Y1,Z1),BY AN ADJACENT SURFACE S2,WITH N2 CONTOUR POINTS
C AND CO-ORD.S (X2,Y2,Z2)
C **SUN GEOMETRY IS DEFINED BY ITS ALTITUDE:ALT0,AZIMUTH:AZ0
C **INITIALISATIONS
0003 CC=3.141592/180.0
0004 AZS1=AZ1-AZ0
0005 AZS2=AZ2-AZ0
0006 CAZ1=COS(AZS1*CC)
0007 CAZ2=COS(AZS2*CC)
C **ENSURE THAT SURFACE S1 IS FACING THE SUN
0008 IF(CAZ1.LT.0.0) GO TO 17
C **AVOID SOLAR ALT APPROACHING 90 DEG.S
0009 IF(ALT0.GT.88.0) ALT0=88.0
C **EQ.OF PLANE SURFACE (N1) IN FORM A*X+B*Y+C*Z+D=0.0
0010 CALL PLEG(N1,X1,Y1,Z1,A,B,C,D)
C **GENERATE THE CO-ORD.S OF THE SHADOW CONTOUR POINTS (XSP,YSP,ZSP)
C ON THE PLANE OF S1 ,CAST BY >2
0011 DO 11 I=1,N2
0012 CALL PSHP(X2(I),Y2(I),Z2(I),AZ0,ALT0,A,B,C,D,
      1XSP(I),YSP(I),ZSP(I))
0013 11 CONTINUE
C
C **ENSURE THAT THE SHADOW GENERATED HAVE THE SAME CONTOUR DIRECTION
C AS SURFACE S1.THEREFORE REVERSE SHADOW CONTOUR DIRECTION WHEN
C COSINE(SURFACE S2 - SOLAR AZIMUTH )< 0.0
0014 IF(CAZ2.LT.0.0) GO TO 12
0015 GO TO 15
0016 12 DO 13 I=1,N2
0017 XT(I)=XSP(I)
0018 YT(I)=YSP(I)
0019 ZT(I)=ZSP(I)
0020 13 CONTINUE
0021 DO 14 I=1,N2
0022 II=N2+1-I
0023 XSP(I)=XT(II)
0024 YSP(I)=YT(II)
0025 ZSP(I)=ZT(II)
0026 14 CONTINUE
0027 15 NSP=N2
C **NO SHADOW IS FORMED ON SURFACE WHEN ALL SHADOW CONTOUR POINTS
C GENERATED ARE BELOW GROUND (ZSP=-VE)
0028 DO 16 I=1,NSP
0029 IF(ZSP(I).GE.0.0) GO TO 18
0030 16 CONTINUE
0031 17 NCD=0
0032 GO TO 30
C **DEFINE SHADOW PROFILE ON S1
0033 18 CALL POLINT(N1,X1,Y1,Z1,NSP,XSP,YSP,ZSP,NS,XS,YS,ZS,NCD)
0034 IF(NCD.LE.2) GO TO 30
C **ENSURE THAT EACH LINE OF SHADOW CONTOUR IS REPRESENTED BY ITS TWO
C END POINTS ONLY
0035 CALL PSTL(NS,XS,YS,ZS,N,X,Y,Z)
0036 IF(N.EQ.NS) GO TO 30
0037 NS=N
0038 DO 19 I=1,NS
0039 XS(I)=X(I)
0040 YS(I)=Y(I)
0041 ZS(I)=Z(I)
0042 19 CONTINUE
0043 GO TO 30
0044 20 WRITE(6,21)
0045 21 FORMAT(1X,' NO SHADOW ON PLANE SURFACE (N1) **/
      110X,'*****')
      GO TO 30
0046 22 WRITE(6,23)XS(1),YS(1),ZS(1)
0047 23 FORMAT(1X,' ONE POINT SHADOW ON SURFACE PLANE (N1) **/3F15.5//
      110X,'*****')
      GO TO 30
0048 24 WRITE(6,25)XS(1),YS(1),ZS(1),XS(2),YS(2),ZS(2)
0049 25 FORMAT(1X,' ONE LINE SHADOW ON PLANE SURFACE N1 **/6F15.5//
      110X,'*****')
      GO TO 30
0050 24 WRITE(6,25)XS(1),YS(1),ZS(1),XS(2),YS(2),ZS(2)
0051 25 FORMAT(1X,' ONE LINE SHADOW ON PLANE SURFACE N1 **/6F15.5//
      110X,'*****')
      GO TO 30
0052 30 RETURN
0053 END
0054

```

```

C*****
0001 SUBROUTINE POLINT(N1,X11,Y11,Z11,N2,X21,Y21,Z21,
1      N3,X31,Y31,Z31,CAF)
0002 DIMENSION Y11(10),Y11(10),Z11(10),X12(10),Y12(10),Z12(10),
1      X21(10),Y21(10),Z21(10),X22(10),Y22(10),Z22(10),
2      X31(10),Y31(10),Z31(10),X32(10),Y32(10),Z32(10),
3      PPF(10),PLF(10),LPF(10),XCC(2),YCC(2),ZCC(2),NPL(2),
4      XC1(10),XC2(10),YC1(10),YC2(10),ZC1(10),ZC2(10),
5      INL1(10),INL2(10),YT(10),YT(10),ZT(10),PPFF(10)
0003 INTEGER PPF,PLF,CAF,PPFF
C ** GIVEN TWO POLYGONS .THIS ROUTINE TEST IF THEY HAVE A COMMON AREA
C ** AND DEFINE ITS BOUNDARY
C ** THE DATA OF THE TWO POLY.S ARE NUMBERED IN A CLOCKWISE DIRECTION
C
C **END POINTS OF LINES OF POLY.(1)
0004 DO 11 I=1,N1
0005 II=I+1
0006 IF(II.GT.N1)II=1
0007 Y12(I)=X11(II)
0008 Y12(I)=Y11(II)
0009 Z12(I)=Z11(II)
0010 11 CONTINUE
C **POLY.(2) : END PT.S OF EACH LINE
0011 DO 12 I=1,N2
0012 II=I+1
0013 IF(II.GT.N2)II=1
0014 X22(I)=X21(II)
0015 Y22(I)=Y21(II)
0016 Z22(I)=Z21(II)
0017 12 CONTINUE
0018 NOP1=0
0019 NOP2=0
C **THE NUMBER OF POINTS OF POLY.(2) INSIDE POLY.(1)
0020 DO 13 I=1,N2
0021 CALL PTPL(X21(I),Y21(I),Z21(I),N1,X11,Y11,Z11,X12,Y12,Z12,PPF(I))
0022 NOP2=NOP2+PPF(I)
0023 13 CONTINUE
0024 IF(NOP2.EQ.N2) GO TO 15
0025 IF(NOP2.GT.0.AND.NOP2.LT.N2) GO TO 26
C **THE NUMBER OF POINTS OF POLY.(1) INSIDE POLY.(2)
0026 DO 14 I=1,N1
0027 CALL PTPL(X11(I),Y11(I),Z11(I),N2,X21,Y21,Z21,X22,Y22,Z22,PPFF(I))
0028 NOP1=NOP1+PPFF(I)
0029 14 CONTINUE
0030 IF(NOP1.EQ.N1) GO TO 17
0031 IF(NOP1.GT.0.AND.NOP1.LT.N1) GO TO 20
C **TEST IF THE CORNERS OF ONE POLY. ARE OUTSIDE THE OTHER ,BUT SOME LINES
C **STILL INTERSECT EACH OTHER
0032 DO 19 I=1,N2
0033 CALL PLLIN(X21(I),Y21(I),Z21(I),X22(I),Y22(I),Z22(I),
1N1,X11,Y11,Z11,X12,Y12,Z12,XCC,YCC,ZCC,NPL,LPF(I))
0034 IF(LPF(I).EQ.2) GO TO 20
0035 19 CONTINUE
C **WHEN NO COMMON AREA IS POSSIBLE
0036 GO TO 71
C **POLY.(2) ENCLOSED WITHIN POLY.(1) :POLY.(2) IS THE COMMON POLY.(3)
0037 15 N3=N2
0038 DO 16 I=1,N2
0039 X31(I)=X21(I)
0040 Y31(I)=Y21(I)
0041 Z31(I)=Z21(I)
0042 16 CONTINUE
0043 GO TO 59
C **POLY.(1) INSIDE POLY.(2) :POLY.(1) IS THE COMMON POLY.(3)
0044 17 N3=N1
0045 DO 18 I=1,N1
0046 X31(I)=X11(I)
0047 Y31(I)=Y11(I)
0048 Z31(I)=Z11(I)
0049 18 CONTINUE
0050 GO TO 59
C **TEST FOR LINES OF POLY.(2) ARE EITHER :-
C **1-COMpletely WITHIN POLY.(1),GIVE POLY.-LINE FACTOR: PLF=1
C **2-PARTLY WITHIN :
C ** A--ONE INTERSECTION,REF.PT.OUT & END PT.IN PLF=2
C ** B--ONE INTERSECTION ,REF.PT.IN & END PT.OUT PLF=3
C ** C--TWO INTERSECTIONS PLF=4
C **3-COMpletely OUTSIDE PLF=0
C
0051 20 DO 29 J=1,N2
0052 II=I+1
0053 IF(II.GT.N2)II=1
0054 IF(PPF(I).EQ.1.AND.PPFF(II).EQ.1) GO TO 25
0055 IF(PPF(I).EQ.1.AND.PPFF(II).EQ.0) GO TO 21
0056 IF(PPF(I).EQ.0.AND.PPFF(II).EQ.1) GO TO 22
0057 GO TO 23
C **REF.PT.IN,BUT END PT.OUT (GOING OUT )
0058 21 PLF(I)=3
0059 GO TO 23

```



```

C   **REF.PT.OUT,BUT END PT.IN (GOING IN )
0060   22 PLF(I)=2
0061   23 CALL PLLIN(X21(I),Y21(I),Z21(I),X22(I),Y22(I),Z22(I),
      1      N1,X11,Y11,Z11,X12,Y12,Z12,XCC,YCC,ZCC,NFL,LPF(I))
0062       XC1(I)=XCC(1)
0063       YC1(I)=YCC(1)
0064       ZC1(I)=ZCC(1)
0065       XC2(I)=XCC(2)
0066       YC2(I)=YCC(2)
0067       ZC2(I)=ZCC(2)
0068       INL1(I)=NPL(1)
0069       INL2(I)=NPL(2)
0070       IF(LPF(I).EQ.0) GO TO 24
0071       IF(LPF(I).EQ.2) GO TO 27
0072       IF(PFF(I).EQ.0.AND.PFF(II).EQ.0) GO TO 24
0073       GO TO 29
C   **BOTH PT.S OUTSIDE POLY.(1) BOUND.
0074   24 PLF(I)=0
0075       GO TO 26
C   **BOTH REF. & END PT.S OF LINE ARE WITHIN POLY.(1) BOUNDARY
0076   25 PLF(I)=1
0077   26 XC1(I)=0.0
0078       YC1(I)=0.0
0079       ZC1(I)=0.0
0080       XC2(I)=0.0
0081       YC2(I)=0.0
0082       ZC2(I)=0.0
0083       INL1(I)=0
0084       INL2(I)=0
0085       GO TO 29
C   **BOTH PT. S OUTSIDE POLY.(1) BOUND.,BUT WITH TWO INTERSECTIONS
0086   27 PLF(I)=4
0087   29 CONTINUE
C
C   **VERTICES OF THE COMMON POLY.OF INTERSECTION OF TWO POLY.S
0088   30 K=0
0089       I=1
0090   31 IF(PLF(I).EQ.1) GO TO 38
0091   32 IF(PLF(I).EQ.2) GO TO 35
0092   33 IF(PLF(I).EQ.3) GO TO 40
0093   34 IF(PLF(I).EQ.4) GO TO 51
0094       GO TO 39
C   **AS A LINE OF POLY.(2) IS GOING INTO POLY.(1),THE NEXT COMMON POINT
C   **IS THE INTERSECTION POINT
0095   35 K=K+1
0096       X31(K)=XC1(I)
0097       Y31(K)=YC1(I)
0098       Z31(K)=ZC1(I)
C   **IF THE ABOVE LINE WAS THE LAST LINE OF POLY.(2),THIS MEANS WE HAVE
C   **ALREADY FOUND POLY.(3)
0099   IF(I.LC.N2) GO TO 58
C   **THE COMMON POLY.(3) FOLLOWS POLY.(2) UNTIL ANOTHER INTERSECTION IS REACHED
0100   IN=I+1
0101   DO 36 J=IN,N2
0102       IF(PLF(J).GE.3) GO TO 37
0103       K=K+1
0104       X31(K)=X21(J)
0105       Y31(K)=Y21(J)
0106       Z31(K)=Z21(J)
0107   36 CONTINUE
0108       GO TO 58
C   **FOUND A LINE THAT IS GOING OUT
0109   37 I=J
0110       GO TO 33
C   **WHEN A LINE OF POLY.(2) IS COMPLETELY WITHIN POLY.(1) THE COMMON POINT
C   **OF POLY.(3) IS THAT OF POLY.(1)
0111   38 K=K+1
0112       X31(K)=X21(I)
0113       Y31(K)=Y21(I)
0114       Z31(K)=Z21(I)
0115   39 IF(I.EQ.N2) GO TO 58
0116       I=I+1
0117       GO TO 31
C   **AS A LINE OF POLY.(2) IS COMING OUT OF POLY.(1),THE REFERENCE POINT OF
C   **THAT LINE IS THE NEXT POINT OF THE COMMON POLY.(3)
0118   40 K=K+1
0119       X31(K)=X21(I)
0120       Y31(K)=Y21(I)
0121       Z31(K)=Z21(I)
C   **THE NEXT COMMON POINT IS THE INTERSECTION POINT
0122   K=K+1
0123       X31(K)=XC1(I)
0124       Y31(K)=YC1(I)
0125       Z31(K)=ZC1(I)
0126       IN1=INL1(I)
C   **FIND THE NEXT LINE OF POLY.(2) WHICH INTERSECTS POLY.(1):
C   **A LINE THAT IS EITHER GOING IN OR HAVING TWO INTERSECTIONS WITH POLY.(1)
0127   41 DO 42 J=1,N2
0128       JJ=I+J
0129       IF(JJ.GT.N2) JJ=JJ-N2
0130       IF(PLF(JJ).EQ.2.OR.PLF(JJ).EQ.4) GO TO 47
0131   42 CONTINUE

```

```

C
0132 43 WRITE(6,44)
0133 44 FORMAT(2X,'ITSEEMS THERE IS SOMETHING WRONG HERE'/
0134 12X,'POLY.(2) NOT CLOSED,CHECK DATA ENTRY,PROG. LOGIC **')
GO TO 75

C
0135 47 IN2=INL1(JJ)
C **WHEN THE TWO INTERSECTION POINTS ARE ON THE SAME LINE,CHECK TO END PROG
0136 IF(IN1.EQ.IN2) GO TO 50
C **THE FOLLOWING COMMON POINTS ARE ALONG POLY(1) TILL ANOTHER INTERSECTION
C **IS REACHED
0137 48 DO 49 J=1,N1
0138 JN=J+1
0139 IF(JN.GT.N1) JN=JN-N1
0140 K=K+1
0141 X31(K)=X11(JN)
0142 Y31(K)=Y11(JN)
0143 Z31(K)=Z11(JN)
0144 IF(JN.EQ.IN2) GO TO 50
0145 49 CONTINUE
0146 GO TO 42

C AS AN INTERSECTION OF A LINE GOING IN IS REACHED *CHECK IF THIS LINE
C **WAS NOT CONSIDERED BEFORE
0147 50 IF(I.GE.JJ) GO TO 58
0148 I=JJ
0149 GO TO 32

C **WHEN A LINE OF POLY.(2) MAKES TWO INTERSECTIONS WITH POLY.(1)
C **THE NEXT COMMON POINT IS THE FIRST INTERSECTION POINT
0150 51 K=K+1
0151 X31(K)=XC1(I)
0152 Y31(K)=YC1(I)
0153 Z31(K)=ZC1(I)

C **IN CASE THE LAST LINE TESTED HAD TWO INTERSECTIONS
C **THE NEXT COMMON POINT IS THE SECOND INTERSECTION POINT
0154 K=K+1
0155 X31(K)=XC2(I)
0156 Y31(K)=YC2(I)
0157 Z31(K)=ZC2(I)
0158 IN1=INL2(I)
0159 GO TO 41

C **THE NUMBER OF POINTS OF THE COMMON POLY.(3)
0160 58 N3=K
C **WHEN TWO CONSECUTIVE POINTS COINCIDES REDUCE THE NUMBER OF THE SIDES
C **OF THE COMMON POLY(3) BY ONE
0161 59 IF(N3.EQ.1) GO TO 72
0162 I=1
0163 60 II=I+1
0164 IF(II.GT.N3) II=II-N3
0165 XDF=ABS(X31(I)-X31(II))
0166 YDF=ABS(Y31(I)-Y31(II))
0167 ZDF=ABS(Z31(I)-Z31(II))

C **WHEN THE DIFFERENCE BETWEEN THE TWO POINTS IS SMALL :ASSUME THAT
C **THE TWO POINTS COINCIDE
0168 IF(XDF.GT.0.001) GO TO 62
0169 IF(YDF.GT.0.001) GO TO 62
0170 IF(ZDF.GT.0.001) GO TO 62

C **AS THE CONSECUTIVE POINTS COINCIDES REDUCE THE NUMBER OF POINTS BY 1
0171 N3=N3-1
0172 IF(N3.EQ.1) GO TO 72
0173 IF(II.EQ.1) GO TO 64

C **SET THE FOLLOWING POINTS
0174 DO 61 K=II,N3
0175 KK=K+1
0176 X31(K)=X31(KK)
0177 Y31(K)=Y31(KK)
0178 Z31(K)=Z31(KK)
0179 61 CONTINUE
0180 GO TO 60
0181 62 I=I+1
0182 IF(I.GT.N3) GO TO 64
0183 GO TO 61
0184 64 IF(N3.EQ.1) GO TO 72
0185 IF(N3.EQ.2) GO TO 73
0186 GO TO 74

C **COMMON AREA FACTOR : CAF
C **NO COMMON AREA CAF=0
0187 71 CAF=0
0188 N3=0
0189 X31(1)=0.0
0190 Y31(1)=0.0
0191 Z31(1)=0.0
0192 GO TO 75

C **ONE COMMON POINT FOR TWO POLY.S CAF=1
0193 72 CAF=1
0194 GO TO 75

C **ONE COMMON LINE FOR TWO POLY.S CAF=2
0195 73 CAF=2
0196 GO TO 75

C **COMMON AREA OF 3 OR MORE POINTS OF TWO POLY.S CAF=3
0197 74 CAF=3
0198 75 RETURN
0199 END

```

```

C*****
0001  SUBROUTINE PLLIN(XR1,YR1,ZR1,XE1,YE1,ZE1,NS,XR,YR,ZR,XE,YE,ZE,
      1  XCC,YCC,ZCC,NPLS,LPF)
0002  DIMENSION XR(NS),YR(NS),ZR(NS),XE(NS),YE(NS),ZE(NS),
      1  XCC(2),YCC(2),ZCC(2),NPLS(2)
C  **ROUTINE TO EVALUATE IF A GIVEN LINE INTERSECTS ONE OR TWO LINES
C  **OF THE BOUNDARY OF A GIVEN POLYGON,ALL ON THE SAME PLANE
C  **LPF = 0   FOR NO INTERSECTION
C  **LPF = 1   FOR ONE LINE INTERSECTION
C  **LPF = 2   FOR TWO LINES INTERSECTIONS

0003  KK=0
0004  LPF=0
0005  XCC(1)=0.0
0006  YCC(1)=0.0
0007  ZCC(1)=0.0
0008  XCC(2)=0.0
0009  YCC(2)=0.0
0010  ZCC(2)=0.0
0011  NPLS(1)=0
0012  NPLS(2)=0
0013  DO 11 I=1,NS
0014  CALL INTS(XR1,YR1,ZR1,XE1,YE1,ZE1,XR(I),YR(I),ZR(I),
      1  XE(I),YE(I),ZE(I),XC,YC,ZC,LPF)
0015  IF(LPF.EQ.0) GO TO 11
0016  KK=KK+LPF
0017  XCC(KK)=XC
0018  YCC(KK)=YC
0019  ZCC(KK)=ZC
0020  NPLS(KK)=I
0021  IF(KK.EQ.2) GO TO 12
0022  11 CONTINUE
0023  IF(KK.EQ.1) LPF=1
0024  GO TO 13
0025  12 LPF=2
C  **WHEN THE LINE MAKING TWO INTERS.S WITH THE POLY.(1) BOUND.,CHECK
C  **THE INTERS. LINE AND THE GIVEN LINE ARE IN THE SAME DIRECTION
0026  DFX1=0.0
0027  DFY1=0.0
0028  DFZ1=0.0
0029  DFX2=0.0
0030  DFY2=0.0
0031  DFZ2=0.0
0032  XS1=XE1-XR1
0033  YS1=YE1-YR1
0034  ZS1=ZE1-ZR1
0035  S1=XS1*XS1+YS1*YS1+ZS1*ZS1
0036  AL1=SQRT(S1)
0037  CDX1=XS1/AL1
0038  CDY1=YS1/AL1
0039  CDZ1=ZS1/AL1
0040  IF(CDX1.LT.0.0) DFX1=-1.0
0041  IF(CDY1.LT.0.0) DFY1=-1.0
0042  IF(CDZ1.LT.0.0) DFZ1=-1.0
0043  XS2=XCC(2)-XCC(1)
0044  YS2=YCC(2)-YCC(1)
0045  ZS2=ZCC(2)-ZCC(1)
0046  S2=XS2*XS2+YS2*YS2+ZS2*ZS2
0047  AL2=SQRT(S2)
0048  CDX2=XS2/AL2
0049  CDY2=YS2/AL2
0050  CDZ2=ZS2/AL2
0051  IF(CDX2.LT.0.0) DFX2=-1.0
0052  IF(CDY2.LT.0.0) DFY2=-1.0
0053  IF(CDZ2.LT.0.0) DFZ2=-1.0
0054  IF(DFX1.NE.DFX2) GO TO 14
0055  IF(DFY1.NE.DFY2) GO TO 14
0056  IF(DFZ1.NE.DFZ2) GO TO 14
0057  GO TO 13
0058  14 TX1=XCC(1)
0059  TX2=XCC(2)
0060  TY1=YCC(1)
0061  TY2=YCC(2)
0062  TZ1=ZCC(1)
0063  TZ2=ZCC(2)
0064  TL1=NPLS(1)
0065  TL2=NPLS(2)
0066  XCC(1)=TX2
0067  YCC(1)=TY2
0068  ZCC(1)=TZ2
0069  XCC(2)=TX1
0070  YCC(2)=TY1
0071  ZCC(2)=TZ1
0072  NPLS(1)=TL2
0073  NPLS(2)=TL1
0074  13 RETURN
0075  END

```

```

C      SUBROUTINE PTPL(XP,YP,ZP,NS,XR,YR,ZR,XE,YE,ZE,PPF)
0001      DIMENSION XR(NS),YR(NS),ZR(NS),XE(NS),YE(NS),ZE(NS),XC(2),YC(2),
0002      1          ZC(2),IXR(10),IYR(10),IZR(10),IXE(10),IYE(10),IZE(10)
0003      INTEGER PPF
C      **ROUTINE TO TEST IF A POINT (XP,YP,ZP) IS WITHIN THE BOUNDARY OF A
C      **POLYGON OF (NS) SIDES .EACH SIDE IS DEFINED BY ITS REF.PT.(XR,YR,ZR)
C      **AND ITS END PT.(XE,YE,ZE).POLY. AND POINT ON THE SAME PLANE
0004      XC(1)=0.0
0005      YC(1)=0.0
0006      ZC(1)=0.0
0007      XC(2)=0.0
0008      YC(2)=0.0
0009      ZC(2)=0.0
0010      NK=0
C      **PLANE POINTS ARE HELD IN INTEGER FORM FOR EQUALITY TEST
0011      DO 8 I=1,NS
0012      IXR(I)=XR(I)
0013      IYR(I)=YR(I)
0014      IZR(I)=ZR(I)
0015      IXE(I)=XE(I)
0016      IYE(I)=YE(I)
0017      IZE(I)=ZE(I)
0018      8 CONTINUE
C      **DECIDE ON THE TESTING PLANE EITHER :X-Y,X-Z, OF Y-Z
0019      9 IF(IZR(1).EQ.IZE(2).AND.IZR(1).EQ.IZE(3)) GO TO 10
0020      IF(IYR(1).EQ.IYR(2).AND.IYR(1).EQ.IYR(3)) GO TO 15
0021      IF(IXR(1).EQ.IXR(2).AND.IXR(1).EQ.IXR(3)) GO TO 20
C      **THE TEST IS CARRIED HERE ON THE X-Y PLANE.ALL PT.S ARE PROJECTED
C      **ON X-Y PLANE .TAKE A LINE PT. PARALLEL TO Y-AXIS:Y=YP
C      **FIRST TEST FOR PARALLELISM,DECIDE ON INTERSECTION PT.S*2 PT.S ENOUGH
0022      10 DO 12 I=1,NS
0023      IF(IXR(I).EQ.IXE(I)) GO TO 12
C      **TEST FOR LINE WITHIN X CO-ORD. S LIMITS OF PLANE LINE
0024      IF(XP.GE.XR(I).AND.XP.LE.XE(I)) GO TO 11
0025      IF(XP.LE.XR(I).AND.XP.GE.XE(I)) GO TO 11
0026      GO TO 12
C      **INTERSECTION POINT.
0027      11 NK=NK+1
0028      XC(NK)=XP
0029      C1=XE(I)-XR(I)
0030      C2=YE(I)-YR(I)
0031      C3=YR(I)*XE(I)-XR(I)*YE(I)
0032      YC(NK)=(XP*C2+C3)/C1
0033      IF(NK.EQ.2) GO TO 14
0034      12 CONTINUE
0035      GO TO 24
C      **TEST FOR PT. Y CO-ORD. IS BETWEEN THE Y CO-ORD. OF THE 2 INTER.PT.S
0036      14 IF(YP.GE.YC(1).AND.YP.LE.YC(2)) GO TO 25
0037      IF(YP.LE.YC(1).AND.YP.GE.YC(2)) GO TO 25
0038      GO TO 24
C      **X-Z PLANE
0039      15 DO 17 I=1,NS
0040      IF(IXR(I).EQ.IXE(I)) GO TO 17
0041      IF(XP.GE.XR(I).AND.XP.LE.XE(I)) GO TO 16
0042      IF(XP.LE.XR(I).AND.XP.GE.XE(I)) GO TO 16
0043      GO TO 17
0044      16 NK=NK+1
0045      XC(NK)=XP
0046      C1=XE(I)-XR(I)
0047      C2=ZE(I)-ZR(I)
0048      C3=ZR(I)*XE(I)-ZE(I)*XR(I)
0049      ZC(NK)=(XP*C2+C3)/C1
0050      IF(NK.EQ.2) GO TO 18
0051      17 CONTINUE
0052      GO TO 24
0053      18 IF(ZP.GE.ZC(1).AND.ZP.LE.ZC(2)) GO TO 25
0054      IF(ZP.LE.ZC(1).AND.ZP.GE.ZC(2)) GO TO 25
0055      GO TO 24
C      **Y-Z PLANE
0056      20 DO 22 I=1,NS
0057      IF(IYR(I).EQ.IYE(I)) GO TO 22
0058      IF(YP.GE.YR(I).AND.YP.LE.YE(I)) GO TO 21
0059      IF(YP.LE.YR(I).AND.YP.GE.YE(I)) GO TO 21
0060      GO TO 22
0061      21 NK=NK+1
0062      YC(NK)=YP
0063      C1=YE(I)-YR(I)
0064      C2=ZE(I)-ZR(I)
0065      C3=ZR(I)*YE(I)-ZE(I)*YR(I)
0066      ZC(NK)=(YP*C2+C3)/C1
0067      IF(NK.EQ.2) GO TO 23
0068      22 CONTINUE
0069      GO TO 24
0070      23 IF(ZP.GE.ZC(1).AND.ZP.LE.ZC(2)) GO TO 25
0071      IF(ZP.LE.ZC(1).AND.ZP.GE.ZC(2)) GO TO 25
0072      24 PPF=0
0073      GO TO 26
0074      25 PPF=1
0075      26 RETURN
0076      END

```

```

*****
0001 SUBROUTINE THPT(NPT,X,Y,Z,NP,XP,YP,ZP,LCD)
0002 DIMENSION X(3),Y(3),Z(3),XP(3),YP(3),ZP(3)
C **THIS ROUTINE TEST IF THREE POINTS ARE ON THE SAME LINE,ACCORDINGLY
C **POINT IS ELIMINATED
C **THE LINE IS TAKEN AS JOINING THE TWO ENDS POINTS ONLY ,THE INTERMEDIATE
C **LCD :IS THE LINE FACTOR INDICATING IF THE THREE POINTS ARE ON THE LINE
C **LCD=0 :THREE POINTS NOT ON LINE
C **LCD=1 :THREE POINTS ON LINE
C **DIRECTIONS RATIOS
0003 XL=X(2)-X(1)
0004 YM=Y(2)-Y(1)
0005 ZN=Z(2)-Z(1)
C **DECIDE ON THE TESTING PLANE,X-Y ,X-Z ,Y-Z
C **THIS TO ENSURE THAT,AT LEAST ONE OF THE POINTS CO-ORD.S IS VARIABLE
C **ON THE TESTING PLANE
C TEST FOR X
0006 ABX12=ABS(X(2)-X(1))
0007 ABX13=ABS(X(3)-X(1))
0008 ABX23=ABS(X(3)-X(2))
0009 IF(ABX12.GT.0.0) GO TO 10
0010 IF(ABX13.GT.0.0) GO TO 10
0011 IF(ABX23.GT.0.0) GO TO 10
C **EQN. FOR Y-Z PLANE
0012 A=(Y(3)*ZN)-(Z(3)*YM)
0013 C=(Y(1)*ZN)-(Z(1)*YM)
0014 GO TO 12
C TEST FOR Y
0015 10 ABY12=ABS(Y(2)-Y(1))
0016 ABY13=ABS(Y(3)-Y(1))
0017 ABY23=ABS(Y(3)-Y(2))
0018 IF(ABY12.GT.0.0) GO TO 11
0019 IF(ABY13.GT.0.0) GO TO 11
0020 IF(ABY23.GT.0.0) GO TO 11
C **EQN. FOR X-Z PLANE
0021 A=(X(3)*ZN)-(Z(3)*XL)
0022 C=(X(1)*ZN)-(Z(1)*XL)
0023 GO TO 12
C **EQN. FOR X-Y PLANE
0024 11 A=(X(3)*YM)-(Y(3)*XL)
0025 C=(X(1)*YM)-(Y(1)*XL)
0026 12 DAC=ABS(A-C)
0027 IF(DAC.LT.0.001) GO TO 13
0028 GO TO 18
C **WHEN THE THREE POINTS ARE ON THE SAME LINE ,DECIDE ON THE TWO
C **EXTREME POINTS MAKING THE LINE
0029 13 X13=X(3)-X(1)
0030 Y13=Y(3)-Y(1)
0031 Z13=Z(3)-Z(1)
0032 Y12=Y(2)-Y(1)
0033 Y23=Y(3)-Y(2)
0034 Z12=Z(2)-Z(1)
0035 Z23=Z(3)-Z(2)
0036 AL13=SQRT((X13*X13)+(Y13*Y13)+(Z13*Z13))
0037 AL12=SQRT((X12*X12)+(Y12*Y12)+(Z12*Z12))
0038 AL23=SQRT((X23*X23)+(Y23*Y23)+(Z23*Z23))
0039 ALL12=AL13+AL23
0040 ALL13=AL12+AL23
0041 NP=2
0042 XP(1)=X(1)
0043 YP(1)=Y(1)
0044 ZP(1)=Z(1)
0045 IF(AL13.GE.ALL13) GO TO 16
0046 IF(AL12.GE.ALL12) GO TO 14
0047 GO TO 15
0048 14 XP(2)=X(2)
0049 YP(2)=Y(2)
0050 ZP(2)=Z(2)
0051 GO TO 17
0052 15 XP(1)=X(2)
0053 YP(1)=Y(2)
0054 ZP(1)=Z(2)
0055 16 XP(2)=X(3)
0056 YP(2)=Y(3)
0057 ZP(2)=Z(3)
0058 17 LCD=1
0059 GO TO 20
0060 C **THE THREE POINTS NOT ON LINE
0061 18 LCD=0
0062 NP=3
0063 DO 19 I=1,NP
0064 YP(I)=X(I)
0065 YP(I)=Y(I)
0066 ZP(I)=Z(I)
0067 19 CONTINUE
0068 20 RETURN
0069 END
0070

```

```

C*****
0001 SUBROUTINE INTS(X1,Y1,Z1,X2,Y2,Z2,X3,Y3,Z3,X4,Y4,Z4,XC,YC,ZC,LNF)
C **ROUTINE TO FIND THE CO-ORD.S OF INTERSECTION POINT OF TWO LINES
C **BOTH LINES ON THE SAME PLANE
0002 YS1=X2-X1
0003 YS1=Y2-Y1
0004 ZS1=Z2-Z1
0005 XC2=X4-X3
0006 YS2=Y4-Y3
0007 ZS2=Z4-Z3
0008 XS3=X3-X1
0009 YS3=Y3-Y1
0010 ZS3=Z3-Z1
C **LENGTH OF EACH LINE
0011 S1=XS1*XS1+YS1+YS1+ZS1*ZS1
0012 S2=XS2*XS2+YS2+YS2+ZS2*ZS2
0013 AL1=SQRT(S1)
0014 AL2=SQRT(S2)
C **DIRECTIONAL COSINES OF EACH LINE
0015 A1=XS1/AL1
0016 B1=YS1/AL1
0017 C1=ZS1/AL1
0018 A2=XS2/AL2
0019 B2=YS2/AL2
0020 C2=ZS2/AL2
0021 A11=ABS(A1)
0022 B11=ABS(B1)
0023 C11=ABS(C1)
0024 A21=ABS(A2)
0025 B21=ABS(B2)
0026 C21=ABS(C2)
C **TEST FOR PARALLELISM AND CHOOSE THE AXES SYSTEM OF THE LINES
C **FOR EGN.SUBSTITUTION.TWO LINES ARE PARAL.WHEN THEIR COSINE ARE EQUAL
0027 IF(A11.NE.A21) GO TO 10
0028 IF(B11.NE.B21) GO TO 11
0029 IF(C11.NE.C21) GO TO 12
C WHEN LINES ARE PARAL LINE FACTOR =0
0030 GO TO 19
0031 10 IF(B1.EQ.0.0.AND.B2.EQ.0.0) GO TO 14
0032 IF(C1.EQ.0.0.AND.C2.EQ.0.0) GO TO 13
0033 GO TO 13
0034 11 IF(A1.EQ.0.0) GO TO 15
0035 IF(C1.EQ.0.0.AND.C2.EQ.0.0) GO TO 13
0036 GO TO 13
0037 12 IF(A1.EQ.0.0) GO TO 15
0038 IF(B1.EQ.0.0) GO TO 14
C
C **SOLUTION FOR INTERSECTON POINT
C WHEN THE DEN.APPROACHES 0.0 ,THE TWO LINES ARE NEARLY PARALLEL*
C **HENCE TAKEN AS PARALLEL.THIS TO AVOID THE DIVIDE ERROR FOR THE MACHINE
C **EGN.S(1)&(2)
0039 13 CON12=(A1*B2-A2*B1)
0040 CONA12=ABS(CON12)
0041 IF(CONA12.LT.0.000001) GO TO 19
0042 U=(B2*XS3-A2*YS3)/CON12
0043 V=(B1*XS3-A1*YS3)/CON12
0044 GO TO 16
C **EGN.S (1)&(3)
0045 14 CON13=(A1*C2-A2*C1)
0046 CONA13=ABS(CON13)
0047 IF(CONA13.LT.0.000001) GO TO 19
0048 U=(C2*YS3-A2*ZS3)/CON13
0049 V=(C1*XS3-A1*ZS3)/CON13
0050 GO TO 16
C **EGN.S (2)&(3)
0051 15 CON23=(B1*C2-B2*C1)
0052 CONA23=ABS(CON23)
0053 IF(CONA23.LT.0.000001) GO TO 19
0054 U=(C2*YS3-B2*ZS3)/CON23
0055 V=(C1*YS3-B1*ZS3)/CON23
C **CHECK FOR THE INTERS.PT. LIES WITHIN THE TWO LINES
0056 16 UAL=AL1-U
0057 IF(U.GE.0.0.AND.UAL.GT.-0.0001) GO TO 17
0058 GO TO 19
0059 17 VAL=AL2-V
0060 IF(V.GE.0.0.AND.VAL.GT.-0.0001) GO TO 18
0061 GO TO 19
C **EVALUATE THE CO-ORD.S OF INTERS.PT.
0062 18 LNF=1
0063 YC=A1*U+X1
0064 YC=B1*U+Y1
0065 ZC=C1*U+Z1
0066 GO TO 20
C **FOR PARAL.LINES & INTERS.PT.OUTSIDE LINES :LINE FACTOR=C.0
0067 19 LNF=C
0068 XC=0.0
0069 YC=0.0
0070 ZC=0.0
0071 20 RETURN
0072 END

```

```

C*****
0001      SUBROUTINE FLFG(NS,X,Y,Z,A,B,C,D)
0002      DIMENSION X(NS),Y(NS),Z(NS)
C      **ROUTINE TO EVALUATE EQ. OF A PLANE GIVEN 3 POINTS ON THE PLANE
C      **EQ. OF THE FORM A*X+B*Y+C*Z=D=0.0
C      **THE ROUTINE CALCULATE THE COEFFICIENTS:A,B,C,D
C      **THE CO-ORD.S OF POINTS:X,Y,Z
0003      A11=X(1)
0004      A12=Y(1)
0005      A13=Z(1)
0006      A21=X(2)
0007      A22=Y(2)
0008      A23=Z(2)
0009      A31=X(3)
0010      A32=Y(3)
0011      A33=Z(3)
0012      E1=A12*(A23-A33)
0013      E2=A13*(A32-A22)
0014      E3=A22*A33-A23*A32
0015      F=E1+E2+E3
0016      F1=A11*(A23-A33)
0017      F2=A13*(A31-A21)
0018      F3=A21*A33-A23*A31
0019      P=-F1-F2-F3
0020      G1=A11*(A22-A32)
0021      G2=A12*(A31-A21)
0022      G3=A21*A32-A22*A31
0023      C=G1+G2+G3
0024      H1=A11*E3
0025      H2=-A12*F3
0026      H3=A13*G3
0027      D=-H1-H2-H3
0028      RETURN
0029      END

C*****
0001      SUBROUTINE PTSTL(N,XX,YY,ZZ,NW,X,Y,Z)
0002      DIMENSION XX(N),YY(N),ZZ(N),XN(3),YN(3),ZN(3),
0003      1X(10),Y(10),Z(10),YT(10),XT(10),ZT(10)
C      **COPY THE ENTERED CO-ORD. INTO A NEW ARRAY WITH A DIFFERENT NAME
0003      NPT=3
0004      NP=0
0005      DO 9 I=1,N
0006      X(I)=XX(I)
0007      Y(I)=YY(I)
0008      Z(I)=ZZ(I)
0009      9 CONTINUE
0010      10 I=0
0011      11 IJ=1
0012      II=1
C      **DECIDE ON THE THREE TESTING POINTS
C      **THE LAST THREE POINTS ARE THE LAST TWO AND THE FIRST ONE
0013      DO 12 J=1,3
0014      II=II+1
0015      IF(II.GT.N)II=1
0016      XT(J)=X(II)
0017      YT(J)=Y(II)
0018      ZT(J)=Z(II)
0019      12 CONTINUE
C      **THE NO. OF THE LAST OF THE 3 POINTS TESTED ABOVE
0020      NL3=II
C      **THE POINT FOLLOWING THE LAST OF THE 3 TESTED
0021      NF=NL3+1
0022      CALL THPT(NPT,XT,YT,ZT,NP,XN,YN,ZN,LCD)
0023      IF(LCD.EQ.0) GO TO 15
C      **WHEN COMING TO THE LAST POINT,WHICH MEANS COMING TO THE STARTING POINT
0024      IF(NL3.EQ.1) GO TO 20
C      **THE CO-ORD.S OF THE TWO POINTS MAKING THE LINE
0025      DO 13 J=1,2
0026      IJ=IJ+1
0027      X(IJ)=XN(J)
0028      Y(IJ)=YN(J)
0029      Z(IJ)=ZN(J)
0030      13 CONTINUE
C      **THE NO. OF THE LAST POINT TAKEN HERE
0031      NL2=IJ
0032      IK=NL2
C      **SHIFTING THE FOLLOWING POINTS ONE STEP BACKWARD
0033      IF(NF.GT.N) GO TO 141
0034      DO 14 J=NF,N
0035      IK=IK+1
0036      X(IK)=X(J)
0037      Y(IK)=Y(J)
0038      Z(IK)=Z(J)
0039      14 CONTINUE
0040      141 N=N-1
0041      IF(N.EQ.2) GO TO 21
0042      GO TO 11
0043      15 I=I+1
C      **TO END TEST HERE,CHECK IF THE LAST OF THE 3 POINTS WAS POINT NO.1 OF POLY.
0044      IF(NL3.EQ.1) GO TO 21
0045      GO TO 11
0046      20 N=N-1
0047      21 NW=N
0048      RETURN
0049      END

```

```

C*****
0001 SUBROUTINE FSHP(X1,Y1,Z1,AZ,ALT,A,B,C,D,XS,YS,ZS)
C **ROUTINE TO FIND THE CO-ORD.S OF THE SHADOW OF ANY POINT ON ANY PLANE
C **SUN GEOMETRY,SIN(AZ),COS(AZ),TAN(ALT)
C **POINT GEOMT.CO-ORD.S X1,Y1,Z1
C **PLANE GEOMT.,EQ.OF PLANE A*X+B*Y+C*Z+D=0.0
C
C **FOR COMPUTATIONAL PURPOSES SOLAR ALT.=90 DEG.S IS AVOIDED HERE
C **AS TAN(90) IS INFINITY THIS IS BOUND TO PRODUCE A DIVIDE ERROR AND
C **TERMINATE THE COMPUTATION,ACCORDINGLY 90LEG.S IS APPROX. TO 89 DEG.S
C **THIS WILL PRODUCE A SLIGHT SHIFT IN THE SHADOW POSITION AND PROFILE
0002 IF(ALT.GT.90.0) ALT=90.0
C
0003 CC=3.1415927/180.00
0004 AZR=AZ*CC
0005 ALR=ALT*CC
0006 CAZ=COS(AZR)
0007 SAZ=SIN(AZR)
0008 TAT=TAN(ALR)
0009 ST=SAZ/TAT
0010 TS=TAT/SAZ
0011 CT=CAZ/TAT
0012 TC=TAT/CAZ
0013 CS=CAZ/SAZ
0014 SC=SAZ/CAZ
0015 EX1=(A+B*CS+C*TS)
0016 EX2=(B*X1*CS+C*X1*TS-B*Y1-C*Z1-D)
0017 EY1=(A*SC+E*CT)
0018 EY2=(A*Y1*SC+C*Y1*TC-A*X1-C*Z1-D)
0019 EZ1=(A*ST+E*CT)
0020 EZ2=(A*Z1*ST+B*Z1*CT-A*X1-B*Y1-D)
0021 XS=EX2/EX1
0022 YS=EY2/EY1
0023 ZS=EZ2/EZ1
0024 RETURN
0025 END

C*****
0001 SUBROUTINE TRANS(NP,Y0,Y0,Z0,AZ,ALT,X1,Y1,Z1,X,Y,Z)
0002 DIMENSION C(3,3),XYZ(3),X1(NP),Y1(NP),Z1(NP),X(NP),Y(NP),Z(NP)
C THIS ROUTINE EVALUATES THE CO-ORD.S OF POINTS ON A PLANE WITH
C **RESPECT TO AN ASSUME PRIME CO-ORD. SYSTEM
C **NP=NO.PT.S DEFINING EACH PLANE
C **ALT,AZ :ALTITUDE AND AZIMUTH FOR THE PLANE
C **X1,Y1,Z1 :UNPRIME SYSTEM CO-ORD.S
C **X0,Y0,Z0 :CO-ORD.S OF REF.PT.S FOR EACH PLANE WITH RESPECT TO
C **PRIME AXES
C **X,Y,Z :PRIME SYSTEM CO-ORD.S
0003 CC=3.1415927/180.0
0004 AZR=A7*CC
0005 ALR=ALT*CC
0006 CAZ=COS(AZR)
0007 SAZ=SIN(AZR)
0008 CAL=COS(ALR)
0009 SAL=SIN(ALR)
0010 C(1,1)=SAZ*CAL
0011 C(1,2)=CAZ*CAL
0012 C(1,3)=SAL
0013 C(2,1)=-CAZ
0014 C(2,2)=SAZ
0015 C(2,3)=0.0
0016 C(3,1)=-SAZ*SAL
0017 C(3,2)=-SAL*CAZ
0018 C(3,3)=CAL
0019 DO 10 I=1,NP
0020 CALL PTRANS(C,X1(I),Y1(I),Z1(I),XYZ)
0021 X(I)=X0+XYZ(1)
0022 Y(I)=Y0+XYZ(2)
0023 Z(I)=Z0+XYZ(3)
0024 10 CONTINUE
0025 RETURN
0026 END

C*****
0001 SUBROUTINE PTRANS(C,X1,Y1,Z1,XYZ)
C **ROUTINE TO TRANSFORM CO-ORD.S OF POINT FROM UNPRIME SYSTEM TO
C **PRIME SYSTEM,3-DIMENSIONAL CO-ORD.SYSTEM,COMMON REF. POINT FOR
C **PRIME AND UNPRIME SYSTEMS
C **CO-ORD.S X,Y,Z :ARE TRANSFORMED TO XYZ
0002 DIMENSION C(3,3),XA(3),XYZ(3)
0003 XA(1)=X1
0004 XA(2)=Y1
0005 XA(3)=Z1
0006 DO 10 I=1,3
0007 XYZ(I)=0.0
0008 DO 10 J=1,3
0009 XYZ(I)=XYZ(I)+XA(J)*C(J,I)
0010 10 CONTINUE
0011 RETURN
0012 END

```


APPENDIX A.7 EXAMPLE FOR ALTERNATE PRACTICAL INTERPRETATION
OF THE DIMENSIONS AND PROPORTIONS OF THE SIDES
OF THE BLOCKS AND THE CONFIGURATION OF THE
SURROUNDING FOR MINIMUM FINAL IRRADIANCE LOAD
ON THE BLOCKS

All the examples shown below are taken with the following main constraints :

- (i) All streets are of equal width;
- (ii) All facades are of the same colour and have equal average reflectance; and
- (iii) The ground is taken as bare dry soil with average reflectance value of $\rho_g = 0.2$.

Example 1

Let all the blocks be of equal size and have the same proportions of sides. Thus the obstruction height on all sides of a block $R_h = 1$, see Figure 6.19(a) in Chapter VI.

Variable Parameters of Form :

Assumed Values

Orientation axis

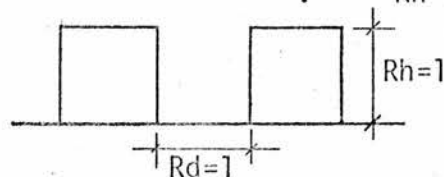
: N-S Axis, $\alpha_s = 0^\circ$

Street width proportion with respect to block height:

$R_d = 1$

Obstruction height proportion with respect to
 block height

: $R_h = 1$



The optimum plan proportion P_f , is mainly determined by the orientation axis.

The recommended plan proportion, given in part 6.1.10 of

Chapter VII and from Figure 7.22

: $P_f = 0.66$

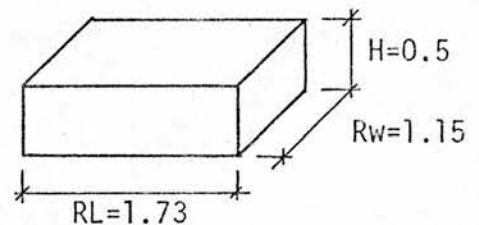
The facade reflectance mainly affects the interreflected irradiance. A high reflecting surface is assumed for minimum absorption, eg, new whitewash : $\rho_f = 0.8$

The proportions of the sides of an equivalent unit volume block are determined by its base area A . The final irradiance load decreases with increase of base area.

Let base area for unit volume block be : $A = 2$

The height proportion of the unit volume block : $H = 1/A = 0.5$

The side proportions for the unit volume block derived by the relations given in Table 6.8 .

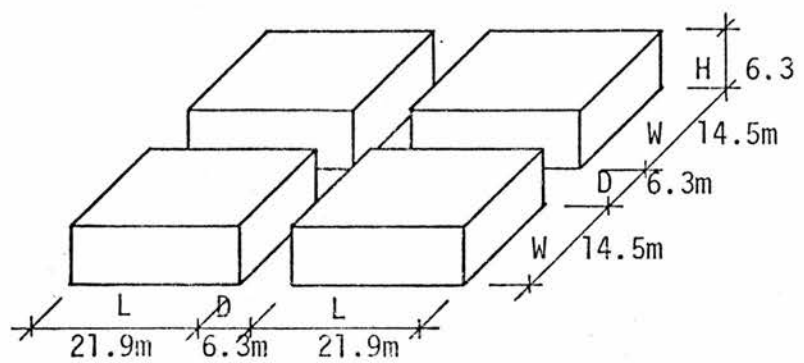


The final dimensions for a block are determined by its volume derived with the volume correction factor given by equation 6.20.

Let volume of block be : $V = 2000 \text{ Cu.m.}$

Volume correction factor : $C_p = 12.6$

The final configuration of blocks, dimensions of sides and street width are illustrated by the following diagram :



Example 2

Let the blocks on each pair of parallel rows be of different height proportion, but with all the blocks on each row having equal height, size and proportioning of sides, see Figure 6.19(b) in Chapter VI.

Constraints :

- (i) All blocks are of equal length
- (ii) The height proportion of shorter to higher block equals 0.6.

Variable Parameters of Form :

Assumed Values

Orientation axis

: N-S axis, $\alpha_s = 0^\circ$

Street width proportion with respect to the higher block

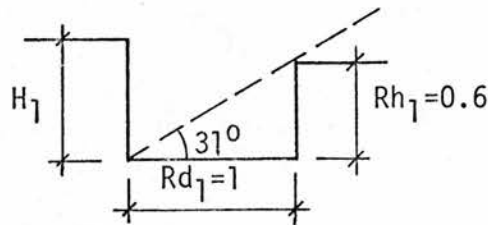
: $Rd_1 = 1$

Obstruction angle to the higher block

: $\gamma_{om1} = 31^\circ$

Obstruction height proportion for the higher block

: $Rh_1 = 0.6$



Street width proportion with respect to shorter block

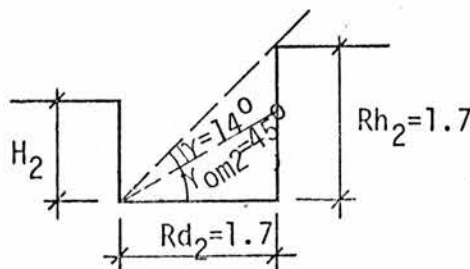
: $Rd_2 = 1.7$

Obstruction angle to the shorter block

: $\gamma_{om2} = 45^\circ$

Obstruction height proportion to the shorter block

: $Rh_2 = 1.7$



Higher Block :

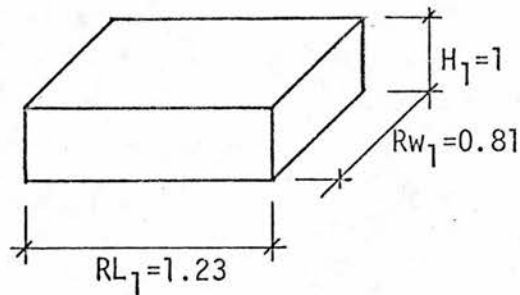
The optimum plan proportion is determined by the orientation axis.

The recommended plan proportion, Figure 7.22 : $P_{f1} = 0.66$

The proportions of the sides for a unit volume block are determined by its base area, expressed by the relations in Table 6.8.

Let base area proportion be : $A_1 = 1$

This gives the following proportions for the sides of the unit volume block



The final dimensions of the sides of the block are determined by its volume.

These are derived using the correction factor for volume, equation 6.20.

Let block volume be : $V = 1000 \text{ Cu.m.}$

Correction factor : $C_p = 10$

The final dimensions of the block are therefore :

$H_1 = 10\text{m}, L_1 = 12.3\text{m}, W_1 = 8.1\text{m}, D = 10\text{m}$

Shorter Block :

The optimum plan proportion is mainly determined by the difference of obstruction angle due to the increase in obstruction height above the level of the block

$$: \gamma = 14^{\circ}$$

Facade reflectance ρ_f , take a low value to minimise interreflected irradiance load, eg, concrete surfaces

$$: \rho_f = 0.3$$

The rate of variation for optimum plan proportion/degree of obstruction angle, given in part 6.1.12 of Chapter VII

$$: -1.7\%/degree$$

The recommended plan proportion calculated according to the modification of γ and ρ_f

$$: P_{f2} = 0.5$$

The dimensions of the sides of the short block are calculated with P_{f2} according to the constraints for the length and height proportions for the two blocks.

The height of the shorter block

$$: H_2 = 6 \text{ m}$$

The block length

$$: L_2 = 12.3 \text{ m}$$

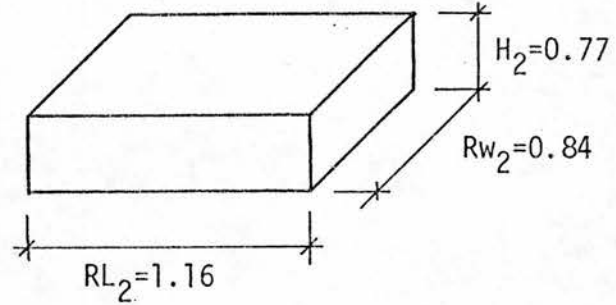
The block width

$$: W_2 = 6.2 \text{ m}$$

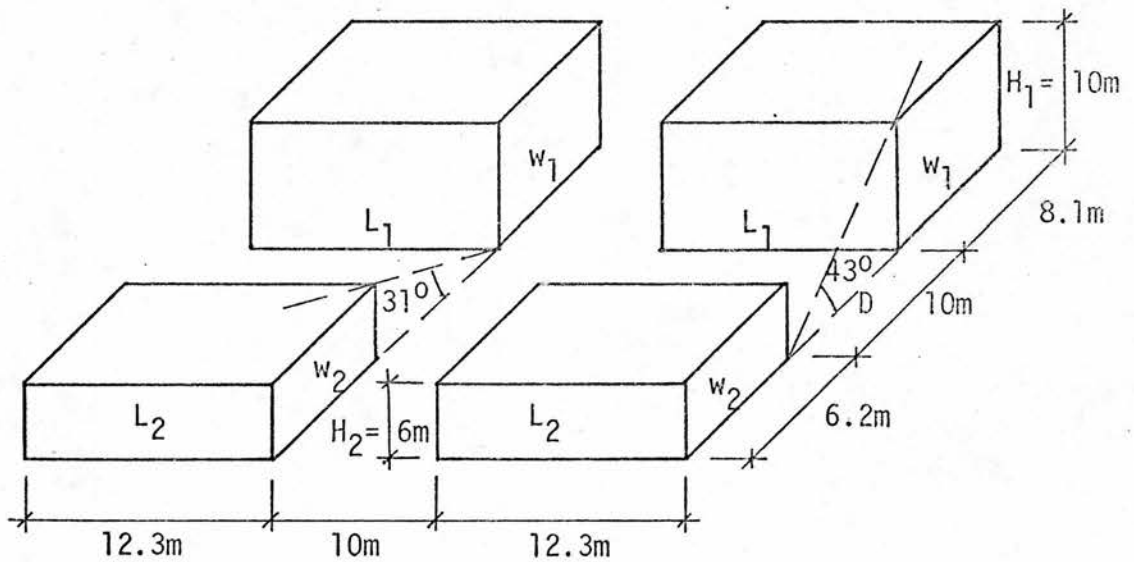
The base area for an equivalent unit volume block

$$: A_2 = 1.3$$

The proportions of the sides for an equivalent unit volume block :



The final configurations and dimensions of the blocks :

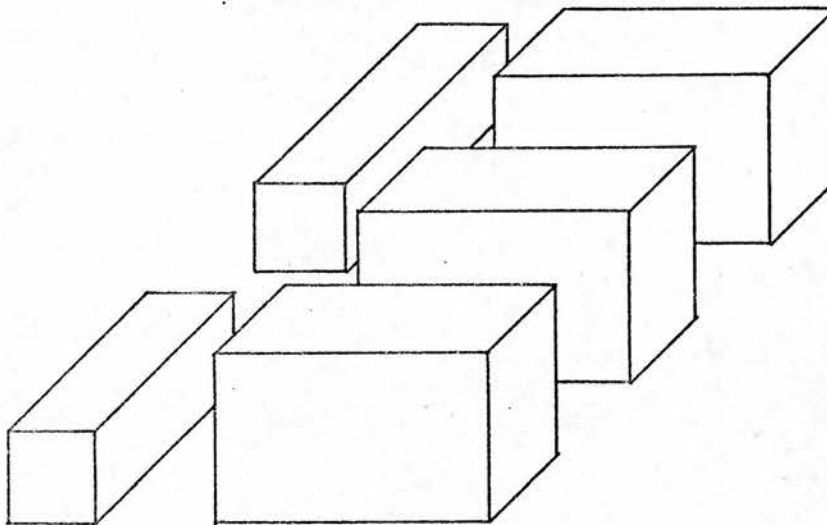


More irradiance/unit area is received on the shorter block than on the higher block by about 7 percent.

However, the magnitude of the total irradiance on the higher block is bigger because of its greater surface area.

Example 3

Take a row of equal size parallel blocks standing at right angles to a row of equal size blocks, but of shorter height. An illustration of the blocks' configuration is shown in the diagram.



Main Constraints :

- (i) The higher blocks are oriented on an N-S axis and the shorter block on an E-W axis.
- (ii) The height of the higher block is three times that of the shorter block.
- (iii) The length of the shorter block is twice the width of the higher block.

Variable Form Parameters :

Assumed Values

Higher Block :

Orientation angle : $\alpha_{s1} = 0^\circ$

Street width proportion with respect to block's height : $Rd_1 = 1$

Obstruction height proportion with respect to block's height : $Rh_1 = 0.3$

The optimum plan proportion of the block is mainly determined by the block's orientation.

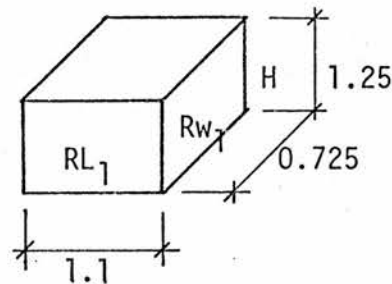
The recommended value : $P_f = 0.66$

The proportions of the sides of an equivalent unit volume block are determined by the base area A.

Take the base area : $A = 0.8$

The block height proportion : $H = 1/A = 1.25$

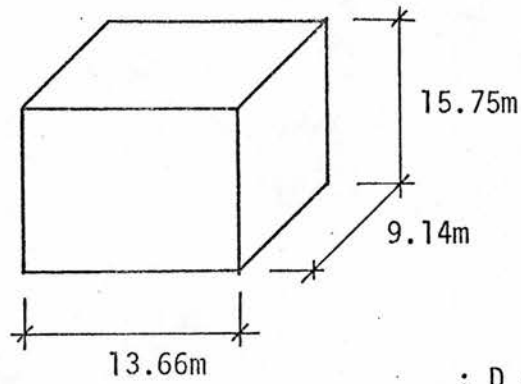
The final proportion for the sides of a unit volume block :



The final dimensions of the sides of the block are determined by the volume of the block.

Take a volume : $V = 2000$

Volume correction factor, equation 6.20 : $C_p = 12.6$



The street width

$$: D = H = 15.75 \text{ m}$$

Shorter Block :

Orientation angle

$$: \alpha_{s2} = 90^\circ$$

Street width proportion with respect to block height

$$: Rd_2 = 3.3$$

Obstruction height proportion with respect to block height

$$: Rh_2 = 3.3$$

Obstruction angle

$$: \gamma_{om2} = 45^\circ$$

The optimum plan proportion of the block is determined by the obstruction height above its level and the reflectance of the facades.

Obstruction angle above block level

$$: \gamma = 28^\circ$$

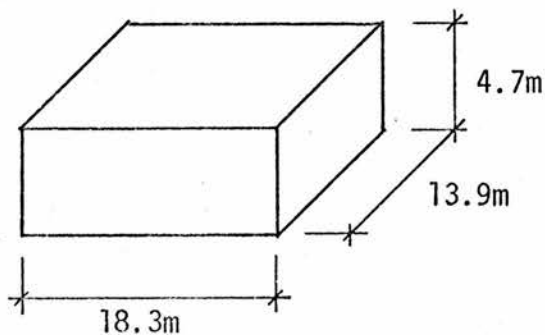
Take a facade reflectance for brick

$$: \rho_f = 0.3$$

The optimum plan proportion is derived from rate of variation with γ_{om} and ρ_f

$$: P_f = 0.76$$

Final dimensions of the block :

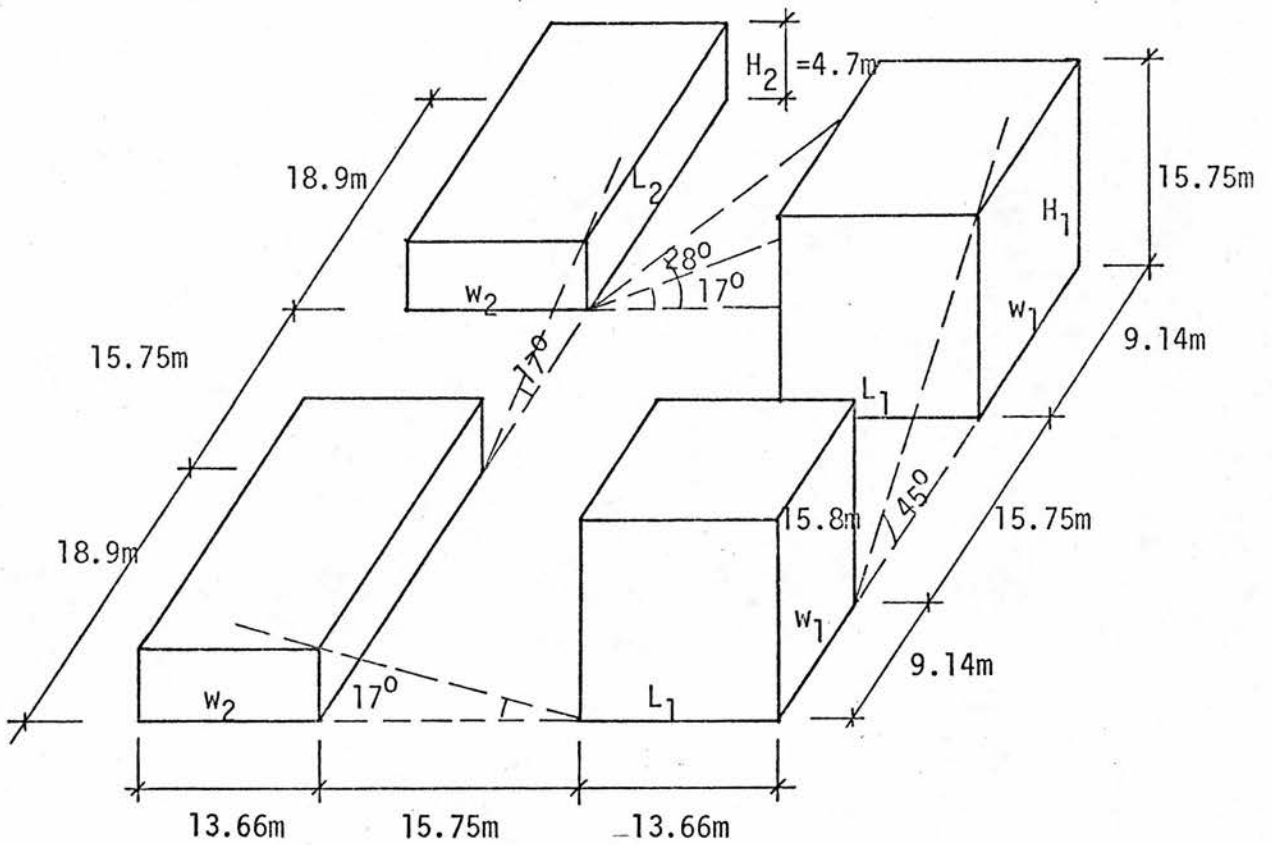


The volume of the block

: $V = 1200 \text{ Cu.m.}$

The following configuration

may be suggested for the blocks :



BIBLIOGRAPHY

- Allen, W. : "Daylighting of Buildings in Urban Districts", R.I.B.A. Journal, Feb 1943, pp 85-87.
- Allen, W. and D. Crompton : "A Form of Control of Building Development in Terms of Daylighting", R.I.B.A. Journal, Aug 1947, pp 491-499.
- Angus, T.C. : "The Control of Indoor Climates", London : Pergamon Press, 1968.
- Annals of the International Geophysical Year : Vol.V, Part VI, Pergamon Press, 1958.
- ASHRAE : Hand Book of Fundamentals, American Society of Heating, Refrigerating and Air Conditioning Engineers, 1963.
- Ballantyne, E.R. : "Sun Data for the Building Designer", Activities of Research, Documentation and Information Institutes in the Field of Building, C.I.B. No 41964, pp 22-26.
- Ballantyne, E.R. and J.W. Spenser : "Solar Radiation Incident on Building Surfaces and Solar Heat Gains Through Windows", Symposium on Environmental Physics as Applied to Buildings in the Tropics, C.B.R.I. Roorkee, India, February 1969.
- Beckett, H.E. : "The Reflecting Powers of Rough Surfaces at Solar Wavelengths", Proc. Phys. Soc., 1931, No 43, pp 227-239.

- Beckett, H.E. : "Population Density and the Heights of Buildings", Trans. Illum. Eng. Soc., (London), July 1942.
- Billington, N.S. : Thermal Properties of Buildings, London : Cleaver-Hume Press, 1952.
: Building Physics : Heat, Pergamon Press, 1967.
- Brinkworth, B.J. : Solar Energy for Man, Salisbury, G.B. : The Compton Press, 1972.
- Buchberg, H. and J Naruishi : "On the Importance of Radiation Exchange in the Amelioration of Thermal Stresses in Enclosures", International Journal of Biometeorology, 1967, Vol. 11, No 1, pp 59-78.
: "A Rational Evaluation of Thermal Protection Alternatives for Shelter", Building Science, Vol. 2, 1967, pp 37-52.
- Burns, J. G. : Edinburgh Multi Access Systems, Edinburgh Regional Computing Centre, 1972.
- Bussat, P. and S. Jorgen : Sun Protection, ASCATEP, Bierut : November 1972.
- Button, D.A. : "Control of Daylight, Noise and Heat by the Building Structure", Lighting Research and Technology, Vol. 2, No 4, 1970, pp 225-231.
- Chroscicki, W. : "Calculation Methods of Determining the Value of Daylight's Intensity on the Ground of Photometrical and Actinometrical Measurement Unobstructed Planes", C.I.E., XVII Session, Barcelone, 1971, Pub. C.I.E. No 21B, p 71.24, 1972.

- C.I.E. Technical Committee : "Standardisation of Luminance Distribution on Clear Skies", Pub. C.I.E. No 22, (TC-4.2), 1973.
- Cowan, H.J., J.S. Gero, G.D. Ding and R.W. Muncey : Models in Architecture, Elsevier Publishing Company, 1968.
- Crogan, D. : "Daylight and the Form of Office Buildings", A.J., Dec 1965, pp 1501-1508.
- Curtis, D.M. and J. Lawrence : "Atmospheric Effects on Solar Radiation for Computer Analysis of Cooling Loads for Buildings at Various Location Heights", J.I.H.V.E., Feb 1972, Vol. 39, pp 254-260.
- Datta, K.L. : "Contribution of Landscape to Building Comforts", Indian Construction News, pp 80-82.
- Department of Environment - Welsh Office : Sunlight and Daylight : Planning Criteria and Design of Buildings, London : HMSO, 1971.
- Dorn, W.S. and D.D. McCracken : Numerical Methods with FORTRAN IV : Case Studies, J. Wiley Inter. Edition, 1972.
- Dresler, A. : "The Reflected Component in Daylighting Design", Trans. Illum. Eng. Soc. (London), Vol. XIX, No 2, 1954, pp 50-60.
- : "Simplifying Daylight Design", Arch. Sc. Review, Vol. 1, No 1, Nov 1958, pp 39-47.
- Echenique M : Models : A Discussion, Centre for Land Use and Built Form Studies, working paper No 6, Cambridge : March 1968.

- Fathy, H. : Architecture for the Poor, Chicago : The University of Chicago Press, 1973.
- Fitch, J.M. : American Building : The Environmental Forces that Shape It, Boston : Houghton Mifflin Company (2nd Ed.), 1972.
- Givoni, B. : Man, Climate and Architecture, Amsterdam: Elsevier Publishing Company, 1969.
- Giedt, W.H. : Principles of Engineering Heat Transfer, Van Nostrand Company, 1957.
- Hawkes, D. : Building Bulk Legislation : A Description and Analysis, Centre for Land Use and Built Form Studies, Working Paper No 4, Cambridge : 1969.
- Hawkes, D. : The Environmental Evaluation of Buildings : 5 Explorations, Centre for Land Use and Built Form Studies : Working Paper No 30, Cambridge:Sept 1970.
- Hawkes, D. : The Use of an Evaluative Model in Architectural Design : Case Studies, Centre for Land Use and Built Form Studies, Working Paper No 31, Cambridge : September 1970.
- Hawkes, D. : A History of Models of the Environment in Buildings, Centre for Land Use and Built Form Studies, Working Paper No 34, Cambridge : September 1970.
- Hawkes, D. and R. Stibbs : The Environmental Evaluation of Buildings: 1 A Mathematical Model, Centre for Land Use and Built Form Studies : Working Paper No 15, 2nd Ed., Cambridge : 1970.

- Hawkes, D. and R. Stibbs : The Environmental Evaluation of Buildings : 2 Technical Specification of the Model, Centre for Land Use and Built Form Studies : Working Paper No 27, Cambridge: Feb 1970.
- : The Environmental Evaluation of Buildings : 3 A worked Example, Centre for Land Use and Built Form Studies : Working Paper No 28, Cambridge: Feb 1970.
- Hamilton, D.C. and W.R. Morgan : Radiant-Interchange Configuration Factors, N.A.C.A., TN 2836, 1952.
- Hassall, D. : Reflective Insulation and the Control of Thermal Environment, St. Regis, ACI, Sydney, 1969.
- Holden, T.S. : "Low Temperature Radiation", J.ASHRAE, Vol. 3, No 4, April 1963, pp 51-54.
- Holden, T.S. and J.J. Greenland : The Coefficient of Solar Absorptivity and Low Temperature Emissivity of Various Materials, C.S.I.R.O. Report R.6, 1951.
- Hopkinson, R.G. : Architectural Physics : Lighting, London : HMSO, 1963.
- Hopkinson, R.G. and J.D. Kay : The Lighting of Buildings, London : Faber and Faber, 1972.
- Hopkinson, R.G., P. Petherbridge and J. Longmore : Daylighting, London : Heinemann, 1966.

- Hutchinson, D.W. : "Building Form", Construction Research and Development Journal, Vol. 2, No 3, Oct 1970.
- IBM Application Program : System/360 Scientific Subroutine Package, Version III, Programmer's Manual, 5th Ed., New York : 1970.
- Kinzey, B.Y. and H.M. Sharp : Environmental Technologies in Architecture, New Jersey : Prentice Hall, Inc., 1963.
- Kittler, R. : "Standardisation of Outdoor Conditions for the Calculation of Daylight Factor with Clear Skies", C.I.E. Inter-Sessional Conference 'Sunlight in Buildings', Newcastle-upon-Tyne, April 1965.
- × : "A Simple Method of Measuring and Evaluating the Atmospheric Diffusion of Sunlight when Seeking the Tropical Luminance Patterns of the Clear Sky", Symposium on Environmental Physics as Applied to Buildings in the Tropics, C.B.R.I., Roorkee, India, Feb 1969.
- × : "Standardisation of Solar Radiation with Regard to Prediction of Insolation and Shading of Buildings", C.I.B./W.M.O. Colloquium on Building Climatology, 'Teaching the Teachers', Stockholm, September 1972.

- Koenigsberger, O.H.,
T.G. Ingersoll, A. Mayhew,
and S.V. Szokolay
Krochman, J.
- : Manual of Tropical Housing and Building, Part One : Climatic Design, London : Longman, 1973.
- : "The Calculation of Daylight Factor for Clear Sky Conditions", C.I.E. Intersessional Conference 'Sunlight in Buildings', Newcastle-upon-Tyne, April 1965.
- : "On Quantities of Radiation and Light of Sun and Clear Sky", Symposium on Environmental Physics as Applied to Buildings in the Tropics , C.B.R.I., Roorkee, India, Feb 1969.
- : "Quantities of Illuminating Engineering for Daylight", UNESCO International Congress 'The Sun in the Service of Mankind', Paris : July 1973.
- Kuba, G.K.
- : Solar Heat Control of Buildings, N.B.R.S. (Khartoum), Building Research Digest No 4, Feb 1969.
- : "New Multi-Latitudinal Solar Shart", Build International, Vol. 5, No 4, July-August 1972, pp 209-213.
- Liu, B.Y.H. and
R.C. Jordan
- : "The Inter-Relationship and Characteristics Distribution of Direct and Total Solar Radiation", Solar Energy, Vol. IV, No 3, July 1960, pp 1-19.

- Loudon, A.G. : "The Interpretation of Solar Radiation Measurements for Building Problems", C.I.E. Intersessional Conference, 'Sunlight in Buildings', Newcastle-upon-Tyne, April 1965.
- : "Heat from the Sun", A.J., Vol. 143, No 2, January 1966, pp 138-143.
- McGuire, J.H. : Heat Transfer by Radiation, D.S.I.R. Fire Research Special Report No 2, HMSO, London : Reprint 1962.
- March, L : Some Elementary Models of Built Forms, Centre for Land Use and Built Form Studies, Working Paper No 56, Cambridge : July 1971.
- March L.J. and M. Trace : The Mathematical Description of Built Forms, Centre for Land Use and Built Form Studies, Working Paper No 1, Cambridge, 1968.
- March L. and P. Steadman : : The Geometry of Environment, London : R.I.B.A. Publications 1971.
- MOHLG : Planning for Daylight and Sunlight, Planning Bulletin No 5, London : HMSO 1964.
- Mirza, R.H. : "A Technique for Predicting Inter-Reflected Component of Illumination", UNESCO International Congress 'The Sun in the Service to Mankind', Paris, July 1973.

- Moon, P. : "Proposed Standard Solar Radiation Curves for Engineering Use", J.F.I. Nov 1940, pp 583-617.
- : Scientific Basis of Illuminating Engineering, New York : Dover Publication 1961.
- Morris, C.W. and J.H. Lawrence : "A Mathematical Model for Predicting Solar Radiation", ASHRAE Annual Meeting, Denver, Colorado, July 1969.
- Murison, J.M. (editor) : OS User's Guide, Edinburgh Regional Computing Centre, 1976.
- Narasimhan, V. and U.K. Maitreya : "Luminance Predetermination by Digital, Analogue and Model Techniques", Indian J., Pure Appl. Phys., Vol.6, July 1968, pp 394-396.
- : "The Reflected Component of Daylight in Multistoreyed Buildings in the Tropics", Build. Sci., Vol. 4, 1969, pp 93-97.
- Narasimhan, V. and B.K. Saxena : "Measurement of the Luminance Distribution of the Clear Blue Sky in India", Indian. J., Pure Appl. Phys., Vol. 5, 1967, pp 83.86.
- : "Luminance and Illumination from Clear Skies in the Tropics", C.I.E. XVII Session, Barcelone, 1971, Pub. C.I.E. No 21B, p 71.01, 1972.

- Narasimhan, V.,
B.K. Saxena and
V.K. Maitreya
- : "External Reflected Daylight in the Tropics", Symposium on Environmental Physics as Applied for Buildings in the Tropics, C.B.R.I. Roorkee, India, Feb 1969.
- NASA
- : Solar Electromagnetic Radiation, NASA, SP-8005, May 1971.
- Nautical Almanac
- : HMSO, 1964.
- Nicol, J.F.
- : Radiation Transmission Characteristics of Louver Systems, B.R.S. Note No EN66, B.R.S. Garston, U.K., 1964.
- Norden, K.
- : Shadow and Diffusion in Illuminating Engineering, Sir Isaac Pitman, London : 1948.
- O'Brien, P.F.
- : "An Analogue Computer for the Pre-Determination of Luminance Pattern", C.I.E. Quatorzieme Session, Bruxelles, June 1959, Pub. C.I.E., No 5B, p 59.18, 1960.
- : "Numerical Analysis for Lighting Design", Trans. I.E.S., J. Of Illum. Engng. Soc., April 1965, pp 169-177.
- : "The Shadow Factor of the Human Form", C.I.E. Seizieme Session, Washington, Pub. C.I.E., No 14B, p 67.06, 1968.

- O'Brien, P.F. and J.A. Howard : "Analogue and Digital Computer Solutions of Daylighting Problems",
J. of Illum. Engng. Soc., March 1959,
pp 177-187.
- : "Predetermination of Luminances by Finite Difference Equation",
Trans. I.E.S. J. of Illum. Engng. Soc.,
April 1959, pp 209-218.
- O'Brien, P.F. and E. Balogh : "Configuration Factors for Computing Illumination within Interiors",
Trans. I.E.S. J. of Illum. Engng. Soc.,
Vol. LXII, No 4, April 1967, pp 169-179.
- Olgay, V. and A. Olgay : Solar Control and Shading Devices,
Princeton : Princeton University Press,
1957.
- Olgay, V. : Design with Climate, Princeton :
Princeton University Press, 1967.
- : "Bioclimatic Orientation Method for Buildings", Int. J. Biometeor., 1967,
Vol. 11, No 2, pp 163-174.
- : "Solar Climates", Symposium on
Environmental Physics As Applied to
Buildings in the Tropics, C.B.R.I.,
Roorkee - India, February 1969.
- Page, J.K. : Climate and Town Planning with Special Reference to Tropical and Subtropical Climates, B.R.S. Overseas Building Notes,
No 52, June 1958.

- Parareda, V.G. : "Some Consideration Concerning Solar Architecture", COMPLES International Conference on Solar Energy, Madrid, Sept 1974.
- Parmelee, G.J. : "Irradiation of Vertical and Horizontal Surfaces by Diffuse Solar Radiation from Cloudless Skies", ASHVE Transaction, Vol. 60, 1954, pp 341-358.
- Petherbridge, P. : "Principles of Sun Control", A.J., Vol. 143, No 2, Jan 1966, pp 143-149.
- Plant, C.G.H. : "Predictive Techniques for the Evaluation of Inter-Reflected Illuminance in Interiors", C.I.E. XVII Session, Barcelone, 1971, Pub. C.I.E. No 21B, p 71.41, 1972.
- Plant, C.G.H. and D.W. Archer : "A Computer Model for Lighting Prediction", Build. Sci., Vol. 8, 1973, pp 351-361.
- Plant, C.G.H., J. Longmore and R.G. Hopkinson : "A Study of Interior Illumination Due to Skylight Under Tropical Conditions", C.I.E. Intersessional Conference 'Sunlight in Buildings', Newcastle-upon-Tyne, April 1965.
- "Natural Lighting Design Under Tropical Condition", Symposium on Environmental Physics as Applied to Buildings in the Tropics, C.B.R.I., Roorkee - India, Feb 1969.

- Pleijel, G. : The Computation of Natural Radiation in Architecture and Town Planning, Bulletin No 25, Statens Namnd for Bygghadsforskning, Stockholm, 1954.
- Ragsdale, L.A. and E.A. Raynham : Building Materials Technology, Edward Arnold : G. Britain, 2nd Edition, 1972.
- Rennhachkamp, W.H.H. : Sky Luminance Distribution in Warm Arid Climates, N.B.R.I., C.S.I.R., No R/BOU 20, Pretoria, S.A., 1967.
- Roa, K.R. and T.N. Seshadri : "Solar Insulation Curves", Indian Journal of Meteorology and Geophysics, 12, No 2, April 1961, pp 264-272.
- Robinson, N. (ed) : Solar Radiation, Elsevier Publishing Company, 1966.
- Robertson, R.G. : "Measurements of the Diffuse Solar Radiation and its Distribution over the Sky Hemisphere", C.I.E. Intersessional Conference 'Sunlight in Buildings', Newcastle-upon-Tyne : 1965.
- Roux, J.L. : "Approche Methodique des Problems de l'Ensoleillement dans l'Habitat", UNESCO International Congress, 'The Sun in the Service of Mankind', Paris, July 1973.
- Sharma, M.R. and R.S. Pal : "Interrelationships between Total, Direct and Diffuse Solar Radiation in the Tropics", Solar Energy, Vol. 9, No 4, Oct - Dec 1965, pp 183-192.

- Sharma, M.R. and A. Sharafat : "An Improved Method of Computing the Incident Solar Radiation on Buildings", Symposium on "Environmental Physics as Applied to Buildings in the Tropics", C.B.R.I., Roorkee - India, Feb 1969.
- Smart, W.M. : Spherical Astronomy, Cambridge University Press, 1962, (fifth edition).
- Sparrow, E.M. : "A New and Simpler Formulation for Radiative Angle Factors", Trans. of ASME, J. of Heat Transfer, May 1963, pp 81-88.
- Steadman, P. : Energy, Environment and Building, Cambridge University Press, 1975.
- Stibbs, R. : The Prediction of Surface Luminances in Architectural Spaces, Centre for Land Use and Built Form Studies, Working Paper No 54, Cambridge : 1971.
- Sun, T.Y. : "Computer Evaluation of the Shadow Area on a Window Cast by the Adjacent Building", ASHRAE J. , Sept 1968, pp 66-68.
- : "Shadow Area Equation for Window Overhangs and Side Fins and their Application in Computer Calculation", ASHRAE TRANS., Vol. 74, Part 1, 1968.
- Tappuni, R.R. : A Generative Approach to the Thermal Design of Buildings in Hot Dry Climate, PhD Thesis, Edinburgh University, 1973.

- Thekaekara, M.P. : "Solar Energy Outside the Earth's Atmosphere", Solar Energy, Vol. 14, 1973, pp 109-127.
- Tonne, F. : "Some Problems of Insolation and Daylight in the Planning of Building", WMO/WHO Symposium on Urban Climates and Building Climatology, Docc. 22, Brussels, 1968.
- Toups, K.A. : A General Computer Program for the Determination of Radiant-Interchange Configuration and Form Factors: CONFAC II, Space and Information Systems Division Report No SID 65-1043-2, North America Aviation Inc, Los Angeles , Oct 1965.
- Valko, P. : "Short Wave Irradiation of Cylindrical and Rectangular Bodies", Fifth International Biometeorological Congress, Study Group for Architectural, Urban and Engineering Biometeorology, Montreux, Sept 1969.
- : Radiation Load on Buildings of Different Shape and Orientation Under Various Climatic Conditions, Reprint from Building Climatology, Technical Note No 109, WMO - No 225 TP 142, 1970.
- : "The Effect of Shape and Orientation on the Radiation Impact on Buildings", C.I.B./WMO Colloquium on Building Climatology 'Teaching the Teachers', Stockholm : Sept 1972.

- Van Bremen, H. : "Daylight Requirements and Calculation in Tropical Regions", Build International, May 1969, pp 36-39.
- Van Deventer, E.N. : "Sun Light and Shade Design", Build International, Vol. 5, No 4, July-August 1972, pp 205-208.
- Van Deventer, E.N. and T.B. Dold : Some Initial Studies on Diffuse Sky and Ground Reflected Solar Radiation on Vertical Surfaces, Reprint, C.S.I.R., Reference No R/Bou 106, Pretoria - S.A., 1966.
- Van Deventer, E.N., T.B. Dold and J. Wessels : Diffuse Solar Radiation on Vertical Surfaces, N.B.R.I., C.S.I.R. Research Report 303, Pretoria - S.A., 1971.
- Van Straaten, J.F. : Thermal Performance of Building, Elsevier Publishing Company, 1967.
- Van Straaten, J.F., F.J. Lotz and E.N. Van Deventer : "The Sun and the Design of Buildings for Tropical Climates", Symposium on Environmental Physics as Applied to Buildings in the Tropics, C.B.R.I., Roorkee - India , Feb 1969.
- Wiebelt, J.A. : Engineering Radiation Heat Transfer, Winston : Holt Rinehart 1966.
- Wilson, C.B. : "Physical Relationships in Architecture", Cooperative Phenomena, (ed. by H Haken and M Wagner), Springer Verlag, Berlin - Heidelberg - New York : 1973.